CIVIL ENGINEERING SERIES

Frederic T. Mavis, Consulting Editor

Soil Mechanics, Foundations, and Earth Structures

Soil Mechanics, Foundations, and Earth Structures

AN INTRODUCTION TO THE THEORY AND PRACTICE OF DESIGN AND CONSTRUCTION

GREGORY P. TSCHEBOTARIOFF

Professor of Civil Engineering
Princeton University

FIRST EDITION

1951

McGRAW-HILL BOOK COMPANY, INC.

New York Toronto London

SOIL MECHANICS, FOUNDATIONS, AND EARTH STRUCTURES

THE MAPLE PRESS COMPANY, YORK, PA.

TO

PRINCETON UNIVERSITY

in grateful acknowledgment of
the sabbatical leave during which
a large part of this book was written

FOREWORD

This book has characteristics which will, I believe, lead to its recognition as a publication of real importance. It should, first of all, be of great value to the student as a text. Secondly, its clarity and readability commend it to the engineer who wishes to improve and broaden his knowledge of soil mechanics and allied subjects. Finally, it should prove an invaluable reference to the practicing engineer who handles foundation work and the engineering of earth structures. This is because it not only describes the way in which the techniques of soil mechanics can lead to sound solutions of many problems in these fields but it also acknowledges the limitations of these techniques, and, indeed, of our present-day knowledge of many soil phenomena.

Over a quarter of a century has passed since Dr. Karl Terzaghi coined the German term "Erdbaumechanik" which, freely translated, gave to English-speaking engineers the term "soil mechanics." Since then many books, papers, and publications on soil mechanics have appeared in English. Many of these possess great merit and practically all contain information of value either to the student, the teacher, or the practicing engineer.

The great value of this new book by Professor Tschebotarioff stems, I believe, from the unusually broad and firm foundation of practical experience upon which it rests. Its author is firstly an engineer of wide experience both in America and abroad. Teaching has enabled him to develop, to an unusual degree, his native gift for imparting knowledge to others. Finally, his teaching career has been carried on simultaneously with consulting and research work which have not merely kept him abreast of the times, but made him an outstanding pioneer in the investigation of such important phenomena as earth pressures. The results of his extensive research in this field are given in this book and should alone make it invaluable to practicing engineers. In addition it is a general text of outstanding merit on *Soil Mechanics, Foundations, and Earth Structures.*

W. MACK ANGAS
Vice Admiral, Civil Engineer Corps
United States Navy, Retired

PREFACE

This book has been developed from lecture notes for courses which the author has given at Princeton University since 1937, when undergraduate instruction in soil mechanics was started in the Department of Civil Engineering. Instruction at a graduate level followed a few years later.*

In this work the author was guided by the following thoughts. Every civil engineer should be prepared to deal with soil engineering and foundation problems and should therefore have a general knowledge of the fundamentals involved. However, the first thing to be learned about soils is that they differ in several important aspects from other materials which civil engineers have to handle. An essentially different approach to their study is therefore indicated. The strength and the deformation characteristics and other engineering properties are not constant for a given soil but may be altered appreciably with time and by the manner in which construction operations are carried out. Stress analyses in soil masses are much more complex than in other civil engineering structures. Rigorous solutions are therefore often based on oversimplified assumptions and hence have only a limited value. By contrast, experimental procedures, which include measurements on full-scale structures, often yield information of decisive importance. Previously accepted theories frequently have to be modified or even rejected on the basis of new experimental data. Such data are far from easy to obtain and at present are rather limited, so that some latitude is still left for the exercise of judgment as to the proper use of existing theories. Hence the strong element of art in all soil and foundation engineering work should not be overlooked. The acknowledgment of its existence is necessary for the understanding of the present status of this field of knowledge and endeavor, as well as of the methods of approach which are essential for its further advancement. This requires the cooperation of the entire civil engineering profession.

These facts lead to the conclusion that an introductory presentati of the theories of soil mechanics should be closely linked to a brief description of the related design and construction practices of soil and foundation engineering. This principle has been followed in this book, which is

* See Refs. 376 and 394.

intended for use at undergraduate and graduate levels and as a general reference.

The past quarter of a century has seen an exceptionally rapid growth of our knowledge concerning the engineering properties of soils. Many time-honored concepts have been proved invalid by the new semiempirical techniques of correlated field observations, laboratory testing, and theoretical analyses. New concepts have been introduced. Many of these concepts have successfully withstood the test of repeated checks in the field. The understandable pressure from practicing engineers for the accelerated development of new simplified guiding rules, combined with the incomplete data as yet available concerning many essential points, however, has led in some instances to the premature acceptance of generalizations which later were shown to be unwarranted. This has been the case in a number of special fields of considerable practical importance; for instance, in problems concerned with the effects of sensitivity of different types of clay to remolding; with the effects of plastic flow on the shearing strength and on the lateral pressures of clay; with the natural frequency of soils subjected to vibrations; and with the effects of so-called "arching" on the lateral pressures of sands. An uninterrupted continuation of this process of reexamination and reevaluation is necessary for the further healthy development of soil engineering. A constructively critical attitude is a prerequisite to that end; to be effective, it has to be combined with a thorough knowledge of the factual basis on which our modern concepts have been erected.

Considerable space in this book has therefore been devoted to records of failures, of field measurements and to other experimental evidence. Emphasis has been placed on differentiation between hypotheses and proven facts. The importance of understanding by civil engineers of allied geotechnical sciences, especially geology and soil physics, is demonstrated by examples. The effect on the soil engineering practice in different countries of varied geological, climatic, and economic conditions has been stressed. Whenever possible, theoretical concepts have been developed from first principles along lines most familiar to American engineers. For instance, the equations of the so-called "classical" earth-pressure theories, instead of being explained by references to conjugate stresses, have been derived from the equilibrium conditions of a small prism, as is done in most undergraduate textbooks on mechanics of materials when developing the concept of principal stresses. Evaluations have been made of the limits of practical application of theories and of points of view, especially when some of them are in conflict with each other.

The wide field covered by the book compelled numerous cross references

and a very condensed presentation, which was facilitated by the provision of a large number of diagrams (approximately 400) and of other illustrations. Case problems and their numerical solutions have been used for the same purpose. Repetition of material available in regularly used textbooks on other subjects has been avoided. For instance, the determination of the depth of concrete and of the steel reinforcement of footings and of retaining walls has not been included in the book. A few selected references are given at the end of each chapter to permit a more detailed study of the subject matter treated in that chapter. In addition, an extensive list of more than 440 references has been provided at the end of the book in support of statements made and to facilitate further advanced studies, including work of a research character.

Our present knowledge of the engineering properties of soils is the result of work by many men in different countries all over the world, and every effort has been made to give in the text of the book proper credit to the pioneers in this field, as well as to their successors.

The author acknowledges the valuable experience he gained on the banks of the Nile while in the service of the Egyptian Government (1929 to 1936) and the splendid opportunities for further research which arose for him at Princeton University from projects in the field of applied soil mechanics sponsored by the Technical Development Service of the Civil Aeronautics Administration (1943 to 1946) and, especially, by the Bureau of Yards and Docks of the United States Navy (1943 to 1949) and the Earth Sciences Division of the Office of Naval Research in Washington, D.C. Very valuable data concerning lateral earth pressure measurements in the approach cuts to the Rotterdam subaqueous tunnel became available through the courtesy of Mr. J. P. van Bruggen, Chief Director of Public Works, Rotterdam, The Netherlands. Private consulting work also served to provide a substantial amount of material for this book. The author is particularly indebted to Spencer, White and Prentis, Inc., of New York City, who not only released data obtained by him when serving as their consultant, but supplied further valuable and so far unpublished information. The cooperation in research work by Sprague and Henwood, Inc., of Scranton, Pennsylvania, is much appreciated, as well as the preparation by that firm of several drawings for this book. Other acknowledgments are made in the text.

The author wishes to express his thanks to Dean Kenneth H. Condit for the provision of funds by the Princeton School of Engineering for the typing of this manuscript, to Vice Admiral W. Mack Angas (CEC), USN, Ret., Chairman of the Princeton Civil Engineering Department, for the review of the entire manuscript and for many valuable suggestions, and to his colleague Dr. Hans F. Winterkorn for the review of the articles on

soil physics in Chap. 3 and on soil stabilization in Chap. 11; also to Yasumaru Ishii for reading the manuscript and pointing out some insufficiently clear passages. The manuscript was typed by Mrs. W. Brickley.

GREGORY P. TSCHEBOTARIOFF

PRINCETON, N.J.
June, 1951

CONTENTS

NOTATION

The recommendations of the American Society of Civil Engineers (Ref. 9) and of the American Society for Testing Materials (Ref. 10) concerning soil mechanics nomenclature have been closely observed in this book. The exceptions are few. Symbols of secondary importance, for instance some of the subscripts, are not listed but are defined in the text.

As a general rule, the metric system has been employed in this book in connection with laboratory work, whereas the English system has been used mainly in connection with field tests and design problems. The following conversion factors may be helpful to the reader:

1 ton = 2,000 lb
1 kip = 1,000 lb
1 lb = 454 gm
1 kg = 2.205 lb
1 ft = 30.5 cm
1 in. = 2.54 cm
1 ft^3 of fresh water weighs 62.4 lb
1 kg per $cm^2 \approx 1$ ton per ft^2
1 cm per sec $\approx 1 \times 10^6$ ft per year, Eq. (5-5)

Symbols

A = area; or acceleration, Eq. (18-8)
A_p = anchor pull, Eq. (16-2)
a = small area, Eq. (5-6)
a_v = coefficient of compressibility, Eq. (6-9)
a_c = air content, Eq. (4-15)
b = width
C = coefficient, Eq. (3-5), or Eq. (15-6), or Eq. (16-8); or pounds of detonated dynamite, Eq. (18-12)
C' = coefficient, Eq. (10-32)
C_a = area ratio of a soil sampler, Eq. (12-1)
C_d = coefficient, Eq. (10-43)
C_i = inside clearance ratio of a soil sampler, Eq. (12-2)
c = cohesion per unit of area; or coefficient, Eq. (15-3) (*Engineering News* formula); or damping constant, Eq. (18-2)
c_v = coefficient of consolidation, Eq. (6-27)
D = diameter of disk, Eq. (3-6); or diameter of tube, Eq. (4-18); or depth, Fig 8-9, or Eq. (14-6), or Eq. (16-10)
D' = diameter of sphere, Eq. (3-6)
D_d = relative density of granular soils, Eq. (4-16)
d = diameter, Eq. (3-3), or Eq. (6-34); or distance, Eq. (13-2)
E = modulus of elasticity
E_A = active lateral earth pressure, total

E_P = passive lateral earth pressure (resistance), total
e = void ratio, Eq. (4-2); or base of natural logarithms; or coefficient, Eq. (10-29)
e_{cr} = critical void ratio of sands, Art. 7-16
F = force, total
F_s = factor of safety
f = force per unit of area (unit stress); or coefficient, Eqs. (16-20) to (16-22); or frequency of vibration, Eq. (18-8)
f_e = effective force per unit of area (effective stress), Eq. (6-1)
f_n = natural frequency of undamped vibration, Eq. (18-1)
f_{nd} = natural frequency of damped vibration, Eq. (18-2)
f_{nr} = reduced natural frequency of undamped vibration, Eq. (18-7)
G = specific gravity, Eq. (3-1); or modulus of elasticity in shear, Eq. (10-28)
g = acceleration of gravity
H = height; or depth; or thickness
H_{max} = limit depth of a braced cut, Eqs. (14-8) to (14-10)
h = hydraulic head, Eqs. (5-1) to (5-8); or height of specimen, Eqs. (6-3) to (6-10)
h_{cr} = critical height of an unsupported vertical cut, tensile stresses neglected, Eq. (8-4)
h_{cr}' = critical height of an unsupported vertical cut, tensile stresses considered, Eq. (8-10)
I = moment of inertia of a section
I_c = consistency index, Eq. (4-21)
I_p = plasticity index, Eq. (4-17)
I_L = liquidity index, Eq. (4-22)
J = seepage force, total, Eq. (5-17)
j = seepage force per unit of volume, Eq. (5-18)
K = lateral earth pressure coefficient (ratio between lateral and vertical pressures); or constant, Eq. (18-12)
K_γ = ratio between the measured lateral earth pressure and the weight of the overburden at that point, Eq. (10-5*a*)
K_n = coefficient of "neutral" lateral earth pressure; or coefficient of lateral earth pressure "at rest," or "at consolidated equilibrium"
K_A = coefficient of active lateral earth pressure, Eq. (10-4)
K_a = coefficient of active lateral earth pressure, based on Eq. (10-35)
K_p = coefficient of passive lateral earth pressure, Eq. (10-13)
K_s = lateral earth pressure coefficient, based on intergranular pressures
K_{s+w} = lateral earth pressure coefficient, based on intergranular plus free-water pressures, Eq. (10-31)
k = coefficient of permeability, Eq. (5-2); or linear spring coefficient, Eq. (18-1)
k' = dynamic modulus of subgrade reaction, Eq. (18-3)
k_s = modulus of subgrade reaction, static, Eq. (19-1)
L = distance; or length
L_f = load factor, Eq. (16-24)
M = moment; or mass
M_o = overturning moment, Eq. (8-11)
M_r = resisting moment, Eq. (8-12)
m_v = modulus of volume change, Eq. (6-11), cm^2 per gm
m_v' = modulus of volume change, Eq. (6-12), cm^2 per kg
n = porosity, Eq. (4-1); or viscosity, Eq. (3-3); or ratio, Eq. (6-34)
P = force, total; or load, total; or weight of pile, Eq. (15-2)

P_t = tangential force; or tangential load
P_n = normal force; or normal load
p = load per unit of area
p_0 = permissible bearing value (load) per unit of area
p_{max} = bearing capacity (ultimate load per unit of area)
Δp = increment of load per unit of area
Q = discharge, Eq. (5-4)
q_u = unconfined compressive strength, Eq. (7-15)
R = reaction; or resultant force, total; or radius; or ultimate resistance of a pile, Eqs. (15-1) to (15-6)
R_s = safe load on pile, Eq. (15-4)
r = radius
S = sensitivity of a clay to remolding, based on ultimate strengths, Eq. (7-20)
S' = sensitivity of a clay to remolding, based on equal strains, Eq. (7-21)
S = settlement, Eq. (6-2), or Eq. (6-10); or pile set, Eqs. (15-1) to (15-6); or hydraulic gradient, Eq. (5-1)
S_{cr} = critical hydraulic gradient, Eq. (5-21)
S_r = degree of saturation, Eq. (4-14)
s = shearing strength, Eq. (7-1)
T = time factor, Eq. (6-29); or period of vibration, Prob. 18-3
t = time, Eqs. (5-6) to (5-8), or Eqs. (6-19) to (6-27) and others
$U\%$ = average percentage of consolidation, Eq. (6-2)
U = coefficient, Eq. (10-37)
u = neutral stress; or excess pore pressure, Eq. (6-1)
V = volume; or total shear, Eq. (10-40)
v = velocity
W = weight
w = water content
w_L = water content at the liquid limit
w_n = natural water content
w_p = water content at the plastic limit
w_s = water content at the shrinkage limit
x = horizontal distance; or coefficient, Eq. (10-37)
y = horizontal distance; or deflection (displacement)
Z = energy losses, Eq. (15-1)
z = vertical distance
z_0 = depth of a tension crack at the top of a bank, Eq. (10-18)

α = angle, Eq. (4-18); or coefficient, Eq. (10-44)
α_R = angle of repose
β = angle, Fig. 8-10, or Eq. (10-21)
γ = unit weight, Eq. (4-7), or Eq. (4-8) (metric system)
γ_d = unit dry weight, Eq. (4-6) (metric system)
γ' = buoyed unit weight, Eq. (4-9) (metric system)
γ_m = unit weight (English system)
γ_{md} = unit dry weight, Eq. (4-10) (English system)
γ_m' = buoyed unit weight, Eq. (4-11) (English system)
γ_w = unit weight of water (metric system)
Δ = increment
δ = angle of wall friction, Eq. (10-21)

ϵ = unit strain
ϵ_f = vertical strain at failure during unconfined compression test, Table 7-1
θ = angle
θ_{cr} = angle defining the plane with least resistance to shearing along it (failure plane), Eq. (7-10)
λ = coefficient, Eq. (10-27)
μ = micron (= 0.001 mm)
ν = Poisson ratio, Eq. (10-23); or Froehlich's stress-concentration factor, Eq. (9-8)
σ = normal stress (normal component of internal force per unit of area)
σ_n = normal stress on a plane which is not a principal plane
σ_1 = major principal stress
σ_3 = minor principal stress
τ = shearing stress (tangential component of internal force per unit of area)
ϕ = angle of internal friction
ω = angle, Eq. (10-21)

CHAPTER 1

SPECIAL FEATURES OF FOUNDATION AND SOIL ENGINEERING

1-1. The Purpose and the Importance of a Foundation. The term *foundation* is used to designate the part of a structure which serves to transmit to the soil beneath it its own weight, the weight of the superstructure above it, and any forces which may act upon them. A foundation is therefore the connecting link between the superstructure and the soil.

The function of a properly designed foundation is to support the loads resting on it and to distribute them in a satisfactory manner over the contact surfaces of the soil layer on which it rests. In order to be satisfactory, this distribution must not produce excessive stresses within the soil mass at any depth beneath the foundation. One must obviously consider as excessive stresses which would cause a complete rupture within the supporting soil mass and a noticeable tilting and sinking of the structure as a whole. This is not a frequent occurrence where buildings are concerned, as may be seen from Fig. 9-25, but it is not unknown. Damages to roadbeds or earth dams due to rupture failures and slides of the soil or supporting embankments also happen occasionally (Figs. 19-1 and 17-2).

Stresses are also to be rated as excessive if the cumulative action of the strains they produce causes a settlement of the supporting soil surface so uneven that the structure above it would be cracked or otherwise damaged while undergoing deformations required to adapt it to this uneven settlement. Extreme cases of this type of damage due to unsatisfactory foundations are illustrated by Figs. 13-6(II) and 13-14. The importance of foundations is self-evident, since no structure can endure without an adequate foundation.

When the surface soil layers are too weak, the foundation has to be carried down to more resisting layers if such are present within easy reach. According to circumstances, this can be done by open excavation, by driving piles, or by sinking caissons to the desired depth. But, whatever

may be the type of foundation or the depth below the soil surface to which the foundation reaches, the loads that it will transmit to these layers will always cause stresses and therefore strains in the supporting soil mass. As in all other materials, the magnitude of the unit strains will depend on the magnitude of the corresponding unit stresses and on the elastic and plastic properties of the supporting soil. These strains will always be present and their sum will always produce some deformation and settlement of the contact surfaces between the foundation and the supporting soil.

1-2. The Interaction between the Superstructure, the Foundation, and the Soil beneath It. A foundation will naturally tend to follow any settlement of the soil on which it rests. In turn, the superstructure will follow the settlement of the foundation which supports it. Both will tend to equalize uneven settlements by resisting deformation and thereby transmitting more load to those parts of the soil surface which have settled least. No deformation of the soil surface beneath a structure can take place without a corresponding deformation of both the foundation and the superstructure above it. This remains true for any type of structure, be it a building, a bridge, a road, or a dam.

The supporting soil, the foundation, and the superstructure form one single unit and should therefore always be considered as a whole. The interaction between them is very complicated and will be discussed in greater detail later (Art. 13-3). However, it is most important to bear in mind the fact of such interaction from the very start of studies in this field. It has been too often disregarded in the past, largely because of the complexity of the problem, analysis of which was not even attempted with the more limited knowledge available in earlier periods in the history of engineering. As a result of this complexity of foundation problems the scientific development of foundation engineering has remained far behind that of structural engineering proper. For the same reason even present-day foundation work requires methods of approach which differ from those usual in structural engineering.

1-3. The Causes of the Past Lag in the Scientific Development of Foundation Engineering. As compared with the structural engineer, the foundation engineer was, and still is, in a much less favorable position.

The analysis of stress distribution in soil masses is a complicated problem of a highly indeterminate nature requiring a thorough knowledge of advanced higher mathematics and of the theories of elasticity and plasticity. For new problems the help of specialists in these fields has to be resorted to. Their solutions for idealized conditions then have to be critically examined by the engineer in order to be adapted as closely as possible to the actual and generally much more complicated field condi-

tions. Such adaptations often reduce the value of the mathematically exact solution to that of a simple estimation. Frequently no direct use of the solution can be made, although it generally retains the value of an indication of likely limit conditions.

The main difficulty lies in the much more complicated engineering properties of soils as compared with other building materials. Most soils are three-phase systems; that is, they are composed of solid matter, of water, and of air. Their behavior under stress is strongly affected by their density and by the relative proportions of water and of air filling their voids. These properties may vary with time and depend to a limited extent on a number of other factors. The time element becomes very important in the study of the stress-strain relationships of soils.

Other factors which are relatively negligible in the study of these relationships for other building materials, such as the rate and the manner of application of loads, may become of cardinal importance where some soils are concerned. Changes in the moisture content of most soils may greatly alter many of their important engineering properties. These properties may also be strongly affected by vibrations and by changes in the condition of lateral confinement of the soil. All the above is true both for undisturbed natural soil deposits supporting foundations and for artificially selected and compacted soils used as a construction material for earth structures such as dams and embankments.

In the case of undisturbed natural soil deposits which support structures erected on them, the difficulties of the determination of their engineering properties are still further increased by their frequent lack of uniformity due to the erratic processes of their formation by nature. It is therefore not always possible to proceed in a manner identical with that used for other building materials and to judge accurately the average engineering properties of a large soil mass on the strength of tests on a few samples. Further, it is extremely difficult to extract for testing small samples from the depth of a natural deposit without changing their properties. Under the circumstances it is not surprising that the scientific development of foundation engineering lagged far behind that of structural engineering.

1-4. Nonengineering and Early Engineering Soil Studies. Many soil studies have been made for other than civil engineering purposes but their results could not be directly applied to foundation work. Very extensive soil studies have been carried out by agricultural soil scientists and by geologists, naturally for purposes of their own specialty.

Agricultural soil scientists are concerned mainly with the properties of a few upper feet of the soil crust which are of importance to the growth of plants. Nevertheless, some of the work performed by them is valuable

for the understanding of the properties of all soil materials. For instance, the chemical processes of soil deterioration and leaching, the effect of the prevailing climate on the nature of the chemical changes accompanying such decomposition, and some drainage and various other problems have been extensively treated by agricultural soil scientists. These investigations have a special character, but the study of their development is, nevertheless, recommended to civil engineers specializing in laboratory soil research or in highway or airport soil stabilization. The same may be said concerning some interesting aspects of research on clays performed by ceramic engineers and chemists.

The approach of geologists to soil problems naturally differs from that of engineers. A geologist will call *rock* any material of which the earth is composed, no matter whether it is hard or soft, and is mainly interested in its origin and manner of formation. The systematic study of the behavior of soils under stress, with which engineers are mainly concerned, has not been undertaken by geologists. Nevertheless, in other respects they can provide assistance of an indispensable nature to engineers. Cooperation between geologists and engineers is therefore essential (Art. 2-9).

Civil engineers were thus compelled to solve their own soil problems. One of the earliest efforts on record in this field was made by Coulomb (1776) and was connected with the determination of earth pressures on retaining walls. Although true for granular soils and rigid walls only, it is particularly notable because with some restrictions its results are to be considered valid to this day.

Other early attempts consisted mainly of field load tests on small footings and single piles, and of the measurement of the resistance of piles to driving. Their interpretation was purely empirical in view of the general lack of basic knowledge concerning the stress-strain relationship and other important physical properties of soils as well as of the laws governing the stress distribution within them. A number of fallacious conceptions resulted.

1-5. Scientific Soil Studies by Civil Engineers. The Appearance of the Term Soil Mechanics. A better understanding of the limitations of small-scale field load tests was reached after a series of laboratory-model tests in several countries, involving the actual measurement of pressures within sand fills. The similarity under certain conditions of the pressure distribution thus obtained and of the pressure distribution derived from a purely mathematical analysis of homogeneous elastic bodies led to cooperation between foundation engineers and the specialists in the field of the theory of elasticity.

The understanding of the basic physical properties of soils in general

and of the plasticity of clay in particular was advanced at the beginning of this century by the Swedish scientist Atterberg and through studies of landslides by the Geotechnical Commission of the Swedish State Railways. The systematic study of the shearing characteristics of soils was begun at about the same time by Dr. Krey in Germany.

A particularly important advance was made through the work of Dr. Terzaghi, who in 1923 published a mathematically rigorous solution of the rate of consolidation of clays under applied pressures. This theory was confirmed experimentally and explained the strong time lag of settlements on fully waterlogged clay deposits. Dr. Terzaghi is a rare example of a practicing civil engineer combining extensive field experience with advanced scientific training and an aggressive pioneer spirit. Apart from his theory of consolidation and other original research, the engineering profession is indebted to him for the first attempts to coordinate and systematically apply to foundation practice the results of engineering research on soils and to correlate their field performance to their numerically defined engineering properties. The term *soil mechanics* was coined by him in 1925 when one of his books appeared under the equivalent German title *Erdbaumechanik.* Although written in German, this book was dedicated to the American Robert College in Istanbul. In the same year Dr. Terzaghi came to the United States to serve as a research consultant to the U.S. Bureau of Public Roads. Since that time his further work and the work of many men he helped to initiate to the new science of soil mechanics in different countries have exercised a great influence on foundation engineering practice all over the world.

At present most of the important engineering schools are equipped with soil mechanics laboratories. Many important organizations, for instance, the U.S. Army Engineers, the Public Roads Administration, and the U.S. Bureau of Reclamation, maintain numerous soil laboratories both for research and for field control testing. The principles of soil mechanics are applied to their engineering design work as a matter of routine.

Nevertheless, civil engineers with little practical experience with soils often expect too much at first from the new science and sometimes are disappointed when they find that the results of mathematical derivations contained in its theory, or the results of its laboratory soil tests, cannot always be directly applied to actual practice in a manner similar to that to which they are accustomed in structural engineering. Many critical remarks by practicing engineers in the past may be traced to an insufficient understanding of the special nature of soil mechanics. Also, it is much too often believed that scientific engineering and a rigorous treatment of a design problem are synonymous.

A common fallacy is to attempt to assume simplified conditions differ-

ent from those actually existing, in order to permit a mathematically rigorous treatment, and to forget afterward that the result refers to idealized conditions only. Actually mathematics should be considered by engineers as only *one* of the tools designed to help them. The scrutiny of *all* factors affecting a foundation problem is essential and must be followed by an approximate estimation of their combined action on the basis of known facts concerning these factors and by an exercise of sound judgment as to their relative importance. This method involves a strong element of experience and personal skill and therefore of art.

The following chapters of this book will attempt to outline how this desirable approach to soil and foundation problems can be realized in actual present-day practice. The present stage of development is far from complete. Much further development is yet to be expected in this field as a result of continued research. But before starting on its study, it is well to realize its special features, and to realize that there should be a basically different approach to the problems of earth structures and to the problems of foundations.

1-6. Difference in the Advisable Approach to the Study of Foundations and of Earth Structures. The erection of earth structures, such as earth dams, embankments, airports, roads, and other fills, involves the artificial removal of soil from its natural deposit, the selection of suitable material, and the placing of this material in the new structure in a definite, controlled manner. The average nature, the composition, and other properties of the soil in the structure can be known to the engineers, as well as the extent of likely variation from this average. It is therefore possible to reproduce fairly closely in the laboratory conditions approximating the ones which will prevail in the finished structure and to test under these conditions the same types of soil material as the ones of which it will be composed. It is therefore further possible to approach the study of earth structures in a manner not very different from the one used in branches of structural engineering which work with ordinary man-made building materials.

The approach to foundation engineering proper should be entirely different. Here one has to deal with natural soil deposits performing the engineering function of supporting the foundation and the superstructure above it. Nature has erected most of these deposits in an extremely erratic manner, producing an infinite variety of possible combinations of factors affecting the choice and the execution of foundations. In many cases foundation engineers do not have the option of selecting a more suitable site for a structure, but have to meet soil conditions as they find them on sites selected for geographical, traffic, commercial, and other considerations.

The most modern methods of soil exploration and testing cannot at present provide completely accurate information concerning the actual average engineering properties of the whole undisturbed, naturally deposited soil mass under the structure, and probably will never be able to do so. All they can do is to give indications as to what these properties are likely to be. This is already a very great step forward as compared to previous pure guesswork in this field. The foundation engineer has to weigh these indications in the light of recorded experiences with similar structures under similar conditions, and then act on the basis of his judgment. The recording in a suitable manner of foundation experiences thus assumes a very important function. Foundation engineering is likely always to retain features of an art, with soil mechanics maintaining the position of its most important auxiliary science. The solutions provided by soil mechanics necessarily refer to idealized conditions. These idealized conditions should be so selected as to provide solutions for *limit* conditions likely to be met in the field. Determination of such limits becomes very important, since the designs should then take into account possible variations within the limits.

1-7. Rupture and Deformation Problems in Foundation and Soil Engineering. It is further important to differentiate between problems involving complete rupture of a soil mass and problems involving only its deformation. The maximum bearing capacity of a spread foundation and the maximum unsupported height of a vertical cut or of a slope in clay soils are examples of rupture problems, governed by the shear strength of the soil. The latest methods of determining the ultimate shearing strength of soils, including field sampling and laboratory testing procedures, have been found fairly reliable.

On the other hand, deformation problems, such as the settlement of a structure, are much more difficult to handle in practice. Experience has shown that in many cases laboratory tests may give not entirely accurate values, especially in the case of natural undisturbed soils. Any slight disturbance or swelling of such soils during or after sampling strongly affects the numerical values of coefficients by which are defined the deformation characteristics of soils. Corrections based on full-scale observations of the performance of actual structures in the field become essential. Because of the great variety of soil types, such studies have to be performed on a regional basis. A semiempirical approach of this kind has actually been tried in several localities with satisfactory results.

A number of problems, such as the lateral pressures exerted by different types of soils against the timbering of cuts or against other earth-retaining structures, may involve both rupture and deformation characteristics of soils.

It should be noted that soil-deformation problems may have great practical importance. Thus excessive differential settlements of the soil surface under a building may not involve any rupture of the soil itself, but may cause cracking and other types of failure in the superstructure unless it is specially designed to resist such differential settlements.

Problems involving gravitational and nongravitational flow of water through soils are also in a separate class, since such water movements may affect both the rupture and the deformation of soils.

References Recommended for Further Study

"Ends and Means in Soil Mechanics," by Karl Terzaghi, *Journal of the Engineering Institute of Canada*, December, 1944. Contains discussion of the past and of the likely future trends in soil mechanics with emphasis on the importance of semi-empirical procedures.

"Early History and Bibliography of Soil Mechanics," by Jacob Feld, *Proceedings of the Second International Conference on Soil Mechanics and Foundation Engineering*, Rotterdam, Vol. I, pp. 1–7, 1948.

CHAPTER 2

THE FORMATION OF SOILS, GEOLOGY, AGRICULTURAL SOIL SCIENCE, AND CIVIL ENGINEERING

2-1. Transformation Cycles of the Rocks and Soils of the Earth Crust. Present-day volcanic activities provide us with direct evidence that part of the interior of the earth is in a molten state. This fact, coupled with other considerations, leads to one of the two existing hypotheses concerning the formation of the earth. According to this hypothesis, the original solid earth crust was formed by the cooling and the resulting hardening of the molten magma. Because of the great age of the earth and the transformations which its crust underwent, no rocks existing at present can be identified as having belonged to the *original earth crust.* But some rocks which have been formed later by cooling and hardening of the molten magma exist to this day close to the present soil surface, apparently without having undergone changes in their original composition or texture. Rocks of this type are called *primary* or *igneous* rocks.

Their texture may vary according to the speed of their cooling during formation. If the molten magma cooled very slowly beneath the ground surface, permitting separate crystallization of the minerals of which it was composed, a coarse-grained structure results (*granite, syenite, diorite, gabbro*). More rapid cooling leads to a finer grained dense structure (*rhyolite, basalt, traprock*). *Porphyries* form an intermediate type, with a dense ground mass and embedded larger crystals. Finally, extremely rapid cooling of the magma leads to a glassy (*obsidian*) or to a frothy structure (*pumice*).

All soils and nonigneous rocks of which the earth crust is formed have been derived from weathered igneous rocks. The *weathering*, or rock disintegration, may be due to the mechanical splitting or abrasive action of water, ice, and wind, or to chemical processes involving the transformation or the dissolution of the rock minerals. The chemical composition of the igneous rocks may vary considerably. It is very important, since it governs the nature of the soil formed through their disintegration (Art.

2-4). The processes of this decomposition may further be strongly affected by the prevailing climate and other surrounding conditions, that is, by the so-called *environment* (Art. 2-8).

The *sands* (coarse particles of soil), *clays* (fine particles), and *silts* (particles of intermediate size) resulting from the disintegration of igneous rocks may then be carried away by forces of gravity, water (Art. 2-5), wind (Art. 2-6), or ice (Art. 2-7), and redeposited elsewhere. The general name for such deposits is *sediments.* With decreasing velocity of the water or of the wind transporting the particles, the coarser particles, or sands, are deposited first, then the silts, and then the clays. A certain segregation of particles as to size may result in separate sand or clay deposits with a great variety of possible mixtures of sands, silts, or clays. Geologists call such mechanically formed sedimentary deposits and their transformations *clastic rocks.*

These soil deposits may then be further transformed to form sedimentary rock deposits in the engineering sense of the word *rock* (Art. 2-2).

Compression of impure clays leads to the formation of *shales.* The cementation of sands by calcium carbonate ($CaCO_3$), silica (SiO_2—white, buff, or gray color), or by iron oxides (red color), deposited from percolating water between these grains leads to the formation of *sandstone.* The similar cementation of sand-gravel deposits leads to the formation of *conglomerates.*

Another type, the *nonclastic* variety of sedimentary rocks, may be formed through nonmechanical agencies. Some of these agencies may be of organic nature. Thus calcareous shell fragments of water animals lead to the formation of *chalks* and some *limestones.* Other animals form coral beds. Compressed and altered vegetable matter forms *coal* and *peat.* Silica secretions of tiny organisms compose the hollow shells of *diatomaceous earths.* Other sedimentary nonclastic rocks may be formed by chemical precipitation. Precipitation of calcareous matter dissolved in water forms *dolomites* and some *limestones.* Precipitation of silica forms *flints.* Deposits of *gypsum* and of *salt* are also due to the chemical precipitation from solutions.

As a result of temperature and other physical and chemical changes in the interior, the earth gradually contracts. This shrinkage causes considerable stresses in the earth crust with resulting continuous deformations and movements. Such movements cause the formation of mountains or the sinking of plains beneath the sea level. As a result, all rocks forming the earth crust may be bent to form folds or sheared to form faults. They may also have numerous cracks, called fractures or joints. Molten magma may be forced upward along faults or other planes of weakness and solidify before reaching the earth surface, forming new *intrusive igneous rocks.* Old igneous or sedimentary rocks may be forced downward and become completely molten, thereby losing their identity.

Both old igneous and old sedimentary rocks may undergo considerable changes, *i.e.*, *metamorphose,* as a result of tremendous pressures developed by the shrinkage of the earth crust or of heat due to the closer presence of molten magma.

Metamorphic igneous rocks are sometimes very similar to *metamorphic sedimentary rocks* as a result of the changes they have undergone. Thus, *schists* may be formed either from fine-grained igneous or from clastic sedimentary rocks. They are foliated;

that is, they have cleavage planes lying parallel to each other. There are many varieties, depending on the mineral composition and the extent of recrystallization under high pressure. *Gneiss* is a rock similar to schists, because of foliation, but of a more granular, banded type. *Slates* are formed through compression and recrystallization of shales. *Marble* results from the recrystallization of limestones or of dolomites under pressure and heat. *Quartzites* are products of the cementation under pressure by quartz silica of quartz grains.

Both sedimentary and metamorphic rocks may undergo disintegration when exposed to weathering on the earth's surface. The continued
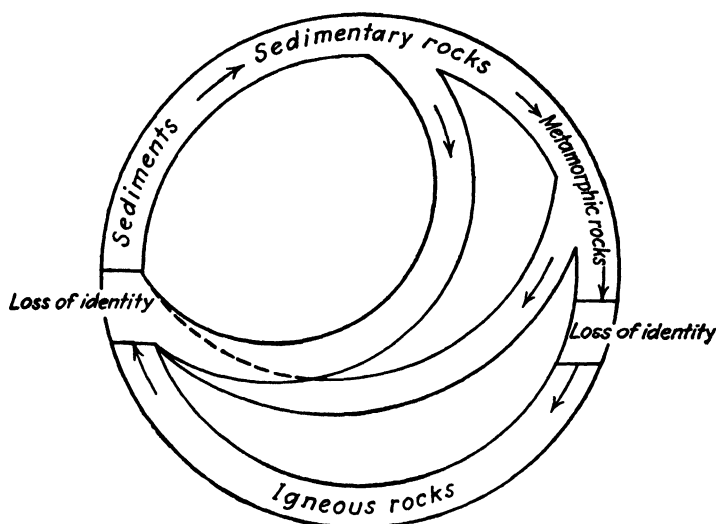
FIG. 2-1. The cycles of metamorphism, or rock transformation. The change is indicated as clockwise, and it will be seen that there are two places of loss of identity. The loss of identity indicated on the right is through reduction of the rock to liquid form. The one on the left through destruction by disintegration and decomposition. (From *W. H. Twenhofel, Ref.* 404.)

process of such disintegration followed by transportation and deposition of its product then again leads to new soil formations of the type described, completing a cycle of rock transformation. Figure 2-1 illustrates the types of transformation cycles just discussed.

Such cycles may be repeated many times. The age of the earth has been estimated from studies of radioactive minerals at 2 billion years or more. Figure 2-2 illustrates the sequence of geologic periods and eras.

The Archeozoic (oldest life) era covers the period of the first formation of the earth crust concerning which nothing very definite is known. The Proterozoic (old-life) era furnishes evidence of the formation of sedimentary rocks over a billion years ago.

During the last billion years, numerous cycles of further rock transformations have probably occurred. Thus, large parts of North America have been more or less widely flooded by ice 20 times or more. The present-day mountains are the product

of successive movements of the earth crust at different ages and of subsequent erosion. The Laurentian uplands of Canada were first formed over a billion years ago in the Proterozoic era. The Appalachian Mountains, of which the Alleghenies are a successor and remnant, were formed in the Permian epoch of the Paleozoic (early life) era 200 million years ago. The Rockies were formed in the Cretaceous period of the Mesozoic (middle-life) era some 70 million years ago. Changes of climate, which also greatly influence the nature of soil formation and deterioration (Arts. 2-4 and 2-8),
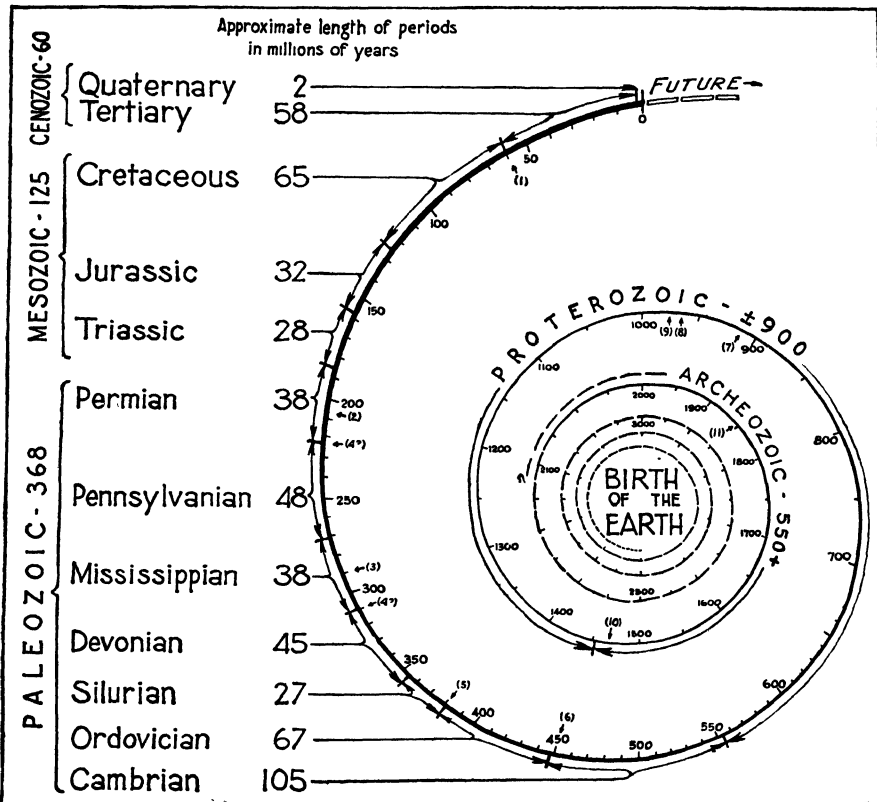
FIG. 2-2. Diagram representing the length of geologic periods and eras. (*From Raymond C. Moore, Ref. 236.*)

occurred several times. Intensely cold periods with resulting glaciation alternated with tropical moist or tropical arid climates.

The process of rock transformation described is not completed and continues to this day. Most of the present unconsolidated soil deposits are a product of the Cenozoic (recent-life) era, although there are exceptions, such as compact plastic clay of Devonian age (Ref. 299). The Tertiary period of the Cenozoic era is successively subdivided into the Eocene, Oligocene, Miocene, and Pliocene epochs, followed by the Pleistocene (ice-age) and Recent epochs of the Quaternary period.

The complexity of the nature and structure of the present earth surface is apparent.

It is so great that in some cases foundation engineers should call on geologists and on soil chemists for cooperation (Arts. 2-9 and 12-2).

2-2. Agricultural, Geological, and Engineering Definitions of the Terms "Rock" and "Soil." Geologists define as *rock* all the materials of which the earth crust is composed, irrespective of their hardness. Even soft clay may be designated as rock by a geologist. The solid part of the earth crust is termed *bedrock*. The products of bedrock disintegration overlying the bedrock are termed *mantle-rock*.

In agricultural soil science the term *soil* is applied only to the thin upper part of the mantle-rock penetrated by the roots of plants, which supplies them with the water and other substances necessary for their existence.

The civil engineering concept of the word "soil" is wider than the agricultural one. This term includes all the loose or moderately cohesive deposits such as gravels, sands, silts, or clays, or any of their mixtures. The term *rock* is applied to natural beds or to large hard fragments of the original igneous, sedimentary, or metamorphic rocks. *In this book the terms "soil" and "rock" will be used only in the civil engineering sense just defined.*

2-3. The Mechanical Agencies of Rock Disintegration. Temperature changes, the splitting action of plant roots, of ice, and of salt crystals, and the impact action of flowing water, of ice, and of wind-borne sand particles, all belong to the mechanical agencies of rock disintegration. The relative importance of these agencies may vary according to the prevailing climate and to the nature of the rock.

The heating of the surface of exposed rock beds by the rays of the sun causes it to expand more than the cooler interior. This sets up stresses in the rock bed on surfaces below and parallel to the exterior face. The direction of these stresses may be reversed during a rainstorm or at night, since the rain water or the air is cooler than the heated rock. The *fatigue* produced by the repeated reversal of these stresses finally causes failure of the so-called exfoliation or spalling type, which causes rock scales to break off from the surface. This type of disintegration is most frequent in dense igneous rocks of glassy (obsidian) or very fine grained structure (basalt).

Coarser grained igneous rocks, like some granites, are subject to a further type of disintegration due to temperature action. The minerals of which such rocks are composed (quartz, feldspar, mica) have different coefficients of thermal expansion and are present in the form of separate crystals. Repeated temperature changes may therefore induce stresses finally producing a separation of these crystals from each other.

Sedimentary rocks (sandstones and limestones) have a less compact and more porous structure than igneous rocks. In engineering terms this circumstance is reflected in the smaller values of their weight per unit of volume, of their Young moduli, and of their coefficients of thermal expansion. As a result of this structure, they are less affected by temperature changes than are igneous rocks.

But, for the same reason of their relatively greater porosity, sandstones and lime-

stones may be more strongly affected by the action of freezing water. Water increases its volume by about 10 per cent when it freezes and forms ice crystals. Pressures up to 150 tons per ft^2 may be thereby developed. Thus, water repeatedly freezing in the voids of porous sandstones may break them up completely.

The repeated freezing of water in small cracks or in joints of any rocks, whether igneous or sedimentary, may progressively widen these cracks and split surface rock beds into many fragments. Pressures developed against the sides of existing cracks by growing roots of plants and by growing crystals of salts deposited there by infiltrating water may have a similar action. Further, chemical transformation of some rock minerals may be accompanied by an increase of their volume and by a secondary mechanical disintegrating action as a result of the pressures thereby developed.

Other mechanical agencies may be at work locally. Thus, the continuous impact action of flowing water may erode even rocks, evidenced by wave action on seashores or by the changes in rocks under waterfalls. The abrasive action of large moving masses of ice in glaciers is also considerable. An abrasive (sandblast) action of wind-borne sand particles occurs sometimes but is not very frequent.

2-4. Rock Minerals and Their Chemical Decomposition. Since all soils are derived through the disintegration or decomposition of some *parent rock,* the properties of the minerals composing such rocks will now be examined. A *mineral* is an inorganic substance having a definite chemical composition, usually a definite molecular arrangement, and therefore fairly definite chemical and physical properties.

The more important physical properties of minerals are crystal form, color, hardness, cleavage, luster, fracture, and specific gravity. All are of importance for the identification of minerals. Only two are of some direct foundation engineering interest—the specific gravity and the hardness.

The *specific gravity of the minerals* affects the specific gravity of soils (Art. 3-1) derived from them and should therefore be noted. By specific gravity of a mineral is meant the ratio of the weight of a unit volume of this mineral to the weight of the same volume of water. In other words, it expresses the density of the mineral as compared to water. The specific gravity of most rock- and soil-making minerals varies within relatively small limits, from 2.50 (some feldspars) and 2.65 (quartz) to 3.5 (augite or olivine). Gypsum has a smaller value of 2.3, and salt ($NaCl$) has 2.1. Some iron minerals may have much higher values, for instance, magnetite, 5.2.

The *hardness of minerals* is measured by comparison to a scale in which 10 selected minerals are arranged and numbered in order of increasing hardness, as shown in Table 2-1.

The modern physicochemical conceptions of the structure of matter and of the nature of chemical transformations will be outlined later in connection with the discussion of the chemistry of soils (Art. 3-4). The possible nature of the *chemical weathering of rock minerals* will be outlined now.

The main types of such decomposition are hydration, oxidation, carbonation, desilication, direct solution by water, or combined actions of these processes. Chemical weathering can transform hard rock minerals into soft, easily erodable matter.

Oxygen and carbon dioxide (CO_2) are always present in the air. In a dry atmosphere they do not combine readily with other elements, but they do so actively in the presence of moisture both aboveground and underground.

Oxidation. This occurs most frequently in rocks containing iron, which decomposes in a manner similar to the rusting of steel when in contact with moist air.

Carbonation. Carbon dioxide (CO_2) and water form carbonic acid, which can decompose minerals containing iron, calcium, magnesium, sodium, or potassium. Thus practically all igneous rocks may be decomposed in this manner. Limestones can be particularly easily dissolved by water containing carbonic acid. Great caverns can be formed in this way. Dolomites are much more resistant to this type of weathering, being composed of less soluble magnesium carbonate.

TABLE 2-1. Scale of Hardness*

Mineral	Property
1. Talc 2. Gypsum	Can be scratched with fingernail
3. Calcite	Can be cut with penknife
4. Fluorite 5. Apatite	Can be easily scratched with penknife
6. Orthoclase feldspar	Difficult to scratch with penknife
7. Quartz 8. Topaz 9. Sapphire (corundum) 10. Diamond	Cannot be scratched with penknife. Quartz (7) scratches glass

* The numbers of the scale are a direct measure of hardness.

It should be noted that silica (SiO_2) is not decomposed by carbonation. Thus, *quartz,* which is composed of pure silica, is one of the most stable minerals, not only mechanically, because of its hardness (7) and absence of cleavage, but chemically as well. *Acid igneous rocks, i.e.,* rocks containing much silica (which gives them a light color), such as granite, are therefore much more resistant to chemical weathering than are *basic igneous rocks* (generally dark-colored), such as basalt and gabbro. But even granite can be decomposed chemically. Orthoclase feldspar is attacked by carbonic acid with the resulting formation of a new soft clay mineral, *kaolinite,* and other by-products. The quartz grains originally embedded in the feldspar are not decomposed but are loosened and can be then easily carried away by wind or water.

The average mineral composition of igneous rocks is about as given in Table 2-2. Feldspars are the most common rock minerals, which accounts for the abundance of clays derived from the feldspars on the earth's surface. Quartz comes next in order of frequency. Most sands are composed of quartz.

Hydration. This consists in the taking up of water, which is then chemically bound to form new minerals. It seldom occurs alone, except in such processes as the hardening of cement pastes in man-made concrete. In nature it is generally coincident with carbonation, as, for instance, in the case of granite decomposition by combined carbonation and hydration of orthoclase feldspar.

The chemical binding of free water during hydration generally produces a con-

siderable increase of volume of the decomposed rock. The pressures thereby developed are one of the factors affecting further mechanical disintegration of the not yet decomposed rock.

TABLE 2-2. Mineral Composition of Igneous Rocks

Mineral	Per cent
Quartz	12–20
Feldspars	60–50
Ca, Fe, and Mg silicates	17–14
Micas	4–8
Others	7–8

Desilication. This also seldom occurs alone but consists in the washing out of dissolved or colloidal silica freed in the course of other chemical processes.

Direct Solution by Water. This affects not only by-products of chemical reactions but can have quite important effects where salt (NaCl) deposits are concerned. Gypsum ($CaSO_4$) can also be dissolved and carried away by flowing water.

Some sedimentary rocks, like sandstones, are less susceptible to chemical weathering than are many igneous rocks. This is largely due to the fact that they already are a product of chemical weathering of igneous rocks. Sandstones cemented by silica (white or gray color) do not effervesce in contact with hydrochloric acid (HCl), but are particularly stable in this respect. Sandstones cemented by lime (white or gray color), which effervesce if sprinkled with HCl solution, or those cemented by iron oxides (red color), are less stable, since these cementing materials may be decomposed, dissolved, and carried away.

Sometimes the products of weathering of bedrock remain in place instead of being carried away. Such deposits are termed *residual.* It also frequently happens that in excavations for dams, or in tunnels, even igneous or metamorphic rocks (such as granite or schist), although covered by thick soil deposits, may be found decomposed to a considerable depth and so soft that they cannot support a foundation and have to be removed. This can happen when the decomposition is of a purely chemical nature and is caused by the leaching effect of continuously percolating underground water charged with carbonic acid. Such continued percolation and decomposition are particularly easy along rock planes inclined toward faults permitting the further downward seepage of water.

On the surface, both mechanical and chemical weathering often occur simultaneously. As they are formed, the products of weathering are then generally carried away by forces of gravity, flowing water, wind, or moving glaciers.

2-5. Soils Transported and Deposited by Water Action. The combined action on the products of weathering of the forces of gravity and of flowing water is illustrated by Fig. 2-3. Blocks of loosened rock roll

down the slope of the hill into the valley and form at first so-called *talus* at its base. Finer grained products of weathering are then washed down by rain water. They penetrate into the spaces between the larger blocks and cover them up gradually, filling the entire valley with detritus.

Depending mainly on the intensity and seasonal distribution of rainfall, different types of stream formations may result. Flowing water can carry with it soil particles in suspension or roll them along the bottom (traction). The latter type of movement causes abrasion of sharp edges
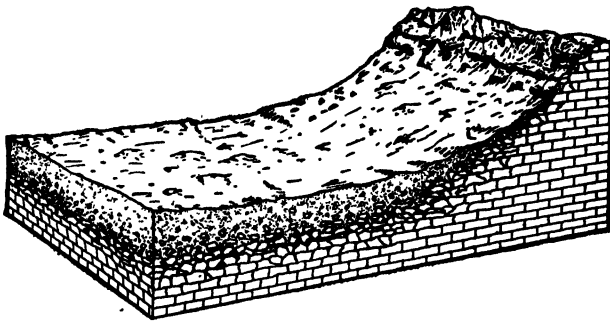
FIG. 2-3. Diagram illustrating the formation of soil on the side of a hill. The solid rock in the valley grades upward to partly decayed rock, which in turn grades into soil. On the steep slope no soil has accumulated, because it is carried away. (*From W. H. Emmons, G. A. Thiel, C. R. Stauffer, and I. S. Allison, Ref.* 115.)

and tends to reduce further the size of particles. With increasing velocity, water is able to move larger and larger particles. Since changes in the velocity of streams occur constantly, both deposition of soil particles with decreasing velocity and their erosion (or *degradation*) with increasing velocity may succeed each other at irregular intervals of time and place. Most *river* (*fluvial*) *deposits* are therefore rather erratic in regard to their granular composition. The following are some of the most important general types of river deposits:

1. Mountain torrents, especially after sudden cloudbursts in semiarid regions, are apt to carry great quantities of coarse debris and to deposit most of it at the mouth of the valley, where their velocity suddenly decreases, in what is called an *alluvial fan*. The larger sized particles are left at the mouth of the valley and the finer ones along the outside periphery of the fan.

2. Slower flowing rivers may at first carry away detritus washed down the slopes of a valley. Later, in overflowing during floods, they may help to fill the valley up. Such overflowing considerably decreases the velocity outside of the main channel, with resulting deposition there of silt and of clay, and the gradual formation of a *flood plain*. Later, as shown in Fig. 2-4, the level of the plain rises, and a river may have to cut into its own deposits and form *terraces*. Some meandering rivers continually change their twisting course along a flood plain by undercutting some banks and depositing sand and silt against others. When a river reaches the sea, its velocity

decreases considerably, with the resulting deposition of most of the soil particles it carries in suspension. A *delta* is thereby formed which resembles an alluvial fan in shape but is composed mostly of very fine soil particles (silts and clays). The fine clays of the Mississippi Valley and Delta are called *gumbo*.

Lake (lacustrine) deposits generally are very fine as to size of particles because of the small velocity with which water flows through most lakes. Small lakes are apt to be filled up with vegetable matter, which decomposes into very compressible *peat*.
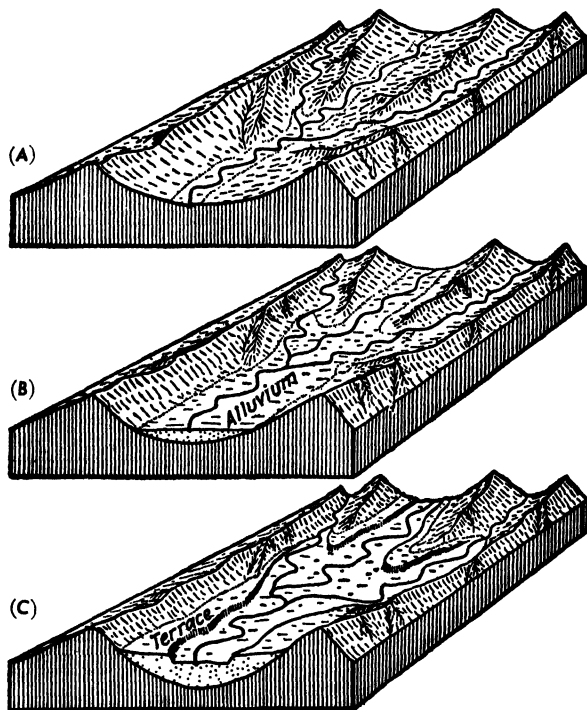
FIG. 2-4. Diagram showing the development of stream terraces. (A) Stream degradation; (B) Aggradation with the development of flood plains; (C) Terraces carved from the flood plain by river, which erodes part of its earlier deposits. (*From W. H. Emmons, G. A. Thiel, C. R. Stauffer, and I. S. Allison, Ref.* 115.)

Marine deposits are always stratified; that is, they possess *bedding planes*. Further, they reflect the physiographical characteristics of the adjoining coasts. This is illustrated by Fig. 2-5.

In shallow seas along coasts with many river mouths detritus (*terraginous deposits*) predominates. When the supply of river-transported fine-soil particles is small, recent limestone deposits formed from chemical precipitates or remains of organisms (also coral beds), may predominate. Of course, along the beaches themselves most of the deposits are created by the destructive and subsequent sorting action of waves on the shore line. At greater depths located farther away from the shore, the deposits consist mainly of very fine clays and muds (oozes). With increasing distance from the shore, the fine particles of land origin become scarcer and the ooze is composed of

mud of wind-borne volcanic or meteoric origin and of organic sediments. Variations in the composition of such muds may be considerable.

It may, nevertheless, be seen that the factors affecting the composition of marine deposits are less erratic than those affecting fluvial deposits. For this reason deposits of marine origin are as a rule much more uniform
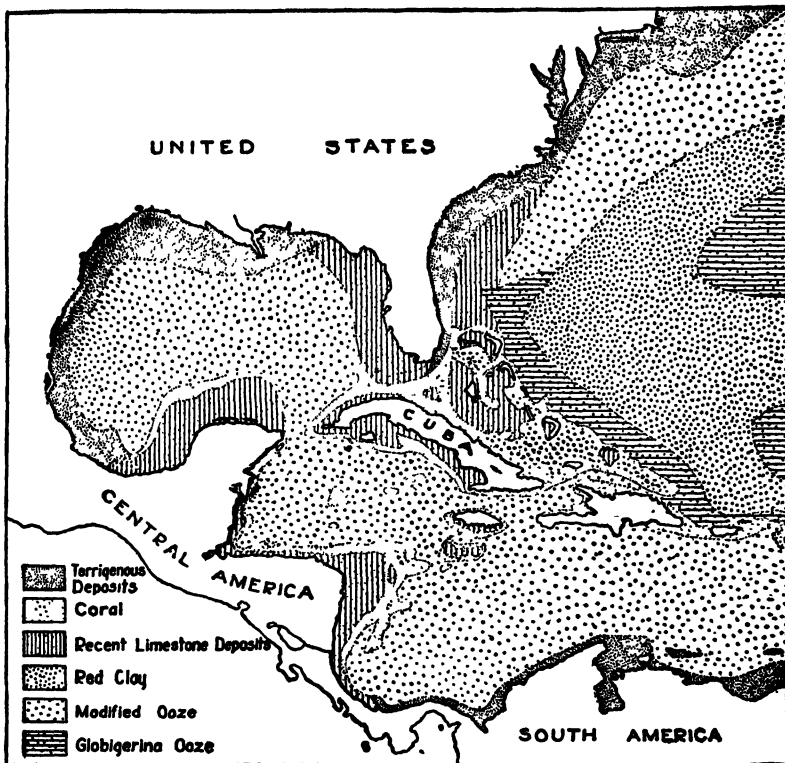
FIG. 2-5. Map showing the distribution of bottom deposits along the western margin of the Atlantic Ocean basin in the vicinity of the Caribbean Sea, the Gulf of Mexico, and the southern coastal plain of the United States. (*From W. H. Emmons, G. A. Thiel, C. R. Stauffer, and I. S. Allison, Ref.* 115.)

in composition than are deposits of fluvial origin. Deposits of lacustrian origin occupy an intermediate position.

Figure 2-6 gives a schematic profile through an ancient lake on which Mexico City is founded. It is filled to a great depth by clay interbedded with sand lenses. The upper 100 ft of the clay is very soft. This location presents what are probably the most difficult foundation conditions in the world (Art. 14-7). The clay was formed by particles of fine and sometimes decomposed volcanic ash deposited by the combined action of

water flowing into the lake and of wind blowing over it. An unusually loose structure of the clay resulted.

Some very stiff clays, overconsolidated by the weight of temporary overburden, by drying, or by chemical action are weakened by many small hair cracks. When resaturated with water, the clay around the cracks is liable to soften up. Such *stiff-fissured* or *slickensided* clays can be very misleading in respect to their over-all strength.

2-6. Wind-blown Soil Deposits. The dust storms of the western part of Oklahoma and of Kansas are well known to everybody in the United States. They are a good illustration of the erosive power of wind and of
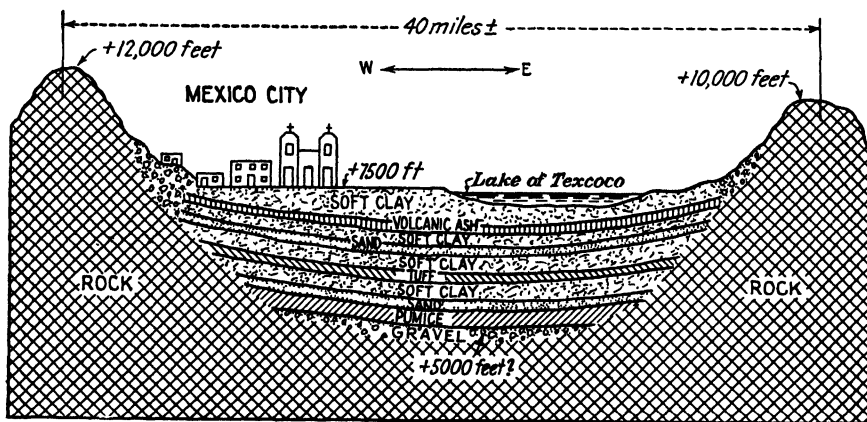
FIG. 2-6. Profile illustrating what are probably the most difficult foundation conditions in the world—the old lake bed on which Mexico City is founded. (*Courtesy of A. E. Cummings.*)

its capacity to transport soil. It has been estimated that in one year 850 million tons of dust has been moved by wind for a distance of 1,500 miles in the West of the United States. Similarly deposited wind-blown or *aeolian* soils occur in China, Europe, and South America.

Figure 2-7 illustrates the formation of such soils. The zone of wind erosion necessarily lies in an arid or semiarid region. Such regions may occur both in very hot and in very cold climates. Most periods of glaciation were accompanied by the formation of cold arid deserts, on the outwash plains of glaciers, from which winds carried away large quantities of dust. Dry dust and loose sand grains are picked up by the wind and carried away. As the velocity of the wind decreases, the sand is deposited first. Finer particles, of silt size (smaller than 0.05 mm), are deposited farther away and form so-called *loess* deposits well segregated as to size. Such deposits may attain thicknesses of many hundreds of feet and have very definite characteristics of considerable importance in engineering

work. First, they are very uniform; that is, all their particles are nearly of the same size. Also, they have relatively little cohesion and therefore are unstable on exposed slopes and are readily eroded there by water. They stand up much better in cuts as almost vertical walls (Fig. 8-18), because their permeability is greater in the vertical direction than horizontally, due to the presence of small vertical channels left by roots of decayed plants which had been covered up by loess during its deposition. For this reason, there is very little surface runoff on gentle slopes, and most of the rainfall seeps directly downward through the loess.
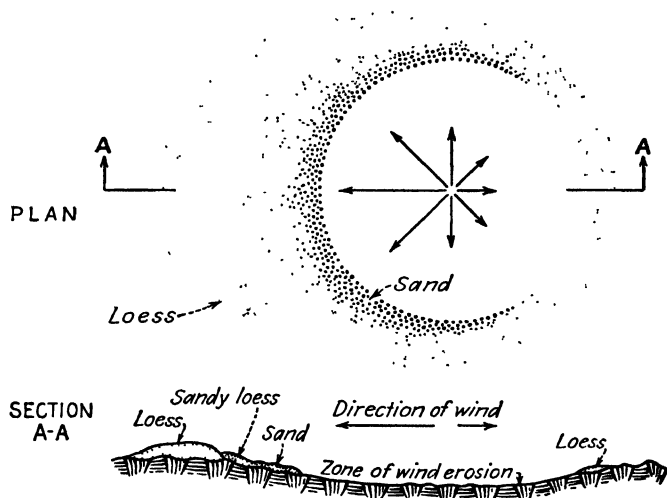
FIG. 2-7. Diagram showing relationship between the direction and strength of prevailing winds and the formation of wind-blown deposits. (*After Obruchev, Ref.* 251, 1911 *and Scheidig, Ref.* 302, 1934.)

Sometimes wind-deposited loesses on steep slopes are eroded and redeposited elsewhere by rain water. The new formation may then lose many of its original characteristics. It should further be noted that the word "loess" has often been misused and applied to soils of nonaeolian origin with characteristics of ordinary loam.

The loess deposits in the United States are shown in Fig. 2-8. Most of them have been formed by dust carried both eastward and westward from the Great Plains. Dust from the periodically dried flood plains westward of the Mississippi is probably responsible for the creation of the loess belt along its more elevated western bank.

European loesses appear to be a by-product of the glaciation era. In North America there are also loesses of glacial origin, but most of them have been since covered by other deposits (Fig. 2-11).

Deposits of uniformly sized sand may be easily moved by the wind and
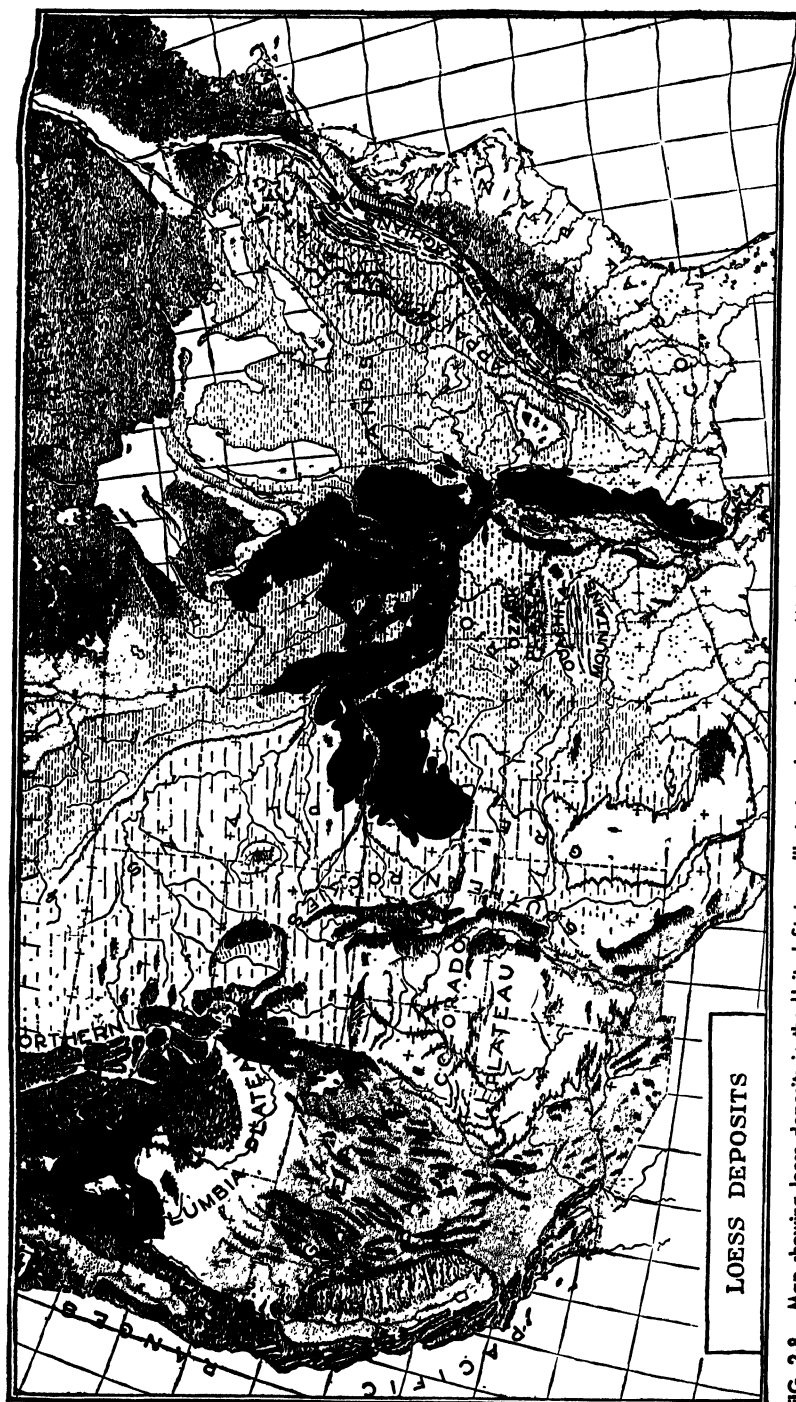
FIG. 2-8. Map showing loess deposits in the United States. Illustrates close relation to Mississippi River system and to the Great Plains. (From A. K. Lobeck, Ref. 214.)

are called dunes. Their grading as to size may be due to their deposition either by wind (inland dunes) or by sea waves (shore dunes).

2-7. Soil Deposits of Glacial Origin. There is evidence of repeated glaciations in the past, the first of which dates back to the Proterozoic era more than 500 million years ago. These early glaciations have left no nontransformed deposits of any special engineering importance. However, the opposite is true of the four recent glaciations during the last million years of the Pleistocene epoch, which is the last one preceding recent, historically recorded times. Their action should therefore be carefully studied.
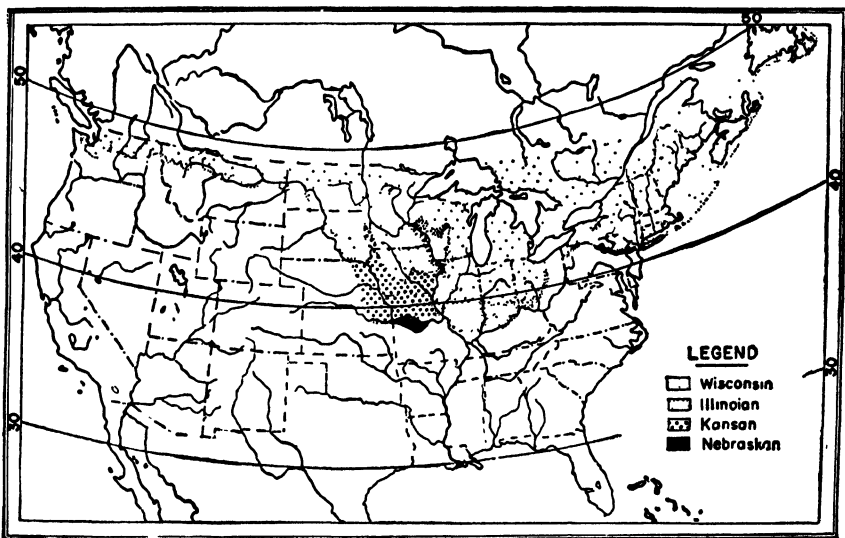
FIG. 2-9. Limits of the glacial drift in the United States. *(Reproduced by permission of C. Schuchert and C. O. Dunbar from Ref. 306. Courtesy of John Wiley & Sons, Inc.)*

During this epoch there were four successive glaciations which lasted about 100,000 years each. They had long interglacial periods between them, each lasting from 200,000 to 300,000 years. During these interglacial periods the ice receded. The oldest of these glaciations is known in North America as the Nebraskan (first), followed by the Kansan (second), Illinoian (third), and Wisconsin (fourth) glaciations, the latter ending some 25,000 years ago. Figure 2-9 illustrates the areas covered by ice in North America.

Colder periods appear to have alternated with warmer ones on the earth surface. During the cold periods, abundant snowfalls compress the lower lying snow to ice and form ice sheets several thousand feet thick. In the summer some of the surface ice melts and the water percolates

downward through fissures and cracks where it subsequently freezes under increase of volume. It is believed that the enormous pressures thereby developed are mainly responsible for the movement of glaciers. The slowly moving ice carries along with it any loose boulders or other debris which it may find on the ground surface. This wears down such debris by grinding it up and at the same time loosens up other blocks of rock.

Whole valleys may become filled up with such debris (termed *glacial drift* or *till* and sometimes designated as *ground moraine*) of all sizes,
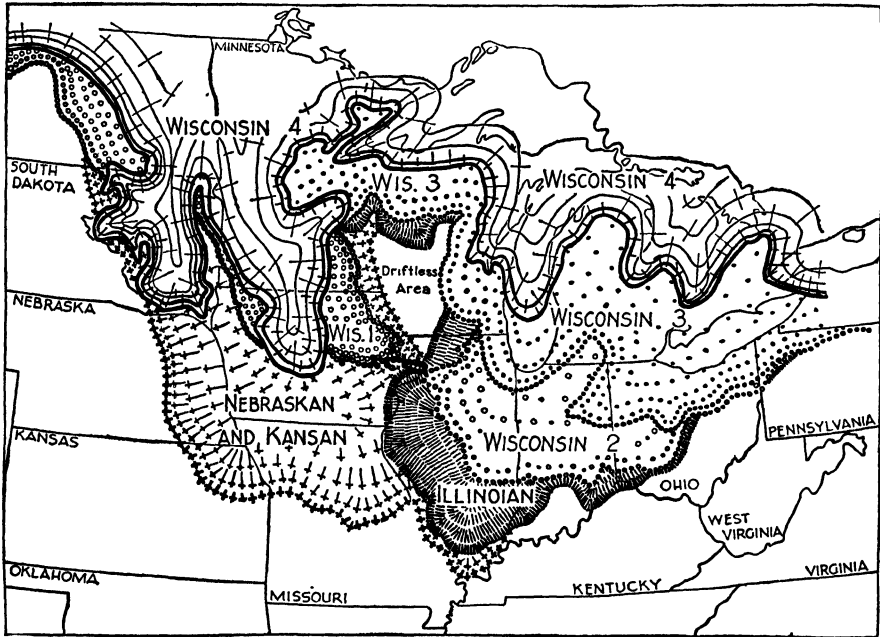
FIG. 2-10. Map of the north central United States, showing distribution of glacial drift of the successive Pleistocene stages. (*From Raymond C. Moore, Ref. 236.*)

ranging from rock flour to huge boulders. With a high clay content, it is sometimes referred to as *boulder clay*. When cemented together by products of chemical rock weathering, and especially if compressed by the pressure of ice during subsequent periods of glaciation, such glacial till is called *hardpan* and generally represents an excellent foundation material. The word "hardpan" is often misused, especially by foremen in charge of borings, by being applied to shales and other hard deposits in regions where there never was any glaciation.

In its movement a glacial sheet finally reaches a line where it melts away. The till carried by the ice is then deposited at its limit in what is

called a *terminal moraine*. The melting water carries the finer particles away and deposits them on the outwash plains bordering the limits of the glaciation. A great variety of soil formations may result from constant ice-sheet changes and the varying velocity of glacial water flowing in streamlets directly off the ice sheet, in larger streams, and into lakes. Most recent surface glacial till deposits (sand-gravel mixtures) are very irregular in respect to their compressibility and require careful investigation if they are to support heavy foundations. Lakes at the end of outwash plains are generally filled by finely stratified *varved clays* (Figs. 7-17 and 12-11). A varve is a yearly deposit of fine particles in a lake. In
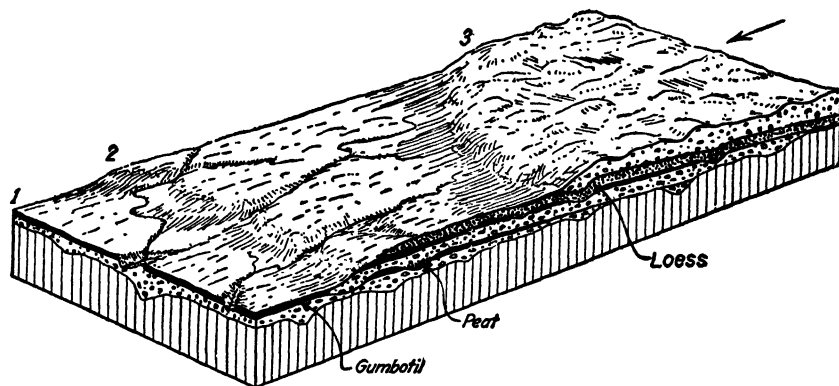
FIG. 2-11. Idealized block diagram, showing the relations of three superimposed drift sheets. The block represents an area many miles across, and the vertical scale is exaggerated. The first glaciation spread till across the entire region. In the long interglacial age that followed, the surface of this first drift sheet was weathered to gumbotil (black). The second ice advance fell short of the first, overriding the older till, gumbotil, and peat deposits in a broad marginal belt. During a second interglacial age this till, in turn, was overridden by the glacier ice, which fell short of the middle of this area. No gumbotil has yet formed on the youngest till. (*Reproduced by permission of C. Schuchert and C O. Dunbar from Ref. 306. Courtesy of John Wiley & Sons, Inc.*)

each varve, the coarser silt is deposited first during the summer thaw of the ice sheet. The finer clay remains in suspension longer and settles down during the winter.

Particularly complicated soil formations may result in regions where several recent glaciations have occurred. This has been the case in the north central United States, as illustrated by a map in Fig. 2-10. The surface of a glacial drift sheet is exposed to chemical weathering during the interglacial periods. The soluble products of such weathering are then washed downward and the insoluble ones remain on the surface in the form of a sticky clay called *gumbotil*, which may attain 10 ft in depth. This indicates a very slow rate of weathering—more than 1,000 years for each inch in depth. Later, gumbotil may be covered in places by wind-

blown loess deposits, which in turn may be covered by a drift sheet from a later glaciation, as illustrated by Fig. 2-11. As shown on this diagram, *peat bogs* may be covered up by later drift. Peat is extremely compressible and may cause unequal settlement and damage of buildings founded on the overlying drift. A situation of this kind arose in New York City, on Manhattan Island near Canal Street. Deep borings are always advisable in regions of former glaciation.

Many more freak formations of engineering importance may occur in such regions. For instance, an advancing lobe of ice had blocked and dammed up a river, and a torrential overflow occurred later into an adjoining valley. The bottom of this valley was therefore covered by a thick layer of large boulders, all finer particles having been carried away and redeposited further on. Later deposits covered up these boulders without filling up the voids between them, except at the very surface of the layer. This layer was located below ground water and its removal became impossible. Since sheet piling could not be driven through the boulders, no dam could be founded on them in view of the extreme permeability of such a deposit. A condition of this kind would, of course, affect the choice of location for a dam.

2-8. The Surface Maturing of Soils as a Result of Recent Climatic Effects. Work on the *maturing* of soils was inaugurated by Russian agricultural soil scientists at the beginning of the present century (Ref. 191) and has been also taken up since and further developed in other countries, and especially in the United States. It has shown that most soils, irrespective of their original composition as governed by the nature of the parent rocks, with time tend to lose their original characteristics under the influence of various climatic factors prevailing in a certain region. As a result, all the surface soil layers of a certain region tend to assume the same type of chemical composition.

These studies, embodied in the science of *pedology*, are of direct interest only for engineers dealing with surface soil layers. They are of practical importance in highway and airport soil-stabilization work (Art. 11-7), but a general understanding of the essential points is necessary to all foundation engineers.

The most important climatic agencies affecting the maturing of surface soil layers are the quantities of surface rainfall, the prevailing temperature, and the type of vegetation. There may be many subdivisions, but the main types of soil-maturing processes are as follows:

1. The *podzolization* consists in the leaching of iron and alumina oxides from the upper soil layers. This occurs mainly in humid northern climates where the topmost soil layer (or topmost *horizon*) contains much *humus*, that is, only partially decayed organic matter. The *humic acids*, the formation of which accompanies such slow decomposition, help the percolating rain water to leach the iron and alumina oxides from the upper layers immediately beneath the topmost horizon into deeper lying ones, where the oxides are deposited and may even act as cementing agents. The iron and alumina oxides are collectively designated as sesquioxides by the symbol R_2O_3. The

upper layers are then relatively rich in silica. This is expressed by a relatively high value of the *silica-sesquioxide ratio* SiO_2/R_2O_3. Soils which have high values of this ratio (up to 7) are termed *podzols*. Because of their acidic nature they then possess a greater degree of chemical stability than do soils with lesser values of this ratio. They are therefore very satisfactory from a highway engineering point of view, but most undesirable from an agricultural point of view since, in addition to the loss of the sesquioxides, most other mineral substances of importance for plant growth, such as calcium and magnesium, have also been leached into deeper lying layers. The surface soils of the forest-covered northeastern part of the United States are mostly podzols.
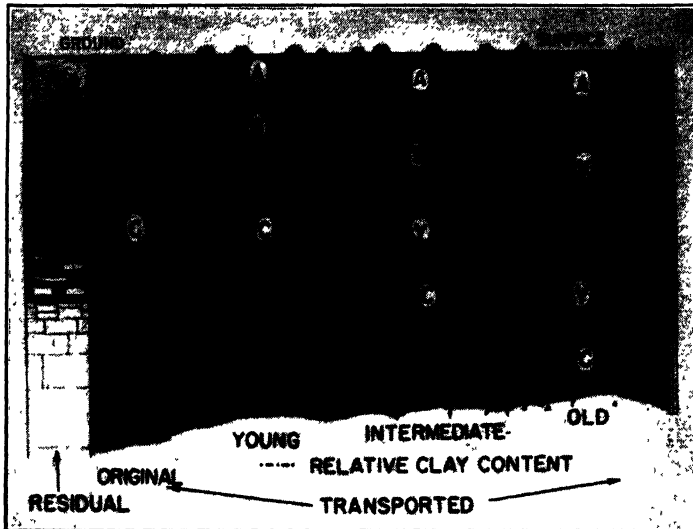
FIG. 2-12. A diagram showing the effect of age on the development of soil profiles. (From *Highway Research Bulletin* 10, *Purdue University, Ref.* 22, 1943.)

2. Another extreme type of soil maturing is the *laterization* which occurs in humid tropical regions. Because of the rapid decomposition of organic matter, hardly any humus is present. As a result the soluble silicates and all soluble salts are washed away more easily than the sesquioxides. The resulting soils are called *laterites* and have a low value of the silica sesquioxide ratio (less than 2). Then fertility is very low. There are hardly any true laterites in the United States. The surface soils of the southeastern United States are an intermediate product of combined podzolization and laterization. All soils matured under humid conditions, including podzols and laterites, are termed *pedalfers*.

3. Soils maturing under arid or semiarid conditions do so as a result of a process termed *calcification* and are called *pedocals* in agricultural terminology. These soils are neutral or alkaline and develop in regions where the rainfall is less than 25 in. per year, and therefore insufficient to keep up a continuous downward movement of water. As a result, most of the soluble mineral substances remain in the lower part of the upper horizon. The resulting concentration of calcium gives this maturing process its name. Most of the surface soils in the southwest of the United States belong to this group.

It should be carefully noted that all the processes of soil maturing just described can occur only with continued downward *movement of moisture*.

For this reason their effects cannot reach below the permanent subsoil water table.

In some very arid regions upward movement of moisture may occur by capillarity from deep soil layers with artesian water. Such water may bring with it salts leached from layers it has traversed and may produce their concentration near the soil surface where it evaporates.

The sequence of layers in any given soil within the zone of maturing is known as the *soil profile*. It is generally considered as having at least three typical layers or horizons, as illustrated by Figs. 2-12 and 2-13.
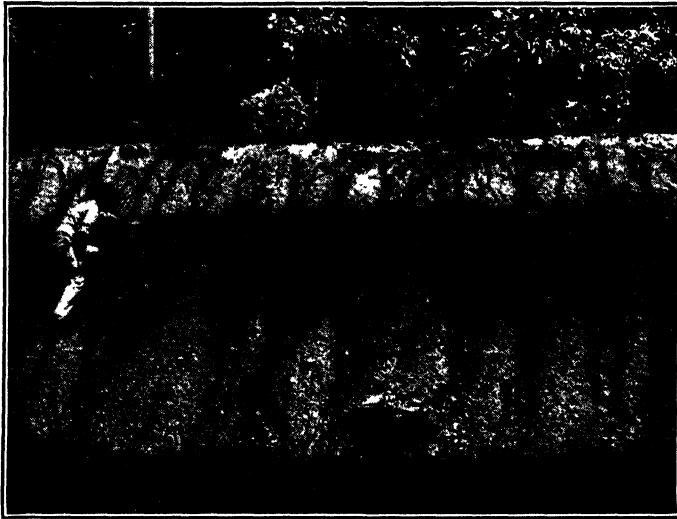
FIG. 2-13. Weathered profile of the Clermont soil exposed in an Indiana highway cut. Note the three general horizons. (*From Highway Research Bulletin* 10, *Purdue University, Ref.* 22, 1943.)

The upper *A* horizon represents in its upper part the zone of accumulation of organic matter and in its lower part the zone from which percolating water has washed out soluble constituents. The *B* horizon represents the zone in which downward-seeping water has deposited material washed out from the *A* horizon. The *C* horizon represents the parent material. The relative position of the three horizons changes with age, as shown in Fig. 2-12. More complex profiles can also result. In Fig. 2-12 the *Y* horizon represents a slightly weathered parent material and the *X* horizon a highly weathered clay pan.

Surface soils having the same type of profile are called a *soil series* by pedologists and are given the name of some locality near which they were first identified. The *Clermont soil* referred to in Fig. 2-13 is an example of such designation.

2-9. The Fields of Cooperation between Civil Engineers, Geologists, and Agricultural Soil Scientists. Every engineer specializing in founda-

tion work should make a careful study of geology. However, few engineers can attain the skill which is often necessary properly to interpret complicated local geological features, since such skill can be attained only through constant practice.

The cooperation of geologists is therefore essential in all problems connected with ground-water supply, in tunnel and dam construction work, and where particularly large and heavy bridges are concerned. Such cooperation should be sought at the very outset of the investigations related to the choice of suitable sites (Art. 12-2). Geologists can detect much more quickly than engineers the presence of local geological features of engineering importance, such as dangerous faults in the bedrock or pervious, water-bearing, or soluble veins. Further, geophysical methods of exploration represent an important accessory for engineers, but require specialists for their proper handling (Art. 12-4).

Where less important structures are concerned, such as bridges or buildings of medium or minor size, the employment of special geological consultants may not be warranted economically. But engineers engaged in foundation work of this type can gain a better understanding of their problems, and therefore benefit, from a study of the geological features of the region in which they are working and from personal contact with geologists familiar with it.

In turn, engineering geologists should study the problems of foundation engineering and of soil mechanics in order better to understand the point of view of engineers and subsequently to adapt their own studies more efficiently to engineering requirements. This should be done to a greater extent than is usual at present, but a healthy trend in this direction is beginning to be noticeable.

Attempts are also being made to apply findings of agricultural soil science to engineering work. This can mainly be done in respect to highway and airport pavement and base-course construction, since upper soil layers are generally used for these purposes. For instance, the surface chemistry of soils, first studied in agricultural and ceramic work, is beginning to find engineering application in the new science of soil stabilization by means of admixtures of cement, of bituminous products, and of various chemicals.

Agricultural soil maps are beginning to be used for engineering work. U.S. Soil Survey maps classify and indicate the location of surface soil deposits according to their texture, drainage, soil material, and other characteristics. These maps can be used to advantage as a direct accessory for preliminary highway and airport soil surveys (Art. 12-3). Advance correlation to engineering properties of soils of the soil types indicated on U.S. Soil Survey maps is desirable. Because of extensive investigations required for the purpose, such correlations have not been

performed very often so far. A notable and successful example are the studies performed by the joint highway research project of Purdue University in Indiana.

Geological maps can also be used for preliminary soil surveys. They are of advantage in cases where a rough idea of the general nature of the soil conditions in a certain area is desired. Information of this kind provided by military geologists has been of great value to Army Engineers in the Second World War for the preliminary selection of airfield sites and for the location of sand and gravel deposits needed in airport and road construction.

Review Questions

2-1. What is the main difference between limestone and dolomite deposits which is of importance in dam construction?

Answer. Dolomites are less easily dissolved by water containing carbonic acid. Caverns and crevasses therefore occur less frequently in dolomites than in limestones.

2-2. Where is the likelihood greater of encountering soft clay deposits: in a steep mountain valley, or in flood plains and delta regions?

Answer. Stretches of stagnant or of very slowly flowing water where clays could be deposited are not very likely to occur in a steep mountain valley.

2-3. Would you consider it possible to find soft peat under a sand-gravel layer in Oklahoma or in Connecticut?

Answer. Peat could be found below sand-gravel deposits in Connecticut which is located in a zone of repeated glaciation. This is not the case in Oklahoma.

2-4. Why are most sands composed of quartz?

Answer. Because of the chemical stability of silica, of which quartz is composed.

2-5. What is the natural process of formation of clay?

Answer. Chemical decomposition of parent rock minerals.

2-6. Would a soil with a high content of gypsum be desirable for the construction of an earth dam?

Answer. Leaching of large amounts of gypsum from a soil used for rolled-earth fill might increase its permeability and decrease its stability to a degree detrimental in earth-dam construction.

References Recommended for Further Study

Geomorphology. An Introduction to the Study of Landscapes, by A. K. Lobeck, McGraw-Hill, 1939.

Pedology, by J. S. Joffe, Rutgers University Press, 1936.

Factors of Soil Formation, by H. Jenny, McGraw-Hill, 1941.

The Formation, Distribution and Engineering Characteristics of Soils, by D. J. Belcher, L. E. Greggs, and K. B. Woods, of the joint highway research project, Purdue University, 1943.

"Engineering Uses and Limitations of Pedology for Regional Exploration of Soils," by Hans F. Winterkorn, *Proceedings of the Second International Conference on Soil Mechanics and Foundation Engineering*, Rotterdam, Vol. I, pp. 8–12, 1948.

"Glossary of Selected Geologic Terms," by William Lee Stokes, *U.S. Geological Survey Bulletin* (in preparation).

CHAPTER 3

DEFINITIONS AND TESTS RELATED TO THE PROPERTIES OF THE SOLID SOIL PARTICLES

3-1. The Absolute Specific Gravity of a Solid Substance. The Effect of Organic Matter. The absolute specific gravity of a solid substance is determined as follows:

$$G = \frac{W_s}{V_s} \tag{3-1}$$

where G = absolute specific gravity of the solid substance
W_s = weight of the solid substance, gm
V_s = volume of the solid substance, cm^3

Thus the specific gravity represents the weight per unit of volume of the solid substance. Its value depends on the value of the specific gravity of the original rock minerals from which the soil is derived. This is true only when no chemical decomposition has occurred under chemical binding of water with a resulting increase of volume and therefore decrease of the specific gravity of the new mineral.

The specific gravity of the solid substance of most inorganic soils varies between 2.60 and 2.80. Sand particles composed of quartz have a specific gravity around 2.65. Clays can have values as high as 2.90.

Most minerals of which the solid matter of soil particles is composed will have a specific gravity greater than 2.60. Therefore values of specific gravity smaller than that figure are an indication of the possible presence of organic matter in the soil in appreciable quantity and show that caution is required. Soils with considerable organic content are very compressible, as for instance peat, which is composed almost entirely of vegetable matter, with the result that it may burn when dry. Apart from the high compressibility which results from their structure, soils with high organic content are undesirable in engineering work because of the possibilities of decay of the organic matter. They are also undesirable in soil-stabilization work (Art. 11-7).

The organic content of soils is sometimes assumed to equal the loss in

weight suffered by a soil held over a flame until the soil particles are red hot, *i.e.*, the so-called *ignition loss*. This method is liable to give too high values, since, in addition to the destruction of the organic matter, chemically bound and adsorbed water may be liberated and removed at temperatures exceeding 105°C.

The specific gravity of soils is generally determined through the measurement of the volume of water displaced by the solid soil particles. The adsorbed water films (Art. 3-5) are included in the volume of the solid particles. However, these films are so thin that their presence does not appreciably change the values of the specific gravity of solids which have adsorbed them.

The specific gravity can be determined as follows:

$$G = \frac{W_s}{V_s} = \frac{W_s}{W_s - (W_2 - W_1)} \tag{3-2}$$

where G = specific gravity of the solid substance
W_s = weight of the solid substance, gm
V_s = volume of the solid substance, cm³
W_2 = weight of flask (taken from calibration chart for each flask) with distilled water and with soil at t°C, gm
W_1 = weight of flask with distilled water only at t°C, gm

For techniques of testing, see Refs. 102 and 190.

This test is not very important by itself; it is performed in connection with computations required for other tests.

3-2. Sand, Silt, and Clay Defined in Terms of Grain Size. According to their grain size, soil particles are classified as sand, silt, and clay, subject to limitations indicated in Arts. 3-8 and 12-11. The metric system is used in this classification. Metric measures are currently employed by soil laboratories in the United States, just as these measures are generally used in chemistry and physics.

The ASTM (American Society for Testing Materials) classifies soil particles according to their size as indicated by Table 3-1.

It should be noted that the ASTM definitions of clay, silt, and sand, although used in several other countries, do not represent an international standard. In European engineering practice a definition is often used according to which particles smaller than 2 μ (microns) (instead of 5 as defined by the ASTM) are considered as clay, and particles between 0.02 and 0.002 mm as silt. The latter definition of clay and silt sizes is also internationally used in agricultural soil work (see Fig. 3-1).

3-3. The Determination of Grain Size by Sieving. The size of particles larger than 0.074 mm (74 μ) may be determined by sieving. This size corresponds to the opening of the U.S. Standard sieve No. 200, the
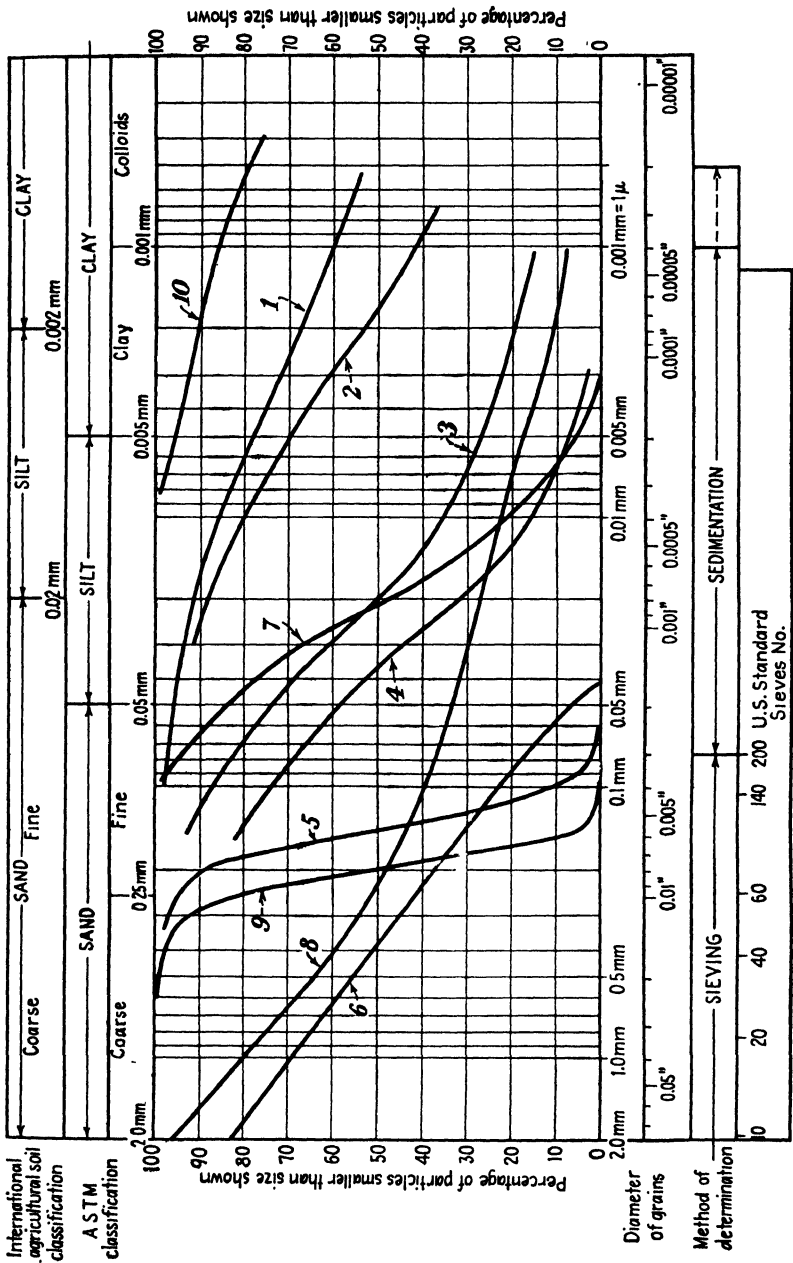
FIG. 3-1. Some grain-size-accumulation curves. 1 and 2—clay soils of the Nile Delta; 3 and 4—silts from the Nile Delta; 5—Port Said beach sand; 6—sand artificially graded for maximum density; 7—Vicksburg loess; 8—New Mexico adobe brick; 9—Daytona Beach sand; 10—Wyoming bentonite. Soils 1 to 9 were tested by G. P. Tschebotarioff. Data on soil 10 are taken from Ref. 6.

number 200 designating the number of meshes per inch length of the sieve tissue. There are sieves of still finer mesh (No. 325), but work with them becomes difficult.

Since silt is composed of particles smaller than 50 μ, neither the quantity of silt nor of clay particles in a soil may be determined by sieving alone. At the same time, most of the important engineering properties of soils, especially the permeability, depend on the silt and clay content. Thus, sieving alone is an entirely inadequate test, except where predominantly sandy soils are concerned. Sedimentation tests have to be

TABLE 3-1. ASTM Soil Classification

Soil	Size, mm
Sand, coarse	2.0 –0.25
Fine	0.25–0.05
Silt	0.05–0.005
Clay	Smaller than 0.005
Colloidal clay	Smaller than 0.001 (= 1 micron = 1 μ)

resorted to for silt- and clay-content determinations (Art. 3-6). In order to understand properly the properties of such very fine particles, it appears advisable first to review briefly some of the factors affecting the structure of all matter, as conceived by modern physics and chemistry.

3-4. Some Physicochemical Concepts. Clay Minerals. Colloidal Soil Particles. During the past decade rapid advance has been made in our understanding of the structure of matter. This development is continuing and is far from complete.

The *atoms*, or smallest particles of any of the elements of which the earth is composed, are at present conceived as having a planetary structure. They are the smallest particles possessing definite chemical characteristics.

Around the nucleus of the atom revolves a cloud of much smaller negatively charged particles, termed *electrons*. The electric and magnetic attractions between the electrons and the nucleus are counterbalanced by the centrifugal force of the electrons. Any chemical reaction consists of an exchange or sharing of electrons between atoms.

Chemically combined atoms form *molecules*, which represent the smallest indivisible particle of the new compound. The atoms of the molecule are firmly held together by the electrochemical bonds formed through the exchange or the sharing of electrons. Some molecules are *dipoles; i.e.*, they act as if they had opposite electrical charges at their opposite ends. Water is a *dipole;* paraffin oil is not.

Attraction between the molecules of liquids is evidenced by the phenomenon of *surface tension*. This is very pronounced in water (owing to its dipolar nature). *Capillary phenomena*, which strongly influence the

shrinkage, the cohesion, and many other properties of soils of importance in engineering work, are a result of the surface tension of water. This surface tension is caused by a downward pull due to attraction of the surface molecules by adjoining and by lower lying molecules.

X-ray studies of clays have shown that they are composed of extremely small crystals, in spite of the amorphous appearance of the whole clay mass. In this manner the existence of at least two definite *clay minerals* of extreme types, *kaolinite* and *montmorillonite*, and of some intermediate types has been established (Refs. 116, 161 to 163). Kaolinite was found to have a very rigid crystal structure, whereas montmorillonite can expand by admitting water between its crystal planes. Its crystal structure thus had an accordionlike nature which explained the swelling tendencies of bentonite clays largely composed of the montmorillonite type of clay minerals.

The diameter of the nucleus of an atom is of the order of 10^{-11} mm. The diameter of an atom is 10^{-7} mm = 1 A, designated in chemistry as 1 angstrom. The diameter of an atom is therefore approximately equal to 0.1 mμ (millimicron) or to 10^{-4} μ (micron). Thus the atoms are still too small to be seen even in an electron microscope, the limit of visibility of which is about 5 mμ. Particles smaller than 1 mμ are said to be in true solution if dissolved in a liquid.

The electron microscope has a 20 to 50 times greater resolving power than the light microscope. Its use, however, is subject to certain limitations. Specimens are examined in a vacuum, with resulting evaporation of all surface moisture films. The images appear dark and the openings appear bright on the fluorescent screen. Indications concerning the third dimension can sometimes be obtained from intensity differences in the case of very thin specimens (see Ref. 275 and Figs. 3-7 and 3-8).

Chemists call particles larger than 1 mμ but smaller than 0.2 μ (or 200 mμ) *colloids* and their solutions *colloidal solutions*. The upper limit represents the resolving power of the best possible optical microscope.

In engineering soil work, particles smaller than 1 μ (0.001 mm) have been defined as colloidal clay. Particles smaller than this diameter cannot be accurately determined by sedimentation methods. The reason for this is that below this size the speed of sedimentation is extremely slow and ceases completely for particles smaller than 0.2 μ (0.0002 mm). Such colloidal particles remain indefinitely in suspension.

The particles of colloidal solutions (or *sols*) are therefore so small as not to be seen by the naked eye, and execute rapid movements in all directions, called *Brownian movements*. These movements are caused by the impacts of the molecules of the liquid in which the colloidal particles are dispersed. The velocities thus gained by the particles are sufficient to

prevent their sedimentation. Another characteristic of colloids is that all particles carry a like electric charge. This like electric charge prevents the particles from attracting each other. The charge of most soil dispersions is negative.

By adding to the colloidal solution an electrolyte, *i.e.*, a chemical solution some of the ions of which have opposite charges to that of the colloid particles, the charges of the colloid particles can be neutralized. These particles then *flocculate* or *coagulate* and cling to each other, forming much larger grains which then sediment rapidly.

This circumstance has some practical applications. Thus, electrolytes are added to the water in settling tanks of water works to accelerate the clarification of muddy water.

Exactly the same thing can happen during a sedimentation test in a laboratory if the soil tested contains salts liable to form an electrolyte. This effect is most undesirable, as the grain diameter obtained from the test is then not that of the real particles, but the diameter of the much larger honeycombed bunches of coagulated particles. Other chemical solutions of opposite action, so-called dispersers or stabilizers, have then to be used.

The presence of dissolved salts in sea water is responsible for its clarity. The presence or absence of such salts in appreciable quantities in the water of rivers generally explains why some rivers are perfectly clear and others very muddy.

3-5. Moisture Films Adsorbed on the Surface of Soil Particles and Their Effect on the Engineering Properties of Soils. Base Exchange. Further investigations of the chemical composition and crystal structure of soils show that individual ions of different minerals may be attached (adsorbed) to the surface of a soil crystal. Figure 3-2 illustrates a relatively simple structure of this type.

Univalent ions, like Na^{+}, are loosely bound to the soil crystal. The bivalent ions Ca^{++} and Mg^{++} are attached to it somewhat more firmly. The slightly dissociated H ion and the trivalent cations of Al^{+++} and Fe^{+++} can be bound very strongly.

At the same time water molecules, being dipoles, are attached (adsorbed) both to the surface of the crystal lattice and to the cations. Some water molecules may even penetrate into the interior of the lattice.

The number of water molecules adsorbed by a cation increases with an increase of its charge and is also a function of the ionic radius. Thus, a Ca^{++} ion will attract more water molecules than an Na^{+} cation, their atomic radii being 1.06 and 0.93, respectively; but two Na^{+} cations may be adsorbed on the surface of the crystal for each Ca^{++} cation. Also, the volume of two Na^{+} cations equals 7.88 A^3 and that of one Ca^{++} cation is

4.99 A^3 (Ref. 332). Therefore the Na^+ cations will have a thicker layer of adsorbed water around them, which together with the cation may form a particularly thick *film of adsorbed water* around the soil crystal.

This adsorbed water film has properties different from those of ordinary water, because of the great pressure to which it is subjected by the electrostatic forces of adsorption.

Winterkorn and Baver (Ref. 433, 1934–1935) compute the average adsorption pressure of water to be of the order of 20,000 tons per ft^2. Bridgman (Ref. 41, 1912), continuing the work of Tamman (Ref. 239, 1899), has shown that at pressures exceeding 6,000 tons per ft^2 the freezing temperature of water steadily increases beyond the normal freezing point. Pressures of 10,000 tons per ft^2 raise this temperature to +30°C (+96°F). Below pressures of 6,000 tons per ft^2 the freezing point of water lies below the normal temperature and reaches a low of −20°C (−4°F) at 2,000 tons per ft^2 pressure. At high pressures in the above ranges five types of ice of varying density can be obtained depending on the pressure and the temperature. From the above data Winterkorn (Ref. 437, 1943) concludes that close to the surface of soil particles of clay size adsorbed water films must have the properties of solid ice. Observed volume changes of clays during freezing and thawing are explained by the above hypothesis.

FIG. 3-2. The fixation of exchangeable cations of different water-adsorbent capacity on the edge of an SiO layer of a clay-mineral crystal, exemplifying the broken-bond type of ion exchange. (*After K. Endell and U. Hoffman, Ref. 116.*)

By *base exchange* is meant the capacity of colloidal particles to change the cations adsorbed on their surface. Thus a hydrogen clay (colloid with adsorbed H cations) can be changed to a sodium clay (colloid with adsorbed Na cations) by a constant percolation of water containing dissolved Na salts. Such changes can be used to decrease the permeability of a soil (Ref. 208). Not all adsorbed cations are exchangeable. The quantity of exchangeable cations in a soil is termed *exchange capacity*.

Exchange capacity increases with the acidity of the soil crystals, as expressed by higher values of the silica-sesquioxide ratio SiO_2/R_2O_3. Another measure for the acidity of a soil, if considered as a suspension, is its pH value, which, however, refers mainly to the acidity of the soluble particles.

The greater the acidity of a soil, as expressed by a low pH value, the greater will be the activity of the H ions and also its corrosive action on metals. Both can become effective only in the presence of moisture. Acid solutions have a pH value smaller than 7, and basic or alkaline solutions have a pH value greater than 7.

The rate at which the base exchange takes place will increase with the concentration of the solution of the base and with the velocity at which this solution will percolate through the soil. The nature of the changes in the physical properties of a soil as caused by base exchange depends on the nature both of the soil and of the exchangeable bases.

The corrosion of iron and of steel embedded in soils is also only possible in the presence of soil moisture. It increases with the acidity (small pH value) of the soil, because acid solutions facilitate the formation on the iron surface of electric couples between the iron and some impurities it may contain. Electrolytic action results and the liberated oxygen combines with the iron progressively forming what is known as rust. Electric currents of external origin can have a similar but much stronger effect, for instance, on water mains. This circumstance sometimes forms the source of litigation between electric-streetcar and water-supply companies. The use of water pipes made of different metals such as iron, brass, and lead, embedded close to each other in a moist acid soil, can also facilitate strong corrosion by the formation of electric couples.

The chemical processes involved are very complicated and depend on so many factors that the base-exchange treatment of natural soils will always have to be dealt with by specialized chemists. At present it is still in the research stages, but some facts already disclosed are of considerable general interest and can help engineers to understand better the causes of differences in the behavior of clays under stress. For instance, during tests made by J. D. Sullivan (Ref. 332, 1939) a natural clay was first transformed into a hydrogen clay, which served as a basis of comparison. Samples of this hydrogen clay were then separately treated with various cations, and it was found that, for the same free-water content, in the semisolid range the shearing strength is very appreciably altered (Art. 7-19), decreasing in the sequence of the cations given in Table 3-2. The plasticity changes in approximately the same, but reversed, order. This phenomenon can be explained by the formation of thin, strongly viscous water films adsorbed by the exchangeable cations on the surface of the soil particles. As explained previously, these films are apt to be relatively thick in the case of strongly water-adsorbent cations like Li^+ and Na^+, but very thin for H^+. The films of other cations have intermediate values in accordance with the series in Table 3-2. Therefore soils with adsorbed Li^+ and Na^+ cations are relatively more plastic and,

at low water content, have a relatively smaller shearing strength because their particles are separated by a thicker viscous film with semisolid properties. In the semiliquid consistency range a reverse relationship may be obtained.

TABLE 3-2. Cations Listed in the Order of Decreasing Beneficial Effect on the Shearing Strength of a Clay

NH_4^+	H^+	K^+	Fe^{+++}	Al^{+++}	Mg^{++}	Ba^{++}	Ca^{++}	Na^+	Li^+

When chemists speak of hydrogen, calcium, or sodium clays, they do not refer to the composition of the soil particles, but only to the kind of cations (H, Ca, or Na) adsorbed on their surfaces. *Sodium clays* in nature are a product either of the deposition of clays in sea water or of their saturation by salt-water flooding or capillary action. *Calcium clays* are formed essentially by fresh-water sediments. *Hydrogen clays* are a result of prolonged leaching of a clay by pure or acid water, with the resulting removal of all other exchangeable bases. In most natural clays the soil particles may have different cations adsorbed on their surfaces (Fig. 3-2).

Further, the base-exchange processes are reversible and do not appear to follow any definite sequence, depending only on the freedom of movement of solutions through the soil and the presence of an excess of one of the exchangeable cations. For these reasons the changes in the engineering properties of chemically treated natural soils may be much more unpredictable and erratic (Ref. 434) than in the Sullivan tests (Ref. 332), which started from a pure hydrogen clay.

A phenomenon of engineering importance caused by adsorbed water films of a different kind is the bulking of sand. Bulking should not be confused with swelling, which may cause an increase of volume of a clay even if it absorbs water in situ. Swelling is not reversible when the clay is submerged, whereas the bulking of sands disappears entirely when the sand is submerged (Fig. 3-3). *Bulking* represents an increase of volume of moist sand, as compared to dry sand, but will take place only if moist sand is loosely reshoveled. The moisture films are sufficiently viscously rigid to prevent the sand grains from touching each other once the films are formed, but they cannot push them apart during the process of their formation, as is the case in the *swelling of clays*. The amount of bulking increases with the fineness of sand particles because of the increase in the total surface area of the particles per unit of volume (Fig. 3-3). Its effects can be considerable and are the main reason why in all important modern concrete work the aggregates are measured by weight and not by volume. The films are comparatively thick and readily evaporate at

room temperature. Since bulking disappears when the sand is fully saturated, surface tension of the water is probably responsible for the phenomenon. It should be noted that bulking is present only in loosely dumped sand. Moist sand can be compacted by high pressures just as well as dry sand (Art. 11-2). This is an indication that the thick water films which produce bulking can offer only a relatively small amount of resistance to pressure.
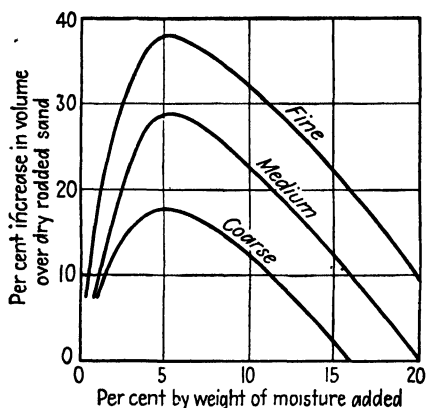
FIG. 3-3. Diagram illustrating the bulking of originally dry sand, that is, its increase of volume after having been moistened and reshoveled. The effect of surface tension of the water films on the sand particles appears to reach a maximum at about 6 per cent water content. It then decreases and disappears entirely shortly before the voids are quite filled with water. (*Courtesy of the Portland Cement Association.*)

3-6. The Determination of Grain Size by Sedimentation. The silt and clay content of a soil has to be determined by sedimentation. There are several methods of doing this. They are based on the fact that smaller sized particles take a longer time to sink through a liquid than do larger particles. The equation by G. G. Stokes for the speed with which a sphere of a given diameter sinks through a liquid is used for the computations. The sedimentation methods therefore do not give the actual diameter of the particles but only the diameter of an equivalent sphere. Stokes' formula generally is written as follows:

$$v = \frac{(G - G_w)gd^2}{1{,}800n} \text{ cm per sec} = \frac{(G - G_w)gd^2}{30n} \text{ cm per min} \qquad (3\text{-}3)$$

where v = velocity of settlement
d = diameter of sphere, mm
G = specific gravity of the soil solid
G_w = specific gravity of the liquid (water = 1.00)
n = viscosity of the liquid, gm per cm per sec, or poises
g = acceleration of gravity, cm per sec^2

$$v = \frac{L}{T} \qquad (3\text{-}4)$$

where L = distance through which particles fall, cm
T = corresponding time, min

Hence

$$d = \sqrt{\frac{30n}{980(G - G_w)}} \sqrt{\frac{L}{T}} = C \sqrt{\frac{L}{T}} \qquad (3\text{-}5)$$

Since for all practical purposes $G_w = 1.00$ when water is used, the coefficient C in Eq. (3-5) depends only on the values of the specific gravity G of the soil solids and the viscosity n of the water. The viscosity depends on the temperature.

The limitations of grain-size determinations should, however, be clearly understood. They are:

1. The results of tests performed by L. and W. Squires (Ref. 325, 1937) at the Massachusetts Institute of Technology give an idea of the amount of error introduced by the use of the Stokes formula when soil particles are not of spherical shape.

According to these tests, the following relationship was found for equal velocity of sedimentation:

$$D = 0.752D' \sqrt{\alpha} \qquad (3\text{-}6)$$

where D' = diameter of sphere
D = diameter of disk
$\alpha = D/H$; where H = height of disk

Correction factors ($= 0.752 \sqrt{\alpha}$) therefore have to be considered.

Since most clay particles are of a scalelike shape and not spheres (Art. 3-8), it follows from Table 3-3 that the actual diameter of a clay scale may be at least five times greater than the one determined from Stokes' law.

2. Another possible source of error is the coagulation of particles. Most soils contain salts which cause their particles to coagulate. To prevent this, and also to loosen the separate particles from each other, the soil has to be treated first with dispersing and stabilizing chemicals.

The addition of stabilizing electrolytes is therefore necessary to permit sedimentation testing. This involves the change of the charge on some of the colloidal soil particles. However, the charge on colloidal particles cannot be removed without causing changes which may amount to the partial destruction of the particles themselves.

3. Particles of different size in the same soil may have a different mineralogical origin and therefore different specific gravities. Only the average value of the specific gravity of the whole soil sample is used during the test.

4. The Stokes formula is based on the motion of one sphere and does not take into account the reciprocal influence of particles of different sizes settling past each other at different speeds in a suspension.

All these and other circumstances justify the statement that the sedi-

mentation test, no matter how accurately performed, gives only a general indication of the *order of magnitude* of the size and quantity of colloidal soil particles. Excessive refinements in the technique of this test therefore are not justified when it is performed for engineering purposes.

TABLE 3-3. Shape Correction Factors

α	D
1.00	$0.752D'$
1.77	$1.00D'$
10.00	$2.38D'$
100.00	$7.52D'$
500.00	$16.80D'$

This consideration, and the fact that the standard hydrometer test takes over two days to perform, have prompted attempts to simplify the whole procedure. One such attempt was made by R. Valle-Rodas (Ref. 413, 1945), and another by W. H. Mills, Jr., (Ref. 231, 1944). Only the total quantities of sand, silt, and clay are determined by siphoning.

The most common procedure involves the use of a glass hydrometer which will float on water, the initial graduation of its stem coinciding with the surface level of clean water. A mixture of soil particles and water will have a greater density, so that in such a mixture the hydrometer will sink less than in clean water. As the coarser particles settle out, the density of the suspension decreases, and the hydrometer sinks deeper. Readings on the stem of the hydrometer are combined with stop-watch and temperature readings taken from the moment the suspension was shaken up. These data, and the known initial dry weight of the soil particles, permit the computation of the diameter and of the weight of soil particles still in suspension at a given time.

3-7. The Classification of Soils According to Grain Size, and Its Limitations. The combined results of sieve and sedimentation tests are sometimes referred to as the *mechanical analysis*.

The results of the analysis are plotted in the manner indicated in Fig. 3-1. The weight of particles which are smaller than a certain diameter is expressed in per cent of the total weight and is plotted against that diameter on a semilogarithmic scale. The grain-size-accumulation curve thus obtained shows at a glance the distribution of particles of different sizes within a sample. It also makes it possible to judge the degree of uniformity in the composition of a sample with respect to grain size.

The *coefficient of uniformity* is defined as the ratio between the grain diameter corresponding to the 60 per cent line in the diagram to the grain diameter corresponding to the 10 per cent line ($=D_{60}/D_{10}$). A small value of this coefficient corresponds to a steeply inclined curve and to a more uniform composition of the sample. The degree of uniformity of

grain size may have a certain influence on the stability of granular soils (Art. 18-4).

Figure 3-1 gives also the corresponding grain diameters in inches, although inch measures are never used for this purpose. They are indicated in Fig. 3-1 merely to help those unfamiliar with metric measures to visualize them.

The terms *clay*, *silt*, and *sand* were applied here to grains of a specific size. The same terms are, however, often used for definite soil formations
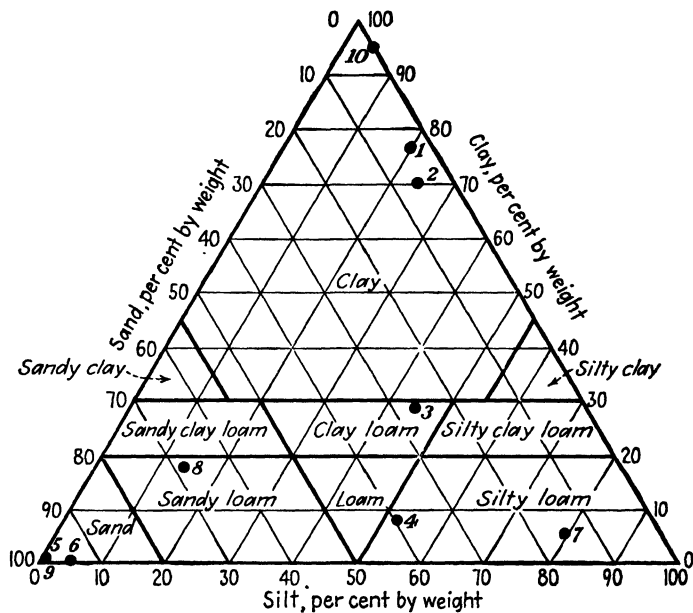
FIG. 3-4. Triangular soil classification chart of the U.S. Bureau of Soils and of the Public Roads Administration, based on the content of sand, silt, and clay. Note: The 10 soils of Fig. 3-1 have been marked by corresponding numbers in this chart.

which do not consist exclusively of clay or of silt or of sand, but which represent mixtures of all three types of grains in varying proportions. There is so far no generally recognized definition concerning the percentage of, for instance, clay particles that a soil must have to be classified as clay, etc.

Figure 3-4 gives a classification of the U.S. Bureau of Public Roads using a triangular diagram for the definition of the percentages of clay, silt, and sand particles in materials to be called, *clays*, *loams*, *silty loams*, etc. A loam is a mixture of sand, silt, and clay particles in varying proportions. The term "loam" originated in agricultural soil work and was

taken over by highway engineers who have to deal mainly with surface soil layers.

A recent trend is to eliminate the rather ambiguous term "loam" from foundation engineering use. Figure 3-5 shows a triangular soil-classification chart of the Mississippi River Commission which does not use the term *loam* at all and replaces it by such terms as *silty clay, silty sand, sandy clay,* etc. This appears logical, since the whole classification is based only on the sand, silt, and clay content.
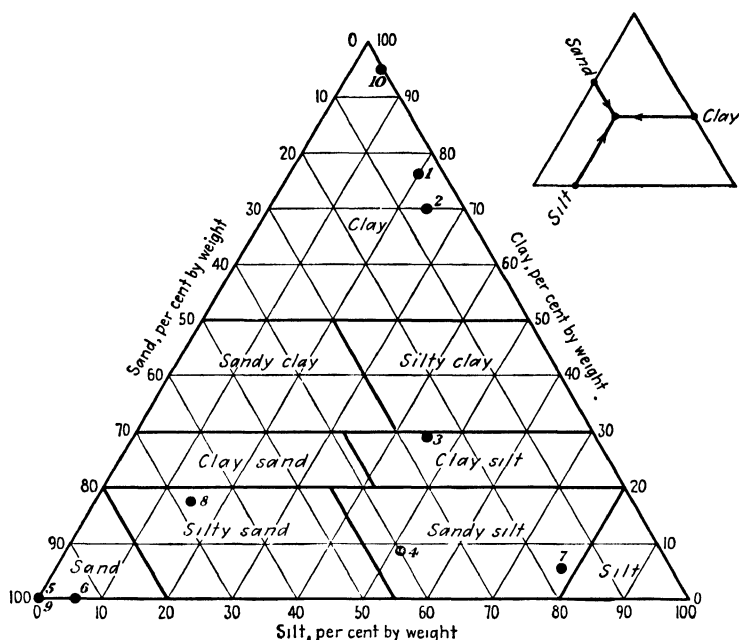
FIG. 3-5. Triangular soil classification chart of the Mississippi River Commission. The term *loam* has been omitted. *Note:* The 10 soils of Fig. 3-1 have been marked by corresponding numbers in this chart. (*Courtesy of the President, Mississippi River Commission, Vicksburg, Mississippi.*)

Figure 3-1 gives the grain-size-accumulation curves of 10 different soils. The same 10 soils are marked on the two triangular charts, Figs. 3-4 and 3-5. The proper way to use these charts is indicated by a diagram in the upper right-hand corner of Fig. 3-5. The sand, silt, or clay content of a soil is expressed in per cent of the total dry weight and is scaled off on the corresponding side of the diagram. Three lines are then drawn as shown in Fig. 3-5. They will always intersect in one point. Diagrams of this kind are used in granular-soil-stabilization work (Art. 11-7).

The classification of soils according to their grain size is the simplest

possible, but it has the limitation that its relation to the main engineering properties of soils is of an indirect kind only.

The size of the grains of a soil is only one of the factors on which depend some of the physical properties of direct importance to engineers, such as the cohesion and the permeability of a soil.

If the grains of a soil are small, the openings between them will also be small, and consequently water will have more difficulty in flowing through such a soil than it would have through a soil with larger grains and larger openings between them.

Smaller grains and openings in a soil may cause a greater cohesion as a result of larger total surfaces of contact between the more numerous small grains. Greater capillary forces in the narrower channels can develop in a not entirely water-logged soil as a result of entrapped air.

However, the knowledge of the grain size alone does not allow any accurate estimation of such properties as permeability and cohesion. Supplementary data are required, giving at least indications as to how closely the grains are packed, *i.e.*, data concerning the density of the soil. Generally speaking, all that the knowledge of the grain size of a soil conveys to us is a certain idea of some of the potential properties the material of the soil possesses.

The determination of the grain size is therefore done mainly in cases where one has to deal with soils which are to be used as an engineering material which must first be disturbed and then artificially recompacted (earth dams, roads, etc.). In such cases the selection of the material possessing the potential properties required is facilitated by the knowledge of its grain-size distribution.

Additional classification tests are, however, required; for instance, the determination of the limits of consistency (Art. 4-7). They are needed because grain-size determinations alone are apt to be misleading concerning such important properties of the basic soil material as plasticity, which appears to depend in part on the shape of the grains.

3-8. The Effects of the Shape and of the Hardness of Soil Grains. The shape of the soil grains has been found to be of considerable importance for the explanation of many phenomena. It was suspected for some time that the plasticity and also the considerable compressibility of clays might be due to the scalelike shape of their particles. The Swedish scientist Atterberg proved this by pulverizing various minerals and separating the particles of colloid size. Only the minerals which were apt to split along parallel planes into scale-shaped fragments gave particles of colloid size possessing plasticity. Similar quartz particles were not plastic. By *plasticity* one generally understands the ability of a substance easily to undergo considerable shearing deformations without rupture.

This consideration leads to another limiting definition of clay, *i.e.*, that it is plastic. According to this definition, quartz powder particles of 1 μ diameter should not be classified as clay, but as silt. No generally accepted terminology concerning soil classification has been developed so far, although many attempts are under way (Ref. 66 and Art. 12-11).

Figure 3-6 shows the results of compression tests on sand-mica mixtures of the same weight. It may be seen that both the volume and the compressibility of the mixture increased with the percentage of mica. This was probably due to the *bridging action* of the mica scales between the sand grains and to the subsequent flexibility of these scales under increased pressure. Other experiments showed that numerous clays are composed of scale-shaped particles.

FIG. 3-6. Compression produced by a pressure of 1 kg per cm^2 (approximately 1 ton per ft^2) on 200-gm samples of various sand-mica mixtures. The compression increased with an increasing content of the scalelike mica particles. (*Reproduced by permission of The Public Roads Administration from paper by K. Terzaghi, Ref.* 350, 1927.)

Figure 3-7 shows a dickite clay mineral crystal lying flat and standing on edge photographed through an electron microscope. In this case the axial ratio of width to thickness is approximately 10:1. Intensity differences of electron microphotographs permitted the estimation that the axial ratio of Wyoming bentonite clay minerals is of the order of magnitude of 250:1 for unit plates. A photograph of this mineral is shown in Fig. 3-8. The penetration of water between these thin unit plates is sometimes believed to be the cause of the pronounced swelling properties of Wyoming bentonite, rather than the penetration of water into the crystal structure.

Figure 3-9 shows a photograph of a quartz sand from the Daytona Beach race track in Florida. This sand is of uniform size, as are most beach sands (Fig. 3-1).

In most cases the *hardness of individual soil grains* is of little importance. Most sands are composed of very hard quartz grains with rounded edges. The foundation pressures normally considered as permissible on such deposits are not sufficient to crush or to split any grains.

If in some exceptional cases the sand is composed of some other

mineral, softer than quartz and with sharp edges, the effects on these grains of the unit pressures which are planned to be applied to the sand deposit may be investigated as follows: The granular composition of a sand sample is first accurately determined by sieving, and its grain-size-
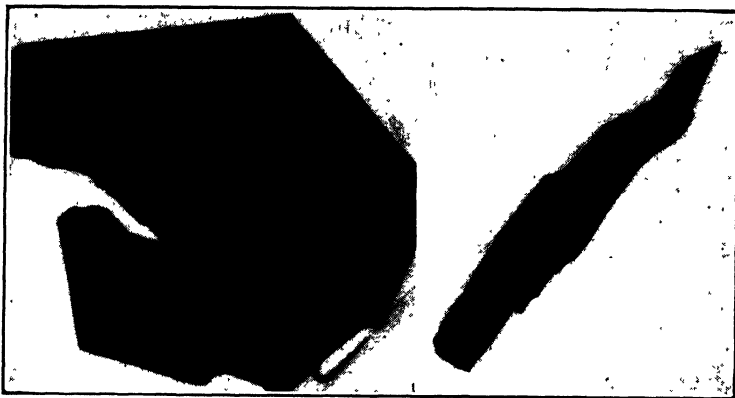
FIG. 3-7. Photograph through an electron microscope of a dickite (clay mineral) crystal lying flat and of the same crystal standing on edge. (*From Albert F. Prebus, Ref. 275, 1944.*)
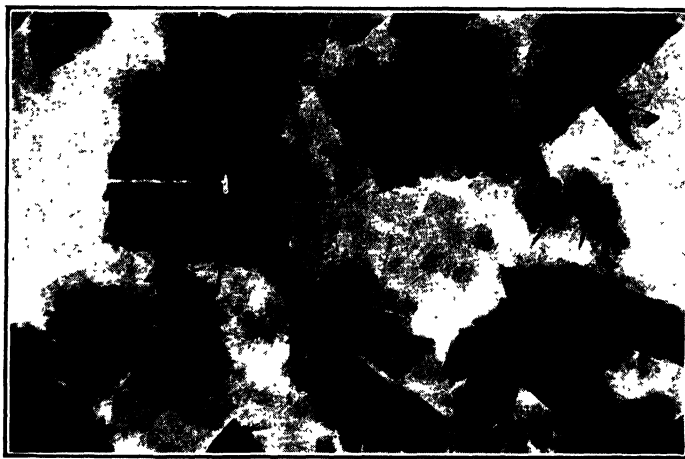
FIG. 3-8. Photograph through an electron microscope of 2 mμ to 1 μ fraction of Wyoming bentonite (soil 10, Fig. 3-1). (*From Albert F. Prebus, Ref. 275, 1944.*)

distribution curve is plotted. Then the same sample is compressed by unit pressures equal to or by some 50 per cent larger than the pressures planned for design use. After this test the sample is sieved again. If the comparison of the grain-size-distribution curves before and after the compression test shows an appreciable increase in the percentage of smaller

sized grains and of dust, this is an indication that crushing of the grains has occurred and that the design pressures should be reduced accordingly. Considerations of the above kind impose a limit on the height of rock-fill dams.

The presence in some sand deposits of *hollow shells* sometimes causes considerable compression of the deposit when loaded, with resulting foundation trouble, because of the ease with which such shells are crushed. Their presence should, therefore, be carefully noted during all preliminary
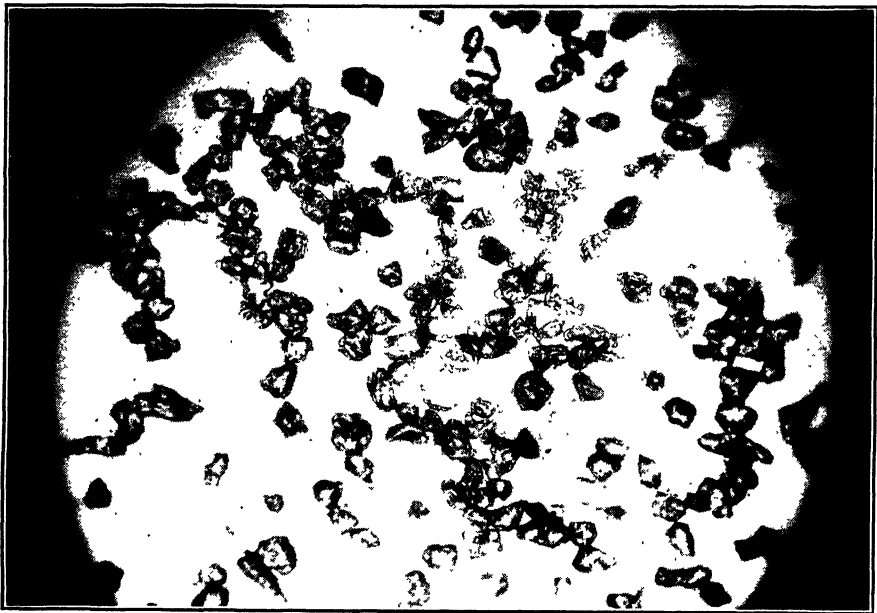
FIG. 3-9. Optical microphotograph of quartz sand particles from the Daytona Beach race track (soil 9, Fig. 3-1; particle size between 0.15 and 0.25 mm). (*From Tschebotarioff and McAlpin, Refs.* 381 *and* 382.)

soil investigations for foundation purposes. Shell fragments or clam-shaped shells filled with sand do not present an additional hazard.

Practice Problems

3-1. What facts of engineering importance will be conveyed to you by a statement that the specific gravity of the solid substance of a soil is equal to 2.3?

Answer. A high organic content may be indicated.

3-2. Determine the respective percentages of sand, silt, and clay content for the 10 soils referred to in Fig. 3-1. Use their grain-size-distribution curves and check by using the data given about them in Figs. 3-4 and 3-5.

Answer:

Soil No.	Sand, per cent	Silt, per cent	Clay, per cent	
1	5	17	78	100%
2	5	25	70	100%
3	26	45	29	100%
4	40	52	8	100%
5	100	0	0	100%
6	95	5	0	100%
7	17	78	5	100%
8	67	15	18	100%
9	100	0	0	100%
10	0	5	95	100%

3-3. The mechanical analysis of a soil has given the following results: Total weight of dry sample, 59.1 gm. Retained on the U.S. Standard sieves No. 20, 40, 60, 140, and 200, respectively, 2.8, 3.4, 8.5, 6.7, and 10.2 gm. The sedimentation test showed that 24.6 gm were smaller than 0.05 mm and 10.2 gm were smaller than 0.005 mm. Plot the grain-size-distribution curve of this soil sample and classify it according to the chart in Fig. 3-5.

Answer:

Total weight: W_s = 59.1 gm

Sieve No.	W_1 = weight retained on sieve, gm	$W_2 = W_s - \sum W_1$ = total weight smaller than corresponding size, gm	$\frac{W_2}{W_s} \times 100$ = fraction smaller than corresponding size, per cent
20	2 8	56 3	95 2
40	3 4	52 9	89.5
60	8 5	44.4	75.2
140	6 7	37 7	63 8
200 (0 074 mm)	10 2	27 5	46.5
0.05 mm		24 6	41 6
0 005 mm		10.2	17.3

Clay: 17.3 per cent; silt: 41.6 − 17.3 = 24.3 per cent; sand: 100 − 41.6 = 58.4 per cent. According to Fig. 3-5 this soil should be classified **as a silty sand.**

References Recommended for Further Study

Any textbook of college chemistry.

"The Clay Minerals and Their Significance," by R. E. Grim, *Proceedings, Purdue Conference on Soil Mechanics*, 1940, pp. 216–223.

"The Condition of Water in Porous Systems," by Hans F. Winterkorn, *Soil Science*,

August, 1943. Shows the significance of the special properties of the adsorbed films of water.

"Physico-chemical Properties of Soils," by Hans F. Winterkorn, *Proceedings of the Second International Conference on Soil Mechanics and Foundation Engineering*, Rotterdam, Vol. I, pp. 23–30, 1948.

"Procedures for Testing Soils," *American Society for Testing Materials*, July, 1950, pp. 43–56. Mechanical analysis.

Laboratory Manual in Soil Mechanics, By Raymond F. Dawson, Pitman, 1949, pp. 74–89 and 104–111. Techniques for the determination of the specific gravity and of the grain-size distribution of soils.

CHAPTER 4

DEFINITIONS AND TESTS RELATED TO THE DENSITY AND TO THE CONSISTENCY OF SOILS. CAPILLARY PHENOMENA

4-1. The Structure of Soils. The structure of soils may be either of a granular or of a flocculent type. By *granular* is meant the structure of a soil skeleton composed of rounded or angular but essentially massive individual grains, such as occur in coarse-grained, *i.e.*, sand soils. The volume of voids (the pore space) of such soils is relatively small and is apt to vary within comparatively restricted limits.

In the case of fine-grained soils, that is, of clays, a similarly compact structure of the soil skeleton is prevented by electrochemical forces of attraction between the tiny scale-shaped particles. During sedimentation, as the clay deposit is formed, these forces may cause the particles to stick together (*coagulate*) in loose bunches, called *floccules*. A *flocculent* or a *honeycombed* structure results, the pore space of which is much greater than that of a granular-type structure. Any breaking down of the originally very loosely honeycombed skeleton of clay soils may cause it to compress considerably. These circumstances are largely responsible for the fact that the possible porosity and water content of clays are relatively high, and that the range of the possible density variations is great, when compared with those of sands (see Fig. 4-9).

The disturbance of the structure of a fine-grained soil, the so-called *remolding* is known to cause sometimes considerable difficulties in actual foundation practice by appreciably decreasing the shearing resistance of the soil and increasing its compressibility. Some clays are very strongly affected by it, others only slightly, and a few hardly at all (Art. 7-22). Several explanations exist for this different behavior (Ref. 440). Caution is to be recommended in carrying out all operations on a clay type not tested in a laboratory, if such operations are likely to disturb its structure. This refers to pile driving into some clays and to deep excavations which may produce heaving (see Arts. 14-6 and 15-2).

Figure 4-1 illustrates a tentative explanation by A. Casagrande (Ref. 61, 1932) of the reason why some clays can support a considerable load when undisturbed and why they become quite soft if remolded. The flocculated clay particles between the silt grains are compressed at the points of contact of these grains by the weight of the upper layers, forming a supporting skeleton framework. Within this skeleton is much looser material. Remolding of the whole therefore destroys the supporting
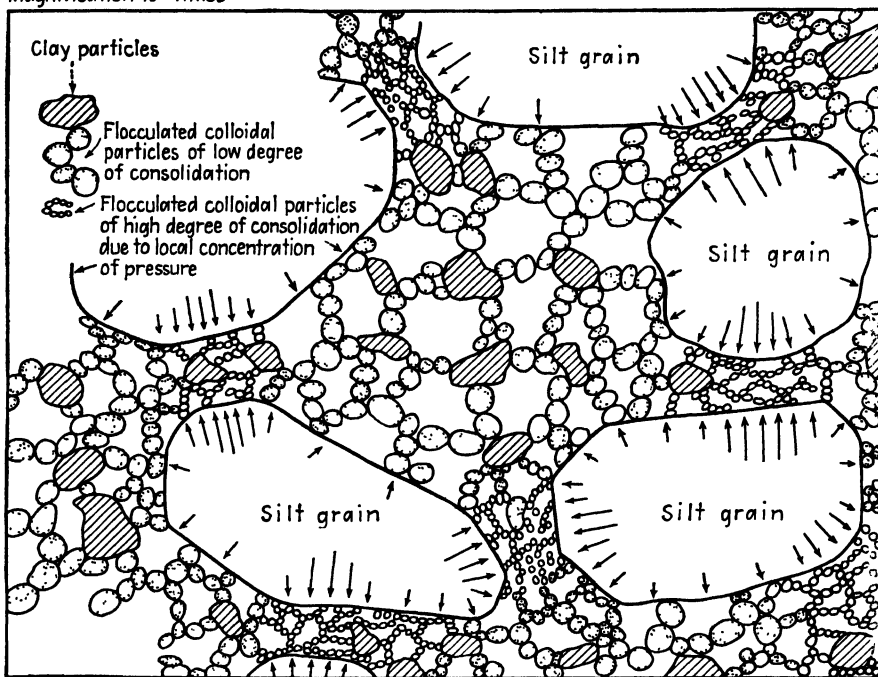
FIG. 4-1. A hypothesis concerning the structure of undisturbed marine clay. (*After A. Casagrande Ref. 61, 1932.*)

skeleton and mixes it up with the not compacted part, the compressibility of the whole being thereby increased.

Some remolded soils appear to regain with time their initial rigidity without any further decrease of volume—so-called *natural hardening* (Ref. 238). These and other similar phenomena (*thixotropy*) are not yet fully understood but show that the Casagrande hypothesis does not cover all the factors which act here, some of them apparently being of a more complicated electrochemical nature, involving cementation of the soil grains at their surface of contact (Refs. 359 and 440).

4-2. The Porosity and the Void Ratio. The volume of voids is generally expressed in per cent of the total volume and is termed *porosity*.

$$n = \frac{V_v}{V} \times 100 \tag{4-1}$$

where n = volume of voids, per cent of total volume
V_v = volume of voids
V = total volume

The porosity of sands can vary between 30 and 50 per cent. The lower values are generally met in deposits formed in slow-flowing water, such as on lake bottoms. Natural clays can have a porosity as high as 89 per cent (Fig. 4-9).
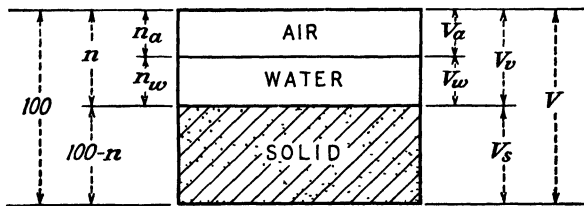
FIG. 4-2. Diagram illustrating the terms porosity (*n*) and void ratio (*e*).

Another expression, the void ratio e, is used for most computations. It is defined as the ratio of the volume of voids to the volume of solids (Fig. 4-2).

$$e = \frac{V_v}{V_s} = \frac{n}{100 - n} \tag{4-2}$$

$$n = \frac{e}{1 + e} \times 100 \tag{4-3}$$

The use of the void ratio e is more convenient for computation purposes than that of the porosity n, because e gives the ratio of voids in respect to a constant value, that of the volume of solids, whereas the total volume, in respect to which the ratio n is given, undergoes changes with every alteration in the volume of voids following changes of pressure. On the other hand, values of the porosity n are easier to visualize. This accounts for the existence and parallel use of both expressions n and e which define the same soil characteristic—the volume of its voids or pore space. See Fig. 4-10 for a graphical presentation of Eq. (4-2).

The values required for the determination of n and e are obtained as follows: The total volume V is measured directly, that is, either by immersion in mercury or, if the sample is sufficiently large and of a regular shape, by direct measurement or by measurement of the volume of the hole from which the sample has been extracted (Art. 11-6). The volume

of solids V_s is computed from Eq. (3-1). The weight of solids W_s is obtained by direct weighing before and after drying in an electric oven. The specific gravity of the solid substance G is determined by a separate test (Art. 3-1).

4-3. The Water Content. The *water or moisture content* w is generally expressed as a ratio of the weight of water to the weight of solids, and not to the total weight, the latter not having a constant value under varying conditions.

$$w = \frac{W_w}{W_s} \times 100 \tag{4-4}$$

where w = water content, per cent of weight of solids
W_w = weight of water
W_s = weight of solids

Both W_w and W_s are obtained by direct weighing before and after drying in an electric oven at 105 to 110°C.

Therefore, in the water content thus obtained is included the gravitational, the capillary, and the hygroscopic moisture, but not the film moisture (Art. 3-5).

As *hygroscopic moisture* is defined the moisture which is still contained in an air-dried soil, but which evaporates if the soil is dried at over 100°C, *i.e.*, over the boiling point.

Provided all the voids are filled with water, *i.e.*, when the soil is *saturated* (*waterlogged*), as shown in Prob. 4-2, the void ratio is equal to

$$e = \frac{w}{100} G \tag{4-5}$$

For fully waterlogged conditions the water content of sands may accordingly vary only from about 12 to 36 per cent, but that of clays may vary from 12 to 325 per cent (Fig. 4-9). The value of 325 per cent water content should not be surprising, since it is to be found only in freshly deposited clay or in particularly loosely sedimented, very fine volcanic ash, such as is found beneath Mexico City (Ref. 4), and since it is given in respect to the weight of solids, and not to the total weight. The reason for this now generally accepted method of expressing the water content is similar to the reason for the use of the void ratio e instead of the porosity n. The total weight of a clay sample changes as the sample dries out or is otherwise compressed, whereas the weight of solids remains unchanged. It is therefore preferable to determine the water content in respect to this constant value.

Generally the water content of soils is determined by weighing the soil specimen in a fairly airtight container, such as a pair of watch glasses with

ground edges held together by a clip, or in so-called *petri dishes*, to prevent evaporation before and during drying. The containers are made of resisting pyrex glass, so that the soil specimen can be dried in an electric oven without being removed from the opened containers (see numerical example, Prob. 4-4).

4-4. The Bulk Specific Gravity (Unit Weight of Soil Mass). The *bulk specific gravity* γ = unit weight of soil mass *above the ground-water table*, is given by the ratio of the total weight of the soil in air to the total volume of the soil, all voids included. It expresses the ratio of the weight of the solid and liquid phases of a soil to the weight of a volume of water equal to the sum of the volumes of the solid, liquid, and gas phases of the same soil.

If no moisture is present, or if the bulk specific mass gravity of the solid phase only has to be determined,

$$\gamma_d = \frac{W_s}{V} = \frac{G}{1 + e} \tag{4-6}$$

If all voids are filled with capillary water,

$$\gamma = \frac{G}{1 + e} + \frac{G_w e}{1 + e} = \frac{G + e}{1 + e} \tag{4-7}$$

If the voids are only partially filled with capillary water,

$$\gamma = \frac{W}{V} = \frac{G(1 + w/100)}{1 + e} \tag{4-8}$$

When entirely *submerged* in water the soil weighs less than in air because of the effects of buoyancy (law of Archimedes).

$$\gamma' = \frac{W_s - (V_s G_w)}{V} = \frac{G - 1}{1 + e} \tag{4-9}$$

Equations (4-6) to (4-9) give not only the bulk mass gravity of a soil, expressing the soil weight as a ratio in respect to a corresponding volume of water, but also give the unit weight of the soil in the metric system, in grams per cubic centimeter, since 1 cm^3 of water weighs 1 gm. To express the unit weight γ_m in the foot-pound system the ratios given by the preceding four equations should be multiplied by the weight of a cubic foot of water, 62.5 lb.

$$\gamma_{md} = \gamma_d \times 62.5 \tag{4-10}$$

$$\gamma_m' = \gamma' \times 62.5 \tag{4-11}$$

In Eqs. (4-10) and (4-11) G_w = 1.00 is the specific gravity of water in grams per cubic centimeter.

The expression $1/1 + e$ appears in all the above equations and it will occur later in some other equations. It is therefore advisable to understand its physical significance. The derivation of the preceding equations will then become apparent. This expression can be transformed as follows:

$$\frac{1}{1+e} = \frac{1}{1 + V_v/V_s} = \frac{V_s}{V_s + V_v} = \frac{V_s}{V} \tag{4-12}$$

The absolute specific gravity G, which appears in Eqs. (4-6) to (4-9), when multiplied by V_s gives the weight of the solids W_s, and the division by V reduces it in proportion to the total volume, thus giving γ, the bulk specific gravity of the whole mass (voids + solids). Similarly, the multiplication of G_w by V_s expresses the effects of buoyancy in accordance with the law of Archimedes. Also

$$\frac{e}{1+e} = \frac{V_v/V_s}{1 + V_v/V_s} = \frac{V_v}{V_s + V_v} = \frac{V_v}{V} = \frac{n}{100} \tag{4-13}$$

This expression appears in Eqs. (4-7) and (4-3). The multiplication of $G_w = 1.00$ by V_v gives the weight of water W_w when the soil is fully saturated.

4-5. The Degree of Saturation of Soils. Sometimes not all the voids of a soil are filled with water, but some air is present (Fig. 4-2). The degree of saturation S_r is then given by the ratio of the volume of voids filled with water to the total volume of voids, expressed as a percentage.

$$S_r = \frac{V_w}{V_v} \times 100 = \frac{n_w}{n} \times 100 \tag{4-14}$$

The *air content* a_c is given by the ratio of the volume of voids filled with air to the total volume of voids expressed as a percentage (see Fig. 4-2).

$$a_c = \frac{V_a}{V_v} \times 100 = \frac{n_a}{n} \times 100 = 100 - S_r \tag{4-15}$$

4-6. The Relative Density of Sands. The relative density of sands is expressed by a relation between the void ratios in the loosest possible state, in the densest possible state, and in the actual state in nature of the particular sand specimen.

$$D_d = \frac{e_{max} - e}{e_{max} - e_{min}} \tag{4-16}$$

where D_d = relative density
e_{max} = void ratio of the sand in the loosest possible state
e = void ratio of the sand in the actual state in nature
e_{min} = void ratio of the sand in the densest possible state

Thus, the relative density D_d expresses the ratio of the decrease of the voids from the loosest possible state to the actual state in nature to the maximum possible decrease through compaction from the loosest to the densest state. Sometimes it is expressed as a percentage, as shown in Table 4-1.

TABLE 4-1. Relative Density of Sands

Loose sand.............	D_d varies from 0 to ⅓ (or 0 to 33%)
Medium sand...........	D_d varies from ⅓ to ⅔ (or 33 to 66%)
Dense sand.............	D_d varies from ⅔ to 1.0 (or 66 to 100%)

For reasons explained in Art. 4-10 the void ratio e is not actually determined in some field investigations, and only the dry density of the soil, expressed in pounds per cubic foot, is available. Equation (4-16) has to be modified to meet such cases. Equations (4-6) and (4-10) can be transformed to read

$$e = \frac{G \times 62.5}{\gamma_{md}} - 1 \tag{4-10a}$$

Substituting the above expression for e in Eq. (4-16), and remembering that $\gamma_{md(\min)}$ corresponds to $e_{\max}$, we obtain after some transformations

$$D_d = \frac{\dfrac{1}{\gamma_{md(\min)}} - \dfrac{1}{\gamma_{md}}}{\dfrac{1}{\gamma_{md(\min)}} - \dfrac{1}{\gamma_{md(\max)}}} = \frac{\gamma_{md} - \gamma_{md(\min)}}{\gamma_{md(\max)} - \gamma_{md(\min)}} \, \frac{\gamma_{md(\max)}}{\gamma_{md}} \tag{4-16a}$$

For sands of different granulometric composition, $e_{\max}$ and $e_{\min}$ can assume different values. In the case of spheres of equal size, the following values are obtained (Fig. 4-3):

$$e_{\max} = 0.91 \qquad n_{\max} = 48\%$$
$$e_{\min} = 0.35 \qquad n_{\min} = 26\%$$
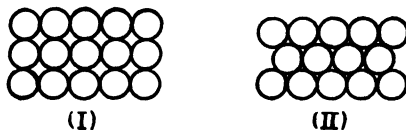
FIG. 4-3. Spheres of equal size (I) arranged in the loosest state possible; (II) arranged in the densest state possible.

The more uniform a sand is (sieve curve 5 in Fig. 3-1) the nearer its $e_{\max}$ and $e_{\min}$ will approach the above values for equal spheres. Less uniform—that is, better *graded*—sands (for instance, curve 6 in Fig. 3-1) will have smaller values for both $e_{\max}$ and $e_{\min}$. This would also be the case for an idealized soil composed of spheres if a sufficient number of smaller spheres were present to fill the voids between the larger ones (Fig. 4-4).

In actual sands the effect of the presence of smaller particles is

offset by the more angular shape of sand grains. The result is that the observed approximate density limits of actual sands, as given in Art. 4-2 (n_{max} = 50 per cent and n_{min} = 30 per cent), correspond very closely to the same limits of spheres of equal size, as given above.

The determination of both e_{max} and e_{min} can be made in a laboratory, but the reproduction of e, that is, of the actual natural state of a deposit, is not possible in a laboratory. The determination of e in the field is difficult because of the difficulty of extraction of really undisturbed samples of sand. It requires great care and is possible only for the upper layers which are accessible by open excavation. No fully reliable methods have been devised so far for the really undisturbed extraction of sand samples from below the water level or from bore holes (Art. 12-6).

FIG. 4-4. Maximum density is obtained when all the voids between larger particles are filled by smaller particles.

For this reason such determinations are seldom made in field practice, in spite of their considerable practical value, but have been used successfully for research on the comparative efficiency of different methods of sand compaction in artificial fills.

The procedure for the laboratory determination of e_{max} and e_{min} of sands has not yet been standardized. Until this is done, the following procedure is suggested: The densest state of sands (e_{min}) may be determined by means of the standard Proctor compaction test (see Art. 11-2). The loosest state of sands (e_{max}) may be determined by filling a 1,000-cm^3 measuring cylinder from a receptacle held 2 in. above the top of the cylinder. The sand is allowed to drop freely from that elevation. It should be completely dry, since otherwise bulking (Art. 3-5) will occur and raise the value of e_{max}. According to Eq. (4-16), this will lower the value of the relative density D_d to an inadmissible extent. Since sands in nature are deposited either by flowing water, in which case they are completely submerged, or by wind, in which case they are quite dry, bulking is not possible in a naturally deposited sand.

The relative humidity and the relative density are terms used mainly in connection with sands or other similar coarse-grained soils. For fine-grained soils, such as clays, other expressions (for instance, the limits of

consistency in relation to the water content) are generally used to define their potential limit states of stability.

4-7. The Limits of Consistency of Clays. A clay deposit in the process of formation, *i.e.*, during sedimentation at the bottom of a lake, of a pond, or of other slow-flowing waters, has at first the consistency of *liquid* mud. In this state, if removed from the deposit, it will not keep its shape by itself and will easily flow.

As the volume of voids of the deposit decreases, (either as a result of the applied weight of newly deposited upper layers or as a consequence of water evaporation, if the deposit has become exposed to the air), the clay becomes more compact and loses its capacity to flow. However, it is still fairly soft and *plastic*, *i.e.*, a laterally unrestrained clay has the capacity of altering its shape under the effect of an applied force without any appreciable change of volume, and of subsequently retaining the newly acquired shape.

Under further compression or drying a clay loses its plastic properties and is apt to crumble if remolded; it has reached the *semisolid* state.

After still further drying the clay finally reaches a state when it will not reduce its volume any further, *i.e.*, it will stop *shrinking*. This corresponds to a change in color; the clay takes on a lighter shade. It has then reached the *solid* state.

The limits between the liquid, the plastic, the semisolid, and the solid states of a fine-grained soil are respectively termed the liquid, the plastic, and the shrinkage limits.

They have a collective name of *consistency limits* and are sometimes referred to as *Atterberg limits*, being given the name of the Swedish scientist who first introduced them. These limits are generally expressed by the water content w of a given soil at a particular limit or by the corresponding void ratio e. Table 4-2 illustrates the relationship between the state of a fine-grained soil and the consistency limits. By *consistency* is meant the degree of resistance of a fine-grained soil to flow or to deformation in general.

The difference between the water contents at the liquid and at the plastic limit indicates the range of plasticity of a given soil and is sometimes termed the *plasticity index* I_p (or PI).

$$I_p = w_L - w_p \tag{4-17}$$

where I_p = plasticity index, per cent

w_L = water content at liquid limit, per cent of weight of solids

w_p = water content at plastic limit, per cent of weight of solids

For instance, if a clay has $w_L = 63$ per cent and $w_p = 22$ per cent, its

plasticity index I_p will be equal to 41 per cent. The higher the plasticity index, the greater the plasticity of that soil.

TABLE 4-2. Consistency Limits of Cohesive Soils

State of Soil (Consistency)	Lower Limit of Consistency
Liquid	Liquid limit w_L (or LL)
Plastic	Plastic limit w_p (or PL)
Semisolid	Shrinkage limit w_s
Solid	

The symbols LL, PL, and PI are sometimes still used by highway engineers in the United States, although both the ASCE (Ref. 9, 1941), and the ASTM (Ref. 10, 1944) recommend the use of the symbols w_L, w_p, and I_p.

A further limit, the so-called *sticky limit,* is used in agricultural soil science to determine the water content at which a soil ceases to stick to metal. Attempts have been made to correlate this limit with desirable properties of a dam-construction material in regions where the soil was of volcanic origin (Ref. 128).

4-8. Capillary Phenomena and the Shrinkage of Soils. The liquid and plastic limits have a certain physical significance, as already explained, but their exact values are determined by an arbitrary agreement between research workers to provide a common basis of comparison.

The *shrinkage limit* w_s of a soil is, however, directly defined in its exact value by changes in the physical characteristics which depend on *capillary phenomena.* These shall therefore be discussed first.

Water has a certain surface tension, which has been found to equal 75 dynes (= 0.0764 gm) across a width of 1 cm. In very narrow tubes, termed capillary tubes, the water will rise by itself, whereby a so-called meniscus is formed. The thinner a tube, the higher the water will rise. When equilibrium is reached the meniscus takes the shape of a semisphere of a diameter equal to that of the capillary tube.

This phenomenon is caused by the surface tension of the water and its molecular attraction to the walls of the tube. A prerequisite for this attraction and for all the ensuing phenomena of capillary rise is a greater *affinity* between the liquid and the material which it wets than would exist between that material and air.

Such greater affinity exists between water and glass, metals, rocks, and soils. Some other materials, for instance, paraffin oil, have greater affinity for air than for water. A coating of oil covering all soil grains may therefore prevent capillary phenomena.

Equilibrium requires that the weight of water pulled up by the force of

surface water tension should equal the vertical component of that force (Fig. 4-5).

$$\frac{\pi D^2}{4} H = 0.0764 D\pi \cos \alpha \tag{4-18}$$

Equilibrium is reached when the angle α equals zero; hence

$$H_{\max} = \frac{0.306}{D} \tag{4-19}$$

where H = height of capillary rise, cm
D = diameter of tube, cm
α = angle formed by the walls of the tube and a tangent to the meniscus at the point of contact with the wall

The force which pulls up the water in a capillary tube, as shown in Fig. 4-5, is balanced by a force which compresses the walls of such a tube. The existence and the action of this force may be visualized by considering the behavior of compressible capillary tubes under the effect of the evaporation of water within them. Suppose such a tube had been entirely filled with water by submerging it and was then exposed to drying. Just after the evaporation has started, causing the appearance of a slightly curved meniscus, a slight shortening of the column of water and of the tube will occur. Under the effect of continued evaporation the meniscus gets more and more curved as the water column gets shorter. The component of the force exerted by the surface tension of the water in the direction of the walls of the tube is correspondingly increased, causing these walls to shorten too, if they are compressible. No further shortening will occur when the increasing resistance of the tube equals the maximum possible value of the compressive force. After that, with further evaporation, the meniscus will withdraw within the tube. If the tube is submerged again the force acting on the tube disappears, so that if the material of the tube is perfectly elastic, it will expand back to its original length.

FIG. 4-5. The rise of water in capillary glass tubes of different length.

The knowledge of the height of active capillary rise in a soil is important in many practical cases; for instance, when determining whether a soil beneath a road pavement is likely to heave during frost by drawing up water from an underlying subsoil water table and thus allowing the growth of ice crystals.

The height of capillary rise is measured either by direct observation of

soil filling a glass tube—active capillarity—or by measuring in a special apparatus the suction required to overcome the capillary forces in the voids of the soil—passive capillarity—(Ref. 412). The latter comes into play in nature during lowering of the ground-water table by drainage.

The maximum possible compressive pressure which can be exerted by capillary forces in a soil subjected to drying has been estimated by Terzaghi (Ref. 350, 1927) to equal

$$p' = \frac{0.306}{b} \quad \text{gm per cm}^2 \tag{4-20}$$

where p' = maximum conceivable compressive pressure per unit of area
b = length of side of capillary opening, cm, assuming the openings to be squares and to cover the whole area

Table 4-3 may serve to give an idea of the theoretical values of maximal capillary compressive pressure p' under the assumption that the size of the opening is equal to that of the particles.

FIG. 4-6. Shrinkage cracks on the surface of a dried-out layer of originally liquid clay.

Such great active capillary rises in clays as are indicated in Table 4-3, however, seldom occur in nature, sometimes because of the formation of shrinkage cracks, but mainly because of the decrease of the free diameter of the voids by the adsorbed water films. There are, however, indications that the theoretical values of H_{max} for passive capillarity and the values of maximum capillary pressures are not estimated too high (Art. 6-4).

The decrease of volume, or *shrinkage*, of a fine-grained soil during drying is caused by the capillary forces. It ceases at the so-called *shrinkage limit* w_s, and the menisci of the water in the voids then recede into the interior of the sample. This induces a change of color from a dark to a

light shade. Very great pressures can be exerted in particularly fine grained soils by capillary forces at this stage. A characteristic pattern of shrinkage cracks is formed on the surface of an originally liquid clay layer after it dries out (Fig. 4-6). The pattern is induced by the resistance to shrinkage offered along the lower restrained surface of the new layer as it dries out.

If the soil is again submerged, the capillary forces cease to act and the soil expands, it *swells*. Generally, being imperfectly elastic, the clay does not reach its full original volume, especially if it had a high water content prior to drying.

The shrinkage limit is sometimes used for the rapid preliminary determination of the effects of the remolding of a clay (Ref. 61). A clay unfavorably affected by remolding will have a lower shrinkage limit in a remolded state than in the undisturbed state, since remolding decreases the strength of the skeleton of solid soil grains and its resistance to compression. A more convenient way to estimate the sensitivity of a clay to remolding, however, is provided by the unconfined compression test (Art. 7-22).

TABLE 4-3. Theoretical Effects of Capillarity

Soil	Size of particles and of openings, mm	H_{max}		p'	
		cm	in.	kg per cm²	lb per in.²
Sand, coarse......	2.00–0.025	1.5–12	⅝–5	0.0015–0.012	0.021–0.171
Fine............	0.025–0.05	12–61	5–24	0.012–0.061	0.171–0.87
Silt..............	0.05–0.005	61–610	24–240	0.061–0.610	0.87–8.7
Clay.............	0.005–0.001	610–3050	240–1200	0.610–3.05	8.7–43.5
Colloids..........	0.001 and finer	3050 and more	1200 and more	3.05 and more	43.5 and more

There are several ways for the laboratory determination of the shrinkage limit (Refs. 10 and 102). One of the possible procedures is outlined in Prob. 4-6.

4-9. The Determination of the Liquid and of the Plastic Limit. The Consistency Index and the Liquidity Index. The *plastic limit* (see Art. 4-7) is defined and determined as the lowest water content at which a soil can still be rolled into threads of ⅛ in. diameter without the threads breaking into pieces, *i.e.*, without crumbling. A small piece of plastic soil is rolled by hand on a glass plate; the threads of the soil are folded and rolled again; some moisture is lost as a result. The process is repeated until the threads cannot be rolled without crumbling. The water content is then determined by weighing the soil threads, drying them in an oven,

and weighing again. This water content is considered to represent the plastic limit w_p of the soil tested (Refs. 10 and 102).

The *liquid limit* w_L is defined as the water content at which a soil will just begin to flow if slightly jarred several times. Atterberg (1912) originally determined it by jarring a pat of soil in a porcelain dish by hand. The personal factor involved in such a determination is at present almost entirely eliminated by the general use of the mechanical device developed by A. Casagrande (Ref. 60, 1932) which is illustrated in Fig. 4-7. A brass dish C is hinged at one end P and can be repeatedly lifted and dropped by
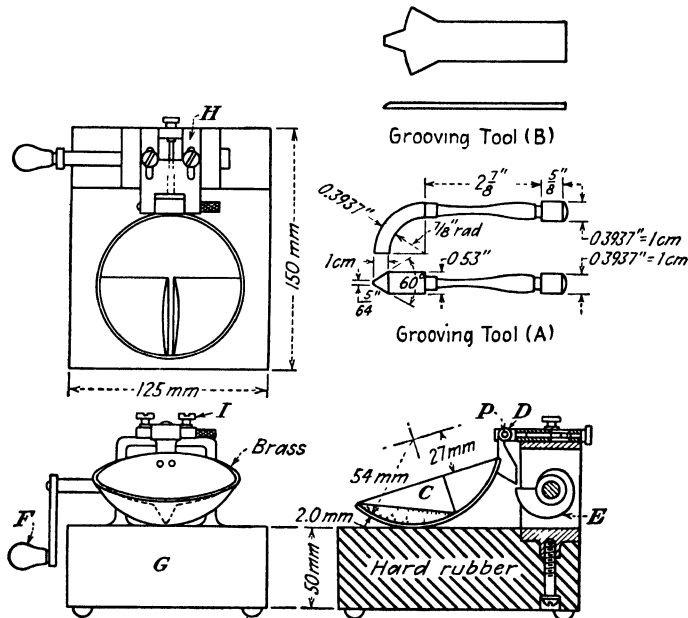
FIG. 4-7. The standard liquid-limit device and the two types of grooving tools. (A) ASTM (Ref. 10). (B) Casagrande (Ref. 60).

the cam E if the handle F is turned. The height of drop of the dish is adjusted to be exactly 1 cm. This apparatus is used the world over. The existence of two types of grooving tools (Fig. 4-7) does not seem to affect the results materially. The grooves cut by each are identical. Type B automatically removes any soil which may be pushed up at the edges of the groove.

Prior to the test the soil is completely remolded and is pressed into the cup. A groove is cut along the center of the soil pat as shown in Fig. 4-7. The handle is then rotated and the number of times the cup drops (the number of "blows") is counted until the groove closes over a distance of ½ in. Some of the soil around the groove is removed and its water con-

tent is determined. The process is repeated three or four times under addition of water or of drier soil, until a couple of water-content determinations have been made for consistencies corresponding to less than 25 blows and a couple more for a larger number of blows. The results of these water-content determinations are then plotted, as shown in Fig. 4-8, to a semilogarithmic scale against the corresponding number of blows. The points thus obtained usually fall along a straight line. The intersection of this straight line with a vertical line through 25 blows gives the
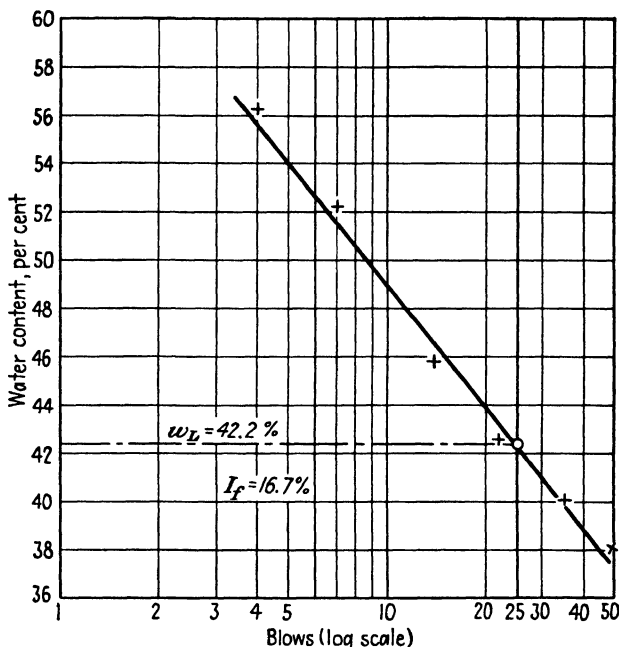
FIG. 4-8. Graphical method of liquid-limit determination.

water content corresponding to the liquid limit. The slope of this straight line is termed the *flow index* I_f, which is determined as the difference of the water contents at 4 and at 40 blows, or at 5 and 50 blows, etc.

The *consistency index* I_c is expressed as a percentage and defines the consistency of the soil in its natural state, as expressed by its natural water content w, in respect to its plastic and liquid limits.

$$I_c = \frac{w_L - w}{w_L - w_p} \times 100 = \frac{w_L - w}{I_p} \times 100 \tag{4-21}$$

The physical significance of the consistency index I_c for clays is similar to that of the relative density D_d for sands (Art. 4-6). If the water content of the soil in its natural state corresponds to the plastic limit, a very

dense state, the value of I_c will be 100 per cent. Water contents below the plastic limit will give I_c values higher than 100 per cent. A natural water content corresponding to the liquid limit will give an I_c value of 0 per cent and a still higher natural water content will give negative I_c values.

A reverse relationship is given by the *liquidity index* I_L.

$$I_L = \frac{w - w_p}{I_p} \times 100 \tag{4-22}$$

When $w = w_p$, $I_L = 0$ per cent; when $w = w_L$, $I_L = 100$ per cent.

4-10. The Practical Value and the Limitations of the Tests Described in This Chapter. The relative density D_d of sands indicates the extent to which the natural soil is capable of further increasing its density as a result of heavy loads, shocks, vibration, and other external influences. Thus, the value of D_d gives direct data concerning the stability of the sand in its natural state. The knowledge of this value therefore is of direct practical importance. Its determination in the field can become somewhat complicated (Arts. 11-6 and 12-6).

By comparison, the consistency index I_c, or the liquidity index I_L, of clays can be easily determined. However, this is not usually done as a matter of routine since, taken alone, their values are insufficient to express the actual consistency of the soil in its natural state, because the liquid limit is determined for the completely remolded state of the soil. It can therefore happen that in the case of highly sensitive clays (Art. 7-22) the natural water content of a clay corresponds to its liquid limit, although that clay in its natural state safely carries multistoried buildings.

The liquid and plastic limits are, however, generally determined for all cohesive soils, since they are easily and quickly obtained and are very helpful in the classification of the potential properties of the soil material, which they define better than the grain-size determinations (Art. 3-7). They belong to the so-called *index* or classification tests.

The liquid limit gives a measure of the shearing resistance which a soil has when mixed with water. In other words, it measures the potential true cohesion of a material which, in turn, depends on the total size of the contact areas, *i.e.*, on the fineness and shape of the grains. The finer and flatter the grains of a clay, *i.e.*, the "richer" or "fatter" a clay is, the greater will be the total contact area between grains, and the higher will be the amount of water required to coat the grains. The liquid limit of the clay will therefore also be higher. In other words, one will have to add more water to it to make it flow.

With the admixture of sand or of silt, the clay will become leaner, and its liquid limit will have a lower value. The plastic limit will decrease at

the same time but not so rapidly as the liquid limit, so that the admixture of coarser particles causes a simultaneous decrease of the plasticity index I_p. For sands I_p equals zero.

The plastic limit is strongly affected by organic content, which raises its value without simultaneously raising the liquid limit. Therefore soils
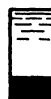
Sands $G = 2.65$	Well graded	$D_d = 100\%$, $w = 21.5\%$	$n = 36.5\%$, $e = 0.57$, $\gamma_{md} = 105.5$, $\gamma'_m = 65.5$	$n = 44.7\%$, $e = 0.81$, $\gamma_{md} = 91.5$ lb per cu ft, $\gamma'_m = 57.0$ lb per cu ft; $D_d = 0\%$, $w = 30.5\%$
	Uniform.	$D_d = 100\%$, $w = 27.2\%$	$n = 41.2\%$, $e = 0.72$, $\gamma_{md} = 96.5$, $\gamma'_m = 60.0$	$n = 48.7\%$, $e = 0.95$, $\gamma_{md} = 85.0$ lb per cu ft, $\gamma'_m = 53.0$ lb per cu ft; $D_d = 0\%$, $w = 35.9\%$
Normal inorganic clays $G = 2.70$	$I_p = 10\%$	$w_p = 25\%$	$n = 40.2\%$, $e = 0.675$, $\gamma_{md} = 100.5$, $\gamma'_m = 63.5$	$n = 48.5\%$, $e = 0.945$, $\gamma_{md} = 86.5$ lb per cu ft, $\gamma'_m = 54.5$ lb per cu ft; $W_L = 35\%$
	$I_p = 20\%$	$w_p = 27\%$	$n = 42.2\%$, $e = 0.730$, $\gamma_{md} = 97.3$, $\gamma'_m = 61.5$	$n = 56.0\%$, $e = 1.270$, $\gamma_{md} = 74.0$ lb per cu ft, $\gamma'_m = 46.8$ lb per cu ft; $W_L = 47\%$
	$I_p = 40\%$	$w_p = 30\%$	$n = 44.7\%$, $e = 0.810$, $\gamma_{md} = 93.0$, $\gamma'_m = 58.5$	$n = 65.4\%$, $e = 1.890$, $\gamma_{md} = 58.2$ lb per cu ft, $\gamma'_m = 36.7$ lb per cu ft; $W_L = 70\%$
	$I_p = 60\%$	$w_p = 35\%$	$n = 48.5\%$, $e = 0.945$, $\gamma_{md} = 86.5$, $\gamma'_m = 54.5$	$n = 72.0$, $e = 2.570$, $\gamma_{md} = 47.0$ lb per cu ft, $\gamma'_m = 29.7$ lb per cu ft; $W_L = 95\%$
Diatomaceous earth $G = 2.65$ $I_p = 0\%$		$w_p = 115\%$	$n = 75.2\%$, $e = 3.05$, $\gamma_{md} = 40.7$, $\gamma'_m = 25.4$	$n = 75.2\%$, $e = 3.05$, $\gamma_{md} = 40.7$ lb per cu ft, $\gamma'_m = 25.4$ lb per cu ft; $W_L = 115\%$
Mexico City clay $I_p = 375\%$		$n = 76.8\%$, $e = 3.31$, $\gamma_{md} = 38.4$, $\gamma'_m = 23.9$; $w_p = 125\%$	$n = 89.5\%$, $e = 8.62$, $\gamma_{md} = 17.2$, $\gamma'_m = 10.7$; $w = 325\%$	$n = 93.0\%$, $e = 13.25$, $\gamma_{md} = 11.6$, $\gamma'_m = 7.3$; $w_L = 500\%$

FIG. 4-9. Examples of density variations of some types of soils.

with organic content have low plasticity indices corresponding to comparatively high liquid limits. This circumstance is used in some classifications of soils (Ref. 66).

Figure 4-9 illustrates the density variations of some types of soils. It should be understood that the figures of that diagram give only the order

of magnitude of the corresponding values, so as *to help in visualizing their* significance, and that minor deviations from these figures are entirely possible. It will be noted from Fig. 4-9 that the range of density variations of sands is relatively small (Figs. 18-8 and 18-9) and of the same order of magnitude as that of lean clays ($I_p < 10$ per cent), but that both the range of density variations and the porosity of possible structures for fat clays increase with increasing values of the plasticity index I_p of a clay. The diatomaceous earth and the Mexico City clay represent special and not too frequent types of soils. The low unit weight, the high
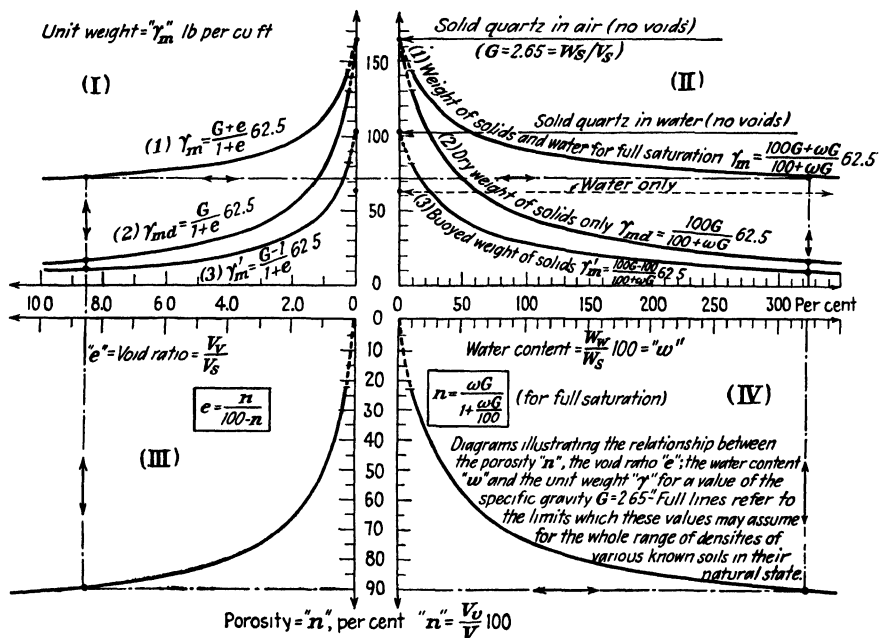
FIG. 4-10.

porosity, and the absence of plasticity of the diatomaceous earth is accounted for by the round shape of the *hollow* silica shells of which it is composed. The Mexico City clay is of volcanic origin. Its high plasticity and porosity are caused by the special properties of the clay minerals of which it is formed. These appear to have an accordionlike structure of scale-shaped particles, somewhat similar to that of bentonites. [The sodium bentonites from Wyoming have liquid-limit values up to 700 per cent. In contact with water they swell and increase their dry volume more than 10 times. They are used commercially as an admixture to granular soils to decrease the permeability (Ref. 6).]

The natural water content and the consistency limits of cohesive soils

can be easily and quickly determined by weighing, drying, and again weighing a soil sample. The dry unit weight (bulk specific gravity) γ_{md} of a cohesive soil can also be easily determined in the field. Here, in addition to the dry weight of a soil specimen, the volume of the space originally occupied by the specimen in the ground has to be determined by one of the methods described in Art. 11-6. On the other hand, calculation of the porosity n and the void ratio e requires knowledge of the volume of solids of a sample, which can be obtained from its weight once the specific gravity G is known. The determination of G has to be performed in a laboratory and requires considerable care. For that reason the porosity n and the void ratio e are used to define the consistency of soils mainly in connection with laboratory investigations, whereas the unit weight, that is, the *dry density* γ_{md} expressed in pounds per cubic foot, is more generally used for field reports of the density of soils. Figure 4-10 gives four charts which illustrate the interrelationship between the void ratio e; the porosity n; the natural water content w; and the dry (γ_{md}), the saturated (γ_m), and the submerged (γ_m') unit weights of soils.

The *centrifuge moisture equivalent* and the *field moisture equivalent* are index tests performed for the purpose of classification of cohesive soils (Ref. 10). They were developed in connection with highway soil problems. They provide information similar to that given by the liquid-limit test, but they are not as universally accepted. For that reason they will not be discussed further in this book.

Practice Problems

4-1. In some old publications the water content is expressed as a percentage w' of the total weight. Derive a relationship between w' and the water content w, conventionally expressed as a percentage of the dry weight [Eq. (4-4)].

Answer:

$$w' = \frac{W_w}{W} \times 100 = \frac{W_w}{W_w \times W_s} \times 100 = \frac{W_w/W_s}{W_w/W_s + 1} \times 100$$
$$= \frac{w/100}{w/100 + 1} \times 100 = \frac{w}{w + 100} \times 100$$

The relationship expressed in the above equation is presented in graphical form in Fig. 4-11.
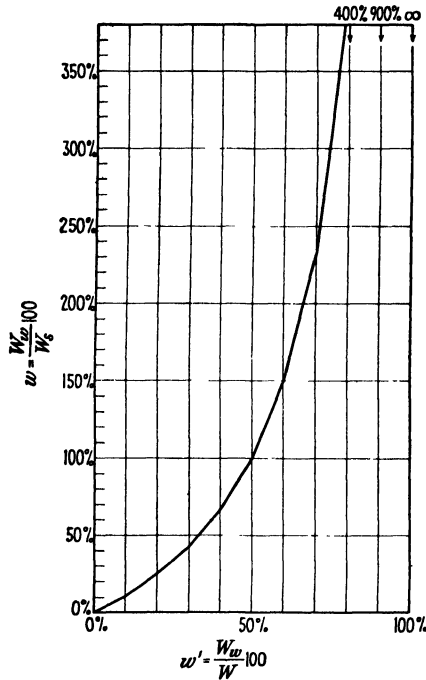
FIG. 4-11. Relationship between the water content w, expressed as a percentage of the dry weight, and the water content w′, expressed as a percentage of the total weight.

4-2. Derive Eq. (4-5), which gives the relationship between the void ratio e, the specific gravity G, and the water content w for full saturation.

Answer:

$$e = \frac{V_v}{V_s} = \frac{W_w/G_w}{W_s/G} = \frac{W_w}{W_s}\frac{G}{1.0} = \frac{w}{100}G \tag{4-5}$$

The relationship expressed by Eq. (4-5) is presented in graphical form in Fig. 4-12.
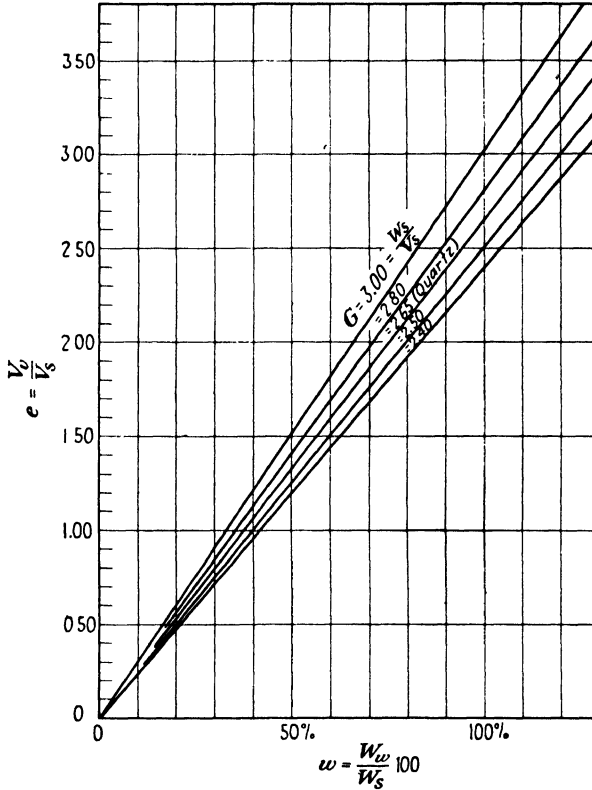
FIG. 4-12. Relationship between the void ratio e and the water content w for full saturation and for limit values of the specific gravity G.

4-3. Present in graphical form the relationship between the void ratio e, the specific gravity G, and the unit dry weight γ_{md}, as expressed by Eqs. (4-6) and (4-10), for $G = 3.0$, $G = 2.65$, and $G = 2.40$.

Answer. See Fig. 4-13. $G = 2.65$ is the specific gravity of quartz, and most inorganic soils have values of G differing by not more than 5 per cent from that of quartz. $G = 3.0$ and $G = 2.4$ represent extreme limit values. It will therefore be noted from Figs. 4-12 and 4-13 that likely deviations of G from 2.65 have only a slight effect on the results.
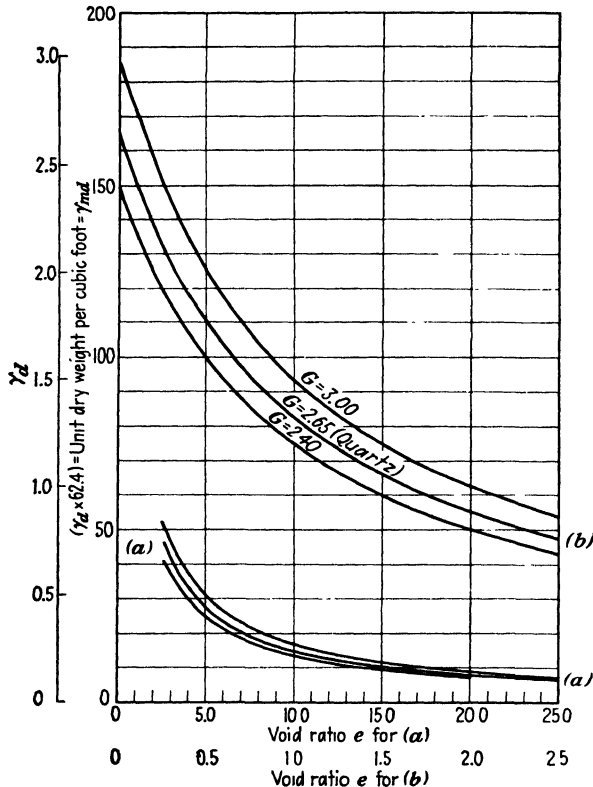
FIG. 4-13. Relationship between the void ratio e and the unit dry weight γ_{md} for limit values of the specific gravity G.

4-4. A clay sample was placed in a glass petri dish marked "37." The total weight of the wet sample plus dish was found to be $A = 72.49$ gm before drying and $B = 61.28$ gm after drying in an electric oven at 105°C for more than 5 hr. The laboratory list gives the weight of the petri dish "37" as $C = 32.54$ gm. A separate test showed that the absolute specific gravity of the solid substance was $G = 2.69$. Assume that the sample was fully saturated with water and compute the water content w, the porosity n, the void ratio e, and the unit weights γ of the soil both in the air and under water.

Answer:

$$W_s = B - C = 61.28 - 32.54 = 28.74 \text{ gm}$$
$$W_w = A - B = 72.49 - 61.28 = \underline{11.21 \text{ gm}}$$
$$W = W_s + W_w = 39.95 \text{ gm}$$

$$w = \frac{W_w}{W_s} \times 100 = \frac{11.21}{28.74} \times 100 = 39.1\%$$

$$V_s = \frac{W_s}{G} = \frac{28.74}{2.69} = 10.68 \text{ cm}^3$$
$$V_v = \frac{W_w}{G_w} = \frac{11.21}{1.00} = \underline{11.21 \text{ cm}^3}$$
$$V = V_s + V_v = 21.89 \text{ cm}^3$$

$$n = \frac{V_v}{V} \times 100 = \frac{11.21}{21.89} \times 100 = 51.3\%$$
$$e = \frac{V_v}{V_s} = \frac{11.21}{10.68} = 1.05$$
$$\gamma = \frac{W}{V} = \frac{39.95}{21.89} = 1.83$$

or

$$\gamma = \frac{G(1 + w/100)}{1 + e} = \frac{2.69(1 + 39.1/100)}{1 + 1.05} = 1.83$$
$$\gamma_d = \frac{W_s}{V} = \frac{28.74}{21.89} = 1.31$$

or

$$\gamma_d = \frac{G}{1 + e} = \frac{2.69}{1 + 1.05} = 1.31$$
$$\gamma' = \frac{W_s - V_s}{V} = \frac{28.74 - 10.68}{21.89} = 0.825$$

or

$$\gamma' = \frac{G - 1}{1 + e} = \frac{2.69 - 1}{1 + 1.05} = 0.825$$

Thus the unit weight of this clay in the air will be $\gamma_m = \gamma \times 62.5 = 114.5$ lb per ft^3, the unit dry weight will be $\gamma_{md} = \gamma_d \times 62.5 = 82.0$ lb per ft^3, and the unit buoyed weight of the submerged clay will be $\gamma_m' = \gamma' \times 62.5 = 51.5$ lb per ft^3.

4-5. Prior to drying, the volume of the sample of clay described in Prob. 4-4 was determined by immersing the sample in mercury and measuring the volume of mercury displaced. It was found to equal $V = 22.31$ cm^3. Compute the air content a_c and the degree of saturation S_r, and indicate the changes which these findings will produce in the values of w, n, and e, and in the unit weights computed in the answer to Prob. 4-4 where the sample was assumed to be fully saturated.

Answer. The volume of air is $V_a = 22.31 - 21.89 = 0.42$ cm^3. The air content is $a_c = (0.42/11.21)100 = 3.7$ per cent. The degree of saturation is

$$S_r = (11.21/11.63)100 = 96.3 \text{ per cent.}$$

The value of the water content w will remain unchanged. The porosity n will be increased to $n = (11.63/22.31)100 = 52.3$ per cent. The void ratio will be increased to $e = 11.63/10.68 = 1.09$. All the unit weights will be increased by $(2.09/2.05)100 = 2.0$ per cent.

4-6. A pat of clay was dried in an oven. Its dry weight was then found: $W_s =$ 11.26 gm. Its volume was determined by immersion in mercury and measurement of the displaced mercury: $V = 5.83$ cm³. A separate test indicated that the specific gravity of the solid substance was $G = 2.67$. Determine the shrinkage limit w_s of that clay.

Answer. The volume of solids is $V_s = 11.26/2.67 = 4.22$ cm³. The volume of voids is $V_v = V - V_s = 5.83 - 4.22 = 1.61$ cm³. The void ratio is $e = 1.61/4.22 = 0.382$. All the voids, as determined above, were still filled with water at the shrinkage limit since no further decrease of volume had occurred, by definition, once the shrinkage limit has been passed as the drying progressed. Therefore, according to Eq. (4-5), $w_s = 100e/G = 38.2/2.67 = 14.3\%$.

4-7. The in-situ volume of a sand sample was determined by one of the methods outlined in Art. 11-6. Its porosity was then found, by the procedure shown in Prob. 9-1, to be $n = 43$ per cent. Compute its relative density D_d for two assumptions: first, that the sand had the limit density values indicated in Fig. 4-9 for well-graded sand; and, second, that it had the limit density values indicated in Fig. 4-9 for uniform sand.

Answer. According to Eq. (4-2), the void ratio corresponding to $n = 43$ per cent is $e = 43/57 = 0.755$. In the case of well-graded sand, according to Eq. (4-16),

$$D_d = \frac{0.810 - 0.755}{0.810 - 0.570} \times 100 = \frac{0.055}{0.240} \times 100 = 22.9\%$$

and in the case of uniform sand

$$D_d = \frac{0.950 - 0.755}{0.950 - 0.720} \times 100 = \frac{0.195}{0.230} \times 100 = 84.7\%$$

Thus a sand with a porosity $n = 43$ per cent would have to be classified as loose (see Table 4-1) if it were well-graded and as dense if it were uniform.

References Recommended for Further Study

"Procedures for Testing Soils," *American Society for Testing Materials*, July 1950, pp. 56–59 liquid-limit determination; pp. 59–61 plastic-limit determination; pp. 66–70 shrinkage-limit determination.

Laboratory Manual in Soil Mechanics, by Raymond F. Dawson, Pitman, 1949, pp. 28–30 plastic-limit determination; pp. 36–39 liquid-limit determination; pp. 40–47 shrinkage-limit determination.

PERMEABILITY OF SOILS. GROUND-WATER MOVEMENTS. FROST ACTION

5-1. The Coefficient of Permeability of Soils. By *permeability* is meant the property of a soil which allows the flow of water through it. Computations of gravitational permeability are based on the *law of*
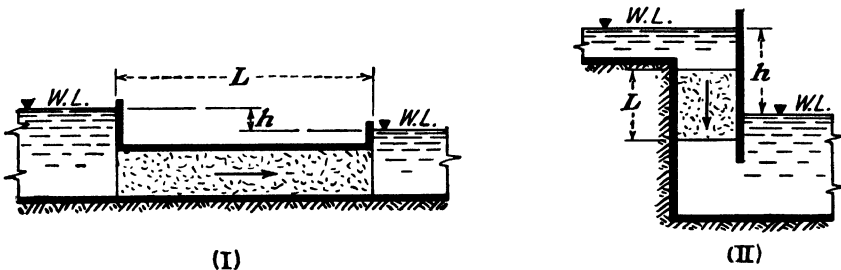
FIG. 5-1. Significance of the term *hydraulic gradient* ($S = h/L$) for (I) horizontal direction of gravitational flow; (II) vertical direction of gravitational flow of water through soils.

Darcy (1856), according to which the velocity of percolation is directly proportional to the hydraulic gradient (see Fig. 5-1).

$$v_p = k_p S \tag{5-1}$$

where v_p = actual velocity of percolating water
k_p = coefficient of percolation, that is, the actual average velocity of flow through the voids of the soil when $S = 1.0$
S = hydraulic gradient = h/L
h = difference between the ground-water levels on either side of a soil layer, that is, the drop of head over the distance L
L = thickness of the soil layer, measured in the direction of the flow

The law of Darcy is valid for laminar flow; no turbulence of flow is possible in most natural soils (Ref. 343), except in coarse sands or gravels of uniform size.

In practical problems it is more convenient to deal with the total cross-

sectional area A of a soil mass, than with the average area of the voids. Accordingly, the *coefficient of permeability* k of a soil is defined as the imaginary average velocity of flow v which will occur under the action of a hydraulic gradient of unity ($S = 1.0$) through the total cross-sectional area (voids + solids) of the soil.

$$v = kS \tag{5-2}$$

The assumption is made that the average area of the voids is directly proportional to the volume of the voids V_v. With reference to Eq. (4-13),
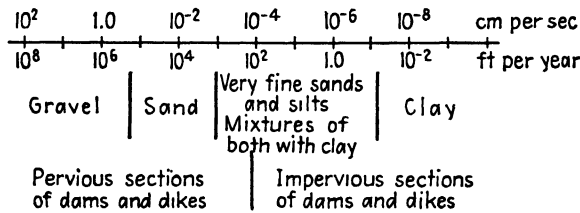
FIG. 5-2. Permeability coefficients *k* of different types of soils. *(After A. Casagrande and R. E. Fadum, Ref. 64, 1940.)*

the following relationship will exist between the coefficient of permeability k and the coefficient of percolation k_p:

$$k = \frac{V_v}{V} k_p = \frac{n}{100} k_p = \frac{e}{1 + e} k_p \tag{5-3}$$

The discharge Q during the time t through a total cross-sectional area of soil A can then be computed from

$$Q = kSAt \tag{5-4}$$

The coefficient of permeability k is expressed in the metric system either in centimeters per minute or in centimeters per second. The latter units have the advantage of providing a simple relationship with English measures.

$$1 \text{ ft per year} = 0.96 \times 10^{-6} \text{ cm per sec} \approx 1.0 \times 10^{-6} \text{ cm per sec} \tag{5-5}$$

Figure 5-2 gives the wide range of the variation of coefficients of permeability k for different types of natural soils.

5-2. Laboratory Methods for the Determination of the Coefficients of Permeability of Soils. The knowledge of the permeability of soils, as expressed by the coefficient k, is of considerable importance for many practical engineering problems, such as the water-retaining capacity of earth dams, the capacity of pumping installations for the lowering of the ground-water level during excavations, and the rate of settlement of buildings.

Two types of apparatus are most frequently used in laboratories for the numerical determination of the permeability coefficients k: the constant-head and falling-head permeameters. They are illustrated in Fig. 5-3. The *falling-head permeameter*, shown in Fig. 5-3(I), is generally used for relatively impervious soils, such as clays, where the discharge is very small. The soil specimen 2, having a cross-sectional area A, is placed between much more porous filter plates 3. The discharge of water Q is measured in a thin glass tube 1 of a small cross-sectional area a. The coefficient of permeability k is computed as follows: During a small
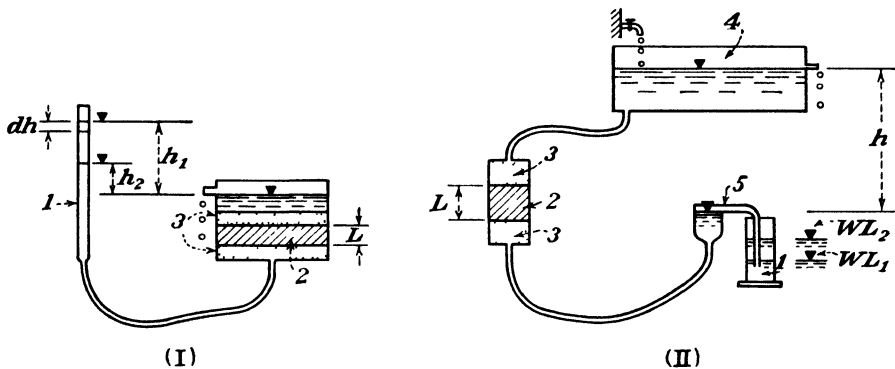
FIG. 5-3. Setup of (I) falling-head permeameter; (II) constant-head permeameter.

interval of time dt the head will decrease by the amount dh. The discharge through the glass tube 1 will then be $(dh\ a)$ and will equal the discharge dQ through the soil sample. With reference to Eq. (5-4), we obtain

$$dQ = -dh\ a = k \frac{h}{L} A\ dt \tag{5-6}$$

or

$$-\frac{dh}{h} = k \frac{A}{La} dt \tag{5-7}$$

The total discharge in the period of time $t = t_2 - t_1$ during which the head decreased from h_1 to h_2 is obtained by integrating Eq. (5-7) between appropriate limits.

$$-\log_e h \Big|_{h_1}^{h_2} = k \frac{A}{La} t \Big|_{t_1}^{t_2}$$

$$k = \frac{La}{A(t_2 - t_1)} \log_e \frac{h_1}{h_2}$$

or

$$k = 2.3 \frac{La}{At} \log_{10} \frac{h_1}{h_2} \tag{5-8}$$

When testing pervious soils, such as sands, it is often advantageous to use a falling-head permeameter of the type illustrated by Fig. 5-4, with $A = a$. For the dimensions shown in Fig. 5-4, Eq. (5-8) is simplified to read (in centimeters per second if t is measured in seconds)

$$k = \frac{16.7}{t} \tag{5-9}$$

The values of the permeability coefficients k are generally reported reduced to a temperature of 20°C. To that end the k values obtained
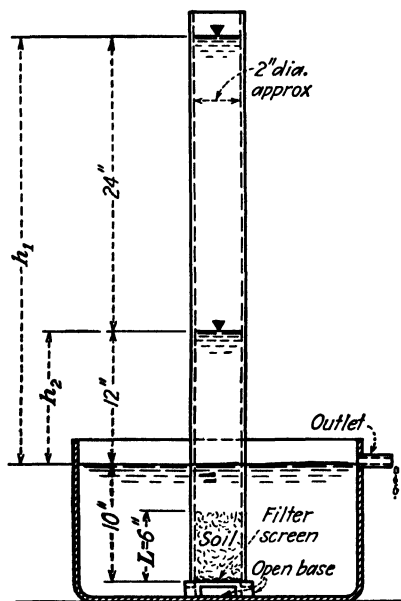
FIG. 5-4. Falling-head permeameter for pervious soils. (*After E. S. Barber, Ref. 10, 1944.*)
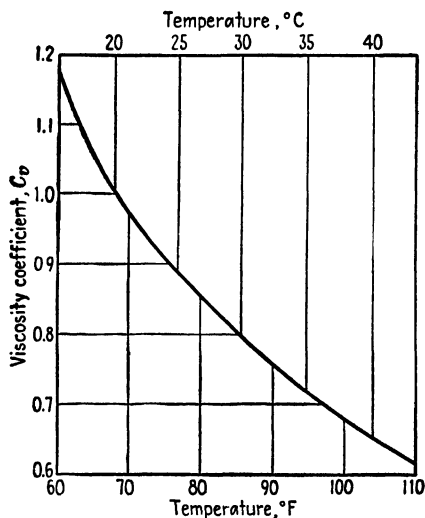
FIG. 5-5. Values of viscosity coefficient C_v.

from Eqs. (5-8) and (5-9) are multiplied by the viscosity coefficient C_v taken from the chart given in Fig. 5-5 and corresponding to the water temperature measured during the performance of the permeability test.

Figure 5-3(II) shows the setup of a *constant-head permeameter*. The water in the reservoir 4 is kept at a constant level. The soil sample 2 of thickness L and cross section A is placed in a container between porous filters 3. The water percolates through the soil to the container 5 with an overflow so disposed that the head h, and therefore the hydraulic gradient S, remain constant. The discharge Q in a given period of time t is measured directly in the container 1, which is graduated for this purpose. Q is determined as the difference between the amount of water contained

at the levels WL_2 and WL_1 corresponding to the time interval $t = t_2 - t_1$. Thus all the data needed for the computation of the permeability coefficient k from Eq. (5-4) are available.

The use of the constant-head permeameter is practicable only for tests with fairly permeable soils, such as sands, where the discharge is considerable. However, even for such soils the use of a falling-head permeameter of the type shown in Fig. 5-4 appears preferable, since the results obtained with the latter are less likely to be unfavorably affected by the formation of air bubbles in connecting pipes, when used as shown in Fig. 5-3(II). The use of deaerated water (Ref. 64) is advisable for accurate measurements.

5-3. Two-dimensional Gravitational Flow of Water through Soils. Flow Nets. The factors which affect the gravitational flow of water through soils can be demonstrated by laboratory seepage experiments. Figure 5-6 illustrates some such experiments performed in the course of undergraduate instruction at the soil mechanics laboratory of Princeton University. Figure 5-6(A) shows the 60- by 24- by 8-in. seepage flume which was used. The front of the flume is of plate glass with a 4-in. square grid of lines painted on its face. The sheet-metal back is perforated at 27 points, marked by small circles on the front view of the flume [Fig. 5-6(A)]. The openings are covered with fine-mesh wire screens. Each opening is connected to a glass standpipe.

An overflow T is provided at one end of the flume to take care of excessive inflow from the faucet R when the outlet faucet U is closed, or when the total discharge through an earth dam in the flume is smaller than the inflow.

When the flume is filled with water only, no soil at all being added, the water in all 27 standpipes will rise to the same elevation, irrespective of the fact that these standpipes are connected to the flume at four different elevations, I, II, III, and IV. One then says that the *head* at all these elevations is the same. Thus a head represents a potential, not a pressure.

Things will be different if we fill the tank with sand. For instance, form an earth dam as shown in Fig. 5-6(C) and (D) and open both faucets R and U to provide constant water levels at the upstream and the downstream faces of the dam, the difference between these two levels being equal to h. It will then be noticed that the water in the standpipes will rise to elevations having intermediate values between those of the upstream and the downstream free-water levels. These elevations are read and written down on a special mimeographed sheet similar to Fig. 5-6(A), each opposite the point marking the corresponding standpipe. Lines of equal head (*equipotential lines*) can then be drawn in between the 27 points at which the head was measured, in a manner similar to the
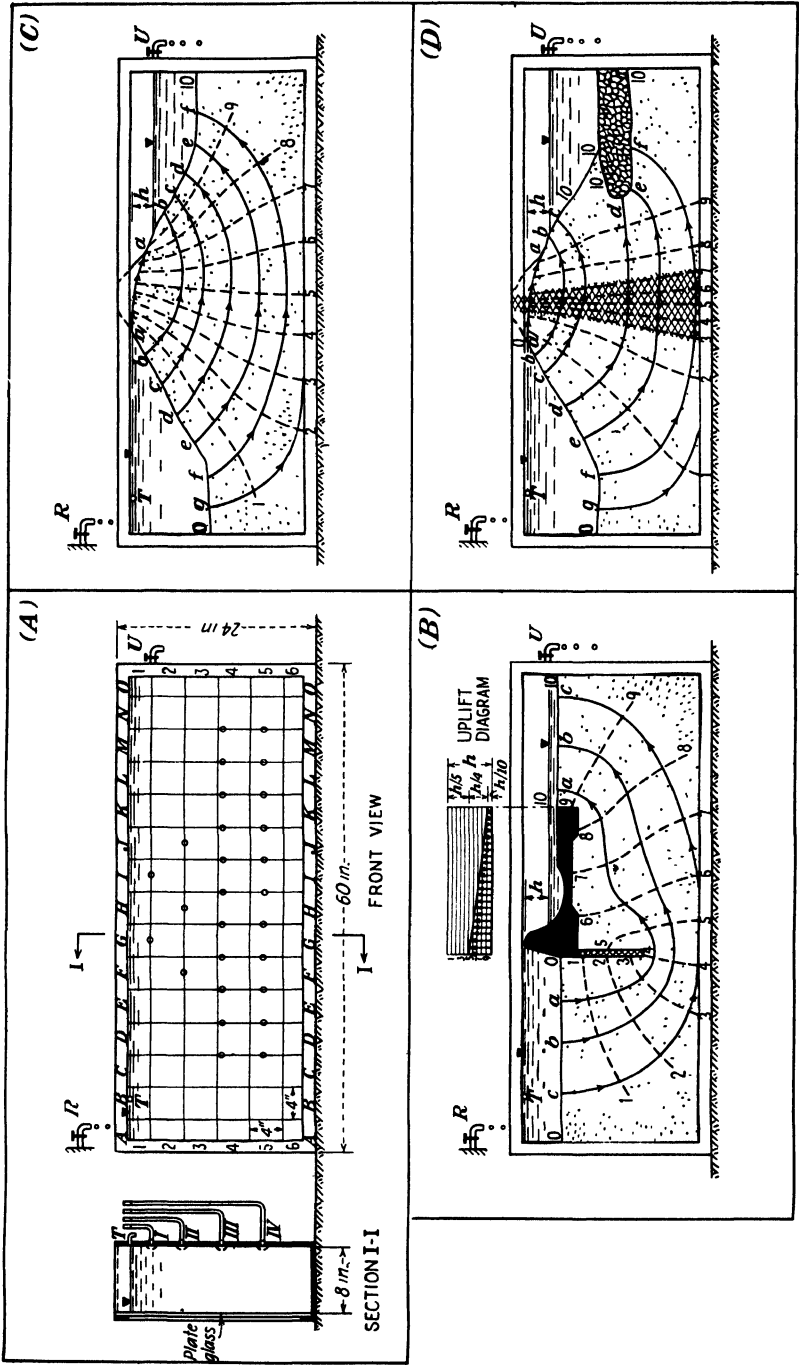
FIG. 5-6. Gravitational flow of water through soils. The general dimensions of flume employed for the laboratory seepage demonstrations are shown in A.

procedure employed when drawing contour lines in land surveying. They are shown by broken lines in Fig. 5-6(*B*), (*C*), and (*D*).

Colored liquid (fluorescein is used as dye) is then allowed to seep into the upstream face of the dam at selected points. A special small tank (not shown in the drawings) is used for the purpose. Several rubber tubes with glass nozzles lead from that tank. Their nozzles are pressed into the sand at the points *a*, *b*, *c*, *d*, *e*, *f*, and *g* on the upstream side next to the glass plate. Clamps fitted to the rubber tubes are loosened so as to release a slight trickle of the fluorescein. A green-colored so-called *flow line* leading from each nozzle can then be observed through the glass side of the flume, as shown by full lines and arrows in Fig. 5-6(*B*), (*C*), and (*D*). The clamps on nozzle *a* have to be loosened more than, for instance, on nozzle *g*, because the velocity of the inflowing water around nozzle *a* is greater than around nozzle *g*. (The head lost in both cases is the same, whereas the path of percolation at *g* is greater, and the hydraulic gradient is therefore smaller there than at *a*.)

The system of interrelated equipotential lines and flow lines is termed a *flow net*. It will be noted that the equipotential lines intersect the flow lines at right angles. This is true because the loss of head, that is, of potential, of seeping water is caused by friction between the moving water and the soil particles and therefore occurs along the lines of flow.

In the flow nets of Fig. 5-6(*B*), (*C*), and (*D*), the total head *h* lost by the percolating water was divided into ten parts, that is, the head lost between each pair of adjacent equipotential lines is equal to $h/10$. The first equipotential line 0-0 coincides with the upstream soil surface, and the last equipotential line 10-10 coincides with the downstream soil surface. It will be noted that when the soil has a uniform composition—for instance, in the case illustrated by Fig. 5-6(*C*), where the dam was built of the same sand throughout—the equipotential lines have a more or less uniform spacing along each flow line. On the other hand, if a less pervious soil is used in parts of the dam—as in Fig. 5-6(*D*), where the central core (shown hatched) was composed of the sand fraction passing the 100-mesh sieve—a greater resistance to flow will be offered by such soil. A greater proportion of the head will therefore be lost within the zone occupied by the less pervious soil. This is indicated by a closer spacing of the equipotential lines. The reverse will be true when part of the soil mass is more pervious, for instance, the gravel filter bed at the toe of the dam shown in Fig. 5-6(*D*). Findings of this kind lead to important practical considerations in the designing of earth dams (Art. 17-5).

Flow nets can be constructed without the help of model seepage experiments. A technique developed by Forchheimer (Ref. 135, 1917) is used for that purpose. Let us consider a section of a flow net represented by

four flow lines 1-1, 2-2, 3-3, and 4-4, as shown in Fig. 5-7. The flow is two-dimensional, so that each flow line remains in the same vertical plane. The distance b between the flow lines 1-1 and 2-2, as well as between the flow lines 3-3 and 4-4, will then remain constant. The discharge Q through the soil enclosed by these four flow lines will also remain constant at all cross sections. This follows from the definition of a flow line as the path followed by a particle of water. Since only nonturbulent laminar flow is considered, none of these paths can intersect another one. The water within the four flow lines shown in Fig. 5-7 behaves essentially
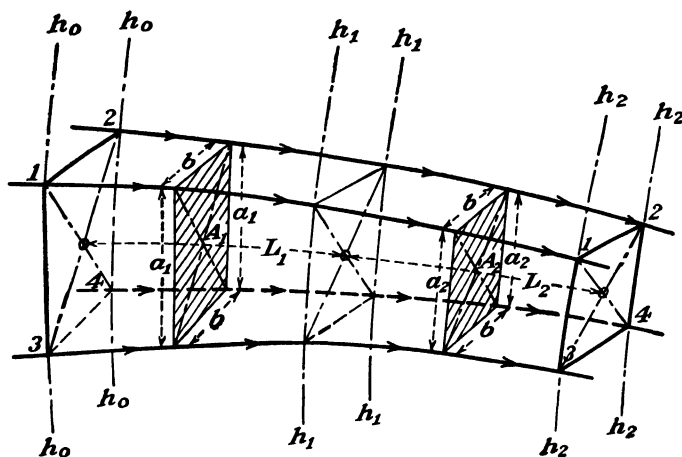
FIG. 5-7. Sketch illustrating the principles of flow-net construction.

as if it were flowing through a pipe limited by these lines. Where the flow lines come closer together, so that the soil cross section bounded by them decreases, the discharge remains the same, but the velocity of flow is increased. Thus the discharge Q_1 through the cross section A_1 must be equal to the discharge Q_2 through the cross section A_2. According to Eq. (5-4),

$$Q_1 = kS_1A_1t = Q_2 = kS_2A_2t \tag{5-10}$$

In a homogeneous soil the coefficient of permeability k will have a constant value throughout. The hydraulic gradients S and the cross sections A will equal

$$S_1 = \frac{h_0 - h_1}{L_1} \quad \text{and} \quad S_2 = \frac{h_1 - h_2}{L_2} \tag{5-11}$$

$$A_1 = a_1b \qquad A_2 = a_2b \tag{5-12}$$

If we decide to draw our equipotential lines in such a way that the drop of head Δh between each pair of adjacent equipotential lines is the same,

then

$$\Delta h = (h_0 - h_1) = (h_1 - h_2) = \text{constant} \tag{5-13}$$

By substituting the values of Eqs. (5-11) to (5-13) in Eq. (5-10) we obtain

$$k \frac{\Delta h}{L_1} a_1 bt = k \frac{\Delta h}{L_2} a_2 bt$$

or

$$\frac{a_1}{L_1} = \frac{a_2}{L_2} \tag{5-14}$$

The physical significance of Eq. (5-14) is that the ratio of the sides of every rectangle of a flow net formed by intersecting flow lines and equipotential lines must have a constant value if the flow net has been drawn correctly. Thus, if one rectangle of a flow net has been drawn as an approximate square with $a_1 = L_1$, then all other rectangles of the flow net must also be approximate squares. This circumstance can be utilized to draw flow nets by a trial and error procedure (see Ref. 343 pp. 161–166). In the case of earth dams the line of saturation has to be determined first; this can be done by means of an approximate method developed by Leo Casagrande (Ref. 69, 1934).

When water flows through soils of different permeability, Eq. (5-10) is simplified to read

$$\frac{k_1 a_1}{L_1} = \frac{k_2 a_2}{L_2} \tag{5-15}$$

Let us assume that the more permeable soil has the permeability coefficient k_1, and that we have begun drawing our flow net in that zone as a system of squares, that is, we have made $a_1 = L_1$. It will then follow from Eq. (5-15) that

$$\frac{a_2}{L_2} = \frac{k_1}{k_2} \tag{5-16}$$

In other words, in the zone of the less permeable soil ($k_2 < k_1$) the flow net will consist of a system of rectangles with the side a_2 being larger than the side L_2 in proportion to the ratio k_1/k_2 of the coefficients of permeability of the two adjoining soil zones. The results of the experiment shown in Fig. 5-6(D) illustrate this point in a general way.

Tridimensional flow involves the use of a variable value b in Eq. (5-10). This complicates the problem to such an extent that graphical solutions become impracticable. An exception is the case of radial flow, which can be treated as a modified two-dimensional flow problem by a method given by D. W. Taylor (Ref. 343, 1948).

5-4. Quicksand and Piping. The loss of head along a flow line occurs because of friction between the water and the soil through which it flows. The soil skeleton resists this friction. So-called *seepage forces*, representing differences of head or potential, are exerted against the soil in the direction in which the water flows. The seepage force J acting against an area A along length L where the loss of head Δh occurs will be

$$J = \Delta h A \gamma_f \tag{5-17}$$

where γ_f is the unit weight of the fluid ($=1.0$ for fresh water, if the metric system is used).

The seepage force j exerted by water per unit of volume of the soil ($A = 1.0$) is

$$j = \frac{\Delta h}{L} \times 1.0 \times 1.0 = S \tag{5-18}$$

where $S = \Delta h/L$ is the hydraulic gradient. In English measures,

$$j = S \times 62.4 \tag{5-19}$$

If a flow line intersects a slope of sand, the seepage force may affect the natural angle of repose α_R (Art. 7-3) of the soil. On the downstream face of a dam the seepage forces j will decrease α_R near the free-water level, since the horizontal components of j along the flow lines *aa* will tend to increase the tangential sliding forces [see Fig. 5-6(C) and (D)]. This circumstance may be partly responsible for the erroneous idea expressed in many old textbooks that the angle of repose of a submerged clean sand is smaller than that of a dry clean sand. Similar conditions are liable to arise after a heavy rainfall on any embankment leading down to a free body of water. The water is seldom clear enough to permit noticing from the bank that, under such conditions, the angle of repose of the sand deeper down is greater than at the water level.

Water flowing into a slope, for instance, on the upstream face of a dam, exerts a stabilizing influence, since the seepage forces increase the tangential resisting forces to sliding. This circumstance is utilized to facilitate cuts in rock-flour types of fine-grained soils with little cohesion by means of suitably located wellpoints with or without electro-osmosis (Arts. 5-6 and 14-9).

In some cases, for instance, on the inner faces of some types of cofferdams [Fig. 16-35(I)], water will flow vertically upward at right angles to the excavation surface if the cofferdam is pumped out. The seepage forces j will then be also directed upward and will be resisted by the unit weight γ_m' of the buoyed sand. According to Eqs. (5-19), (4-9), and (4-11), at limit equilibrium

$$j = S_{cr} \times 62.4 = \frac{G-1}{1+e} \times 62.4 \tag{5-20}$$

so that the critical hydraulic gradient which corresponds to this limit equilibrium is

$$S_{cr} = \frac{G-1}{1+e} \tag{5-21}$$

The absolute specific gravity G of quartz sands is 2.65 and, according to Fig. 4-9, the void ratio e of some naturally deposited sands may vary between the values of 0.57 and 0.95. With these values we obtain from Eq. (5-21) for the loosest possible state of submerged sand $S_{cr} = 0.85$, and for the densest state $S_{cr} = 1.05$. An approximate average value of the critical hydraulic gradient can be taken to equal unity. The corresponding void ratio is then $e = 0.65$ and, according to Eq. (4-3), the porosity $n = 39.3$ per cent.

The significance of the critical hydraulic gradient can be demonstrated in the laboratory with the help of a device illustrated in Figs. 5-8 and 5-9, which give its vertical cross section. It is a metal box, 1 by 1 by 1 ft, with a glass window on one side. Water can flow into the bottom of the box when the stopcock C is opened. A porous filter plate A is located an inch or so above the bottom of the box. The space above that filter plate can be filled with sand almost up to the overflow level. The standpipe B is connected to the free space below the filter plate.

As soon as the stopcock C is opened, water will start to flow vertically upward through the filter plate and the sand. It will be noticed then that the water level in the standpipe B will rise above the free-water level in the box by a height h, which will increase with the velocity of the flow as the stopcock C is opened wider. This height h therefore represents the loss of head of the flowing water due to friction against the solid skeleton of the filter plate and of the sand above it. The flow lines—of which ten, a to j, are shown in Fig. 5-8—are all directed vertically upward. The equipotential lines, by their very nature, have to intersect the flow lines at right angles and, in this case, are therefore horizontal. If we draw the equipotential lines in such a way that the distance between them represents the same value of lost head Δh = constant, the number of equipotential lines will increase with the hydraulic gradient $S = h/L$ as the stopcock C is opened wider. Their spacing ΔL will decrease correspondingly. Thus, as shown in Fig. 5-8, if the equipotential lines $0'$-$0'$ to $3'$-$3'$ correspond to the loss of head h, a greater loss of head with increasing velocity of flow will produce a closer spaced system of equipotential lines, for instance 0-0 to 10-10 as shown.

Finally, a critical condition will be reached when the entire sand mass

will begin to *boil,* it becomes *quick,* as it is loosened up and held in suspension by the upward-flowing water. This is the condition expressed by Eq. (5-21) and $S_{cr} = \Delta h/\Delta L_{cr}$. In this quick condition the sand loses its supporting power; any object placed on the sand surface will sink into it if its unit weight is greater than the unit weight of the fluid sand-water mixture. It should be noted, however, that the placing of a solid object on the sand surface modifies the entire pattern of the flow net (see Fig. 5-9 and compare to Fig. 5-8). Visible boiling of the sand will begin around

FIG. 5-8. Laboratory demonstration of quicksand action.

the edges of the solid object *W*. This is caused by the greater local velocity of flow, as indicated by the more closely spaced flow lines deflected by the object from their original path.

Similarly, it has been observed on underdesigned cofferdams in the field that a quick condition usually begins to develop at their inside corners (Ref. 429), where the concentration of flow lines is greatest.

In the laboratory the direction of the flow can be reversed (Fig. 5-8) by connecting the stopcock *C* to the waste and opening it. It will then be observed that the water level in the standpipe *B* will drop below the free-water level in the box. The value of this *negative head* $-h$ will increase with the escape velocity of the water through the stopcock *C*. The direction of the seepage forces is now reversed, and their effect is added to the effect of gravity. Thus they will have a tendency to slightly compact the soil and to increase its shearing strength.

The preceding discussion shows that any sand can become a *quicksand* and remain continuously in that condition so long as a flow of water and a critical hydraulic gradient have been developed and are maintained by pumping during inadequately planned construction operations (Art. 14-9), or by special drainage conditions, such as under improperly designed dams built on a bed of sand (Art. 17-7). Thus a quicksand is *not* a type of material but a condition thereof which can be prevented by appropriate measures. A special condition may arise in uncompacted, loosely deposited, fully saturated sands, the loose grain structure of which may
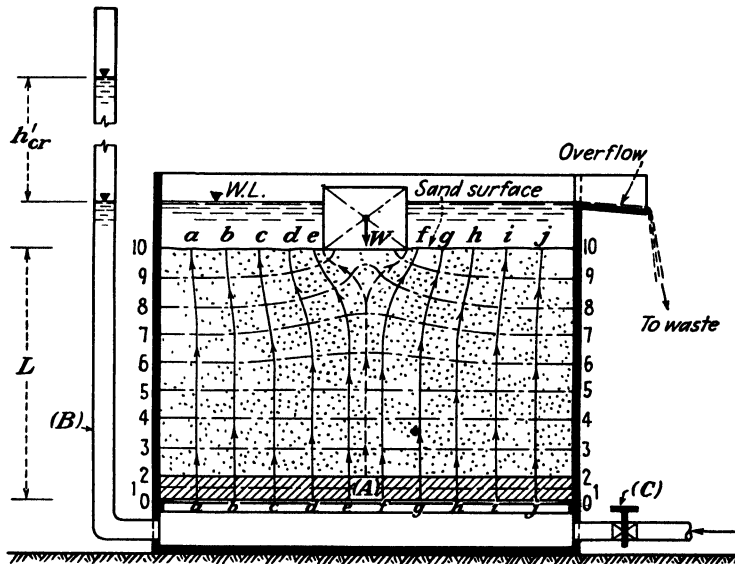
FIG. 5-9. Laboratory demonstration of localized quicksand action.

collapse as a result of a sudden shock, so that the whole mass may be momentarily liquefied, that is, become momentarily quick, with unpleasant consequences (see Arts. 7-16 and 8-11). Some uncompacted, very fine, uniformly loose sands may be particularly susceptible to such momentary liquefaction. Shearing stresses imposed by construction operations may favor momentary liquefaction in all loose, fully saturated sands.

A special type of a localized quick condition is provided by so-called *piping*, where a stream formed by a liquefied sand-water mixture moves through surrounding stable sand as if it were flowing through a pipe. Figure 5-10 illustrates a laboratory demonstration of that effect in the seepage flume shown in Fig. 5-6(A). A temporary vertical partition was placed across the flume. It had, at a quarter of its height above the
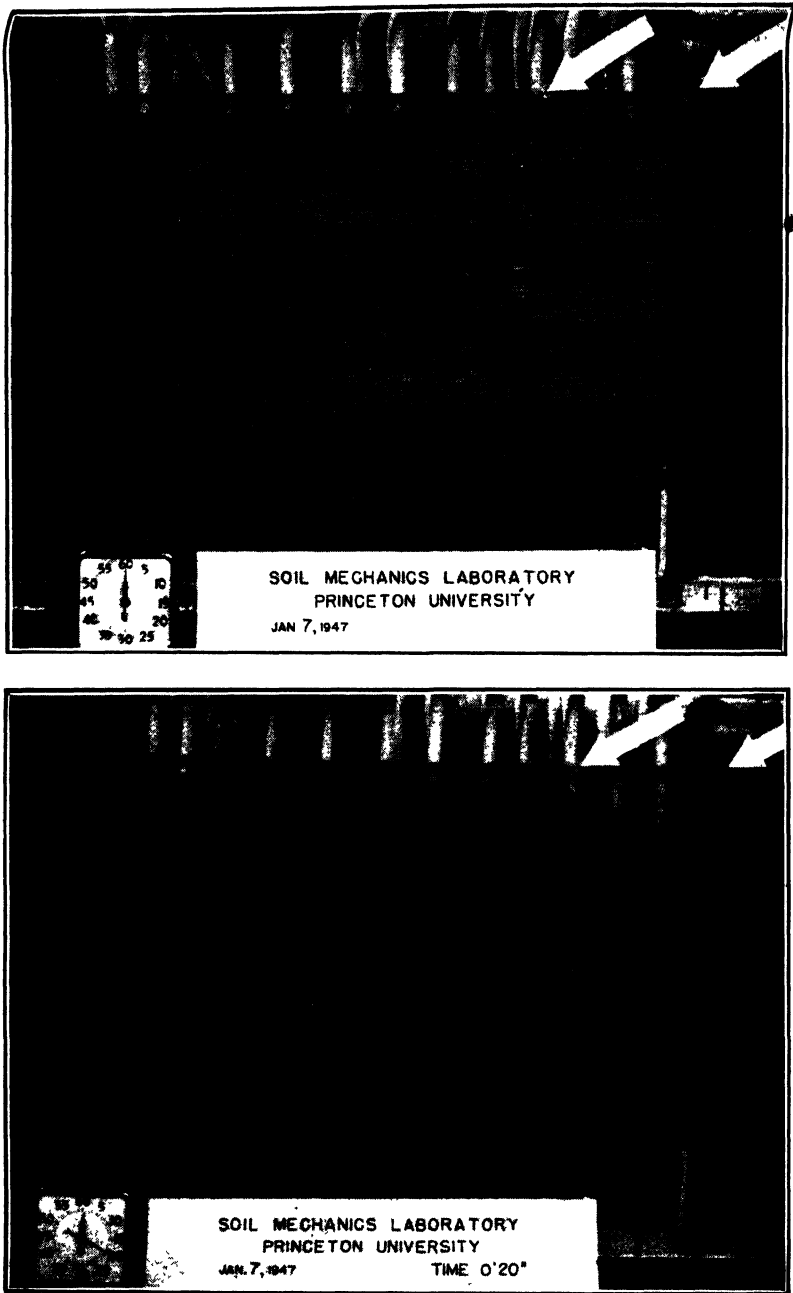
FIG. 5-10. Laboratory demonstration of the formation of a vertical "pipe" during the escape of submerged sand backfill through a small opening in a model sheet-pile retaining structure.

bottom, a small (2-in. diameter) semicircular hole next to the plate-glass side of the flume. The hole was plugged with a removable stopper, and the flume was filled with fine beach sand on one side of the partition. Artificially colored, black sand was placed in horizontal layers at 2-in. elevation intervals. The photographs in Fig. 5-10 show the setup after completed filling. The two white arrows indicate the water level, which was the same on both sides of the partition. When the stopper was removed, and sand began to trickle out laterally through the hole, a column of sand immediately above the hole appeared to be liquefied and was set into downward motion as if it were moving along a pipe. A crater was formed at the surface. Its slope corresponded to the natural angle of repose. The sand rolled down along that slope toward the "pipe," which had almost vertical walls. The lateral pressure exerted by the heavy fluid sand-water mixture must therefore have been sufficient to keep the surrounding sand in place by counterbalancing its active lateral pressure. The latter, of course, must have been relatively small because of arching phenomena around the fluid "pipe," similar to those likely to occur around shafts (Art. 10-16).

5-5. Field Methods of Determining the Permeability of Soils. The correct estimation of the amount of water discharged into an excavation depends on the permeability of the soil and acquires considerable practical importance in sand soils, where that amount may be considerable and may influence the selection of the type of pumping installation to be employed. Permeability tests on sand samples in the laboratory cannot give fully reliable results, partly because it is extremely difficult to obtain an undisturbed sample of noncohesive soil from a bore hole without appreciably changing its density (Art. 12-7). For that reason such permeability tests have to be performed for the densest and for the loosest possible states of the sand sample, where the coefficient of permeability for the loosest condition may be seven or ten times greater than for the densest condition. Further, many sand deposits are stratified and have permeabilities which vary in the vertical and in the horizontal directions, the latter usually having a somewhat higher value.

This situation has prompted attempts to determine the permeability of sandy soils by trial pumping from bore holes (Ref. 305) or from wells (Ref. 343). In the latter case water-level observations have to be made in at least two other adjoining wells. Opinions, however, are divided as to the reliability of such procedures (Ref. 365). Frequently it becomes necessary to rely on the experience of specialized firms who have to a certain extent correlated their pumping data from past jobs with the grain-size curves of the surrounding soil (see Art. 14-9).

In some cases, when the size and importance of the construction

project justified the expense, more extensive preliminary investigations have been undertaken. For instance, when large canals had to be cut through very pervious ground, it sometimes became necessary to determine the magnitude of possible undesirable seepage losses. These were then measured, after deduction of evaporation losses, from specially built experimental basins. Several such basins were sometimes provided, each with a different type of lining. Supplementary water-level check measurements were made in a system of adjoining control wells.

5-6. Nongravitational Flow of Water. Electro-osmosis and Thermo-osmosis. Effect of Vegetation. The most commonly known form of nongravitational flow of water through soils is caused by capillary attraction. It has been explained in Art. 4-8 that this phenomenon is due to the affinity of water to most soils and the ability of water to resist surface tension.

Another but less well known form of nongravitational water movement is the flow which is caused by differences of temperature within a soil layer, known by the general name of *thermo-osmosis*. It has been demonstrated by Bouyoucous (Ref. 37, 1915) that the affinity of water to soil increases with decreasing temperature. This accounts for the observed migration of water from a warmer section of a soil layer to a colder one. Such migration of water in a fluid phase is sometimes accompanied by condensation of water vapor in the air-filled voids of colder sections of not fully saturated soil layers.

A closely related phenomenon is *electro-osmosis*. It was shown as early as 1808 by Reuss (Ref. 288) that the application of an electric potential will produce water movement in a capillary tube. Since then the theory of such movement has been developed by a number of investigators. The water migrates from the anode (+) to the cathode (−). Winterkorn (Ref. 441, 1947), by his experiments at Princeton University, has shown the direct interrelationship which exists between electro-osmotic and thermo-osmotic phenomena. Water moving through soil under the influence of a thermic potential creates thereby an electric potential. Daily and seasonal temperature variations which fluctuate through the soil, starting from its surface, must therefore be accompanied by corresponding electrical waves. Leo Casagrande (Ref. 70, 1947) has shown that a brittle structure of certain remolded clays may be recreated by electrical currents. Studies of these phenomena may therefore lead to a better understanding of the factors which influence the formation of clay structures (Art. 4-1).

Electro-osmosis has found direct practical application in facilitating excavation work through otherwise unstable rock-flour types of soils

(Art. 14-9). Thermo-osmosis is closely related to the frost-heaving phenomena discussed in Art. 5-7.

Water movements may be caused seasonally by growing vegetation and produce volume changes in surface clay layers detrimental to shallow foundations of buildings and roads. The spread of roots and the depth of their penetration vary with the type of tree, the type of soil, and the intensity of summer rainfall. W. H. Ward (Ref. 421, 1948), in his analysis of extensive damage to buildings with shallow foundations on heavy clays in England, points out that the average root spread of trees approximately equals the height of the tree, and that the roots sometimes reach down to a depth of 10 ft. During dry spells trees and shrubs will absorb moisture from the soil around their roots. If the soil is heavy clay, uneven shrinkage may result in the zone of root penetration, accompanied by differential settlements of any shallow foundations founded within that zone. Damage is likely to be considerable when only part of the foundation rests on the zone of root penetration.

5-7. Frost Heaving of Soils. Observations have shown that the surface of frozen soil layers is liable to heave under certain conditions. Heaves of 10 in. and more have been recorded. The main factors which influence the heaving have been found to be:

1. Presence of a free-water table below the depth of frost penetration at a distance H (see Fig. 5-11), when that distance is smaller than the height of capillary rise H_{max} [Eq. (4-19)]
2. The value of the height of capillary rise H_{max}
3. The permeability of the soil
4. The duration of the frost

Excavations in frozen soil which heaved have disclosed the presence of lenses or layers of solid ice, as shown in Fig. 5-11. This indicated that the heaving was caused not just by an expansion of water during freezing, but by a steady growth of the ice crystals as a result of the continuous capillary migration of water from the free-water table into the frozen zone (Art. 5-6). The ice lenses grew in size with time when the frost continued.

Clean sands are not subject to frost heaving because of their negligible height of capillary rise. Clays are liable to heave only when the frost lasts for a long time. Although clays have a considerable height of capillary rise, their permeability is so low that only little additional water can be supplied through them by capillarity to the frost zone. The most dangerous type of frost-heaving soils are the silts, which have intermediate values of the height of capillary rise and of permeability, thus allowing the rapid growth of ice layers. Sands with such a high silt con-

tent that all the spaces between the sand grains are filled with silt are likely to heave as if they were silts.

The danger of frost heaving exists not only when there is a continuous water table within a silt layer underlying a structure such as a road. Particularly dangerous are cases when the silt forms pockets penetrating into a clay layer on a slope. Percolating rain water can then accumulate in these pockets and later cause irregular frost heaving.
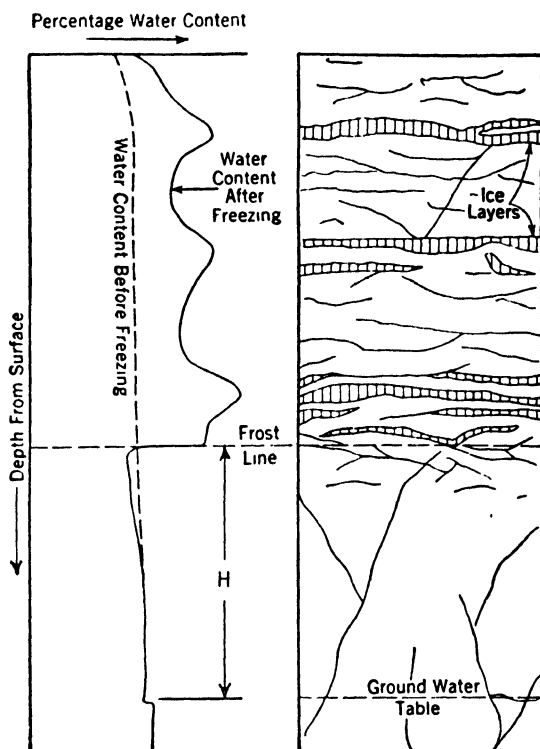
FIG. 5-11. Increase in the water content of a frozen soil layer located close to the ground-water table. (*After G. Beskow, Ref. 23, 1935, and J. O. Osterberg, Ref. 254, 1935.*)

The irregularity in the heaving of a frozen soil surface is the main cause of damages to structures. The second cause is the excessive accumulation of water and the resulting softening of the ground near the soil surface after the thawing of the ice lenses in the spring. Damages can be avoided by the measures outlined in Art. 14-11 for buildings and in Art. 19-6 for highways.

Special civil engineering problems arise in the so-called *permafrost* regions of the far north, where at a certain depth below the soil surface the ground remains eternally frozen (see Arts. 14-11 and 19-7).

Practice Problems

5-1. A falling-head permeameter test was performed on a clay sample in the device illustrated in Figs. 5-3(I) and 6-2. The diameter of the sample was 2.5 in. (A = 31.7 cm²), and its thickness L was 1.0 in. = 2.5 cm. At the start of the test the water in the 1.7 mm inner diameter (a = 0.0227 cm²) glass-tube standpipe was at an elevation h_1 = 32 cm. Six minutes thirty-five seconds later (t = 395 sec) it dropped to h_2 = 30 cm. Compute the coefficient of permeability of the clay.

Answer:

$$\begin{aligned} \log_{10} 32 &= 1.50515 \\ \log_{10} 30 &= 1.47712 \\ \hline \log_{10} (h_1/h_2) &= 0.02803 \end{aligned}$$

According to Eq. (5-8),

$$k = 2.3 \frac{2.54 \times 0.0227}{31.7 \times 395} \times 0.02803 = 2.97 \times 10^{-7} \text{ cm per sec}$$

5-2. A proposed weir on sandy soil, similar to the one illustrated in Fig. 5-6(B) but somewhat shorter, was analyzed with respect to safety against the development of a quick condition at its downstream end. A flow net was drawn to a suitably large scale, and a section of its downstream part is given in Fig. 5-12(I). The relevant dimensions were measured to scale on the flow net and were found to be L_1 = 1.56 ft and a_1 = 1.60 ft. The total difference of head between the upstream and downstream water levels was h = 25 ft; the head lost between the equipotential lines 9-9 and 10-10 was $\Delta h = {}^{25}\!/_{10}$ = 2.5 ft. It was then decided to place a clay blanket on the sand surface behind the weir to some distance upstream of it. The resistance to flow offered by that clay blanket absorbed a large portion of the total head h. A new flow net was drawn to take into account this new condition, and Fig. 5-12(II) shows the resulting changes in the section of the downstream part which is being examined. It was found that the distance between the flow lines bb and cc had not changed, remaining $a_2 = a_1$ = 1.60 ft, but the distance L_2 increased to 3.65 ft.

Assuming that the sand has a porosity n = 35 per cent (void ratio e = 0.54), compute the factors of safety against the development of a quick condition in the two cases illustrated by Fig. 5-12.
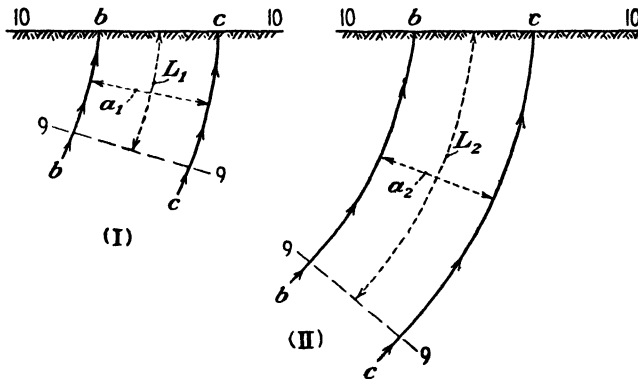
FIG. 5-12.

Answer. The critical hydraulic gradient will be [Eq. (5-21)]

$$S_{cr} = \frac{2.65 - 1}{1 + 0.54} = 1.07$$

The actual hydraulic gradient in the case illustrated by Fig. 5-12(I) will be $S_1 = \Delta h/L_1 = 2.50/1.56 = 1.6$, and the corresponding factor of safety $F_1 = S_{cr}/S_1 = 1.07/1.60 = 0.67$. Thus failure will occur.

In the case illustrated by Fig. 5-12(II) $S_2 = \Delta h/L_2 = 2.50/3.65 = 0.685$, and the factor of safety $F_2 = S_{cr}/S_2 = 1.07/0.685 = 1.57$.

5-3. What will be the discharge per square foot of downstream sand surface area between the flow lines *bb* and *cc* in the case illustrated by Fig. 5-12(II) if the permeability coefficient of the sand is $k = 2 \times 10^{-2}$ cm per sec $= 2 \times 10^4$ ft per year?

Answer. According to Eq. (5-4),

$$Q = 2 \times 10^4 \times 0.685 \times 1.0 \times 1.0 = 13{,}700 \text{ ft}^3 \text{ per year}$$

References Recommended for Further Study

Ground Water, by Cyrus F. Tolman, McGraw-Hill, 1937, 593 pp. Geological aspects of ground-water problems.

Hydraulic Structures, translated from German by A. Schoklitsch, American Society of Mechanical Engineers, Vol. I, pp. 167–197, 1937. Ground-water flow to wells.

"Seepage through Dams," by A. Casagrande, *Journal of the Boston Society of Civil Engineers*, June, 1937. Also *Contributions to Soil Mechanics*, Boston Society of Civil Engineers, 1925–1940, pp. 295–337. Procedures for the construction of flow nets.

Soil Freezing and Frost Heaving, by Gunnar Beskow, translated from Swedish by J. O. Osterberg, Northwestern University, 1947, 145 pp. Experimental and theoretical studies and Swedish highway experiences.

"Fundamental Similarities between Electro-osmotic and Thermo-osmotic Phenomena," by Hans F. Winterkorn, *Proceedings, Highway Research Board*, Washington, D.C., 1947, pp. 443–455. Basic theory of the subject.

Fundamentals of Soil Mechanics, by Donald W. Taylor, Wiley, 1948, Chap. 9, pp. 156–207. Flow net construction, including radial flow.

"Electro-osmosis in Soils," by Leo Casagrande, *Geotechnique*, London, Vol. 1, No. 3, pp. 159–177, June, 1949. Experimental and theoretical data.

CHAPTER 6

THE CONSOLIDATION OF SOILS

6-1. The Process of Consolidation. Neutral and Effective Stresses. The compression of a soil occurs mainly as a function of a decrease of the volume of the voids. By comparison, the component of compression produced by a decrease of the volume of the grains of the solid skeleton is quite negligible. Therefore, if the voids of a soil are entirely filled with water, measurable compression can occur only as a result of the escape of excess water from the voids. Gradual compression of a soil under such conditions, when induced by static forces of gravity, such as the weight of the soil itself or of structures erected upon it, is termed *consolidation.* It is *not* synonymous with *compaction* (Art. 11-1), which is the artificial compression of a soil by mechanical means.

If a saturated soil is quite pervious, for instance if it is a clean sand, its consolidation under newly applied static loads will be almost instantaneous, since excess water has no difficulty in escaping from the voids. On the other hand, if the saturated soil is a clay with low permeability, its consolidation will be quite slow, since any excess water in the voids will take time to be squeezed out toward pervious boundaries of the clay layer.

When a load is applied to a fully saturated cohesive soil in its plastic range of consistency (Art. 4-7), the entire compressive stress p created by the load is at first carried by the water in the voids. It is then said that $p = u$, where u is the stress in the water which resulted from the application of the pressure p. The stress u is termed *neutral stress.* Other terms frequently used to designate the stress u are *hydrostatic excess pressure* or *excess pore pressure.*

As time goes by, some water is squeezed out of the clay and escapes through the pervious boundaries of the clay mass where such pervious boundaries are available. The decrease of the volume of the voids of a fully saturated clay corresponds to the amount of water squeezed out. As a result of this process, the solid grains of the soil skeleton are brought into closer contact with each other and consequently take up some of the newly applied load. The stresses thus created in the soil skeleton are

termed *effective stresses* f_e. Any decrease of the neutral stresses of the water in the voids must correspond to an equal increase of the effective stresses in the solid skeleton, and vice versa. The sum of the effective stresses f_e and the neutral stresses u at any point and at all times must remain constant and equal to the applied pressure p.

$$p = u + f_e \tag{6-1}$$

When all the pressure p has been transferred to the soil skeleton so that $p = f_e$, the neutral stress or excess pore pressure u becomes equal to zero.
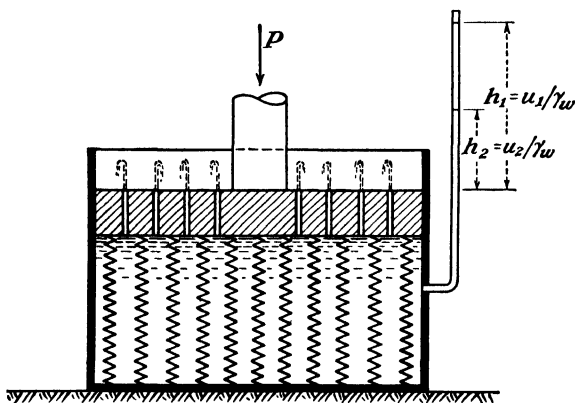
FIG. 6-1. Model of the type used by Terzaghi, Ref. 350, 1927, to explain by analogy the process of consolidation of a saturated clay.

Further expulsion of water from the voids and, hence, further compression of the clay will then cease. The consolidation has reached 100 per cent of its final value. Intermediate stages in this process can be defined by the *percentage of consolidation*

$$U = \frac{S}{S_2} \times 100 \tag{6-2}$$

where S = linear change of length of a soil specimen or settlement of a layer during one-dimensional vertical consolidation at the consolidation stage to be defined

S_2 = linear compression or settlement at the final stage of consolidation

The process of consolidation can be visualized better with the help of the model shown in Fig. 6-1 which Terzaghi used to explain his theory. The sketch shows a cylinder filled with a liquid. A piston fits into the cylinder and is supported by a system of springs which simulates the action of the solid soil skeleton. The piston is provided with a number of small openings through which the liquid can escape if a load P is applied

to the piston. The amount of resistance offered to the load P by the liquid and the rate of the decrease of that resistance are functions of the rate at which the water can escape through the openings and, hence, are also functions, of the diameter of these openings. If the diameter of the openings is made smaller, the rate of the escape of water will decrease. (This principle has been applied for many years in hydraulic shock absorbers in artillery guns.) As the water escapes through the openings, the piston moves downward under the action of the external load P. The springs compress as a result and offer progressively increasing resistance as the downward movement continues. The pressure $u = \gamma_w h$ on the water decreases at the same time, and the level h of the water in the standpipe shown in Fig. 6-1 drops correspondingly. The downward movement and the expulsion of water will stop when the resistance of the compressed springs will equal the external load P, and u and h will then be equal to zero.

A rigorous mathematical solution of the process of consolidation was first published by Terzaghi in 1923 (Ref. 347, see also Art. 6-7). Terzaghi thus became the founder of the new science of *soil mechanics*, which differs from the conventional mechanics of solids by the predominant influence which is exercised on the mechanical properties of soils by the water in the voids of the soil. The time factor becomes all important in this connection. The development of soil mechanics permitted insight into the causes of the long duration of the settlements of structures erected on deep saturated clay deposits, which sometimes last for many years. In addition, insight into the process of consolidation permitted the improved understanding of the variable shearing strength of soils, which was found to increase with the pressures transmitted from grain to grain of the solid soil skeleton, that is, with the so-called intergranular pressures or effective stresses. On the other hand, pressures carried by the water in the voids did not contribute to the increase of the shearing strength of a soil—hence the name "neutral stresses."

6-2. Laboratory Equipment for Consolidation Testing. Laboratory consolidation testing is now generally performed in apparatus of a type designed by Arthur Casagrande, one of the several existing modifications of which is illustrated in Fig. 6-2. An undisturbed clay sample is carefully and tightly fitted into a massive brass ring 1. Special cutting tools are used for this very delicate operation which requires considerable skill and experience for its successful performance. The ring 1 with the clay sample in it is fitted into a brass base 2 and is clamped to the latter by means of a brass cover plate 4 and six screws 5, a rubber gasket 3 providing a watertight joint. The ring 8 is placed on top of the ring 1, and the joint sealed with putty, so that some free water can be maintained

over the surface of the sample to prevent drying due to evaporation. The lower porous filter plate 6 and the underlying channel cavities of the base 2 are filled with water prior to the fitting of the sample into the ring 1. The load P is applied through a yoke 10, a brass plate 9, and an upper porous filter plate 7. The compression of the clay sample is measured by a dial extensometer 11 reading to 1/10,000 in.

The diameter of the ring 1 usually varies from 2.5 to 3.0 in., its height from 1.0 to 0.75 in. A smaller apparatus is sometimes employed, but its use cannot be recommended, since the effect of any disturbances at the
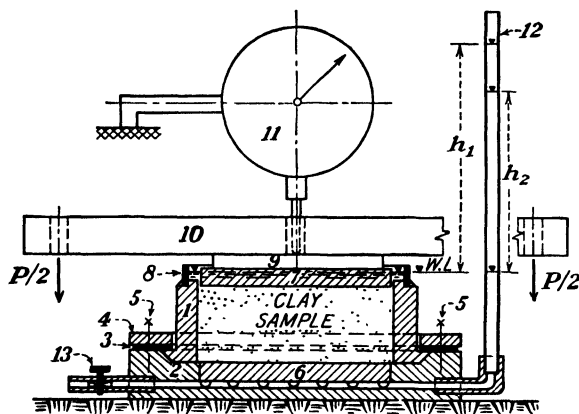
FIG. 6-2. The Casagrande type of consolidometer for combined compressibility and permeability tests.

boundaries of the sample during its cutting down to shape and fitting into the ring then becomes too great. Any economy in the possible use of smaller sized samplers (Art. 12-7) for smaller sized consolidation apparatus is only imaginary, since the results of the tests become highly questionable.

The glass standpipe 12 shown in Fig. 6-2 can be filled with water through the stopcock 13 for the performance of falling-head permeability tests (see Art. 5-2 and Prob. 5-1).

A simplified type of consolidometer, shown in Fig. 6-3, is sometimes employed. The clay sample is fitted into a light thin metal ring 1 and is laid on top of a porous filter stone 3 inside a container 2. The ring 1 hangs on the clay specimen, hence the name *floating-ring* consolidometer. This type of device therefore cannot be used with good results for testing of very soft clays. Also it does not permit the performance of direct permeability tests, so that the coefficient of permeability has to be determined indirectly by computation from the time-compression curve (Art. 6-9). Thus, although this type of device has the advantage of low cost,

it should be employed mainly as an accessory for purely routine testing of clays.

Emphasis has been placed in the preceding description on the use of *clay* samples for consolidation tests. This is so mainly because no satisfactory methods have yet been developed for the extraction of really undisturbed samples of noncohesive soils, such as sands, from bore holes (Art. 12-7). There is therefore, as a rule, no point in any routine testing of their consolidation characteristics, which are greatly affected and modified by any disturbance. It should further be noted that consolidation tests are performed on fully saturated clays. The limitation has
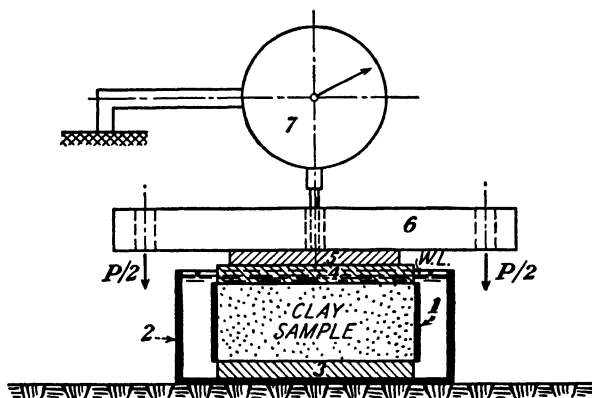
FIG. 6-3. Floating-ring type of consolidometer.

little practical importance, since it is mainly fully saturated clays which create difficulties to engineers in the field because of their compressibility. Dry clays are apt to deform much less under loading, although they may cause other types of engineering trouble, such as irregular swelling when wetted (Art. 14-11).

Further, the compressibility of sands, as opposed to the compressibility of clays, is affected much more strongly by vibratory and by slow repetitional loading than by static loading (Art. 18-4).

The consolidation test is sometimes termed a *compression test with confined lateral expansion.* The height of the test sample should be kept small in respect to its diameter, so as to decrease the effect of friction between the clay and the sides of the enclosing metal ring.

6-3. The Consolidation Testing of Undisturbed and of Disturbed Clays. The load is applied to a clay sample during a standard-type consolidation test in increments, where each increment is equal to the previous total load. Thus, for instance, if the first load applied produces a compressive stress of 0.20 ton per ft^2, successive increments of load should raise the stress to 0.40, 0.80, 1.60, 3.20, 6.40 tons per ft^2 and so on, if

necessary. Sometimes a sequence of 0.25, 0.50, 1.00, 2.00, 4.00, 8.00 tons per ft² is preferred. The reasons which prompt this doubling of load are explained in Art. 6-5.

Each increment of load is allowed to consolidate the clay sample for at least 24 hr. In that time most types of clay can be expected to consolidate fully when the sample thickness equals 1 in. A careful continuous record is kept of the compression of the sample during each increment, as shown in Fig. 6-10, Art. 6-9. The final accumulated compression of the
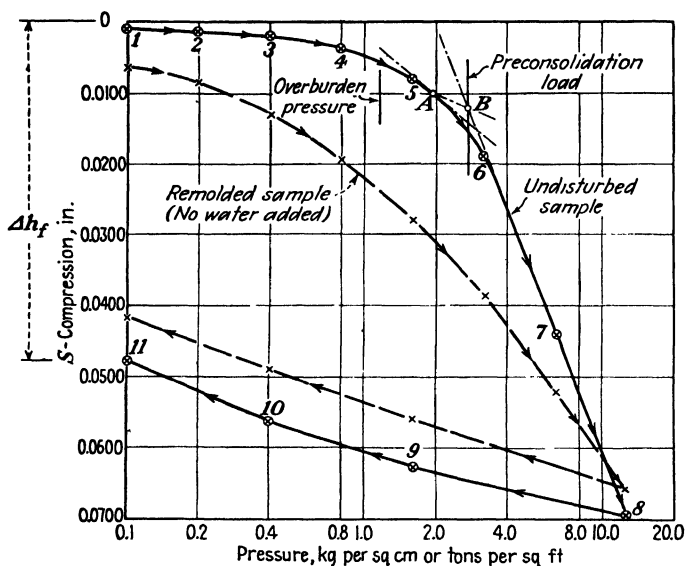
FIG. 6-4. Records of the total (accumulated) compression of clay samples during consolidation tests.

sample at the end of its consolidation period after each increment of loading is then plotted to a semilogarithmic scale, as shown in Fig. 6-4. The points 1 to 8 indicate the total compression obtained during loading of an undisturbed clay sample, and the points 9 to 11 the reduction of the total compression due to expansion during unloading. It should be noted that the clay sample should be allowed to expand for at least 24 hr after each increment of unloading, since the expansion can fully develop only as a result of absorption of water, the rate of the absorption depending on factors similar to those which govern the rate of water expulsion during the compression of the sample (Art. 6-7).

After completed unloading the clay sample is removed from the apparatus and its water content is determined by weighing, drying, and weighing again. The volumes of the solid matter and of the water can then be expressed in terms of the corresponding fractions of the height of the sam-

ple. If the dry weight of the solid is found to be W_s in grams, its specific gravity is G, and the horizontal cross-sectional area of the clay sample within the consolidometer ring is A in square centimeters, then the height h_s in inches of the solid will be

$$h_s = \frac{W_s}{AG \times 2.54} \tag{6-3}$$

Similarly, the height h_{w2} in inches of the water in the sample at the end
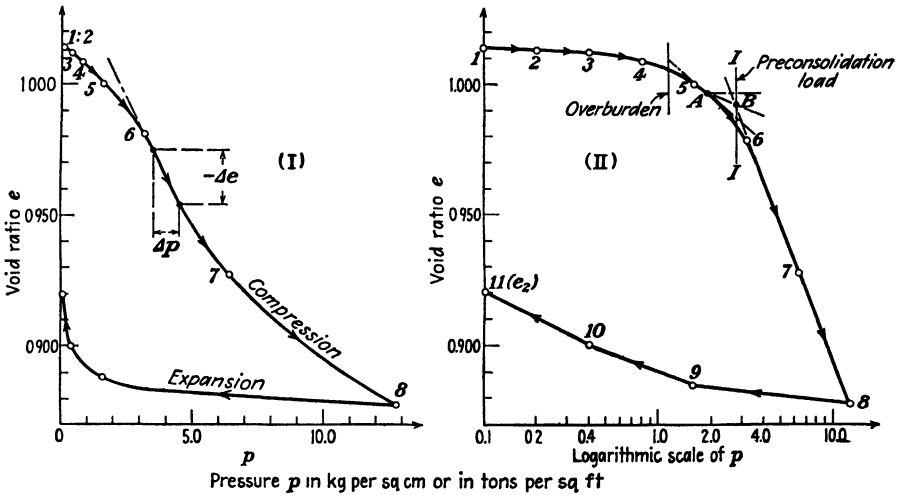
FIG. 6-5. Void ratio–pressure curves of an undisturbed sample of clay (computed from the data given in Fig. 6-4).

of the test will be

$$h_{w2} = \frac{W_{w2}}{A \times 1.00 \times 2.54} \tag{6-4}$$

The following relationship should hold for a fully saturated sample (see Fig. 6-8):

$$H_1 = h_s + h_{w2} + \Delta h_f \tag{6-5}$$

where H_1 = initial height of sample (can be taken as equal to the height of the consolidometer ring 1 in Figs. 6-2 and 6-3)

Δh_f = residual compression after end of test (see Fig. 6-4)

The area A of the sample remains constant during all stages of the test. Therefore the void ratio can be expressed as a ratio of heights instead of volumes.

$$e = \frac{V_v}{V_s} = \frac{h_v A}{h_s A} = \frac{h_v}{h_s} \tag{6-6}$$

and the void ratio at the end of the test is then

$$e_2 = \frac{h_{w2}}{h_s} \qquad (6\text{-}7)$$

The value of e_2 can be plotted as the point 11 of the void ratio–pressure curve, as shown in Fig. 6-5. The subsequent points 10, 9, . . . , 1 of that curve can then be plotted after computing the void-ratio changes Δe for each load decrement or increment.

FIG. 6-6. Void ratio–pressure curve of a disturbed clay sample remolded under addition of water.

$$\Delta e = \frac{\Delta h}{h_s} \qquad (6\text{-}8)$$

where Δh is the total expansion or compression registered by the dial gage for each load stage. The values of Δe are then successively subtracted from e_2 to give the points 10, 9, and 8 of the expansion branch of the void ratio–pressure curve, as shown in Fig. 6-5. The subsequent values of Δe for the compression branch of the void ratio–pressure curve are then successively added to the void-ratio value given by the point 8 in Fig. 6-5, and the points 7, 6, 5, 4, 3, 2, and 1 are obtained in this manner.

6-4. Effect of Preconsolidation on the Compressibility of Clays.

If a clay sample is completely remolded under addition of water up to and above the liquid limit and is then subjected to a consolidation test, its void ratio–pressure curve will be a straight line when plotted to a semilogarithmic scale (see points 1, 2, and 3 in Fig. 6-6). This branch of the curve is sometimes termed the *virgin compression curve* (Ref. 61), since it presumably represents the compression of a naturally deposited clay mass under its own weight. If the load is then removed in specified decrements, points 4, 5, and 6 will be obtained. A second application of the load will produce the curve through points 6, 7, 8, and 9. The continuation of the loading beyond the pressures reached during the first loading will give a straight line parallel to the virgin curve for the void ratio–pressure curve at point 10.

The shape of the recompression curve through points 6 to 10 of Fig. 6-6 is very similar to the shape of the first loading curve of an undisturbed sample of a naturally deposited clay, shown by points 1 and 8 in Fig. 6-5(II).

This circumstance and subsequent comparative tests of the type illustrated by Fig. 6-6 have led Arthur Casagrande (Ref. 61, 1932) to propose an empirical method for the graphical determination of the so-called *preconsolidation load*, that is, the determination of the greatest pressure under which the clay sample had been consolidated during its past geological history. The method is illustrated in Fig. 6-7. A tangent KH is drawn at the point of greatest curvature A of the void ratio–pressure curve. A line AC is drawn so that it bisects the angle formed by the tangent AH and the horizontal line AG. The straight section DE of the void ratio–pressure curve is extended to its intersection at the point B with the line AC. A vertical line I-I through the point B will indicate the pressure corresponding to the preconsolidation load.
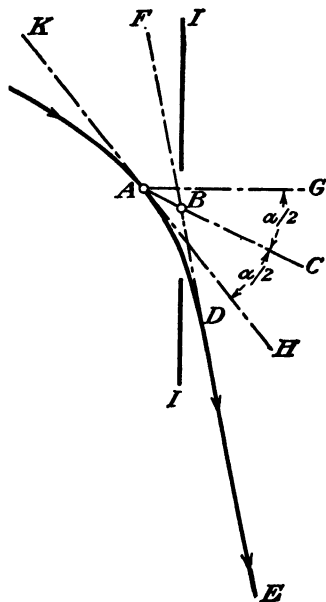
FIG. 6-7. Enlarged section of Figs. 6-5(II) and 6-6, illustrating a method of determining the preconsolidation load. (After A. Casagrande and R. E. Fadum, Ref. 64, 1940.)

Most of the early studies of this type were performed on marine and other naturally consolidated clays which had not been subjected to drying. In such clays the preconsolidation load, when determined by the procedure shown in Fig. 6-7, closely corresponded to the weight of the overburden, that is, to the weight of the soil layers above the sample tested. When the preconsolidation load exceeded the weight of the present overburden, it could usually be shown that the excess corresponded to the weight of soil layers which had been removed by erosion during the preceding ages or to the weight of glaciers which had pressed down on the soil surface during past glaciations (Ref. 61). Later studies have, however, shown that even much more pronounced increases of the preconsolidation load could be attributed to the compressive forces which act on the soil skeleton during drying (Art. 4-8). Thus Tschebotarioff (Ref. 369, 1936) found that some clays of the Nile Valley in Egypt had been precompressed, presumably by repeated drying, to over 9.0 tons per ft^2, whereas the overburden load was only 3.0 tons per ft^2. Similar results have been reported from Texas and other localities.

New investigations show that high values of the preconsolidation load may be attributed to the action of chemicals. A recent silty clay deposit in salt water, studied by Tschebotarioff (Ref. 395, 1946), samples of which had never been subjected to drying or to any overburden load in excess of 0.45 ton per ft^2, nevertheless had a preconsolidation load of 5.70 tons per ft^2. This and other unusual properties of this soil could be attributed to chemical action (Art. 11-8).

Remolding of the clay specimen—even if only partial, for instance that due to a slight disturbance during sampling—is liable to lower the preconsolidation load because of the resulting decreased curvature of the void ratio–pressure curve (see Fig. 6-4). Thus, if a laboratory test shows that the preconsolidation load is smaller than the present overburden, this will not necessarily mean that the consolidation of the soil has not yet been fully completed.

The preceding discussion is intended as a warning against the uncritical attaching of undue importance to the practical significance of laboratory values of preconsolidation loads. Their importance has been exaggerated in the past.

6-5. Effect of the Rate of Application of the Load. It has been stated in Art. 6-3 that during a standard consolidation test each successive increment of load is applied instantaneously and is made equal to the total previous load. In some soils smaller increments of load, and a correspondingly large number thereof, are liable to decrease the amount of final compression. This is presumably due to special characteristics of the *bond* between the individual soil particles. This bond appears to be a function of time and of the load, so that when the load is applied very slowly, the strength of the soil skeleton has time to increase and to offer greater resistance to the next increment of load than would be the case if a large increment of the load was applied suddenly (see Art. 4-1).

A similar explanation is offered for a phenomenon which was first extensively discussed by Terzaghi (Ref. 359, 1941). In a homogeneous, fully submerged deep layer of naturally deposited clay one would expect the water content to decrease with depth if the natural layer follows the same laws as a clay sample during a standard type of laboratory test. Nevertheless it has been repeatedly found that the water content of such natural homogeneous deposits remains constant throughout the depth, with the exception of any surface-dried crust. It appears probable that during the very slow natural formation of the deposit the bond between the clay particles had time to increase and to keep pace with the increase of load due to the addition of the weight of new layers of soil.

Attempts to reproduce this condition in the laboratory were only partially successful. Some soils showed a gain of strength and a decrease

of compressibility when the duration of the consolidation test was increased to the extent feasible under laboratory conditions; other soils did not.

It is customary at present to perform laboratory consolidation tests at the rate given in Art. 6-3. This is liable to give overly safe results (see Art. 13-7).

6-6. The Coefficient of Compressibility and the Modulus of Volume Change. The degree of compressibility of a soil is sometimes expressed by the *compressibility coefficient* a_v.

$$a_v = \frac{-\Delta e}{\Delta p} \times 10^{-3} \qquad \text{cm}^2 \text{ per gm} \tag{6-9}$$

In the Eq. (6-9) Δp is given in kilograms per square centimeter $\approx$ tons per square feet. It will be seen from Fig. 6-5(I) that the coefficient a_v repre-
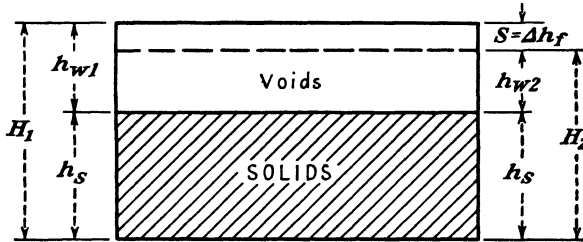
FIG. 6-8. Diagram illustrating computations of the settlement S of a fully saturated clay subjected to compression.

sents the slope of the void ratio–pressure curve. It is given in square centimeters per gram for reasons explained in Art. 6-7.

With reference to Fig. 6-8, the total compression or *settlement* S is

$$S = h_{w1} - h_{w2} = \frac{h_{w1} - h_{w2}}{h_s + h_{w1}} H_1 = \frac{h_{w1}/h_s - h_{w2}/h_s}{1 + h_{w1}/h_s} H_1$$

$$= \frac{e_1 - e_2}{1 + e_1} H_1 = \frac{\Delta e}{1 + e_1} H_1 = \frac{a_v}{1 + e_1} \Delta p \, H_1 \times 10^3 \tag{6-10}$$

Another coefficient, the *modulus of volume change* m_v, is frequently used.

$$m_v = \frac{a_v}{1 + e_1} \qquad \text{cm}^2 \text{ per gm} \tag{6-11}$$

For practical purposes, when estimating settlements, it is more convenient to take the modulus of volume change m_v in square centimeters per kilogram, so that

$$m_v' = m_v \times 10^3 \tag{6-12}$$

and

$$m_v' = \frac{S}{\Delta p\, H_1} \qquad \text{cm}^2 \text{ per kg or ft}^2 \text{ per ton} \qquad (6\text{-}13)$$

Thus the coefficient m_v' has the apparent form of the reciprocal of the Young modulus E and can sometimes be interchanged with it (see Prob. 9-1). Such a substitution should, however, be limited by the consideration that the Young modulus E is conventionally applied to elastic deformations only, whereas the modulus of volume change usually is so computed that it includes both elastic and plastic deformations in addition to the deformations induced by consolidation.

The modulus m_v' represents the final compression in meters of a layer 1 m thick, under an average pressure throughout the depth of that layer 1 kg per cm². The numerical values of this coefficient remain unchanged if both S and H_1 are expressed in feet (or in inches) and Δp in tons per square foot (1 ton per ft² is approximately, within 3 per cent, equal to 1 kg per cm²). The use of this modulus (the symbol X was employed at the time, instead of m_v') was proposed by Tschebotarioff (Ref. 369, 1936) in connection with settlement studies of buildings in Egypt, since it permits the *direct* comparison of compressibility values computed from individual laboratory consolidation tests to the average value computed from observed settlements of full-scale structures in the field. The use of this coefficient has the further practical advantage that it can be computed at any stage of the laboratory consolidation test, without waiting for the water-content and void-ratio determination at the end of the test, directly from the dial readings and Eq. (6-13). The original thickness of the sample H_1 has to be estimated, but the error caused by this approximation does not exceed some 5 per cent. The gain in time which is achieved by this procedure is, however, by no means negligible for cases of rush design jobs when preliminary settlement estimations are needed in a hurry, since a consolidation test may take up to two weeks to complete.

The range of possible variations in the compressibility of different types of soils and the comparison between laboratory values of the coefficient m_v' and values obtained in the field are given in Art. 13-7.

6-7. Terzaghi's Rate-of-consolidation Theory. The publication by Terzaghi (Ref. 347, 1923) of a theory which gave a rigorous solution of the problems concerned with the rate of consolidation of clay layers permitted the development of the modern science of soil mechanics, since the pore-water pressures treated by that theory influenced many other important phenomena, such as the shearing strength of clays. The general outline of Terzaghi's theory follows.

Let us consider a clay layer of the thickness $2H$ (see Fig. 6-9) which is

sandwiched between two pervious sand layers and is stressed by a surface unit load p. Under the influence of this load the clay layer will begin to compress as the excess of the water from its pores is squeezed out toward the two pervious boundaries provided by the sand layers. If the clay is homogeneous, excess pore water from the upper half of the layer, that is, above its center plane 0-0, will flow toward the upper sand layer, whereas
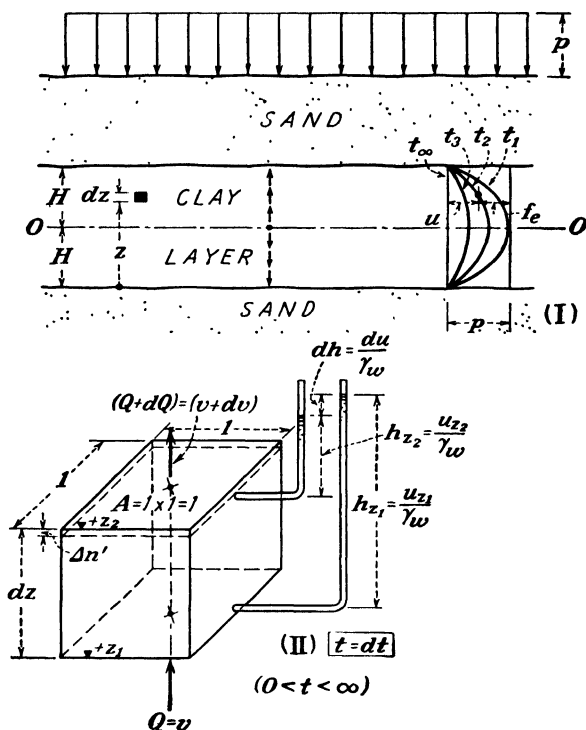
FIG. 6-9. The one-dimensional consolidation of a clay layer and some of the factors which affect its rate.

the excess pore water from the lower half of the layer will flow toward the lower sand layer, as indicated by arrows in Fig. 6-9(I).

Equation (6-1) ($p = u + f_e$) must remain valid at all times and at all points of the clay layer. This is illustrated by the diagram in Fig. 6-9(I). At the moment the load is applied (t_0) all of the pressure p is carried by the pore water, so that $p = u$. This gives a straight line in the diagram. A few instants later, however, water will start escaping into the sand, so that the pore pressures u at both pervious boundaries will equal zero at all times. As time goes by, the line of demarcation over the depth of the layer between the excess pore pressures u and the effective stresses f_e will

be successively indicated by the curves t_1, t_2, and t_3. The slope of these curves at any point indicates the rate of change of u with depth at a given time. This change of u along the depth of the layer represents the hydraulic gradient S upon which depends the velocity v of the expulsion of the excess water from the voids. After a certain period of time (t_∞) consolidation will be complete, and the excess pore pressures will equal zero ($u = 0; p = f_e$), as indicated by the straight line in the diagram.

This process of consolidation will now be analyzed further in respect to a small prism of clay from the upper half of the layer. The prism has a horizontal cross-sectional area equal to unity and a height dz; it is drawn to a large scale in Fig. 6-9(II). Let us assume that two imaginary piezometer tubes (standpipes) have been connected with the pores of the clay in the prism, one of the standpipes at the upper edge and the other at the lower edge of the prism. Since water is flowing in the upward direction, there must be a drop of head in the direction of the flow, and the water in the lower standpipe will rise to a higher elevation. The drop of head dh over the height of the prism is related at a given time to the decrease in the pore-water pressure ∂u over the same distance.

$$dh = \frac{du}{\gamma_w} \tag{6-14}$$

In the Eq. (6-14) γ_w is the unit weight of water. The hydraulic gradient S, by definition [Eq. (5-1)], is the drop of head over a given distance, so that

$$S = -\frac{\partial h}{\partial z} \tag{6-15}$$

or, substituting from Eq. (6-14),

$$S = -\frac{1}{\gamma_w}\frac{\partial u}{\partial z} \tag{6-16}$$

According to the law of Darcy [Eq. (5-2)], the velocity of the flow of excess pore water through the voids at a given time will be $v = kS$. Inserting the value of S from Eq. (6-16), we obtain

$$v = kS = -\frac{k}{\gamma_w}\frac{\partial u}{\partial z} \tag{6-17}$$

The rate of change of the velocity v over the distance dz (at a given time interval dt) is obtained by differentiation from Eq. (6-17).

$$\frac{\partial v}{\partial z} = -\frac{k}{\gamma_w}\frac{\partial^2 u}{\partial z^2} \tag{6-18}$$

Equation (5-4) can be rewritten to read

$$v = \frac{Q}{At} \tag{6-19}$$

and, since the horizontal cross-sectional area A of the prism shown in Fig. 6-9 has been taken to equal unity, it follows from Eq. (6-19) that in a time interval dt the velocity v, as given by Eq. (6-17), will represent the amount of water Q which will flow into the lower face of the prism during that time interval, after having been squeezed out from the underlying clay layers above the elevation 0-0. It also follows that the increment of velocity dv gained over the distance dz (height of the prism) during the same time interval dt will equal the amount of water dQ by which the discharge at the upper face of the prism has been increased by comparison with the inflow Q into its lower face. In other words, dv and dQ represent the amount of water which has been squeezed out of the prism during that time interval. Any expulsion of water from the voids of a fully saturated clay prism must naturally be accompanied by a corresponding decrease Δn of its pore space, as defined by its porosity n (or n'), so that during the same time interval dt

$$-\frac{\partial n'}{\partial t} = \frac{\partial v}{\partial z} \tag{6-20}$$

For purposes of this analysis it will be more convenient to express the porosity as a fraction and not as a percentage, that is, to work with a value $n' = n/100$. With this in mind, and with reference to Eqs. (4-3), (6-9), and (6-11), we can relate $\Delta n'$ to the compressibility coefficient a_v and to the modulus of volume change m_v by writing

$$\Delta n' = \frac{\Delta e}{1+e} = \frac{a_v \, \Delta p}{1+e} = m_v \, \Delta p \tag{6-21}$$

In the above equation, as well as in all other equations of this article, a_v and m_v should be given in square centimeters per gram and the pressures p, u, and f_e in grams per square centimeters. This follows from Eq. (6-14) if h is to be expressed in centimeters and γ_w in grams per cubic centimeter. (1 cm³ of water weighs approximately 1 gm.)

Since the decrease $\Delta n'$ of the pore space is completed when the pressure p is fully carried by the grains of the soil skeleton ($p = f_e$), Eq. (6-21) can be modified to read

$$\frac{\partial n'}{\partial t} = -\frac{\partial f_e}{\partial t} m_v \tag{6-22}$$

During the process of consolidation under a constant unit load p, according to Eq. (6-1), any increase of the effective stress f_e over an

interval of time dt must equal the decrease of the neutral stress u during the same time interval, that is,

$$\frac{\partial u}{\partial t} = -\frac{\partial f_e}{\partial t} \tag{6-23}$$

Combining Eqs. (6-23) and (6-22) we obtain

$$\frac{\partial n'}{\partial t} = \frac{\partial u}{\partial t} m_v \tag{6-24}$$

From Eqs. (6-24), (6-20), and (6-18) we have

$$\frac{\partial u}{\partial t} = \frac{k}{m_v \gamma_w} \frac{\partial^2 u}{\partial z^2} \tag{6-25}$$

or

$$\frac{\partial u}{\partial t} = c_v \frac{\partial^2 u}{\partial z^2} \tag{6-26}$$

This eq uation relates the rate of change of the excess pore pressure u in respect to time to the amount of water which is squeezed out of the voids of a clay prism during the same time interval [Eq. (6-18)].

c_v is the *coefficient of consolidation.*

$$c_v = \frac{k}{m_v \gamma_w} \tag{6-27}$$

The units of c_v are square centimeters per minute if the coefficient of permeability k is given in centimeters per minute.

By deriving the differential equation (6-26) Terzaghi (Ref. 347, 1923) solved the problem, since that equation is analogous to the one which had already been studied in thermodynamics in connection with the rate of heat transfer from a flat plate. The solution of equations of this type is obtained by means of the Fourier series and takes the following form for the boundary conditions illustrated by Fig. 6-9(I):

$$u = p \frac{4}{\pi} \sum_{N=0}^{N=\infty} \frac{1}{2N+1} \left[\sin \frac{(2N+1)\pi z}{2H} \right] e^{-(2N+1)^2 \pi^2 T/4} \tag{6-28}$$

In this equation N is any integer, p is the applied pressure which causes consolidation, z and H are the vertical distances shown in Fig. 6-9(I), e is the base of the natural (Napierian) logarithms, and T is a dimensionless number called the *time factor.*

$$T = \frac{c_v t}{H^2} \tag{6-29}$$

where t = time which elapses until the excess pore pressure u drops to the value defined by Eq. (6-28)

c_v = coefficient of consolidation, as defined by Eq. (6-27)

For any given time t the variation with the depth z of the excess pore pressure u can be computed from Eq. (6-28), expressed as a fraction of the applied consolidation pressure p, and then plotted as shown by the curves t_1, t_2, and t_3 of Fig. 6-9(I).

The percentage of consolidation U_z at a given depth z and time t will equal

$$U_z = \frac{p - u}{p} \times 100 = \left(1 - \frac{u}{p}\right) 100 \tag{6-30}$$

The percentage of consolidation U for the entire layer at a given time t is taken as the average of the U_z values over the full depth $2H$. Since the terms *percentage of consolidation* and *percentage of settlement* are synonymous for the case illustrated by Fig. 6-9(I), the above definition of U is in agreement with Eq. (6-2).

The dimensionless time factor T [Eq. (6-29)] can be related to the average percentage of consolidation U of the entire layer by means of Eqs. (6-28) and (6-30). This relationship is presented graphically by the curve T_p in Fig. 6-11. It should be noted that Eq. (6-29) corresponds only to the boundary and loading conditions illustrated in Fig. 6-9. Different boundary and loading conditions, for instance those for the case of expulsion of surplus water in a horizontal direction toward vertical drains, or the nonuniform distribution of the consolidation load with depth (Art. 6-10) give solutions of Eq. (6-26) which differ somewhat from the solution given by Eq. (6-29) and hence produce a somewhat different relationship between the time factor T and the average percentage of consolidation U (see Fig. 6-11).

6-8. Sequence of Steps for the Computation of the Time Which Will Elapse until a Certain Percentage of Consolidation Is Reached. Let us assume that borings in the field have revealed the thickness of the deposit and the nature of the drainage conditions at its boundaries. In this connection it should be remembered that if these conditions are as shown in Fig. 6-9(I)—except that drainage is possible toward one boundary only, for instance when the clay deposit is underlain by sound, unfissured, and therefore impervious rock—then the center line 0-0 in Fig. 6-9(I) should be moved down to the bottom of the clay layer, so that the value H in Eqs. (6-29) and (6-31) should refer to the entire thickness of the clay stratum instead of just one half (Prob. 6-4).

Let us further consider that the necessary laboratory tests have been performed, so that the values of the permeability coefficient k (Art. 5-1),

of the modulus of volume change m_v (Art. 6-6), and hence of the coefficient of consolidation c_v [Eq. (6-27)] are known. The subsequent steps for the computation of the time which will elapse until a certain percentage of consolidation is reached are as follows:

1. Select the T-U curve in Fig. 6-11 which most closely corresponds to the actual boundary conditions of the case being studied.

2. Read off from the selected curve in Fig. 6-11 the value of T which corresponds to the percentage of consolidation U for which we want to find the time t.
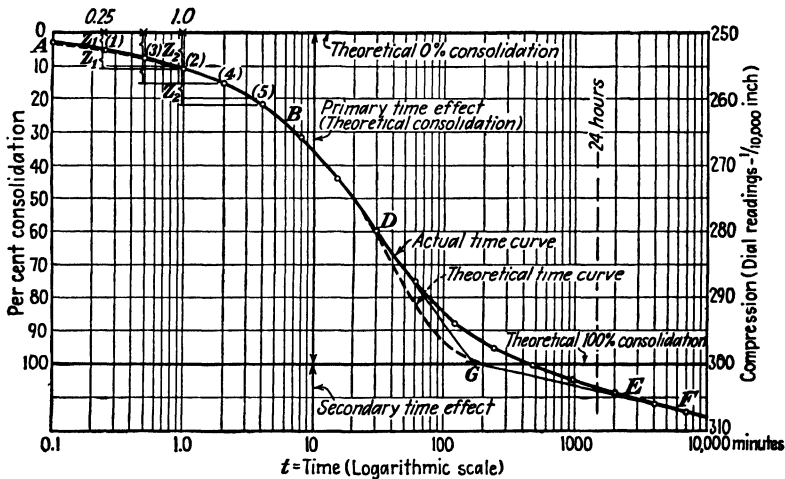
FIG. 6-10. Graphical analysis of a time-compression curve obtained from the dial readings of one load stage during a consolidation test. (After A. Casagrande and R. Fadum, Ref. 64, 1940.)

3. Insert the value of T found under 2 into the modified equation (6-29)—for water $\gamma_w = 1.00$—from which equation the desired value of t can be computed.

$$t = \frac{m_v}{k} H^2 T = \frac{1}{c_v} H^2 T \qquad (6\text{-}31)$$

It will be noted that the time which elapses until a certain percentage of consolidation is reached is independent of the intensity of the applied pressure p which causes the consolidation. The reasons are as follows: A higher value of p produces more total compression of the clay and hence, as compared to a lower value of p, will have to expel from the voids a larger amount of excess water. But, simultaneously, the higher value of p will cause a larger hydraulic gradient S along the depth of the clay layer and hence also a higher velocity of outward flow. The two effects counterbalance each other, and the rate of consolidation theoretically remains unchanged by differences in the intensity of the pressure p.

The two most important factors which influence the rate of consolidation are the permeability coefficient k and the thickness H of the layer, that is, the maximum distance which the excess water has to travel until it reaches a pervious boundary. The relative importance of these two factors is illustrated by Fig. 13-23, Art. 13-7. (See also Art. 6-10.)
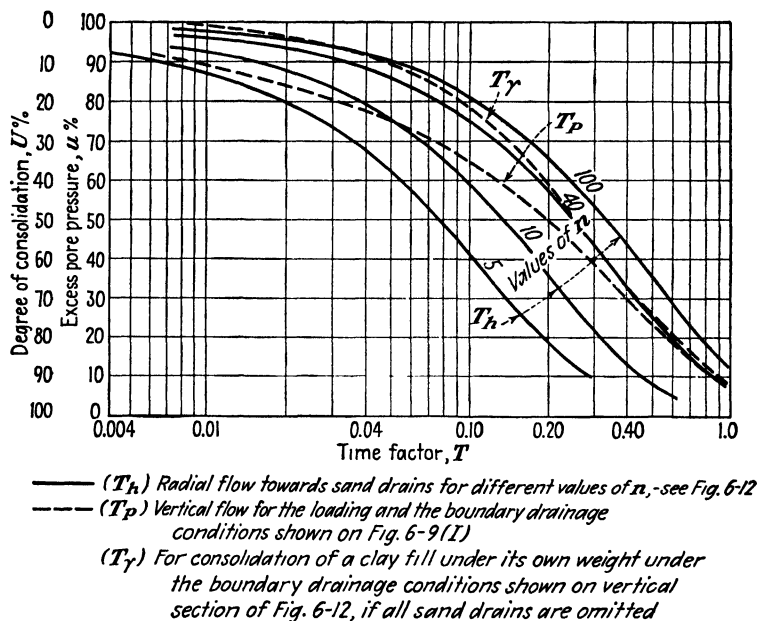
FIG. 6-11. Some time factors T for different conditions of loading and of drainage. (After Reginald A. Barron, Ref. 20, 1948.)

6-9. Computation of the Coefficient of Permeability from Time-Per Cent Consolidation Curves. Secondary Time Effects. The technique of laboratory consolidation testing has been outlined in Art. 6-3. Figure 6-10 illustrates a record, plotted to a semilogarithmic scale, of the dial readings obtained during one load stage. In this particular case the load increment was left unchanged for almost 5 days, that is, for a longer period than the customary 24 hr. This was apparently done for the purpose of emphasizing the so-called secondary time effects.

A comparison of the actually recorded time curve (shown by a full line in Fig. 6-10) with the theoretical time curve (broken line in Fig. 6-10) shows that the shapes of the two curves agree fairly well over the first half AD of their length. In order to make a closer comparison between the recorded and the theoretical values, one first has to establish the theoretical line of 0 per cent consolidation, as shown in Fig. 6-10. Some of the sudden initial compression at the moment of the application of a load

increment during a laboratory test can be attributed to causes other than expulsion of water from the voids, for instance to some squeezing out of the soil itself between the edge of the loaded filter plate and the container ring (see Figs. 6-2 and 6-3).

The theoretical 0 per cent consolidation line is established as follows: The part AB of the consolidation curve has been found to approximate a parabola. Hence, the distance z_1 between the theoretical 0 per cent line and a point 1 of the curve which corresponds to the time t_1 must follow the relationship $z_1^2 = t_1$. Similarly, for a point 2 of the curve we should have $z_2^2 = t_2$. Let us select, as shown in Fig. 6-10, for the point 1, $t_1 = 0.25$ min; and for the point 2, $t_2 = 1.0$ min $= 4t_1$. Then $z_1 = \frac{1}{2}z_2$; we can obtain z_1 graphically as the difference between the compression represented by the points 2 and 1. Then, by plotting the value z_1 once more, but *above* the point 1, a point of the theoretical 0 per cent consolidation curve is obtained and marked by an x in Fig. 6-10. The procedure is repeated again with the points 3 and 4 where $t_3 = 0.5$ min and $t_4 = 2.0$ min; then with the points 2 and 5 where $t_2 = 1.0$ min and $t_5 = 4.0$ min. Two more points marked by x are thereby obtained, and a horizontal line is drawn through these three points to represent the theoretical 0 per cent consolidation line.

The theoretical 100 per cent consolidation line is obtained by a purely empirical procedure based on a number of comparative analyses of actual laboratory test records and theoretical values. This procedure is as follows: A tangent is drawn to the point D of contraflexure of the actual time curve. Another tangent is drawn to the last portion EF of the curve. The intersection of these two tangents gives the point G through which a horizontal line is drawn to represent the theoretical 100 per cent consolidation line. The vertical distance between the theoretical 0 and 100 per cent lines is then divided into 10 equal parts to give intermediate theoretical percentages of consolidation. A somewhat different but basically similar empirical procedure has been developed by Taylor (see Ref. 343).

The coefficients of permeability k and the coefficients of consolidation c_v can be computed from the theoretical percentages of consolidation as illustrated by the following example:

It can be seen from Fig. 6-10 that the actual and the theoretical time curves coincide in their central portion BD. It is therefore customary to compute the c_v and the k coefficients from Eqs. (6-29) and (6-27) by inserting the values of the time factor T and of the actual time t which correspond to a percentage of consolidation U = 50 per cent. The T values for the boundary and loading conditions of a standard consolidation test are essentially the same as the conditions illustrated by Fig. 6-9. They are defined by curve T_p in Fig. 6-11; from that curve we find that for U = 50 per cent, $T = 0.20$. Similarly, we find from Fig. 6-10 that until U = 50 per cent was reached, the actual time which had elapsed during the particular

laboratory test illustrated by that diagram was $t = 19.5$ min. The value of H for a 1-in.-thick laboratory sample (see Fig. 6-2) is equal to $\frac{1}{2} \times 1.0 = 0.5$ in. $= 1.27$ cm. Hence, from Eq. (6-29) we obtain

$$c_v = \frac{TH^2}{t} = \frac{0.20 \times 1.27^2}{19.5} = 0.0166 \text{ cm}^2 \text{ per min} \qquad (6\text{-}32)$$

In order to compute the coefficient of permeability k from Eq. (6-27), we have to know the modulus of volume change m_v which must be given in square centimeters per gram, since the units of γ_w are grams per cubic centimeter. The units of k will then be

$$k = c_v m_v \gamma_w = \text{cm}^2 \text{ per min} \times \text{cm}^2 \text{ per gm} \times \text{gm per cm}^3 = \text{cm per min}$$

With reference to Art. 13-7 and Eq. (6-12), let us assume that the clay tested had a modulus of volume change $m_v' = 0.01$ ft^2 per ton, or approximately 0.01 cm^2 per kg. Thus the corresponding $m_v = m_v' \times 10^{-3} = 1 \times 10^{-5}$ cm^2 per gm, and with $\gamma_w =$ 1.0 gm per cm^3,

$$\begin{aligned} k = 0.0166 \times 1.0 \times 10^{-5} \times 1.0 &= 1.66 \times 10^{-7} \text{ cm per min} \\ &= 2.75 \times 10^{-9} \text{ cm per sec} \qquad (6\text{-}33) \end{aligned}$$

This is a very impervious clay (see Fig. 5-2).

The computation of the permeability coefficient from the primary compression curve of a consolidation test gives accurate results only for comparatively impervious clays with permeability coefficients smaller than 1×10^{-7} cm per sec $= 6.0 \times 10^{-6}$ cm per min. For more permeable clays and silts, direct permeability tests of the falling-head type (Fig. 6-2 and Art. 5-2) have to be performed in order to determine the k values.

In certain types of clays the secondary time effects are very pronounced, to the extent that in some cases the entire time-compression curve has the shape of an almost straight sloping line when plotted to a semilogarithmic scale, instead of the typical inverted S shape of the curve (Fig. 6-10) of clays with pronounced primary consolidation effects. These so-called *secondary time effects* are a phenomenon somewhat analogous to the *creep* of other overstressed materials in a plastic state. A delayed progressive slippage of grain upon grain, or plate upon plate, as the particles adjust themselves to a denser condition, appears to be responsible for these secondary effects. Possibly some creep of the bent platelike clay particles themselves may also be a contributing factor. When the rate of such plastic deformations of the individual soil particles, or of their slippage on each other, is slower than the rate of the expulsion of the excess water from the decreasing volume of voids between the particles, then secondary effects predominate, and this is reflected by the shape of the time-compression curve. The factors which affect the rate of the secondary compression of soils are not yet fully understood, and no methods have yet been developed for the rigorous and reliable analyses and forecasts of the magnitude of these effects (see Arts. 4-1 and 6-5).

6-10. Methods Used in the Field for the Purpose of Accelerating the Consolidation. It will be noted from Eq. (6-31) that the time which elapses until a certain percentage of consolidation is reached changes with the square of the thickness of the layer H, that is, with the square of the maximum distance which a particle of water may have to travel until it reaches the pervious boundary. This circumstance permitted the devel-
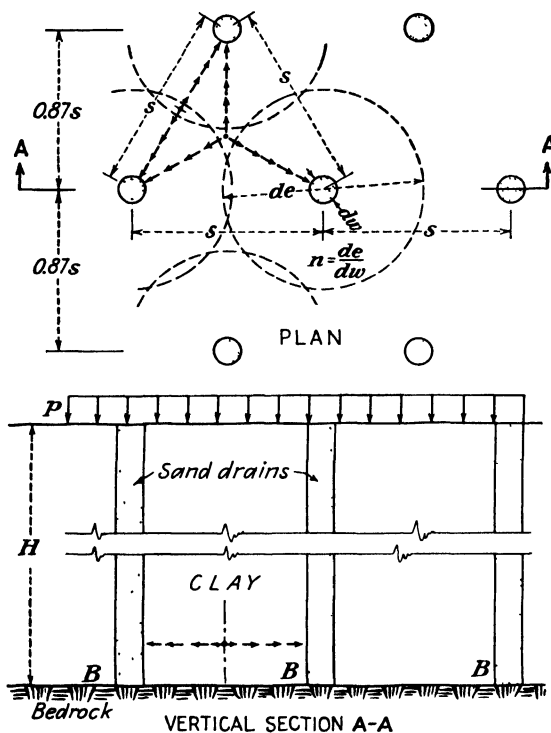
FIG. 6-12. Vertical sand drains accelerate consolidation of clay layer when their spacing s is smaller than the thickness H of the layer.

opment of practical methods for accelerating the consolidation of deep layers of clay under applied surcharges or of hydraulic clay fills under their own weight.

The method is illustrated in Fig. 6-12. Vertical sand drains are driven into the clay in a manner described in Art. 19-4. If their spacing s is appreciably smaller than the thickness of the layer H, the rate of consolidation will be greatly accelerated, since now the excess pore water can escape in a radial direction toward the sand drains along a much shorter distance than was the case previously (see Prob. 6-5).

The field use of sand drains was first effectively tried out in California

by O. J. Porter (Ref. 270, 1936). A complete theoretical analysis of the problem was published by Reginald A. Barron (Ref. 20, 1948). Its results are summarized in Fig. 6-11 which gives curves of the time factor T_h for radial drainage in a horizontal direction and varying values of the ratio

$$n = \frac{d_e}{d_w} \tag{6-34}$$

where d_e = effective diameter of soil cylinder within which water will flow toward drain well

d_w = actual diameter of drain well (see Fig. 6-12)

Equation (6-31) can be used for the solution of such problems if d_e is substituted for H.

The analysis of R. A. Barron is based on the assumption of so-called *free strain* during consolidation, according to which all deformations of the clay during consolidation are influenced solely by the rate of escape of the excess water from the voids. According to this assumption, which was also made by Terzaghi for his original theory, one would have to expect that the settlements of the soil surface, at say 50 per cent consolidation, would be greater in the immediate proximity of the sand drains than at some distance from them, since the local percentage of consolidation of a portion of a clay layer close to a drainage surface is always higher than the local percentage of consolidation of the portions of the layer located further away from the drainage surfaces. This is illustrated for the case of horizontal drainage surfaces by the t curves in Fig. 6-9(I). No such observations have however been made in the field, and the ground surface around the drains was found to settle uniformly at all times. This circumstance indicates that shearing stresses along vertical planes redistribute the weight of the soil in a manner compelling a uniform settlement of the soil surface at all times. A condition of so-called *equal strain* is thereby created which has also been analyzed by R. A. Barron (Ref. 20, Fig. 8). The T_h curves for the case of equal strain show a somewhat slower rate of consolidation, between 0 and 50 per cent consolidation, as compared with the curves given in Fig. 6-11, which refer to the case of free strain. For percentages of consolidation greater than 50 per cent both types of curves coincide almost exactly.

It has been shown experimentally by Tschebotarioff and Welch (see Fig. 10-9) that shearing stresses along rigid vertical pervious boundaries may even prevent the full development of surface settlements of soft clay in their immediate vicinity. These surface settlements are then governed by plastic displacements along curved trajectories of the entire mass of soft clay toward the rigid pervious boundary. It is conceivable that similar conditions may arise in the vicinity of timber or concrete piles (see Ref. 398). They cannot arise near sand drains, since these drains are compressible. Some practical aspects of the use of such drains are discussed in Art. 19-4.

Practice Problems

6-1. The settlement of a building resting on a 60-ft-deep layer of stiff clay was measured from the start of construction. It was found that after a number of years the settlement ceased after reaching a value of 2.07 in. at the center of the building. The average unit pressure on that layer, computed in the manner shown in Prob. 9-2,

was found to be 0.7 ton per ft². Compute the average value of the modulus of volume change m_v' of the clay layer.

Answer. Since 1.0 ton per ft² is approximately equal to 1.0 kg per cm² we obtain from Eq. (6-13)

$$m_v' = \frac{2.07}{0.7 \times 60 \times 12} = 0.0041 \text{ cm}^2 \text{ per kg}$$

6-2. Let us assume that the void ratio–pressure curve shown in Fig. 6-5 was plotted from a laboratory consolidation test of an undisturbed sample of stiff clay obtained 20 ft below the surface of the ground. What will be the value of the modulus of volume change m_v' which will correspond to an increment of pressure on the sample of 0.7 ton per ft²?

Answer. Assuming that the unit weight of the soil is 120 lb per ft³, we obtain the overburden pressure to which the sample is subjected in the soil.

$$p_1 = 120 \times 20 \times 1/2{,}000 = 1.20 \text{ tons per ft}^2$$

As a result of the application of the surcharge the pressure on the sample would be

$$p_2 = p_1 + 0.7 = 1.90 \text{ tons per ft}^2$$

From the curves of Fig. 6-5 we obtain the corresponding void ratios

$$\begin{aligned} e_1 &= 1.0050 \\ e_2 &= 0.9970 \\ \hline \Delta e &= 0.0080 \end{aligned}$$

From Eq. (6-9) we have

$$a_v = 0.0080/0.70 = 0.0114 \times 10^{-3} \text{ cm}^2 \text{ per gm}$$

and from Eqs. (6-11) and (6-12),

$$m_v' = \frac{0.0114 \times 10^{-3}}{1 + 1.0050} \times 10^3 = 0.0057 \text{ cm}^2 \text{ per kg}$$

6-3. A structure has been erected on a 45-ft-thick layer of very impervious clay, the time-compression curve of a sample of which is shown in Fig. 6-10. The boundary drainage conditions are as shown in Fig. 6-9(I). Compute the time which will elapse according to the Terzaghi theory of consolidation until 50 and 90 per cent of the final settlement will be reached.

Answer. Since drainage is possible both at the lower and the upper surfaces of the clay layer, as shown in Fig. 6-9(I), the value of $H = \frac{1}{2} \times 45 = 22.5$ ft $= 686$ cm.

The coefficient of consolidation of that clay sample was computed, as shown by Eq. (6-32), and found to be $c_v = 0.0166$ cm² per min. The time factor values which correspond to the drainage conditions of the case are given by curve T_p in Fig. 6-11. It will be seen from that curve that the value which corresponds to $U = 50$ per cent consolidation is $T_{50} = 0.20$, and to $U = 90$ per cent consolidation, $T_{90} = 0.85$. Therefore, from Eq. (6-31) we obtain the time which will elapse until 50 per cent of the final settlement, that is, of the consolidation, is reached.

$$\begin{aligned} t_{50} &= \frac{0.20 \times 686^2}{0.0166} = 5.68 \times 10^6 \text{ min} \times \frac{1}{60 \times 24 \times 365} \frac{\text{year}}{\text{min}} \\ &= 10.8 \text{ years} \end{aligned}$$

The time which will elapse until 90 per cent of the consolidation is reached is computed from

$$t_{90} = t_{50}\frac{T_{90}}{T_{50}} = 10.8\frac{0.85}{0.20} = 46.0 \text{ years}$$

6-4. Assume that all conditions remain the same as in Prob. 6-3, except that the clay layer is underlain by sound rock, so that drainage is possible only at the upper surface of the clay. What effect will this have on the time which will elapse until a certain percentage of the final settlement is reached?

Answer. The value of H will now be 45 ft, instead of the 22.5 ft of Prob. 6-3. Therefore, according to Eq. (6-31), the time t will be increased in the proportion of $45.0^2/22.5^2 = 4.0$. In other words, settlement will take four times longer to reach a certain value.

6-5. To what extent will the settlement of the case given in Prob. 6-4 be accelerated if sand drains of 18 in. (1.5 ft) diameter are driven down 8 ft (244 cm) on centers, as illustrated in Fig. 6-12? The permeability of the clay in both the vertical and the horizontal directions was found to be the same.

Answer:

$$n = 8.0/1.5 = 5.3$$

From Fig. 6-11 and the T_h curve for radial drainage and a value of $n = 5.0$ we find that the time factor which corresponds to $U = 50$ per cent consolidation is $T_{50} = 0.078$, and to $U = 90$ per cent consolidation, $T_{90} = 0.28$. From Eq. (6-31) we obtain

$$t_{50} = \frac{0.078 \times 244^2}{0.0166} = 2.79 \times 10^5 \text{ min}$$
$$= 194 \text{ days} = 6.4 \text{ months}$$

and

$$t_{90} = t_{50}\frac{T_{90}}{T_{50}} = 6.4\frac{0.280}{0.078} = 23 \text{ months}$$

As compared with the conditions of Prob. 6-4, settlement will be accelerated:

$$\frac{10.8 \times 4}{6.4/12} = 81 \text{ times} \qquad U = 50\%$$
$$\frac{46.0 \times 4}{23/12} = 96 \text{ times} \qquad U = 90\%$$

See Art. 19-4 in this connection.

References Recommended for Further Study

Laboratory Manual in Soil Mechanics, by Raymond F. Dawson, Pitman, 1949, pp. 111–128. Consolidation test.

"Consolidation of Fine-grained Soils by Drain Wells," by Reginald A. Barron, *Transactions of the American Society of Civil Engineers*, 1948, pp. 718–754. Basic theory of consolidation; diagrams and charts related to consolidation due to flow in a vertical direction, in a horizontal direction, or a combination of both, for different values of permeability coefficients in the vertical and in the horizontal directions.

"Studies of Fill Construction over Mud Flats Including a Description of Experimental Construction Using Vertical Sand Drains to Hasten Stabilization," by O. J. Porter, *Proceedings of the International Conference on Soil Mechanics and Foundation Engineering*, Vol. I, pp. 229–234, 1936. Procedures and observations which led to the adoption of this now widely used auxiliary type of construction.

CHAPTER 7

THE SHEARING STRENGTH AND THE SHEARING DEFORMATION OF SOILS

Basic Concepts

7-1. Friction and Cohesion. The Coulomb Equation. It is still customary to separate the shearing strength s of a soil into two components, one due to the *cohesion* between the soil particles, and the other due to the *friction* between them, according to the following equation which is based on the work of the French engineer Coulomb (Ref. 87, 1776):

$$s = c + \sigma \tan \phi \tag{7-1}$$

This equation expresses the assumption that the cohesion c is independent of the normal pressure σ acting on the plane of failure, so that at zero normal pressure $s = c$. Thus, according to the Coulomb equation (7-1), the cohesion is defined as the shearing strength at zero normal pressure on the plane of failure. On the other hand, the frictional component of the shearing strength of a soil is defined as being directly proportional to the normal pressure σ, the value $\tan \phi$, where ϕ is the angle of internal friction, being taken as a constant for a given soil.

It will be shown in the following articles of this chapter that Eq. (7-1) expresses the problem in a greatly oversimplified form. The shearing strength of a soil depends on a number of other factors not considered by that equation. Also, in actual practice, it is extremely difficult, if not impossible, to determine separately the quantitatively correct values of these two components of the shearing strength of an actual soil in situ. Alternative procedures will therefore be considered after an examination of the fundamentals involved.

7-2. Sliding Friction and Adsorbed Water Films. Let us consider the behavior of a solid body resting on a plane surface 1-1, as shown in Fig. 7-1, and subjected to the action of two forces one of which, the force P_n, acts at right angles to the plane 1-1, whereas the other, the force P_t, acts tangentially to that plane. Let us further assume that P_n remains constant during the entire experiment, whereas P_t gradually increases from

zero to the value which will produce sliding. The angle formed by the resultant R of these two forces with the normal to the plane 1-1 is known as the *angle of obliquity*. The solid body will start sliding along the plane 1-1 when the force P_t reaches a value which will increase the angle of obliquity α to a certain maximum value ϕ. The angle ϕ is termed the angle of friction, and the value $\tan \phi$ is termed the coefficient of friction.
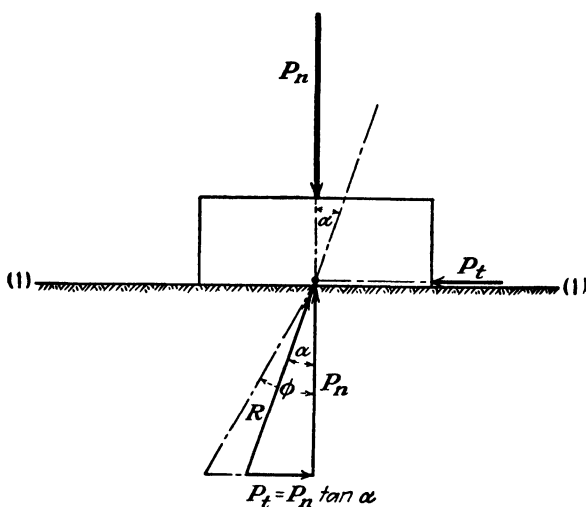
FIG. 7-1. Sketch illustrating the term *angle of friction*.

Experiments show that the critical value of P_t is proportional to P_n, that is,

$$P_t = P_n \tan \phi \tag{7-2}$$

or, since $P_t = sA$ and $P_n = \sigma A$, where A is the over-all contact area,

$$s = \sigma \tan \phi \tag{7-3}$$

Equation (7-3) is identical with Eq. (7-1) when the cohesion c is equal to zero. It states that for $c = 0$ the maximum shearing resistance to sliding is directly proportional to the normal pressure on the plane of sliding.

The physical causes of this relationship are complex and are not yet fully understood. For chemically clean surfaces the value of $\tan \phi$ increases somewhat with the roughness of the surfaces. This indicates that in such cases the resistance to sliding is dependent on the interlocking of the protuberances of the two surfaces. Microscopic protuberances, however, are present even in the case of apparently polished surfaces. Therefore, when two surfaces are brought into contact over an area A,

they will be actually touching each other only over a small fraction of that area, and at the actual points of contact the material may be stressed up to its yield point (Ref. 349) by pressure normal to the plane of contact. Induced sliding will occur when the interlocks of the projections and their areas in direct plane contact with each other are sheared off. An increase of normal pressure presumably increases the percentage of the total over-all area A of contact of the two surfaces which interlocks or which is in actual contact. As a result the total resistance to sliding is increased,
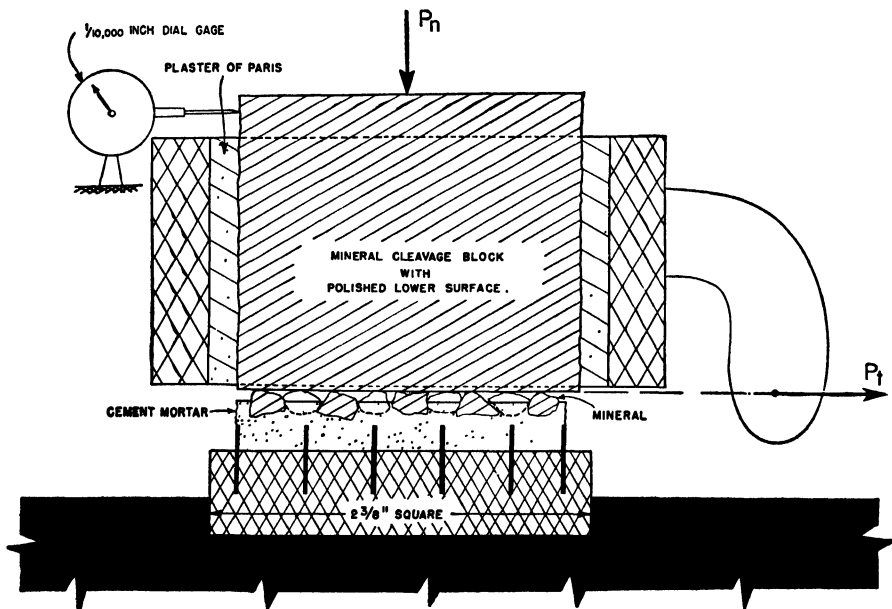
FIG. 7-2. Test set-up for the determination of the friction coefficient between minerals under exclusion of the interlocking effect between individual grains. *(From Tschebotarioff and Welch, Ref.* **393, 1948.)**

since the total cross-sectional area of the material to be sheared off has also been increased.

Adsorbed films of liquid are also known to influence the frictional resistance strongly. Oil has been used for centuries to lubricate metal surfaces and to decrease the friction between them. On the other hand the antilubricating action of water on some substances, for instance on steel or on glass, is less generally known. Since water is of paramount importance in soils, Terzaghi (Ref. 349, 1925) emphasized its antilubricating properties. According to the concept that the frictional resistance between soil grains is equal to the shearing strength of the actual contact layer between them, it was assumed that when a film of liquid separated the two solid surfaces, the frictional resistance equaled the shearing

strength of the adsorbed film. An increase of normal pressure presumably decreased the thickness and thereby increased the shearing strength of the film. The semisolid properties of adsorbed films of water have already been outlined (Art. 3-5).

Since earlier sliding-friction experiments were concerned with metals, glass, and other substances, but not with soil minerals, Tschebotarioff and
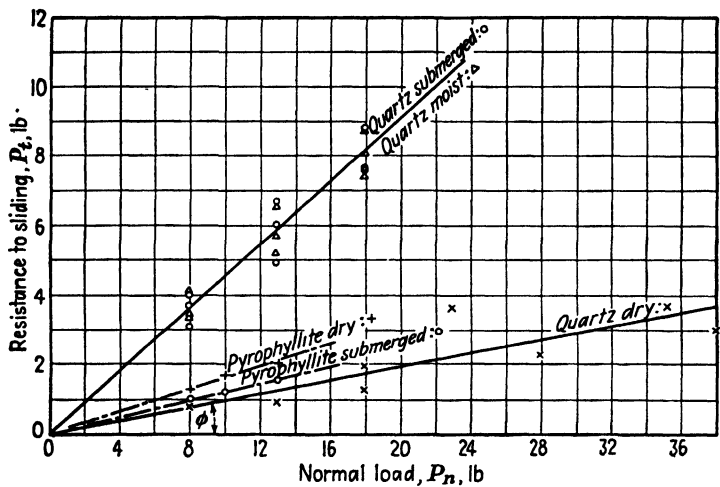
FIG. 7-3. *Relationship between normal load and resistance to sliding of quartz and pyrophyllite. (From Tschebotarioff and Welch, Ref. 393, 1948.)*

Welch (Ref. 393, 1948) performed such tests, which eliminated interlocking on a macroscopic scale between individual grains. The setup for the tests is illustrated in Fig. 7-2. The following four minerals were used:

1. Quartz. .... Hardness 7
2. Calcite . ... Hardness 3
3. Pagodite.............. . Hardness 1 to 2 −
4. Pyrophyllite... .... Hardness 1 to 2 −

The latter two are minerals of the talc variety which sometimes occur in clays. A 2-in. cube of each of the above four minerals was polished on its lower surface and was fitted, by means of plaster of paris, into the upper frame of a standard-type box for direct-shear tests of soils, as shown in Fig. 7-2 (see also Fig. 7-6.) Small fragments of the same block were embedded in cement mortar covering a metal grid plate fixed in the lower portion of the shear box. They were pressed by the upper block into the still soft mortar which was then allowed to harden. Tests were then performed in the controlled-strain manner (see Fig. 7-21) in three conditions: dry, moist, and completely submerged. The tangential forces P_t

required to induce the first motion of sliding are plotted against the corresponding normal forces P_n in Fig. 7-3. They are independent of the amount of motion. The values of the friction coefficients tan ϕ obtained in this manner are plotted in Fig. 7-4.

It was found that an appreciable difference existed between the dry and the moist conditions, and the slightest humidity in the surrounding air could rapidly affect the results, presumably because of the formation of adsorbed moisture films on the surfaces of the minerals. There was a distinct difference between *hydrophilic* minerals, quartz and calcite, which
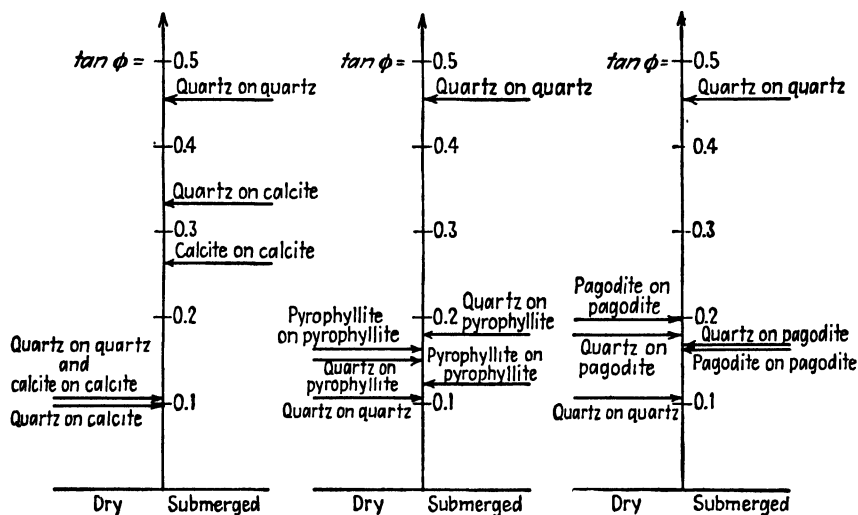
FIG. 7-4. Comparison of the friction coefficients obtained by means of the testing set-up illustrated in Fig. 7-2. (*From Tschebotarioff and Welch, Ref. 393, 1948.*)

have an affinity for water, and the two *hydrophobic* minerals of the talc variety, which are water repellent.

In the case of quartz the friction coefficient in a completely dry condition was found to be 4.5 times smaller than in a completely submerged condition. In the case of calcite it was 2.5 times smaller. For both minerals the friction coefficients in a slightly moist and in a completely submerged condition were practically identical. This indicates that the increase of frictional resistance, as compared with the dry condition, was not caused by any surface-tension phenomena, but by the changed properties of the water in the adsorbed layer, which had acquired semisolid characteristics (Art. 3-5). A reverse relationship was observed in the case of the hydrophobic minerals; water had a slight lubricating effect and decreased the frictional resistance. Tests involving a combination of two different minerals were also carried out. In such tests the harder

mineral was always used to provide the polished surface in the upper part of the box. Figure 7-4 shows that the friction coefficients of such combinations of minerals had values intermediate to the ones obtained from tests in which only one of these two minerals was used.

A test was performed with the quartz mineral after its polished surface was thoroughly roughened up by means of a carborundum stone. The friction coefficients in the moist and in the submerged condition remained practically unchanged at a value of approximately 0.480. In the dry condition, however, the friction coefficient of 0.106 was increased more than three times to a value of 0.370. It is thus apparent that the sliding
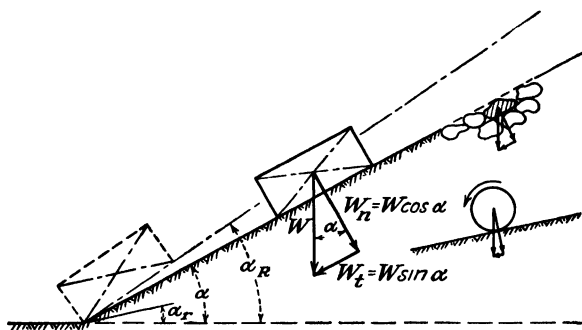
FIG. 7-5. Sketch illustrating the term *angle of repose.*

friction between different types of minerals can vary within wide limits and appears to be primarily dependent on the nature of the films adsorbed on their surface, and only to a lesser extent on the degree of roughness of the mineral surfaces in contact with each other.

Natural soils are composed of mixtures of hydrophilic and of hydrophobic minerals. The exact proportions have not yet been studied in detail, but hydrophilic minerals appear to predominate in most cases.

7-3. Angle of Repose, Rolling Friction, and the Interlocking of Soil Grains. Let us consider the equilibrium of a solid body resting on an inclined surface, as illustrated in Fig. 7-5. The angle formed by that surface with the horizontal is designated by α. The weight of the body is W. Sliding is induced by its tangential component $W_t = W \sin \alpha$ and is resisted by its normal component multiplied by the friction coefficient $W \cos \alpha \tan \phi$. If we increase the angle α of the inclined slope, sliding will finally occur when it reaches a certain maximum value α_R. At that moment

$$W \sin \alpha_R = W \cos \alpha_R \tan \phi \tag{7-4}$$

and

$$\tan \alpha_R = \tan \phi \qquad \text{or} \qquad \alpha_R = \phi \tag{7-5}$$

A body of a spherical shape will start rolling down the slope at a much smaller angle α_r of the slope, since the coefficient of rolling friction of all materials is smaller than the coefficient of sliding friction.

Grains of sand or other granular materials may either *slide* or *roll* over each other when the slope is composed of the same material. In addition, they will *interlock* with each other, as illustrated in Fig. 7-5. The natural slope which a mass of soil will assume is termed the *angle of repose.* In the case of granular materials, subject to certain reservations discussed in Art. 7-17, the angle of repose α_R is frequently taken to equal the angle of internal friction ϕ, in accordance with Eq. (7-5). It should, however, be clearly understood that the resistance of sand to sliding along a plane is composed of sliding and rolling friction and of the interlocking of the grains. A separate evaluation of all three components is not practicable for a mass of soil. All three components are directly proportional to the normal pressure.

7-4. Apparent and True Cohesion. Slaking. The shrinkage of cohesive soils due to the pressures exerted on the soil skeleton by the tension of water along the surfaces of the menisci which are formed in the capillaries during drying has already been discussed (Art. 4-8). Similar pressures, but of lesser intensity, are exerted on the soil skeleton of a saturated mass of granular soil when it starts to dry out. The pressures are smaller, as compared with a similar process in cohesive soils, because the diameters of the voids are much greater. No measurable shrinkage of the sand mass results, since the rounded shape of the sand grains produces a much more rigid skeleton than the one formed by the flexible thin plates of clay particles. Nevertheless, these capillary pressures give the sand a slight shearing strength, even at its surface, by pressing the grains together and thereby inducing friction between them. This slight shearing strength of unconfined moist granular soils is usually referred to as *apparent cohesion,* since it disappears once the surface tension of the free-water menisci in the voids is removed either by renewed submergence or by complete drying. Thus caution is needed when one relies on apparent cohesion in engineering work. A case is on record where a cut was made through slightly moist clean sand on what was believed to be its natural angle of repose of 45°. The 1:1 slope was immediately paved. It proved too steep because the effect of the apparent cohesion was only temporary and disappeared after all the water dried out. The sand, including all of its pavement, then slid out (Ref. 216, Fig. 53), adjusting itself to its true natural angle of repose.

True cohesion is produced by the actual bond which develops at the surfaces of contact of clay particles as a result of electrochemical forces of attraction. It is dependent on a great number of factors, the study of

most of which falls within the provinces of soil physics and colloidal chemistry. A detailed knowledge of these factors is essential in such branches of soil engineering as soil stabilization, where the cohesive properties of relatively small quantities of surface soils are altered and improved by appropriate chemical treatment. In the case of the large masses of natural soils in situ with which foundation engineers or earth-dam builders are concerned, a general understanding of the effect which natural chemical factors may have on the shearing strength of soils will usually suffice. A detailed study of the controllable factors which affect the determination of the over-all shearing strength of soils and its relation to the actual true values in the field is, however, essential for civil engineers of all fields of specialization.

True cohesion can sometimes develop even in sands, if some cementing agent is present to bind the particles together in a dry, moist, or submerged state. In the case of clays in a dry state, the true cohesion cannot be determined separately from the apparent cohesion. Submergence as such does not affect the true cohesion of clays, although, as will be shown later, any increase of volume reduces the shearing strength of clays, presumably by increasing the distance between particles and thereby decreasing the forces of attraction between them. The cohesion of a clay can, however, be gradually but completely destroyed as a result of submergence if it is accompanied by *slaking*. This is essentially a surface phenomenon. If the clay layer at the exposed surface swells first and therefore expands more than the adjoining inner layers, then the induced relative displacements are liable to detach the surface layer and cause it to disintegrate and slough away. The process can then be repeated and gradually progress from the surface inward.

Types and Techniques of Soil Shear Tests

7-5. Direct Shear Tests. Three main types of devices fall into this category: the direct single-shear box apparatus, the direct double-shear ring apparatus, and the torsional-ring direct single-shear apparatus.

Figure 7-6 illustrates the main features of the *direct single-shear box apparatus.* This is the oldest and simplest type of soil shear testing device. The soil specimen is fitted into the apparatus between two indented or grid plates a which help to distribute the tangential force P_t over the whole area of the specimen. The plates a can be made either pervious or impervious, depending on the conditions of drainage desired. The normal load P_n is maintained at a constant value during the test. The tangential force P_t is increased gradually until failure is produced along the plane ss. The lateral and vertical displacements are measured

by sensitive dial gages not shown in Fig. 7-6. Usually the lower half of the apparatus is stationary and the upper half movable. Sometimes a reverse arrangement is used; this does not appear advisable, since it is apt to restrain somewhat the expansion of specimens which occurs during shear in the case of dense granular soils. Too high values of shearing resistance result (Art. 7-15).
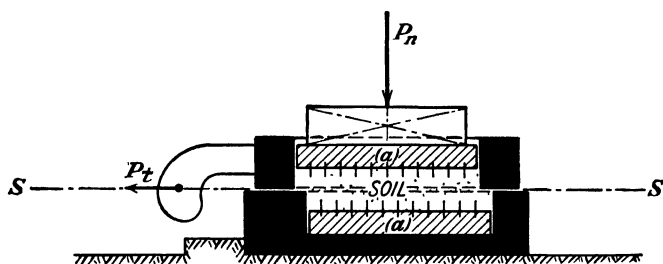
FIG. 7-6. Main features of direct single-shear box apparatus.

Figure 7-7 illustrates the main features of the *direct double-shear ring apparatus.* The tangential force P_t is applied to the central, movable ring, so as to produce shearing along two planes *ss.* Frequently the two outer rings are made somewhat longer than the central one. Not all of the normal force P_n would then be transmitted to the planes *ss*, part of it being taken up by friction along the walls of the outer rings; this would
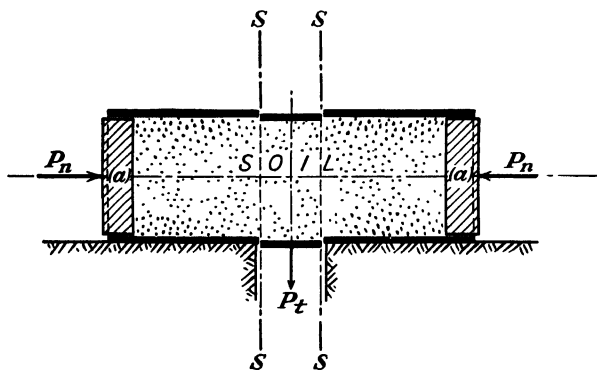
FIG. 7-7. Main features of direct double-shear ring apparatus.

give too low values of shearing resistance. On the other hand, expansion of dense sands might be partially prevented for the same reason; this would give too high values of shearing resistance. Frequently the apparatus is so designed that the inner tube of a special sampler is formed by rings which will fit directly into the shearing device, without having to transfer the soil from them. This procedure does not actually have the

advantages which it appears to have at first glance (see Arts. 7-25 and 12-7).

Figure 7-8 illustrates the main features of the *torsional-ring apparatus for direct single shear.* The tangential stresses P_t are applied by means of an external torsional moment M_t. It will be noted from the diagram that these tangential stresses p_t are liable to be greater at the outer edges of the plane *ss* along which shearing occurs. This is a disadvantage, rendering the correct evaluation of the results difficult. Also, only disturbed or remolded specimens can be conveniently fitted into the soil container, which is shaped like a hollow ring. On the other hand, there
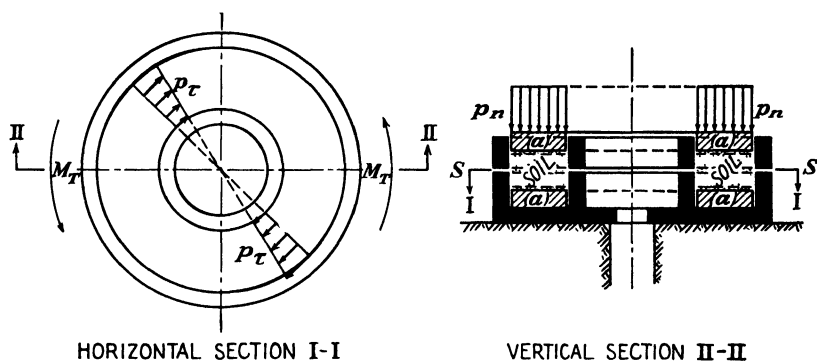
FIG. 7-8. Main features of torsional-ring apparatus for direct single shear.

is no limit to the amount of shearing displacement which can be induced. This is of advantage for the study of some special research problems, such as the restitution with time of the shearing strength of some clays after their remolding.

Figure 7-9 illustrates the conventional manner of graphical presentation and of interpretation of the results of direct shear tests. At least three tests on as many separate specimens from the same sample have to be performed under varying normal pressures p_n. The shearing strengths $s = P_t/A$ obtained from each of the three tests are then plotted against the corresponding normal pressures p_n, giving three points such as 1, 2, and 3 in Fig. 7-9 corresponding to unit normal pressures of, say, 1.0, 2.0, and 3.0 tons per ft.[2] These three points will usually lie on an approximately straight line, some scattering being sometimes caused by experimental errors or by slight variations in the properties of the three specimens tested. The slope of the line through the three points 1, 2, and 3 is tan ϕ, where ϕ is taken to represent the angle of internal friction. In the case of clean granular soils the extension of the line through the three points 1, 2, and 3 will pass through the origin O. This will also happen

in the case of a clay soil which has been completely remolded under addition of water in the laboratory, placed in a semifluid condition into the shear device, and then reconsolidated under the normal pressures p_n, although the angle ϕ obtained in this case will vary greatly, depending on the subsequent manner of testing (Art. 7-21). In the case of a naturally undisturbed clay, as shown in Fig. 7-9, the extension of the line through points 1, 2, and 3 will cut the ordinate through the origin in point 4. The distance O-4 is then taken to represent the cohesion c of the sample. This does not, however, mean that this value will necessarily represent the shearing strength of the clay at zero normal pressure in the sense of Coulomb's Equation (7-1). At normal pressures lower than the ones
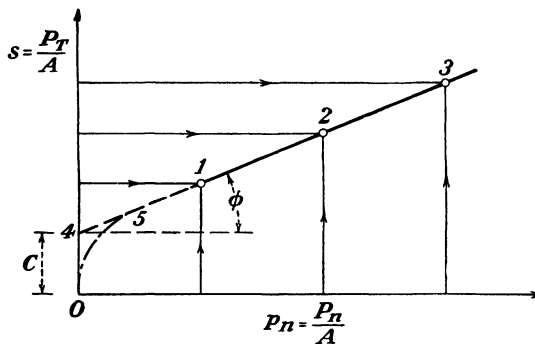
FIG. 7-9. Conventional manner of interpreting the results of direct shear tests.

corresponding to point 5 in Fig. 7-9, the shearing strengths of some clays are apt to lie on the dash-dotted curve and to tend towards zero at zero normal pressure, because, as shown by the void ratio–pressure diagram in Fig. 6-5, the expansion of a fully submerged specimen under decreasing pressure increases rapidly when low normal pressures are reached.

7-6. Types of Confined Compression Tests. The general setup for the so-called *confined compression tests*, the triaxial and cell tests, is illustrated in Fig. 7-10. A soil specimen is enclosed in a cylindrical rubber membrane and is placed in a pressure chamber formed by a cylinder of transparent material, usually lucite, filled with liquid, usually glycerine. The vertical unit pressure σ_1 is applied through a piston with a sufficiently good fit to prevent leakage of the confining liquid from the chamber. Since a tight fit may decrease the normal load because of friction along the piston, for very precise measurements some recent apparatus interpose a load-measuring device, a proving ring, for instance, between the piston and the soil specimen by placing the device inside of the pressure chamber (not shown in Fig. 7-10).

Seiffert (Ref. 307, 1933) made what appears to be the first published

reference to an apparatus of the type illustrated in Fig. 7-10. It indicates that the Prussian Waterways Experiment Station had designed the apparatus for the purpose of studying the consolidation of clay cylinders under elimination of friction along their side walls. The liquid in the pressure chamber was entirely confined, so as to provide an unyielding frictionless lateral support to the clay cylinder and its enclosing rubber membrane. For the same reason the tests had to be performed in a room where the temperature was controlled and kept constant, since otherwise
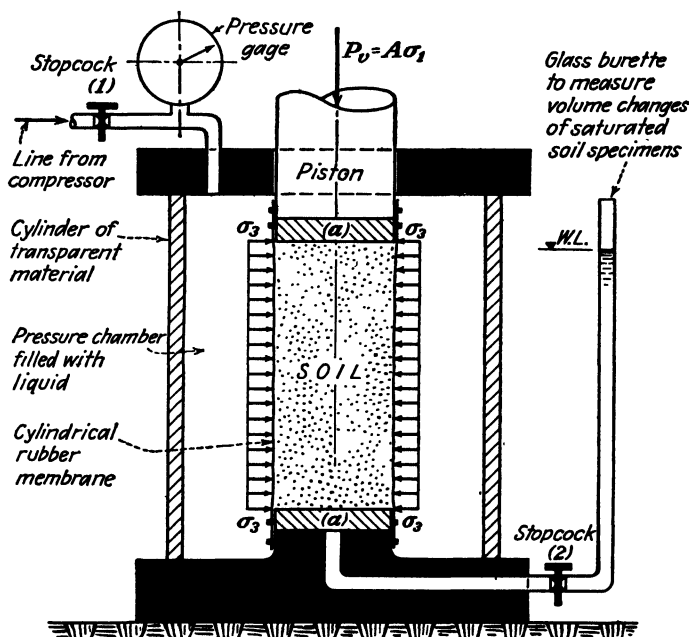
FIG. 7-10. Main features of the triaxial and of the cell types of cylindrical compression apparatus.

the difference between the thermal expansion coefficients of the materials forming the pressure chamber and of the liquid which filled it produced variations in the degree of lateral confinement of the soil specimen to the extent that shear failures were sometimes induced before the consolidation test was completed. Seiffert's diagram (Ref. 307) shows a pressure gage for the measurement of the pressures in the confining liquid, but no mention is made of any related studies. The potentialities of this device for the determination of the ratios σ_3/σ_1 of the lateral pressure σ_3 to the vertical pressure σ_1 over a wide range of pressure intensities not limited to failure conditions, that is, its use for so-called *cell* tests, appear to have been soon realized in the U.S.S.R. and in Holland. In 1936 Gersevanoff (Ref. 147) and Geuze (Ref. 148) reported the results of such tests per-

formed in their respective laboratories. The subsequent developments *in the United States* were centered at Harvard and *M.I.T.* and took a somewhat different line, since they were mainly concerned with the stability of earth dams and related failure conditions. The *triaxial* shear test, reported by Rendulic (Ref. 286, 1936), was further developed in this connection.

7-7. The Triaxial Shear Test. In the *triaxial* test the stopcock 1 shown in Fig. 7-10 is open and thereby connects the pressure chamber with a compressor which in a standard-type test maintains the lateral pressure
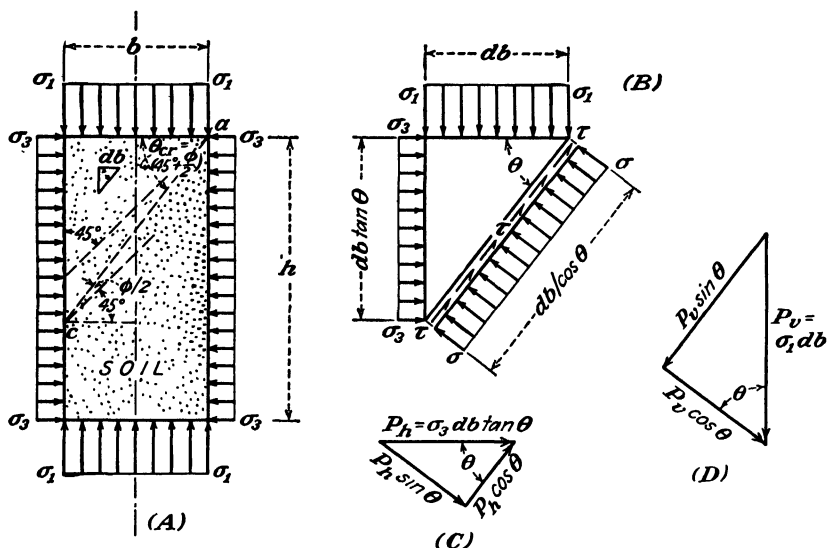
FIG. 7-11. Sketch illustrating equilibrium of external pressures and of internal stresses during a triaxial shear test.

σ_3 in the chamber at a constant value throughout the duration of the test. The vertical pressure σ_1 is then gradually increased until failure occurs. The stopcock 2 may be either open or closed, depending on whether drainage of the specimen through the lower porous stone *a* is or is not desired. In the case of a saturated specimen of granular soil the measurement of its volume changes can be conveniently performed by observing the fluctuations of the water level in a graduated glass burette connected to the open stopcock 2.

Figure 7-11 illustrates the stress conditions of the soil specimen subjected to a triaxial shear test. It is customary to assume that the vertical pressure σ_1 and the lateral pressure σ_3 are *principal stresses*, which are conventionally defined as the stresses normal to planes on which the shearing stresses are equal to zero. In the case of the lateral pressure σ_3 this is

strictly true if the rubber membrane around the soil specimen is sufficiently thin. But in the case of the vertical pressure σ_1 some shearing stresses are bound to develop at the necessarily rigid boundary of the plates *a* (see Fig. 7-10), which at their surface tend to restrain the lateral bulging of the loaded soil specimen. To minimize the influence on the failure conditions of such shearing stresses at the upper and at the lower boundaries of the soil specimen, the height *h* of the specimen should be made at least equal to 1.5 times its width *b*.

7-8. External Pressures and Internal Stresses during a Triaxial Shear Test. Let us now consider the conditions of equilibrium of a small prism of soil of the width *db*, as illustrated by Fig. 7-11(*B*), (*C*), and (*D*). First let us find the inclination of the plane along which there will be the least resistance to shearing, that is, the value of the angle θ_{cr}.

The force normal to an inclined plane forming the angle θ with the horizontal is

$$P_n = P_h \sin\theta + P_v \cos\theta$$

or, in terms of unit stresses,

$$\sigma \frac{db}{\cos\theta} = \sigma_3\, db \tan\theta \sin\theta + \sigma_1\, db \cos\theta$$

$$\begin{aligned} \sigma &= \sigma_3 \sin^2\theta + \sigma_1 \cos^2\theta \\ &= \sigma_3 + \cos^2\theta\,(\sigma_1 - \sigma_3) \end{aligned} \tag{7-6}$$

Similarly, the force tangential to the plane forming the angle θ with the horizontal is

$$P_t = P_v \sin\theta - P_h \cos\theta$$

$$\tau \frac{db}{\cos\theta} = \sigma_1\, db \sin\theta - \sigma_3\, db \tan\theta \cos\theta$$

$$\begin{aligned} \tau &= \sigma_1 \sin\theta\cos\theta - \sigma_3 \sin\theta\cos\theta \\ &= \sin 2\theta\,(\sigma_1 - \sigma_3) \times \tfrac{1}{2} \end{aligned} \tag{7-7}$$

In the case of a purely cohesive frictionless soil the shearing resistance along any plane will be independent of the normal pressure σ against it and will therefore be governed only by the intensity of the shearing stress τ along it. From Eq. (7-7) it can be seen that τ will reach a maximum value when $\sin 2\theta$ equals its maximum value of unity, that is, when the angle θ equals 45°,

$$\tau_{max} = \tfrac{1}{2}(\sigma_1 - \sigma_3) \tag{7-8}$$

If the shearing resistance *s* of a soil depends on both friction and cohesion, sliding failure will occur in accordance with the Coulomb equation (7-1), that is, when

$$\tau = s = c + \sigma \tan\phi \tag{7-8a}$$

Substituting the values of σ and of τ from Eqs. (7-6) and (7-7) into Eq. (7-8a), we obtain

$$\sigma_1 \sin\theta\cos\theta - \sigma_3 \sin\theta\cos\theta = c + \sigma_3\tan\phi + \cos^2\theta\,\sigma_1\tan\phi - \cos^2\theta\,\sigma_3\tan\phi$$

Solving for σ_1,

$$\sigma_1(\sin\theta\cos\theta - \cos^2\theta\tan\phi) = c + \sigma_3\tan\phi + \sigma_3(\sin\theta\cos\theta - \cos^2\theta\tan\phi)$$

$$\sigma_1 = \sigma_3 + \frac{c + \sigma_3\tan\phi}{\sin\theta\cos\theta - \cos^2\theta\tan\phi} \tag{7-9}$$

The plane with the least resistance to shearing along it will correspond to the minimum value of σ_1 which can produce failure in accordance with Eq. (7-9). σ_1 will be at a minimum when the denominator in the second member of the equation is at a maximum, that is, when

$$\frac{d}{d\theta}(\sin\theta\cos\theta - \cos^2\theta\tan\phi) = 0$$

Differentiating, we obtain

$$\cos^2\theta_{cr} - \sin^2\theta_{cr} + 2\tan\phi\cos\theta_{cr}\sin\theta_{cr} = 0$$

or

$$\cos 2\theta_{cr} = -\tan\phi\sin 2\theta_{cr}$$
$$\cot 2\theta_{cr} = -\tan\phi = \cot(90° + \phi)$$
$$\theta_{cr} = 45° + \frac{\phi}{2} \tag{7-10}$$

Substituting this value in the denominator of Eq. (7-9), and remembering that

$$\tan\phi = \cot(90° - \phi) = -\cot(90° + \phi) = -\cot 2\theta_{cr}$$
$$= \tfrac{1}{2}(\tan\theta_{cr} - \cot\theta_{cr})$$

we obtain

$$\sin\theta_{cr}\cos\theta_{cr} - \cos^2\theta_{cr}\tan\phi$$
$$= \sin\theta_{cr}\cos\theta_{cr} - \cos^2\theta_{cr}\left(\frac{\sin\theta_{cr}}{\cos\theta_{cr}} - \frac{\cos\theta_{cr}}{\sin\theta_{cr}}\right)\frac{1}{2}$$
$$= \frac{\cos\theta_{cr}}{2\sin\theta_{cr}}(\sin^2\theta_{cr} + \cos^2\theta_{cr}) = \frac{1}{2\tan\theta_{cr}} \tag{7-10a}$$

Substituting in Eq. (7-9),

$$\sigma_1 = \sigma_3\tan^2\left(45° + \frac{\phi}{2}\right) + 2c\tan\left(45° + \frac{\phi}{2}\right) \tag{7-11}$$

if $c = 0$,

$$\sigma_1 = \sigma_3 \tan^2 \left(45° + \frac{\phi}{2}\right) \tag{7-12}$$

if $\phi = 0$,

$$\sigma_1 = \sigma_3 + 2c \tag{7-13}$$

7-9. The Mohr Circle. The results of the foregoing analysis of a triaxial test can be conveniently presented in graphical form by means of the so-called *Mohr circle*, as illustrated in Fig. 7-12 for a granular material with $c = 0$.
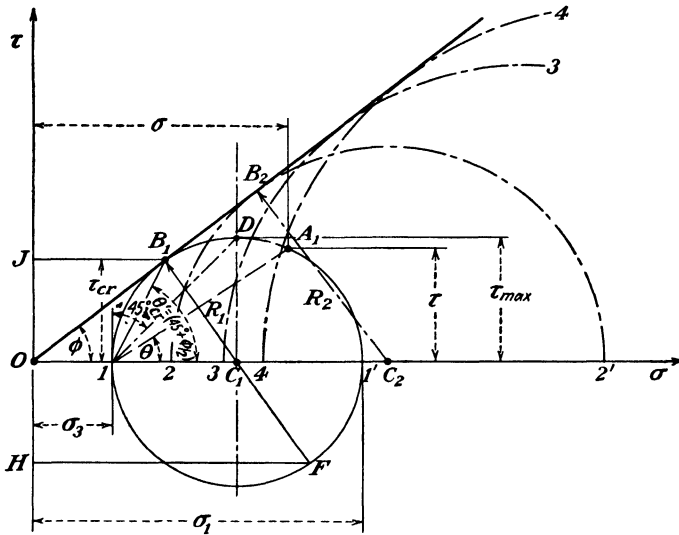
FIG. 7-12. Conventional presentation of the results of triaxial shear tests by means of the Mohr-circle diagram (a noncohesive granular soil).

The distance 0-1 is made equal to σ_3, and the distance 0-1′ to the value of σ_1 at which failure occurred. A circle is then drawn through the points 1 and 1′ with the point C_1, located midway between these two points, as center. It will be noted that the ordinates of any point, for instance point A_1, located on the circumference of that circle give us the value of the shearing stress τ on the plane forming the corresponding angle θ with the plane on which the major principal stress σ_1 is acting, the latter plane being in the present case horizontal, according to Fig. 7-11(A). This is simply a graphical expression for Eq. (7-7). Similarly, the abscissa of the same point A_1 expresses Eq. (7-6) and represents the normal stress σ on the plane forming the same angle θ with the major principal plane.

Let us assume that three other triaxial tests have been performed with progressively increasing values of the lateral pressure σ_3, so that for the

second test σ_3 will be equal to the distance 0-2, for the third test to the distance 0-3, and for the fourth test to the distance 0-4, all as shown in Fig. 7-12. Mohr circles will then be drawn for each of these tests. If the soil tested has no cohesion ($c = 0$), for instance if it is clean sand, then the envelope for all four tests will be found to be approximately a straight line forming the angle ϕ with the horizontal and passing through the origin O as shown in Fig. 7-12. It will be noted from that diagram that, because of the relationship expressed by Eq. (7-8a), the shearing stress τ_{cr} along the failure plane forming the angle θ_{cr} with the major principal plane, is somewhat smaller than the greatest shearing stress τ_{max}, which occurs under an angle of 45°.
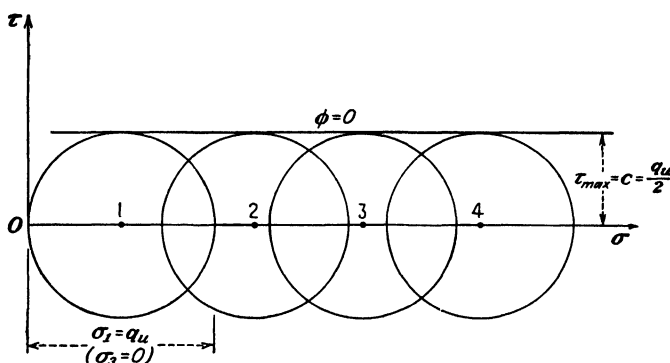
FIG. 7-13. Mohr-circle diagrams of unconfined and of triaxial compression tests at constant water content on a fully saturated clay.

A number of other relationships can be presented by means of the Mohr circle. It is particularly convenient as an accessory for the analysis and visualization of conditions related to cases more complex than the one analyzed in the preceding paragraph, for instance when the major principal plane is not horizontal (Ref. 343). Such conditions may arise, for instance within the mass of soil behind a slope, and may require analysis.

It should be noted that the analysis by means of the Mohr circle, strictly speaking, is possible only in respect of two-dimensional problems, since the effect of the third principal stress σ_2, acting normal to the plane of the drawing, cannot be taken into account. In the case of a triaxial test σ_2 is always equal to σ_3. However, according to Taylor (Ref. 343), the effect on the strength at failure of variations in the value of σ_2 is likely to be very small.

The value of $(\sigma_1 - \sigma_3)$ is termed *deviator stress*, and the value at failure is known as the *compressive strength* of a soil. According to Fig. 7-12 and Eq. (7-8), the latter is equal to $2\tau_{max}$. If we have a frictionless soil, for instance a fully saturated clay, the water content of which has not been

permitted to change during the tests, then the results of triaxial tests under increasing values of σ_3 give a series of circles of equal radius, the envelope of which is horizontal ($\phi = 0$), as shown in Fig. 7-13. This indicates that the compressive strength and therefore also the shearing strength of such a clay are constants which are independent of the normal pressure, any increment of the latter being carried by the neutral pressures in the water filling the voids of the clay. These neutral pressures in the water naturally do not contribute to an increase of the frictional component of the shearing strength of the soil, which depends only on the effective stresses $(\sigma - u)$, where u represents the neutral stresses or excess pore pressures (Art. 6-1). Therefore, the Coulomb equation reads

$$s = c + (\sigma - u) \tan \phi \tag{7-14}$$

when $\sigma = u$, then $s = c$, and the results are as shown in Fig. 7-13.

7-10. Unconfined Compression Tests. Triaxial tests performed with no lateral confining pressure ($\sigma_3 = 0$) are known as unconfined compression tests. Standard-type compression tests on concrete cylinders fall into this category. The value of σ_1 at failure is known in soil mechanics as the *unconfined compressive strength* and is designated by the symbol q_u. An examination of Eq. (7-9) shows that the value of θ_{cr}, as given by Eq. (7-10), remains unchanged. On the other hand, Eq. (7-11) is simplified to read

$$\sigma_1 = q_u = 2c \tan \left(45^\circ + \frac{\phi}{2}\right) \tag{7-15}$$

from which the cohesion c is found.

$$c = \frac{q_u}{2 \tan (45^\circ + \phi/2)} \tag{7-16}$$

and, if $\phi = 0$,

$$c = \frac{q_u}{2} \tag{7-17}$$

The Mohr diagram of an unconfined compression test, as shown in Fig. 7-13, becomes a circle tangent to the point of origin O. τ_{max} is equal to the cohesion c, in accordance with Eq. (7-17), and this value remains unchanged during triaxial texts if no change of water content is permitted. Therefore, under such conditions the unconfined compression test has considerable advantages over the triaxial test because of its simplicity. As shown in Fig. 7-14(I) and (II) and Table 7-1, the unconfined compression test can be used as a classification test not only in respect to the ultimate strength of a clay soil, but also in respect to its deformation characteristics, as expressed by the strain at failure. It will be shown

later (Art. 7-21) that the value of the strain at failure may be strongly influenced by large differences in the rate of loading. However, within the customary limit of approximately 10 min for the duration of a test, which can easily be achieved through adjustment of the rate of loading,

TABLE 7-1. Classification of Natural Clays*

	ϵ_f, per cent
Brittle clay (curve *B*)	3–8
Semibrittle clay (curve C)	8–14
Plastic clay (curve *D*)	14–20

* Arranged according to their strains at failure during an unconfined compressive-strength test, as shown in Fig. 7-14(II).

there is not much variation to be expected in the values of the strain at failure ϵ_f.

The stress-strain diagrams shown in Fig. 7-14(II) refer to the controlled-stress type of tests (Art. 7-13). In the controlled-strain type of tests the curve *B* would be likely to approximate the line *ef*, in which case the point
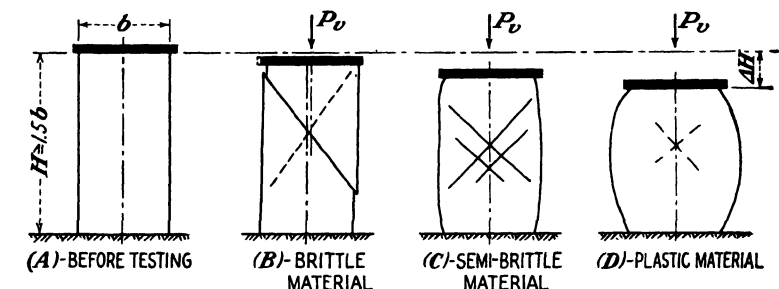
(I)-APPEARANCE OF CLAY SPECIMENS. (BEFORE AND AFTER TESTING)
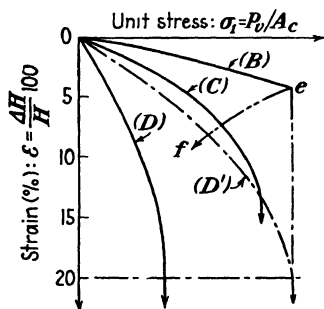
(II)-STRESS-STRAIN DIAGRAM
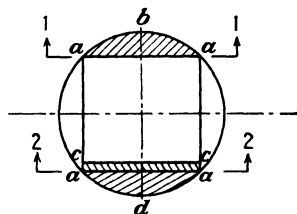
(III)-TRIMMING SAMPLE FOR TESTING AND PHOTOGRAPHY

FIG. 7-14. Unconfined compression tests. (I and II *after Rutledge, Ref. 293, 1935.*)

e giving the *peak stress* would have to be taken in determining the value of ϵ_f for classification purposes.

In some cases plastic clays have a high strength (curve *D'*), but usually it is much lower (curve *D*) than that of brittle clays. This circumstance
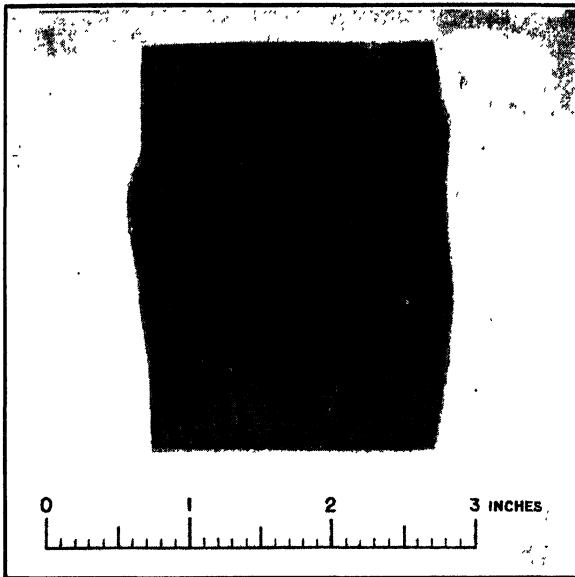
FIG. 7-15. Unconfined compression test. The development of planes of failure on a completely remolded clay sample from Greenville, Mississippi. (*Unpublished report by Tschebotarioff, 1947.*)
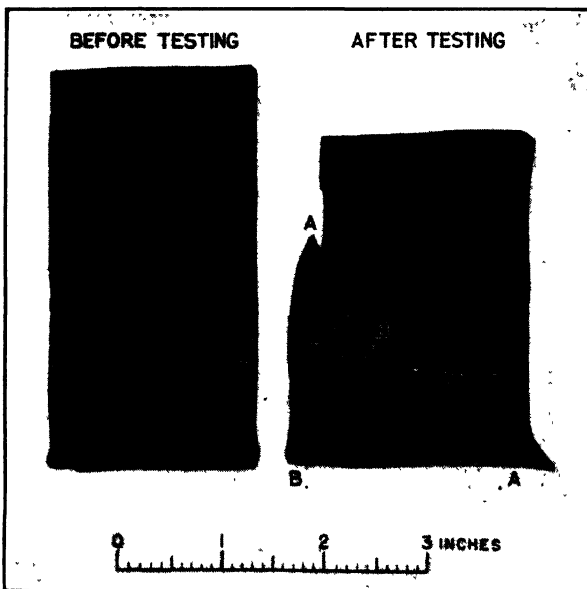
FIG. 7-16. Unconfined compression test. Brittle failure of a varved clay specimen from Albany, New York (see Art. 12-7). (*Tschebotarioff and Bayliss, Ref.* 385, 1948.)

can be utilized for the determination of the sensitivity of clays to remolding (Art. 7-22). Some clays develop fracture planes even after remolding. (See Fig. 7-15, which shows a side view of the outer face of a clay prism.)

Figure 7-14(III) shows how, for testing, a cylindrical sample is usually trimmed down to a prism, marked by the letters *a* at the corners. One of the segments, for instance *aba*, can then be photographed before testing (Figs. 7-16 and 7-17). After the end of the test, a slice *acca* can be cut for photographing the deformations which accompanied failure. When
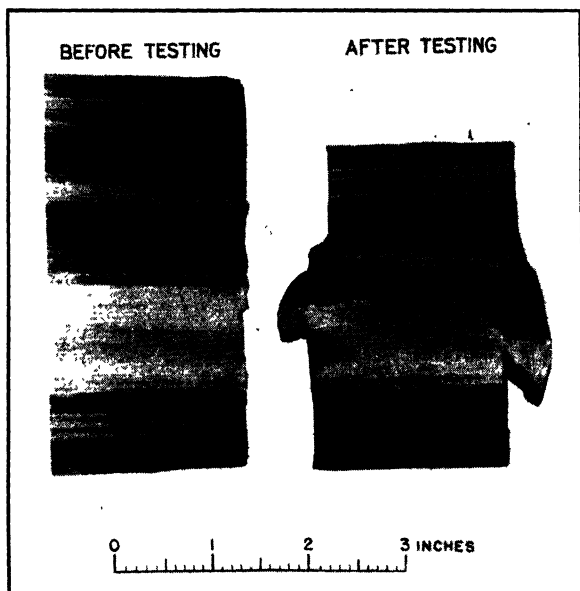
FIG. 7-17. Unconfined compression test. Failure by lateral squeezing of a single varve of a clay specimen from Albany, New York (see Art. 12-7). (*Tschebotarioff and Bayliss, Ref. 385, 1948.*)

the same specimen is then remolded for a repeated test to determine its sensitivity (Art. 7-22), the loss of the material of slice *acca* can be made up from one of the remaining three segments, for instance *ada*.

7-11. Cell Tests. The *cell* test derives its name from the fact that the liquid which provides lateral support to the soil specimen is sealed off in the pressure chamber as in a cell. This is achieved by means of a setup which is essentially the same as in triaxial tests, except that the stopcock labeled 1, shown in Fig. 7-10, is closed during a cell test. Thus in a triaxial test the lateral pressure σ_3 is maintained at a constant value during the test until failure occurs as a result of an increase of the vertical pressure σ_1. In the cell test, however, the lateral pressure σ_3 is measured on the pressure gage not only at failure but at all intermediate stages of
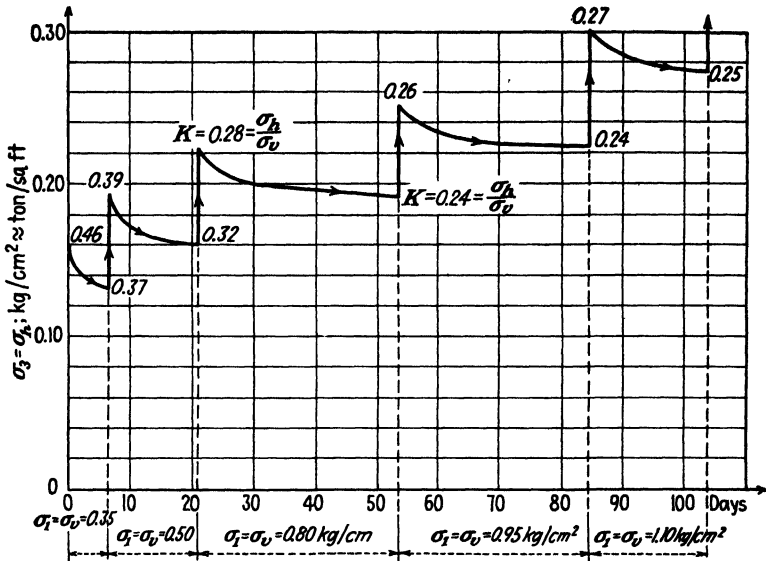
FIG. 7-18. Variation of lateral supporting pressures with time during a slow (S) cell test with peat. (After E. C. W. A. Geuze, Ref. 148, 1936.)
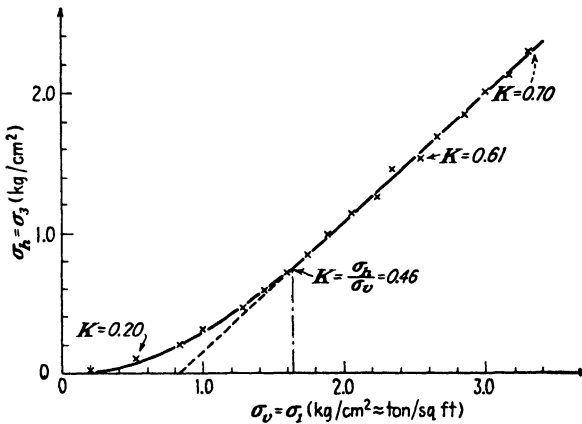
FIG. 7-19. Variation of lateral supporting pressures with increasing vertical pressures during a quick (Q) cell test with undisturbed peaty clay. (After E. C. W. A. Geuze, Ref. 148, 1936.)

loading intensity σ_1. The manner in which the presentation of the results of different types of such cell tests has been developed in Holland is illustrated by Figs. 7-18 and 7-19.

The cell test therefore has an important advantage over the triaxial test in that it permits the direct determination of the ratio σ_3/σ_1 at all intermediate stages of loading. This is of great importance in all studies of lateral earth pressures against retaining walls and sheet-pile bulkheads.

It will be shown later that designs involving lateral earth pressures frequently represent a problem of deformation and not of rupture. Another advantage of the cell test is that a test of only one specimen covers the entire range of possible pressures. At least three to four specimens have to be tested in triaxial tests.

Figure 7-20 illustrates the manner of presentation of the results of some cell tests in the U.S.S.R., giving the variation of the ratio σ_3/σ_1 as a function of an increasing vertical pressure σ_1.

Failure conditions may be induced during any cell-test stage by bleeding a few drops of the supporting liquid (for instance by opening the stopcock 1 shown in Fig. 7-10) and recording the corresponding minimum
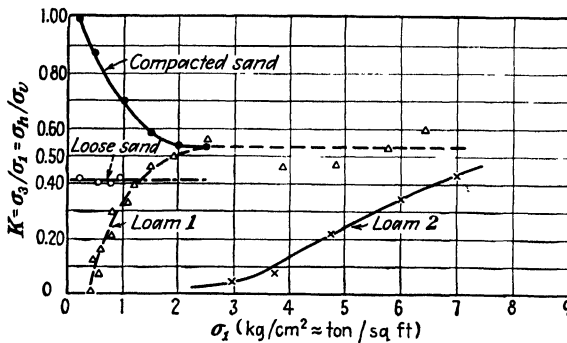
FIG. 7-20. Some results of cell tests. (*After Gersevanoff, Ref.* 147, 1936.)

lateral pressure σ_3. This is taken to correspond to the limit equilibrium of pressures at failure. The procedure can be repeated several times, and the results plotted on a Mohr diagram of the usual type, such as is illustrated in Figs. 7-12 and 7-13. According to DeBeer (Ref. 105), the envelope of a Mohr diagram obtained in this manner consists of two straight lines intersecting at a so-called *singular point.* The ordinate of that point was taken to correspond to the shearing resistance of the material in its natural state in the ground. It was found to be somewhat smaller than the shearing strengths obtained by means of conventional triaxial shear tests for σ_1 values equal to the natural overburden pressure on the sample in the ground.

A disadvantage of the cell test is the difficulty which it presents in operation. First of all, a space with constant temperature control is required for any tests exceeding a few hours duration. Further, it is difficult to prevent any leakage whatsoever of the supporting liquid from the sealed pressure chamber during long-duration tests. Finally, the models available at present appear to be too lightly built and to yield excessively under high internal pressures. This induces uncontrollable

deformation of the soil specimen, which is particularly undesirable in the case of sensitive clays, since it may cause their partial remolding and may result in their weakening. There also is some *spring action* of the entire apparatus during the reduction of the supporting pressures σ_3, for instance, during consolidation of a clay specimen. Nevertheless, improvements which will minimize these defects appear entirely feasible and should be carried out in view of the great potentialities of this type of apparatus.

7-12. Shear Tests In Situ. Cone-penetration and Auger-vane Tests. The attempt is sometimes made to determine the shearing strength of soils from the results of cone-penetration tests in deep soundings (Art. 12-9). In the case of sands the practical value of the results of relevant computations (Ref. 103) is somewhat questionable, since the resistance to the penetration of the cone is a composite one. Both the compressibility of the sand and its shearing strength affect the recorded data. Nevertheless, in connection with other studies (Art. 12-9), the cone-penetration test can serve to evaluate the sand density in situ. The cone test therefore has considerable potentialities for the indirect and empirical evaluation of the shearing strength of sands in situ, since it will be shown later that this shearing strength is closely related to the sand density (Art. 7-17).

In the case of natural clays the cone, as it is pressed down, is liable to remold some of the clay ahead of it and therefore to register too low resistance and, consequently, too low shear values, especially in the case of sensitive clays. The rotating-auger or vane test in some cases appears to give good correlation with the results of laboratory shear tests (Refs. 58 and 312) and even seems to present certain advantages over them (Art. 7-23).

In-situ shear tests of surface layers of soil have sometimes been attempted. For instance, Burggraf (Ref. 50, 1938), developed a portable unit for the purpose. It involves shearing by means of horizontal pressure and may be employed in conjunction with conventional-type load tests (Art. 19-6), although no correlations between the two types of test have yet been made. Its use is limited to shallow surface exploration in connection with highway or airport pavement-design studies.

7-13. Controlled-stress and Controlled-strain Tests. Figure 7-21 illustrates the difference between these two types of tests, as applied to direct-box single-shear tests. In the first type [Fig. 7-21(*A*)] the load P_t which induces shear is gradually increased until complete failure occurs. This can be done by placing weights on a hanger or by filling a counter-weighted bucket of original weight W with water. The shearing displacements are measured by means of the dial gage a as a function of the increasing load P_t. A stress-strain curve of the shape b in Fig. 7-24 is a

result of this procedure, which is known as the *controlled-stress* type of test. Because of the relative simplicity of its setup, it was exclusively used for soil testing up to about 1938.

In the *controlled-strain* type of test, illustrated by Fig. 7-21(*B*), the shearing displacements are induced and controlled in such a manner that they occur at a constant fixed rate. This can be achieved by turning the wheel *d*, either by hand or by means of an electrically operated motor, so that horizontal motion is induced through the worm gear *e* while the dial
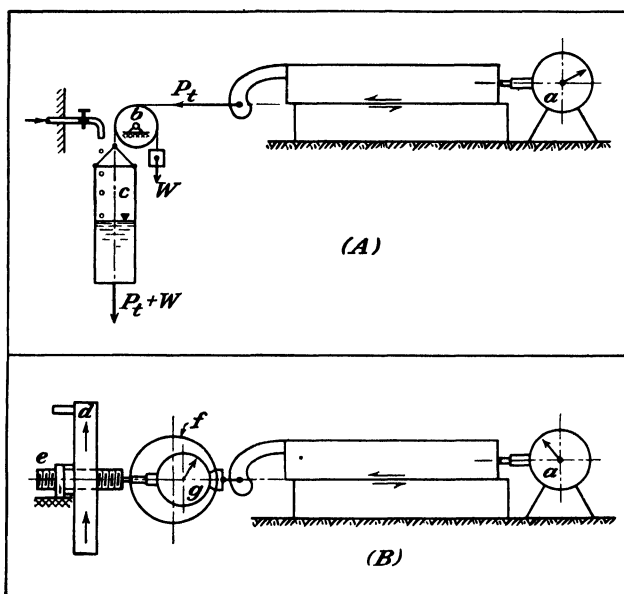
FIG. 7-21. (A) Controlled-stress direct shear test. (B) Controlled-strain direct shear tests.

gage *a* registers the desired constant rate of displacement. The shearing resistance offered to this displacement by the soil specimen is measured by the proving ring *f*. Such proving rings are frequently manufactured from roller bearing races (Ref. 134). Their load-axial deformation relationship is linear within a certain range of load. Thus they can be calibrated so that a change of their diameter, as measured on the dial gage *g*, indicates the load the ring is transmitting at that moment. The stress-strain curves of tests of this type have the shape *ac* in Fig. 7-24. Nearly all compression and tension machines for the testing of such materials as steel and concrete are operated on the controlled-strain principle.

Both the controlled-stress and controlled-strain types of test can be and are used in connection with all the direct, triaxial, and unconfined

soil shear tests described in the preceding paragraphs. Only the controlled-stress type of test is used in connection with cell tests.

The controlled-strain type of test is easier to perform, although not to install, and has the advantage of readily recording not only the peak resistance (*a* in Fig. 7-24), but also the smaller resistances after greater deformations have broken down in part the structure of the soil. The controlled-stress type of apparatus has some advantages, mainly in connection with some special problems of a research character (Ref. 296).

7-14. The Rate of Shearing and the Conditions of Specimen Drainage. Some shear tests are performed under so-called *drained* conditions, that is, the escape of water from the voids of the specimen, which tends to take place as a result of increased pressures during the test, is permitted at the boundaries of the soil specimen. This is achieved by making the plates *a* in Figs. 7-6, 7-8, and 7-10 porous. The stopcock 2 shown in Fig. 7-10 is kept open.

The amount of drainage which can actually take place prior to failure will strongly affect the results. In the case of cohesive soils of low permeability the amount of drainage which can take place during a test largely depends on whether consolidation under normal load (or σ_3) was or was not permitted prior to shearing, and on the rate at which the shearing force (or σ_1) was applied.

Arthur Casagrande suggested on the basis of the above considerations the following classification of shear tests, which will be followed in this book:

1. *Quick Tests* (Symbol: Q). No consolidation or drainage of water from the voids is permitted. It is an *undrained* test, quickly performed. It is easier to achieve this fully on a triaxial device (by closing the stopcock 2, Fig. 7-10), than on a direct-box shear device.

2. *Unconfined Compression Tests* (Symbol: U). When carried out on a saturated clay within 10 to 20 min, this test gives results which are essentially identical to those of Q tests (Fig. 7-13).

3. *Consolidated Quick Tests* (Symbol: Q_c). Full consolidation under the normal load, or σ_3 and $\sigma_1 = \sigma_3$, is allowed to take place prior to the start of the shear test proper, after which the tangential force (direct tests) is applied, or σ_1 is increased (triaxial tests) to produce a rapid failure.

4. *Slow Tests* (Symbol: S). After completed consolidation, as in the Q_c tests, the shear test proper is conducted so slowly under drained conditions that any excess pore pressures u which may be induced by shearing deformations will have time to be completely dissipated under additional consolidation.

Comparison of the results of the preceding types of shear tests indicates

that, for saturated cohesive soils, the S tests give the highest values of shearing strength, the Q tests give the lowest, and the Q_c tests give intermediate values. Therefore, in the case of drained tests, the shearing strength of a cohesive soil increases with a decrease of the rate at which the shearing stresses are induced.

A reverse relationship is obtained in the case of undrained tests, where no decrease of water content, that is, no consolidation, is permitted. In such cases the so-called *creep* or *plastic flow* effects appear to exercise a predominant influence on the results of shear tests with undrained saturated cohesive soils. The resistance to a slowly applied shearing stress under the above conditions may therefore be found to be appreciably smaller than the resistance to a rapidly applied shearing stress.

Shearing Characteristics of Sands

7-15. Volume Changes during Shear. *Dense sands* expand during shear. This is illustrated by Fig. 7-22(I). If shear is to occur along the
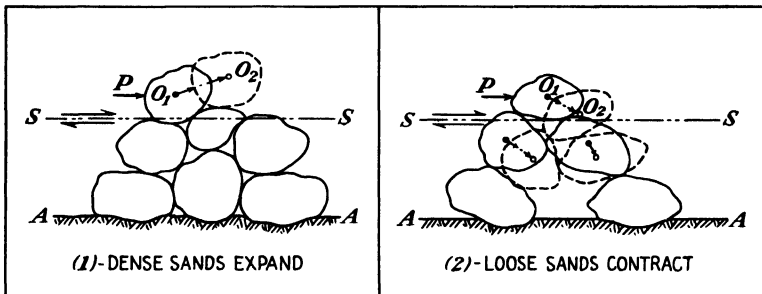
FIG. 7-22. Diagram illustrating volume changes of sands during shear. (1) Dense sands expand. (2) Loose sands contract.

plane ss, the one sand grain shown above that plane in the diagram would have to slide or to roll over the underlying closely packed grains, thus moving from O_1 to O_2. Other sand grains above the plane ss would have to do the same, thus causing the sand mass to expand. Under natural conditions in the field such expansion usually appears possible. Should expansion of a dense sand be artificially prevented under laboratory conditions, for instance, during a direct single- or double-shear test, then appreciable shearing displacements would become possible only as a result of the partial crushing or splitting of individual sand grains. The ultimate shearing resistance would thereby be increased to unnaturally high values. This sometimes occurs during double-shear direct-ring tests, such as are illustrated by Fig. 7-7.

The expansion of dense sands during shear can be demonstrated in the

laboratory by means of a simple experiment illustrated by Fig. 7-23. A rubber cylinder (*b*) is filled with dense sand, which is then saturated with water, introduced through the stopcock (*C*) until it rises to the top of the capillary glass tube *a*. To prevent bulging and creep of the rubber as a result of the head of water thus developed, electricians' tape is wrapped around the cylinder. The sand is then thoroughly shaken down. If one exerts lateral pressure on the cylinder with two fingers, as indicated by
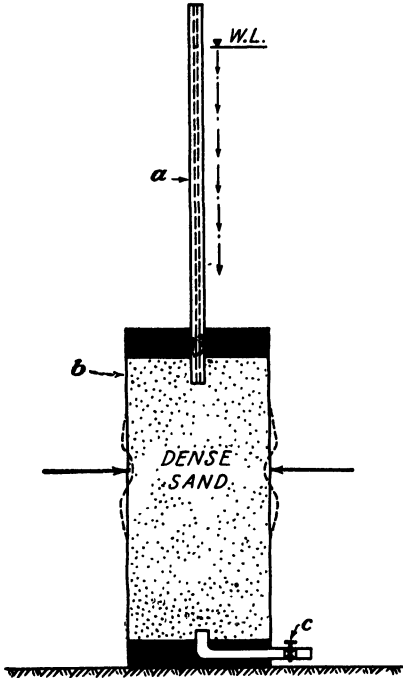
FIG. 7-23. Simple device to demonstrate the expansion of dense sand during shear.

FIG. 7-24. General shape of stress-strain curves. Controlled-strain direct-box shear tests. (*After H. A. Fidler, Ref.* 134, 1938.)

arrows, then the dense sand inside will have to bulge slightly, as shown by the broken lines in Fig. 7-23. Such bulging is essentially due to shearing deformations (Figs. 9-5 and 9-8). A local increase of the total sand volume and, hence, of the volume of its voids will take place. This circumstance will be confirmed visually by a drop of the water level in the glass tube *a*, since some of the water in the tube will go to fill up the additional void space. The harder one presses on the rubber cylinder, the lower the water level will drop in the glass capillary tube above it. The original water level may be restored by shaking down the sand again.

The point *a* of the stress-strain curve of Fig. 7-24(II), which represents

the greatest (peak) shearing resistance of a well-graded dense sand, probably corresponds to the moment when the dense structure of the sand just begins to be loosened up. In any case, experiments show that expansion of dense sand continues well beyond that point (Ref. 343).

Loose sands contract during shear. This is illustrated by Fig. 7-22(2). If shear is to occur along the plane *ss*, then any lateral movement of the one grain shown in the diagram above that plane is liable to bring about a general readjustment of the sand grains below it to the positions indicated by broken lines. This, of course, is accompanied by a general decrease of the total volume and of the volume of the voids. The stress-strain curve of a shear test on loose sand has the shape given in Fig. 7-24(2). It should be noted that, once the loose structure of the sand has collapsed, the decrease of volume ceases and, after it has thus been *densified*, further shearing deformations of the sand are accompanied by an increase of its volume (Ref. 343).

FIG. 7-25. Effect of intensity of confining pressure σ_3 on the values of the critical void ratio. Triaxial shear tests on sand. (*After Palmer, Ref. 257, 1948.*)

7-16. The Critical Void Ratio and Liquefaction Phenomena.

Since dense sands expand and loose sands contract during shear, there must be an intermediate density at which shearing deformation may take place without any change of volume. The void ratio which corresponds to this intermediate density has been termed *critical void ratio* by Arthur Casagrande (Ref. 62, 1936).

Direct shear tests are not well suited for the determination of the critical void ratio of sands; triaxial tests on completely saturated sands have to be used. The change of volume of a sand specimen during the test is measured by recording the variations of the water level in the graduated glass burette attached to the stopcock 2, which is kept open, as shown in Fig. 7-10. At least three to four separate triaxial tests, with as many different initial sand densities, have to be performed in order to determine the critical void ratio for a given intensity of the minor principal stress σ_3. As shown in Fig. 7-25, the volume change at the failure

load of each test is plotted against the initial void ratio at which the sand specimen had been placed into the apparatus for testing (it is necessary to have at least one test with very dense sand and another with very loose sand). A line is then drawn, as shown in the diagram, through the points thus obtained. Its intersection with the line representing the ordinates of zero volume change gives the value of the critical void ratio e_{cr}.

It may be seen from Fig. 7-25 that an increase in the value of the confining pressure σ_3 brings about a decrease in the recorded value of e_{cr}.
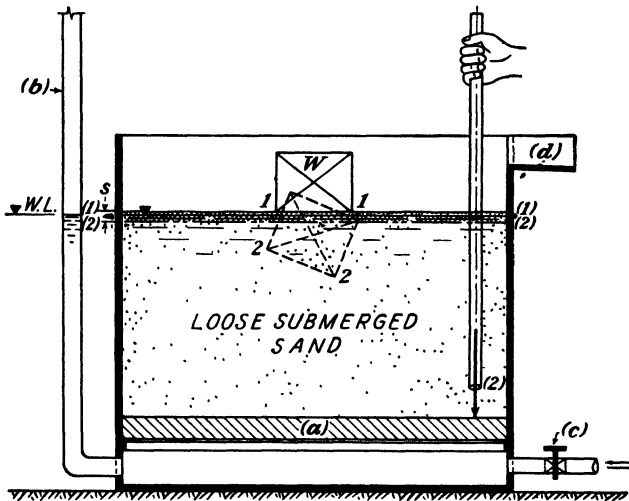
FIG. 7-26. Laboratory demonstration of the contraction and of the temporary loss of supporting capacity of a loose submerged sand as a result of a sudden strong shock.

This means that if the sand used for the tests illustrated by that diagram had an initial void ratio of, say 0.80, then under a confining lateral pressure of $\sigma_3 = 1$ kip per ft^2 ($=0.5$ ton per ft^2) it would tend to expand during shear, whereas under a higher confining lateral pressure of $\sigma_3 = 6$ kips per ft^2 it would tend to contract.

All the above considerations are of considerable practical importance in connection with *liquefaction* phenomena of saturated loose sands, which sometimes lead to the so-called *flow slides* of embankments or earth dams (Art. 8-11).

The liquefaction of a loose sand as a result of a sudden shock may be demonstrated in the laboratory by means of the apparatus employed for the demonstration of quicksand conditions (Art. 5-4). The metal box shown in Fig. 7-26 is filled with sand. The stopcock c is connected to a water line and is opened wide. Water is thus allowed to surge through

the filter stone *a* upward through the sand and out over the overflow *d*; this completely loosens up the sand. The stopcock *c* is then closed; it is disconnected from the water line and is opened to permit downward drainage of the water at a sufficiently slow rate, so as not to compact the loose structure of the sand. When the water level drops approximately ¼ in. below the surface 1-1 of the sand (as seen from the glass standpipe *b*), the stopcock *c* is closed, and a weight *W* is carefully placed on the sand surface. A metal rod is then rammed through the sand, so as to hit the bottom of the box and jar it. Two things will then be observed. The entire surface of the sand will fall by the amount *s* to the level 2-2 and will sink slightly below the water level. Thus the shock will have caused the compaction of the entire mass of the saturated loose sand. The weight *W* will, however, be found to have sunk down to the position 2-2 by an amount several times greater than the settlement *s* of the sand surface. This indicates that immediately after the shock the whole mass of the sand was liquefied for a few moments. In this condition it had no shearing strength whatsoever and could not offer any resistance to the shearing stresses which are always caused in the soil by a load resting on its surface (Figs. 9-5 and 9-22).

The practical importance of the compaction of sands becomes therefore evident for all cases where earthquake tremors, sudden shocks due to blasting, or forge-hammer action and the like may momentarily decrease or nullify its shearing resistance. It is difficult, however, to establish an exact numerical criterion for the minimum densities which are compatible with safety. It can only be stated at present that no danger of liquefaction is to be expected if the sand is so dense that its natural void ratio lies well below the value of e_{cr}. If its density is insufficient to meet this requirement, then a suddenly induced shearing displacement may produce a tendency toward a decrease of volume, which will set up for a few moments excess pore pressures u, since the excess water will be unable to escape instantaneously from all the voids of the saturated sand mass. Therefore the shearing strength of the mass of sand will be decreased in accordance with Eq. (7-14), so that with an increased value of u (for saturated sands $c = 0$), liquefaction may result (Art. 8-11). Full-scale field-test measurements under conditions simulating shock waves of intensities corresponding to actually possible values are needed to establish possible limit values of the resulting transitory excess pore pressures u compatible with stability.

7-17. The Ultimate Strength of Sands as a Function of Their Density. Figure 7-27 gives the results of shear tests performed with so-called Ottawa sand, 20 to 30 mesh, at different densities. This sand is used for standard-type cement tests (see ASTM Standard C190-44) and is of a

fairly uniform composition and has rounded grains. It may be seen that the angle of internal friction ϕ of the sand is directly dependent on the sand density and increases with it. A negative value of the initial relative density D_d was obtained with the help of bulking, by placing the sand in the shear boxes in a moist condition without compacting it at all (Art. 3-5).

The controlled-stress-type tests illustrated by this diagram were performed as a part of a cooperative research study sponsored by the Committee D-18 of the ASTM. Results very similar to those of Fig. 7-27

Curve No	ϕ	n	e	D_d	w
1	39°	31%	0.45	100%	Dry
2	35°	35%	0.54	62%	6%
3	33°	41%	0.69	0%	Dry
4	30°	47%	0.89	-83%	6%
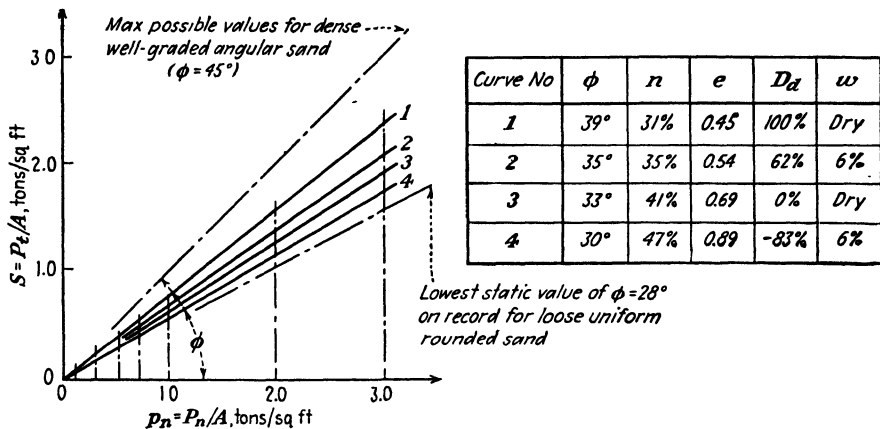
FIG. 7-27. **Effect of sand density on its shearing strength. Direct-box shear tests on standard Ottawa sand.** (*Soil mechanics laboratory, Princeton University,* 1938.)

were obtained at Columbia University with the same type of sand by means of controlled-strain-type tests, as reported by Burmister (Ref. 51, 1939).

Greater density thus means better interlocking and hence greater shearing strength. The test data given in Fig. 7-27 show that the increase of shearing strength due to interlocking is directly proportional to the normal pressure applied.

The direct relationship between the density of a sand and its laboratory angle of internal friction ϕ has been established by numerous tests in different localities. There is no evidence that under static conditions in the field the actual angle ϕ would be any different from the laboratory value. The lowest static values of ϕ to be recorded for any sand by triaxial or direct-box shear tests equal 28°, the highest 45°, depending on the absolute density of the sand. Values up to ϕ = 60° have been obtained by means of double-ring shear tests on sand, but this appears to indicate jamming of grains in this type of apparatus.

The angle of internal friction ϕ is essentially the same for a completely

dry sand and for a fully submerged sand. Engineering manuals of some 20 years ago frequently prescribed 20 to 30 per cent lower values of ϕ for submerged sands, as compared with the dry condition. This differentiation is not warranted and appears to have been based not on actual tests, but on observations of the angle of repose of natural slopes in the field. Wave action and sometimes seepage forces exerted by percolating rain water tend to flatten out somewhat the slope of banks at the free-water level [see Fig. 5-6(*C*)], thus leading to the incorrect assumption of lower ϕ values in the submerged condition.

In this connection it should further be noted that a natural slope of sand, by its very nature, cannot restrict at its surface the expansion of sand, which is associated with the rolling of grains over each other, and which is restricted in the interior of a dense mass of sand by the interlocking of the individual grains. For this reason the angle of repose α_R, as defined by Fig. 7-5, cannot reflect the changes of density of the entire sand mass in the same manner in which this is done by the angle of internal friction ϕ, as defined by the preceding paragraphs.

7-18. The Tensile and "Beam" Strength of Sands. When the potential shearing strength of a sand is rendered effective by confining pressures, the sand will behave essentially like a solid body. Under such conditions sand has "beam" strength and will resist bending. This can be demonstrated in the laboratory by an experiment illustrated in the two photographs of Fig. 7-28. A football rubber bladder is filled with sand. When a suction pump is connected to the bladder, a partial vacuum is created inside. The unbalanced excess of external air pressure against the rubber of the bladder presses the sand grains together and makes the whole sand mass feel solid to the touch. In this condition, as shown in Fig. 7-28(*A*), the sand-filled rubber bladder becomes a beam by virtue of the prestressing to which it is subjected and will support without visible deflection a concentrated 15-lb load at its center. However, as shown in Fig. 7-28(*B*), the sand "beam" will immediately collapse under the loading applied, once the suction pump is disconnected from the football bladder. It should be noted that the "beam" strength illustrated by Fig. 7-28(*A*) was developed as a result of an all-round pressure not exceeding 1 atm, or approximately 1 ton per ft^2. Assuming 105 lb per ft^3 for the unbuoyed weight of a soil, and 62 lb per ft^3 for its buoyed weight, we find that an effective vertical pressure σ_1 approximately corresponding to 1 atm would be exerted by the weight of only 19 ft of soil above the free-water level or by 33 ft of submerged soil.

The corresponding lateral pressure σ_3 within a mass of sand at these depths is, however, dependent on a number of variables and will usually not exceed 0.4 or 0.5 of σ_1 (Art. 10-9). Thus the conditions illustrated by

Fig. 7-28 are hardly ever exactly reproduced in nature within a mass of sand. This experiment therefore serves only for a qualitative demonstration of the transformation of a confined sand into a solid body, and it cannot be used for any quantitative evaluations of "beam" strength.

The *vacuum* method of triaxial testing of sands is based on a similar arrangement and has the advantage of not requiring any liquid-filled pressure chamber of the type needed for conventional tests, as illustrated by Fig. 7-10. The confining pressure σ_3 is then equal to the drop of

(A) (B)
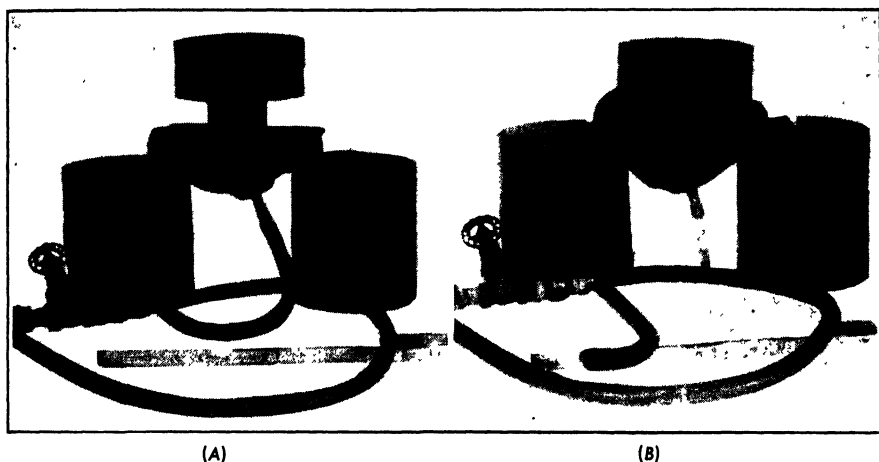
FIG. 7-28. Simple experiment illustrating the properties of sand in a confined and loaded condition. (*Soil mechanics laboratory, Princeton University,* 1945.)

atmospheric pressure inside of the rubber cylinder, which is produced by a suction pump and is measured by a pressure gage.

Partial saturation by capillarity may give a sand mass some slight apparent cohesion (Art. 7-4) and therefore some slight tensile strength.

Shearing Characteristics of Clays

7-19. Effect of Adsorbed Ions on the Shearing Strength of Clays. Figure 7-29 illustrates the results of torsional tests performed by Sullivan (Ref. 332, 1939) on cylinders of the same clay but with different ions adsorbed on the surface of the particles of the original clay mineral. The natural or *raw* clay was first transformed into a hydrogen (H) clay by removing all the originally adsorbed cations. It was then divided into nine specimens, each of which was treated with a different solution containing one type of cation. The results of the tests show the considerable influence which the nature of the adsorbed ions has on the torsional resistance and therefore on the shearing strength of the same clay, the mineral composition of which has not been changed. For instance, at

the same free-water content, the specimens of the clay with adsorbed iron (Fe) or aluminum (Al) cations had a shearing strength almost double that with sodium (Na) cations. This is to be attributed to the adsorbed films of semisolid water, which are apt to be particularly thick in the case of the Na cations (Art. 3-5). In the stiffly plastic consistency range, in which Sullivan performed his experiments, this circumstance leads to lower shearing strengths of the Na and Ca clays at the same free-water content. The reverse relationship, however, will be observed in the semiliquid range, since it was found by Winterkorn and Moorman (Ref. 436, 1941) that the Na clay of the same original mineral composition had higher liquid-limit values as compared to the same clay treated by other less hydrophilic cations.
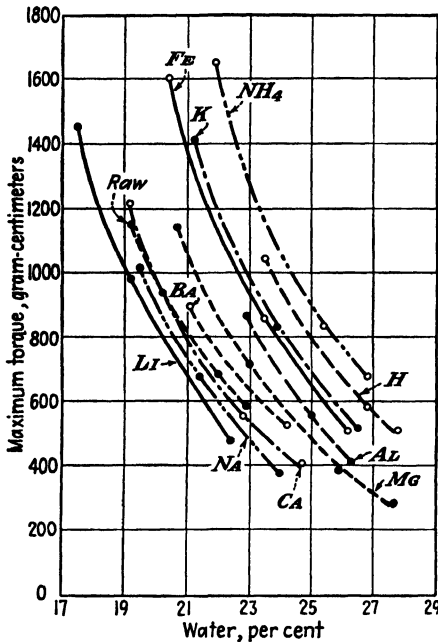
FIG. 7-29. Effect of changes in the nature of adsorbed cations on the shearing strength of the same clay. Torsional shear tests. (After Sullivan, Ref. 332, 1939.)

Sullivan's tests were performed in connection with practical problems of the ceramic industry in a search for means to facilitate the handling of clays in the stiffly plastic range of consistency. Studies of the same kind, but with the opposite objective, are of direct practical importance for civil engineers specializing in soil stabilization. A general understanding of the factors involved is necessary for all civil engineers, if only to show the need for considering supplementary factors when making efforts to establish simplified and universally valid relationships between such values as the liquid limit and the shearing strength of a soil (Ref. 312). Such relationships may be strongly affected not only by the geological but also by the pedological history (Art. 2-8) of the particular deposit.

7-20. Effect of the Preconsolidation Load on the Shearing Strength of a Saturated Clay. Experiments show that if a natural clay is completely remolded under addition of water to a semiliquid consistency, that is, to a water content exceeding the liquid limit, and then several specimens of the material are reconsolidated under pressures of varying intensity and are subsequently sheared off, the shearing stresses at failure

will fall on approximately the same straight line OB, passing through the origin O, as shown in Fig. 7-30. The slope of this line, that is, the angle ϕ_1, conventionally termed the angle of internal friction, will vary with the rate of shearing, as will be shown in Art. 7-21.

However, if the same semiliquid material is first allowed to consolidate in all shear boxes under a given normal stress, say 3 or 4 tons per ft², and is sheared off under smaller unit stresses of 3, 2, and 1 tons per ft², respectively, then the points would lie on approximately straight lines FE and DC. According to Hvorslev (Ref. 180, 1937), the angle ϕ would have the same value in both cases and could be considered to represent the true
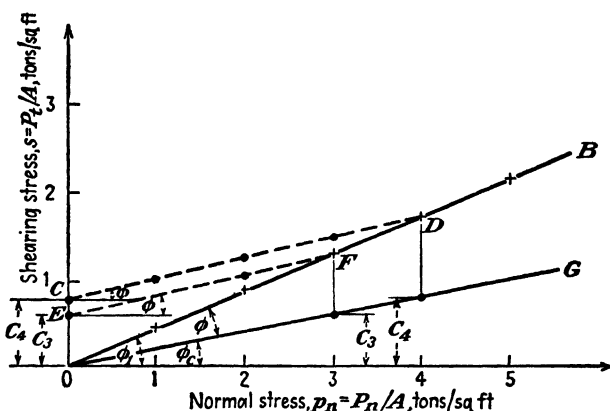
FIG. 7-30. Effect of the preconsolidation load on the shearing strength of remolded clays, as determined by means of direct-box shear tests. (After Hvorslev, Ref. 180, 1937.)

angle of internal friction. The values of the cohesion c_3 and c_4, determined in the conventional manner, as shown in Fig. 7-30, when plotted against the corresponding preconsolidation loads of 3 and 4 tons per ft², would also lie on a straight line GO through the origin forming the angle $\phi_c = \phi_1 - \phi$ with the horizontal. Results of this kind led to the formulation of the so-called Krey-Tiedemann criterion for failure, which represents an elaboration of the Coulomb criterion [Eq. (7-1)], and which is expressed by the following equation:

$$s = p_c \tan \phi_c + \sigma \tan \phi \tag{7-18}$$

Similar results were reported by Hogentogler (Ref. 177, 1937), except that the angle ϕ was found to increase somewhat with the value of the preconsolidation load (Art. 6-4), suggesting that with increasing pressures the relative importance of cohesion, as conventionally defined, decreased in comparison with that of friction. It is likely that the difference between these findings and those reported by Hvorslev is due to unequal

opportunities for sample expansion and unequal amounts thereof after the decrease of the maximum preconsolidation load. As explained under Art. 7-5, with reference to Fig. 6-5, the expansion of a fully submerged specimen under decreasing pressure increases rapidly at low pressures. This is particularly pronounced if the preconsolidation load p_c was high.

The Krey-Tiedemann failure criterion, as expressed by Eq. (7-18), does not take into account these additional important factors. Nevertheless, it represents an important milestone in the development of engineering thought in this field, since it abandons Coulomb's concept of the cohesion having a constant value for a given material and indicates that in the case of clay soils the cohesion is strongly influenced by the maximum preconsolidation load (Art. 6-4) to which it had been subjected during its past geological history.

This finding somewhat blurs the conventional clear-cut and simple separation between friction and cohesion in clays. The true cohesion is generally attributed to electrostatic forces of attraction between clay particles at their boundaries in contact with each other. Increasing external pressures bring these particles closer together and thereby apparently increase the effectiveness of these electrostatic forces of attraction and the "cohesion" which they produce, possibly in part by mobilizing friction between the clay particles. Thus both friction and cohesion of a clay actually depend on external forces, although to a different extent, and, in the final analysis, both may depend on the friction between the clay particles. The wisdom of trying to determine in practice a clear dividing line between these two conventional components of the shearing strength of a saturated clay therefore becomes very questionable.

The above investigations paved the way for the present trend toward abandoning oversimplified past attempts to determine friction and cohesion separately for cohesive soils, and recognizing instead that the over-all shearing strength is what matters for the solution of practical problems, and that this over-all shearing strength is directly dependent on the density and therefore on the water content which the particular saturated clay under investigation has at the time of failure (Art. 7-23).

7-21. Numerical Evaluation of the Effect of the Rate of Shearing and of the Type of Specimen Drainage. As explained earlier (Arts. 7-9 and 7-14), quickly performed (Q) tests on saturated clays at the same water content give a value of $\phi = 0$. Consolidated quick (Q_c) tests give values of ϕ ranging from 12° to 20°. Slow (S) tests give values of ϕ close to 30° for almost all clays. The variations in the value of ϕ appear to be primarily a question of the degree of consolidation and of the resulting changes in water content of the clay which can occur prior to failure.

Figure 7-31 gives the results of a series of consolidated tests, sheared at seven different rates. The maximum value of $\phi = 29°40'$ was obtained when the shearing stresses were increased so slowly that failure occurred after 96 hr. This can be taken as the value of an S test. The shearing resistance established by a test which took 4 hr (240 min) was only 4 per cent smaller, indicating that most of the additional consolidation induced by shearing deformation was completed by that time. With a further decrease of the time of the test the values of ϕ decreased along a parabolic curve, and for a 1-min test duration equaled approximately 60 per cent ($\phi = 19°$) of the value established by the S test.

FIG. 7-31. Effect of rate of application of the shearing stress on the ultimate strength of a completely remolded sample of Detroit clay during consolidated drained box-type direct shear tests. (From Tschebotarioff, Ref. 374, 1939.)

The tests illustrated by Fig. 7-31 were performed on a rather lean clay from Detroit with a liquid limit $w_L = 36$ per cent and a plasticity index $I_p = 18$ per cent. A richer and therefore less pervious clay would take a longer time to consolidate and to reach its maximum value of ϕ during an S test. This would also be the case for the same material within a large mass of soil, since the time required to reach a certain percentage of consolidation increases with the square of the thickness of the layer (Art. 6-7). Therefore in many cases in the field the behavior of a large mass of clay should correspond to the action of undrained clay specimens in the laboratory, that is, it should be in accordance with the results of tests conducted in a manner preventing a decrease of the water content during shear.

Tests performed with undrained clay specimens, however, indicate that in such cases the rate of shear has a reverse effect on the ultimate strength as compared with drained clay specimens. The plastic or viscous flow effects appear to dominate the situation in such cases and to reduce the shearing strength of a clay with time. For instance, the results of M.I.T. tests on remolded Boston clay, reported by Rutledge (Ref. 296, 1947), indicate a drop of 16 per cent in the strength of a clay when the induced velocity of the shearing strain was decreased to one-thousandth of the original value. This may be one of the reasons why in structures in the field failures due to rupture in shear do not always occur immediately, but some time after completion of the construction (Art. 9-10).

The attempt was made by Housel (Ref. 178, 1943) to take into account the probability of strong viscous or plastic flow effects under such conditions. To that end, undrained slow controlled-stress tests were performed in the double-shear ring device illustrated by Fig. 7-7. It was
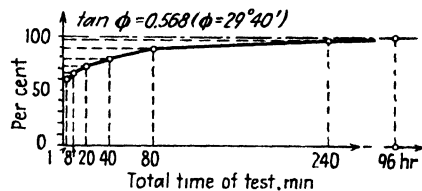
found that the plastic flow effects became more and more pronounced with increasing intensity of shearing stresses. Deformations finally became progressive, and the soil continued to yield without any increase of load until failure occurred. The shearing resistance at which progressive yielding of the soil begins was determined graphically and was considered to represent the actual strength of the clay. Comparisons with the results of field measurements, however, indicated that the strength values thus obtained were too low (Ref. 178). A. E. Cummings (Ref. 97, 1943), pointed out that these values represented the elastic limit or the yield
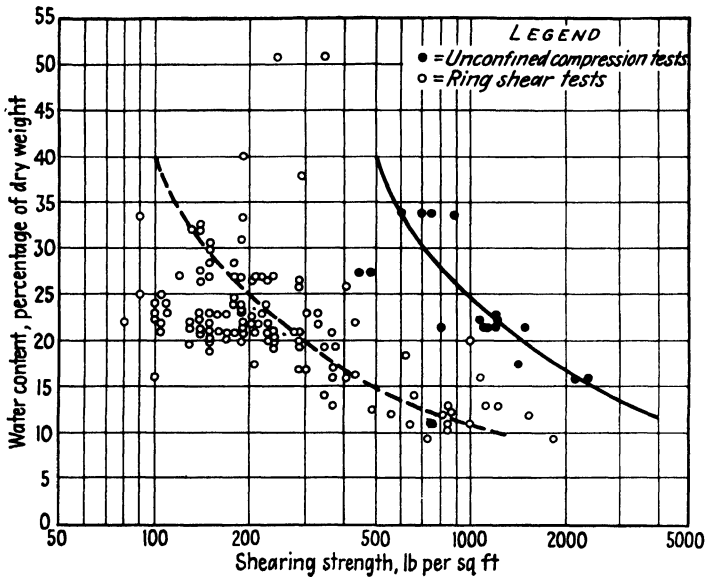
FIG. 7-32. Comparison of the shearing strength of the same clay as obtained by means of the unconfined compression tests to the shearing strength, as obtained by means of the direct-ring shear test. (*After A. E. Cummings, Ref. 97, 1943.*)

point of the clay, and not its ultimate strength, and that the unconfined compressive-strength test gives better agreement with field observations. Figure 7-32 gives a comparison of the shearing strength of a clay from a site near Indiana Harbor, Indiana, as determined from unconfined compressive-strength tests and Eq. (7-17), and as evaluated by means of the undrained slow double-shear ring tests. It may be seen that on the average the ultimate shearing strength, as represented by one-half of the unconfined compressive strength, is approximately five times greater than the *yield-point* strength determined from the slow double-shear ring tests. For other clays the difference may be smaller. The average value of the ratio may be taken as four.

7-22. Unconfined Compression Tests. Determination of the Sensitivity of Clays to Remolding. Comparisons between the results of different types of shear tests and of analyses of various shear failures of clay slopes led Terzaghi (Ref. 361, 1943) to express the belief that the closest agreement between the actual shearing strength at failure in the field and laboratory values could be obtained by the use of one-half of the unconfined compressive strength, in accordance with Eq. (7-17). This equation expresses the assumption that the compressive strength of a saturated clay is equal to twice the value of its cohesion c, where the angle of internal friction is taken to be zero ($\phi = 0$). Numerous later observations and studies have confirmed in a general way, with some limitations (Art. 7-23), the over-all correctness of Terzaghi's finding.

In some cases the inclination of the planes of failure of saturated clay specimens subjected to an unconfined compressive test is somewhat steeper than 45°, thereby indicating, in accordance with Eq. (7-10), that the angle of internal friction ϕ is greater than zero. This is, however, of no practical importance, since according to the suggested procedure and Eq. (7-16),

$$s = \frac{q_u}{2} = c \tan\left(45° + \frac{\phi}{2}\right) \tag{7-19}$$

Thus, by taking in all cases the shearing resistance as being equal to one-half of the unconfined compressive strength, there is no separate determination of the cohesion and of the friction. Both values are included in the over-all shearing strength of the clay, in accordance with Eq. (7-19). The somewhat arbitrary nature of the conventional separation between the terms friction and cohesion has been demonstrated by the preceding articles. As shown by Eq. (7-19), the use of Eq. (7-17) as a criterion of the shearing strength may be equivalent to the tacit abandonment of attempts to separate these two values for practical use. The review of extensive research on triaxial shear testing led Rutledge (Ref. 296, 1947) to take a further step in the same direction. This will be outlined in Art. 7-23 in connection with a discussion of the merits of the unconfined compression test.

An important practical routine application of this test will be pointed out first, that is, its use for the determination of the so-called sensitivity of a clay, by which is meant the degree of its weakening as a result of a breakdown of its structure (Art. 4-1) by remolding. Terzaghi suggested (Ref. 363, 1944) that the sensitivity S of a clay be defined as the ratio of the unconfined compressive strengths in the undisturbed and in the remolded conditions.

$$S = \frac{q_u}{q_{ur}} \tag{7-20}$$

Most naturally deposited and really undisturbed clays exhibit brittle types of failure at relatively small strains (Art. 7-10). Remolding usually increases the strain at failure of sensitive clays up to the ultimate value of 20 per cent, which characterizes fully plastic failure. In some cases it may be advisable to base the definition of the sensitivity of clays on the ratio S' of the strengths of the undisturbed and of the remolded samples *at equal strains*, as proposed by Tschebotarioff (Ref. 380, 1946) and by Tschebotarioff and Bayliss (Ref. 385, 1948), in accordance with Fig. 7-33 and the following equation:
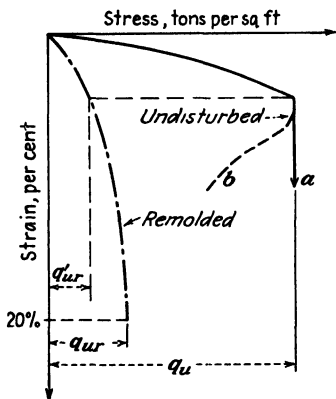
FIG. 7-33. Determination of the sensitivity of a clay by means of an undisturbed and of a remolded unconfined compression test on the same specimen. Curve a—controlled stress; curve b—controlled-strain type of test. (*After Tschebotarioff and Bayliss, Ref. 385, 1948.*)

$$S' = \frac{q_u}{q_{ur}'} \tag{7-21}$$

The direct use of Eq. (7-21) is predicated on the construction of stress-strain diagrams of the type illustrated by Fig. 7-33 and is therefore more time-consuming than the use of Eq. (7-20). However, the approximate value of S' may be estimated from Eq. (7-20) and the following data, based on the strain ϵ_f corresponding to failure in the undisturbed condition:

If $\epsilon_f = 5\%$, then $S' = 2.50S$ to $3.00S$
$\epsilon_f = 10\%$, then $S' = 1.30S$ to $2.00S$
$\epsilon_f = 15\%$, then $S' = 1.05S$ to $1.30S$
$\epsilon_f = 20\%$, then $S' = S$

It should be noted that in the case of controlled-strain tests q_u should refer to the peak value and not to the strength at final failure.

On the basis of data reported by A. Casagrande (Ref. 61, 1932), it was originally believed that all clays are strongly weakened by remolding. Tests on Egyptian clays reported by Tschebotarioff (Ref. 369, 1936), however, showed that some clays were even strengthened by remolding. Buisson (1936), in his discussion D-29 of Ref. 369, reported similar results with some French clays, and other data have become available from other localities, showing that a generalization of damaging effect of remolding is unwarranted. This point is of considerable practical importance (see Art. 15-2).

7-23. The Strength of Clays as a Function of Their Water Content. Tests reported by Tschebotarioff (Ref. 384, 1948) and illustrated by Fig. 7-34 showed that some clays increase their compressive strength in an almost direct proportion to the preconsolidation pressure. The material

used for these tests was a silty red-colored clay from Princeton, New Jersey, a product of in-situ weathering of shale, with a liquid limit $w_L = 30$ per cent and a plasticity index $I_p = 7$ per cent. It was remolded under addition of water to a consistency corresponding to 3 blows on the liquid-limit device. Curve III shows the results of tests on specimens reconsolidated in the laboratory, and curves IV, V, and VI the results of tests on specimens extracted from a large mass of soil reconsolidated in an 18- by 13- by 9-ft tank. All show the same general trend, with an approximate value of $\tan \phi_q = q_u/p$ varying from 0.50 to 0.42. If the shearing strength s is taken as one-half of this ratio q_u, a variation of the
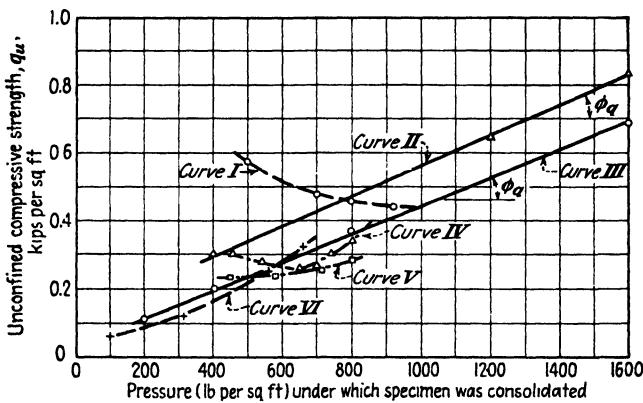
FIG. 7-34. Relationship between consolidation pressure and the unconfined compressive strength of a clay completely remolded with addition of water and then reconsolidated in the laboratory. (*Tschebotarioff, Ref. 384, 1948.*)

ratio s/p from 0.25 to 0.21 is possible. The slight decrease is probably due to some capillary drying pressures on the outer faces of the specimen, producing an effect similar to the application of a slight constant value of σ_3 for all of the tests. The lower values of the above ratios are therefore more reliable. Curves I and II refer to the results of tests with a mixture of 50 per cent of the clay which was used for the preceding tests with 50 per cent clean sand. Surface drying occurred in the tank (curve I).

Skempton (Ref. 312, 1948) computed a ratio $(c/p)_n$ for naturally consolidated clays from several localities, where c is the cohesion, or shearing strength, taken as one-half of the compressive strength, and p is the weight of the overburden. When plotted against the liquid limit, this ratio was found to show a trend to increase from values of 0.18 for $w_L = 40$ per cent to values of 0.38 for $w_L = 110$ per cent. Subject to the reservations given in Art. 7-19, these field values are in approximate agreement with the s/p ratio computed above from the laboratory data of Fig. 7-34. A high

value of the liquid limit indicates a high percentage of very fine particles of colloidal size and therefore a very large total effective surface area of the particles per unit of volume of the soil. The electrostatic forces of attraction upon which the cohesion depends should, therefore, also increase somewhat with the value of the liquid limit.

It should, however, be noted that the unconfined compressive strength of natural clays frequently has been found not to increase with depth, but to remain at a constant value. Terzaghi (Ref. 359, 1941) described
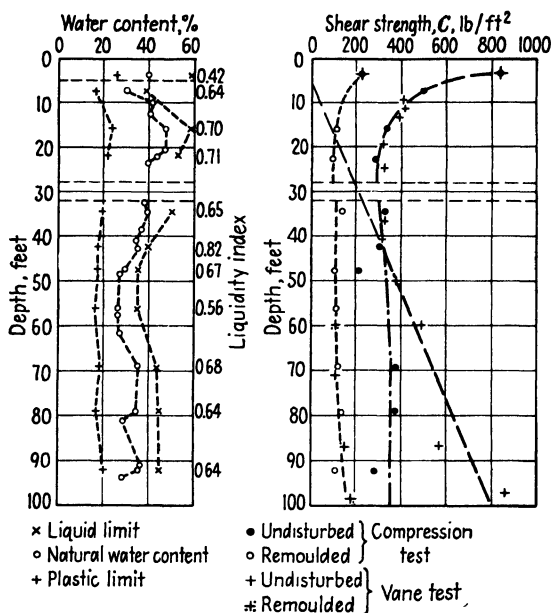
FIG. 7-35. Comparison of the shearing strength of a natural clay deposit, as determined by laboratory unconfined compression tests and as obtained by vane torsional tests in situ. (*After Skempton, Ref.* 312, 1948.)

several such cases in which the water content as well as the unconfined compressive strength had approximately the same value for a considerable depth of a fully submerged clay never exposed to drying in the past, where its liquid limit also did not vary to any extent with depth. A similar case investigated in England by Skempton (Ref. 312, 1948) is illustrated by Fig. 7-35. The ground-water level at the time of the borings was at a depth of approximately 5 ft, which accounted for the high strength of the samples down to a depth of 10 ft, since drying is equivalent to compressing a sample by high loads (Art. 4-8). Between the depths of 15 and 45 ft the shearing strength, as determined in the laboratory by compression tests, agreed quite well with the values obtained by means of the rotating-

auger-vane test in situ (Art. 7-12). Below the depth of 45 ft the compressive strength, and to a slightly lesser degree the water content, remained unchanged, whereas the in-situ strength, as determined by vane tests, increased slightly with depth. This cannot be attributed to any defects of the vane-test method, since both the laboratory and the field values of the test on remolded clay agreed very closely for the entire 100-ft depth of the test. Even more pronounced differences were obtained in Sweden by Lyman Carlson-Cadling (Refs. 58, 1948, and 55, 1950). The vane test gave shearing strengths which in two cases were in good agreement with values computed from actual landslides. These values, at depths smaller than 25 ft, were some 50 per cent, and at greater depths, were some 150 per cent higher than the values obtained by means of laboratory compression tests on undisturbed samples. The field cone-penetration test gave intermediate values only slightly higher than the laboratory ones. These large differences may perhaps be attributed to the difficulties of sampling Swedish clays (Art. 12-7). Some reports indicated that triaxial Q_c tests gave values of the shearing strength which exceeded the values obtained in the field by the vane test.

All these data serve to confirm the view that the shearing strength, when determined in the laboratory and taken as one-half of the unconfined compressive strength, comes reasonably close to the actual strength of the clay in the field, so long as the clay has not been remolded by sampling operations or did not expand owing to any causes after removal from the soil. Reconsolidation of an "undisturbed" sample to overburden pressures in the triaxial apparatus gives it a slightly greater density as compared with the original values, and therefore a greater strength. The findings of Rutledge (Ref. 296, 1947), summarized in simplified form in Fig. 7-36, lead to the recognition that the clay density is the governing factor in this respect. Curve A of Fig. 7-36 represents the relationship between the pressure and the water content of a clay obtained by a consolidation test (Art. 6-3). Thus curve A is a standard-type void ratio–pressure curve (compare with Fig. 6-5). Curve B is a similar void ratio–pressure curve, but obtained by means of triaxial tests, the water content being plotted not against the consolidation pressure but against the compressive strength $(\sigma_1 - \sigma_3)$ at failure. Point 1 of the curve corresponds to the unconfined compressive strength q_u as determined in the laboratory. Point 2 is determined from curve B in the same manner in which the preconsolidation load is determined on standard void ratio–pressure curves (Art. 6-4). Point 3 represents the maximum possible value of q_u of the clay in situ at the natural water content, and the distance d gives the maximum possible range of weakening and of the decrease of q_u because of normal expansion *not* due to remolding during

and after sampling. The additional consolidation and corresponding decrease of the water content during a consolidated quick (Q_c) test increases the compressive strength of the clay sample well above any actually possible in-situ value at unchanged water content. A slow (S) test does this to an even greater extent.

Thus once the curve B for a certain type of clay is established, the knowledge of the water content of the clay under a given loading should
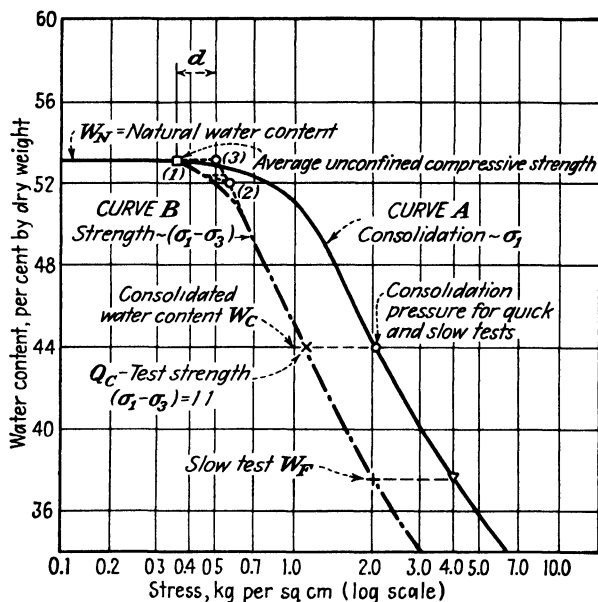
FIG. 7-36. Comparison of the water content of a natural undisturbed clay at the end of consolidation tests and at the end of unconfined compression tests and of consolidated quick and consolidated slow triaxial shear tests. (*After Rutledge, Ref. 296, 1947.*)

be sufficient to determine its over-all shearing strength (Ref. 296). The implementation of these findings in routine investigations of practical design problems is, however, still a matter for further research.

Recommended Practice of Shearing-strength Determination for Design Problems

7-24. Clean Sands. To date there is no sure way of extracting a really undisturbed sample of sand from a deep borehole without changing its density (Art. 12-7). At the same time, it has been shown by research that the angle of internal friction of a sand is primarily affected by its density and varies within the maximum limits of 28° to 45°, the usual range being 30° to 40° (Art. 7-17).

Since it is very difficult to reproduce in the laboratory the exact density of a natural layer of sand deep below the surface, there is no point in carrying out laboratory shear tests with sand in connection with routine investigations, unless they are performed for projects of major importance, such as large dams, where the desired density of sand is achieved by compaction above ground level.

In this respect the author concurs with the following recommendations of the 1946 U.S. Engineer Corps conference on Shearing Resistance of Soils (Ref. 296):

> It was emphasized that, in general, it is better to estimate the shearing strength values for sands than to perform a limited number of tests on a large number of samples. It was recommended that for such estimates an angle of internal friction of 30° be used for loose sands and an angle of internal friction of 35° be used for dense sands where the materials consist of bulky grains. If higher values are used they should be justified by a comprehensive investigation.

As shown earlier (Art. 7-17), the values of $\phi = 30°$ for loose sands and $\phi = 35°$ for dense sands are conservative and safe in most cases of static loading. The simplest and most effective way of estimating the in-situ density appears to be by means of penetration tests (Art. 12-9), which permit the classification of a sand as loose or dense.

7-25. Saturated Clays. The unconfined compression tests (Art. 7-22) on fully undisturbed samples (Art. 12-7) appear to give the best agreement with the actual in-situ performance of a natural deposit of saturated clay. Opportunities for the expansion of the sample should be reduced to a minimum. One method of doing this is to perform the compression test on the site of the boring immediately after the extraction of the sample. The British Building Research Station has developed a portable unit for the performance of such tests. It is of the controlled-strain type and automatically registers the stress-strain curve on a sheet of paper. This testing unit was described by Cooling (Ref. 85, 1946) and can be obtained in the United States.* Parallel unconfined compression control tests and other classification tests should be run upon delivery of the samples to the laboratory. In view of the frequent and considerable strength variations from sample to sample (see Fig. 7-32), a sufficiently large number of samples should be obtained and tested in order to provide a representative average. This average should not be based on the ultimate strength of samples from layers of different rigidity, since this might lead to *progressive failure* of the whole soil mass. Instead, one should use the average of the resistances of all samples corresponding to the unit strain at which the more brittle samples reached the peak of their resistance (Fig. 7-14).

* For instance, from Soil Testing Services, Evanston, Illinois.

The rotating-auger-vane tests in situ (Arts. 7-12 and 7-23) appear to have considerable promise. Although still in the research stages of development, they should be performed whenever at all possible simultaneously with unconfined compression tests.

Triaxial shear tests appear justified for routine investigations only under very special circumstances, for instance, in the case of naturally overconsolidated stiff-fissured clays (Art. 2-5), which are liable to fly apart in an unconfined compression test even under a slight pressure. A reasonable confining pressure σ_3 is essential for the investigation of such clays. Triaxial tests are also useful in cases where the clay deposit is liable to receive appreciable additional consolidation as a result of later construction operations, for instance, that due to its loading by a heavy fill. A comprehensive investigation to obtain data of the type illustrated by Fig. 7-36 is then indicated. A detailed description of the techniques of such an investigation is beyond the scope of this book.

Direct single-shear box-type tests can also be sometimes used for similar purposes, but the accurate control of water-content changes is more difficult than in the triaxial tests. The torsional-ring single-shear test (Art. 7-5) is essentially an instrument for special types of research only. The double-shear direct-ring test (Art. 7-5) is sometimes claimed to have the advantage that the clay specimen does not have to be transferred in the laboratory from the sampling-tube liner to the testing device. This is a somewhat questionable feature, since the use of special ring liners in a sampler necessarily increases the over-all wall thickness of the sampler and its area ratio (Art. 12-7), thereby increasing the danger of remolding and weakening the clay sample.

7-26. Other Types of Soils. The problems connected with the determination of the shearing strength of two extreme types of soils, clean sands and saturated clays, have been clarified to a considerable extent. Much less has been done concerning the numerous intermediate types of soils.

Specifically, much remains to be learned concerning the various possible mixtures of sand and clay. There is sometimes a tendency (Ref. 125) to treat as a sand any soil which in a consolidated quick (Q_c) test gives a value of $\phi > 20°$ and to neglect its cohesion in computations of shear strength, and to treat any material with $\phi < 20°$ in a Q_c test as a clay and to rely only on its cohesion. Such a division is entirely arbitrary, and much further combined field and laboratory research is needed before any simple and definite rules can be set up on this point.

Partially saturated clays, because of the high compressibility of the entrapped air in the voids, are known to respond much quicker than fully saturated clays to applied pressure and to increase their shearing strength accordingly. There is hardly any difference between the results of Q and

Q_c tests of such soils, and their laboratory shearing strength is strongly influenced not only by their water content but also by the intensity of the confining lateral pressure σ_3 (Ref. 296).

Gravels have sometimes been reported to have angles of internal friction higher than 45° (Ref. 296). This may be due to insufficient opportunities for expansion in too small testing devices. Until further research data become available on the point, gravels should be handled similarly to sands (Art. 7-24).

Sands with a high content of mica may have lower shearing strengths than indicated earlier (Art. 7-24). They should be made the subject of comprehensive investigations.

No simple testing rules can be set up for the time being in connection with the above and other similar cases. The advice of specialized soil mechanics research laboratories should be sought for such problems, in accordance with the general procedures recommended for soil investigations (Art. 12-1).

Practice Problems

7-1. What will be the theoretical inclination of failure cracks in a mass of soil subjected to vertical loading if the angle of internal friction has the following values: (a) $\phi = 0$, (b) $\phi = 20°$, (c) $\phi = 30°$, (d) $\phi = 45°$?

Answer. According to Eq. (7-10), the angle formed by failure planes with the horizontal should be (a) $\theta_{cr} = 45°$, (b) $\theta_{cr} = 55°$, (c) $\theta_{cr} = 60°$, (d) $\theta_{cr} = 67.5°$.

7-2. Estimate the approximate shearing resistance at failure of a loose sand per unit of area at a depth of 20 ft below the ground surface (water level 5 ft below ground surface). The failure is to be induced by a gradual yielding of the lateral support of the sand and a corresponding reduction in the value of σ_3.

Answer. According to Art. 4-4, the effective unit weight of the loose sand above water level may be taken at 100 lb per ft³ and below the water level at 60 lb per ft³ Thus

$$\sigma_1 = 100 \times 5 + 60 \times 15 = 1{,}400 \text{ lb per ft}^2$$

According to Art. 7-24, the value of $\phi = 30°$ may be selected for the loose sand and, according to Eq. (7-12), the minimum value of σ_3, that is, its value at failure, will be

$$\sigma_3 = \sigma_1/\tan^2 (45° + 30°/2) = 0.333\sigma_1 = 467 \text{ lb per ft}^2$$

The pressure normal to the failure plane ($\theta_{cr} = 60°$), according to Eq. (7-6), will be

$$\sigma = 467 + \cos^2 60°(1400 - 467) = 700 \text{ lb per ft}^2$$

The shearing resistance at failure will be, according to Eq. (7-8a),

$$s = 700 \tan 30° = 404 \text{ lb per ft}^2$$

7-3. What will be the value of the least shearing resistance at failure of a sand under the general conditions of Prob. 7-2, except that the sand is denser, and its angle of internal friction is found to be (a) $\phi = 35°$, (b) $\phi = 40°$, (c) $\phi = 45°$?

Answer. Substituting the above values in the computations of Prob. 7-2, we obtain:

(a) $\sigma_3 = 0.271\sigma_1 = 380$ lb per ft²; $\sigma = 597$ lb per ft²; $s = 417$ lb per ft²
(b) $\sigma_3 = 0.217\sigma_1 = 304$ lb per ft²; $\sigma = 500$ lb per ft²; $s = 419$ lb per ft²
(c) $\sigma_3 = 0.172\sigma_1 = 241$ lb per ft²; $\sigma = 410$ lb per ft²; $s = 410$ lb per ft²

7-4. Three triaxial shear tests were performed with a certain type of sand. During the first test (*a*) the confining lateral pressure was $\sigma_3 = 0.20$ ton per ft², and failure occurred under a vertical pressure $\sigma_1 = 0.82$ ton per ft². During the second test (*b*) $\sigma_3 = 0.40$ ton per ft², and at failure $\sigma_1 = 1.60$ tons per ft². During the third test (*c*) $\sigma_3 = 0.60$ ton per ft², and failure occurred at $\sigma_1 = 2.44$ tons per ft². Draw the Mohr diagram for these three tests. Determine from that diagram the value of the angle of internal friction ϕ and the values of the shearing stresses τ_{cr} on the failure planes in each of these three tests.

Answer. A diagram similar to Fig. 7-12 is obtained. $\phi = 37°20'$.

(*a*) $\tau_{cr} = 0.24$ ton per ft² = 480 lb per ft²

(*b*) $\tau_{cr} = 0.48$ ton per ft²

(*c*) $\tau_{cr} = 0.72$ ton ft²

7-5. The results of rotational-auger-vane in-situ tests shown in Fig. 7-35 indicate an increase of the shearing resistance of the clay with depth below the depth of 40 ft. Compute the rate of increase of shearing resistance of that clay in terms of overburden pressure, that is, determine its angle of shearing resistance ψ on the basis of the values of shearing resistance obtained by the vane test, according to Fig. 7-35, at a depth of 40 ft ($s = 320$ lb per ft²) and at a depth of 97 ft ($s = 860$ lb per ft²). The approximate average saturated unit weight of the clay can be taken at 110 lb ft³.

Answer. From Eq. (4-7) and the saturated unit weight of 110 lb per ft³, assuming a value of the specific gravity of solids $G = 2.65$, we obtain the corresponding value of the void ratio $e = 1.17$. This, in conjunction with Eqs. (4-9) and (4-11), gives us a value of the buoyed effective weight of the clay of 47.6 lb per ft³. Therefore the increment of shearing stress between these two elevations is

$$\Delta s = 860 - 320 = 540 \text{ lb per ft}^2$$

and the increment of effective vertical pressure is

$$\Delta\sigma_1 = (97 - 40) \times 47.6 = 2{,}710 \text{ lb per ft}^2$$

Hence

$$\tan\psi = 540/2{,}710 = 0.20 \qquad \psi = 11°20'$$

References Recommended for Further Study

Fundamentals of Soil Mechanics, by Donald W. Taylor, Wiley, 1948, Chaps. 13, 14, and 15, pp. 310–405. Discussion giving supplementary points concerning the shearing strength and the shear-testing procedures of soils.

"Theories of Failure of Materials Applied to the Shearing Resistance of Soils," by P. C. Rutledge, *Proceedings of the Purdue Conference on Soil Mechanics*, pp. 191–204, 1940. Discussion of the maximum-stress, maximum-strain, maximum-shear, Navier, Mohr, constant-energy of distortion, and Brandtzaeg theories of failure.

"Review of the Cooperative Triaxial Shear Research Program of the Corps of Engineers," by P. C. Rutledge, Waterways Experiment Station, Vicksburg, Mississippi, April, 1947. Discussion of the findings concerning shear-testing procedures of sands and clays in the laboratory, and their summary.

"Vane Tests in the Alluvial Plain of the River Forth, near Grangemouth," by A. W. Skempton, *Geotechnique*, London, Vol. I, No. 2, December, 1948. Description of the techniques of the in-situ determination of the shearing strength of natural clays by means of the rotating auger vane; comparison of the results with laboratory values.

"Proceedings of the Conference on the Measurement of Shear Strength of Soils in Relation to Practice," *Geotechnique*, London, Vol. II, No. 2, December, 1950, and Vol. II, No. 3, June, 1951.

THE STABILITY OF VERTICAL CUTS AND OF SLOPES

8-1. Conventional Analysis of the Stability of Unsupported Vertical Cuts. Let us determine the limit conditions for the stability of an unsupported vertical cut of a height h, as shown in Fig. 8-1. At first the assump-
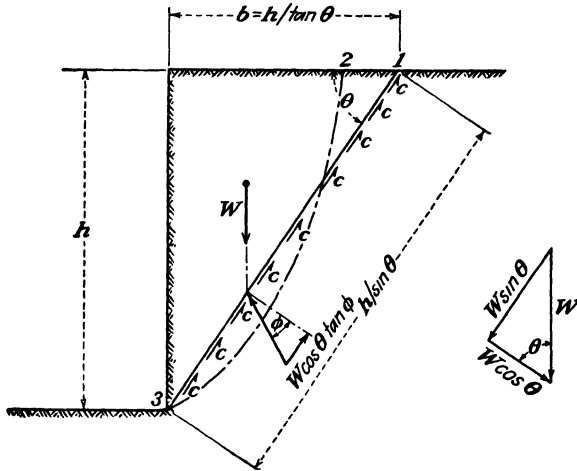
FIG. 8-1. Stability analysis of a vertical cut.

tion will be made that failure can occur only along plane surfaces, for instance, along the surface 1-3 forming the angle θ with the horizontal. The length of the line 1-3 will be $h/\sin\theta$. The weight W per foot depth of the sliding wedge thus formed is

$$W = \frac{\gamma h^2}{2 \tan \theta} \tag{8-1}$$

where γ is the effective unit weight of the soil, according to Eqs. (4-6) to (4-11). The component of the forces of gravity tending to produce sliding will be $W \sin \theta$. It will be resisted by the cohesive and frictional forces

along the surface 1-3. Thus at failure,

$$W \sin \theta = \frac{ch_{cr}}{\sin \theta} + W \cos \theta \tan \phi \tag{8-2}$$

or

$$\frac{\gamma h_{cr}^2}{2} \frac{\sin \theta}{\tan \theta} - \frac{\gamma h_{cr}^2}{2} \frac{\cos \theta \tan \phi}{\tan \theta} = \frac{ch_{cr}}{\sin \theta}.$$

$$\frac{\gamma h_{cr}^2}{2} (\sin \theta \cos \theta - \cos^2 \theta \tan \phi) = ch_{cr} \tag{8-3}$$

It is apparent from Eq. (8-3) that a vertical cut must have a limit height, called the *critical height*, which is directly proportional to the cohesion c of the soil. The cohesive resistance to sliding is proportional to the first power of the height h, whereas the forces which induce sliding, after deduction of the frictional resistance, are proportional to the second power of the height h of the cut and therefore increase more rapidly than the resistance as the height h increases.

The limit height h_{cr} will reach its minimum value when the expression $\sin \theta \cos \theta - \cos^2 \theta \tan \phi$ is at a maximum. This expression is identical with the denominator of Eq. (7-9), which, as has already been shown by the derivation of Eq. (7-10), reaches a maximum when $\theta_{cr} = 45° + \phi/2$. By substituting this value, as shown by the derivation of Eq. (7-10*a*), we obtain

$$\sin \theta_{cr} \cos \theta_{cr} - \cos^2 \theta_{cr} \tan \phi = \frac{1}{2 \tan \theta_{cr}}$$

Substituting this value in Eq. (8-3), we obtain

$$\frac{\gamma h_{cr}^2}{4 \tan (45° + \phi/2)} = ch_{cr}$$

from which, with reference to Eq. (7-16),

$$h_{cr} = \frac{4c}{\gamma} \tan \left(45° + \frac{\phi}{2}\right) = \frac{2q_u}{\gamma} \tag{8-4}$$

Thus, so long as no additional consolidation and corresponding increase of density has occurred, the critical height may be expressed in terms of the unconfined compressive strength, whether it includes a frictional component of resistance to shear or not (Art. 7-22).

Equation (8-4) can be presented in a somewhat different form

$$\frac{c}{\gamma h_{cr}} = 0.25 \tag{8-5}$$

where the term $c/\gamma h_{cr}$ is called the *stability factor* (Art. 8-8), and it is assumed that $c = q_u/2$ when $\phi = 0$.

The above analysis was based on the assumption of plane surfaces of failure. Observations of failures in the field, however, show that slides occur along curved surfaces of a type corresponding to the curve 2-3 in Fig. 8-1. An analysis of such curved surfaces led Fellenius (Ref. 133, 1927) to derive the expression

$$h_{cr} = \frac{3.86s}{\gamma} \tag{8-6}$$

This value is only 3.5 per cent smaller than the one given by Eq. (8-4) for plane surfaces of failure. Nevertheless, field experience shows that both values are too high, because tensile stresses near the ground surface weaken the soil there.

8-2. Tensile Stresses near the Ground Surface and Their Effect on the Critical Height of Unsupported Vertical Cuts. The preceding conventional analysis of the equilibrium of the entire sliding wedge of soil was made without consideration of the fact that the forces taken as acting on the wedge are not concurrent. This point is illustrated by Fig. 8-2(II). Let us consider the equilibrium of a slice, Δh high, shown in that diagram. The weight ΔW of the slice will form a couple $\Delta W l_1$ with the vertical component ΔR_v of ΔR, which acts along the surface of failure as a resultant of the shearing and of the normal resistances along that surface. (Any vertical pressures transmitted to that slice from the soil above it are not shown in the diagram, since they can be assumed as being balanced by reaction pressures from the soil beneath the slice.) This couple produces an overturning moment ΔM_o. The same thing will happen with all other slices of the sliding wedge of soil. Equilibrium will therefore require the presence of a restoring moment.

$$M_R = Tl_2 = Cl_2 = \sum \Delta M_o \tag{8-7}$$

The causes of tensile stresses near the ground surface, and of the tensile cracks which have been observed there in the field prior to the failure of unsupported banks, have thus been demonstrated in a qualitative manner. However, very little is known so far about the tensile strength and the tensile strains of soils, so that no precise quantitative analysis of the problem is yet possible. Terzaghi (Ref. 360, 1943) estimates the maximum depth to which tensile cracks may reach down from the surface to be one-half of the unsupported height of the cut. The formation of tensile cracks near the surface destroys any shearing strength of the soil there and thereby increases the shearing stresses along the lower portion of the surface of sliding. Thus the critical height h_{cr} of a bank unweakened by tensile cracks, as given by Eq. (8-6), will be reduced by such cracks to a value h_{cr}', which can be determined in accordance with the

above conservative assumption of Terzaghi from

$$h_{cr}' = h_{cr} - \tfrac{1}{2}h_{cr}' \tag{8-8}$$

or

$$h_{cr}' = \tfrac{2}{3}h_{cr} \tag{8-9}$$

Substituting the value of h_{cr} from Eq. (8-6), we obtain

$$h_{cr}' = \frac{2.58s}{\gamma} = \frac{1.29q_u}{\gamma} \tag{8-10}$$

8-3. The Brandtzaeg Theory and the Compression Failures of Brittle Clays in Tension. Figure 8-2(I) shows that no conditions similar to a
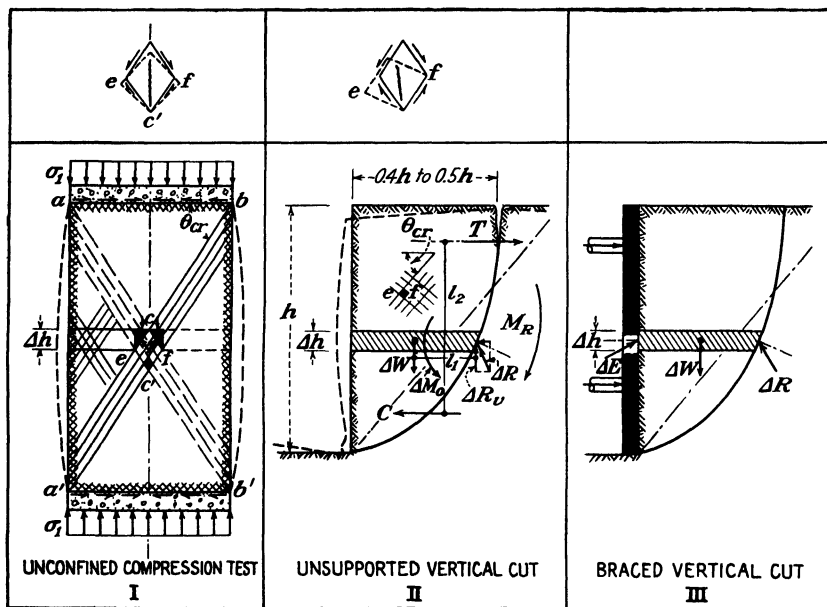
FIG. 8-2. The causes of tension cracks at the ground surface behind an unsupported vertical cut illustrated by comparison with other types of failure conditions.

vertical cut exist during an unconfined compression test. The forces which induce failure are a function of the externally applied stresses σ_1 and are not body forces. The deformation of a slice of soil Δh is symmetrical in respect to the center line of the entire soil prism. Any local overturning moments of individual prisms cancel each other out and are further restrained by shearing stresses along the upper and the lower boundaries ab and $a'b'$.

The effects which these boundary shearing stresses have on the nature

of the failure conditions are clearly brought out during compression tests with concrete cylinders, which practically every civil engineering student has either performed or seen. Cones *abc* and *a'b'c'* usually are found to be intact at the end of a concrete-cylinder compression test, whereas the concrete outside of these cones has split along vertical planes. This is true because the concrete in that zone is not affected by the restraining shearing stresses along the boundaries *ab* and *a'b'*. If the surfaces of these boundaries are well polished and oiled, *all* of the concrete will be found to break up along vertical planes of failure, even within the cones *abc* and *a'b'c'*. An examination of the upper sketch of Fig. 8-2(I) shows that this can be accounted for by horizontal tensile strains, since the diagonal *ef* of the prism *cfc'e* is elongated by the shearing stresses acting along its surfaces. Observations of this kind form the basis of the Brandtzaeg (Ref. 289, 1928) theory for the failure of nonisotropic materials, such as concrete, under the influence of tension governed by the maximum tensile stress or by the maximum tensile strain (Ref. 295).

Lubrication of the boundary surfaces *ab* and *a'b'* in Fig. 8-2(I), for instance, by using a thoroughly moisted porous stone there, will frequently produce similar failure by splitting along vertical planes in the case of brittle undisturbed natural clays. This indicates that the Brandtzaeg theory, and not the conventionally used Mohr theory developed from the Coulomb equations (7-8) and (7-8*a*), may correspond more closely to the actual behavior of undisturbed brittle clays. The use of the Brandtzaeg theory for rigorous solutions, however, is not yet practicable. This circumstance further emphasizes the uncertainties attached to all attempts to obtain generally valid, rigorous solutions of problems involving the strength of soils and demonstrates the need for a semiempirical approach to such problems, as illustrated by Art. 8-5 in respect to the stability of vertical cuts.

8-4. The Failure of a Vertical Cut Illustrated by Model Experiments with Gelatine. A series of model experiments with gelatine was performed by D. Harroun in W. Housel's laboratory at the University of Michigan (Ref. 170, 1940). The results are summarized in Fig. 8-3. Molten gelatine was poured in a cold room between two lubricated vertical glass plates parallel to the plane of the drawing. After the gelatine cooled and solidified, the temporary vertical support 1-1 was removed; as a result the gelatine bank sagged to position 2. It will be noted from Fig. 8-3 that in position 2 no tension cracks had as yet developed. Tension at the upper surface of the bank is, however, indicated by the relatively greater outward movement of the lower portion of the bank. The start of the development of a curved surface of shearing failure was revealed there by four photoelastic pictures, shown ringed by circles in Fig. 8-3.

During the third stage of the experiment (marked "3" in the diagram) the temperature of the room was raised somewhat. This decreased the shearing strength of the gelatine and induced further deformations of the bank. Pronounced tension cracks appeared on its upper surface, and some crushing of the material occurred at the toe.

It was only during the fourth stage of the experiment (marked "4"), when the temperature of the room was raised further, that sliding occurred along the curved surface of failure, which was somewhat displaced as compared with its original position. The gelatine sloughed out at the toe as a result of this sliding.
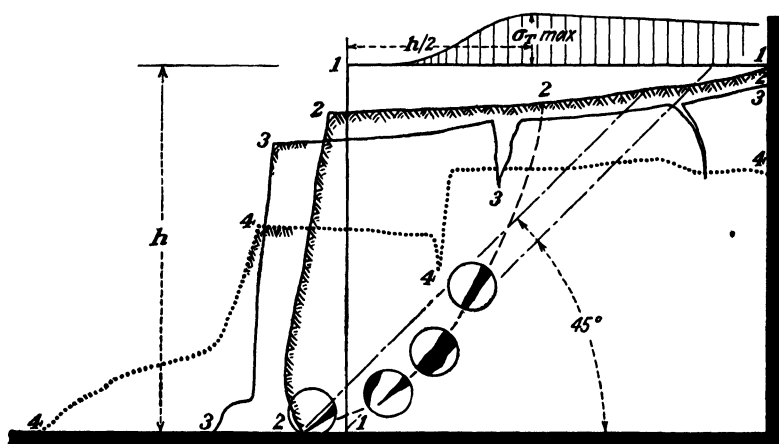
FIG. 8-3. Successive stages in the failure of a vertical bank of cohesive material. Model laboratory tests with gelatine. (*After D Harroun, Ref. 170, 1940, and K. Terzaghi, Ref. 360, 1941.*)

At approximately the same time, Terzaghi (Ref. 360, 1941) reported the results of measurements performed at his Vienna laboratory on gelatine of a somewhat stiffer consistency than the one used by Harroun. The tensile strains were actually measured at the upper surface of the unsupported gelatine bank prior to the appearance of tensile cracks. Their general trend is plotted in Fig. 8-3. The greatest value of the tensile strain, and therefore of the tensile stress, was reached at a distance from the edge of the cut equal to approximately one-half of its height.

No precise quantitative evaluations can be made from experiments of this type, but they permit the visualization of the mechanics of the failure of unsupported vertical cuts in cohesive soils. No similar changes in the strength of a cohesive soil are, of course, possible in nature, but according to Eq. (8-10), a change of shearing strength at a constant height of cut should have the same general effect as the change in the height of the cut in a material of constant strength. Thus Fig. 8-3 may be taken to repre-

sent, at reduced scales, the deformations and the failure of banks of different height in the same material. An examination of this diagram shows that the nature of the material below the horizontal plane through the toe of the bank should have an appreciable influence on the behavior of the bank.

8-5. Comparison of the Estimated and of the Actual Field Values of the Critical Height of Unsupported Vertical Cuts. Figure 8-4 illustrates one of the very few numerical comparisons of this kind which have so far been carried out. An excavation for a two-story basement was to be made (1929) in varved clay, the surface of which was sloping so that at one edge of the cut it was 9.5 ft lower than at the opposite side. The excavation was made without any bracing to the full depth required, with a height of vertical cut of 22.0 ft on one side and 31.5 ft on the other. Then the installation of the timber bracing was begun. Figure 8-4(I) shows the stage it had reached just before the failure of the higher side of the cut. It may be seen that the cross bracing was not yet in place, except in part at the surface. Thus no cross stiffening was at all available to the main braces at the lower level, where, as a result, the cut was entirely unsupported. Figure 8-4(II) shows the same location after the failure of the 31.5-ft-high side of the cut. The opposite 22.0-ft-high side did not fail.

None of the modern methods of clay testing had yet been developed at the time. However, a very careful laboratory study was made in 1946 on undisturbed samples extracted from an adjoining site (see Tschebotarioff and Bayliss, Ref. 385). The average unconfined compressive strength of selected samples (see Fig. 7-16) was found to be $q_u = 1.05$ tons per ft^2, and the unit weight of the clay $\gamma = 120$ lb per ft^3 $= 0.06$ ton per ft^3. Inserting these values in Eqs. (8-4) and (8-10) we obtain $h_{cr} = 35$ ft and $h_{cr}' = 22.6$ ft. This latter value is in quite good agreement with the situation illustrated by Fig. 8-4. The failure occurred in upper New York State during the month of March. It is therefore possible that it was temporarily retarded by the increased tensile strength of the partially frozen upper crust of the ground, which disappeared when the thaw set in, as it did at the time of the failure.

It would thus appear that the weakening of the ground surface by tensile cracks should be taken into account when designing unbraced cuts of excavations. Equation (8-10) appears to take care of this in a reasonably conservative manner. However, further comparative field studies of this type in respect to both stable and unstable past cuts are needed to provide further checks.

Figure 8-2(III) shows that, as compared with unsupported cuts, in the case of rigidly braced cuts there is much less tendency for overturning

(I)
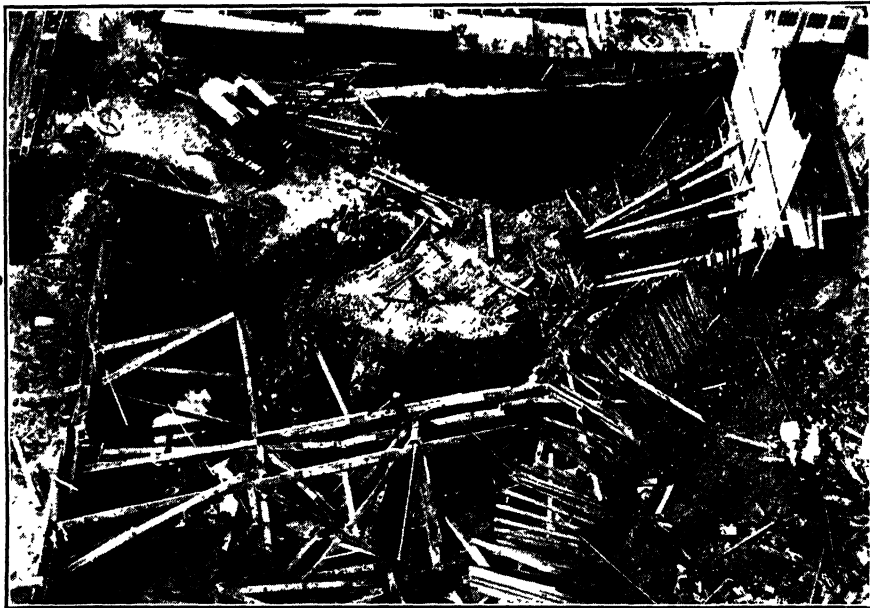
(II)

FIG. 8-4. Failure of a 31.5-ft-deep cut in varved clay. The cross-stiffening timbers of the bracing, as shown in (I), were not yet in place at the time of failure. Therefore the cut was unsupported. (I) Photograph just before failure. (II) Photograph just after failure.

moments, and hence for tensile cracks, to develop. The point will be discussed further in Chap. 10.

8-6. The Stability of Submerged Unsupported Vertical Cuts. Complete submergence as such does not destroy the cohesion in the interior of a clay soil mass. However, as a result of slaking phenomena (Art. 7-4), disintegration may start at the surface and progressively undermine the stability of the entire vertical cut. Figure 8-5 illustrates this point.

At the end of one of the large-scale earth-pressure experiments at Princeton University (Refs. 384 and 397), involving the use of a vertical sand blanket, the removal of the soil from the testing tank was started by
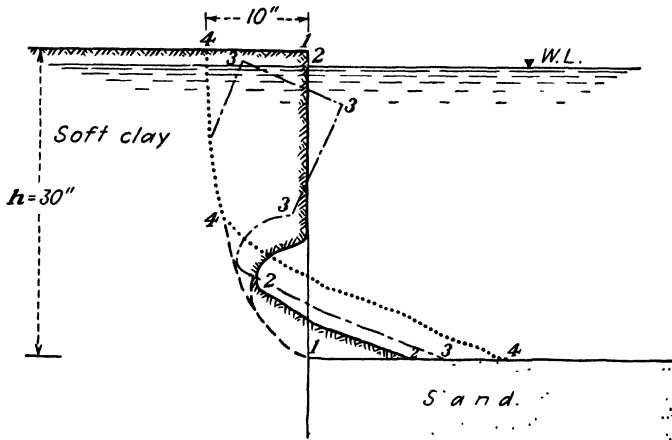
FIG. 8-5. Successive stages in the failure of a submerged vertical bank of cohesive material, started by slaking at the toe. Model tests with soft clay. (*Soil mechanics laboratory, Princeton University,* 1946.)

excavating the sand first. This permitted the observation of the stability of the submerged vertical face of the adjoining soft silty clay exposed in this manner. The silty clay (I_p = 7 per cent) had been completely remolded to a semifluid condition at the start of the test and, at the time of excavation of the sand, had reconsolidated to a plastic consistency corresponding to an unconfined compressive strength of approximately q_u = 200 lb per ft^2. Its buoyed unit weight γ was 60 lb per ft^3. According to Eq. (8-10), the corresponding value of h_{cr}' would be 4.3 ft or 52 in.

The depth of 30 in. was reached at the time work had to be interrupted for the night. At first there was no sign of instability whatsoever. Then some local disintegration of the slaking type was found to take place at the toe of the cut (line 2-2 in Fig. 8-5). The zone of disintegration gradually spread, until after approximately 3 hr the top of the bank was undermined and toppled over. The experiment shows that the usual type

of stability analysis cannot be generally applied to the case of submerged unsupported vertical cuts. Fortunately they are seldom required in practice.

8-7. The Quay-wall Failure in the Harbor of Gothenburg, Sweden. The large number of embankment slides on soft clays in Sweden prompted the appointment by the State Railroad Administration of a special Geotechnical Commission (1913) for their study. The work of the commission and of other Swedish engineers led to the development of a
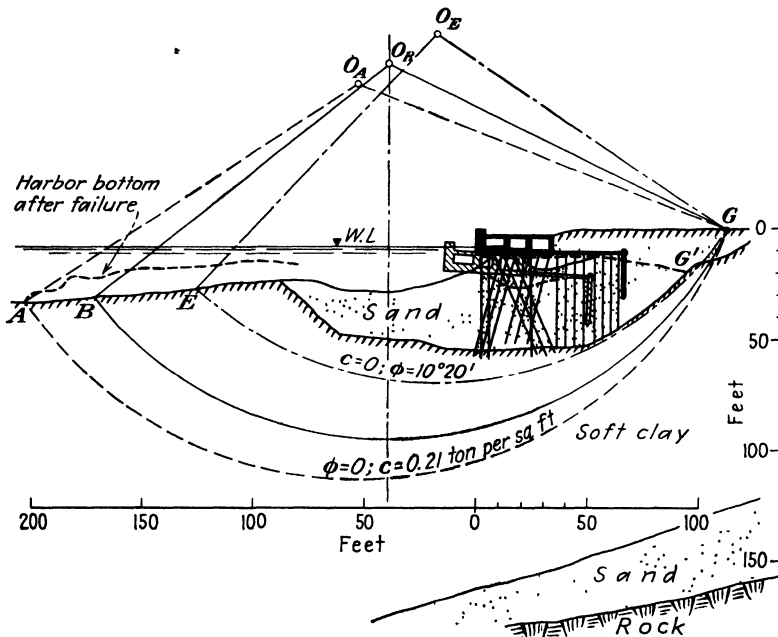
FIG. 8-6. Harbor of Gothenburg (Sweden) quay-wall failure on March 5, 1916. (*After Petterson, Ref. 265, 1916, and Fellenius, Ref. 133, 1927.*)

method of slope-stability analysis which has become generally known as the Swedish cylindrical-surface (or circular-arc) method, first proposed by K. E. Petterson (Ref. 265, 1916). Figure 8-6 illustrates the kind of field observations which formed the basis for this method.

The full lines in Fig. 8-6 give the cross section of a 25-ft water-depth quay wall of Gothenburg Harbor. Since the deposit of soft clay was over 150 ft deep, some 50 ft of it was dredged out, as shown in the sketch, and was replaced by sand fill into which the piles supporting the cellular-type reinforced-concrete relieving platform (Art. 16-15) of the quay wall were driven.

On March 5, 1916 several hundred feet of the quay wall slid out

seaward, coming to rest in a position indicated by lighter lines in Fig. 8-6. This position, the exposed part GG' of the slip surface, as well as the heave of the harbor bottom (shown by broken lines), indicated that a rotational type of failure had taken place. Modern methods of undisturbed sampling from deep borings and of testing the shear strength of soft clays had not yet been developed at the time. For that reason trial computations were performed later by Fellenius (Ref. 133, 1927), involving various assumptions concerning possible limit combinations of the cohesion c and of the angle of friction ϕ which would correspond to a factor of safety of unity along different possible cylindrical surfaces of failure. Only one end, point G of the break at ground surface, was common to all such possible surfaces of failure. The other end would have to pass somewhere between points A and E, point B being one of the most probable ones. With these limiting conditions in mind, a large number of trial computations were performed with various possible positions of the center O. The positions indicated in Fig. 8-6 were found to give the most unfavorable values for any of the centers O tried. It may be seen that the assumption of a purely frictional resistance ($c = 0$) to sliding gave the *shallowest* arc GE. This is logical, since the assumption of $\phi > 0$ means that the shearing strength of a soil increases with depth, thus making deep-seated failures unlikely.

For similar reasons the assumption of $\phi = 0$ gave the deepest arc GA. The intermediate arc GB corresponded to intermediate values of c and ϕ ($\phi = 4°$). A somewhat flatter arc GB than the one shown in Fig. 8-6 had been originally drawn by Petterson (Ref. 265, 1916) under the assumption of $c = 0$ and gave a value of $\phi = 9°40'$ for a factor of safety of unity. This means that a purely frictional failure along GB is somewhat less likely than along GE, since a higher shearing strength of the soil along GE corresponding to $\phi = 10°20'$ would be required to produce equilibrium just on the verge of failure.

The preceding discussion shows that the rotational character of some slides along curved surfaces in deep layers of soft clay is established beyond any doubt. It also shows, however, that slight variations in the assumed location of the sliding surface have much less effect on the actual over-all stability, than do changes in the assumed shearing strength of the clay (Art. 7-25).

8-8. Analysis of the Stability of Slopes by the Swedish Cylindrical-surface Method for Uniform Soil Conditions. The suggestion has been made by Rendulic (Ref. 285, 1935) that the surface of failure be assumed to have the shape of a logarithmic spiral. This assumption has certain theoretical advantages and is sometimes used for that reason. However, it has been shown by Taylor (Ref. 342, 1937) that the results obtained by

this method differ only slightly from those obtained by procedures based on the assumption that the surface of failure is a circle. Moreover, the former take about twice as long to compute as the latter. For this reason the logarithmic-spiral method will not be given further consideration in this book.

Petterson's cylindrical-surface method (Ref. 265, 1916) was developed further by Fellenius (Ref. 133, 1927). As shown in Fig. 8-10, the soil mass above the failure surface was subdivided into *slices*—nine slices in the case illustrated by that diagram. The equilibrium of each slice, for
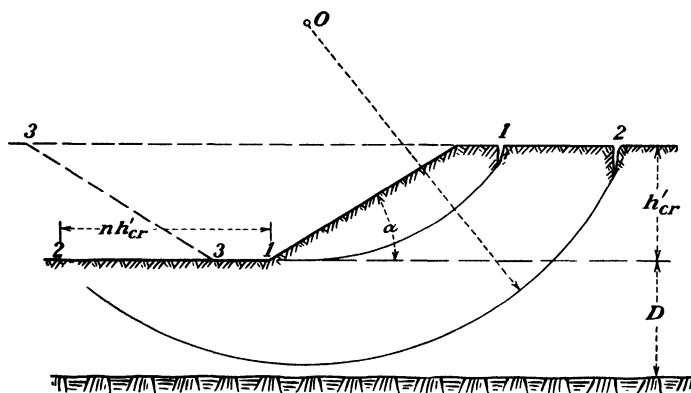
FIG. 8-7. Key to the symbols used in Figs. 8-8 and 8-9.

instance, that of the third slice of Fig. 8-10 represented by the trapezoid $mnm'n'$, is considered independently of the others. This requires simplifying assumptions, such as that the forces on the faces mm' and nn' of the slice are equal and opposite to each other, and that the nonconcurrent nature of the weight W_3 of the slice and of the shearing resistance along the surface $m'n'$ may be overlooked. Graphical procedures of analysis were then developed, in part by means of the so-called *ϕ-circle* method. Once a center of rotation has been selected, a small circle can be drawn around the center with the radius $r' = R \sin \phi$. The resultants for all slices, formed by the weight W and by the frictional resistance along the corresponding segment of the failure surface, will then be tangent to the so-called ϕ circle of radius r'. This helps in drawing the polygon of forces for all the slices into which the entire sliding mass is subdivided.

Taylor (Ref. 342, 1937) utilized this method to compute tables and charts which gave the relationship between the angle α of the slope and its critical height h_{cr} on the one hand, and the properties of the soil, as expressed by its unit weight γ, its cohesion c, and its angle of internal friction ϕ, on the other. The numerical values of the *stability factor*

$c/F_s\gamma h$, where F_s is the factor of safety [compare with Eq. (8-5), where it equals unity], were given in terms of the angle α of the slope and of the *depth factor* $h + D/h$. Each point on the charts was obtained after 10 to 20 trial computations, which proved necessary to determine the most unfavorable location of the center of rotation O. No consideration was given to the weakening of the bank by tension cracks. Similar charts had been developed by Fellenius (Ref. 133, 1927).

The above data were used as a basis for the computation of the charts given in Figs. 8-8 and 8-9. The significance of the symbols used is illustrated by Fig. 8-7. The values of h_{cr}' corresponding to $F_s = 1.00$ are given directly in feet for different angles of slope α as a function of the cohesion c of the soil and for depths D of the same soil below the toe of the slope equal to 0 ft, 20 ft, 50 ft, and 100 ft, followed by strata with higher shearing strength, such as sand or rock. The values of h_{cr}', in accordance with Eq. (8-9), were in all cases taken to equal two-thirds of the height h_{cr} unweakened by tension cracks at the surface. As explained earlier, no precise data are available on this point, but the above assumption is believed to be of a conservative and safe nature. The charts of Figs. 8-8 and 8-9 have been computed for an effective unit weight of the soil $\gamma = 100$ lb per ft^3. If the actual unit weight of the soil has a different value γ', the values of h_{cr}' obtained from the charts of Figs. 8-8 and 8-9 should be multiplied by $100/\gamma'$. This is rigorously correct only when $D = 0$. However, the error involved when $D > 0$ is slight and is on the safe side. The charts also give the values of n by which the corresponding values of h_{cr}' should be multiplied if one wishes to estimate the length nh_{cr}' of the possible *mud wave* which may occur in the case of a slide, as shown in Fig. 8-7. None of the charts of Figs. 8-8 and 8-9 are valid in the case where the toe of the opposite slope, if any, of the cut falls within the distance nh_{cr}', thereby restricting the development of the sliding surface 2-2 assumed for the computation of the charts. In such an eventuality reference is made to Taylor's original article (Ref. 342), which considers in its charts the case when points 1 and 3 of the toes of the opposite slopes coincide.

It will be noted that only Fig. 8-8(I), for $D = 0$, gives curves involving a value of $\phi > 0$, namely, $\phi = 10°$. For other values see Ref. 342. This is true because the most unfavorable failure surface for any soil with $\phi > 0$, that is, for a soil whose shearing strength increases with depth, tends to pass through the toe of the slope, but not beneath it. This will also be the case if $\phi = 0$, but $\alpha > 53°$.

It will also be noted from Fig. 8-9 that an increase of depth D of the same soil beneath the toe of the slope tends to decrease the value of h_{cr}', especially in the case of the flatter slopes. For an infinitely great depth
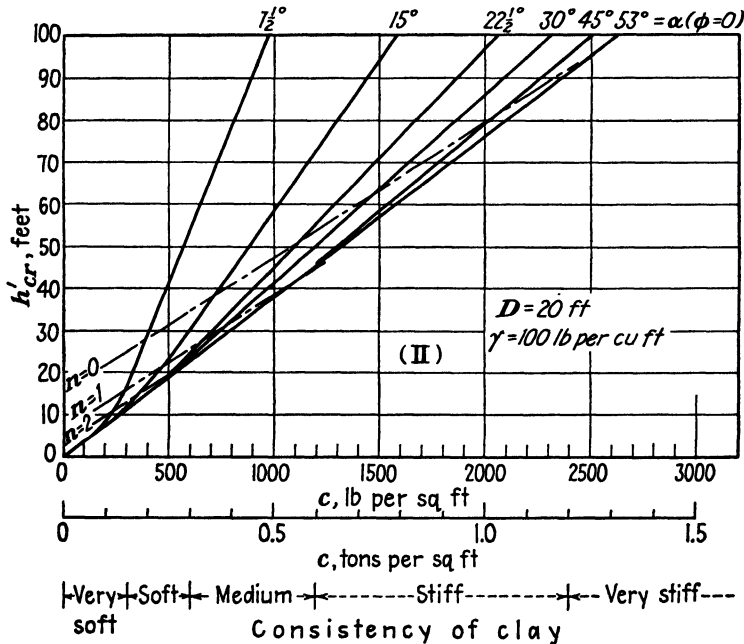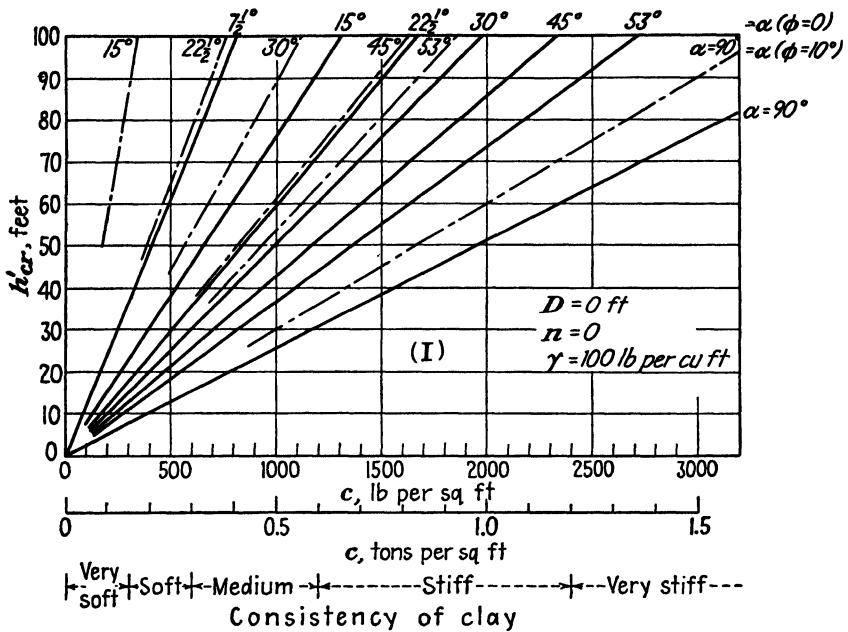
FIG. 8-8. Four diagrams illustrating the relationship between the critical height h_{cr}' of different slopes and the cohesion c of a clay weighing 100 lb per ft^3. (*Developed from D. W. Taylor, Ref. 342, 1937.*)
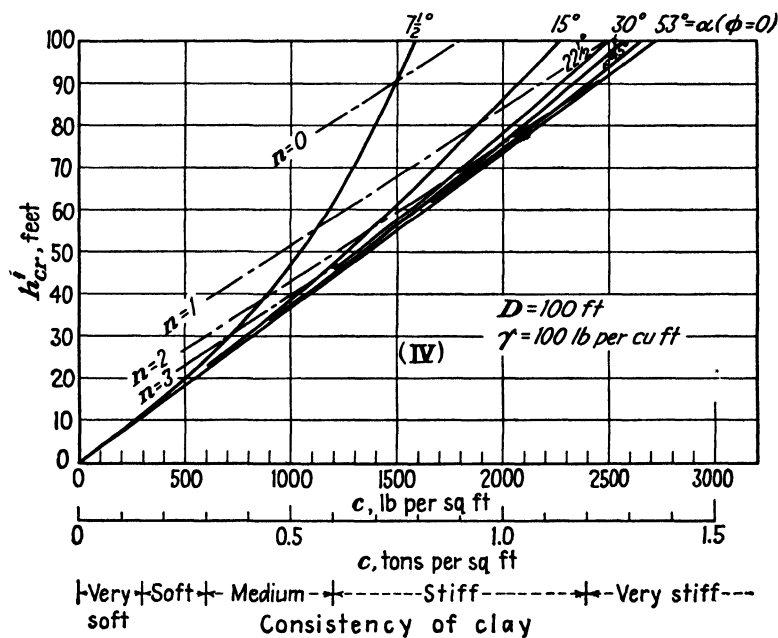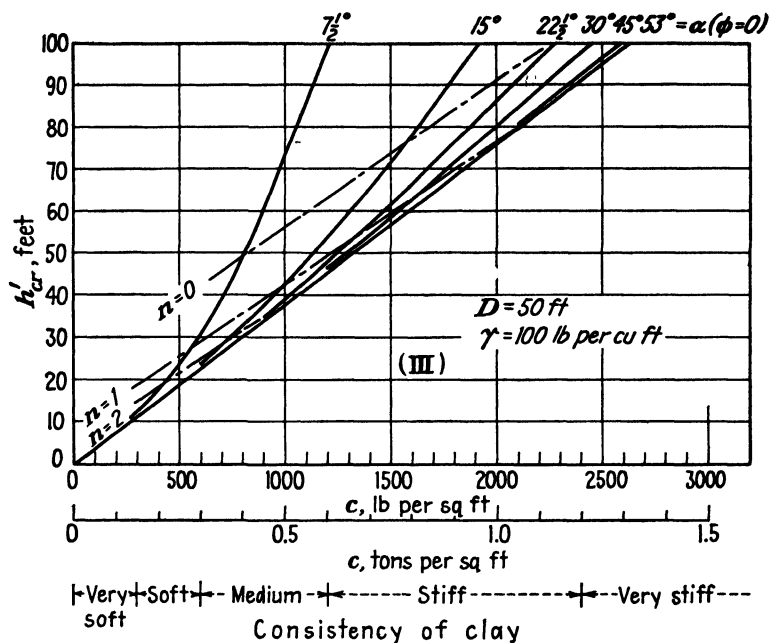
FIG. 8-8.—(*Continued*).
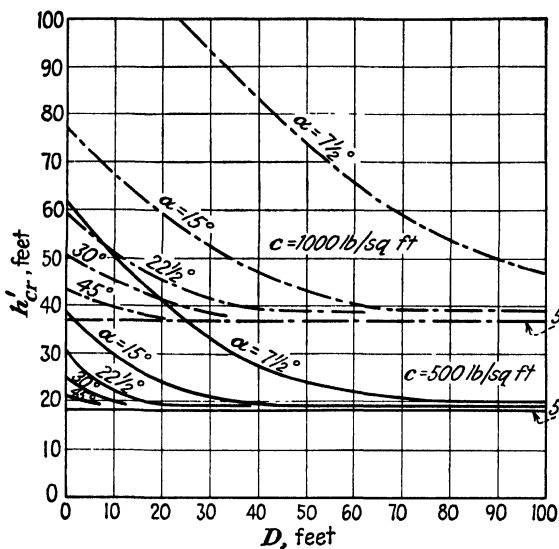
FIG. 8-9. Diagram illustrating the decrease of the critical height h_{cr}' with an increase of the depth D of the clay layer beneath the toe of the slope. (Based on Fig. 8-8; $\phi = 0$, $\gamma = 100$ lb per ft^3.)
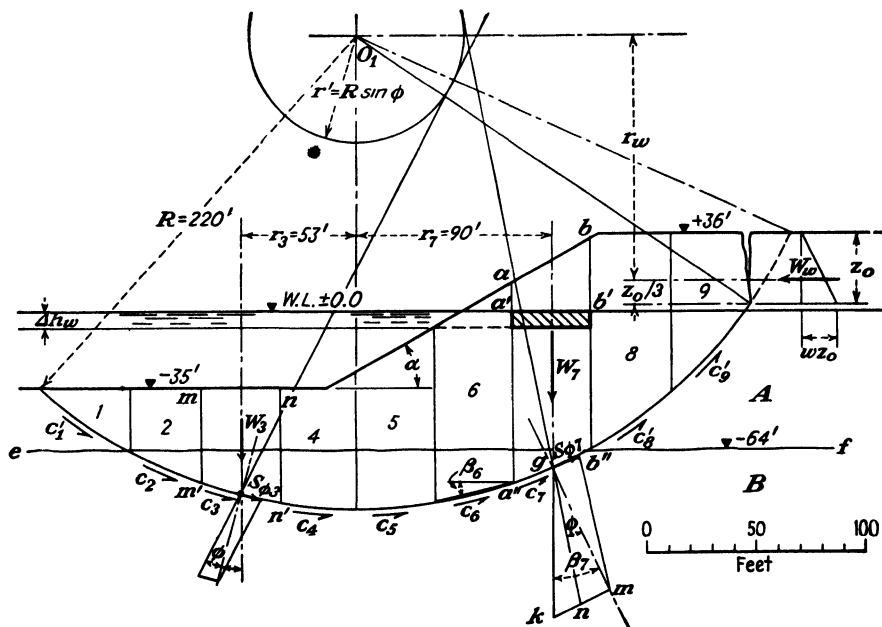
FIG. 8-10. Example of slope-stability computations for nonuniform soil conditions.

D all slopes with $\alpha > 53°$ tend toward the same value of h_{cr}' which a slope with $\alpha = 53°$ has for $D \geq 0$.

The critical height of cohesionless soils ($c = 0$) is infinitely great, so long as the angle of slope α is equal to or smaller than the natural angle of repose of the soil.

Uniform soil conditions of the type illustrated by Fig. 8-7 are seldom encountered in the field. The data given by the charts of Figs. 8-8 and 8-9, however, are helpful in visualizing the interrelationship and the relative importance of the various factors involved, and also in making rough preliminary estimations for field use.

8-9. Analysis of the Stability of Slopes by the Swedish Circular-arc Method for Nonuniform Soil Conditions. Nonuniform soil conditions of the type illustrated by Fig. 8-10 are much more frequent than uniform ones. The effective unit weight of the soil above the free-water level ± 0.00 has to be taken in accordance with Eqs. (4-7) and (4-10), and in accordance with Eq. (4-11) below that level. The shearing strength of the soil layers A and B may be different. Thus the surface of failure shown in Fig. 8-10 is drawn on the assumption that the deeper lying layer B has a lower shearing strength than the overlying layer A. Several trial computations and their comparison with each other would, however, be necessary to determine the most unfavorable surface and the location of its center O.

The customary computation procedure is as follows: After selection of the surface of failure, the soil above it is subdivided in cross section, as shown in Fig. 8-10, into a number of slices. The effective total weight W of each slice is then computed, as shown for parts of slice 7 by Prob. 8-4. The product of each weight W and the distance r from its line of action to the vertical line through the center of rotation O contributes to the overturning moment M_o, the forces to the right of that line by increasing that moment, and the forces to the left of the line by decreasing it. Thus, with reference to Fig. 8-10,

$$M_o = \sum_{5}^{9} Wr - \sum_{1}^{4} Wr \tag{8-11}$$

The resisting moment M_r is governed by the sum of the cohesive and frictional forces acting along the surface of failure. Thus, if we take slice 7 as an example, the component of the resisting moment provided by its cohesive resistance will be (cl_7R) where l_7 is the length $a''b''$. Similarly, the component of its frictional resistance will be $(W_7 \cos \beta_7 \tan \phi)$, where β_7 is the angle formed by the line $a''b''$ with the horizontal, and $W_7 \cos \beta_7$ is the component of the weight of slice 7 normal to the line

$a''b''$. Accordingly,

$$M_r = R \sum_1^9 cl + R \sum_1^9 W \cos \beta \tan \phi \tag{8-12}$$

The values of c and ϕ corresponding to the properties of the soil layer at the bottom of each slice should be used in the above summation.

The factor of safety F_s against sliding is then determined from

$$F_s = \frac{M_r}{M_o} \tag{8-13}$$

As an additional precaution, the possible effect of the accumulation of rain water in tension cracks at the ground surface may be taken into account by adding to the overturning moment M_o the value $W_w r_w = \frac{1}{2}(62.4 z_o^2 r_w)$.

The value of the depth z_o to which tension cracks may reach is usually taken as one-half of the critical height of an unsupported vertical cut, as given by Eq. (8-4), that is, $z_o = q_u/\gamma$. See Art. 8-2 for a discussion of the limitations of this assumption.

The main uncertainty involved in the performance of stability evaluations of the type described in this article lies in the proper estimation of the shearing strength of the soil, as expressed by the values c and ϕ. In view of the still unclarified points related to such estimations (Arts. 7-21 and 7-23), computations of this type should not be attempted for design use without the participation of experienced soil engineers. No opportunity should be missed to perform "post-mortem" analyses of actual slides in conjunction with modern methods of determining the shearing strength of soils (Art. 7-25). This is the only way to perfect existing techniques.

8-10. Effect of Seepage Forces on the Stability of Slopes. Saturation with water above the free-water level increases the effective unit weight of the soil somewhat. An examination of Fig. 8-10 shows that this will increase the weight of slices 6, 7, 8, and 9, and therefore also the overturning moment.

A similar but even more pronounced effect is caused by a sudden drawdown, that is, by a drop of the water level, caused by, for instance, rapid tidal variations in estuaries. Suppose the free-water level in the channel dropped by the amount Δh_w, as shown in Fig. 8-10. Some time will elapse before the water in the soil will drain out and adjust itself to that new level. Meanwhile the weight of, for instance, slice 7 will be increased, since the effective weight of the prism $a'b'$ long and Δh_w thick depended on the buoyed unit weight of the soil prior to the drawdown and will depend

on the unbuoyed saturated weight of the soil after the drawdown. Thus the effective unit weight of that prism is almost doubled (Prob. 8-4).

In some cases it is possible to attempt drawing a flow net, so as to evaluate the seepage forces from it. Figure 8-11 gives an example. It illustrates the cross section of part of the upstream face of the Fort Peck Dam both before and after a slide. This is a hydraulic-fill dam (Art. 17-3), and the failure occurred during construction. Data provided by observation wells showed that the saturation line was as indicated in Fig. 8-11(I). As drawn in Fig. 8-11(II), the saturation line can be taken to represent the upper stream line *aa*. The position of the lower stream line *bb* is also defined, as shown by considerations of symmetry of the dam
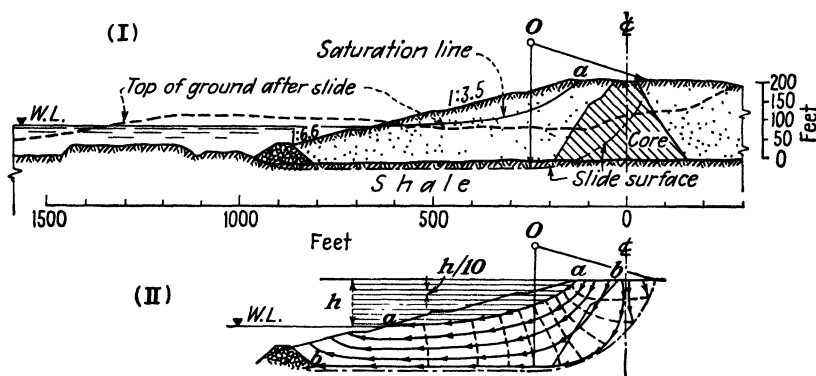
FIG. 8-11. Local slide failure on the upstream face of the hydraulic-fill dam at Fort Peck, Montana. (I) General profile (*after Middlebrooks, Ref 229, 1942*). (II) Probable flow net prior to failure.

and by the location of the impervious shale surface. The points of intersection between the saturation line and the equipotential lines can be determined by means of the graphical procedure indicated in Fig. 8-11(II). It will be noted that these intersection points are spaced more closely in the upper part of the saturation line *aa*, indicating that the soil there is less pervious than in the lower part of that line. In other words, the transition from the impervious inner core to the pervious outer shell is gradual. With this in mind, after several trials the rest of the flow net can be drawn, as shown in Fig. 8-11(II) in accordance with the procedures given in Art. 5-3. The seepage force of each rectangle of the flow net can then be estimated, and the increment to the overturning moment provided by it can be determined. The sum of these increments from the entire flow net can then be added to the overturning moment determined from Eq. (8-11); it should, however, be noted that in this case, to avoid duplication, the unit weight of the soil beneath the entire saturation line *aa* should be taken as buoyed, in accordance with Eq. (4-11).

The construction of flow nets for drawdown conditions is even more difficult and uncertain, since the saturation line usually is not known and has to be estimated. Thus the alternative procedure illustrated by Fig. 8-10 for the estimation of sudden drawdown effects appears preferable in view of its simplicity.

The presence of thin horizontal lenses of sand in a bank of clay at times may have a very detrimental effect on its stability if such lenses are connected to an adjoining large mass of sand. During rainy seasons the free-water level in the sand mass may rise considerably and thereby produce considerable uplift pressures in the sand seams and lenses. Thus the tendency to slide out may be increased (Ref. 365).

8-11. Flow Slides. It will be noted from Fig. 8-11(II) that the slide-failure surface, as determined by later borings, was found to have the form of a circular arc only along part of its length and that it follows the surface of the shale in a straight line along the rest of its length. This formed the basis of the opinion that the primary cause of the failure lay in the weakness of the partially disintegrated shale surface (Refs. 229 and 86). It will, however, also be noted that the location of the top of the ground after the slide indicates that the soil of the outer shell of the dam spread out some 600 ft beyond its original toe. Thus the loose sand of the shell must have been liquefied (Art. 7-16) by the deformations induced by the sliding. The slide, which started as a shear failure along a definite surface, appears to have ended as a *flow slide* (Ref. 153).

Under that name are known slides which involve the complete liquefaction of a mass of loose granular material, which then spreads out at a very flat slope. Geuze (Ref. 149, 1948) reports the results of density analyses of sands in Holland in parts of embankments near sections which had failed by slides of the flow type. In every case the laboratory values of the critical void ratio of the sands (Art. 7-16) showed that the field densities were below the critical values. Other data are given by Kappejan *et al.* (Ref. 202, 1948). The preventive measure against flow slides is proper compaction of the sand (Arts. 11-3 to 11-5).

Ehrenberg (Ref. 114, 1933) described a flow slide of loose sand in a soft-coal mine in Germany. The soft coal was covered by a 155-ft-thick layer of sand, which was removed to permit open-pit mining, and which was dumped in parts of the excavation where the coal had already been taken out. One of these dumps of sand reached to a height of 62 ft above the open level of the adjoining coal surface and was partially saturated with water seeping down a slope into the pit. Without any warning over a million cubic yards of that sand flowed out into the pit, spreading out within a few minutes over the uncovered coal to a distance of 2300 ft. Fortunately the slide occurred in the evening when only four men oper-

ating emergency equipment were in the pit. Two were close enough to the far edge and succeeded in climbing out in time; the other two perished.

8-12. Construction and Design Measures to Increase the Slope Stability of Cuts and of Embankments. Any measure which decreases the overturning moment M_o in Eq. (8-11) will increase the stability of a slope. This may be done, for instance, by cutting it back, as shown in
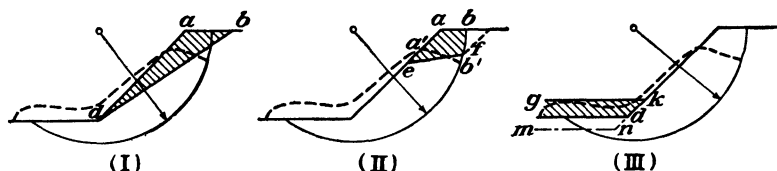
FIG. 8-12. Three types of measures for the purpose of stabilizing a slope which had failed along a cylindrical surface.

Fig. 8-12(I), from *da* to *db* to decrease the angle of the slope. The overturning moment will then be decreased by the moment of the area shown hatched in the diagram. A similar result may be achieved after a slide, as shown in Fig. 8-12(II), by not building the surface *a'b'* of the mass of soil which has slipped out up to its original position *ab*, but cutting it down to *ef*, prior to restoring the original slope.

A third method is shown by Fig. 8-12(III). It consists in leaving some of the soil which has slid out at the toe of the slope. A somewhat similar
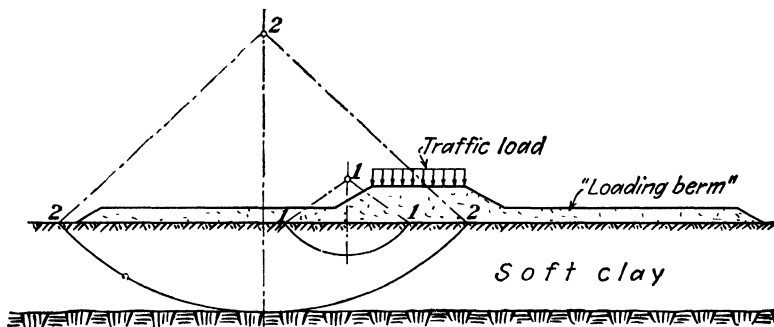
FIG. 8-13. The use of loading berms to permit the construction of railway or highway embankments on beds of soft clay in Sweden. (*After B. Jakobson, Ref. 185, 1948.*)

procedure is employed in Sweden (Ref. 185) to permit the construction of railway or highway embankments on very soft clay. It is illustrated by Fig. 8-13 and consists in the use of so-called *loading berms* to decrease the overturning moments both of possible shallow slides 1-1 and of deep slides 2-2.

With reference to Fig. 8-12(III), it should be noted that a reverse procedure—that is, the deepening of the cut by excavation, for instance, to

the level *mn*—will increase the overturning moment and thereby increase the danger of sliding. Some slides of canal banks have been caused by dredging to deepen the channel.

The creation of conditions of the type illustrated by Fig. 8-14 should be avoided under all circumstances. First of all, the overturning moment is increased by the weight of the excavated material placed at the top of the cut. In addition, the free runoff of surface water is prevented. The seeping water weakens the soil in the zone of possible failure and increases its unit weight. The resisting moment is thereby decreased, and the overturning moment is increased.
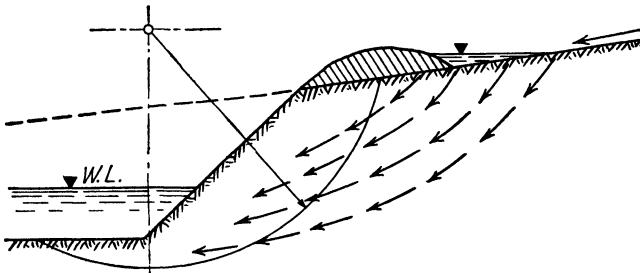
FIG. 8-14. Wrong way of placing part of the excavated material.

8-13. Additional Factors Influencing the Stability of Slopes. Figure 8-15 illustrates the results of model tests performed by Ek Khoo Tan (Ref. 340, 1948) at Columbia University. Sand was placed between two glass plates; its surface was covered by a rubber membrane, and the interior was subjected to a vacuum, in a manner somewhat similar to that of the experiment illustrated by Fig. 7-28 (Art. 7-18). Subjected, as a result, to outside atmospheric pressure throughout its depth, the sand acquired the properties of a cohesive material. Point *b* of the base of the 3- by 1.5- by 1.5-ft box was raised gradually, the entire box being tilted around point *a*, until failure occurred. The displacements of the sand at failure are illustrated by Fig. 8-15. They were obtained from measurements of the smudges made by the moving sand grains along a network of lines drawn on the interior of the glass plates with a softly plastic mixture of lampblack and turpentine.

It will be noted that the curve of sliding failure passed through points where the shearing strain reached values of approximately 7°. An appreciable zone of disturbance with smaller values of shearing strain extended below the surface of failure. It is therefore reasonable to assume that the nature of the soil material below the surface of failure is likely to affect the location of that surface. There is as yet no way to evaluate this additional factor numerically, nor do experiments of the

type illustrated by Fig. 8-15 provide the means for such an evaluation. However, they permit better visualization of the mechanics of deep slide failures of slopes and emphasize the important but conventionally neglected effect of boundary conditions. This point will be referred to
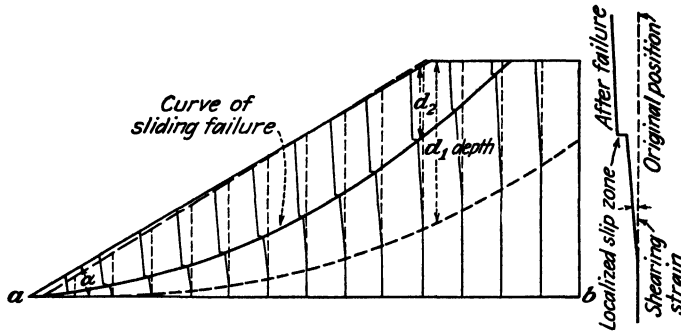
FIG. 8-15. Model tests indicate effect of boundary conditions on the location of the curve of sliding failure. (*After Ek Khoo Tan, Ref. 340, 1948.*)

further in connection with problems of lateral earth pressure against retaining structures (Art. 10-20).

8-14. Surface-detritus Slides of the "Creep" Type. When a surface layer of relatively loose and permeable detritus, that is, disintegrated material, is underlain by a layer of compact impervious shale, water is liable to percolate through the detritus and along the surface of the shale,
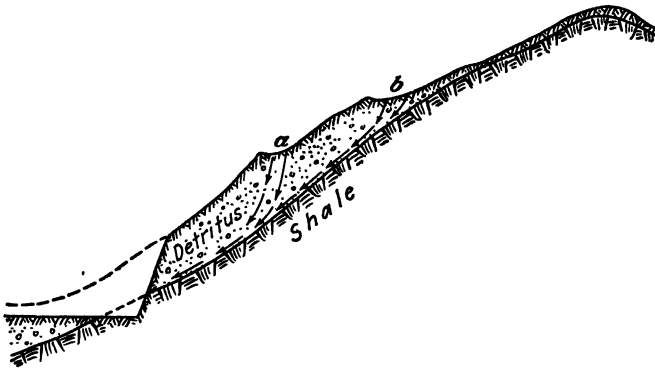
FIG. 8-16. Profile showing drainage conditions which facilitate detritus slides into cuts of the type illustrated by the photographs of Fig. 8-17.

thereby softening it up and making it slippery. If a cut, for instance for a highway, is made under such conditions as are illustrated by Fig. 8-16, then the entire surface detritus layer is liable to start sliding into the cut along the shale surface.

(I)

(II)

FIG. 8-17. Movement of a detrital bank along a wet slippery plane on top of hard shale (see Fig. 8-16). (*Courtesy of H. F. Peckworth*, 1938.)

The two photographs of Fig. 8-17 illustrate a case of this type. Photograph I shows the face of the cut and its intersection with the plane of slippage. Photograph II shows an uncovered portion of the surface of slippage with scratches left by pebbles of the overlying and moving detritus on the softened surface of the shale. Proper surface drainage is the most effective remedy. It can be facilitated by providing impervious

(clay) surfacing at points where water is likely to accumulate, for instance *a* and *b* in Fig. 8-16, and channels to carry the water away.

In humid climates, for instance in England (Ref. 310), dangerous slides of this type may occur periodically even without a cut, once the detritus cover of steep slopes gets sufficiently sodden. Alternating sloping layers of waterbearing porous sandstone and of shale may aggravate the situation further. Draining the water away is the only effective remedy in such cases. Drainage tunnels may be used in extreme cases.

8-15. Stability of Cuts in Stiff-fissured Clays. None of the methods described in the preceding articles for the numerical estimation of the stability of vertical cuts or of slopes in homogeneous plastic clay can be applied to overconsolidated so-called *stiff-fissured clays* (Art. 2-5). Terzaghi (Ref. 355, 1936) gave a sound explanation of the causes of sudden failures of clay banks which should have had an ample factor of safety if their behavior had been governed by the strength of the unfissured portions of the clay mass. An excavation produces tensile stresses in the upper zone of the slope or cut (Art. 8-2). The resulting expansion opens up the fissures of the clay in that zone, especially near to the soil surface. Water can then gradually seep into the fissures, thereby softening the adjoining clay. After a while, the resistance to shear of the clay mass will be governed, down to a considerable depth, by the strength of these softened thin layers. Four of the five cases quoted by Terzaghi in the above reference indicated that failure had occurred at effective shear strengths of approximately 0.30 ton per ft^2, whereas the compressive strength of samples of the unweakened clay between the fissures was 10 to 20 times greater. One case corresponded to a failure strength of 1.0 ton per ft^2.

Stiff-fissured, sometimes referred to as *slickensided*, clays of the above type have caused many troublesome slides in England (Ref. 73). Attempts have been made, by means of field studies of such slides, to evaluate the softening of the clay in the fissures as a function of the time elapsed since the cut was made. The results of such studies, reported by Skempton (Ref. 311, 1948), indicate that this is a promising line of approach to the problem. Of course, separate field studies have to be performed for different geological formations in different regions. They are not likely to have universal validity.

Slickensided clays of the stiff-fissured type in the so-called Cucaracha formation caused repeated trouble during the construction of the Panama Canal. The strength at failure was found to vary between 15 and 28 per cent of the undisturbed shear strength (Ref. 30, 1948). Nevertheless, it was several times higher than the failure strength of most of the clays reported by Terzaghi (Ref. 355) or that of the English clays reported by Skempton.

8-16. Cuts in Loess Soil. Experience with such cuts has shown that a vertical or almost vertical cut of the kind illustrated in Fig. 8-18 proves to be most stable and lasting. This is true because of the predominantly silty composition of loess soils (Art. 2-6), and because of their resulting low cohesion, which renders them very susceptible to rapid erosion by rain water trickling down inclined slopes. In the case of vertical cuts

FIG. 8-18. A vertical cut in loess soil along a highway near Vicksburg, Mississippi. (*Photo by Tschebotarioff, Ref. 375, 1939.*)

FIG. 8-19. Deep stepped cut with vertical faces in loess soil on a highway in Iowa. (Ref. 120).

most of the rain water will not reach the edge of the cut and flow over it but will seep into the loess surface behind the slope. This is particularly pronounced in the case of loess soils in their primary deposit, since the vertical permeability in such cases is much greater than the horizontal permeability. Draining of water away from the cut is usually advisable, however.

Turnbull (Ref. 402, 1948) reports good results with similar techniques during the construction of canals in Nebraska. Back slopes of 1 on ¼ were used up to a height of 40 ft in sandy loess, and up to a height of 55 ft in silty loess. This applies to the slope above the water level. Special treatment such as sand berms, flatter slopes, and blanketing with treated material, was needed below water level.

Figure 8-19 illustrates a method used for an 80-ft-deep cut in the construction of a highway in Iowa (Ref. 120, 1940). It had approximately 15-ft-high steps with vertical faces. A slight (1 on 24) slope was provided to drain water away from the edge of each cut. To avoid erosion of the

FIG. 8-20. The use of cheesecloth to prevent erosion along a gentle slope (silty soil with little cohesion) until the seeded grass has taken root. (*Photo by Tschebotarioff, Ref.* 375, 1939.)

toe of the next higher step, the region *a* was paved, and the drainage of the accumulating water was facilitated in a longitudinal direction (that is, at right angles to the plane of the drawing) by provision of a gentle slope in that direction.

8-17. Protection of Slopes against Erosion. The growth of grass is one of the simplest and least expensive means for the protection of slopes against erosion by wind and by rain-water action. Once a good turf has been formed, the grass will absorb most of the impact of rain drops, and its roots will hold the surrounding soil in place and prevent it from being washed down the slope.

It is very important to permit the grass to form a continuous cover before erosion has time to develop. Otherwise seeding will be entirely ineffective, as shown in Fig. 8-21. Erosion is apt to develop particularly

rapidly on slopes formed by soils with little cohesion, that is, by true silts, very fine sands, rock flour, or loess. Covering the slope with sod, when available, is an effective but expensive countermeasure. Figure 8-20 illustrates an attempt to hold down a soil of this type on a gentle slope next to a highway by the use of cheesecloth for the time needed by grass to take root. Otherwise the soil would be blown or washed away together with the grass seeds.

In the case of steep slopes the velocity of the water flowing down the slope can be strongly decreased by the method illustrated in Fig. 8-22.
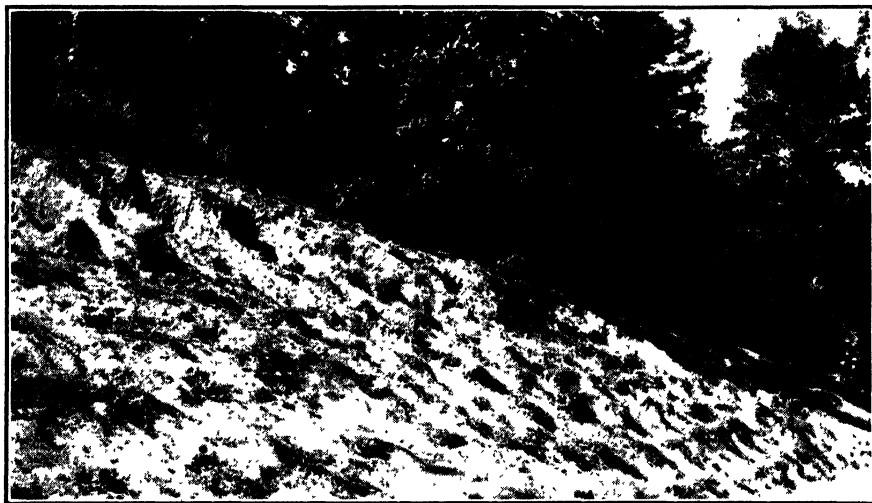
FIG. 8-21. Erosion of a highway slope in a cut before the seeded grass had fully taken root. *(Photo by Tschebotarioff, Ref. 375, 1939.)*

It is similar to the so-called *contour plowing* or *terracing* (Ref. 17) used for soil conservation purposes in agricultural work. Water then tends to flow slowly along the gently inclined grooves between the plowed ridges, which run almost parallel to the toe of the slope. The erosive power of the water is thereby reduced to a minimum.

Special precautions are required for the protection of slopes close to the water line of canals, lakes, or dams, against erosion by wave action. This is usually accomplished by means of rock riprap, where the size of the blocks of rock has to be increased with the height of the waves to be expected. A sufficient weight of such blocks prevents their displacement by the impact of waves. In addition, it is necessary to prevent gradual washing out of the soil between the blocks by water running down the slope as each wave recedes. Something in the nature of an inverted filter is helpful for this purpose. A layer of sand is placed immediately on top

FIG. 8-22. Protection of a highway slope by a method similar to the contour plowing or terracing of the U.S. Soil Conservation Service. (*Photo by Tschebotarioff, Ref. 375, 1939.*)
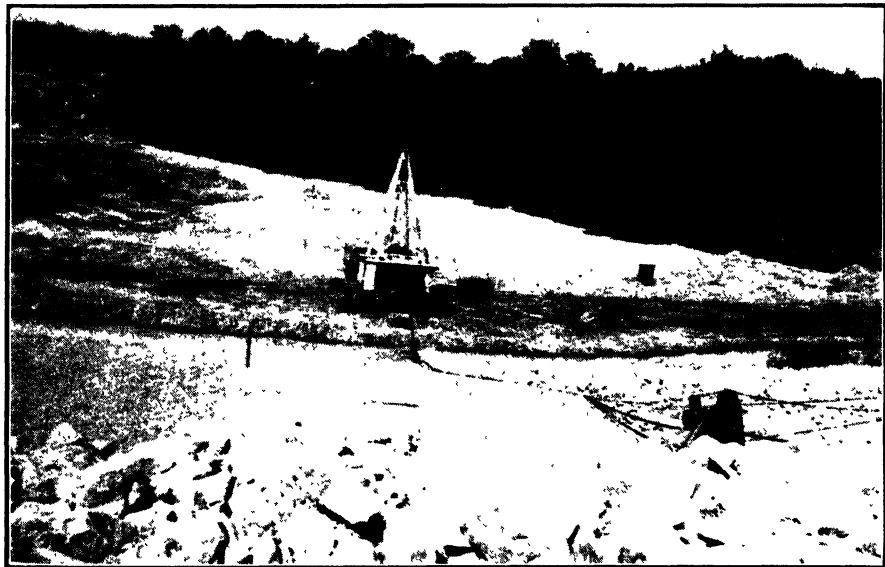
FIG. 8-23. Protection of the upstream slope of the dam at Sardis, Mississippi, against erosion by wave action. Rock riprap over gravel and sand. (*Photo by Tschebotarioff, Ref. 375, 1939.*)

of the natural soil of the slope and is followed by layers of gravel, of broken stone, and finally of rock riprap. Figure 8-23 illustrates this method. *One of the two towers of the movable cableway used in placing the riprap on the slope is shown at its toe.*

Practice Problems

8-1. An unsupported vertical cut 23 ft deep is to be made in a stiff clay layer, the relevant properties of which have been determined in the laboratory from tests on undisturbed samples as follows: $q_u = 1.40$ tons per ft², $\gamma = 125$ lb per ft³. What will be the factor of safety F_s against rupture of the bank?

Answer. According to Eq. (8-10):

$$h_{cr}' = \frac{1.29 \times 1.40 \times 2{,}000}{125} = 28.9 \text{ ft}$$

$$F_s = \frac{28.9}{23.0} = 1.26$$

8-2. On what approximate slope would one have to make a 23-ft-deep cut to obtain a factor of safety $F_s = 1.26$, if the clay is softer than that in Prob. 8-1 ($q_u = 0.70$ ton per ft², $\gamma = 110$ lb per ft³), reaches to a depth $D = 30$ ft below the bottom of the cut, and is followed by much stiffer material at a greater depth?

Answer. According to Eq. (7-17) $c = q_u/2 = 700$ lb per ft². To obtain a factor of safety $F_s = 1.26$ one should calculate a value of c to be used in the computations as follows: $c = 700/1.26 = 560$ lb per ft², corrected further to $560(100/110) = 510$ lb per ft², since the unit weight of the soil is greater than that used in the charts. From Fig. 8-8(III), where $D = 50$ ft, we find $\alpha = 10°$ (1:5.7), and from Fig. 8-8(II), where $D = 20$ ft, we find $\alpha = 16°$ (1:3.5). Extrapolating we obtain a slope of 1:4, which value should be satisfactory for purposes of preliminary estimation. Note that the corresponding value of n is 1.5, that is, a steeper slope would be permissible if the width of the base of the cut is smaller than $1.5 \times 23 = 34.5$ ft.

8-3. What slope would be permissible if the clay of the cut were underlain by stiffer material, that is, if $D = 0$, all other conditions remaining the same as in Prob. 8-2?

Answer. From Fig. 8-8(I) we find $\alpha = 45°$ (1:1).

8-4. By what value would the overturning moment of slice 7 in Fig. 8-10 be increased as a result of sudden drawdown $h_w = 7.5$ ft? The void ratio of the soil is $e = 0.84$, and its buoyed weight, according to Eq. (4-11) and a value of $G = 2.65$, is 56 lb per ft³.

Answer. According to Eqs. (4-7) and (4-10), the unit weight immediately after the drawdown within its zone, which is shown hatched for slice 7 in Fig. 8-10, would be

$$56.0 \times \frac{2.65 + 0.84}{2.65 - 1.00} = 118.4 \text{ lb per ft}^3$$

The unit increase would be $118.4 - 56.0 = 62.4$ lb per ft³. Thus it is equal to the removal of the effect of buoyancy per unit of total volume (voids + solids) of the soil. The distance $a'b'$ being equal to 36 ft, the total increase of weight in slice 7 (1 ft deep) will be $62.4 \times 7.5 \times 36.0 \times 1.0 = 16{,}850$ lb $= 16.85$ kips. The corresponding increase in the overturning moment will be $16.85 \times 90.0 = 1{,}515$ ft-kips.

8-5. What is the resisting moment of slice 7 in Fig. 8-10 if the unconfined compressive strength of undisturbed samples from layer B was found to be $q_u = 0.90$ ton per ft²?

Answer. According to Eqs. (7-17) and (7-19), we can take $\phi = 0$ and $c_7 = q_u/2 = 0.90$ kip per ft². The length of the arc $a''b''$ is measured from the diagram to equal 40.0 ft. Thus the resisting moment of slice 7 will be

$$0.90 \times 40.0 \times 220.0 \times 1.0 = 7{,}920 \text{ ft-kips}$$

References Recommended for Further Study

"Stability of Earth Slopes," by Donald W. Taylor, *Journal of the Boston Society of Civil Engineers*, July, 1937. Also *Contributions to Soil Mechanics*, Boston Society of Civil Engineers, 1925–1940, pp. 337–386. Comparison of the Culmann, Résal-Frontard, circular-arc (cylindrical-surface) and logarithmic-spiral methods. Charts of stability numbers obtained by the ϕ-circle method.

Soil Mechanics in Engineering Practice, by Karl Terzaghi and Ralph B. Peck, Wiley, 1948, Art. 49, pp. 354–372. Stability of hillside slopes in open cuts. Examples of different types of slides and of their handling. Includes special cases, such as the slides influenced by the presence of thin water-bearing seams of sand.

Soil Erosion and Its Control, by Q. C. Ayres, McGraw-Hill, 1936, 365 pp. Practical methods for the control of different types of erosion.

CHAPTER 9

THE STRESS DISTRIBUTION IN SOILS. THE BEARING CAPACITY OF SOILS

9-1. Some General Considerations Concerning the Surface Settlements of Loaded Areas and the Stress Distribution in the Soil beneath Them. Practicing engineers frequently make the simplifying assumption
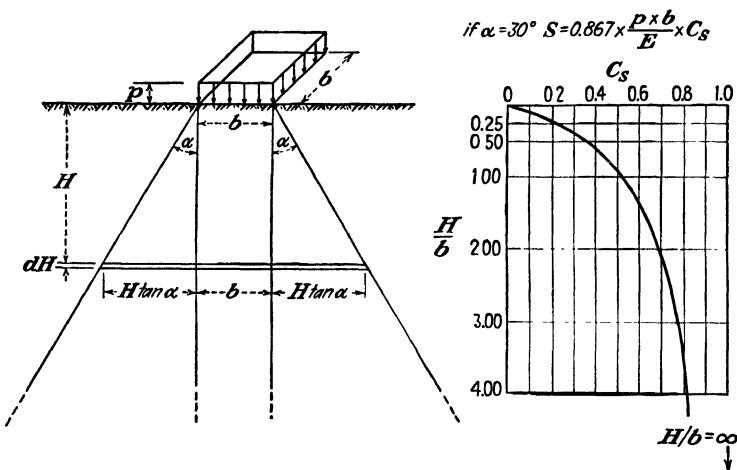
FIG. 9-1. Compression S of a truncated pyramid of elastic material uniformly loaded over its top surface.

that the pressures transmitted to the soil by a foundation footing are spread out through the soil under a certain angle α, usually taken to equal 30° with the vertical, and are thereby uniformly distributed on the underlying layers at a reduced intensity. It will be shown later that in many respects this assumption is inaccurate or even incorrect, but it can nevertheless serve as a basis for an introductory discussion of the entire problem of stress distribution through soils.

As shown in Fig. 9-1, in the case of a square footing the above procedure is equivalent to assuming that the surface load $P = pb^2$ is carried by a

truncated pyramid. The surface settlement S will then equal the compression of the entire pyramid of height H. This will be the sum of the compressive strains ϵ of all of the successive horizontal layers dH of the pyramid. Each of these successive layers occupies a horizontal area $A = (b + 2H \tan \alpha)^2$. If the Young modulus of the material of the pyramid is E, its compression S will be

$$S = \int_{H=0}^{H=H} \epsilon \, dH = \int_{H=0}^{H=H} \frac{P}{AE} \, dH = \frac{pb^2}{E} \int_{H=0}^{H=H} \frac{dH}{(b + 2H \tan \alpha)^2}$$

$$= \frac{pb^2}{E} \Big|_{H=0}^{H=H} - \frac{1}{2 \tan \alpha} \frac{1}{(b + 2H \tan \alpha)}$$

$$= \frac{pb^2}{E} \left(- \frac{1}{2 \tan \alpha} \frac{1}{b + 2H \tan \alpha} + \frac{1}{2b \tan \alpha} \right)$$

$$= \frac{pb}{E \times 2 \tan \alpha} \left[1 - \frac{1}{1 + 2(H/b) \tan \alpha} \right] \tag{9-1}$$

If $\alpha = 30°$ ($\tan \alpha = 0.577$), then (for a square)

$$S = 0.867 \frac{pb}{E} C_s \tag{9-2}$$

This value is only 39 per cent smaller than that given by the rigorous solution of Timoshenko [Ref. 367, Eq. (206)] for a square footing and $\nu = 0.5$.

For values of $H < \infty$ the value of the compression S, as given by Eq. (9-2), must be multiplied by a coefficient $C_s < 1$. Values of this coefficient, computed from Eq. (9-1), are given in graphical form on the right-hand side of Fig. 9-1. That diagram, as well as Eq. (9-2), indicates the following circumstance, which is of the greatest practical importance.

When the depth of the compressible layer of soil, as represented in the preceding analysis by the height H of the pyramid, is very large by comparison with the size of the loaded area ($A = b^2$), then the surface settlement of square foundation footings, which transmit to the soil average unit pressures of the same intensity p, will increase in direct proportion to the length b of the sides of the square footings. Such conditions may occur in practice. For instance, let us assume that a layer of clay or of loose sand, say some 80 ft deep, is underlain by rock and is loaded at the surface by widely spaced individual foundation footings varying in size from 4 ft square (4 by 4 ft) to 8 ft square (8 by 8 ft). If we load all footings to the same intensity of pressure, say 1 ton per ft², then an 8-ft-square footing will tend to settle twice as much as a 4-ft-square footing if the soil beneath both is fully homogeneous in respect to its compressibility. This will be true because in the case of the larger footing a greater depth of soil

will be compressed at the same average intensity than will be the case beneath a smaller footing. This difference will be somewhat less pronounced when the depth H of the compressible layer is relatively small and comes closer to the size of the footings (see variation of the coefficient C_s in Fig. 9-1 for $\alpha = 30°$ in terms of the ratio H/b).

This general principle has been shown to be true by more rigorous analyses of the problem, by laboratory experiments, and by field observations, which will be discussed in the following articles. Equation (9-2)
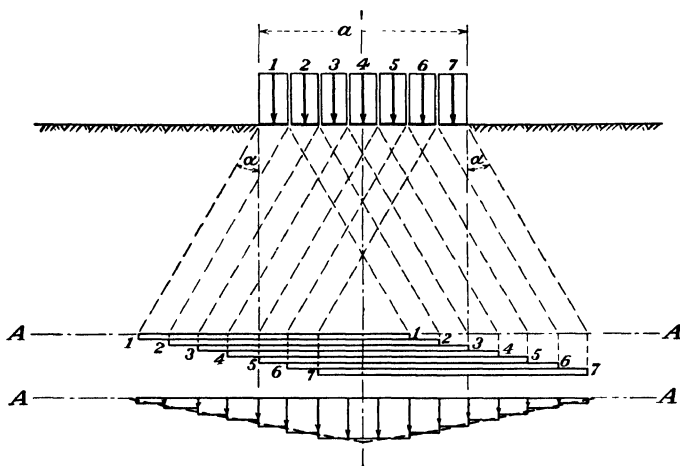
FIG. 9-2. Simplified proof of the fact that vertical pressures transmitted to the soil by a surface load cannot be distributed uniformly on deeper lying horizontal planes. (*After Koegler and Scheidig, Ref. 201, 1938.*)

and Fig. 9-1 may in some cases be applied to practical problems (see Prob. 9-1).

Equation (9-2) holds for a square footing. For a footing of the width b and of an infinite length we can obtain in a similar manner, for $\alpha = 30°$

$$S = 2.0 \frac{pb}{E} \log\left(1 + \frac{1.154H}{b}\right) \tag{9-2a}$$

The preceding simplified analysis is incorrect in one respect which has practical importance, namely, in the assumption that pressures are spread out through the soil at a well defined angle and are uniformly distributed over underlying horizontal planes. Figure 9-2 illustrates in a simplified manner the fallacy of this assumption. Let us split up the width a of the footing into several sections of equal size and then assume that each of these sections spreads its load out through the soil under an angle $\alpha = 30°$ with the vertical, as shown by broken lines in Fig. 9-2. The truncated

pyramids within which the soil is compressed by the load of each of the component sections of the footing will overlap. Therefore, if we add up the pressures transmitted to a plane AA by each of the overlapping pyramids, as shown in Fig. 9-2, greater pressures on the plane AA will be recorded beneath the center of the footing than beneath its edges. As a result, the center of the uniformly loaded footing will tend to settle more than its edges. This has been frequently observed on actual structures. The point is illustrated by Fig. 9-3. According to Prentis and White (Ref. 276), the middle ordinate of the parabolic deflection curve is about 4 ft. This case is an extreme one, since the depth and the compressibility

FIG. 9-3. Cornice deflection of an old Mexico City masonry building shows that the center of its façade settled more than its ends. (*Photo by Boris Ashurkoff.*)

of the soft clay at Mexico City is greater than anywhere else in the world (see Art. 2-5 and Fig. 4-9). Nevertheless, similar observations have been made on full-scale structures in many other places (Fig. 13-10).

Another essential point revealed by an examination of Fig. 9-2 is that the vertical pressures on underlying soil layers spread out well beyond the vertical planes through the edges of the footing. Since a large part of the surface settlements can be represented by the summation of the compressive strains of all underlying soil layers, it follows that there will be no sharp differential settlement between the footing and the immediately adjoining surface of the ground; a gently curved so-called *settlement crater* will be formed around the footing (Art. 13-4).

9-2. Rigorous Analysis by Boussinesq of the Stress Distribution in a Semi-infinite Elastic Solid. The simplified treatment of the stress-distribution problems, as outlined in the preceding article, omitted to take into consideration the effect on the stress distribution of the lateral and shearing deformations of the soil under load, and of the soil properties

which influence the magnitude of these deformations. A rigorous analysis of the problem was first carried out by the French mathematician Boussinesq (Ref. 36, 1885), in respect to a concentrated load applied to the surface of a so-called *semi-infinite elastic solid*, that is, to a mass of elastic material limited on one side by a horizontal plane surface and extending to an infinite distance in all directions below that plane. The soil beneath a horizontal surface may be considered to represent a semi-infinite solid when its depth is large in comparison to the dimensions of the loaded surface area.
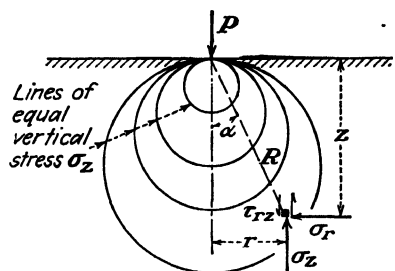
FIG. 9-4. Diagram illustrating the symbols of the Boussinesq solutions.

A presentation of the Boussinesq solution in a modern English-language publication was made by Timoshenko (Ref. 367, pp. 328–333). With reference to the symbols shown in Fig. 9-4, the following values were obtained for stresses produced by a concentrated surface load P at a point within the elastic soil mass located at a depth z and a horizontal distance r from the vertical line of action of the load P: The vertical stress

$$\sigma_z = -\frac{3P}{2\pi} z^3(r^2 + z^2)^{-5/2} \tag{9-3}$$

The shearing stress

$$\tau_{rz} = -\frac{3P}{2\pi} rz^2(r^2 + z^2)^{-5/2} \tag{9-4}$$

The horizontal radial stress

$$\sigma_r = \frac{P}{2\pi}\left\{(1 - 2\nu)\left[\frac{1}{r^2} - \frac{z}{r^2}(r^2 + z^2)^{-1/2}\right] - 3r^2z(r^2 + z^2)^{-5/2}\right\} \tag{9-5}$$

The expression for the horizontal tangential stress σ_θ may be found in Ref. 367.

The following facts are revealed by an examination of Fig. 9-4 and of Eqs. (9-3) to (9-5): All stresses are independent of the value of the Young modulus E of the material. The vertical stress σ_z and the shearing stress τ_{rz} in addition are independent of the value of the Poisson ratio ν. Lines drawn through points of equal vertical stress σ_z have the approximate shape of circles; this is also true in the case of lines drawn through points of equal shearing stress τ_{rz}. The horizontal radial stress σ_r, that is, the radial lateral pressure, however, *is* dependent on the value of the Poisson ratio ν.

Indirect evidence of the correctness of the Boussinesq solution for elastic materials has been provided by laboratory *photoelastic experiments*. This type of study is based on the fact that the crystals of an elastic medium are reoriented to an equal degree by shearing stresses of the same intensity, so that when polarized light is sent through stressed bakelite, gelatine, or similar materials, points of equal shearing stress appear as lines of the same color (see Ref. 140). Under conditions of loading corresponding to Fig. 9-4, the lines of equal shear during a photoelastic experiment have the approximate shape of circles, as should be the case according to the Boussinesq solution.
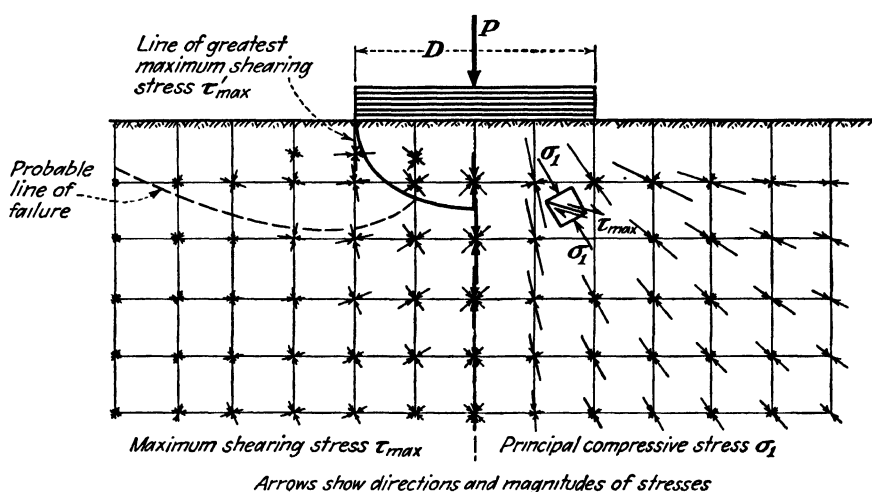
FIG. 9-5. Distribution of stresses under a circular loaded area. (After Converse, Ref. 83, 1939.)

Of course many soils are plastic and not elastic materials. The theory of plasticity (Ref. 244) has not yet been developed to the point permitting the rigorous mathematical treatment of such problems. Nevertheless, observations of the behavior of soils indicate that the Boussinesq solutions can be applied with reasonable accuracy to cohesive soils and even, with some limitations, to granular soils, such as sands. This will be discussed in the following articles.

The way stresses are distributed through the soil under a circular loaded area is shown in Fig. 9-5, where it is assumed that the soil behaves like a semi-infinite elastic solid. The relevant equations are given by Timoshenko (Ref. 367, pp. 333–337). The graphical evaluation given in Fig. 9-5 was performed by Converse (Ref. 83, 1939) (see also Jurgenson, Ref. 195, 1934). It will be noted from the small cube shown on the right-hand side of the diagram that the maximum shearing stress at that point,

τ_{max}, occurs on planes inclined 45° to the direction of the principal compressive stress σ_1 [see Eqs. (7-7) and (7-8)].

The location of the greatest values τ_{max}' of the maximum shearing stresses at any point of the entire soil mass is indicated on the cross section by an elliptical curve. According to Timoshenko (Ref. 367, p. 337), this curve will intersect the vertical axis through the center of the loaded area at a depth $z = 0.638\ (D/2)$. This will hold for a value of the Poisson ratio $\nu = 0.3$. The corresponding value of the greatest maximum shearing stress will then be

$$\tau_{max}' = 0.33p \tag{9-6}$$

where $p = P/A$ is the average unit load on the area of contact between the footing and the soil. It should be noted that, whereas the shearing stress on vertical planes τ_{rz} due to a concentrated surface load was independent of the Poisson ratio [Eq. (9-4)], the value of the greatest maximum shearing stress under a loaded footing is dependent thereon, although only to a slight extent. Thus it may be shown, by substituting the limit value of $\nu = 0.5$ in Eqs. (h) and (k) of Ref. 367, p. 337, that

$$\tau_{max}' = 0.29p \tag{9-7}$$

and $z' = 0.692\ (D/2)$. Thus the possible variation of τ_{max}' because of uncertainties in the value of the Poisson ratio of soils is negligible and does not exceed 15 per cent. The actual value of τ_{max}' is of practical importance (see Arts. 9-10 and 14-2).

9-3. Model Tests to Determine the Stress Distribution in Sands. Many attempts to determine experimentally the stress distribution in sands have been made during the past century with gradually improving instrumentation and testing techniques. Sands were experimented with first, since it is comparatively easy to embed pressure-measuring devices in sand.

Particularly noteworthy are the extensive tests with footings of different sizes which were carried out by Koegler and Scheidig at the Mining Academy of Freiberg, Saxony, in 1927 (Ref. 200). An improved method of vertical-pressure measurement was employed. It consisted in using a very large number of pressure cells, which were placed so closely to each other that they formed continuous horizontal layers at several depths, thereby eliminating inaccuracies in the measurements due to differences in the compressibility of the pressure cells and of the surrounding sand.

The results of one of the Freiberg tests are shown in Fig. 9-6. The curved, pear-shaped lines are drawn through points in the sand mass where vertical pressures of equal intensity were measured. These pressures are expressed in per cent of the average unit surface pressure

$p = P/A$ at the plane of contact between the test footing and the sand, where P is the total load applied, and A is the area of the footing.

It will be noted from Fig. 9-6 that the vertical pressures in the sand were somewhat more concentrated under the footing and were somewhat less spread out laterally than is indicated by the Boussinesq formulas (see Fig. 9-4). Near the sand surface there existed a zone of zero stress, limited by the curve of zero pressure, as shown in Fig. 9-6. The angle φ_0 between that curve and the vertical equaled 35° near the sand surface, then increased gradually till at a certain depth t is approached 90°. This
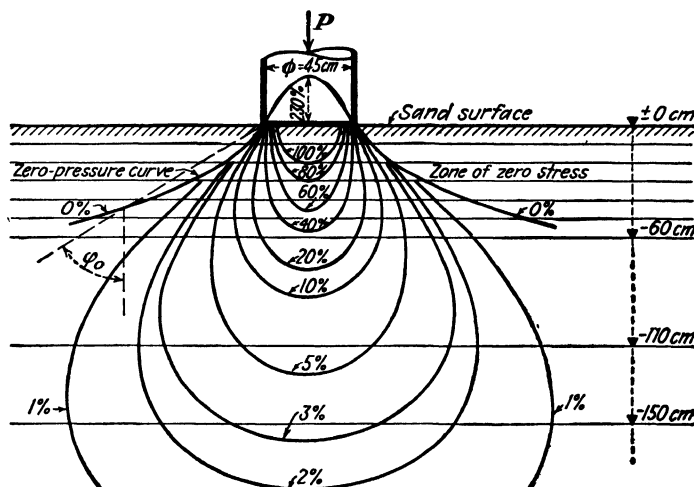
FIG. 9-6. Lines of equal vertical pressure in sand, as measured during the Freiberg tests. (*After Koegler and Scheidig, Ref. 200, 1927.*)

depth t was found at Freiberg to be independent of the size of the footing and to vary between 3 and 4 ft for surface-contact pressures in the range of 0.5 to 1.0 ton per ft^2 and sand of normal density. It did not exceed 6.5 ft for very loose sand. It is reasonable to assume that the depth t will be greater for larger surface-contact pressures. The explanation of these observations follows.

The application of a load to the surface of a homogeneous body produces, as shown by Boussinesq, vertical and lateral pressures within that body. These pressures, together with the weight of the overlying layers of the soil, form a resultant pressure, which has a strong inclination in the upper layers. Here, outside of the surface loaded by the footing, the noncohesive granular soils cannot resist its horizontal component. The resistance to shear of such soils depends only on intergranular friction, which is zero near the sand surface, since there is no overlying soil layer to produce, by its weight, pressures which would render the potential

frictional resistance of the sand effective. Intergranular movements will occur there with little hindrance. Therefore the pressures from the footing cannot spread out laterally in the upper layers of the sand to the same extent as they would in a cohesive material. This produces in sand a greater concentration of vertical pressures below the loaded surface than is indicated by the Boussinesq formulas. Farther below the surface of the sand, conditions change. The inclination of the resultant pressure gradually decreases because of the added weight of the upper soil layers. For the same reason, the value of intergranular friction and therefore of the horizontal resistance of the soil is increased. At a
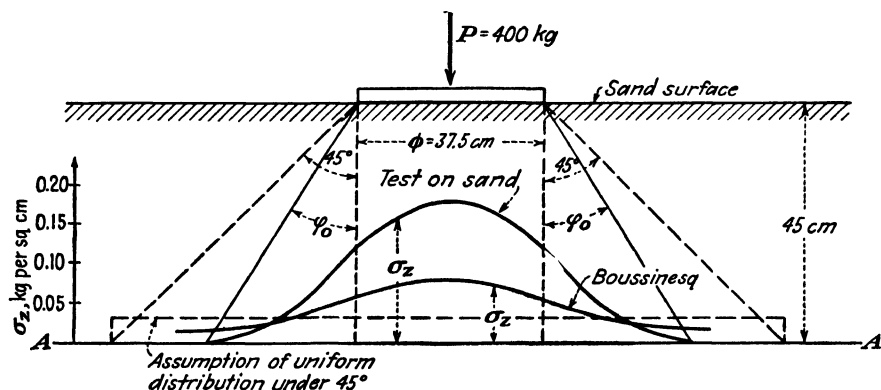
FIG. 9-7. Distribution of vertical pressures on the horizontal plane AA, as established during the Zurich tests on sand and as computed according to the Boussinesq formulas. (*After Hugi, Ref.* 179, 1927 *and Gerber, Ref.* 146, 1929.)

depth t the sand can then behave like a homogeneous elastic body to which the Boussinesq equations may be applied.

Figure 9-7 illustrates this point in respect to the upper layers. It is based on tests performed at Zurich, the results of which closely agreed with those obtained at Freiberg. It also shows that the assumption of a uniform distribution of the vertical pressures, spread out under a certain angle, is entirely inaccurate. However, for larger footings the difference between these three types of pressure distribution should be somewhat smaller than given in Fig. 9-7, even in the upper layers. The point will be discussed further in Arts. 9-4 and 9-5.

Some additional experiments were performed at Freiberg, which demonstrated the nature of the displacements of the sand particles below the loaded footing. Small wooden spheres were embedded in the sand fill as it was placed, and their coordinates were measured. After the loading the sand was carefully removed, and the positions of the spheres were again measured. The results are shown in Fig. 9-8. The displacements

of the particles did not follow too closely the direction of the principal compressive stresses shown in Fig. 9-5 for an elastic material, indicating that shearing stresses influenced these displacements, as well as the heave of the sand surface. Similar results were obtained at Zurich by embedding small lead spheres in the sand and taking an X-ray photograph before
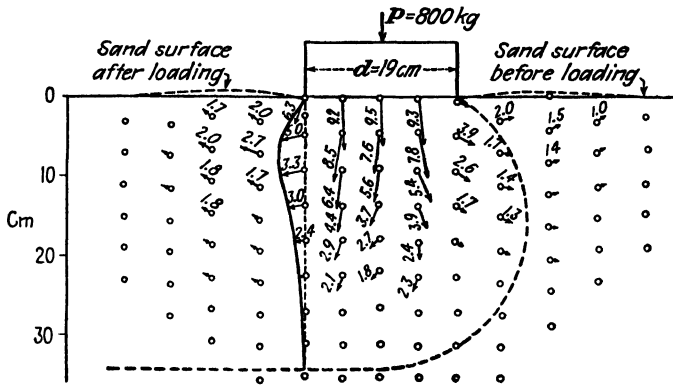
FIG. 9-8. Displacements of small wooden spheres embedded in sand. (*After Aichhorn, Ref.* 3, 1931.)

the application of the load to the footing and a second photograph (on the same film) after the application of the load (Gerber, Ref. 146, 1929).

9-4. The Distribution of Soil Reactions at the Plane of Contact with the Foundation. The distribution of the reactions of the soil to the foundation loads depends on the condition of the soil at the boundary of the loaded footing. Sand with no surcharge around the footing, that is, with no overlying layers of soil, will not have any shearing strength at the footing boundary for reasons explained in Art. 9-3. The sand there will
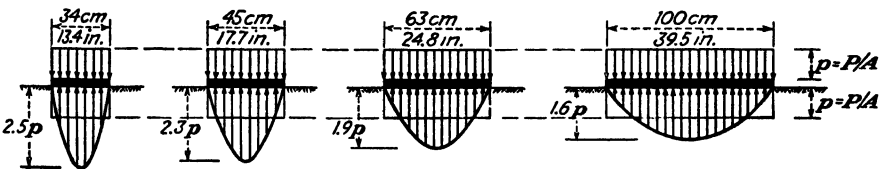
FIG. 9-9. The effect of the size of a footing resting on sand on the distribution of the soil reactions against the footing, as determined during the Freiberg tests. (*After Koegler and Scheidig, Ref.* 200, 1927.)

therefore yield readily, reducing the reactions against the footing at the boundary. Equilibrium will then require an increase of the intensity of the soil reactions at the center of the footing to values higher than the average uniformly distributed unit pressure $p = P/A$. In the case of the test illustrated by Fig. 9-6 pressure-measuring cells were embedded

on the lower face of the footing. The reaction pressure at the center was measured and found equal to 230 per cent of P/A. The magnitude of this increase was found to be a function of the size of the footing, as shown in Fig. 9-9. The length of the circumference of a footing increases linearly with an increase of the diameter or of the side length of the footing. It is therefore reasonable to expect that the influence of any boundary effects on the distribution of unit pressures will decrease with an increase of the size of a footing, since the unit pressures are dependent on its area, that is, on the second power of the diameter or of the side length of the footing. It is even probable that for very large footings or for entire buildings founded on sand the boundary effects will affect only a small adjoining portion of the entire area, with a resulting distribution
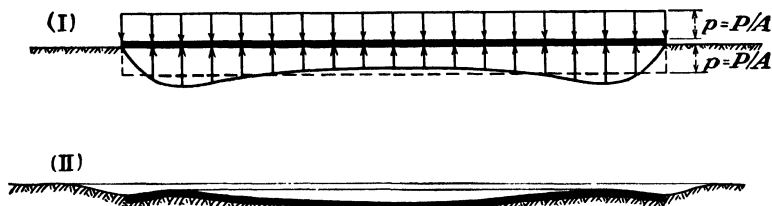
FIG. 9-10. (I) The probable distribution of the soil reactions and (II) the resulting deflection of a large flexible foundation on sand.

of soil-reaction pressures of the type shown in Fig. 9-10(I) and a tendency for a flexible superstructure to settle and to deflect as shown in Fig. 9-10(II).

That the curvatures of a uniformly loaded, flexible footing may be reversed, depending on the nature of the soil reactions, is illustrated by Fig. 9-11. The type of curvature shown in Fig. 9-11(I) has actually been measured on sand (Ref. 201), but only for very small footings, where the effect of the yielding of the surface sand grains at the boundary of the footing overbalanced the effect of the greater compression beneath the center of the footing of the deeper lying soil layers (see Fig. 9-7). The curvature shown in Fig. 9-11(II) has been frequently measured on structures erected on clay soils (Figs. 9-3 and 13-10); it is the natural result of the stress-distribution pattern shown in Fig. 9-11(II). This pattern is in agreement with the rigorous Boussinesq solution and can be explained as follows: In a *firm* cohesive soil the material immediately outside of the boundary of the footing will receive some of the load, which will be transferred to it by shearing stresses which, in contrast to noncohesive sand, can be resisted by a clay at the ground surface irrespective of any surcharge pressures around the footing. Thus the clay at the outer boundary of the footing will offer more resistance to the load of the footing than

will that at the center of the footing. A concentration of reaction pressures at the perimeter of the footing will result, as shown in Fig. 9-11(II). This concentration is a discontinuous localized phenomenon; deeper down below the contact surface between footing and soil the distribution of vertical pressures on a horizontal plane will be as shown in Fig. 9-7. It will be noted that a greater deflection at the center of a flexible, uniformly loaded footing on clay is in agreement both with the soil-reaction diagram of Fig. 9-11(II) and with the vertical-pressure diagram of Fig. 9-7, if we
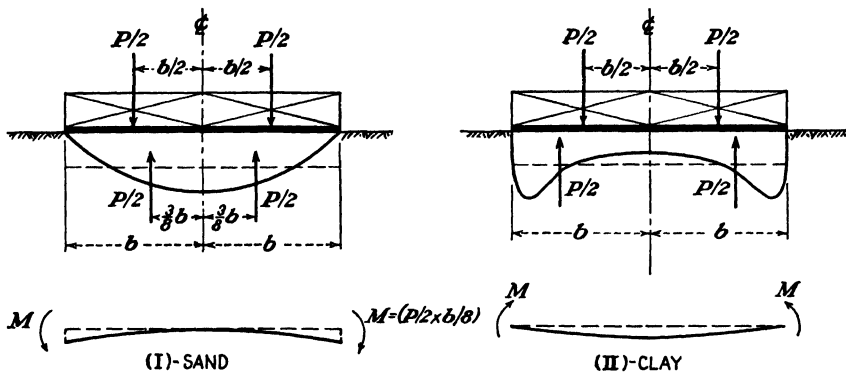
FIG. 9-11. The relationship between the distribution of soil reactions and the curvature of small, uniformly loaded flexible footings on sand and on clay.

consider that most of the surface settlements represent the sum of the vertical compressive strains of all underlying layers.

A noteworthy series of soil-reaction measurements was performed by Oscar Faber (Ref. 129, 1933) in London. The special test footing employed is illustrated in Fig. 9-12. It consisted of two $\frac{3}{4}$-in.-thick steel plates of 12 in. diameter. The lower plate was in direct contact with the soil; it was formed by six concentric rings so dimensioned that the areas of all six rings were equal. The upper plate was of one solid piece and received the test load at its center. Each of the six rings of the lower plate was connected to the upper plate by means of three steel rods on which strain measurements were performed. The increment of strain registered on a rod as a result of a load increase on the footing, when multiplied by the Young modulus of steel and by the cross-sectional area of the rod, gave the load carried by the rod. The sum of the loads carried by the three rods which supported a ring, divided by the area of the ring, gave the unit pressure on the ring. In this manner the diagrams shown in Figs. 9-13 to 9-15 were obtained.

It will be noted from Fig. 9-13 that the unit pressure at the center of the plate was approximately equal to 2.5 times the average unit pressure

FIG. 9-12. The design of the special footing employed by Oscar Faber (Ref. 129, 1933) for the measurement of soil reactions.

FIG. 9-13. The distribution of soil reactions against the test footing illustrated in Fig. 9-12. Clean sand, no surcharge around the footing. (After O. Faber, Ref. 129, 1933.)

$p = P/A$ over the entire footing. Actually it varied between $2.3p$ and $2.7p$—except for the first load, which produced a very low unit pressure—when the reaction pressure at the center was only $1.8p$. Thus these results agree quite well with those of the Freiberg tests, where on a footing of a comparable size (34 cm) the reaction pressure at the center equaled $2.5p$ (see Fig. 9-9).

The application by Oscar Faber of a surcharge around the perimeter of the same footing increased the shearing resistance of the sand, as shown in Fig. 9-14. This was particularly noticeable under higher unit pressures, where the reaction pressure at the center of the footing dropped to
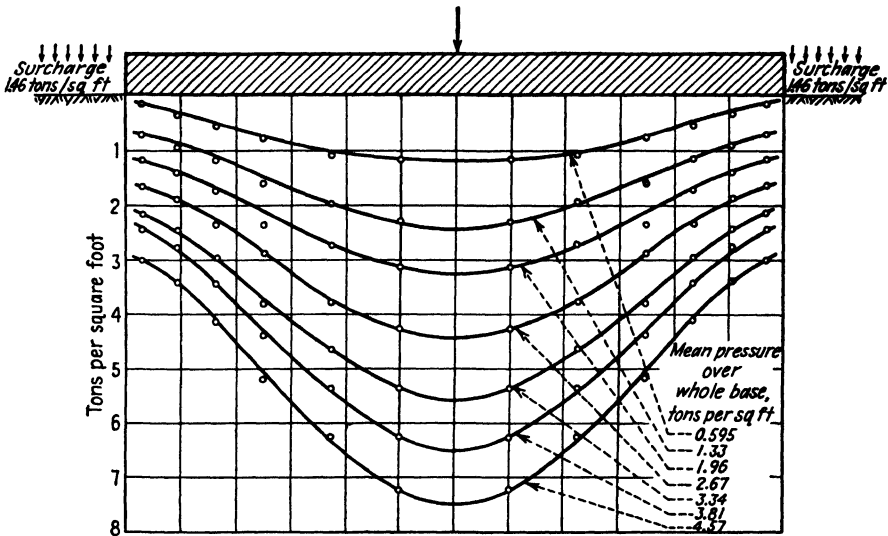
FIG. 9-14. The distribution of soil reactions against the test footing illustrated in Fig. 9-12. Clean sand, 1.46 tons per ft² surcharge around the footing. (*After O. Faber, Ref. 129, 1933.*)

approximately $1.6p$. The surcharge applied equaled 1.46 tons per ft². This surcharge is the equivalent of the overburden weight of 24 ft of soil weighing 120 lb per ft³. It is reasonable to believe that for greater surcharge pressures there would be even less tendency for the sand to yield at the boundary of the footing, so that the reaction pressures would be even more nearly uniform.

Of particular interest is the test made on a stiff London clay, the results of which are shown in Fig. 9-15. The curve of reaction pressures has the shape that is to be expected on the basis of the Boussinesq solution for a homogeneous elastic body with greatest pressures at the edges of the footing. This circumstance provides further indirect proof of the fact that the Boussinesq equations can be applied to clay soils and give results

of satisfactory accuracy (see also Art. 13-7). The application of a surcharge around the perimeter of the test footing did not produce any noticeable difference in the shape of the soil-reaction curves, as compared with Fig. 9-15, when the footing rested on clay. This result is also in agreement with theory, since the shearing strength of clays depends on cohesion only (Art. 7-22).
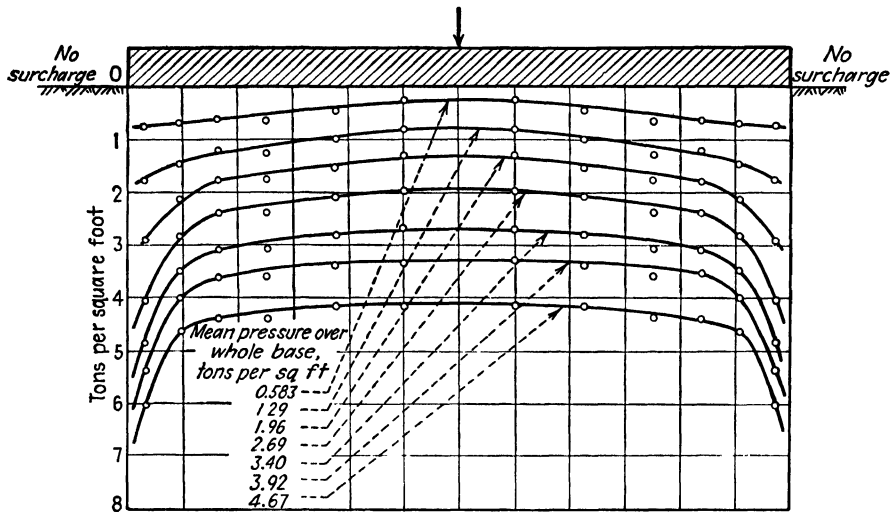
FIG. 9-15. The distribution of soil reactions against the test footing illustrated in Fig. 9-12. Stiff clay, no surcharge around the footing. (*After O. Faber, Ref. 129, 1933.*)

9-5. Froelich's Stress-concentration Factor

The following attempt was made by Froehlich (Ref. 141, 1934) to express different degrees of stress concentration beneath a concentrated load applied to the surface of a semi-infinite solid. With reference to the symbols of Fig. 9-4, the equation for the vertical stress σ_z was proposed by Froehlich to read

$$\sigma_z = -\frac{\nu P}{2\pi} z^\nu (r^2 + z^2)^{-(\nu+2)/2} \qquad (9\text{-}8)$$

where ν is a statically indeterminate parameter, called the *concentration factor.* A comparison with the Boussinesq solution for an elastic medium shows that for a value of the stress concentration factor $\nu = 3$, Eq. (9-8) becomes identical with the conventional Boussinesq equation (9-3). Figure 9-16 illustrates the change in the curvature of the σ_z isobars, that is, of the lines passing through points of the same vertical stress, for values of ν equal to 2, to 4, and to 6, in accordance with Eq. (9-8). The isobar for $\nu = 2$ is a circle.

On several occasions attempts have been made to integrate Eq. (9-8) over the area of a footing in much the same manner as this is done for the Boussinesq equation (9-3) (see Art. 9-6). The purpose of this operation was to find convenient expressions for the determination of stresses in sandy soils, where tests on small footings had shown a lesser degree of stress distribution, that is, a greater stress concentration,

than in the case of cohesive soils, as expressed by the Boussinesq equation (9-3) (see Fig. 9-7). Attempts of this kind, however, disregard the fact that, as explained in Art. 9-4, differences in vertical-stress concentration in the soil are primarily caused by *boundary effects* at the perimeter of a loaded footing. Any integration of Eq. (9-8) for a unit load over the area of a footing, when based on the assumption of a constant value of the concentration factor ν over that area, therefore is not compatible with the physical nature of the observed phenomena. It should be noted that in his original publication on the matter, Froehlich did not extend his analysis beyond the problem presented by a concentrated load.

FIG. 9-16. Lines of equal vertical pressure σ_z for varying values of the stress concentration factor ν [see Eq. (9-8)]. (*After Froehlich, Ref. 141, 1934.*)

9-6. Charts for the Computation of Stress Distribution in Soils.

In the early stages of the development of soil mechanics the following procedure was used when it was necessary to compute the stresses within a soil mass due to pressures applied to the soil surface by foundations or by earth fills. The contact area between the foundation and the original soil was subdivided into a number of squares sufficiently large to permit the replacement of the total unit pressures over the area of the square by a concentrated load at its center. The stress induced by such a concentrated load at any point within the soil mass was then computed by means of Eqs. (9-3) and (9-5). The procedure was repeated for the concentrated loads of all squares, and the stresses, as computed for each of the loads, were added up. Needless to say, the procedure was extremely time-consuming and laborious. Several types of auxiliary computation charts were then developed to permit quicker operation. There are two main types of such charts.

The first type is illustrated by Figs. 9-17 and 9-18. It permits the determination of the vertical stress σ_z at a depth z below the corner A of a rectangular footing of width b and length a, uniformly loaded by a unit pressure p. Let us consider an infinitely small square unit of area $(da\ db)$, shown in Fig. 9-17. The pressure acting on that small square may be replaced by a concentrated load dP applied to the center of that square, so that

$$dP = p\ da\ db \tag{9-9}$$

The increase of the vertical stress σ_z due to the load dP can be expressed

by rewriting Eq. (9-3) to read

$$d\sigma_z = -dP \frac{3z^3}{2\pi} (r^2 + z^2)^{-5/2} \tag{9-10}$$

The stress σ_z produced by the pressure p over the entire rectangle $a \times b$ can then be obtained by combining Eqs. (9-9) and (9-10), expressing
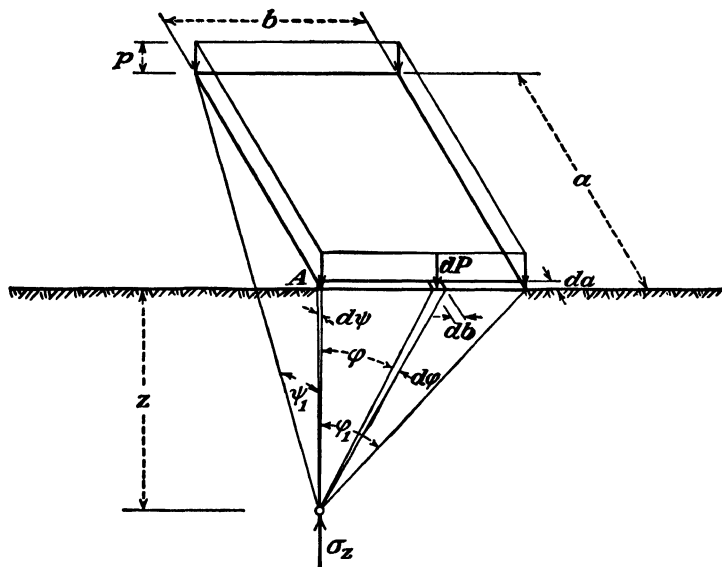
FIG. 9-17. Diagram illustrating the symbols of Eqs. (9-9) to (9-12), on which the chart of Fig. 9-18 is based.

da, db, and r in terms of the angles φ and ψ, and integrating

$$\sigma_z = \int_{\varphi=0}^{\varphi=\varphi_1} \int_{\psi=0}^{\psi=\psi_1} d\sigma_z \tag{9-11}$$

Solutions of Eq. (9-11) can be presented in several forms (Ref. 370). Steinbrenner (Ref. 333, 1936) published the following solution:

$$\sigma_z = -\frac{p}{2\pi} \left\{ \arctan \left[\frac{h}{z} \frac{a(a^2 + b^2) - 2az(R - z)}{(a^2 + b^2)(R - z) - z(R - z)^2} \right] + \frac{bz}{b^2 + z^2} \frac{a(R^2 + z^2)}{(a^2 + z^2)R} \right\} \tag{9-12}$$

where $R = \sqrt{a^2 + b^2 + z^2}$.

Equation (9-12) is presented in graphical form in Fig. 9-18. The chart can be used for computation of pressures (see Prob. 9-2). It also serves to illustrate the influence of the ratio a/b of the lengths of the sides of the loaded rectangle (see Prob. 9-2).

The chart of Fig. 9-18 is well suited for the computation of pressures in cases where the loaded areas are continuous, such as foundation mats or rafts, and are composed of only a few rectangular areas. When the foundation consists of a large number of individual footings, a chart developed by Newmark (Ref. 248, 1942), is more practical. It is based on the following procedure: The vertical stress σ_z at a depth z beneath the
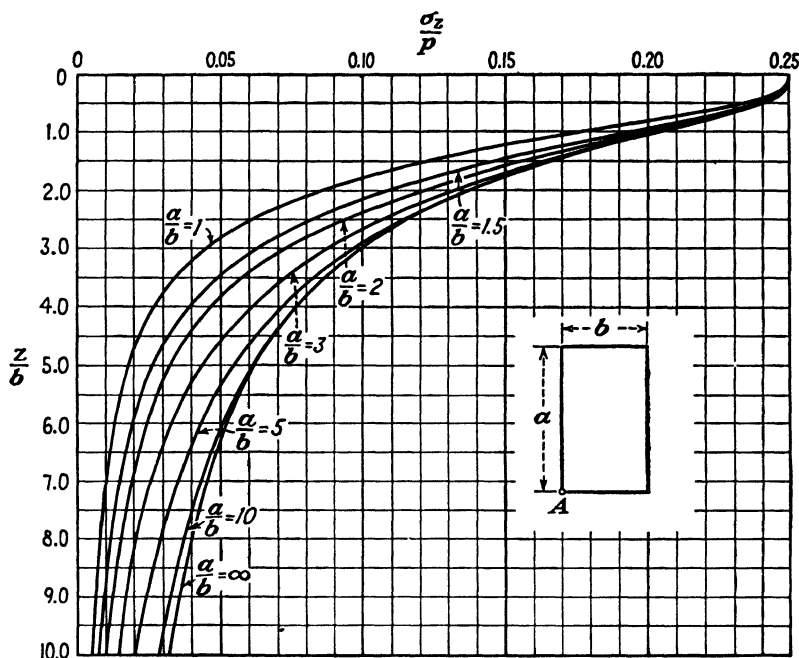
FIG. 9-18. Chart for the computation of vertical stresses in the soil under the corner of a mat foundation (see Fig. 9-17). (*After Steinbrenner, Ref. 333, 1936.*)

center of a circular, uniformly loaded area of radius r is equal to

$$\sigma_z = p\left[-1 + \frac{z^3}{(r^2 + z^2)^{3/2}}\right] \tag{9-13}$$

where p is the unit load on the circular area. For the derivation of this equation see Timoshenko (Ref. 367, pp. 333–335). It can be transformed to read

$$\frac{\sigma_z}{-p} = 1 - \left[\frac{1}{1 + (r/z)^2}\right]^{3/2} \tag{9-14}$$

It will be noted that when $r = \infty$, $\sigma_z/p = 1.0$, that is, $\sigma_z = p$. It is possible to determine from Eq. (9-14) the ratios r/z for which the ratio

$\sigma_z/p = 0.8$, [Eq. (9-14)] gives $r/z = 1.387$. By selecting some definite scale, for instance, the length OQ, as shown in Fig. 9-19, to represent the depth z, we obtain the length of the radius $r_{0.8}$ which corresponds to $\sigma_z/p = 0.8$ by dividing the distance OQ by 1.387 and drawing a circle with that radius. This procedure can then be repeated for other values of σ_z/p, for instance, for $\sigma_z/p = 0.6$ and 0.4, as shown in Fig. 9-19. The diagram thus obtained represents an influence chart for a surface unit load of unity ($p = 1.0$). Thus the vertical stress σ_z will equal 0.8 if the entire circular area of radius $r_{0.8}$ is loaded by $p = 1.0$. If only a ring between the radii $r_{0.8}$ and $r_{0.6}$ is loaded with $p = 1.0$, then $\sigma_z = 0.8 -$
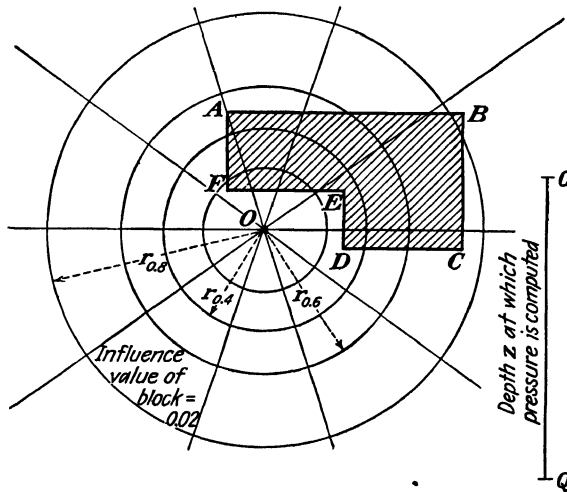
FIG. 9-19. Diagram illustrating the use of the Newmark chart for the computation of vertical stresses in soils. (*After Newmark, Ref. 248, 1942.*)

$0.6 = 0.2$. It will be noted from Fig. 9-19 that each ring is subdivided in that diagram into 10 equal blocks. Therefore a load of $p = 1.0$ covering one of these blocks will produce a vertical unit stress of $\sigma_z = 0.1 \times 0.2 = 0.02$. In other words, the influence value of each loaded block is 0.02. For values of p other than unity, the influence value of 0.02 of each loaded block should be multiplied by the actual value of p.

The computation procedure is as follows: A plan of the foundation is drawn on tracing paper to such a scale that the distance OQ of the chart corresponds to the depth z at which the stress σ_z is to be computed (a different tracing has to be made for each different depth z). The tracing of the foundation plan is then laid over the chart in such a way that the surface point, at a depth z beneath which the stress σ_z is to be computed, coincides with the center O of the chart. The number of blocks covered

by the foundation area *ABCDEF* (see Fig. 9-19) is then counted. This number is multiplied by the influence value of the blocks and by p. The product thus obtained gives the value of σ_z for that particular point. The charts used for actual computations have a much larger number of subdivisions than are shown in Fig. 9-19. The influence values of the resulting blocks are correspondingly smaller, so that the evaluation of the areas covered by irregular-shaped foundation surfaces becomes easier. Such charts, both for vertical and for horizontal stresses, are joined to Ref. 248.

9-7. Effect of the Rigidity of the Superstructure and of Soil Stratification on the Stress Distribution in Soils. The stress-distribution computations described in Art. 9-6 assume that the foundation is perfectly flexible. This is true in the case of such structures as steel tanks for the storage of oil and other liquids, or of long brick buildings of one to three stories height (see Art. 13-3). On the other hand, such structures as bridge piers or reinforced-concrete silos can be considered as entirely rigid. They will therefore be unable to adapt themselves to the curvature of the settlement crater of the soil surface and will tend to span it, thereby increasing the pressures transmitted to the soil at the foundation perimeter to the extent necessary to enforce uniformity of settlement. There are a number of partially rigid types of superstructure which will deflect somewhat and yet redistribute pressures at the soil surface to a certain extent. Under such conditions considerable stresses are apt to be engendered in the superstructure (see Art. 13-3).

Nonuniformity of the soil may also produce deviations from the computed stress distribution which cannot always be evaluated accurately. For instance, as shown in Fig. 9-20(I), a stiff upper crust of clay may act as a foundation mat, so that the pressures on a plane *AA* of an underlying layer of soft clay will be distributed to a somewhat greater extent and will therefore be somewhat smaller than the values computed from charts based on the Boussinesq solution. A stiff layer, when underlying the foundation at a shallow depth, as shown in Fig. 9-20(II), will have a reverse effect on the stress distribution within the compressible layer above it. A rock surface *BB* will tend to restrain along that plane the lateral expansion of the overlying clay, so that a greater concentration of pressures will take place under the foundation on a plane *AA* than would be the case for a uniform layer of great depth. This concentration of pressures will increase with decreasing values of the ratio H/L.

Stratification, if considered as providing within a clay mass at small intervals thin layers of relatively great rigidity, will tend to spread out the pressures and therefore to reduce them somewhat as compared with the Boussinesq solution for a homogeneous soil. A solution for layers of

infinite rigidity has been proposed by Westergaard (1938) (see Taylor, Ref. 343).

The results of stress computations in soils are therefore liable to be affected by so many numerically uncertain secondary factors, that one should not expect to obtain rigorously exact values. Nevertheless, satisfactory agreement between theory and measurements, insofar as the order of magnitude of the values obtained is concerned, has frequently been recorded (see Fig. 13-10) in the case of a flexible or semiflexible superstructure. In the case of a very rigid superstructure there is some justification for the use of the simplified Equations (9-2) and (9-2a), instead of
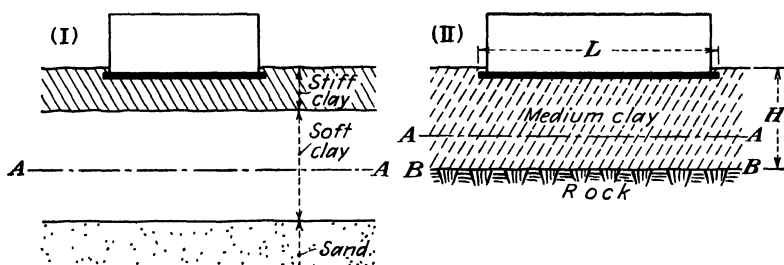
FIG. 9-20. (I) A stiff upper layer distributes pressures to a greater extent than indicated by the Boussinesq solution, whereas (II) a stiff underlying layer has a reverse effect on the stress distribution above it.

the rigorous solutions valid only for a fully flexible superstructure (see Prob. 9-1). In any case, theoretical stress-distribution studies have firmly established a number of facts which are of primary importance for the general guidance of foundation engineers. These facts had been frequently disregarded in the past.

9-8. Some Misconceptions Which Have Been Dispelled by Studies of Stress Distribution in Soils. A number of practically important misconceptions, widely accepted by professional engineers as facts only some 20 to 25 years ago, have been shown to be fallacious by the theoretical and experimental studies of stress distribution described in the preceding articles. Here are a few of the more essential ones:

1. *Fallacy:* "If the loads are uniformly distributed over a certain area on the surface of a homogeneous soil mass, the settlement of that area will also be uniform." We now know that the settlement will be greatest at the center of the area and that the soil surface will tend to assume a dishlike shape.

2. *Fallacy:* "The soil layers immediately beneath the foundation will cause most of the settlement that it may undergo." We now know that weak soil layers at considerable depths beneath the foundation may still

in some cases be the cause of surface settlements and of resulting appreciable damage to the superstructure.

3. *Fallacy:* "The settlement of a foundation depends only on the nature of the underlying ground and on the intensity of the pressure applied to the soil surface." We now know that under the same unit pressure, on the same ground, a foundation of larger area will tend to settle more than a foundation of smaller area.

9-9. The Bearing Capacity of Soils. The term *bearing capacity* of a soil, as used in this book, shall refer to the ultimate value of the average
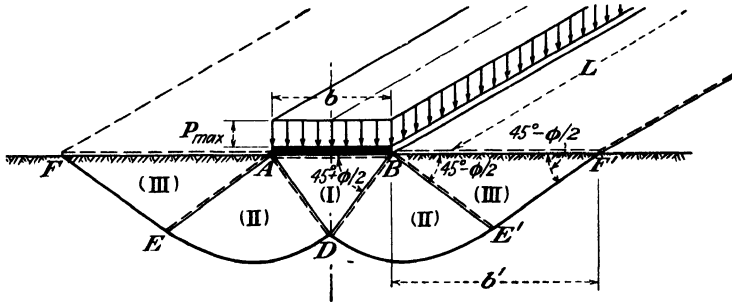
FIG. 9-21. Diagram illustrating the determination of the ultimate bearing capacity p_{max} of a very long footing ($L/b \rightarrow \infty$) under the assumption of simultaneous upward yielding of the soil on both sides of the footing. (*After Prandtl, Ref. 274, 1921.*)

unit contact pressure between a foundation mat or footing and the soil which will produce a shear failure within the soil mass.

Many modern analyses of this problem are based on a solution by Prandtl (Ref. 274, 1921). Prandtl investigated the plastic failures of metals. A special case (horizontal surface) of his general solution is applicable to foundations and is illustrated by Fig. 9-21. Since Prandtl was mainly concerned with the penetration of punches into metals, where movement of these punches was *guided*, a basic assumption of his solution is that a loaded footing of width b and a very great length L will sink vertically downward into the underlying material, thereby producing shear failures on both sides of the footing. The wedge-shaped soil zone I immediately beneath the footing is assumed to move downward without any deformation together with the footing. Soil zones II are assumed to be in a plastic state and to push soil zones III upward as units. The assumed displacements are shown by broken lines in Fig. 9-21 (compare this simplifying assumption with Fig. 9-8).

Prandtl's analysis covered varying values of the angle of internal friction ϕ. For $\phi = 0$ his solution was

$$p_{max} = 2.571q \tag{9-15}$$

where q = the compressive strength of the soil. For $\phi > 0$, p_{max} increased rapidly with the value of ϕ, as shown by Table 9-1.

TABLE 9-1. Values of p_{max} According to Prandtl*

ϕ	b'/b	p_{max}/q
0°	1.000	2.571
10°	1.572	3.499
20°	2.530	5.194
30°	4.290	8.701
40°	8.462	17.560

* Ref. 274, 1921.

Of practical importance in actual foundation work are the values of p_{max} for $\phi = 0$, since experience shows that complete shear failures of the soil under overloaded foundations occur only on plastic clays, for which the angle of internal friction ϕ may be taken as zero (Art. 7-22) or, at least, the shearing strength of which may be taken as one-half of the unconfined compressive strength [see Eq. (7-19)]. With this assumption, Eq. (9-15) becomes

$$p_{max} = 2.571q_u = 5.14c \qquad (9\text{-}16)$$

In the above derivations Prandtl did not consider the effect of the weight of the soil in zones II and III (Fig. 9-21). However, in some recent publications (Ref. 104), this effect is included in modifications of the original Prandtl equation. Further, Terzaghi (Ref. 362, 1943) restricted the validity of Eq. (9-16) to foundations with a perfectly smooth base in contact with the soil. Shearing stresses along a rough base were believed to exert a restraining effect on the soil, and p_{max} was claimed to be increased thereby to a value of $5.7c$. The application to all foundation designs of the above suggestions to increase to this extent the original values obtained by Prandtl, however, appears questionable in the light of the following considerations.

In a great many cases the nature of the possible downward movement of a foundation is not restrained in any manner, so that the foundation is *free to rotate* about any one of its edges. Thus the basic assumption of the Prandtl solution, illustrated by Fig. 9-21, does not necessarily hold in all cases. Actual records of shear failures of the clay underlying large foundations usually indicate rotational displacements of the soil, as shown in Figs. 9-24 and 9-25. The clay deposit cannot always be absolutely homogeneous to such an extent that a shear failure would develop in it simultaneously on both sides of the foundation (Fig. 9-21). It is likely to be somewhat weaker on one side than on the other, so that a rotational

failure would result. Therefore an analysis such as is illustrated by Fig. 9-22 is usually indicated.

If we assume that the rotational axis of the cylindrical failure surface coincides with the edge O [Fig. 9-22(I)], limit equilibrium will require the following approximate relationship of moments in respect to O:

$$p_{\max}\frac{b^2}{2} = c(\pi b^2 + hb) + \gamma h\frac{b^2}{2} \tag{9-17}$$

or

$$p_{\max} = c\left(2\pi + \frac{2h}{b}\right) + \gamma h$$

$$= 6.28c\left(1 + 0.32\frac{h}{b} + 0.16\frac{\gamma}{c}h\right) \tag{9-18}$$
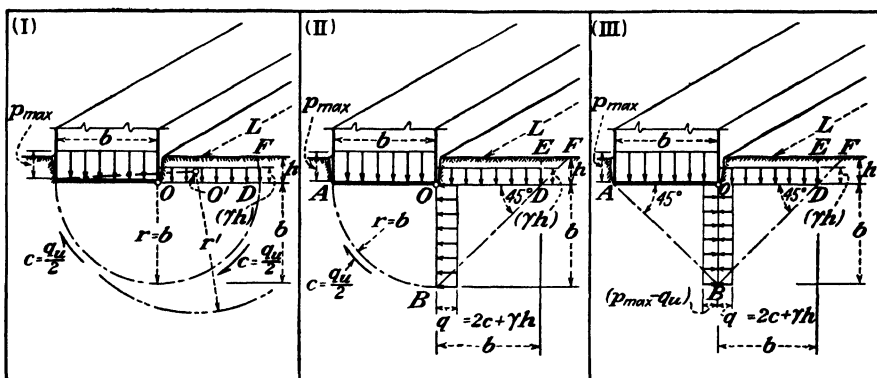
FIG. 9-22. Diagrams illustrating different conceptions concerning the surfaces of failure in a purely cohesive soil ($\phi = 0$) under the assumption of lateral and upward yielding of the clay on one side only of a very long footing ($L/b \rightarrow \infty$).

When the foundation rests on the ground surface ($h = 0$),

$$p_{\max} = 6.28c \tag{9-19}$$

This value is somewhat too high. Studies made by Fellenius (Ref. 133, 1929), have demonstrated that the most unfavorable cylindrical surface of failure is obtained for a center of rotation O' located as shown in Fig. 9-22(I). For surface loading ($h = 0$) Fellenius obtained

$$p_{\max} = 5.52c \tag{9-20}$$

This analysis was extended by Guthlac Wilson (Ref. 431, 1941) to a general analytical solution giving the coordinates of the center of rotation O' and the ultimate load on an infinitely long footing for other than surface loading ($h > 0$).

Wilson's results, as given by his chart (Fig. 6), may be expressed as follows:

$$p_{max} = 5.52c\left(1 + 0.377\frac{h}{b}\right) \tag{9-21}$$

Two other assumptions concerning possible surfaces of failure are given in Fig. 9-22 for purposes of comparison. The first consists in assuming the center of rotation O at the edge of the foundation, as shown in Fig. 9-22(II). The rotational equilibrium of the sector OAB is assumed to be provided in part by the passive lateral resistance of the adjoining clay. In accordance with Eqs. (10-12) and (10-5), Fig. 10-1(II), and Eq. (7-8), this passive resistance for $\phi = 0$ will equal $2c + \gamma h$. Equilibrium will then require

$$p_{max}\frac{b^2}{2} = c\frac{\pi b}{2}b + 2c\frac{b^2}{2} + \gamma h\frac{b^2}{2} \tag{9-22}$$

or

$$p_{max} - \gamma h = c(\pi + 2) = 5.14c \tag{9-23}$$

For surface loading ($h = 0$) this result is identical with that of the original Prandtl solution [Eq. (9-16)].

Figure 9-22(III) illustrates the assumption of plane surfaces of failure, on which, according to Ref. 431, some early (1929) analyses by Terzaghi were based. With reference to Fig. 10-1(II) and Eqs. (10-12), (10-5), and (7-19), equilibrium along the plane OB will require

$$p_{max} - q_u = q_u + \gamma h \tag{9-24}$$

or

$$p_{max} - \gamma h = 2q_u = 4.0c \tag{9-25}$$

It will be noted that in the preceding analyses of rotation stability the weight of the rotating cylindrical soil sectors could be neglected, since it is in approximate equilibrium in respect to the center of rotation. Shearing stresses along a rough base AO (Fig. 9-22) cannot affect the stability in respect to the center of rotation O.

All the preceding equations of this article are valid for very long foundations for which the ratio L/b tends to approach infinity. The resistance to rotation of somewhat shorter foundations will be increased by the shearing strength of the soil on vertical planes beneath the two ends of the foundation strip. The increased bearing capacity of the entire foundation can then be roughly estimated, as illustrated by Fig. 9-23.

When the shearing resistance on the cylindrical surface $ADBGEF$ of radius b reaches its maximum value of c, the conservative assumption can be made that at some smaller distance ρ from the axis of rotation OO the

unit shearing resistance c on a vertical plane through the short ends AB or EF of the rectangular foundation will be reduced in direct proportion to the distance from O, so that

$$c_\rho = c\frac{\rho}{b} \tag{9-26}$$

The rotational resistance dR around O of a ring $d\rho$ thick, located at a distance ρ from O, will then be

$$dR = c\frac{\rho}{b}\pi\rho^2\,d\rho \tag{9-27}$$

and of the entire sector ADF

$$R = \frac{\pi c}{b}\int_{\rho=0}^{\rho=b}\rho^3\,d\rho = \frac{\pi c}{b}\bigg|_{\rho=0}^{\rho=b}\frac{\rho^4}{4} = 0.25\pi cb^3 \tag{9-27a}$$

By dividing Eq. (9-27a) by the resistance πcb^2L offered by the cylindrical surface $ADBGEF$ to rotation around the axis OO, we obtain $0.25b/L$ as an
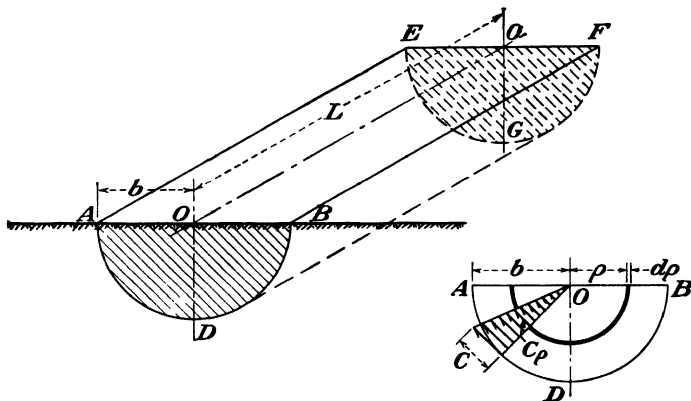
FIG. 9-23. Diagram illustrating method of evaluating the resistance to rotational sliding of cohesive soil beneath foundations with values of the ratio $b/L > 0$.

expression for the increment of rotational resistance offered by one end sector ADB, if the resistance of the cylindrical surface is taken to equal unity. For both end surfaces this value becomes $0.50b/L$. It corresponds to the conditions for which Eq. (9-19) had been derived. It has, however, been shown that the value $p_{max} = 6.28c$ given by that equation is somewhat too high, the $5.52c$ of Eq. (9-20) being more nearly correct. In addition, the three-dimensional failure surface may be somewhat smaller than the one assumed on the basis of the preceding simplified two-dimensional analysis. We can therefore reduce the value $0.50b/L$ at least to read $0.44b/L$. By adding this value to Eq. (9-21) we obtain

the following general expression for the approximate value of the ultimate unit load on clay soils:

$$p_{max} = 5.52c\left(1 + 0.38\frac{h}{b} + 0.44\frac{b}{L}\right) \tag{9-28}$$

For a square footing ($b = L$) on the surface of the ground ($h = 0$), we obtain

$$p_{max} = 7.95c \tag{9-29}$$

Terzaghi and Peck (Ref. 365, 1948) suggest for a square footing $p_{max} = 7.4c$.*

The factors of safety advisable in actual design for use in conjunction with Eqs. (9-28) and (9-29) will be given in Art. 14-2.

9-10. Comparison of Foundation Loads Which Caused Actual Shear Failures in Underlying Clay with Values Computed from Laboratory Tests. The type of collapse illustrated by Figs. 9-24 and 9-25 is by no means infrequent. For instance, Scheidig (Ref. 303, 1937) reproduced photographs of four other similar cases. They had one common characteristic; all were heavy silos or stockhouses erected on plastic cohesive soil. However, no numerical data concerning the shearing strength of the underlying clay were reported in these cases, nor were any available at first in respect to the structure illustrated in Fig. 9-24. The study of that failure by Lazarus White (Ref. 428, 1940) had to be limited to the selection of a more suitable site for the new structure which was to replace the one destroyed. The only data available were old records of borings made prior to the construction, giving the number of blows of a 360-lb hammer, dropped 18 in., per foot of penetration of a sampling spoon, the average of which is shown in Fig. 9-24. However, the diameter of the spoon, necessary for the evaluation of the strength of the clay (see Art. 12-9), was not indicated in these records. The only thing one could therefore definitely conclude was that the strength of the clay was approximately constant between the depths of 15 and 60 ft below the bottom of the foundation mat. The possibility of a higher strength of a dry crust above 15 ft was, however, indicated by the water-level elevation, which appeared to vary in depth between 7 and 15 ft. The permission was therefore obtained by Tschebotarioff (1949) to check the properties of the upper 20 ft of that clay. Thin-walled 2-in.-diameter Shelby tubing was used for sampling (see Art. 12-7). The results are shown in Fig. 9-24. The unconfined compressive strength dropped from $q_u = 2.0$ tons per ft^2 at the elevation of the foundation mat to $q_u = 1.0$ ton per ft^2 18 ft below

* Rigorous solutions for circular footings give somewhat smaller values (by some 15 per cent). See A. W. Skempton, "The Bearing Capacity of Clays," paper presented to the Building Research Congress, London, 1951.

it. The corresponding water content increased with depth from 34 to 46 per cent. The soil was a varved clay of glacial origin, of a mottled, brown-gray coloring, caused by oxidation, near the surface. The brown-colored sections of the clay decreased with depth and disappeared entirely at a depth of 15 ft. The sensitivity (see Art. 7-22) increased with depth from $S = 2.0$ and $S' = 2.5$ to $S = 5.0$ and $S' = 10.0$. This is therefore a clay which is quite sensitive to remolding.

A number of extensive laboratory investigations have been performed in recent years on varved clays of the general region where the structure illustrated by Fig. 9-24 is located. The lowest average unconfined compressive strength of any layer found so far was $q_u = 0.8$ ton per ft². This is therefore the minimum value which can be reasonably assigned to the layer below a depth of 20 ft. Further, if we compare the q_u values with the blows-per-foot penetration of the spoon shown in Fig. 9-24, it does not appear likely that this value could be higher than $q_u = 1.0$ ton per ft². The total depth affected by the failure is approximately 60 ft. The average strength of the upper 20 ft has been shown to equal $q_u = 1.5$ tons per ft². Therefore, if we assume $q_u = 1.0$ ton per ft² for the following 40 ft, we obtain $(1.5 \times 20 + 1.0 \times 40)\frac{1}{60} = 1.16$ tons per ft² as an average q_u value for the site. If we assume $q_u = 0.8$ ton per ft² for the lower 40 ft, the average value will be $q_u = 1.02$ tons per ft². In accordance with Eq. (7-19), for $\phi = 0$ we then obtain the possible variation of the shearing strength $s = c = q_u/2$ within the limits of 0.58 and 0.52 ton per ft².

The actual value of $s = c$ at failure can then be computed from Eq. (9-28). Failure occurred when the unit load on the soil reached the value of $p_{max} = 3.05$ tons per ft². With $h = 3$ ft, $b = 49$ ft, and $L = 225$ ft, we obtain

$$\begin{aligned} 3.05 &= 5.52c[1 + 0.38(\tfrac{3}{49}) + 0.44(\tfrac{49}{227})] \\ &= 5.52c(1 + 0.023 + 0.096) = 6.20c \end{aligned}$$

or

$$c = \frac{3.05}{6.20} = 0.49 \text{ ton per ft}^2$$

This value is only 3 to 15 per cent smaller than the one estimated from the laboratory tests. The agreement can be considered quite good, since it appears probable that prior to failure this sensitive clay was somewhat weakened by the remolding which it underwent as a result of shearing deformations. Evidence of such deformations is provided by the following observations (Ref. 428).

The pressures on the ground due to the weight of the silos proper, equal to approximately $p = 0.3p_{max}$, had produced a negligible settlement of ⅛ in. at the side A and 1⁄16 in. at the side O of the silos (see Fig. 9-24). The

filling of the silo was then begun, so that within a month the pressure on the ground equaled $p = 0.82p_{max}$. During that month the tilt of the structure reversed itself, the settlement reaching the values of 1.0 in. at A and $1\frac{5}{16}$ in. at 0. For the following six months the silos remained partially filled, so that the pressure on the ground varied within the limits of $p = 0.82p_{max}$ and $p = 0.71p_{max}$. The settlement during the same period however increased rapidly and at a constant rate, so that at the end of
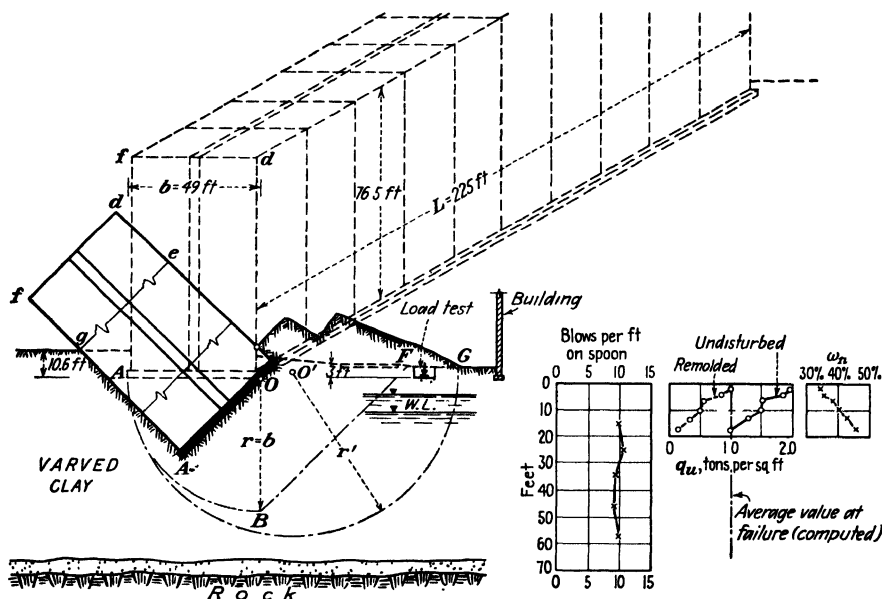
FIG. 9-24. Profile before and after failure of the silos shown in the photographs of Fig. 9-25. (After Lazarus White, Ref. 428, 1940.)

that period the settlement at A was $8\frac{7}{8}$ in. and at O $10\frac{3}{4}$ in. This settlement could not have been caused by consolidation during that short time. The modulus of volume change (see Art. 6-6) of varved clays in that region can be estimated from observations on other structures to be of the order of magnitude $m_v' = 0.005$ (see Art. 13-7 and Fig. 13-22). If we consider that in Eq. (9-2a) the value $1/E$ can be replaced by m_v' (see Art. 6-6) and then substitute the relevant figures in that equation, we obtain the following estimate of the maximum possible value of settlement due to 100 per cent consolidation:

$$\begin{aligned} S &= 2.0pbm_v' \log\left(1 + 1.154\frac{H}{b}\right) \\ &= 2.0 \times 0.82 \times 3.05 \times 49 \times 12 \times 0.005 \log\left[1 + 1.154(\tfrac{60}{49})\right] \\ &= 4.8 \text{ in.} \end{aligned}$$

FIG. 9-25. Collapse of heavy reinforced-concrete silos due to a shear failure of the underlying varved clay (see Fig. 9-24). (*From Lazarus White, Ref.* 428, 1940.)

Therefore more than half of the settlement measured during that six-month period must have been caused by shearing deformation which induced lateral and upward squeezing of the soil at the side O of the foundation. The constant rate of the settlement also indicated some form of plastic flow. An attempt was then made to complete the filling of the silos. During one more month the continued filling increased the pressure on the ground from $p = 0.71p_{max}$ to its final value. The rate of settlement increased, so that at the time of the failure the settlement had reached $11\frac{7}{16}$ in. at A and $13\frac{7}{8}$ in. at O. At the time of the failure the tilting first increased toward the side O to such an extent that attention was attracted by the noise produced by buckling members of a steel bridge (not shown in Fig. 9-24) which connected the silos to the building to the right of the side O. Then the direction of tilting suddenly changed and within approximately 2 min the silos assumed the position shown in the photographs of Fig. 9-25. The upper portion, marked *degf* in Fig. 9-24, broke off, thereby indicating that the silos may have come to rest with some impact.

This sequence of events suggests the following explanation. No important deformations of the clay occurred so long as the pressure p on the surface of the ground did not induce shearing stresses within the soil which exceeded its shearing strength at any point. For a circular footing the limit value of p which corresponds to such a condition can be estimated from Eqs. (9-6) and (9-7) to read

$$p = \frac{\tau'_{max}}{0.30} = \frac{c}{0.30} = 3.33c = 1.62q_u \tag{9-30}$$

The foundation was not circular in this case, and the value obtained from Eq. (9-30) therefore is only approximate: $p = 1.62 \times 1.16 = 1.88$ tons per ft^2 $= 0.62p_{max}$. For a long foundation it may be somewhat smaller. In the six-month period during which the considerable settlement occurred the actual pressure exceeded this limit value, having varied between $0.71p_{max}$ and $0.82p_{max}$. Thus the shearing strength of the clay was exceeded in places, excessive deformations resulted, which weakened the sensitive clay further, especially on the side O of the foundation, where most of the preliminary lateral squeezing, which must have followed a pattern similar to Figs. 9-21 and 9-8, occurred. This weakening of the clay on that side then facilitated the development of the rotational failure, as shown in Fig. 9-24. Increasing of the factors of safety for very sensitive clays is therefore indicated (see Art. 14-2).

The position of point G in Fig. 9-24 suggests that the first rotational movement may not have occurred around the edge O of the foundation. The location of the probable center of rotation O' appears to confirm the

considerations on which Fellenius based his equation (9-20), and which are also valid for Eqs. (9-21) and (9-28) derived from it. The final position of the silos shown in Fig. 9-24 may be a result of a combined secondary rotation and lateral and upward displacement of the silos which developed after the original rotational movement around the center O' was already underway and had destroyed part of the cohesion of the clay.

Another point is of interest with reference to Fig. 9-24. Prior to construction, a surface load test on a 1-ft square footing had been conducted
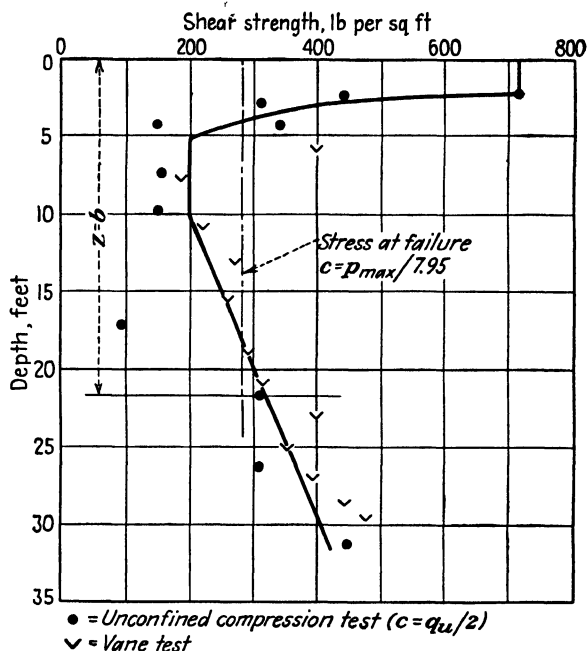
FIG. 9-26. Comparison of the actual shearing strength of the clay at Shellhaven to the average value computed from the failure load of a 22-ft-diameter steel tank. (After I. K. Nixon, Ref. 250, 1949.)

for a short time with apparently satisfactory results. Since the unconfined compressive strength q_u of the clay close to the surface, which alone mattered in the case of such a small footing, was almost twice as large as the average value of the entire deposit, the satisfactory performance of the test footing is not surprising and illustrates how misleading the results of such tests can be, unless supplemented by other data and properly interpreted.

I. K. Nixon reported (Ref. 250, 1949) the results of an experimental filling of a 22-ft-diameter and 30-ft-high steel tank at Shellhaven. The tank was placed on a layer of soft clay with a slightly stiffer upper crust,

as shown in Fig. 9-26. Both $q_u/2$ values and data from vane tests (see Art. 7-12) are given. The filling was continued over a period of four days until the clay failed and the tank overturned. The unit pressure on the surface of the ground at the moment of failure was $p_{max} = 2{,}230$ lb per ft². According to Eq. (9-29), the average shearing strength of the clay at failure was $c = 2{,}230/7.95 = 280$ lb per ft². This value is plotted in Fig. 9-26. There was some discussion in Ref. 250 as to whether a distributing effect of the stiffer upper crust should be considered. It can be seen from Fig. 9-26 that the failure value $c = 280$ lb per ft² corresponds fairly closely to the average shearing strength of the entire layer down to the depth likely to be affected by a rotational failure, that is, approximately, $r = b = 22$ ft. The agreement will be particularly good if the vane-test results are disregarded, and only the unconfined compressive strength test results are considered.

The cases discussed in this article show that there are a number of points of detail which still have to be cleared up, but that modern methods of sampling, testing, and analysis permit a reasonably accurate forecast of the conditions under which failure of a heavy foundation is likely to occur when it is supported by a clay layer. Hence, a satisfactory semiempirical basis for a rational procedure of design has been laid (see Art. 14-8).

Practice Problems

9-1. Prior to the construction of the heavy stockhouse illustrated by Figs. 12-18 and 13-9 a load test was performed on a 2- by 2-ft footing which rested on the surface of the 70-ft-deep sand layer. The settlement of the footing under a unit load of 3.7 tons per ft² was 0.36 in. What will be the probable settlement of the 90- by 100-ft structure under the same unit loading if we assume that the coefficient of compressibility of the sand has the same value throughout its depth?

Answer. With reference to Fig. 9-1, the ratio H/b of the footing is $^{70}\!/_{2} = 35$ and hence approaches infinity in respect to its influence on the coefficient C_s, which can therefore be taken as $C_s = 1.0$. Substituting the relevant values in Eq. (9-2), we obtain

$$0.36 = 0.867 \times 3.7 \times 2.0 \times 12 \times 1.0 \times 1/E = 77.0 \times 1/E$$

or

$$1/E = 0.0047 (= m_v')$$

For the building itself, $H/b = {}^{70}\!/_{90} = 0.78$ and, from Fig. 9-1, $C_s = 0.45$. Substituting these values in Eq. (9-2), we obtain

$$S = 0.867 \times 3.7 \times 90 \times 12 \times 0.78 \times 0.0047 = 7.3 \text{ in.}$$

It will be noted from Fig. 13-9 that the final settlement of the structure proved to be approximately 3.5 in. The actually measured value is thus approximately half of that to be expected from the surface test. The explanation of this discrepancy lies in the fact that the density of the sand layer increased with depth, as evidenced by its increased resistance with depth to penetration testing (see Fig. 12-18).

9-2. A 50- by 30-ft foundation mat is uniformly loaded to an average intensity of $p = 1.7$ tons per ft² over its entire area. Compute the resulting unit vertical pressure σ_z on a plane $z = 45$ ft below the bottom of the mat under points A, F, K, and N in Fig. 9-27.
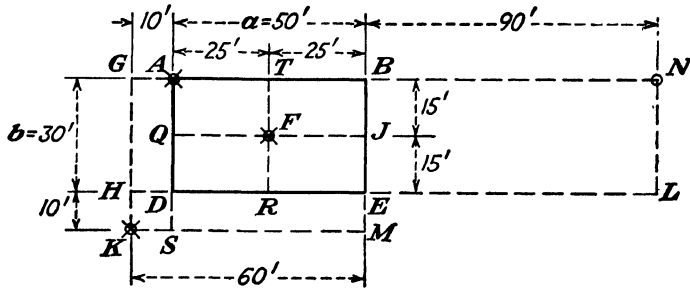
FIG. 9-27. Diagram illustrating Probs. 9-2 and 9-3.

Answer:

1. Point A (also points B, D, and E). With reference to Fig. 9-18, we obtain the ratios $z/b = 45/30 = 1.5$ and $a/b = 50/30 = 1.67$, with which we find from the chart $\sigma_z/p = 0.15$, so that $\sigma_z = 0.15 \times 1.7 = 0.255$ ton per ft².

2. Point F at the center of the mat. We have to find the effect of one-quarter of the area of the mat (rectangle $ATFQ$) and multiply it by four. For the area $ATFQ$ $z/b = 45/15 = 3.0$ and $a/b = 25/15 = 1.67$, so that, from the chart in Fig. 9-18, $\sigma_z/p = 0.067$ and $\sigma_z = 4 \times 0.067 \times 1.7 = 0.455$ ton per ft².

3. Point K outside the area of the mat. We have to find the effect of the rectangle $GBMK$, subtract from it the effects of $ASKG$ and $HKME$, and add the effect of $HDSK$.

Rectangle $GBMK$: $z/b = 45/40 = 1.12$; $a/b = 60/40 = 1.5$; from chart $\sigma_z/p = 0.185$
Rectangle $ASKG$: $z/b = 45/10 = 4.5$, $a/b = 40/10 = 4.0$; from chart $\sigma_z/p = 0.055$
Rectangle $HKME$: $z/b = 45/10 = 4.5$; $a/b = 60/10 = 6.0$; from chart $\sigma_z/p = 0.065$
Rectangle $HDSK$: $z/b = 45/10 = 4.5$; $a/b = 10/10 = 1.0$; from chart $\sigma_z/p = 0.022$
The total effect is

$$\sigma_z = (0.185 - 0.055 - 0.065 + 0.022) \times 1.7 = 0.148 \text{ ton per ft}^2$$

This last computation illustrates the circumstance that in order to compute the effect of a number of isolated footings, the use of the chart in Fig. 9-19 (Ref. 248) is more convenient.

4. Point N outside the area of the mat. We would have to take the effect of the rectangle $ANLD$ and subtract from it the effect of $BNLE$; for the latter $z/b = 45/30 = 1.5$ and $a/b = 90/30 = 3.0$. From the chart in Fig. 9-18 we find that the curve $a/b = 3.0$ almost merges with the curve $a/b = \infty$ for the ratio $z/b = 1.5$. Therefore, even if the loaded area extended from BE well beyond AD to infinity, no measurable increase of σ_z would be produced at a depth $z = 45$ ft below the point N.

9-3. A 16-story building is erected on a 70- by 100-ft mat resting on a 120-ft-deep layer of clay with an average unconfined compressive strength $q_u = 1.1$ tons per ft². The unit pressure on the clay is $p = 2.0$ tons per ft². What is the factor of safety against a shear failure of the clay if the bottom of the mat is 3 ft below the ground surface? Compare the result with Table 14-4.

Answer. From $c = q_u/2 = 0.55$ ton per ft² and Eq. (9-28)

$$p_{max} = 5.52 \times 0.55[1 + 0.38\,3/70 + 0.44\,70/120] = 3.87 \text{ tons per ft}^2$$

The factor of safety is

$$F_s = p_{max}/p = 3.87/2.00 = 1.93 \qquad \text{(too low!)}$$

References Recommended for Further Study

"Influence Charts for the Computation of Stresses in Elastic Foundations," by Nathan M. Newmark, *University of Illinois Engineering Experiment Station Bulletin Series*, No. 338, 1942, Urbana, Illinois. Charts are provided for the computation of vertical and horizontal stresses; the scale of the charts is convenient for practical use.

Soil Mechanics in Engineering Practice, by K. Terzaghi and R. B. Peck, Wiley, 1948, Art. 29, pp. 169–173. Approximate methods for the computation of the bearing capacity of foundations under consideration of both friction and cohesion of the soil.

"Correspondence on $\phi = 0$ Analysis," by I. K. Nixon and B. F. Saurin, *Geotechnique*, London, Vol. I, Nos. 3 and 4, pp. 208, 272–276. Data on the complete failure of a 22-ft-diameter steel tank and on the partial failure of a 116-ft-diameter steel tank.

Theory of Elasticity, by S. Timoshenko, McGraw-Hill, 1948, pp. 338–339. Equations for the settlement of a loaded, absolutely rigid footing of a circular shape.

CHAPTER 10

LATERAL EARTH PRESSURES

10-1. General Concepts. Let us assume that a massive gravity retaining wall shown in Fig. 10-1(III) rests on a hard but slippery layer 3'3 of shale. The backfill behind the wall will exert a lateral pressure E_A, the so-called *active lateral earth pressure*, which will tend to push the wall to
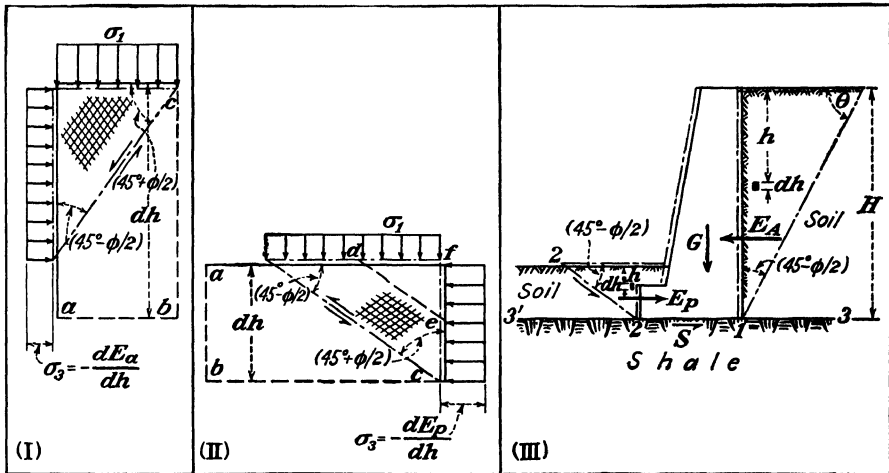
FIG. 10-1. Diagrams illustrating the terms *active* and *passive earth pressure.* (I) Active state: $\sigma_1 > \sigma_3$. (II) Passive state: $\sigma_3 > \sigma_1$. (III) Active and passive earth pressure in the case of a massive gravity wall slipping along plane 3-3'.

the left to a position shown by the dash-dotted lines. The stress condition of a small element of the backfill close to the wall, if we neglect the friction between the wall and the soil, will be very similar to the condition illustrated by Fig. 7-11 and reproduced in Fig. 10-1(I). The vertical unit pressure σ_1, which usually can be taken as being equal to the weight of the overburden γh, is greater than the lateral unit pressure σ_3. Thus the so-called *active state* of deformation or of rupture in a soil mass is taken to represent a condition where lateral expansion of the soil is possible and is induced by the weight of the soil or by a surcharge resting on its surface.

Equation (7-11) can be rewritten as follows:

$$\sigma_3 = \frac{\sigma_1 - 2c \tan (45° + \phi/2)}{\tan^2 (45° + \phi/2)} \tag{10-1}$$

or, since

$$\tan\left(45° + \frac{\phi}{2}\right) = \frac{1}{\tan (45° - \phi/2)} \tag{10-2}$$

$$\sigma_3 = -\frac{dE_A}{dh} = \sigma_1 \tan^2\left(45° - \frac{\phi}{2}\right) - 2c \tan\left(45° - \frac{\phi}{2}\right) \tag{10-3}$$

The ratio of lateral to vertical pressure in the active state is termed the *coefficient of active lateral earth pressure* K_A. The limit value at failure will be

$$K_A = \frac{\sigma_3}{\sigma_1} = \tan^2\left(45° - \frac{\phi}{2}\right) - \frac{2c}{\sigma_1} \tan\left(45° - \frac{\phi}{2}\right) \tag{10-4}$$

Unless horizontal arching (Art. 10-14) relieves the vertical pressure σ_1, it will be equal to

$$\sigma_1 = \gamma h \tag{10-5}$$

so that

$$K_A = K_\gamma = \frac{\sigma_3}{\sigma_1} = \frac{p_h}{\gamma h} \tag{10-5a}$$

where K_γ is the ratio of the actual lateral pressure p_h to the unrelieved unit weight of the overburden at that elevation. Then

$$K_A = \tan^2\left(45° - \frac{\phi}{2}\right) - \frac{2c}{\gamma h} \tan\left(45° - \frac{\phi}{2}\right) \tag{10-6}$$

For a granular cohesionless soil ($c = 0$),

$$K_A = \tan^2\left(45° - \frac{\phi}{2}\right) \tag{10-7}$$

The coefficient K_A for granular cohesionless soils is sometimes expressed by means of two other equations:

$$K_A = \frac{1 - \sin \phi}{1 + \sin \phi} \tag{10-8}$$

or

$$K_A = \frac{\sqrt{\tan^2 \phi + 1} - \tan \phi}{\sqrt{\tan^2 \phi + 1} + \tan \phi} \tag{10-9}$$

Equation (10-8) was originally derived by Rankine, (Ref. 283, see also Art. 10-3) and is commonly used in England; Eq. (10-7) is more frequently used on the continent of Europe; Eq. (10-9) is also employed occasionally (Refs. 203 and 320). Any one of the three equations can be derived from one of the other two by direct trigonometric transformation. Equation (10-7) will be used in this book.

For a frictionless cohesive soil ($\phi = 0$) Eq. (10-6) will read

$$K_A = 1 - \frac{2c}{\gamma h} \tag{10-10}$$

or, under consideration of Eq. (7-17),

$$K_A = 1 - \frac{q_u}{\gamma h} \tag{10-11}$$

As the wall shown in Fig. 10-1(III) slips outward along the plane 3-3′ under the influence of the active earth pressure E_A, its movement will be resisted by the soil in front of its toe, that is, by the so-called *passive lateral earth pressure* E_p. The stress condition of a small element of the soil close to and in front of the wall, again neglecting the friction between the wall and the soil, is shown at a larger scale in Fig. 10-1(II). Essentially it represents the condition of the prism shown in Fig. 10-1(I), if it were laid on its side by rotating it clockwise through 90°. The procedure of the analysis is exactly the same in both cases, except that σ_3 is now greater than σ_1 and can be interchanged with it in Eq. (10-3), which will then read

$$\sigma_3 = -\frac{dE_p}{dh} = \sigma_1 \tan^2\left(45° + \frac{\phi}{2}\right) + 2c \tan\left(45° + \frac{\phi}{2}\right) \tag{10-12}$$

Thus the so-called *passive state* of deformation or of rupture in a soil mass is taken to represent a condition where vertical expansion of the soil occurs as a result of lateral contraction produced by lateral pressures transmitted to the soil by a structure or by a part thereof. The weight of the soil itself and any surcharge resting on its surface will contribute to the *passive pressure*, that is, to the *resistance* offered by the soil to this type of deformation. The unit vertical pressure will have to be much smaller than the lateral external pressure if this type of failure is to occur.

The ratio of lateral to vertical pressure in the passive state is termed the *coefficient of passive lateral earth pressure* K_p. Assuming that Eq. (10-5) is valid, the limit value at failure will be

$$K_p = \frac{\sigma_3}{\sigma_1} = \tan^2\left(45° + \frac{\phi}{2}\right) + \frac{2c}{\gamma h} \tan\left(45° + \frac{\phi}{2}\right) \tag{10-13}$$

For a cohesionless granular soil ($c = 0$) this expression is simplified to read

$$K_p = \tan^2\left(45° + \frac{\phi}{2}\right) \tag{10-14}$$

Therefore, under consideration of Eqs. (10-2) and (10-7),

$$K_p = \frac{1}{K_A} \tag{10-14a}$$

For a frictionless cohesive soil ($\phi = 0$) Eq. (10-13) will read

$$K_p = 1 + \frac{2c}{\gamma h} = 1 + \frac{q_u}{\gamma h} \tag{10-15}$$

The values of K_A and of K_p given by the preceding equations represent the limit values which are reached at the point of failure, where the assumption is made that both the full frictional resistance and the full cohesive resistance reach their maximum values simultaneously after the same amount of deformation and maintain both these maximum values even after further deformation. This assumption is somewhat questionable from a quantitative point of view, but it is acceptable for a preliminary qualitative description of the influence exerted by these factors. K_A will always be smaller than unity [see Eq. (10-4)], whereas K_p will always be greater than unity [see Eq. (10-13)]. Their limit values, as given by these two equations, represent the minimum value of K_A which is reached as a result of full lateral expansion of the soil prior to failure and the maximum value of K_p which is reached as a result of full lateral compression of the soil prior to failure. It therefore follows that for a soil in its natural condition in situ, that is, for a soil which neither expanded nor contracted laterally after its formation, the lateral pressure within its undisturbed and undeformed mass must have some intermediate value between the values of the active and of the passive pressures of the same soil. This value of the lateral earth pressure existing in the undeformed mass of natural soil is called the *lateral earth pressure at rest*. Other terms used to designate the same condition are the *neutral lateral earth pressure* or the *lateral earth pressure at consolidated equilibrium*. The ratio of lateral to vertical earth pressure in this natural state is termed the *coefficient of earth pressure at rest* K_n (Art. 10-8).

10-2. Coulomb's Sliding-wedge Analysis. Several experimental earth-pressure studies were made during the early part of the eighteenth century (Ref. 131). None of them led to the development of a rigorous basis for the design of earth-retaining structures. Coulomb (Ref. 87, 1776) was the first to succeed in developing one as a result of a purely

theoretical study. He considered the limit equilibrium of the entire wedge of soil behind a retaining wall in very much the same manner as this has been done in Art. 7-8 for an infinitely small element of soil. Accordingly, the limit value of the earth pressure at failure of the soil was expressed by him in terms of the total pressure E and not of unit pressures.

Coulomb did his work at a time when trigonometric functions were not yet in use; accordingly, he expressed all his values as ratios. This circumstance may be responsible for the rather surprising fact that Coulomb is generally credited at present only with the study of purely granular, cohesionless soils. Actually, his investigation was much more comprehensive. Philip Brown (Ref. 42, 1948) transformed Coulomb's original (1776) equation to correspond to present-day terminology and obtained the following expression:

$$E_A = \frac{\gamma H^2}{2} \tan^2\left(45° - \frac{\phi}{2}\right) - 2cH \tan\left(45° - \frac{\phi}{2}\right) \qquad (10\text{-}16)$$

It will be noted that Eq. (10-16) includes the cohesion c, consideration of which for the first time is usually attributed to Résal (Ref. 287, 1910) as a development of Rankine's theory (Art. 10-3). It will be further noted that Eq. (10-16) is identical with Eq. (10-19), which is derived by graphical integration of Eq. (10-3) for unit lateral active earth pressures. Coulomb's analysis was limited to plane surfaces of failure, in order to simplify the mathematics involved. Nevertheless, he admitted the possibility of curved surfaces of failure, as shown by his original diagrams (Ref. 87). Thus this early investigator had a very clear conception of most of the factors which influence the lateral pressures of soils. Since his basic assumption of a "sliding wedge of least resistance" limits his analysis to the actual failure of the soil, Coulomb's basic approach is sounder than the one of some later investigators.

It should also be noted that Coulomb was the first to derive Eq. (8-4), except for the part relating q_u to c, giving the critical height h_{cr} of an unsupported cut unweakened by tension cracks (Refs. 87 and 42).

10-3. Rankine's Theory. Rankine (Ref. 283, 1857) studied the state of stress within a loose granular mass with zero cohesion. His analysis was based on the assumption that the slightest deformation of the soil is sufficient to bring into play its full frictional resistance and immediately to produce an "active state" if the soil tends to expand parallel to its surface, and a "passive state" if it tends to compress parallel to its surface. Terzaghi (Ref. 354, 1936) pointed out that "The fundamental assumptions of Rankine's earth pressure theory are incompatible with the known relation between stress and strain in soils, including sand. Therefore the use of this theory should be discontinued."

This recommendation is believed to be sound and will be followed in the present book, even though in later publications Terzaghi (Ref. 362) described the theory at some length.

Rankine's analysis was extended by Résal (Ref. 287, 1910) to include a soil with both friction and cohesion. The same objections apply to this extension.

It should be noted that the derivation of Rankine's equation is based on the use of conjugate pressures and of the stress ellipse. The procedure therefore involves techniques which are somewhat less generally familiar in the United States than the ones used by Coulomb and in the preceding articles of this book. At the same time, the equations obtained in both cases for the unit and for the total lateral pressures are identical if the soil surface is horizontal and if the friction between the wall and the soil is taken to be zero (Art. 10-2). The Coulomb approach of "wedge of least resistance" permits a clearer analysis of the effect on lateral earth pressures of wall friction of various intensities (Art. 10-5) than the Rankine-Résal "state of stress" approach. This factor is very important in its influence on passive pressures. A further description of the Rankine methods of analysis and of the derivation of his formula will therefore be omitted as unnecessary ballast for the general civil engineering practitioner.

10-4. The Distribution of Lateral Earth Pressures. Figure 10-2(I) illustrates the distribution of active lateral earth pressures σ_3 along the depth of a retaining wall, in accordance with Eq. (10-3), where $\sigma_1 = \gamma h$, that is,

$$\sigma_3 = \gamma h \tan^2\left(45° - \frac{\phi}{2}\right) - 2c \tan\left(45° - \frac{\phi}{2}\right) \qquad (10\text{-}17)$$

The surface of the ground is horizontal, and friction between the wall *ab* and the soil behind it is assumed to be zero. If the soil had no shearing strength whatsoever ($c = 0$, $\phi = 0$), then at all depths the lateral pressures would be equal to the weight of the overburden γh, as in a fluid. The distribution of lateral pressures against the wall would correspond to the line *ag*, as shown in Fig. 10-2(I), and the ratio of lateral to vertical pressures would equal unity at all elevations ($K_A = 1.00$).

If the soil has no cohesion but some friction ($c = 0$, $\phi > 0$), then the distribution of active lateral earth pressures would correspond to a somewhat steeper line *ad*. The coefficient of active earth pressure K_A would be smaller than unity and would have a constant value throughout the entire depth.

Finally, if the soil has both friction and cohesion, the distribution of active lateral earth pressures would follow the line *mfe*, and there would

be tension between the wall and the soil down to a depth z_o. The value of this depth can be computed from the ratio $H/(H - z_0) = \gamma H \tan^2(45° - \phi/2)/\sigma_3$ to read

$$z_o = \frac{2c}{\gamma}\tan\left(45° + \frac{\phi}{2}\right) \tag{10-18}$$

Accordingly, under the above assumptions, the total active lateral earth pressure E_A will be equal to the area *abd* less the area *amed* (Fig. 10-2).

$$E_A = \frac{\gamma H^2}{2}\tan^2\left(45° - \frac{\phi}{2}\right) - 2cH\tan\left(45° - \frac{\phi}{2}\right) \tag{10-19}$$

This equation is identical with Eq. (10-16), originally derived by Coulomb. It is therefore apparent that the equations giving the total
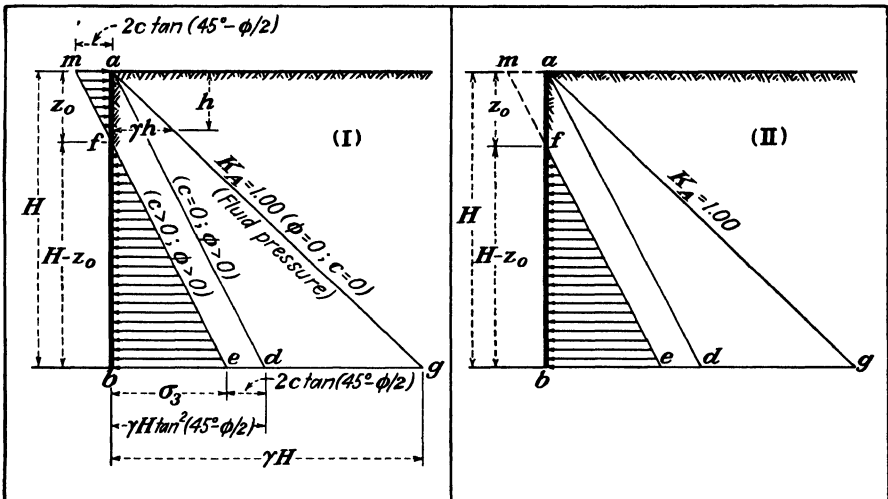
FIG. 10-2. The distribution of active lateral earth pressures. [(I) *After Coulomb, Ref. 87, 1776, and Rankine, Ref. 283, and Résal, Ref. 287, 1857–1910*). (II) *After Cain, Ref. 56, 1916.*]

lateral earth pressure E_A acting against a wall, when based on the Coulomb and on the Rankine-Résal analyses, involve the assumption that the soil will adhere to the material of the wall—that is, to masonry, concrete, steel, or timber—so strongly that the bond developed between the soil and the wall will be able to withstand appreciable tension. This assumption is not in qualitative agreement with actual experience, although practically no exact numerical data are yet available on the actual tensile strength of such a bond.

Cain (Ref. 56, 1916) recognized the unsound basis of the above assump-

tion and proposed to neglect the tension between the soil and the wall. In other words, he suggested to consider that there is no pressure at all against the wall down to a depth z_o (Ref. 42). This assumption is illustrated by Fig. 10-2(II). The value of E_A will then be equal to the area *fbe*, that is, to the value of E_A as expressed by Eq. (10-19), plus the area *maf*. With reference to Eq. (10-18), the area *maf* will be equal to $2c^2/\gamma$, and the total pressure against the wall will be

$$E_A = \frac{\gamma H^2}{2} \tan^2\left(45° - \frac{\phi}{2}\right) - 2cH \tan\left(45° - \frac{\phi}{2}\right) + \frac{2c^2}{\gamma} \quad (10\text{-}20)$$

Neither Eq. (10-19) nor Eq. (10-20) takes into account the possibility of tension cracks forming in the soil itself near the surface and of the resulting increase of pressures against the lower half of the wall, as happens in the case of an unsupported cut (Art. 8-2). With reference to Fig. 8-2, it should, however, be noted that in the case of a braced (supported) vertical cut [Fig. 8-2(III)] the overturning moment M_o will be much smaller than in the case of an unsupported vertical cut [Fig. 8-2(II)], since the force ΔE will partially balance ΔR in respect to ΔW. It should further be noted that ΔE is likely to decrease with an outward motion of the wall, so that ΔM_o will become a function of the nature of the wall displacements and deformations. These displacements and deformations of the supporting wall strongly affect the distribution of lateral earth pressures against a retaining structure also in other ways (Art. 10-14) but have in no way been considered in the preceding conventional forms of analysis.

10-5. Effect of Wall Friction on the Values of the Active and of the Passive Earth Pressure of Cohesionless Soils. The equations derived in the preceding articles were based on the simplifying assumption that no shearing stresses were being transmitted to the soil along the vertical face of the wall, so that the direction of the resultant lateral earth pressure was horizontal, both in the active and in the passive case. The angle of wall friction was then equal to zero ($\delta = 0$). This condition seldom occurs in practice.

As shown by the dash-dotted lines in Fig. 10-3, in the active case the soil tends to slip downward along the wall. This is equivalent in its effect to a relative upward movement of the wall in respect to the soil, a condition which is designated by a plus (+) sign in Fig. 10-3 for the angle of wall friction δ. It will be noted from the diagram of Fig. 10-3(I) that the resultant total earth pressure reaction $-E_A$ necessary to support the sliding wedge of soil at limit equilibrium will then be directed upward. Its component parallel to the plane of failure *ab* will be increased. This in turn will increase the resistance S to sliding, and the value of E_A itself will

become smaller as a result. However, at the same time the component of E_A normal to the plane of failure *ab* will be decreased. This will decrease the frictional component of the resistance S to sliding along *ab*, which in turn will tend to induce a higher value of E_A. The effects of the changes of the two components will thus partially cancel each other. The net result will be that any increase in positive values of the angle of wall friction δ will only slightly decrease E_A, as shown in Table 10-1 and Fig. 10-4.

If the angle of wall friction has a negative value, that is, if the wall tends to move downward past the active wedge of soil, then a reverse situation will arise, and the values of E_A will be increased slightly, as
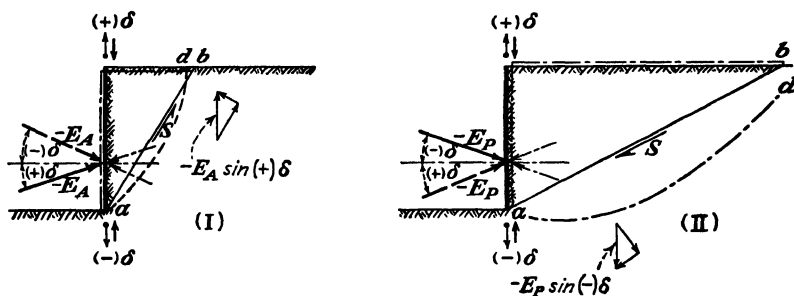
FIG. 10-3. Key to the symbols in the chart of Fig. 10-4 and in Table 10-1.

shown in Table 10-1. In actual practice such a condition is not likely to arise frequently. It is conceivable only in special cases when a heavy concentrated load, for instance, from a crane, is placed at the surface on the wall, forcing it into the ground, as if the wall consisted of piling.

In the passive case, illustrated by Fig. 10-3(II), the angle of wall friction δ will usually have a negative value. The value of E_p will then be strongly increased, since the changes of both its components will tend to increase the relative importance of the resistance S to sliding along the plane of failure *ab* as compared with the case of $\delta = 0$. The component of E_p which induces sliding parallel to *ab* will become smaller, and the component normal to *ab* will become greater, thereby increasing the frictional resistance S. The over-all effect is considerable, as shown in Table 10-1 and Fig. 10-4.

A positive value of δ will have an opposite effect on the value of E_p, that is, the latter will become smaller, as shown in Table 10-1 and Fig. 10-4. This condition will seldom occur in practice, since to create it, the wall would have to be pulled out of the soil. This may conceivably happen as a result of rotational movements of a structure of which the wall forms part, for instance, when a sheet-pile wall is placed at the back of a relieving platform (Fig. 16-21).

The earth pressure coefficients K_A and K_p given by the chart of Fig. 10-4 are based on Eqs. (10-21) and (10-22), that is, on the assumption that failure occurs along plane surfaces, such as are shown by the lines *ab* in Fig. 10-3. Table 10-1 gives, in parentheses, the values of the K_A and K_p

TABLE 10-1. Lateral Earth Pressure Coefficients*

δ	Values of K_A				Values of K_p			
	ϕ				ϕ			
	25°	30°	35°	40°	25°	30°	35°	40°
−40°				0.77 (0.88)				92.3 (17.5)
−30°		0.87 (0.98)	0.50	0.36		10.0 (6.4)	15.3 (9.7)	25.1 (14.6)
−20°	0.61	0.47 (0.48)	0.36	0.28	4.6 (4.1)	6.1 (5.4)	8.3 (7.5)	11.9 (10.4)
−10°	0.47	0.38	0.30	0.24	3.3 (3.3)	4.2 (4.2)	5.3 (5.3)	7.0 (7.0)
± 0°	0.41 (0.41)	0.33 (0.33)	0.27 (0.27)	0.22 (0.22)	2.5 (2.5)	3.0 (3.0)	3.7 (3.7)	4.6 (4.6)
+10°	0.37	0.31	0.25	0.21	1.9	2.3	2.7	3.3
+20°	0.36	0.30 (0.30)	0.25	0.20	1.4	1.7	2.0	2.4
+30°		0.30 (0.31)	0.25	0.20		0.87 (0.53)	1.3	1.7
+40°				0.20 (0.22)				0.77 (0.52)

* See also Table 10-2.

coefficients computed under the assumption of curved surfaces of failure (Refs. 203 and 57), as shown by the curves *ad* in Fig. 10-3. It will be noted that there is very little difference between the values computed on the basis of these two different assumptions, except in the passive case for high negative values of the angle of wall friction. The simplifying assumption of plane surfaces of failure leads then to excessively high

values of K_p. The use of the tables developed by Caquot and Kerisel (Ref. 57, 1948) for curved surfaces of failure is therefore recommended for such cases.
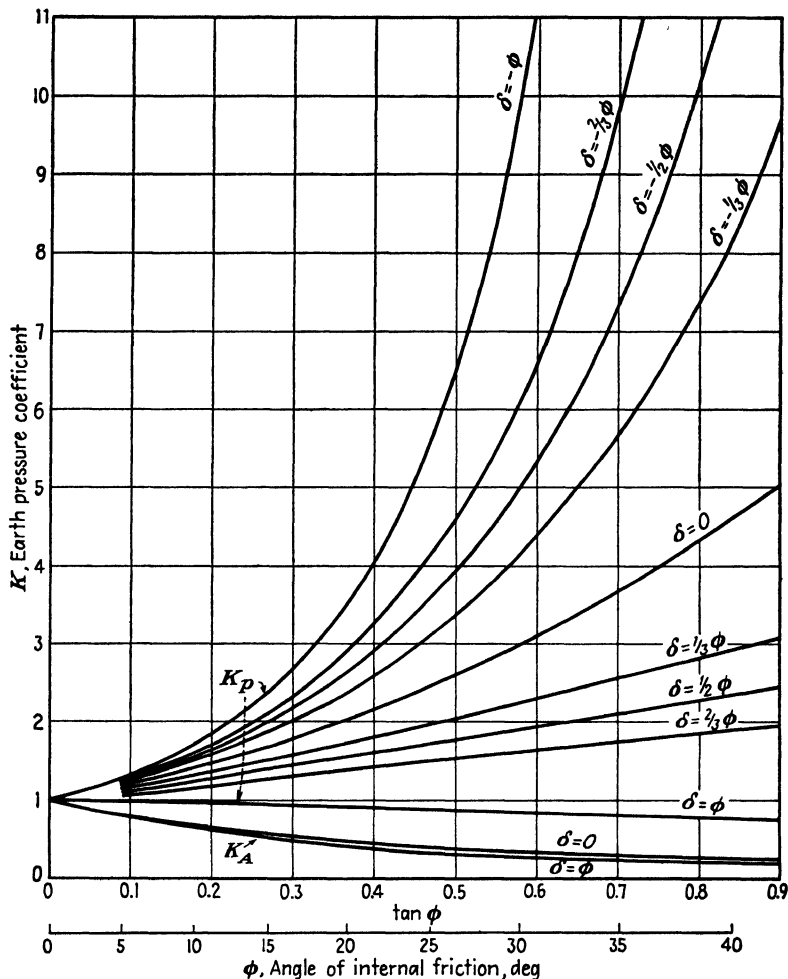
FIG. 10-4. Effect of variation of the angle of internal friction ϕ and of the angle of wall friction δ on the values of the active and passive earth pressure coefficients K; $c = 0$ (wall vertical and soil surface horizontal; plane surfaces of failure). (See Refs. 203 and 42.)

10-6. Effect of Sloping Ground and Wall Surfaces on the Values of the Active and of the Passive Earth Pressure of Cohesionless Soils. The general trends of this effect are illustrated by the values of the K_A and K_p coefficients of Table 10-2, for the specific case of a cohesionless soil ($c = 0$) with $\phi = 30°$ (loose sand) and a zero value of the angle of wall

friction δ. The figures in parentheses refer to curved surfaces of failure, (Ref. 57).

The following two equations, derived by Mueller-Breslau (Ref. 241, 1906), can be used for the computation of earth pressure coefficients for other combinations of ϕ, δ, ω, and β when $c = 0$:

$$K_A = \frac{\cos^2(\phi - \beta)}{\cos^2\beta\cos(\delta + \beta)\left[1 + \sqrt{\dfrac{\sin(\phi + \delta)\sin(\phi - \omega)}{\cos(\delta + \beta)\cos(\omega - \beta)}}\right]^2} \tag{10-21}$$

$$K_p = \frac{\cos^2(\phi + \beta)}{\cos^2\beta\cos(\delta + \beta)\left[1 - \sqrt{\dfrac{\sin(\phi - \delta)\sin(\phi + \omega)}{\cos(\delta + \beta)\cos(\omega - \beta)}}\right]^2} \tag{10-22}$$

TABLE 10-2. Lateral Earth Pressure Coefficients

	ω =	-30°	-12°	±0°	+12° (1:4.7)	+30° (1:1.7)
β = +20°	K_A Values	0.34	0.43	0.50	0.59	1.17
+10°	K_A Values	0.30	0.36	0.41	0.48	0.92
±0°	K_A Values	0.26 (0.26)	0.30 (0.30)	0.33 (0.33)	0.38 (0.38)	0.75 (0.85)
-10°	K_A Values	0.22 (0.22)	0.25 (0.24)	0.27 (0.26)	0.31 (0.30)	0.61 (0.63)
-20°	K_A Values	0.18 (0.18)	0.20 (0.18)	0.21 (0.20)	0.24 (0.22)	0.50 (0.45)
β = +20°	K_p Values	0.50	1.5 (1.0)	2.3 (1.8)	3.1 (2.8)	4.9 (4.6)
+10°	K_p Values	0.62	1.8 (1.4)	2.5 (2.3)	3.6 (3.4)	6.2 (5.9)
±0°	K_p Values	0.75 (0.40)	2.1 (1.8)	3.3 (3.1)	4.4 (4.2)	8.8 (7.4)
-10°	K_p Values	0.92 (0.52)	2.6 (2.4)	3.8 (3.6)	5.9 (5.7)	16.7 (9.3)
-20°	K_p Values	1.17 (0.67)	3.4 (3.0)	5.3 (4.8)	9.6 (7.2)	45.7 (11.6)
$c = 0$;			$\phi = 30°$;		$\delta = 0°$	

When δ, β, and ω all equal zero, Eqs. (10-21) and (10-22) become identical with Eqs. (10-8) and (10-14), respectively.

Tables of earth pressure coefficients based on Eqs. (10-21) and (10-22) were published by Krey (Ref. 203, 1912–1936). Similar but more extensive tables based on curved surfaces of failure have been published by Caquot and Kerisel (1948). An English translation is available (Ref. 57).

10-7. Some Early Experimental Attempts to Determine the Value of the Neutral or At-rest Lateral Pressure of Soils

The so-called *classical* earth pressure theories, the Coulomb and the Rankine-Résal theories, described in the preceding articles do not determine the amount of deformation which is necessary in order to fully mobilize the shearing resistance of the soil
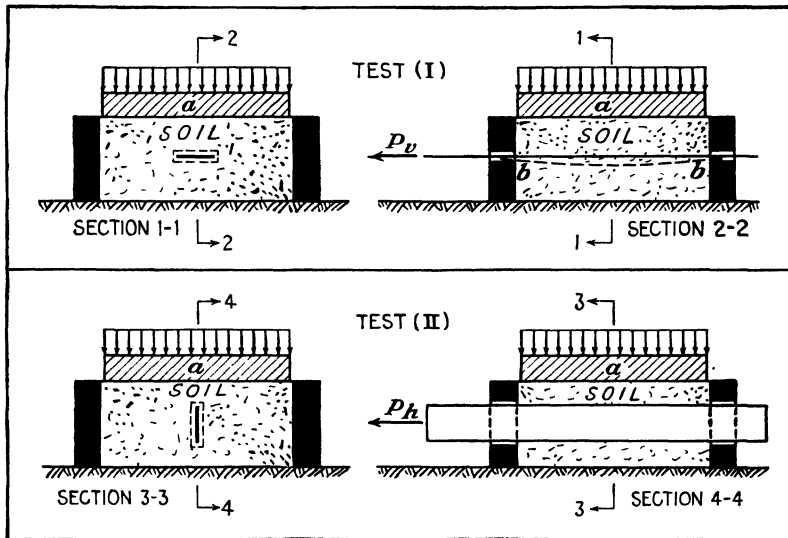
FIG. 10-5. Setup used by Terzaghi (Ref. 346, 1920, and Ref. 348, 1925) for the determination of the at-rest coefficient of lateral earth pressure.

and to transform the soil from an at-rest state to an active or to a passive state (Art. 10-1). These classical theories simply assume that the above two limit conditions are reached after a certain amount of lateral motion has taken place. Coulomb does not specify this amount, whereas Rankine assumes it to be infinitesimal. At the same time, modern research has shown that the resistance of all soils to shearing deformations is a function of the amount of such deformations (Art. 7-15). A study of the relationship between lateral earth pressures and the amount of lateral displacement of the earth-retaining structures therefore become imperative.

As a first step in that direction Terzaghi (Ref. 346, 1920 and Ref. 348, 1925) undertook an experimental study for the purpose of determining the value of the at-rest or neutral coefficient of earth pressure, that is, the value of the K coefficient for a condition where no lateral deformation of the soil is taking place. Figure 10-5 illustrates the device he used for this purpose.

Two thin strips of metal were placed inside of soil-consolidation devices. In one of these devices (test I) the strip was placed horizontally, in the other (test II) it was

placed vertically within the soil mass. Of course, the tests could be performed only with sands and completely remolded clays. After completed consolidation of the soil under the normal load the metal strips were pulled out, and the forces required to make them move were measured. It was considered that the ratio of the forces P_h/P_v represented the value of the coefficient of earth pressure at rest K_n. The following values were obtained:

Sands: $K_n = 0.42$

Clays: $K_n = 0.70$ to 0.75 (remolded and reconsolidated)

These values are still frequently quoted (Refs. 205 and 13). Later investigations however, have, shown that the above value of K_n for sand is too low in some cases, and that the range of values given for clays is too high (Ref. 392). It should be noted that these values refer to intergranular pressures only, that is, they are K_s coefficients in the sense of Art. 10-13. A possible explanation of why the above K_n values are so high follows: During the consolidation of the clay in test I the clay beneath the horizontal strip near the wall of the consolidation device, that is, in the zones b in Fig. 10-5, was only partially consolidated as a result of the probable deflection of the strip, shown at an exaggerated scale by a broken line. This would have the effect of decreasing the value of P_v and hence would have increased K_n beyond its true value. Any adhesion of the clay to the metal of the strips in both tests would have had the same effect.

The term *earth pressure at rest* was introduced by Donath (Ref. 108, 1891), who made the first attempts to estimate its value.

10-8. The Theory of Elasticity and the Values of the Neutral Earth Pressure

The general equation for the lateral unit strain ϵ_3 within a large elastic body reads as follows (see Timoshenko, Ref. 367, p. 8, 1934):

$$\epsilon_3 = \frac{1}{E}[\sigma_3 - \nu(\sigma_1 + \sigma_2)] \tag{10-23}$$

Within a large mass of soil with a horizontal surface the lateral pressures acting at right angles to each other are equal, that is, $\sigma_2 = \sigma_3$. Further, in the at-rest condition, by definition, there are no lateral deformations, that is, $\epsilon_3 = 0$. Equation (10-23) is then simplified to read

$$\sigma_3 - \nu\sigma_3 - \nu\sigma_1 = 0 \tag{10-24}$$

from which follows the following expression for the coefficient of earth pressure at rest:

$$K_n = \frac{\sigma_3}{\sigma_1} = \frac{\nu}{1 - \nu} \tag{10-25}$$

The Poisson ratio ν has its maximum value of $\nu = 0.5$ for a completely incompressible material. The corresponding value of K_n is then 1.00, as actually measured for unconsolidated clays in a semifluid condition (Art. 10-9). For smaller values of the Poisson ratio, Eq. (10-25) gives the values of K_n shown in Table 10-3.

No reliable method for the direct measurement of the Poisson ratio ν of soils has yet been developed. Such values as have been published (Ref. 205) were computed back from measured values of σ_2 and known corresponding values of $\sigma_1 = \gamma H$, using Eq. (10-25). Therefore the theory of elasticity cannot yet be used for any direct determinations of the values of lateral earth pressure. The K_n values of Table 10-3

are, however, of some theoretical interest for comparison with the results of direct measurements of lateral earth pressures.

TABLE 10-3. Relationship between the Poisson Ratio ν and the Coefficient of Earth Pressure at Rest K_n

ν	K_n
0.50	1.00
0.45	0.82
0.40	0.67
0.35	0.54
0.30	0.43
0.25	0.33
0.20	0.25

10-9. Neutral Earth Pressure Values as Determined by Means of the Lateral Earth Pressure Meter

The *lateral earth pressure meter* is illustrated in Fig. 10-6 (Refs. 21, 425, 420, 390). It is a device capable of testing a cylinder of soil 1 ft in diameter and 1.5 ft high by applying a known normal load at the top and measuring the corresponding lateral pressures and lateral displacements at small increments throughout its depth. Because of its size this device is not suited for testing undisturbed samples of natural soil.

The general shape of the device is that of a thick-walled cylinder cut in half vertically. The left half shown in Fig. 10-6 is solid from top to bottom, but the right half is sliced horizontally into 12 half-circular rings. These rings are mounted on ball bearings, so that each one is free to roll away from the solid half. The end of each ring is connected to the solid half by a dynamometer on which electric resistivity SR-4 strain gages (Art. 10-23) are mounted, thus permitting the determination of the total lateral pressure F_h against one-half of each of the $h = 1.5$ in. high rings. The lateral pressure $\sigma_3 = p_h$ of the soil against each of the rings can then be computed from the relationship $p_hDh = 2F_h$. Outward motions of the rings are measured by mechanical dials.

The normal vertical pressure $\sigma_1 = p_v$ is applied to the top of the soil sample by air pressure, which acts through a thin rubber membrane that is free to adjust its shape to the contours of the soil surface. This procedure ensures that no shearing forces can be transferred to the upper boundary of the soil surface when the vertical pressure is applied and induces a tendency of the soil to expand laterally.

Vertical settlement is measured by a series of indicator rods resting on the rubber membrane in contact with the soil surface. The inner faces of the soil chamber are lined with porous concrete to permit lateral drainage.

At the start of a test the soil sample may be consolidated for a given length of time at any desired pressure up to 3 tons per ft^2. During this period of consolidation the variations in lateral pressure at different depths may be determined from the changes in the dynamometer readings.

The values of $K = p_h/p_v$ can be computed for each ring and for each test stage, where the assumption is made that the vertical pressure p_v remains constant throughout the depth of the soil. As will be shown in the next article, this assumption definitely is not correct, and it is made only for purposes of convenience of presentation of the test results and of their over-all evaluation, since it is not yet possible to measure accurately the actual variation of the vertical pressure p_v with depth.

The lateral pressures against the upper active ring of the device are taken to correspond closely to the at-rest condition within a large mass of soil, since they are not affected by friction along the upper boundary of the soil in the ring when a rubber membrane is used to apply the vertical pressure. Friction along the walls of the upper ring is also negligible, since the ratio of the height of a ring (1.5 in.) to its diam-
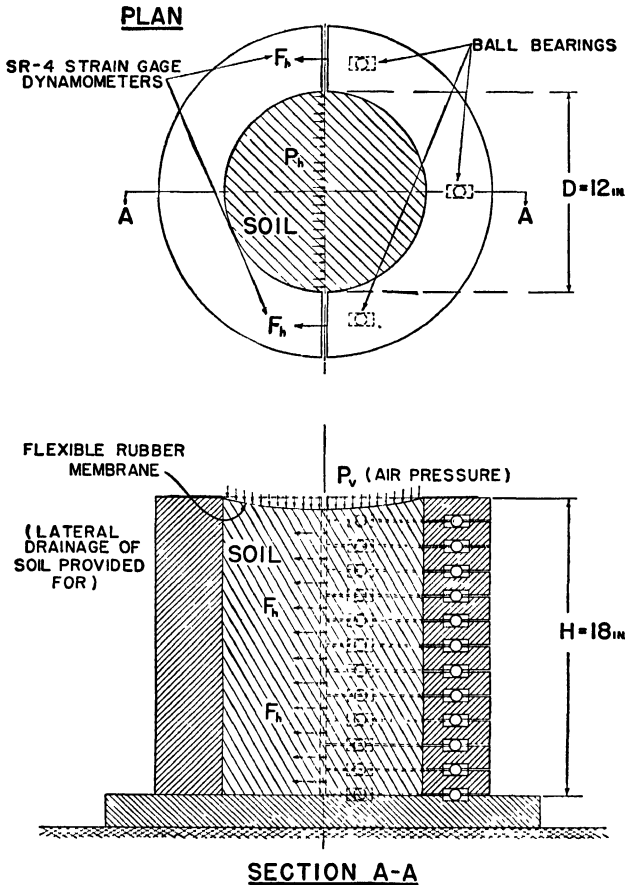
FIG. 10-6. The lateral earth pressure meter. *(After Bayliss, Ref. 21, and Tschebotarioff and Welch, Ref. 390, 1948.)*

eter (12 in.) is only 1:8 (see Art. 10-10). A depth of 16 in. of soil is provided between the upper ring and the lower rigid boundary of the device, minimizing the restraining effects of that boundary. By "upper active ring" is meant the top ring which lies immediately beneath the lowest point of the rubber membrane, and which therefore does not receive any direct lateral air pressure. Thus, for the conditions shown in Fig. 10-6, the second ring from the top would be taken as the upper active ring. A slight dish-shaped depression in the soil surface above it does not seem to affect the results, since check tests performed with a reversed curvature of the soil surface,

artificially created before the start of the test, gave identical values of lateral pressure under otherwise identical conditions.

Figure 10-7 gives the results of a test with sand. It will be noted that the value of K_n against the upper active ring is very close to 0.50. Figure 10-8 gives the variation with time of the K_n values against the upper active ring during the consolidation of a disturbed sample of a "blue" clay which had a liquid limit w_L = 43 per cent and a plasticity index I_p = 18 per cent. The clay was placed in the device after complete remolding with water. It will be seen from Fig. 10-8 that immediately after application of the first vertical load to a previously unstressed, fully saturated specimen, the ratio of vertical to lateral pressures K_n, as measured on the upper active ring, was
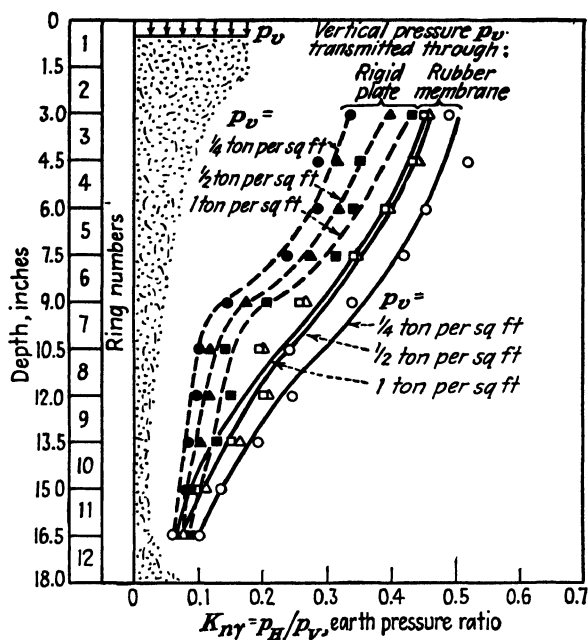
FIG. 10-7. Comparison of the effect of the presence or absence of restraint at the upper boundary in the lateral earth pressure meter. (*After Tschebotarioff and Welch, Ref. 390, 1948.*)

almost exactly 1.00. (K_n = 0.97 within 10 min after the application of the vertical load.) As time went on and consloidation progressed, the value of K_n decreased until it finally stabilized itself at K_n = 0.50. The general shape of the time-K_n curve shows even more similarity to a typical time-consolidation curve than the curve shown in Fig. 10-8 for a separate consolidation test on the same soil, which gives evidence of secondary time effects (Art. 6-9). It therefore follows that the decrease of lateral pressures during consolidation from a condition of completely fluid pressure (K_n = 1.00) to what Tschebotarioff (Ref. 384, 1948) termed a *consolidated-equilibrium state* (K_n equals approximately 0.50) occurs as a result of the dissipation of the excess pore pressures (Art. 6-1) and the transfer of the entire vertical load from the water filling the voids of the clay to the skeleton of soil grains.

Similar results were obtained during tests on a siltier clay with a liquid limit w_L = 30 per cent and a plasticity index I_p = 7 per cent. Again, after completed consolida-

tion the at-rest, neutral, or consolidated-equilibrium earth pressure coefficient was found to be approximately, that is, within ±10 per cent, $K_n = 0.50$. Almost identical values were obtained with the same silty clay during large-scale model earth pressure tests with model flexible bulkheads (Art. 10-23).
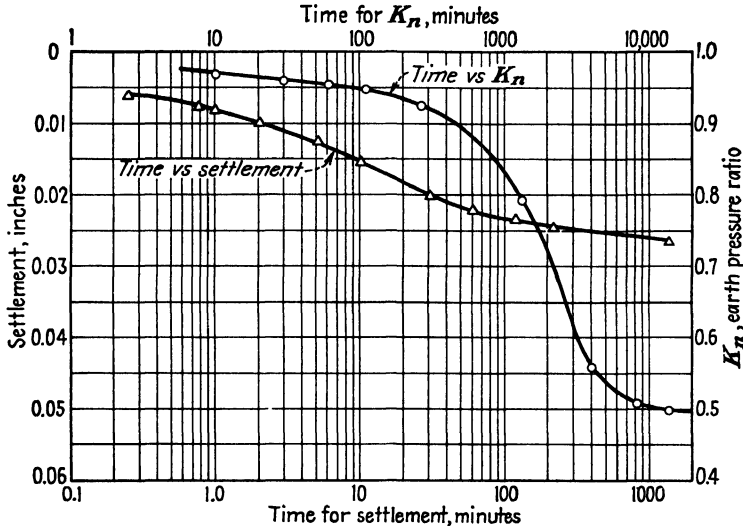
FIG. 10-8. Rate of consolidation of a clay, as affecting the settlements measured in a consolidometer, and the decrease of lateral pressure measured on the upper active ring of the lateral earth pressure meter. (*After Tschebotarioff and Welch, Ref. 390, 1948.*)

10-10. Effects of Restraining Boundaries on Parallel Soil Deformations and on Lateral Earth Pressures. The effect which a rigid restraining boundary may have on the location of a surface of failure was already mentioned in Art. 8-13. The conventional rigorous computation procedures are compelled to ignore this effect, which is too complex for them to handle.

Similarly, the conventional procedures for the computation of settlements of soft saturated clays usually ignore the effects of shearing resistance to displacements parallel to vertical rigid boundaries in their vicinity and assume that the surface settlements at all times are directly proportional to the degree of consolidation of the soil beneath the respective point of the soil surface (Art. 6-7). This means that, say, at 50 per cent average consolidation of the layer, the clay surface near vertical sand drains, if such were used, should settle more than the surface between the drains. No such observations, however, appear to have been reported so far from the field (Art. 6-10).

Tests performed at Princeton University have even shown a reverse relationship (Refs. 390 and 397, 1948). After the completed consolida-

tion of an 8-ft-deep fluid clay mass in a 13- by 18-ft testing tank (see Fig. 10-35), with vertical sand blankets acting as drains at two ends of the tank, a pronounced dip of the clay surface away from the faces of the sand blankets was noticeable. The same phenomenon, but greatly accentuated, was observed during tests with the lateral earth pressure meter, as shown in Fig. 10-9. The silty red clay (I_p = 7 per cent) was placed in the device at a fluid consistency corresponding to three blows
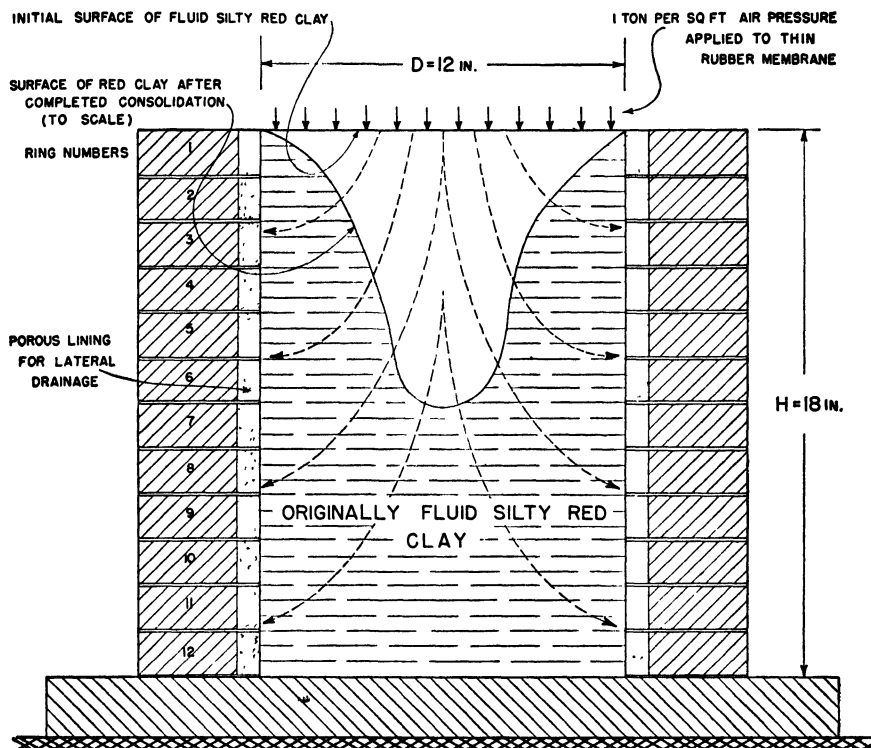
FIG. 10-9. Effect of the wall friction in the lateral earth pressure meter on the settlement of the surface of a clay. (*After Tschebotarioff and Welch, Ref. 390, 1948.*)

on the liquid-limit device. When consolidation was completed under a vertical pressure of 1.00 ton per ft^2, the clay surface was found to have assumed the shape shown in Fig. 10-9. This was a result of the restraining effect of the cylindrical pervious vertical boundaries, friction along which prevented adjoining soil particles from sliding downward along them. Consequently, the rate of the settlements of points on the clay surface was governed not by the rate of consolidation of the clay beneath each point, but by plastic deformations of the clay mass, which must have followed trajectories approximately indicated by broken lines in Fig. 10-9.

The presence of a rigid horizontal boundary at the soil surface has a similar effect, as shown in Fig. 10-7. The lateral expansion of the soil immediately beneath the rigid plate is restrained by it. The shearing stresses thereby engendered decrease the lateral pressures. It will be noted that for a vertical pressure $p_v = 0.25$ ton per ft² the lateral pressures against the upper active ring corresponded to $K = 0.33$, whereas for the same vertical pressure transmitted to the soil surface through a flexible thin rubber membrane they corresponded to $K_n = 0.52$. As the vertical pressure was appreciably increased, the difference between the lateral pressures for the two surface conditions decreased somewhat, presumably because of the unavoidable slight yield of the walls of the apparatus and the resulting very slight expansion of the soil. This effect was observed not only with sand, but also with plastic clay (see Art. 10-23).

The decrease of the K values with depth shown in Fig. 10-7 is not to be taken to mean that the actual ratio of the lateral to the vertical pressures is changing with depth. As already mentioned in Art. 10-9, this method of presentation of test results was adopted solely for purposes of convenience. The actual ratio K of the lateral and vertical pressures probably remains unchanged with depth, and the decrease of lateral pressures with depth measured in the lateral earth pressure meter shown in Fig. 10-7 is the result of the decrease with depth of the corresponding vertical pressures due to friction along the walls of the device. The effect is very similar to the so-called *bin effect* in grain silos (Art. 10-15).

10-11. Effect of Soil Consolidation or Expansion on Its Lateral Pressure

According to the theory of elasticity (see Timoshenko, Ref. 367, p. 11), the following relationship exists between the lateral pressure σ_3, the material constants E and ν, and the unit strains ϵ of an elastic body:

$$\sigma_3 = \lambda e + 2G\epsilon_3 \tag{10-26}$$

where

$$\lambda = \frac{E}{(1 + \nu)(1 - 2\nu)} \tag{10-27}$$

$$G = \frac{E}{2(1 + \nu)} \tag{10-28}$$

$$e = \epsilon_3 + \epsilon_2 + \epsilon_1 \tag{10-29}$$

E is the Young modulus and ν the Poisson ratio. In the above equations the plus sign is used to designate tension or expansion and the minus sign corresponds to compression. This holds both for the stresses σ and the strains ϵ.

Let us consider a cube of soil shown in section in Fig. 10-10. The length of each side of the cube will be taken as unity. Let us assume that the soil surface has settled by the amount $-\epsilon_1$, as shown in Fig. 10-10(I). According to Eq. (10-26), if lateral expansion is prevented, this type of deformation should induce compressive lateral stresses $-\Delta\sigma_3$ in the soil. The reaction pressures of the soil cube against a restraining

boundary, that is, the lateral pressures of the soil, would therefore be increased. Since the reverse relationship is actually observed during consolidation (Fig. 10-8), it follows that the laws of the theory of elasticity cannot be applied to a soil which undergoes the process of consolidation (Art. 6-1). This fact may be taken as obvious, but the physical causes of the observed values of the at-rest or consolidated-equilibrium lateral pressures are not clear. It may be argued, as was done by A. E. Bretting (Ref. 40, 1948) that "the internal friction of the soil will probably at every moment be fully mobilized on account of the great deformations, which are needed to consolidate the fluid clay." This statement may perhaps be illustrated by Fig. 10-10(III). As a result of consolidation, the height of the cube will be decreased by $-\epsilon_1$, and the length of the diagonals *na*, *mb*, *hc*, and *hd* will be shortened to *na'*, *mb'*, *hc'*, and *hd'*, respec-
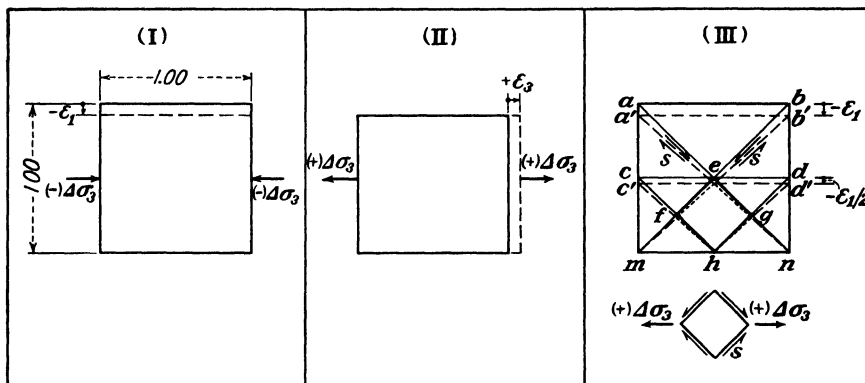
FIG. 10-10. (I) Vertical compression of soil under prevention of lateral expansion increases lateral pressures, according to the theory of elasticity. (II) Induced lateral expansion of soil decreases lateral pressures, according to the theory of elasticity. (III) Internal shearing stresses set up during the consolidation of a soil may tend to decrease lateral pressures, although no over-all expansion occurs.

tively. A square element *efhg*, marked by thick lines in the sketch, will be deformed to the rhomboidal shape shown by dotted lines. This "internal" deformation can only be associated with intergranular displacements and the intergranular shearing stresses *s* shown in the lower sketch of Fig. 10-10(III). The horizontal resultant of these shearing stresses $+\Delta\sigma_3$ will produce a decrease of total lateral pressures by enabling the soil skeleton to take up by internal shear the decrease of excess pore pressures.

The puzzling part of the phenomenon lies in the absence of any apparent generally valid relationship between the measured K_n ratios and the values of the internal friction ϕ of different soils, as determined in the laboratory by different testing procedures (Art. 7-21). Slow (*S*) tests give approximately the same value of $\phi = 30°$ for most clays, silts, and loose sands. According to Eq. (10-8) and Fig. 10-4, the corresponding value of K_n would equal $K_A = 0.33$ if the internal friction were fully mobilized. Actual direct measurements (Arts. 10-9 and 10-12), however, show that the value of K_n in almost all instances is appreciably higher and generally comes very close to $K = 0.50$. The corresponding value of ϕ would be approximately 19° ($\tan \phi = 0.35$), which is sometimes obtained by consolidated quick (Q_c) tests (Art. 7-21), on some clays but is never obtained on sands by any type of test. The hypothesis was

advanced by Tschebotarioff and Welch (Ref. 390, 1948) that the coefficient K_n of internal friction of a soil at rest may not be influenced at all by the cohesion or by the interlocking of grains (Arts. 7-3 and 7-4), since these phenomena depend on motion to be fully mobilized, and that only the component of sliding friction may govern its value, since that component is fully active prior to any motion. This hypothesis could only be valid if the coefficient of sliding friction were found to be the same for different minerals. It was subsequently disproved by its authors (Ref. 393, 1948) and (Ref. 397, 1949), who found a considerable diversity of values of the coefficient of sliding (Art. 7-2).

The equation suggested by Jaky (Refs. 187 and 186, 1944)

$$K_n = 1 - \sin \phi \qquad (10\text{-}29a)$$

happens to fit many of the experimental results, since with $\phi = 30°$, $K_n = 0.50$. However, the basic assumptions on which the derivation of the above equation is based do not appear tenable. They apply to the stress condition along the center line of an embankment with slopes forming the angle ϕ with the horizontal, so that there is a variation of the horizontal shearing stress with the distance from the center line. Jaky's contention (Ref. 186) that these assumptions correspond to the conditions within an infinite mass of soil with a horizontal surface unfortunately cannot be accepted.

The satisfactory numerical correlation between the measured values of lateral pressures of soils at rest and the measured values of their physical properties (ϕ, ν, and any others not yet defined) therefore still awaits further theoretical and experimental research.

Let us now consider the effect of the induced *expansion* of the soil, which causes the change from the at-rest to the active state. As shown in Fig. 10-10(II), an induced lateral strain $+\epsilon_3$, for instance, as a result of a lateral yield of the retaining structure, in accordance with Eq. (10-26), will induce tensile lateral stresses $+\Delta\sigma_3$ in the soil. Therefore the reaction pressure of the soil against the yielding restraining boundary should be decreased in theory. Actual observations on this point are as follows:

In the case of cohesionless sands experiments have shown that a very slight outward yield of the retaining wall, equal to 0.1 per cent of its height, does decrease lateral pressures appreciably (Art. 10–14). The transition from the at-rest to the active state occurs with a minimum of motion.

As regards clays, Terzaghi (Ref. 362, 1943) advanced the suggestion that a very appreciable expansion—corresponding, for instance, to an outward movement of a retaining wall, equal to 5 per cent of its height—would be needed to fully mobilize the shearing resistance of a clay and to decrease the lateral pressures at rest to their active values. This suggestion was presumably based on laboratory shear tests of clays which undergo much greater deformations than sands before failure. Since no corresponding direct observations had yet been made, the idea essentially was a guess which was not substantiated by later observations on models

and in the field. First of all it appears necessary to *differentiate between plastic and brittle clays.*

By "plastic clays" will be meant clays which have not developed a brittle inner structure, which have a value of the sensitivity ratio S close to unity (Art. 7-22), and a strain at failure during unconfined compression tests close to 20 per cent (Art. 7-10). Most of the strongly remolded and reconsolidated natural clays should fall into this category, as do fully consolidated, hydraulically deposited backfills with a high clay content.

Experiments performed at Princeton University (Art. 10-23) have shown that such plastic clays do not decrease their lateral pressures during expansion. This, as well as data obtained by means of the cell tests (Art. 10-12), was in contradiction with the results of Terzaghi's purely theoretical application of the conventional stress-strain concepts to that problem (Ref. 362, 1943) which led him to believe that an outward movement of 5 per cent of the height of a retaining wall would be necessary to achieve a transition from the at-rest to the active state of the clay behind the wall. Tschebotarioff, (Ref. 384, 1949) explained this discrepancy by stating that the very terms "at rest," "neutral," or "consolidated equilibrium" imply a limit state of incipient failure where plastic cohesive backfills or remolded natural clays are concerned. Therefore, in the absence of any adjoining boundaries which may restrain deformations and thereby decrease lateral pressures in their vicinity, the active pressure values of such clays are very close to the values of their pressures at rest. No experimental data have yet become known to disprove this hypothesis but further studies are needed, so as to either confirm or modify it. The point is of considerable practical importance, since, if the above hypothesis is finally confirmed, the determination for design purposes of the lateral pressures of such clays will be greatly simplified (Art. 16-5).

Natural undisturbed clays with a brittle inner structure present a much more complicated problem in this respect, especially if they have a high degree of sensitivity to remolding (Art. 7-22). Measurements on the Chicago subways (Art. 10-20) have indicated that even a slight degree of lateral displacement of the retaining wall was sufficient to reduce the lateral pressures to what was believed to represent their active values. Further expansion (beyond 1 per cent of the height of the retaining structure), however, again increased the lateral pressures (Art. 10-20).

10-12. Lateral Earth Pressure Coefficients Determined from Cell Tests. Effect of Soil Structure and Rate of Load Application. It was shown in Art. 7-11 that the cell tests permit the direct measurement of the lateral pressure σ_3, under varying vertical pressures σ_1. The coefficient of lateral earth pressure K can then be presented as a function of the vertical pressure σ_1, as was done in Fig. 7-20 for three types of soil. The influence

of soil structure on the results is brought out by that diagram. It will be noted that the compacted sand had at first a very high value of K, which under a load of 0.20 ton per ft² equaled $K = 1.00$. This was the natural result of the wedging-in effect of sand grains during their compaction. Similar values were obtained somewhat earlier for compacted backfills by Terzaghi during the large-scale model tests described in Art. 10-13. Similarly, these values dropped rapidly as a result of a slight induced lateral expansion of the sand. The design details of the apparatus with which the results given in Fig. 7-20 were obtained were not published. Presumably it had the usual lightweight design characteristics of other cell and triaxial shear devices, which cannot fail to bulge out slightly under increasing lateral pressures transmitted through the supporting liquid. As a result the original $K_n = 1.00$ value of the compacted sand rapidly dropped to a value of $K = 0.53$.

The two specimens of undisturbed loam acted in a reverse manner. Because of their brittle and unyielding natural structure they did not begin to bulge sufficiently to transmit lateral pressures to the supporting liquid until the vertical pressures reached 0.5 ton per ft² in one case and 3.0 tons per ft² in the other. After that, presumably because of the crumbling of the brittle inner structure, the K values increased rapidly with increasing vertical pressure until they reached the approximate value of $K = 0.54$. It is still an open question whether these final values should be considered as representing the active or the neutral coefficients of lateral earth pressure (Art. 10-1).

The results of a rapidly performed (Q) cell test with a saturated sample of undisturbed peaty clay are illustrated by Fig. 7-19. The effects of soil structure and of its breakdown are even more pronounced here. The lateral pressures and the corresponding K values gradually increased from $K = 0.20$ at a vertical pressure of 0.5 ton per ft² to $K = 0.46$ at a vertical pressure of 1.65 tons per ft². According to Geuze (Ref. 148, 1936), this latter value corresponded to the weight of the overburden. When vertical pressures were quickly increased beyond that value, the K coefficients also increased, first to $K = 0.61$ and then to $K = 0.70$, indicating that, as a result of the breakdown of the soil structure and prior to the subsequent further consolidation, part of the vertical pressures were being temporarily transmitted to the water in the voids. Figure 7-18 illustrates the results of a slow (S) cell test with a specimen of peat, where, by contrast, full consolidation was permitted. The vertical load was maintained at a constant value for several days after the application of each load increment. During that time the lateral pressures and the corresponding K values decreased as consolidation progressed. This result is similar to the one obtained at Princeton with the lateral earth

pressure meter (Fig. 10-8). The consolidated-equilibrium K_n values obtained from these cell tests were, however, much lower, ranging from $K_n = 0.37$ to $K_n = 0.24$. This is probably due to the fibrous character of the peat soil, the lateral expansion of which is very small during compression when water is given time to escape. This means that the values of the Poisson ratio of organic soils must be smaller than the values of that ratio for inorganic soils. According to Eq. (10-25) and Table 10-3, a value of $\nu = 0.19$ would correspond to $K = 0.24$, whereas a value of $\nu = 0.33$ would correspond to $K = 0.50$ for a soil in an elastic state.

David Welch (Ref. 425, 1949) computed the K_n values for consolidated-equilibrium conditions, from cell test results reported by DeBeer (Ref. 105, 1948), for 14 clay samples with not more than 3.6 per cent organic content. The K_n values varied between 0.40 and 0.65 for all 14 samples, with 10 samples having values equal to 0.49, 0.50, 0.51, or 0.52. In the text of his paper, DeBeer (Ref. 105), with reference to the conditions of the test which gave a value of 0.65, states that this value is "probably too high."

The preceding discussion shows that much is yet to be learned concerning the values of lateral earth pressures of natural undisturbed clays. Further progress cannot be expected, however, from a continuation of the "classical" approach to the problem which attempts to relate lateral earth pressures only to the ultimate shearing strength of the soil at failure. Too many other factors affect the results. Direct field measurements and laboratory tests with improved apparatus are therefore essential.

10-13. The K_s and the K_{s+w} Values

Differentiation is essential between the following two conditions: First, both the vertical pressures σ_1 and the lateral pressures σ_3 are purely intergranular pressures; their ratio will be designated by K_s. Second, both σ_1 and σ_3 include a component of free-water pressure which is transmitted through the water in the voids of the soil quite independently of its grain skeleton; their ratio will be designated by K_{s+w}.

Figure 10-11 illustrates the difference. Let us assume that a wall of steel sheet piling with completely watertight interlocks has been driven into a layer of fully saturated soil. It was then excavated on one side and strutted out against the opposite wall of the cut. The lateral forces P_1 and P_2 transmitted from the sheet piling to the struts were measured. The ground-water level has been established in an open pit and in a bore hole, as shown in Fig. 10-11. The density of the soil has been determined, so that its buoyed unit weight, according to Eq. (4-9), or its unbuoyed but fully saturated unit weight, according to Eq. (4-7), can be easily computed.

It is then generally preferable to deal with intergranular pressures. The K_n values at rest determined by means of the cell tests (Art. 10-12) or the lateral earth pressure meter (Art. 10-9) are based on intergranular pressures and are therefore essentially K_s values as defined above.

If the soil of the case illustrated by Fig. 10-11 is of a noncohesive and therefore permeable type, the water in an imaginary standpipe, shown in Fig. 10-11 as being

connected to a sand pocket behind the impervious wall, would gradually rise to the level a. This level would correspond to the free-water level in an open pit or in a bore hole. It is then possible to determine the total intergranular lateral pressures by subtracting the total water pressure, represented by the area *def* in Fig. 10-11, from the strut loads P_1 and P_2. In computing the K_s values, the buoyed weight of the soil should be used below the water level according to Eq. (4-9). The line showing the distribution of intergranular lateral pressures can then be drawn in on the basis of the residual strut-load values.

To facilitate the evaluation of the results of field measurements, Tschebotarioff (Ref. 384, 1948) proposed to draw at least a clear distinction between the possible limit
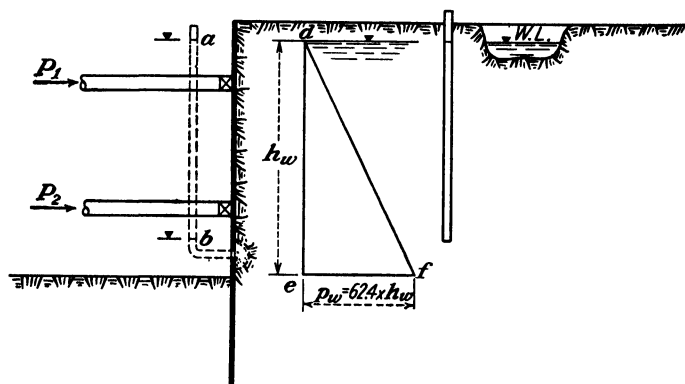
FIG. 10-11. Diagram illustrating the computation of the K_s and K_{s+w} coefficients.

conditions and to numerically relate them to each other by means of the K_s and K_{s+w} coefficients.

If the full water pressure is included in both the horizontal (measured directly) and vertical (computed) component of pressure, then, according to Eq. (4-7), their ratio at a depth h, expressed in metric units, will be equal to

$$K_{s+w} = \frac{p_h}{p_v} = \frac{p_h}{\gamma h} = \frac{p_h(1 + e)}{h(G + e)} \tag{10-30}$$

On the other hand, if only the buoyed intergranular pressures are to be taken into account, that is, if the full water pressure is to be subtracted from both the horizontal and the vertical pressures, their ratio will be

$$K_s = \frac{p_h - 1.0h}{p_v - 1.0h} = \frac{p_h - 1.0h}{h(G + e/1 + e) - 1.0h} = \frac{p_h(1 + e) - h(1 + e)}{h(G + e) - h(1 + e)}$$
$$= \frac{p_h(1 + e)}{h(G - 1)} - \frac{1 + e}{G - 1} = K_{s+w}\frac{G + e}{G - 1} - \frac{1 + e}{G - 1}$$

or

$$K_s = \frac{K_{s+w} - C'}{1 - C'} \tag{10-31}$$

where

$$C' = \frac{1 + e}{G + e} \tag{10-32}$$

where G = specific gravity of the solids [Eq. (3-1)].

The upper part of the chart in Fig. 10-12 illustrates the relationship expressed by Eq. (10-31) for three values of the void ratio ($e = 0.50, 1.00, 1.50$). The lower part of the same chart gives the relationship between the coefficient K_s and the angle of internal friction ϕ for a cohesionless soil according to Eq. (10-7).

The symbol $K_{s+w'}$ will be used to designate the condition where the water filling the voids of the clay is in tension and is suspended from the soil skeleton. The weight of the water will then be transmitted from grain to grain and

$$K_{s+w'} = K_s \tag{10-33}$$

FIG. 10-12. Conversion chart for the K_s and the K_{s+w} coefficients.

10-14. Terzaghi's Large-scale Model Tests with Sand Backfills. Wall Motion and Arching in a Horizontal Direction.

Terzaghi's studies were inspired by the views of Meem (Ref. 225, 1908) and Moulton (Ref. 240, 1920). Their observations of deep cuts of New York subways indicated that lateral earth pressures did not increase linearly with depth, as is assumed by the classical earth pressure theories (see Fig. 10-2). For that reason, Meem, in designing the bracing for a 5,000-ft-long and 30-ft-deep section of the Brooklyn subway, where the soil consisted of sand and gravel, placed the larger braces at the top and smaller braces near the bottom. In no single instance was any failure of the lower and lighter braces observed. Many instances of bending of the upper rangers, *i.e.*, wales, however, were noticed.

Some later measurements, performed in a deep cut in New York by M. Miller (1916) and reported by Moulton (Ref. 240), showed, as illustrated by Fig. 10-13, that on that job the upper struts received the maximum load. The soil there consisted of "coarse sand mixed with about 20 to 30 per cent of clay and some gravel." Some objections could be raised concerning the experimental method employed, which was based on the measurement of ranger deflections, since these were probably reduced by horizontal arching of the sand parallel to the wall. Further, although both Meem and Moulton attributed the observed performance of the timbering to arching of the soil in a horizontal direction at right angles to the wall, similar to the *bin effects* (Art. 10-15), a great variety of opinions was advanced as to whether and when these effects could be active (Refs. 225 and 240). Terzaghi subsequently succeeded in further clarifying this important matter (Ref. 360, 1941).
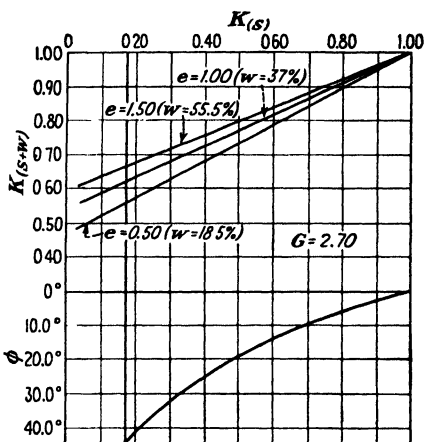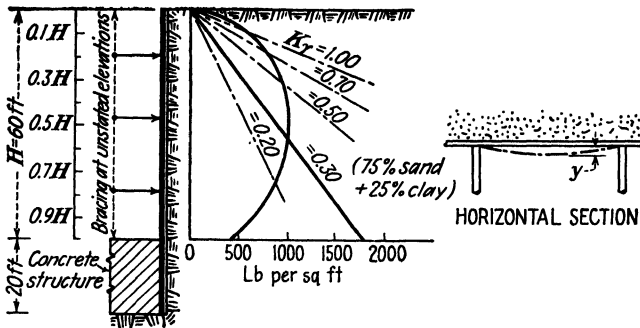
FIG. 10-13. Diagram illustrating the distribution of pressures against the timbering of a subway cut at Flatbush Avenue, Brooklyn, New York, as computed by Max Miller (1916) from the measured deflections y of the rangers. (*After H. G. Moulton, Ref.* 240, 1920.)
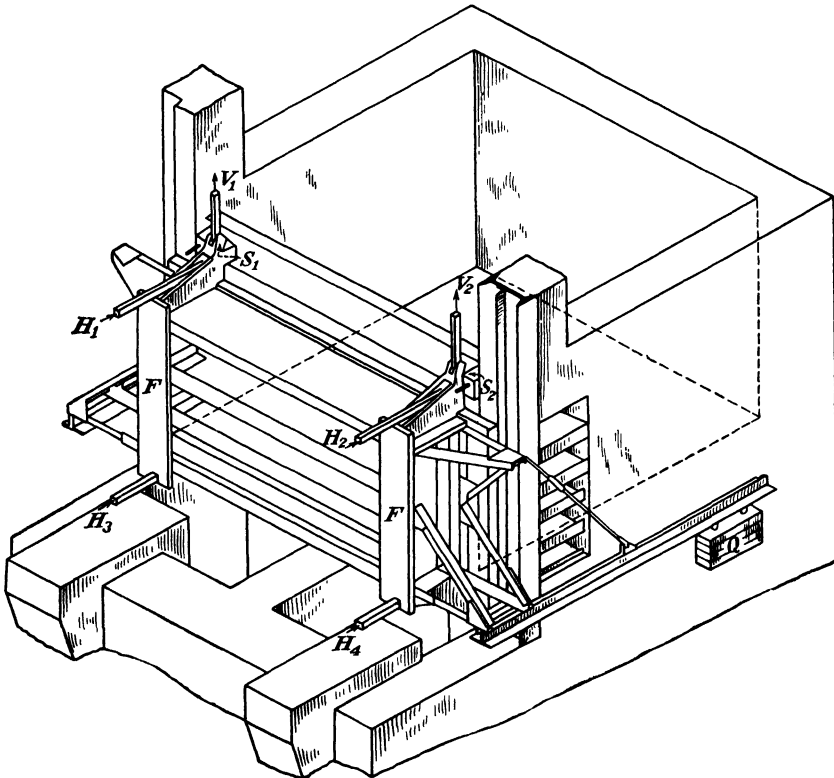
FIG. 10-14. Terzaghi's 1928 setup for tests with rigid walls (14- by 14- by 7-ft bin) (Ref. 352). (Isometric diagram view of earth-pressure testing machine installed at Massachusetts Institute of Technology laboratories.)

The testing installation illustrated in Fig. 10-14 was used by Terzaghi (Ref. 352) in 1928 to 1929 to study the effect of different kinds of motion of a rigid retaining wall on the distribution of lateral pressures exerted against the wall by granular noncohesive backfills. The rigid wall was 14 ft wide and 7 ft high; the bin behind the wall was 14 ft long. A system of levers permitted the measurement of the vertical reaction V as an average of values measured at two points, V_1 and V_2, and of the horizontal reactions at two elevations H' and H''. The upper reaction H' was determined as the average of values measured at two points, H_1 and H_2; the lower reaction H'' was determined as the average of values measured at two points, H_3 and H_4. Both the magnitude and the location of the centroid of the total lateral pressure R acting against the wall could then be determined as the resultant of the upper reaction H' and the lower reaction H''.

FIG. 10-15. Diagram illustrating nature of the rotational displacement of gravity retaining wall resting on soil.

The distribution of pressures was estimated from the elevation of the resultant R. If it was located at one-third of the height, then it was con-
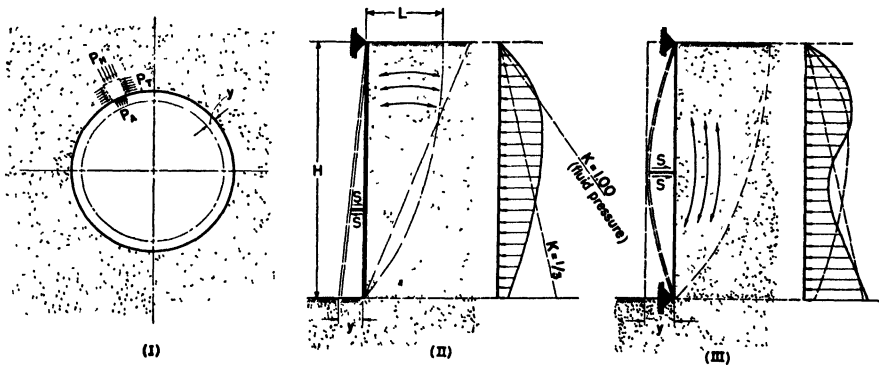
FIG. 10-16. Three types of arching in soils. (I) Arching around a vertical shaft or a horizontal tunnel (Ref. 345, 1925). (II) Horizontal arching in a rigidly sheeted vertical cut with fixed upper edge and yielding lower edge (Ref. 360, 1941). (III) Vertical arching behind a flexible bulkhead (Ref. 360, 1941). (*After Terzaghi.*)

cluded that the lateral-pressure diagram must have a triangular shape of the type shown in Fig. 10–15. If it was located above the lower third of the height, the pressure-distribution curve was assumed to have a para-

bolic shape of the type shown in Fig. 10–16(II). The method is extremely crude, but it was the best possible with the instrumentation available at that period. Although numerical evaluations obtained in this manner could not be relied upon to give quantitatively precise data, some interesting trends were disclosed by these tests.

An outline of the test results was published by Terzaghi in 1934 (Ref. 353). Tests were made with dry and with submerged sand, both in a loose and in a compacted condition. No difference was found between the dry and the submerged conditions so long as the earth pressure coefficients K referred to intergranular pressures, that is, if they were computed on the basis of the corresponding unbuoyed and buoyed unit weights γ [Eqs. (4-7) and (4-9)], and the full water pressure was subtracted in the latter case from the measured lateral pressures.

Prior to any displacement of the wall, that is, in the at-rest condition, the earth pressure coefficient of the sand backfill K_n was found to have the limits of $K_n = 0.70$ (for compacted dense sand backfill) and $K_n = 0.40$ (for loose sand backfill). Intermediate values were obtained, depending on the degree of compaction of the backfill. These values were computed as a ratio of total pressures—the measured value of the resultant of lateral pressures R divided by the computed value of the lateral pressures for $K = 1.00$, that is, by the total fluid pressure $\gamma H^2/2$.

A very slight outward displacement of the wall, not exceeding 0.001 of the wall height, was sufficient to reduce the lateral pressures to their minimum value of $K_A = 0.10$ in the case of originally dense backfill and $K_A = 0.25$ in the case of originally loose backfill. These values were reached when the displacement consisted in a tilting of the wall around its lower edge, the type of displacement illustrated by Fig. 10–15, as well as in the case of a horizontally sliding wall, such as is illustrated in Fig. 10-1(III). The location of the center of lateral pressures, that is, the elevation of the resultant R, was fairly consistently close to $\frac{1}{3}H$ in the case of originally loose sand. In the case of compacted dense sand the elevation of R was approximately $0.4H$ at the start of the test but dropped to $\frac{1}{3}H$ and even lower as the wall yielded.

The possible restraining effect of friction along the rigid bottom of the concrete testing tank was not considered in the layout of these tests and in the evaluation of their results. The elevation of R could be strongly affected thereby. This point was criticized by Anders Bull (Ref. 49, 1934). The same point was found by Tschebotarioff to be of considerable importance during tests at Princeton 10 years later (Art. 10-23).

No tests involving a rotation of the wall around its upper edge, that is, a motion of the type illustrated by Fig. 10-16(II), were actually performed at the time.

Some years later (Ref. 354, 1936) and (Ref. 360, 1941) Terzaghi, by means of the diagram of Fig. 10-16(II), established a basic fact of very great importance, which explained the observations concerning so-called *horizontal arching*, made 30 years earlier by Meem (Ref. 225) and by other builders of the first subways in New York. These basic facts may be summarized as follows:

1. The distribution of pressures against a retaining structure is a function of the nature of the wall displacements.
2. The Coulomb distribution, that is, the hydrostatic distribution, of lateral pressures develops only if a wall tilts by rotating around its lower edge (Fig. 10-15).
3. If a wall slides out as a block [Figs. 10-1(III) and 10-24(*B*)], then the pressure-distribution curve tends to assume a parabolic shape, similar to the one shown in Fig. 10-24. It is, however, still an open question—for sands, and especially for clays—whether this shape is primarily caused by a redistribution of pressures due to horizontal arching or by a transfer of lateral pressures to the underlying soil by shearing stresses along it.
4. If a wall tilts around its upper unyielding edge, as happens during excavations with several vertical rows of struts (see Fig. 10-25), then a redistribution of pressures occurs, with an increase at the top, as shown in Fig. 10-16(II). This is a result of arching in a horizontal direction (see Arts. 10-15 to 10-19), which is somewhat similar to the phenomena observed in grain silos and bins.

10-15. Pressures in Silos and Bins. Observations made of grain silos and bins showed that the increase of pressure on the bottom of the silo and against its side walls was not proportional to the height of grain over the point where the pressures were measured. Numerous experiments have been performed, both on models and on full-sized bins. Figure 10-17 gives the results of a typical example of carefully performed full-scale measurements on an actual structure, reported by Jamieson (Ref. 188, 1904). One of the silo cells, 67 ft deep and having a horizontal 12- by 13.5-ft cross section, was selected for the tests. The vertical pressures p_v and the horizontal pressures p_h were measured by means of hydraulically operated pressure cells, located at the bottom of the silo cell and in the lower part of the side wall, as shown in Fig. 10-17. The adjoining diagram shows the increase of the measured pressures as a function of the corresponding depth h of the grain above the points of measurement. The unit weight of the wheat used during the tests was 49.4 lb per ft^3. Its angle of repose was $\alpha_R = 28°$.

It will be noted from Fig. 10-17 that both the vertical and the horizontal pressures increased at a decreasing rate as the value of h increased. This happened because of the increasing influence of the frictional shearing

stresses s between the wheat and the walls of the silo cell. These shearing stresses are active along the entire depth of wheat and are a function of the corresponding horizontal pressures, the latter, in turn, being a function of the corresponding vertical pressures at the same elevation. The vertical pressures transmitted to the bottom of the silo cell are decreased by the shearing stresses along the entire height to which the silo is filled with wheat. It will be noted from Fig. 10-17 that, when the height of the wheat reached 40 ft above the silo bottom, or approximately three times the width of the cell, no further increase of either horizontal or vertical pressures was measured. This elevation corresponds to the point where the weight of each added layer of wheat is balanced by the increase of shearing stresses which the weight of that layer produces along the entire depth of wall beneath it. It is a function of the width of the cell (compare with Art. 10-25). Among several past mathematical treatments of the problem of pressures in silos, a paper by Jaky (Ref. 187, 1948) should be mentioned as noteworthy.

FIG. 10-17. Results of pressure measurements in a wooden silo filled with Manitoba wheat at St. John, Canada (1900). (*After Jamieson, Ref. 188, 1904.*)

The ratio of the actually measured horizontal and vertical pressures increases somewhat with h from $K_n = p_h/p_v = 0.54$ to $K_n = 0.64$. As already mentioned in Arts. 10-9 and 10-10, the decrease with depth of the coefficient K_γ frequently is only apparent, since K_γ is customarily computed for purposes of convenience as the ratio $p_h/\gamma h$, that is, under the assumption of a constant vertical fluid pressure equal to the full weight of the overburden $p_v = \gamma h$; this assumption is not correct. The vertical pressure changes and not the actual value of K. Nevertheless, the method of relating the measured lateral pressures to the weight of the overburden will be maintained, since it provides the most convenient way for the comparison of the results of field measurements on different types of structures and at different localities (Arts. 10-17 to 10-20).

Observations in cuts through sand (Art. 10-18) indicate that true arching in a horizontal direction [Fig. 10-16(II) and Art. 10-19] may produce local increases of lateral pressures in the upper zone, corresponding to K values well above $K = 1.00$. Possible similar effects have not yet been fully studied in silos.

It may be mentioned in this connection that Krynine (Ref. 204, 1945) has shown that the ratio K_f of the lateral to the vertical pressure in a vertical plane of failure is given by the expression

$$K_f = \frac{\cos^2 \phi}{2 - \cos^2 \phi} = \frac{1 - \sin^2 \phi}{1 + \sin^2 \phi} \tag{10-32a}$$

This expression is derived with the help of the Mohr circle. As shown in Fig. 7-12, the line JB_1 is proportional to the normal pressure on the plane of failure, that is, to the horizontal pressure in the case of a vertical plane of failure, and the line HF is proportional to the pressure on the plane perpendicular to the plane of failure, that is, to the vertical pressure in the case considered. As an approximation, Eq. (10-32*a*) may possibly be applied to the problem of silos, if we consider that the vertical plane of contact between the grain and the walls of the bin is a failure plane. With $\phi = 30°$, we obtain $K_f = 0.60$.

10-16. Arching around a Vertical Shaft. Field experience with shafts sunk through sand has shown that very light bracing can safely be used. This is an indication that lateral pressures against the bracing of such shafts must be much smaller than the pressures exerted at the same depth against the bracing of continuous trenches.

Figure 10-16(I) illustrates the probable causes of the observed smaller pressures p_A against the bracing of shafts. Every soil element of each successive ring of soil outside of the shaft is liable to act as a keystone of a circular sand arc around the shaft. The tangential stresses p_T transmitted from element to element of the arcs will reduce the lateral pressures p_H of the soil to the smaller value p_A transmitted to the bracing.

This is the most stable type of arching, since any yield y of the bracing will only tend to increase the effectiveness of the ring-arch action of the sand.

An approximate mathematical solution of the problem was attempted by Terzaghi (Ref. 345, 1919). A more recent general solution has been given by Westergaard (Ref. 426, 1940).

No actual measurements of pressures against the bracing of shafts sunk in sand appear to have so far been performed, so that no precise information is yet available on the matter. Figure 10-18 illustrates the results of measurements in a 15-ft-diameter shaft sunk through soft clay in Chicago. The lateral pressures were estimated from the forces acting in each of the metal rings which supported the shaft lining. Hydraulic jacks and a special auxiliary device were used for this purpose by Peck and Berman (Ref. 262, 1948). A comparison of the measured pressure curve and of the $K_\gamma = p_h/\gamma h$ lines in Fig. 10-18 (shaft) with the corresponding curves

and lines of Fig. 10-26 (open cut, also at Chicago) shows that relatively little pressure relief was observed in the shaft. In addition, the points a, b, and c indicate limits reached by the measuring device; actual pressures were greater. Further observations of this type are essential in other localities.
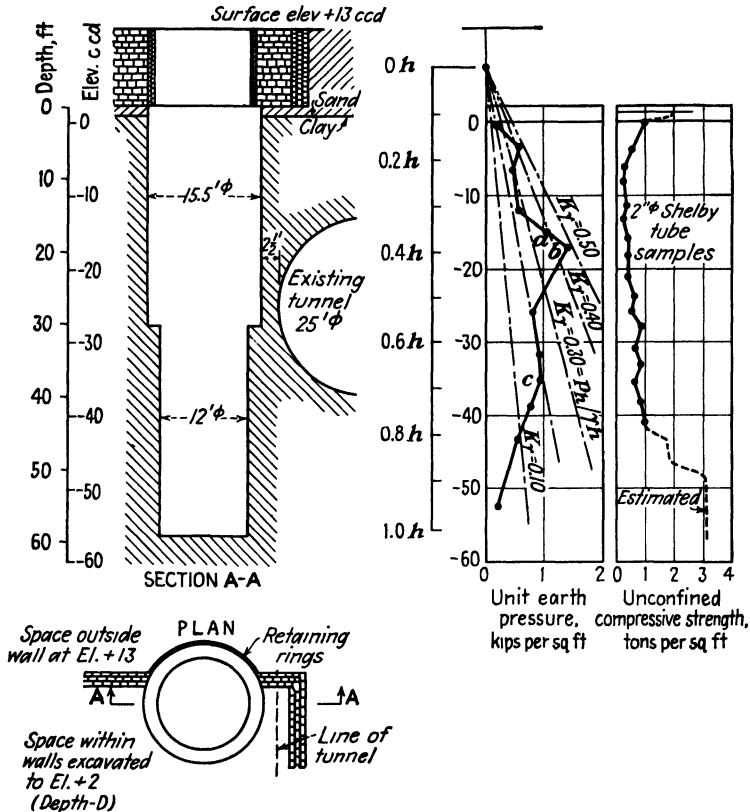
FIG. 10-18. Results of lateral-earth-pressure measurements in a shaft sunk through soft plastic clay at Chicago. (*After Peck and Berman, Ref. 262, 1948.*)

10-17. Records of Full-scale Field Measurements of Lateral Pressures of Backfills against Retaining Walls.

A number of pressure measurements have been performed on massive retaining walls, using pressure cells of various designs for the purpose. Unfortunately, numerical data defining the soil properties are very seldom given. Figure 10-19 illustrates the result of one such measurement reported by Goldbeck (Ref. 156, 1938). The backfill was compacted in layers 12 in. thick. It was described as "earth," thus presumably being a sandy clay material.

The retaining wall formed the abutment of a bridge, so that a slight outward tilting of the type illustrated by Fig. 10-15 appeared likely. It will be noted that the lateral pressures, on the average, increased linearly with depth, as is to be expected with such types of motion. The erratic deviations from a straight line represent an almost inevitable consequence of the use of individual cells of a small size, even though each point in the diagram of Fig. 10-19 gives the average of readings on two separate cells at the same elevation. The cells used here were of the Goldbeck type, of
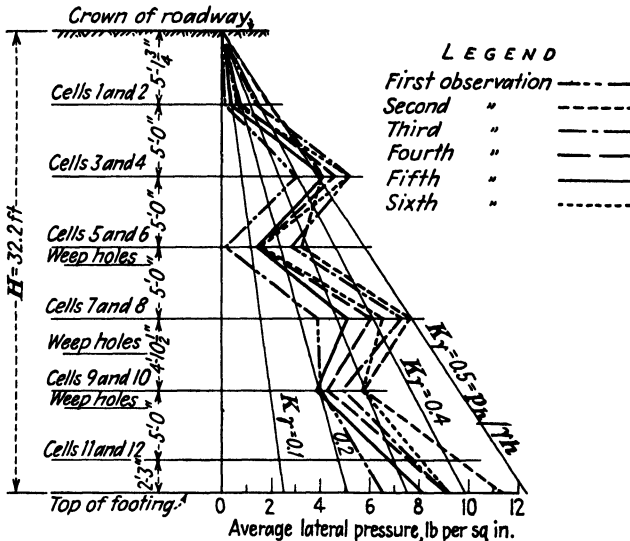
FIG. 10-19. Distribution of lateral pressures against a concrete gravity retaining wall, as measured by Goldbeck cells. (After A T Goldbeck, Ref. 156, 1938.)

5.5 in. diameter, built into the wall, their surface flush with the face of the concrete.

The $K_\gamma = p_h/\gamma h$ lines have been drawn into the diagram for an average unit weight of 110 lb per ft^3 of the backfill. It will be noted that the lowest average lateral pressures correspond to $K = 0.20$. This was an observation taken during a dry period. The highest pressures approximately correspond to $K = 0.40$ and were measured after the fill had been saturated with a spring flood which reached to within a few feet of the roadway crown and then receded.

In the same paper (Ref. 156) Goldbeck reports measurements on the abutments of another bridge with clay backfill which "intercepts both ground water flow and surface drainage and is not provided with any means of drainage." The slope of the greatest pressure curve was such as if these pressures were created by an equivalent liquid weighing 48.4 lb

per ft³ ($K = 48.4/110 = 0.44$). During dry periods the lateral pressures were lower, presumably not so much because of the decrease of the unit weight γ, but as a result of shrinkage stresses in the fill.

Figure 10-20 gives the results of measurements against a 79-ft-high wall which was backfilled with loose clean sand in the manner indicated in the diagram. The wall formed part of a massive reinforced-concrete structure for an underground factory. It could therefore be considered as absolutely rigid and unyielding.

The lateral pressures were measured by means of large (12.0-in. diameter) Maihak- (sonic-) type cells (Ref. 243). Each cell has a load
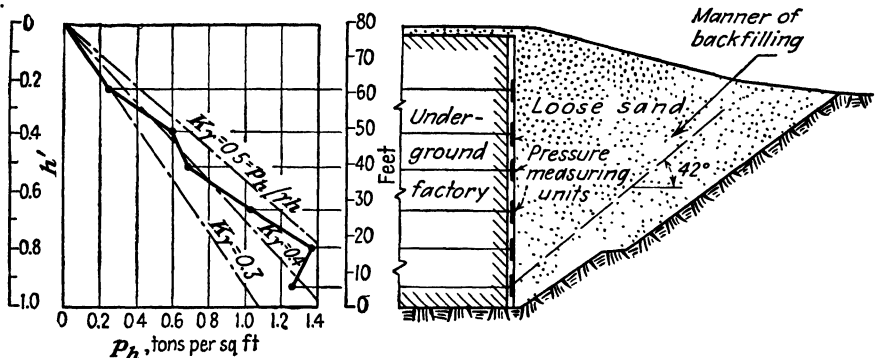
FIG. 10-20. Lateral earth pressures acting against 79-ft-high massive concrete wall of underground German factory, as measured in 1942. (After H. Muhs, Ref. 243, 1947.)

capacity of 8 tons. These cells utilize a vibrating wire which changes its natural frequency, and hence, when vibrating, its tone, with changes of stress, produced in the wire by slight deflections of the metal membrane surface of the pressure cell in contact with the soil. A magnet in the cell induces the vibration of the wire, and an acoustic loading-control device is used to induce the same tone in another calibrated but originally unstressed wire.

The area of the cell in contact with the soil was increased by placing specially designed metal plates between the soil and the two cells. The outer surface of each plate was flush with the surface of the masonry. In this manner, pressures against 54 per cent of the height of the wall were measured over a width of 2 ft. It will be noted from Fig. 10-20 that this method gives a much smoother sequence of measured pressures than can be obtained by the use of small individual cells (see Fig. 10-19).

The factory was built in an open excavation and then backfilled with clean sand. Laboratory direct shear tests gave for that sand a value of the angle of internal friction $\phi = 42°$. The angle of repose in a dry state was found to be $\alpha_R = 34°$.

The backfilling proceeded from the surface of the ground at the edge of the excavation toward the building, as shown in Fig. 10-20, and took about four months to complete. All compaction of the sand was avoided; its unit weight after placing was estimated at $\gamma = 100$ lb per ft^3. Because of its slightly moist condition and the resulting apparent cohesion (Art. 7-4), the angle of repose during backfilling in the field was higher than in the laboratory and equaled 42°.

Taking the lowest of these values, $\phi = 34°$, we obtain, by setting the angle of wall friction equal to zero, from Eq. (7-7) the highest possible value of $K_A = 0.28$. It will, however, be noted from Fig. 10-20 that the actually observed average coefficient of earth pressure was $K = 0.42$. This value was reached a year after construction, having increased slightly, by approximately 5 per cent, during that period. The increase of pressure was presumably due to the slight increase of density of the sand by traffic vibrations and percolating rain water. Thus the pressures actually observed in this structure came very close to the at-rest values obtained for loose sand in the laboratory (Art. 10-9) and by model tests (Art. 10-14), as was to be expected for an unyielding rigid wall. The pressure distribution was essentially hydrostatic, that is, it increased linearly with depth.

10-18. Records of Full-scale Measurements of Lateral Pressures against the Bracing of Open Cuts in Sand. The results of extensive measurements performed during subway construction at Berlin and reported by Spilker (Ref. 323, 1937) are summarized in Fig. 10-21. The heavy curve *db* gives the pressure distribution determined as an average from the measurement of forces on each of the four struts in three adjoining vertical rows of struts. The horizontal distance between these rows of struts was equal to 6.6 ft. The maximum deviation of individual strut loads from the average values given in Fig. 10-21 equaled ± 30 per cent.

The straight line *A* in Fig. 10-21 indicates the officially prescribed assumptions for the design of the bracing, which were based on a unit weight of the soil $\gamma = 112$ lb per ft^3, angle of internal friction $\phi = 37°$, angle of wall friction $\delta = 0°$, a surcharge equal to the weight of 2 ft of soil (Art. 10-21). The soil was clean sand, and the ground-water level was lowered below the bottom of the excavation during the entire period of construction by means of wellpoints (Art. 14-9).

The observed parabolic distribution of lateral pressures, with reference to earlier measurements (Refs. 240 and 353), had been previously explained by Terzaghi (Ref. 356, 1936) solely on the basis of a redistribution of the lateral pressures, the total value of which was to equal the area of the Coulomb triangle for noncohesive soils (Art. 10-2). The possibility of a transfer of lateral pressures to the soil beneath the bottom of the cut due to horizontal shearing stresses at that elevation was not given any con-

sideration. This reasoning appears to have led Spilker to the conclusion that the official design assumptions were incorrect not only in the matter of the "Coulomb shape" of the pressure-distribution curve, but also in respect to the values of the physical constants of the soil. The hatched area between the measured pressure curve and the "official" pressure curve, as shown in Fig. 10-21(I), is much greater in the lower section of the cut than in the upper section. If the total pressure were to remain the same, the two hatched areas should have been equal, as shown in Fig. 10-21(II). Therefore Spilker assumed that the straight line B should represent the correct Coulomb pressures with zero surcharge, $\gamma = 106$ lb
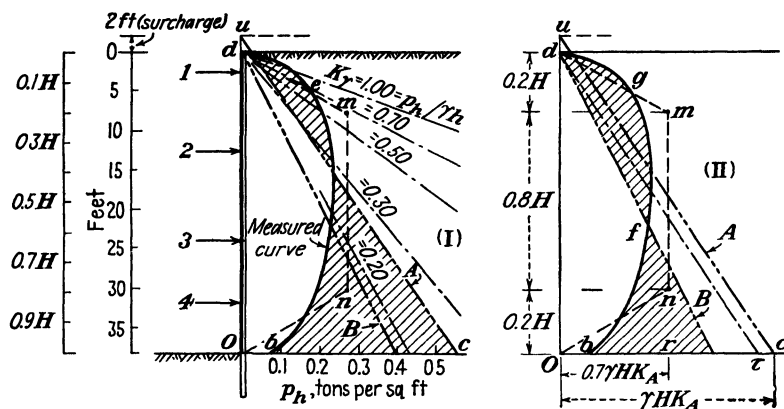
FIG. 10-21. Lateral-earth-pressure distribution determined from an average of several measured strut forces in a 39-ft-deep subway cut through sand at Berlin. (*After Spilker, Ref. 323, 1937, and Terzaghi, Ref. 360, 1941.*)

per ft³, $\phi = 37°$, and $\delta = 26°$. This, of course, is a pure guess, which neglects the restraining effects of the lower boundary. The broken line *dmno* in Fig. 10-21 represents the trapezoidal pressure distribution which Terzaghi (Ref. 360, 1941) recommended for design purposes on the strength of Spilker's measurements. The distance *Or* of the trapezoid was then set at 0.7 of the Coulomb value *Oc*. In later publications Terzaghi (Ref. 365, 1948) recommended increasing of the distance *Or* to 0.8 of *Oc*, presumably to take into account the recorded 30 per cent deviation, as compared with the average curve shown in Fig. 10-21, of the forces acting against individual struts.

At about the same time, similar measurements were performed in New York on the Sixth Avenue Subway and were reported by White and Prentis (Ref. 429, 1940), as shown in Fig. 10-22, for a 120-ft-long cut in sand. Here again higher lateral pressures, which exceeded values corresponding to $K_\gamma = 1.00$, were measured against the upper half of the brac-

ing of the excavation, thus indicating that a redistribution of pressures was the most important of the factors producing the observed shape of the pressure-distribution curve. But it was not possible to determine to what extent the secondary but not negligible restraining effects at the lower boundary were active, since the exact "Coulomb line" is not known.
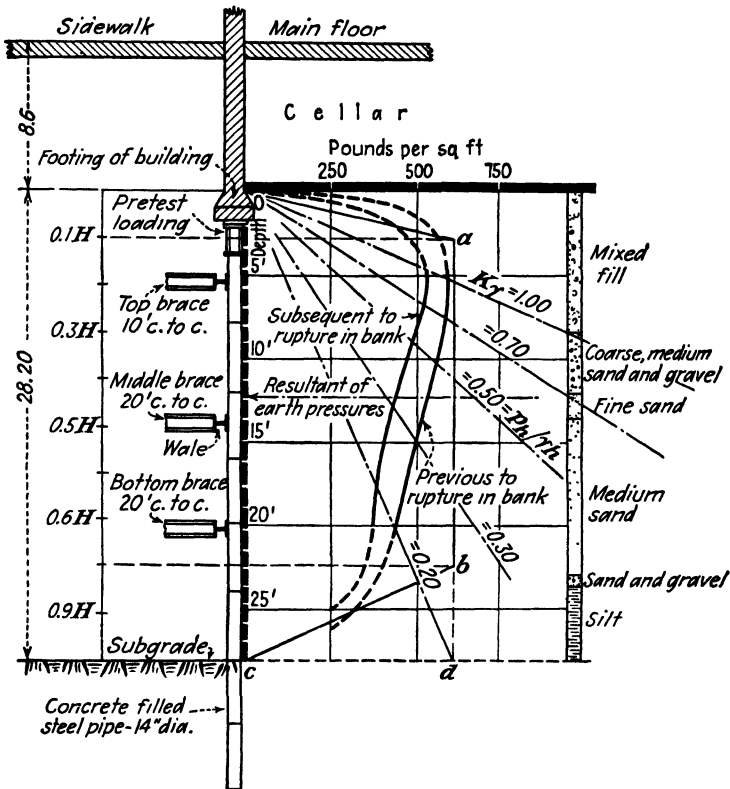
FIG. 10-22. Hydraulically measured lateral earth pressures against braces of subway excavation at Sixth Avenue and 16th Street, New York City. (*After White and Prentis, Ref. 429, 1940—the lines of the hydrostatic pressure ratio K have been superimposed on the original drawing.*)

The trapezoidal pressure line *oabc* shown in Fig. 10-22 represents the diagram suggested by Tschebotarioff (see Art. 16-4) for the design of the bracing of excavations in sand, as a simplification of Terzaghi's original proposals on the matter.

10-19. Difference between True Arching and the Transfer of Pressures by Shear. Terzaghi's General Wedge Theory. It should be noted that the term "arching" is ambiguous since it is sometimes used (Ref. 365) whenever shearing stresses between soil elements transfer pressures

from one part of a bulkhead to another (see Figs. 10-16 and 10-23). Actually the terms "arching" and "transfer of pressures by shear stresses" are *not* synonymous. Arching does involve some transfer of pressures by shear, but pressures can be transferred by shear without any arching being involved. In this book the use of the term "arching" will be limited to conditions where the redistribution of horizontal pressures occurs because of the transfer of either vertical or horizontal pressures toward two more rigid boundaries, since an arch must have two abutments. There is no such thing as a cantilever arch of uncemented grains. For this reason the term "arching" will *not* be applied to the transfer of
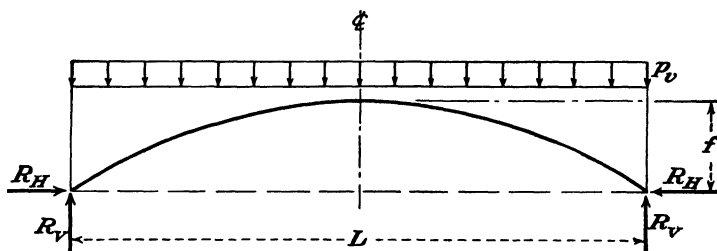
FIG. 10-23. Diagram illustrating the relationship between the dimensions and the forces acting on a true arch.

lateral pressures to the soil beneath the dredge level [see Art. 10-23 and Figs. 10-40 and 10-24(I)] and to similar phenomena.

In a true arch of parabolic shape (Fig. 10-23) the following general relationships hold, according to conventional structural theory: For a uniformly distributed vertical unit load p_v, the vertical reaction is

$$R_v = \frac{p_v L}{2} \tag{10-33a}$$

The horizontal reaction is

$$R_h = \frac{p_v L^2}{8f} \tag{10-33b}$$

If the vertical reaction is to be supported by friction only, then

$$R_v = R_h \tan \phi \tag{10-33c}$$

For $\phi = 30°$, by substituting $\tan \phi = 0.577$ and the values of R_v and R_h from Eqs. (10-33*a*) and (10-33*b*) in Eq. (10-33*c*) and solving for f, we obtain

$$f = 0.15L \tag{10-33d}$$

Thus a relatively flat, horizontal arch may support its own weight by friction at its abutments, provided the grains are *hard* and are really

tightly wedged to form an arch, and provided the two abutments do not yield.

Let us now assume that one of the successive horizontal arches, located at a depth z below the soil surface, has a cross section of unity and carries its own weight only. In that case $p_v = \gamma \times 1.0^3$ and, with $f = 0.15L$,

$$p_h = \frac{R_h}{1.0^2} = \frac{1.0^3\gamma L^2}{8 \times 0.15L \times 1.0^2} = 0.835\gamma L$$

According to Fig. 10-16(II), we can assume, as a maximum value, $L = 0.4H$, where H is the full depth of the cut, so that at an intermediate depth z,

$$p_h = 0.333\gamma H \qquad \text{(constant!)}$$

The hydrostatic earth pressure ratio K_γ, expressed in terms of the weight of the overburden γz, will be

$$K_\gamma = \frac{p_h}{\gamma z} = 0.333\,\frac{H}{z} \tag{10-33e}$$

Thus, at a depth $z = 0.10H$, $K_\gamma = 3.33$; if $z = 0.20H$, $K_\gamma = 1.66$; if $z = 0.333H$, $K_\gamma = 1.00$. Actual observations on cuts in sand (see Fig. 10-22), however, show lesser pressures at these elevations. Thus $K_\gamma = 1.00$ at a depth $z = 0.20H$. This indicates that horizontal arching in the case of cuts in sand does not reach its maximum possible value. Some compression of the sand and readjustment of its grains has to take place before horizontal arching develops fully. Part of the vertical load is transmitted to the lower layers, where the yield of the supports is greater, and the arching is therefore less effective. All this accounts for the smaller K_γ values at the top of the cut and the smaller rate of their observed decrease as compared with Eq. (10-33*e*), which is valid only for full effectiveness of horizontal arching.

The preceding analysis by Tschebotarioff (Ref. 399, 1950) nevertheless shows that true arching, as opposed to load transfer by vertical shear (Fig. 10-47), may better explain the observed shape of the lateral-pressure curves *agehf* in cuts in sand [Fig. 10-24(II)] where only a very small transfer of lateral pressures occurs because of shearing stresses between horizontal slices of the soil [see Fig. 10-24(*C*)]. A mathematical method of analysis proposed by Hertwig (Ref. 172, 1939), based on the latter type of load transfer, therefore appears to have only an abstract theoretical value. The application of the *general wedge theory* of Terzaghi (Ref. 360, 1941) requires an arbitrary assumption concerning the elevation of the resultant lateral earth pressure. Assumptions on that point have to be based on field observations. It therefore appears more logical to base the entire analysis on such observations (see Art. 16-4).

Attempts of the above type to obtain rigorous or semirigorous solutions of the problem are all liable to founder in practice because of the present impossibility to differentiate numerically between the three possible causes of redistribution of lateral pressures: (*a*) true horizontal arching [Figs. 10-16(II) and 10-23], which relieves the vertical pressures at lower elevations; (*b*) horizontal shearing stresses which redistribute lateral pressures along the height of the retaining structure [Fig. 10-24(II)]; (*c*) horizontal shearing stresses which transfer lateral pressures to the underlying soil [Fig. 10-24(I)]. The first cause (*a*) is likely to predominate in sands, since their grains are hard enough to wedge themselves against each other to form an arch in the true sense of the word. Anyone who has
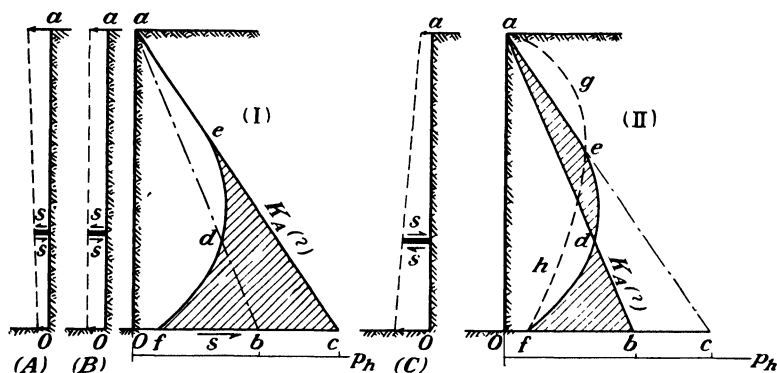
FIG. 10-24. Two possible causes of the observed shape of lateral-earth-pressure curves in cuts through plastic clay.

tried to push soil out of a sampling tube knows that it is almost impossible to do so, no matter how high pressures are applied, if the soil is sand; on the other hand, relatively light pressures can push clay out of such a tube. Therefore it is probable that the two types of pressure transfer by horizontal shearing stresses, as listed above under (*b*) and (*c*), and not arching, will predominate in clays.

10-20. Records of Full-scale Measurements of Lateral Pressures against the Bracing of Open Cuts in Clay. Figure 10-24 illustrates the difficulty of accurately interpreting the causes of the observed shape of curves of lateral pressures against the bracing of cuts through clay. As explained in Art. 10-18, for cuts in sand the shape of observed curves, such as *agehf* in Fig. 10-24(II), can be reasonably ascribed to a redistribution of pressures due to horizontal arching, since the values in the upper zone of the curves exceeded the known K_A (active pressure) or even K_n (at-rest pressure) of sand. In the case of cuts through clay the matter takes on a different aspect. First of all, there is still some uncertainty

concerning the exact values of the active pressures and of the corresponding K_A values of undisturbed natural clays. Second, the slope of the measured pressures against the braces of cuts through clay (curve *aedf*) does not seem to exceed the value of $K = 0.50$, and this value appears to correspond closely both to the active and to the neutral pressures of not overconsolidated natural clays (Art. 10-9). Therefore it cannot yet be definitely said whether the redistribution of pressures within the sliding wedge, as shown in Fig. 10-24(II), or the transfer of pressures to the soil beneath the bottom of the cut by shearing stresses along that boundary, as shown in Fig. 10-24(I), is responsible in all cases of clay soils for the observed shape of the curve of lateral pressures. It appears probable that for reconsolidated clays of a nonbrittle type (Fig. 7-14) the explanation presented in Fig. 10-24(I) is the more likely one if the wall displacements are as shown in Fig. 10-24(*C*). The redistribution of pressures indicated in Fig. 10-24(II) is most unlikely if the wall motion is of the type shown in Fig. 10-24(*A*) or (*B*).

One of the first known series of extensive measurements of lateral pressures against the timbering of open cuts through plastic clay were performed during the construction of the Chicago subways and were reported by R. B. Peck (Ref. 260, 1943). Figure 10-25 gives a typical result of these measurements (for contract S-1A). Of particular interest is the observation according to which an appreciable inward displacement of the MZ38 sheet piling (Art. 15-11) took place on January 3, 1941, when the depth of excavation had reached only 12 ft. The ground next to the sheet piling had been excavated down to a depth of 8 ft and had not yet been backfilled, thus the lateral displacement of the sheet piling was induced by deep-seated movements of the clay toward the excavation, as evidenced by cracks in the old freight tunnel far beneath it. The point is of importance in connection with all excavation problems (Art. 14-6).

The clay at Chicago is of glacial origin and was found to range from a soft consistency with an unconfined compressive strength of $q_u = 0.3$ ton per ft^2, a natural water content of $w_n = 50$ per cent, a liquid limit $w_L = 55$ per cent, and a plasticity index $I_p = 35$ per cent, to a stiff consistency with $q_u = 0.7$ ton per ft^2, $w_n = 22$ per cent, $w_L = 32$ per cent, and $I_p = 12$ per cent (Ref. 260). A layer of sand overlay the clay in most places.

Peck attempted to relate the measured lateral pressures to the shearing strength of the clay at failure, as determined from unconfined compressive-strength tests. Terzaghi (Ref. 361) made the assumptions on which that analysis was based. A correction factor (which changed q_u to q_a) was introduced to take care of the presence of sand layers above the clay. A trapezoidal pressure diagram, similar to the one proposed earlier by

Terzaghi and shown in Fig. 10-21 for sands, was suggested for design purposes on the basis of the field measurements, good agreement with which was claimed (Ref. 260).

The highest possible value of lateral pressures, according to that diagram, was stated to be

$$p_h = \gamma H K_a \tag{10-34}$$

where H is the total depth of the cut and

$$K_a = 1 - \frac{2q_a}{\gamma H} \tag{10-35}$$

It is to be noted that the value of K_a, as expressed by the Terzaghi-Peck equation (10-35), is based on the total pressure E_A, that is, it can be obtained from Eq. (10-16) by setting the angle of internal friction $\phi = 0$ and dividing the remaining values by the total fluid pressure $\gamma H^2/2$. A different expression, and a smaller value of K, as compared with those based on unit pressures, is obtained thereby [see Eq. (10-11)]. The difference is caused by the fact that Eq. (10-16) for the total pressure E_A, as explained in Art. 10-4 and illustrated by Fig. 10-2(I), assumes that tension between the piling and the clay is fully active in the upper soil layers. On the other hand, Eq. (10-11), which is based on unit pressures, will give positive values of K only below the depth of the tensile zone [Eq. (10-18)]. The use of the total Rankine-Résal pressures for the computation of the K values, as introduced by Terzaghi and Peck and expressed by Eq. (10-35), represents a departure from many previous concepts of the matter, for instance, from those of Cain (Art. 10-4), expressed by Eq. (10-20). Cain's views, however, appear to be more rational, since the bond between soil and wall usually cannot resist tension.

Terzaghi and Peck (Ref. 260, 1943) combined the Rankine-Résal equation (10-19) with procedures based on Terzaghi's general wedge theory (Ref. 360), although only two years earlier (Ref. 360, 1941) Terzaghi had specifically excluded this theory "from application to the pressure of soft clay or other highly elastic types of soil on the timbering of cuts or of tunnels." No reference was made to that earlier limitation when advancing the new assumptions. In addition, the statement was made (Ref. 260), concerning the Chicago measurements, that "it is unlikely that important arching in the horizontal direction will develop," although the redistribution of pressures given by Terzaghi's general wedge theory is mainly based on arching in a horizontal direction, as shown in Figs. 10-16(II) and 10-21(II).

All these unexplained contradictions made Tschebotarioff surmise (Ref. 392, 1948) that the agreement, reported by Peck (Ref. 260), between
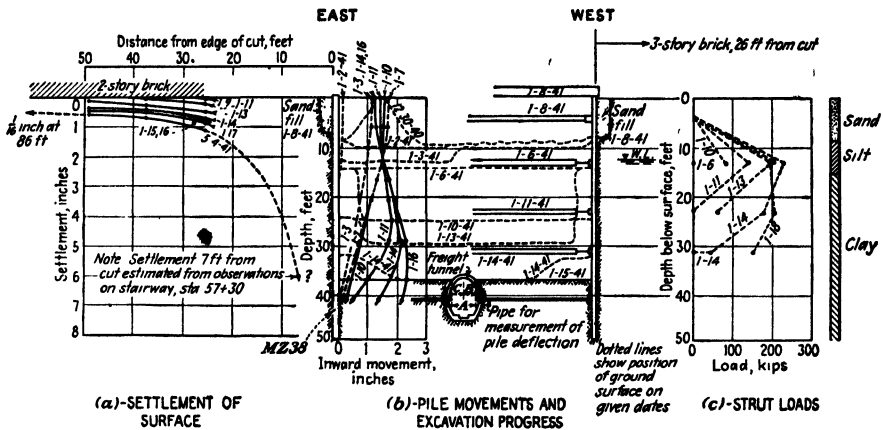
FIG. 10-25. Example of the results obtained by lateral-earth-pressure measurements on the bracing of open cuts through Chicago clay during subway construction (contract S-1A). (a) Settlement of surface. (b) Pile movements and excavation progress. (c) Strut loads. (*After R. B. Peck, Ref. 260, 1943.*)
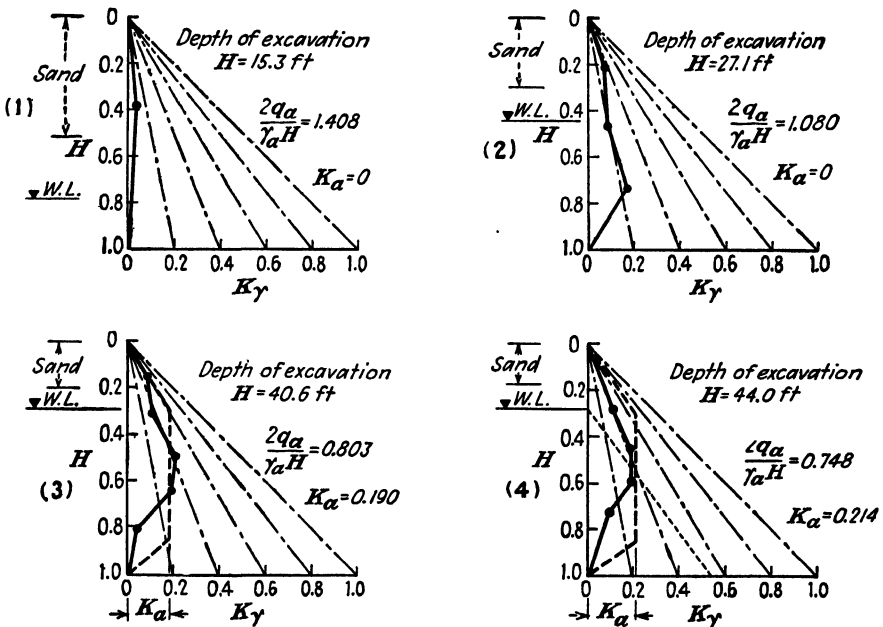
FIG. 10-26. Critical analysis by Philip Brown (Ref. 42) of R. B. Peck's equations and data from Chicago subway cuts (contract S-9c). *Note:* (1) K_a = value of hydrostatic pressure ratio computed from Eq. (10-35). (2) The actually measured strut loads are shown thus: ●.

the lateral pressures as measured in the Chicago subway cuts and as computed from Eq. (10-35) might have definite limitations. An analysis of the data given by Peck in his paper (Ref. 260) was thereupon performed by Philip Brown (Ref. 42, 1948) and confirmed this point of view. Figure 10-26 summarizes Brown's analysis. When the depth of excavation equaled $H = 15.3$ ft, the Terzaghi-Peck equation (10-35) gave a value of $K_a = 0$. Nevertheless, a definite pressure, approximately equal to $K_\gamma = 0.10$, was recorded on the single upper strut which had been placed by that time. The same discrepancy was found when the depth of excavation reached $H = 27.1$ ft. The Terzaghi-Peck equation (10-35) still gave a value of $K_a = 0$, whereas all three struts recorded definite pressures. The pressures against the upper strut, however, had increased and corresponded to a value of $K_\gamma = 0.30$. This one strut was located within the depth of the sand layer. The other two struts were located within the depth of the underlying plastic clay layer, and the pressures against them corresponded to a value of $K_\gamma = 0.20$.

FIG. 10-27. Variation with the depth of excavation H of the K_a values computed from the Terzaghi-Peck equation (10-35).

It was only when the excavation reached depths of $H = 40.6$ ft and $H = 44.0$ ft, the latter value being the greatest on that particular job, that approximate agreement was obtained between values based on Eq. (10-35) and the actually measured pressures. Down to approximately one-half of the depth H the lateral pressures approximately followed the line $K_\gamma = 0.45$; farther on they decreased. The thick broken lines in Fig. 10-26 indicate the trapezoidal pressure distribution recommended by Peck for design purposes (Art. 16-5) and illustrated by Fig. 16-11.

The K_a values obtained from Eq. (10-35) are plotted in Fig. 10-27 against the depth H of the excavation for three values of the unconfined compressive strength: $q_u = 0.5$ ton per ft^2, $q_u = 0.7$ ton per ft^2; and $q_u = 1.0$ ton per ft^2, all for a unit weight $\gamma = 120$ lb per ft^3. It will be noted that down to depths of 34 to 66 ft, respectively, the K_a values thus obtained are smaller than the maximum value $K_n = 0.50$ expected for the at-rest pressures, and hence for the active pressures, of clays (Art. 10-9). At greater depths the Peck K_a values continue to increase and exceed appreciably the maximum likely at-rest value of 0.50. Since the

analysis given in Fig. 10-26 by Brown indicated, for depths smaller than 40 ft, greater pressures of the Chicago clay than the ones obtained from Eq. (10-35), it appeared likely that at greater depths this trend would be reversed. This was later found to be the case, according to a letter of May 28, 1949, to Tschebotarioff from Peck, when the measured pressures in a new 65-ft-deep cut at Chicago were found to be smaller than those expected on the basis of Eq. (10-35).

The same general trends were recorded during the construction of the approaches to the tunnel under the river Maas at Rotterdam in the Netherlands. These measurements were performed in 1939 to 1940, that is, earlier than the ones at Chicago, but because of the war only a very brief outline thereof was published in Holland by van Bruggen (Ref. 44) in 1941. Figures 10-28 and 10-29 summarize some of the results of these very extensive studies. These diagrams are based on detailed records sent to Tschebotarioff through the courtesy of van Bruggen (Ref. 46, 1949) and reveal the same trends as did later independent investigations at Princeton University (1943 to 1948) (Arts. 10-9 and 10-23).

Before comparing the results of the Chicago and Rotterdam measurements, it should first be noted that the Chicago K values plotted in Fig. 10-26 probably should be considered as K_s values in the sense of Art. 10-13, that is, they refer to intergranular pressures caused by the combined weights of the soil solids and of the water in the voids, in spite of the fact that the water level, as shown in Fig. 10-26, according to Peck's paper (Ref. 260) was quite high. The entire problem of the effect of seepage pressures had been originally left out of consideration in Eq. (10-35). The distance between the source of free-water supply (the Chicago River) and the open cuts appears to have been considerable (Ref. 361) and to have exceeded 2,000 ft in the case of the cut illustrated in Fig. 10-25. Therefore the hydraulic gradient (Art. 5-1) should have been very small and approximately equal to 32/2,000 = 0.016, provided sufficient leakage and/or evaporation was possible through the sheeting into the cut to prevent the building up against it of full hydrostatic pressure (see Art. 14-10). The leakage was apparently sufficient, since otherwise, according to Fig. 10-12, the full water pressure alone ($K_s = 0.00$) would have given a K_{s+w} value of 0.55 and the corresponding dotted pressure line in Fig. 10-26(4). With an unhindered flow of water toward the open cut, an approximate pressure of only 32(50/2,000) = 0.8 ft of water would be transmitted to the soil skeleton within a horizontal distance of 50 ft from the edge of the cut. Thus it could well be neglected.

Conditions in this and in other respects were different at Rotterdam. The tunnel itself was built by the trench method (Art. 16-19) between two ventilation towers (Ref. 45) founded on compressed air caissons (Art.

15-14). The approaches to these towers were constructed in open cuts, as shown for the left-bank approach in Fig. 10-29(II). It should, however, be noted that the cut, shown in that diagram for purposes of convenience as approaching the tower at right angles to the river, actually ran in a curve approximately parallel to it at a distance of some 300 ft. The general construction procedure is illustrated by Fig. 16-13 and was as follows: First the 14 ft of soil above the water level (± 0.00) was excavated by shovels in a wide unbraced trench with $1:1\frac{1}{2}$ slopes at its edges.
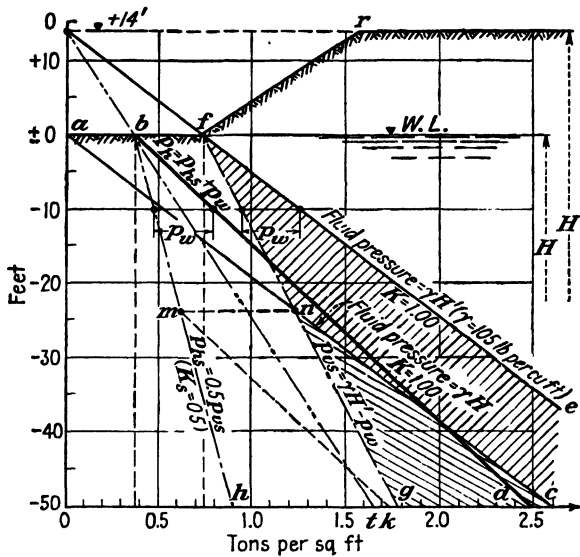
FIG. 10-28. Diagram illustrating the assumptions concerning the lateral pressures of soft clay and peat on which were based the design computations for the bracing of the open cuts on the approaches to the Maas River Tunnel at Rotterdam, Holland. Compare with Fig. 10-29. (*After J. P. van Bruggen, Ref. 44, 1941, and Ref. 46, 1949.*)

Then cast-in-place concrete piles (Art. 15-7) were driven to the sand layer at -66 ft to provide a support for the future concrete tunnel, and Larsen IV (new) steel sheet piles (Art. 15-11) were driven into the sand on both sides of the future cut to prevent squeezing of the overlying soft clay and peat into the cut. For the same purpose wellpoints (Art. 14-9) were driven into the sand along the edge of the cut. They relieved any uplift pressures of the water against the clay plug which remained in place between the bottom of the excavation and the surface of the sand layer by continuous pumping. As the excavation proceeded, successive steel struts were placed in position. Control measurements of all strut forces, during both the excavation and the concreting of the tunnel, were performed at ten locations, *aa* to *ll*, shown in Fig. 10-29(II).
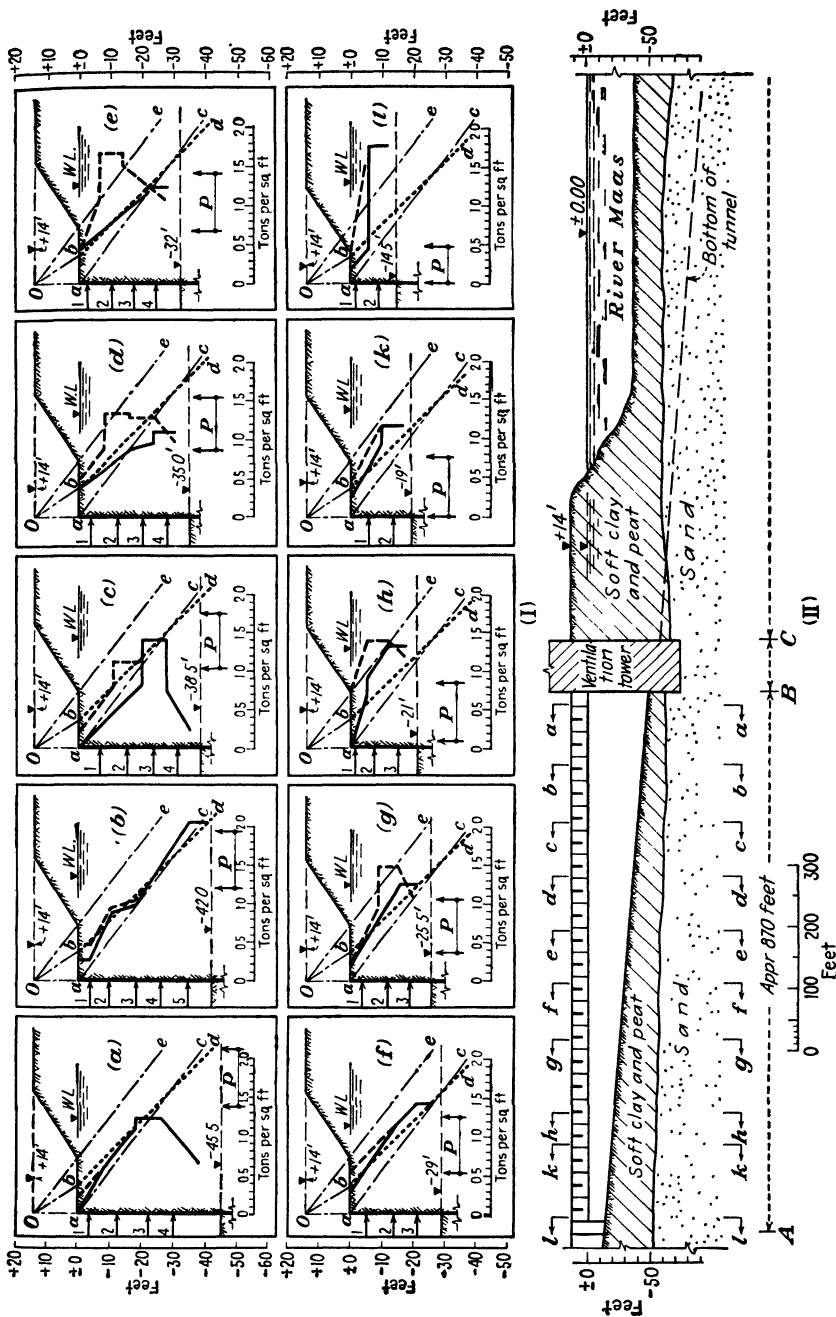
FIG. 10-29. Results of lateral-earth-pressure measurements on braces of open cut through soft clay and peat on left-bank approach to the tunnel under the river Maas at Rotterdam, Holland. (After J. P. van Bruggen, Ref. 44, 1941, and Ref. 46, 1949.)

The layers of soft clay and peat which overlay the sand above elevation −66 ft were found to have an extremely varied composition. Closer to the surface a few of the stiffer and sandier clay samples had a natural water content $w_n = 27$ per cent, a liquid limit $w_L = 57$ per cent, and a plasticity index $I_p = 28$ per cent. The majority of the samples, however, had higher values, ranging up to $w_n = 62$ per cent, $w_L = 109$ per cent, and $I_p = 62$ per cent. One of the peat samples had $w_n = 190$ per cent, $w_L = 247$ per cent, and $I_p = 70$ per cent. Strength tests were performed by the cell method (Art. 7-11), and the values obtained thereby indicated that the approximate corresponding unconfined compressive strength would be of the order of magnitude of $q_u = 0.50$ ton per ft^2.

Nevertheless, the Dutch engineers did not base the design of the bracing of their cut on the ultimate-strength characteristics of the surrounding soil. Instead they based it on the observed fact that in the cell tests the active and the neutral lateral pressures of cohesive soils were found to be approximately equal (Art. 10-11) and, in a consolidated condition, did not exceed values corresponding to $K_s = 0.50$. The following design assumptions were therefore made (Ref. 44): The intergranular lateral pressures are equal to one-half of the corresponding vertical pressures and are not decreased by the removal of part of the original overburden which results from the excavation down to ± 0.00. In addition to the intergranular lateral soil pressures, the full water pressure will act against the sheet piling. The pressure distribution obtained on the strength of these assumptions is indicated by the thick line *bd* in Figs. 10-28 and 10-29.

The question may be raised whether the assumption of full lateral water pressure is not too unfavorable, since wellpoints relieved the uplift in the underlying sand layer. The following analysis, illustrated by Fig. 10-28, will show that the action of the wellpoints introduced another factor which had the same effect.

Assuming that the soil above elevation ± 0.00 is fully saturated by capillarity, the line *Ofe* in Fig. 10-28 will give the values of the fluid pressure, that is, of the vertical pressure due to the combined weight of the soil solids and of the water in the voids, prior to the excavation of the trench. If we subtract from the line *Ofe* the water pressure p_w, the line *Ofng* will be obtained, which will correspond to the vertical intergranular soil pressures p_{vs} in the original condition, under which pressures the soil is fully consolidated. The line *Obmh* will give the corresponding lateral intergranular soil pressures p_{hs}, equal to one-half of p_{vs}.

As a result of the pumping of water from the underlying sand layer by means of wellpoints the uplift is neutralized, and the full fluid pressure will become effective. Immediately next to the sheet-pile wall, that is, beneath the point *a* in Fig. 10-28, the vertical fluid pressure will be repre-

sented by the line *anc*, and the hatched triangle *ngc* will represent the vertical pressures in excess of the original intergranular pressures *Ofng* which correspond to a state of completed consolidation under the original weight of the overburden. Until further consolidation occurs, these excess pressures *ngc* will be carried by the water in the voids of the soil and will be transmitted laterally without any reduction. The line *bmk* will then represent the lateral pressures at that initial pumping stage. It would be fully valid if the excavation down to the elevation ± 0.00 were extended to an appreciable distance from the sheet piling. Since this was not the case, a different condition will prevail along a vertical plane through the point *r* at the top of the slope. The hatched triangle *efng* will then represent the vertical pressures in excess of the original intergranular pressures *Ofng*. Prior to further consolidation they will be transmitted laterally without any reduction, and the line *Obd* will represent the lateral pressures beneath the point *r* at the initial stage of pumping. Since the amount of lateral pressure which can be transmitted to the underlying clay by shear cannot yet be estimated, it is advisable to assume that the full lateral pressures beneath the water level and the point *r* will be transmitted to the sheet piling. The line *bd* is then obtained, which is identical with the line used by the Dutch engineers for their original design. The line *bt* would correspond to the lateral pressures after full consolidation.

As pumping continued during the several months of construction, consolidation of the clay was bound to develop under the additional vertical pressures imposed by the neutralization of the water uplift. That this actually did occur was shown by the settlements of the soil surface in the vicinity, which were measured during the construction operations and were found to be a function of the water-level lowering (Fig. 13-26).

Figure 10-29 gives a graphical comparison of the lateral pressures, as actually measured against the struts at the ten locations *aa* to *ll*, with the design pressure line *bd* and with the fluid pressure lines *ac* and *Oe*. The full thick lines indicate the pressure distribution as measured when the deepest point of the excavation was reached; on the whole they agree fairly closely with the design line *bd*, which is shown dotted. The dashed lines indicate the maximum pressures measured at any construction stage against the individual struts. It will be noted that occasionally these peak values exceeded even the maximum possible fluid pressures given by the line *Oe*. Almost without exception, these high peak values were measured during the concreting of the tunnel immediately after removal of the underlying strut. Presumably the concrete adjoining the sheet piling yielded somewhat before taking up the load previously carried by the strut which had been removed, and this transferred an additional load to

the next strut above. It does not appear necessary to take this possibility into consideration when designing the struts, since the overloading occurs for a very short while only and can be taken care of by the usual factors of safety present in structural-steel members. But it does not appear advisable to reduce these factors of safety appreciably under similar circumstances.

The two vertical arrows with the letter P on the connecting line between them indicate the design pressures which would have been obtained from the Terzaghi-Peck equation (10-35), based on an unconfined compressive strength $q_u = 0.50$ ton per ft^2 and a unit weight of $\gamma = 105$ lb per ft^3. The arrow on the left corresponds to the H next to the sheet piling, and the one on the right to the value of H' up to the level of the natural ground. It will be noted that the same trend is observed here as was brought out by Brown (Ref. 42) in Fig. 10-26 for the Chicago measurements. Equation (10-35) gives unsafe values of lateral pressures for depths of excavation smaller than 34 ft (compare with Fig. 10-27), and leads to uneconomical designs for greater depths.

The determination of lateral pressures exerted by clays appears to be primarily a problem of deformations and not of rupture (Ref. 387). It is therefore not surprising that equations, such as Eq. (10-35), which are based on the strength of clays at failure do not correspond to observations made under a wide variety of conditions. A new approach to the whole question, along the lines used by the Dutch engineers for the Rotterdam tunnel and determined experimentally during the tests at Princeton University, appears necessary (Art. 10-23). It is based on definite values of the coefficient of earth pressure at rest (Arts. 10-9 and 10-12), and the observed fact that the active lateral pressures of plastic clays are no smaller than their pressures at rest (Art. 10-11). The measurements on the Chicago subway cuts have even shown that induced expansion of the clay had an effect which was the reverse of the one to be expected on the basis of conventional stress-strain concepts (Art. 10-11). A yield of the bracing in excess of 1 per cent of the height of the cut was found to increase the lateral pressures (Ref. 260) of the clay, instead of decreasing them. This is to be attributed to a remolding of the natural undisturbed clay by such expansion, to the resulting breakdown of its brittle structure (Art. 4-1), to the tendency for additional consolidation as a result of this remolding, and to the temporary transfer of part of the weight of the overburden to the pore water, with a corresponding temporary increase of the earth pressure coefficient beyond its at-rest value of $K_n = 0.50$.

Figure 10-30 illustrates the results of measurements of lateral pressures performed on the bracing of a cut next to an inadequate retaining wall of the gravity type in London, reported by Cooling (Ref. 85, 1946) and

Golder (Ref. 157, 1948). The old retaining wall had been built in 1901 to 1902 and was found to move outward. Some buttresses were added but did not stop the movement. It was then decided to strengthen it by digging a trench behind it, as shown in Fig. 10-30, in sections, and then filling the trench with concrete, anchored by steel tie rods to the old wall. As the trench was dug, measurements were performed on the timber struts. Preliminary calibrations of the selected struts in the laboratory indicated that compressive strains of the wood could give fairly accurate values of the loads applied, provided they were measured over a 5-ft gage
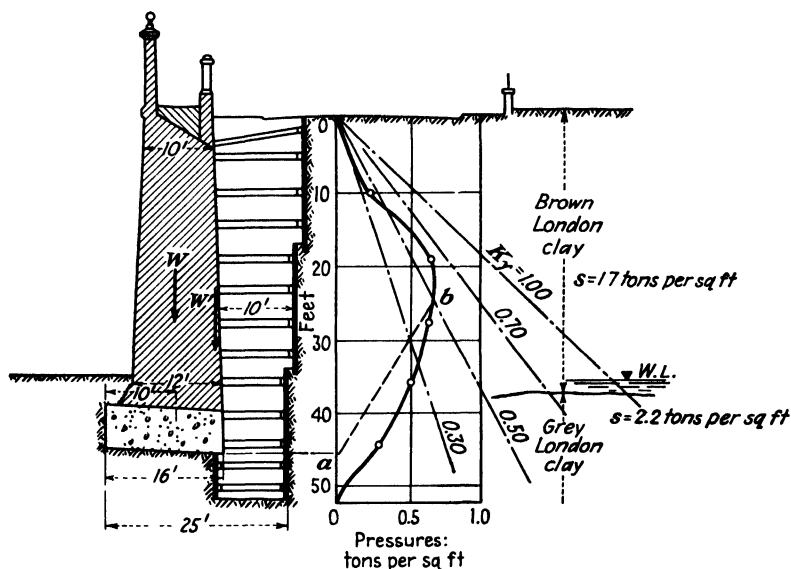
FIG. 10-30. Observations of earth pressure for distribution on timbering of a 52-ft-deep cut in stiff-fissured London clay. (*After Cooling, Ref. 85, and Golder, Ref. 157—the lines of the hydrostatic pressure ratio K have been superimposed on original drawing.*)

length to 0.01 mm, using special metal points screwed into the interior of the wood through a shallow recess subsequently filled with wax. This and other techniques eliminated the otherwise considerable effect of the surface strains of the wood, which are caused by moisture changes (Ref. 157).

The clay behind the wall was of the stiff-fissured or slickensided type, overconsolidated during its past geological history (Art. 2-5). As stated by Golder (Ref. 157), "the behaviour of the London clay in stability problems is usually controlled by the strength, not of the mass of clay, but of the clay surfaces exposed in the fissures." This is typical of other clays of this kind (Art. 8-15). According to Eq. (8-10), a vertical bank in the weakest layer encountered (s = 1.7 tons per ft^2, γ = 120 lb per ft^3) in the

cut shown in Fig. 10-30 should have been able to stand unsupported up to a height of $(2.58 \times 1.7)/0.06 = 73$ ft. Nevertheless, definite lateral pressures exerted by that clay were measured at a depth of excavation of only 52 ft. The intensity of the lateral pressures was found to vary in different sections of the trench with the time of the year. It was smallest during the dry summer months. Figure 10-30 shows the maximum values which were recorded in a section built during December, January, and February, when it was reasonable to assume that the fissures of the overconsolidated clay had been soaked with water and, as a result, were filled with softer clay, the water content of which was likely to have increased to the point corresponding to the water content of semifluid clay consolidated under the weight of the existing overburden. In this connection it is interesting to note from Fig. 10-30 that down to one-half of the depth of excavation the lateral pressures approximately follow the line $K_\gamma = 0.50$, they decrease from there on (compare with Fig. 10-42, curve B).

10-21. Surcharge Effects. Spangler's Tests with Concentrated Loads. It is customary to express a surcharge uniformly distributed on the surface of the soil next to a retaining structure in terms of the weight of an additional layer of soil of the same kind as that beneath the surface. Thus, in the case of the Berlin subway cuts illustrated in Fig. 10-21, the official specifications called for consideration by the designers of a uniform surcharge of 600 kg per m^2 (=123 lb per ft^2). Dividing the latter value by the unit weight of the soil, which in that case equaled $\gamma = 112$ lb per ft^3, we obtain a height of $h_s = 1.1$ ft of soil as the equivalent of the surcharge. As shown in Fig. 10-21(II), the resulting lateral pressures are given by the line uc, which is parallel to the line df of the pressures caused by the weight of the soil itself without considering the effects of the surcharge. The difference between these two lines represents the lateral pressures p_{hs} caused by the surcharge:

$$p_{hs} = h_s \gamma K_A \tag{10-36}$$

The distribution of lateral surcharge pressures is then represented by a rectangle.

An experimental investigation of the effect of a concentrated surcharge load was performed by Spangler at the Iowa Engineering Experiment Station (Refs. 318 and 319, 1938). A 6-ft-high model reinforced-concrete wall was used for the purpose. It was backfilled with pit-run gravel, 13 per cent of which was from ½ to 1½ in. in size, and another 13 per cent passed the 100-mesh sieve. The remainder was sand of intermediate size. The plasticity index was $I_p = 4$ per cent. The concentrated loads were applied to the backfill surface through the wheels of a

loaded truck, which was backed to the desired position. No wall displacements were measured.

The lateral pressures were measured by means of stainless-steel friction-ribbon assemblies, each of which had only 6 in². of contact area with the soil. Thus the scattering of measured results which is to be expected when individual pressure cells are used (see Fig. 10-19), was greatly accentuated, as shown in Fig. 10-31, because of the small size of these pressure-measuring devices and because of their general characteristics.
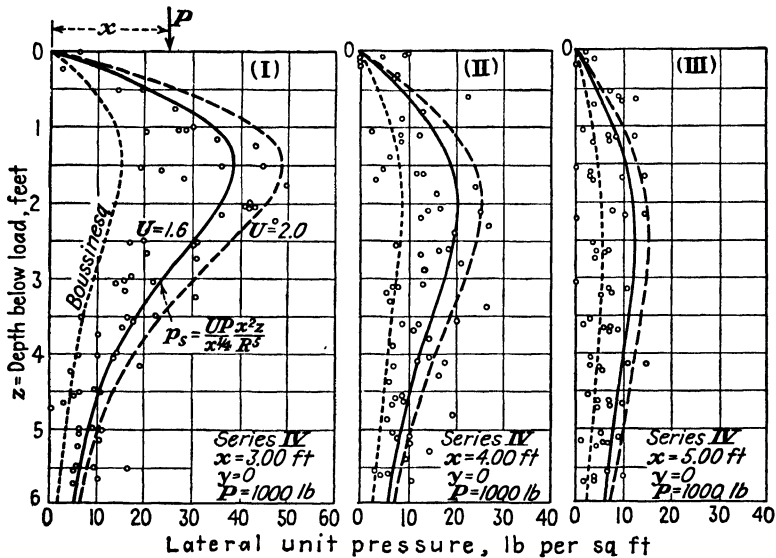
FIG. 10-31. Distribution of lateral pressures against a model concrete retaining wall, as caused by concentrated surface loads and measured by steel friction ribbons. (*After M. G. Spangler, Refs.* 318 *and* 319, 1938.)

It will be noted from Fig. 10-31 that the difference between the maximum and minimum pressures measured at the same elevation frequently exceeded 100 per cent of the smaller values.

Spangler (Ref. 319) set up the following empirical equation to express his measured lateral earth pressure values:

$$\sigma_x = \frac{UPx^2z}{x^nR^5} \tag{10-37}$$

where U and n are empirical constants and the remaining terms have the significance illustrated by Fig. 10-32. The two curves shown in Fig. 10-31 were drawn for a value of $n = \frac{1}{4}$ and for the values of $U = 1.6$ and $U = 2.0$, respectively. All these values appear to be arbitrary. A curve stated to represent the Boussinesq distribution is also given in Fig. 10-31.

Presumably the value of the Poisson ratio was taken at $\nu = 0.5$, since only in that case the general Boussinesq equation (9-5) for lateral earth pressures would be simplified to the expression referred to by Spangler:

$$\sigma_x = \frac{P}{2\pi} 3r^2z(r^2 + z^2)^{-5/2} \qquad (10\text{-}38)$$

where $(r^2 + z^2)^{1/2} = R$, as shown in Figs. 9-4 and 10-32 (where $x = r$).

The choice of the maximum possible value of $\nu = 0.5$ is equivalent to the assumption that the soil is entirely incompressible. Smaller and more likely values of the Poisson ratio ν, according to Eq. (9-5), would give somewhat smaller values of the lateral pressure σ_x. Nevertheless, the Boussinesq pressure distribution shown in Fig. 10-31 for a value of $\nu = 0.5$, according to Spangler, was found to be two to three times smaller than the actually measured values. Spangler correctly attributed this circumstance (Ref. 319) to the restraint of lateral soil displacements which was imposed by the rigid wall, but unfortunately no data had been obtained concerning the actual magnitude of the wall displacements. Probably they were small, and the wall could be considered as unyielding. Under such conditions lateral pressures double the ones given by the Boussinesq equation (9-5) are to be expected, according to Weiskopf (Ref. 424, 1945).

The point is illustrated by Fig. 10-32. The application of a concentrated or linear load P to the surface of a large elastic body will cause an originally plane, vertical surface OO to deform and to take the shape indicated by the curve ab. This deformation will be prevented if the face of a rigid and unyielding wall is located along the plane OO. Exactly the same condition of zero lateral displacement along the vertical plane OO will be produced by the action of a so-called *reflected load* P', that is, of an imaginary load of exactly the same magnitude and distance x from OO as the load P. This imaginary load P' will induce lateral pressures σ_x' against the vertical plane OO which will be equal to the lateral pressures σ_x exerted by the actual load P on that plane in the unrestrained mass of soil. Therefore the actual lateral pressure against an unyielding rigid wall would be equal to

$$\sigma_x'' = \sigma_x + \sigma_x' = 2\sigma_x \qquad (10\text{-}39)$$

where σ_x is defined by Eq. (10-38).

An examination of Fig. 10-31 shows that, when $x = 0.5H$ (case I), a curve of lateral pressures, according to Eq. (10-39), equal to twice the Boussinesq values for $\nu = 0.5$ and Eq. (10-38), would very closely correspond to the measured values, in fact equally well as the first empirical curve given by Spangler, since the scattering of these values is so great

that inherent defects of the type of instrumentation used are indicated, and precise evaluations are not possible. On the other hand, when $x = 0.83H$ (case III), the original Boussinesq equation (10-38) for $\nu = 0.5$ closely corresponds to the measured values, which are much smaller than the values given by Spangler's empirical curves. An intermediate condition is observed when $x = 0.66H$ (case II). All this is entirely logical, since for larger values of x the small lateral yield of the wall, such as it was, would acquire a relatively greater importance.

The integration of the empirical equation (10-37) suggested by Spangler (Ref. 319) to obtain the effect of concentrated area loads does not appear justified, since the empirical coefficient U in that equation actually is not a constant but a function of the distance x and of the displacements y of the wall. During the Spangler tests the slight wall motion probably was of the type shown in Fig. 10-15. Until more is known concerning the effect of such displacements and of the values of the Poisson ratio ν of soils, it appears advisable to use for design purposes Ref. 248 and the definitely conservative relationship given by Eq. (10-39).
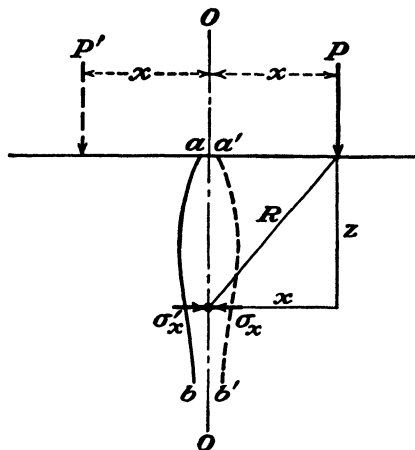
FIG. 10-32. Diagram illustrating the use of reflected loads for the computation of pressures against unyielding rigid walls according to the theory of elasticity. (After W. H. Weiskopf, Ref. 424, 1945.)

10-22. Stroyer's Tests with Model Flexible Bulkheads

Figure 10-33 illustrates the setup used by Stroyer (Ref. 330, 1933) for the purpose of checking the assumptions concerning arching in a vertical direction upon which were based the empirical rules of the Danish Society of Engineers for the design of flexible anchored sheet-pile bulkheads (Art. 16-12). These assumptions were somewhat similar to the ones advanced at a later date (1941) by Terzaghi (Ref. 360) and illustrated by Fig. 10-16(III).

A 3- by 4- by 3-ft wooden bin was used by Stroyer. It was closed at one end by a flexible sheet of metal, which was supported at the levels A and C, as shown by Fig. 10-33. An important point to be remembered is that these supports were unyielding. No actual measurements of the pressure or bending strain distribution over the metal sheet, nor of the total pressure exerted by the fill against the flexible metal sheet, were made. The only measurements taken were those of the forces which had to be applied to the overhanging ends of the flexible plate in order to counterbalance the lateral pressure of the fill. A complicated system of pulleys, illustrated in Fig. 10-33, was used, and the counterbalancing load was applied by filling a water tank H.

Stroyer found that, if the deflection of the plate during backfilling with sand was prevented by supporting it at the levels *a*, *b*, *c* (Fig. 10-33), the total bending moment required to balance the lateral pressure after the removal of these supports was much smaller—it equaled only 50 per cent—than the value needed to balance the theoretical, hydrostatically distributed earth pressures. This might have been caused in part by a decrease of these pressures, for instance, because of the restraining effect of the sloping bottom of the bin, and not by a redistribution of pressures alone. Nevertheless, possible limitations of Stroyer's findings were generally disregarded, and his tests were
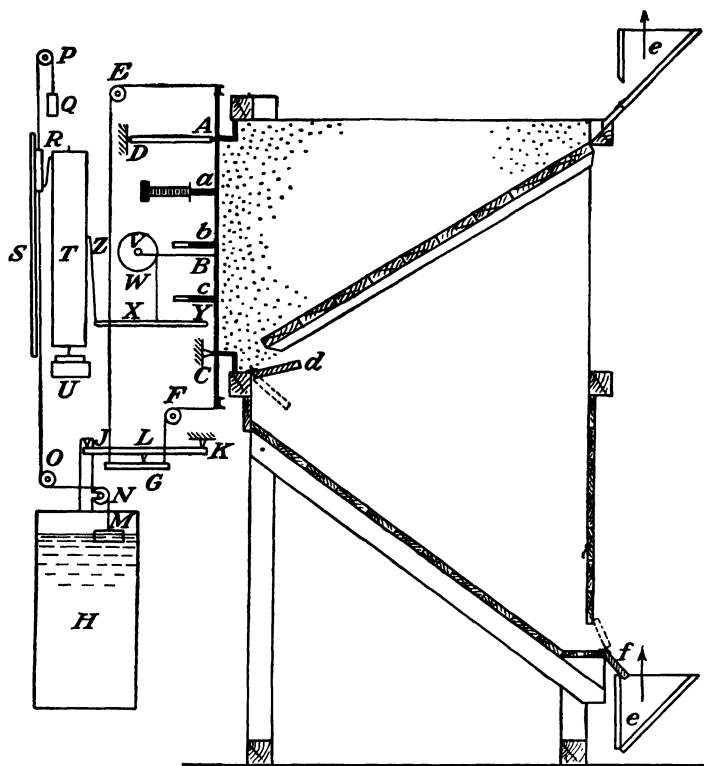
FIG. 10-33. Stroyer's 1933 setup for tests with flexible walls (Ref. 330) (vertical cross section of 3- by 4- by 3-ft bin).

taken to confirm the Danish regulations for the design of flexible bulkheads (Art. 16-12). Stroyer (Ref. 331) even gave a diagram for the reduction of bending moments in sheet-pile walls as a function of the ratio of the wall thickness to the length of the span. The diagram was taken over by some authors, for instance, by Donovan Lee (Ref. 209, 1945). Its purely hypothetical nature appeared to have been gradually forgotten.

The practical implications of a very important finding reported by Stroyer in his original paper (Ref. 330) were disregarded by him and by everybody else at that time. Stroyer found that a slight movement of the sand, induced by opening the trap door *d* (Fig. 10-33), immediately broke down the arching and created what he termed a state

of "flux." The bending moments necessary to counterbalance the lateral earth pressures against the flexible metal plate immediately increased. In the light of later experiments at Princeton University, outlined in Art. 10-23, this finding, when applied to field conditions, should have been interpreted to mean that if an abutment of a flat sand arch moves, as usually happens with all bulkheads, with the possible exception of those connected to an unyielding relieving platform (Art. 16-15) all vertical arching of the type illustrated by Fig. 10-16(III) should immediately disappear because of the collapse of the uncemented flat sand arches.

10-23. Large-scale Earth Pressure Tests with Model Flexible Bulkheads. An extensive research program was carried out at Princeton in
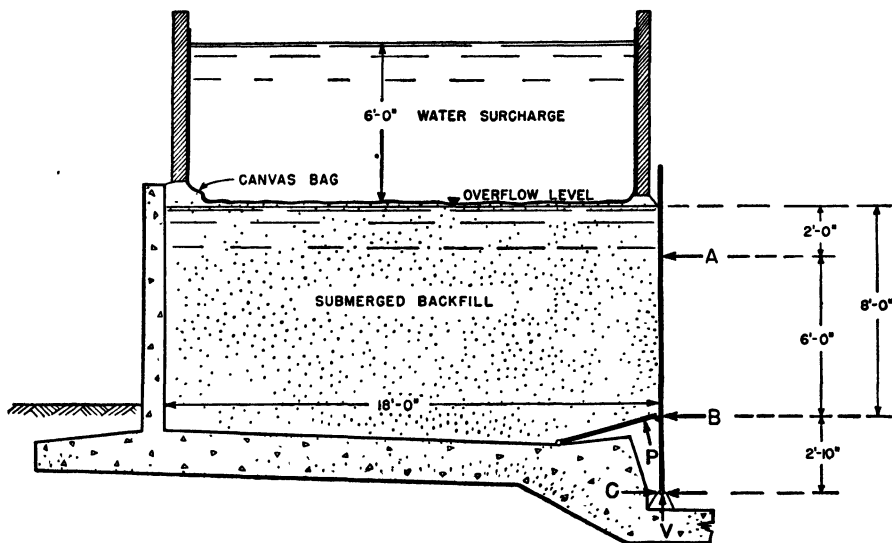
FIG. 10-34. Setup for first series of the Princeton earth pressure tests. (*After Tschebotarioff and Brown, Ref. 387, 1948.*)

1943 to 1948 under the sponsorship of the Bureau of Yards and Docks, U.S. Department of the Navy. A general summary of the results was given by Tschebotarioff in a final report (Ref. 397, 1949). Partial evaluation of the results, in the form of progress reports, had been given earlier (Refs. 384, 387, 390, 396).

The first series of model tests was performed in 1943 to 1945 at a 1:5 scale in a reinforced-concrete testing tank, illustrated in Fig. 10-34. Essentially it was a box, 18 by 13 by 9 ft, open at one end where it was closed by the model steel bulkhead, which consisted of three independent vertical sections. The main measurements were performed on the central 5-ft-wide section, in order to minimize the effects of friction along the side walls of the tank. The following quantities were measured: the reaction pressures A, B, C, and V, the bending strains in the steel plate, the deflec-

tions and displacements of the steel plate, and, when the backfill was of a cohesive type, the pore pressures in the voids of the soil.

The vertical reaction V and the pore pressures were measured by means of pressure cells of the Carlson type. The deflections and the displacements of the steel plate were measured to 0.001 in. by mechanical dial gages of the Federal type. The reactions A, B, and C and the bending strains of the steel bulkhead were measured by means of SR-4 electric-resistivity strain gages. These gages consist of very thin wire, about 1/1,000 in. thick, cemented to a ⅜-in.-wide and 1-in.-long sheet of impregnated paper. This sheet is then cemented to the metal surface where the strain readings are to be taken. The strength of the cement is greater than the strength of the wires, so that they follow the elongations or contractions of the metal surface to which they
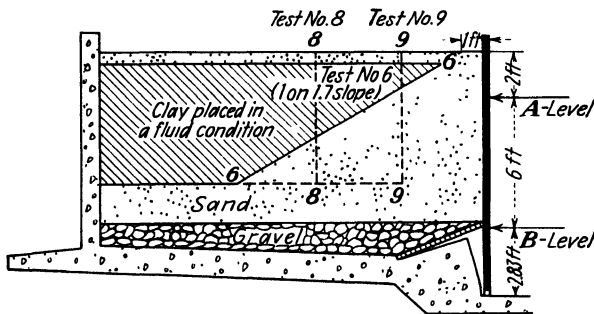
FIG. 10-35. Diagram illustrating the over-all dimensions of three of the first series of Princeton tests (No. 6, No. 8, and No. 9) with sand dikes of different dimensions. (After Tschebotarioff, Ref. 384, 1948.)

are fixed. These longitudinal deformations produce corresponding changes of the cross-sectional area of the wire, which can be measured in terms of varying electrical resistance. The gages are very sensitive to humidity, so that, unless special precautions are taken, erratic volume changes in the glue by which they are cemented may occur, which changes may then be erroneously recorded as strains. Nevertheless, satisfactory methods of insulation were developed during the first series of Princeton tests, as reported by Tschebotarioff (Ref. 379, 1946). A further development by Kimble (Ref. 197, 1946) even permitted the use of these gages under water and led to the improved general testing setup of the third series of Princeton tests, illustrated by Fig. 10-36.

The second series of the Princeton tests was concerned with some supplementary studies of a general character, the results of which have been described in Arts. 7-2 and 10-9.

During both the first series (Fig. 10-34) and the third series (Fig. 10-36) of the Princeton model bulkhead tests—1:10 model scale—different types of backfills were employed; these were clean sand of two different gradings, silty red-colored clay (plasticity index $I_p = 7$ per cent), mixtures of these two materials, and sand dikes of different shapes (Fig. 10-35) interposed between the bulkhead and a fluid silty clay backfill placed in a semiliquid consistency corresponding to 3 blows on the liquid-limit device (Art. 4-9). Surcharges were occasionally applied during tests of both series. Special techniques were employed to ensure fully controlled model similarity of deflections.

Calibrations were performed to determine the section modulus of the bulkhead plate, so that the bending moments M could be accurately computed from the bending strains recorded. The points at which the bending strain readings were taken were sufficiently numerous, and the readings themselves were sufficiently accurate, to permit determination of the shears V by the use of the conventional equation

$$V = \frac{dM}{dh} \tag{10-40}$$

where dM = change of bending moment between two adjoining elevations at which strain readings were taken

dh = vertical distance between these elevations

As shown in Fig. 10-37, a smooth curve was laid through the V (shear) points thus obtained, and values taken from that curve permitted the determination of the lateral
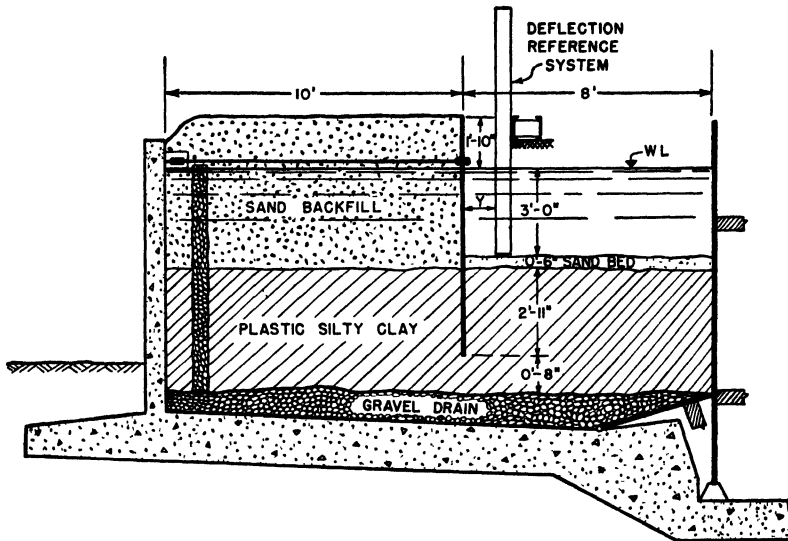
FIG. 10-36. Setup for combined active- and passive-earth-pressure tests at Princeton University. Details shown refer to test 12A. (After Tschebotarioff and Brown, Ref. 387, 1948.)

pressures from the equation

$$p_h = \frac{dV}{dh} \tag{10-41}$$

The derivation of Eqs. (10-40) and (10-41) can be found in most textbooks on mechanics of materials. When drawing the shear curve through the computed points (Fig. 10-37), the following accessory controls were used: First, the shear curve had to pass through the origin at the two points below the anchor level where the bending moment had a maximum. Second, the slope of both branches of the shear curve at anchor level had to be identical. Third, areas of the shear curve between the five points where the bending moments reached limit values had to equal the corresponding difference in bending moments. Similar controls, all based on recognized laws of statics, were applied to the computed points of the lateral-pressure curve. Finally, as shown in Fig. 10-37, a bending-moment curve was computed back from the lateral-
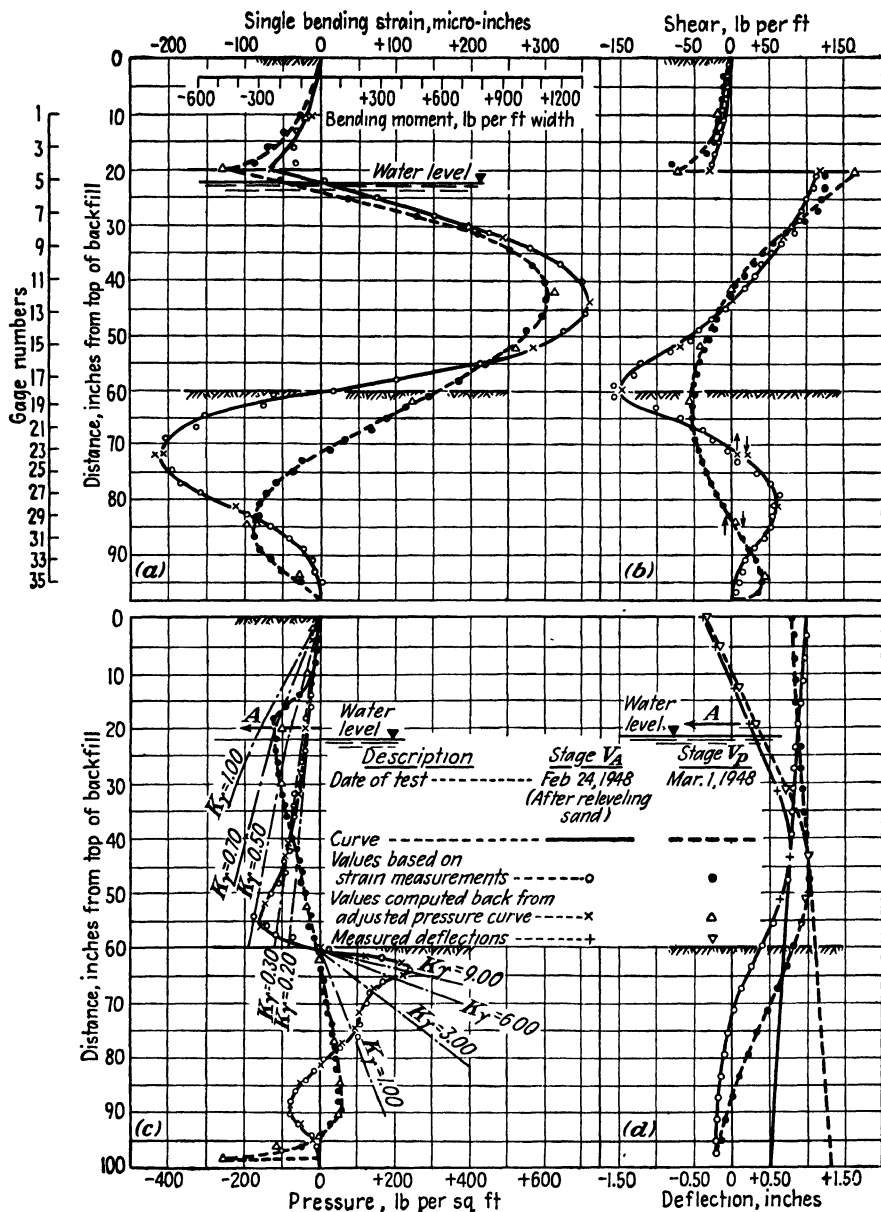
FIG. 10-37. Diagrams giving an example of the results of bending strain and deflection measurements and of lateral-earth-pressure computations during two successive stages of a model bulkhead test (No. 41) at Princeton University. (*After Tschebotarioff, Ref. 384, 1949.*)

pressure curve, which was slightly adjusted when necessary, until equally good agreement with the originally measured bending-moment curve was obtained as that shown in Fig. 10-37. That not more than ±7 per cent difference between the two curves was recorded at any of the essential points indicates the satisfactory accuracy of these novel methods of measurement and of analysis. Tables with complete readings of the bending-strain-measuring instruments and control and other relevant computations showing the determination of lateral pressures were published by Tschebotarioff (Ref. 396, 1948 and Ref. 397, 1949).* Deflection curves were computed from the electrically measured bending strains by the area-moment and elastic-weight methods (see textbooks on structural theory) and were found to agree within ±5 per cent with deflection curves measured by independent mechanical means.

The first series of tests (Fig. 10-34) was limited to the study of active pressures and gave a number of important findings. They were later confirmed by the third series of tests (1947–1948), which involved a study of the simultaneous active and passive lateral earth pressures and of their interaction (Fig. 10-36), at a somewhat smaller (1:10) model scale. The most essential findings were as follows:

1. A sand dike placed at its natural angle of repose between the bulkhead and the fluid-clay backfill (test 6, see Fig. 10-35) was fully effective in reducing the lateral pressures of the fluid clay. The lateral pressures exerted against the bulkhead were no greater than if the entire backfill were composed of clean sand. The interposition between the fluid-clay backfill and the bulkhead of a vertical sand blanket of a width equal to the bulkhead height was found to be just as effective as that of a sand dike (test 8, Fig. 10-35). When the width of the blanket was equal to one-half of the bulkhead height, it was only approximately one-half as effective (test 9, Fig. 10–35), and it was not effective at all when its width was equal to one-tenth of the bulkhead height. In that latter case the lateral pressures transmitted to the bulkhead from the unconsolidated-clay backfill were no smaller than those of a fluid of an equivalent weight.

2. Differentiation is essential between conditions created by backfilling behind a flexible anchored sheet-pile bulkhead or by dredging in front of a "sunk" wall. No clear differentiation between these two conditions had been made in previously published theoretical investigations of the subject of arching in soils. Figure 10-38 shows the five main lateral earth pressure distribution types of *sand* determined in the Princeton tests. No evidence of vertical arching was found when the model bulkheads were backfilled with sand [Fig. 10-38(I) and (II)]. This is true because vertical arching [see Fig. 10-16(III)], as a result of the flatness of the arches, is the

* An almost identical procedure was successfully developed later in Germany (1946–1949) for the computation of pressures against a laterally loaded single model test pile (see W. Loos, "Modellversuche ueber Biegung von Pfaehlen und Spundwaenden," *Der Bauingenieur*, No. 9, pp. 264–275, 1949).

least stable type. Similarly to horizontal arching, it does not develop noticeably behind an anchored bulkhead while backfilling is done, since no soil is present during most of the backfilling to provide an abutment for the arch at and above the anchor level. Further, the elastic elongation of the anchor and the yield of its supports progressively increase as backfilling goes on. This induces the breakdown of any arches in the uncemented sand. Definite evidence of vertical arching was obtained at Princeton only during the stages of a test which simulated dredging in front of a "sunk" wall—that is, when all the backfill was in place, the bulkhead having been driven or "sunk" through it—the anchor support of which did not yield any further [Fig. 10-38(V)]. Of all the theoretical
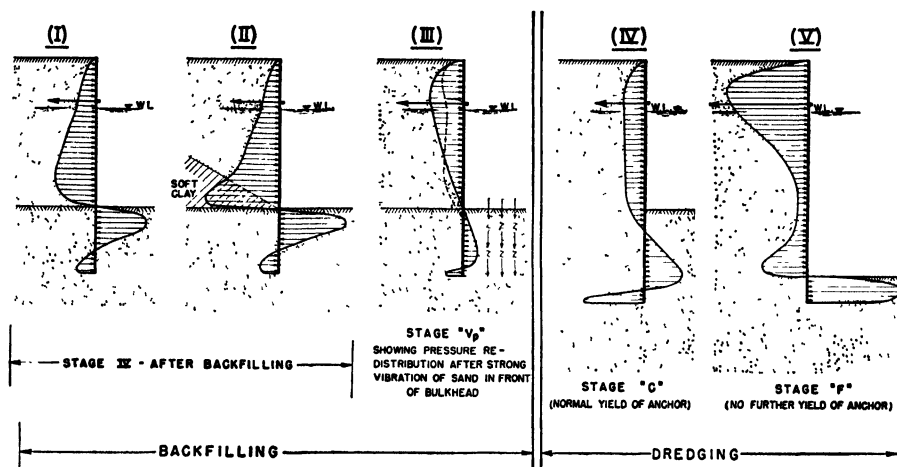
FIG. 10-38. Five main lateral-earth-pressure distribution types determined during the Princeton tests with model flexible bulkheads. (*After Tschebotarioff, Ref.* 384, 1949.)

pressure-distribution curves so far advanced which assume arching of sands, only the one proposed by Ohde [Ref. 252, 1938, see Fig. 10-39(*C*) and Ref. 290] closely corresponded to the one determined at Princeton under the above conditions. Severe vibration of the sand below the dredge line in front of a completely backfilled bulkhead [Fig. 10-38(III), also stage V_p, Fig. 10-37] has an effect similar to dredging. However, even a slight simultaneous natural yield of the anchor strongly reduces the effect on the pressure redistribution of both types of arching and of the passive pressures above anchor level [Fig. 10-38(IV)].

The pressure distributions suggested by the Danish bulkhead regulations [Art. 16-12, see Fig. 10-39(*A*)] and by Terzaghi [Fig. 10-39(*B*)] do not appear probable for reasons made clear in Fig. 10-40. The so far conventional concept of arching [Fig. 10-40(I)] assumes that the bulkhead provides the sole abutment support for the sand arches formed as a result

of the bulkhead deflection. The lateral pressures at the center of the bulkhead span can then be assumed to be decreased. The type of pressure distribution found for sand backfills during the Princeton tests is explained by the *flexible-beam* concept suggested by Tschebotarioff (Ref. 397, 1949) and illustrated by Figs. 10-40(II) and 10-41. The main difference between the two concepts is that, according to the second one, it is the soil below the dredge line and not the bulkhead, which acts as the main support of the flexible beam. The active earth pressures are therefore decreased near restraining boundaries by shearing stresses along them. Not only the soil below the dredge-line level, but even the soil above the free-water level, if possessing some tensile strength, may act as such a
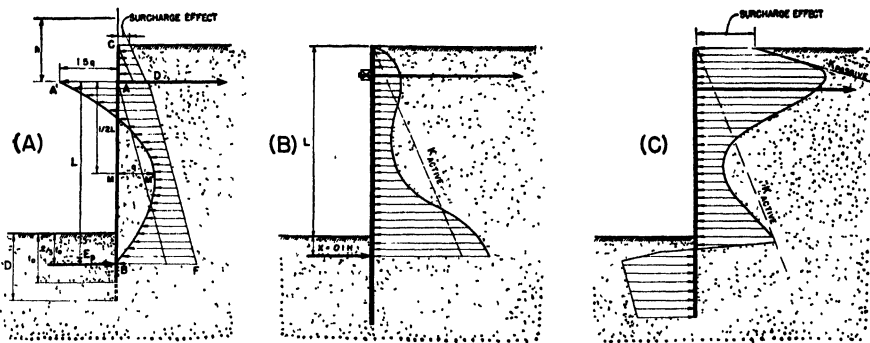
FIG. 10-39. Three concepts concerning the effects of vertical arching on the redistribution of lateral pressures behind flexible bulkheads. (A) Danish regulations, 1937. (B) Terzaghi, 1943. (C) Ohde, 1938. (*After Tschebotarioff, Ref.* 397, 1949.)

restraining boundary. A slight increase of pressure against the bulkhead itself, near the dredge line, is possible only when the depth of embedment of the bulkhead is so small [Fig. 10-38(V)] that failure and general outward plastic movement of the sand together with the bulkhead is induced thereby. If the anchor support is immovable, the strong outward movement of the embedded lower portion of the bulkhead will press the upper portion of the bulkhead against the soil behind it and will induce passive pressures of a high magnitude, which were actually recorded at Princeton [Fig. 10-38(V)] and were considered earlier by Ohde [Fig. 10-39(*C*)], but not by the Danish regulations [Fig. 10-39(*A*)] or by Terzaghi [Fig. 10-39(*B*)]. During backfilling only a very slight increase of pressures above anchor level is possible, owing to passive resistance of the soil, which reaches that level only during the last stages of backfilling [Figs. 10-40(II) and 10-41]. A slight yield of the anchor will destroy the passive resistance of the soil above it.

3. An absence of lateral displacement at the anchor level is conceivable

in actual structures only when the sheet piling is connected to massive relieving platforms (Art. 16-15). The piles supporting such a platform would also have a strong effect on the pressure redistribution against the sheet piling when the latter is placed on the water side of the platform. This effect is, however, not yet known and could probably vary greatly, depending upon the spacing, the inclination, and other characteristics of such piles, as well as of the surrounding soil. It is therefore still an open question whether arching can actually occur under field conditions, even in the case of a "sunk" wall of the above type.

4. The passive pressures below the dredge line in front of the bulkhead reached values which in some cases were three to four times greater than
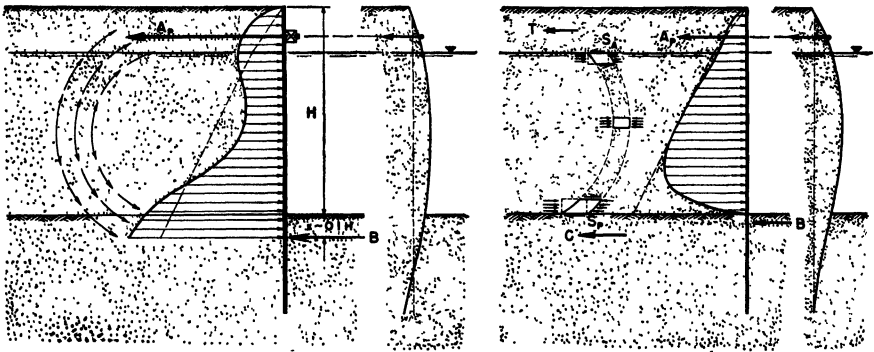
FIG. 10-40. Difference between (I) the conventional concept of *arching* and (II) the suggested concept of a *flexible sand beam* supported by adjoining more rigid soil layers and not by the bulkhead. (*After Tschebotarioff, Ref.* 397, 1949.)

the maximum values which are theoretically possible if the effect of wall friction is neglected. This finding approximately corresponds to the result of Krey's analysis of the problem of passive resistance (see Table 10-1 and Fig. 10-4) for the condition where the angles of internal friction ϕ and of wall friction are assumed to be equal, and the bulkhead sinks somewhat into the soil.

5. The resultant of the residual passive pressures was located much closer to the dredge line than this is usually assumed, these pressures being a function of the bulkhead displacements (see Fig. 10-41). This and the decrease of the active pressures just above the dredge line by shearing stresses, and not by vertical arching, were found to be the main causes of smaller bending moments in the model sheet piling, as compared with values obtained by conventional methods. The flexibility of the bulkhead was of importance to the extent that the bulkhead displacement y_D at the dredge line (Fig. 10-41) increased the shearing stresses

along that boundary and decreased the active pressures behind the bulkhead at that boundary.

6. Exceptionally severe vibration of the sand backfill behind the bulkhead, stage V_A (see Fig. 10-37), increased lateral pressures, so that the resulting bending moments in the bulkhead were increased by 60 per cent and more, as compared with values obtained after normal backfilling. Subsequent vibration of the sand in front of the backfill (stage V_P) decreased the bending moments somewhat.
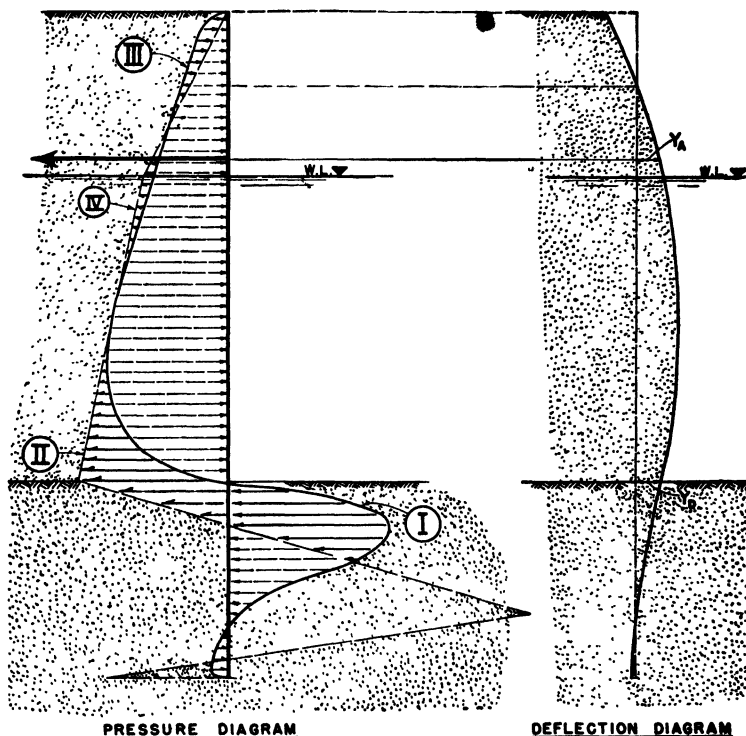
FIG. 10-41. The three main causes of bending moment decrease of the model bulkheads backfilled at Princeton, as compared with conventional assumptions. (*After Tschebotarioff, Ref. 397, 1949.*)

7. The lateral pressures of originally fluid clay backfills were found to decrease with time as a function of the consolidation of the clay, and without any outward movement of the bulkhead being necessary to achieve the pressure reduction. This finding was similar to the one made with the rigid-walled lateral earth pressure meter (Art. 10-9), except that as a result of the spring action of the deflected bulkhead it even moved back toward the backfill during its consolidation (see Fig. 10-42). After completed consolidation the lateral pressures of the clay corresponded to a

value of $K = 0.50$ (curve B, Fig. 10-42), except in the immediate vicinity of more *rigid restraining horizontal boundaries.*

8. A further induced expansion of the consolidated-clay backfills did not reduce their lateral pressures any further in the upper half of the backfill during tests where the water level reached to the backfill surface so that no restraining layer capable of resisting some tension because of capillary saturation was present there. In other words, the active pressures of the consolidated plastic clay backfill were found to equal its
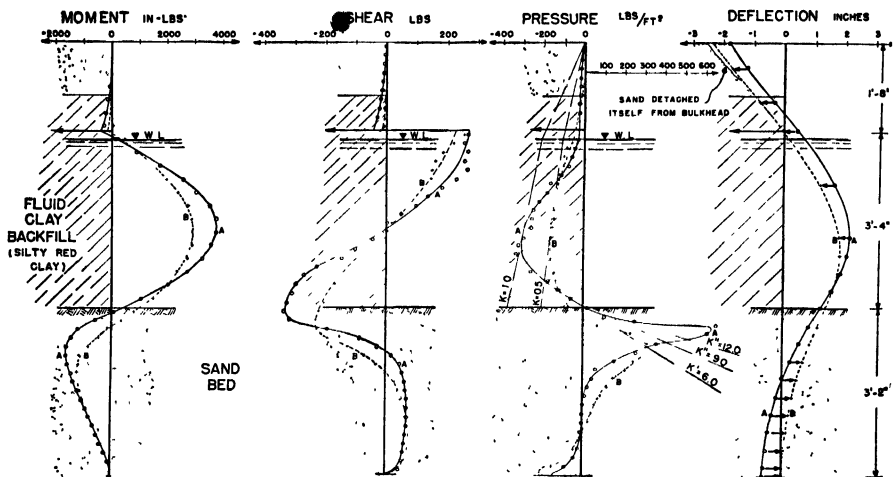
FIG. 10-42. Model bulkhead bending moments, shears, lateral pressures, and deflections at the initial (*A*) and final (*B*) stages of originally fluid clay backfill consolidation during Princeton test 21. (*After Tschebotarioff and Welsh, Ref.* 390, 1948.)

neutral pressures, further confirming laboratory findings on the matter (Arts. 10-9 and 10-12).

9. In the upper zones of cohesive backfills it is customary (Art. 10-4) to assume an absence of lateral pressures, as shown in Fig. 10-43(a). This was not the case during the Princeton tests, where the pressure distribution illustrated by Fig. 10-43(b) was determined for all plastic cohesive backfills of a uniform consistency. A decrease of lateral pressures in the upper zone was observed during the Princeton tests only when a more rigid layer was present there. For instance, during the test illustrated by Fig. 10-42, the upper sand layer was saturated by capillarity and therefore had some tensile strength. After completed consolidation of the underlying, originally fluid clay backfill, although the bulkhead had moved back toward it, the upper sand layer was found to have moved back even more and to have detached itself from the bulkhead, as shown in Fig. 10-42. This was caused by a dip in the surface of the soil, similar

to the one illustrated in Fig. 10-9 and discussed in Art. 10-10. The curvature of the soil surface next to the bulkhead, which acted as a vertical restraining boundary in respect to the consolidating underlying clay mass, induced tension in the upper layer which pulled it back (Ref. 390).

10. No generally valid relationship between the shearing strength at failure and the lateral pressures of plastic cohesive soils or of sand-clay mixtures could be established during the Princeton tests. This lack is due to the fact that once a safe depth of embedment is selected, as should
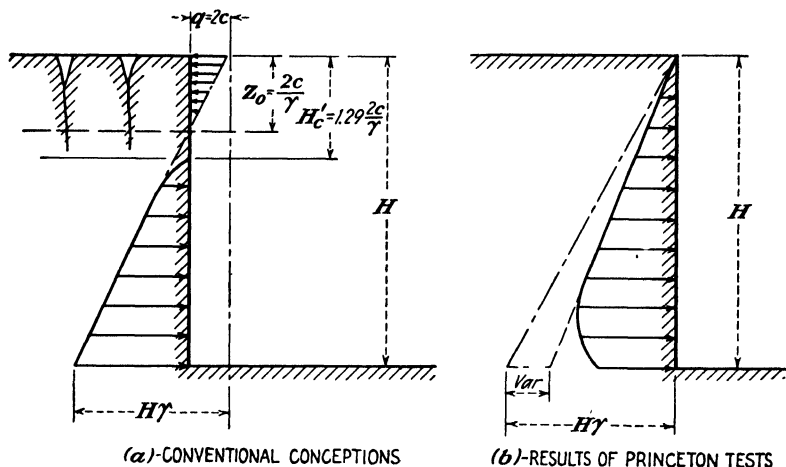
FIG. 10-43. Active lateral pressures of cohesive backfills. (*After Tschebotarioff, Ref. 384, 1948.*)

always be done in proper bulkhead design, the lateral pressures against the bulkhead cease to be a problem of rupture and become a problem of deformations.

The findings listed in this article have served as a basis for the formulation of definite recommendations for the design of flexible anchored sheet-pile bulkheads, which will be given in Arts. 16-14 and 16-15.

10-24. Earth Pressures against Tunnels. The knowledge of the earth pressure values exerted against the lining of a tunnel is of comparatively minor importance where subaqueous tunnels are concerned, that is, tunnels just below the bottom of a river or of a sea channel. As shown in Fig. 10-44(I), full water pressures will be exerted against the tunnel shell and will govern its structural design. The additional pressures exerted by the buoyed weight of the thin layer of overlying and surrounding soil are smaller than the water pressures, and minor errors in the estimation of their values therefore cannot have serious consequences. The situation will be, however, quite different in this respect in the case of tunnels through deep deposits of plastic clay [Fig. 10-44(II)].

Purely theoretical considerations are of little importance for problems of this type, when compared with the results of actual measurements and observations. Only a very limited number of such records is available. One of the more noteworthy and complete sets of such observations was obtained and reported by W. S. Housel (Ref. 178, 1943) from Detroit during construction of sewer tunnels at a depth of some 60 ft below the soil surface. The overlying and surrounding soft plastic clay was fully saturated with water and had a natural water content varying from w_n = 26 per cent to w_n = 37 per cent. The liquid and plastic limits of the clay were not stated, but it would appear from other analyses of the Detroit clay (Art. 7-21) that it is of the same general type as the Chicago
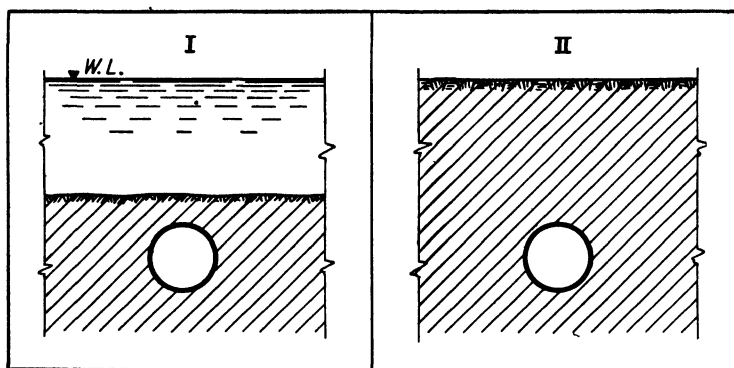
FIG. 10-44. In subaqueous tunnels (I) water-pressure values are of predominant influence on the design. In deep tunnels through plastic clay (II) the design is governed by pressures exerted by the soil.

clay (Art. 10-19). Housel stated (Ref. 178) that the shearing strength of the clay, except for a stiffer surface crust, varied between 150 and 200 lb per ft^2. These values were obtained by direct slow undrained-ring double-shear tests (Art. 7-5). As explained in Art. 7-22, such tests give the yield value which is for clays of this type four to five times smaller than the ultimate shearing strength (see Fig. 7-32). It would therefore appear that the unconfined compressive strength of the Detroit clay was approximately equal to q_u = 0.75 ton per ft^2.

The sewer tunnel cross section had the shape of rings of 9½ ft inner diameter and 17½ in. wall thickness. Goldbeck pressure cells were installed on the outer face of the concrete tunnel lining. The large number of individual cells employed compensated somewhat for the unreliability of this type of cell, when used over long periods of time, and for the inevitable scattering of readings, based on the measurement of pressures over small areas of contact with the soil (Art. 10-17). Figure 10-45 illustrates the general layout of the cells and some typical readings.

A summary of the results obtained over a period of 10 years of observation is given in Fig. 10-46. The tunnel was built with the use of compressed air to minimize the loss of ground and the resulting surface settlements of buildings. After completion of the tunnel and release of the compressed air on December 12, 1930, as shown in Fig. 10-46, all cells recorded an increase of soil pressure which corresponded fairly closely to the drop in air pressure of 3,880 lb per ft^2. Then for a period of three months the pressures decreased somewhat. The horizontal pressures remained practically unchanged thereafter, but during the following five years the vertical pressures increased steadily until they stabilized them-
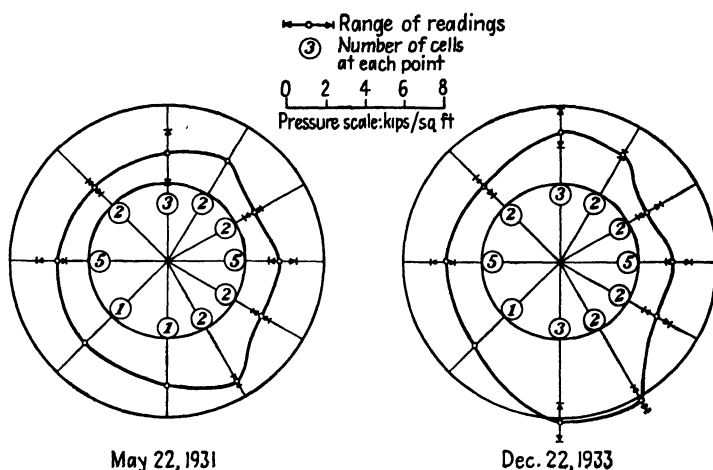
FIG. 10-45. Some sample readings of Goldbeck pressure cells on Detroit sewer tunnels. (*After Housel, Ref. 178, 1943.*)

selves at values corresponding to the weight of the overburden at the respective elevations, referred to as *static head* by Housel. There were no significant changes in the next five years. The ratio of lateral to vertical pressure in this *reconsolidated-equilibrium* condition, according to Fig. 10-45, was equal to $K_n = 5.4/8.2 = 0.66$. It is not clear whether this should be considered a K_s or a K_{s+w} ratio (Art. 10-13). It is possible that it occupies an intermediate position and that some water pressure had built up against the tunnel lining in addition to the intergranular soil pressures. It should be noted further that a high value of K is favorable for the structural design of tunnels (Art. 16-19).

Skempton reported (Refs. 309 and 310, 1943) the results of pressure measurements between cast-iron ring plates which lined a 12-ft-diameter tunnel through London clay of the stiff-fissured type (Art. 2-5). During

the first two weeks after the ring had been built and grouted the pressures gradually increased and finally leveled off at values corresponding to the full weight of 109 ft of overlying clay. In this respect Skempton's findings on London clay (Art. 10-19) corresponded to Housel's findings at Detroit, but the method of measurement he employed permitted the determination of the maximum thrust only.

No measurements appear to have been made concerning the soil pressures exerted against tunnels driven through sand, but available data seem to indicate that arching around the tunnel [Fig. 10-16(I)] appreci-
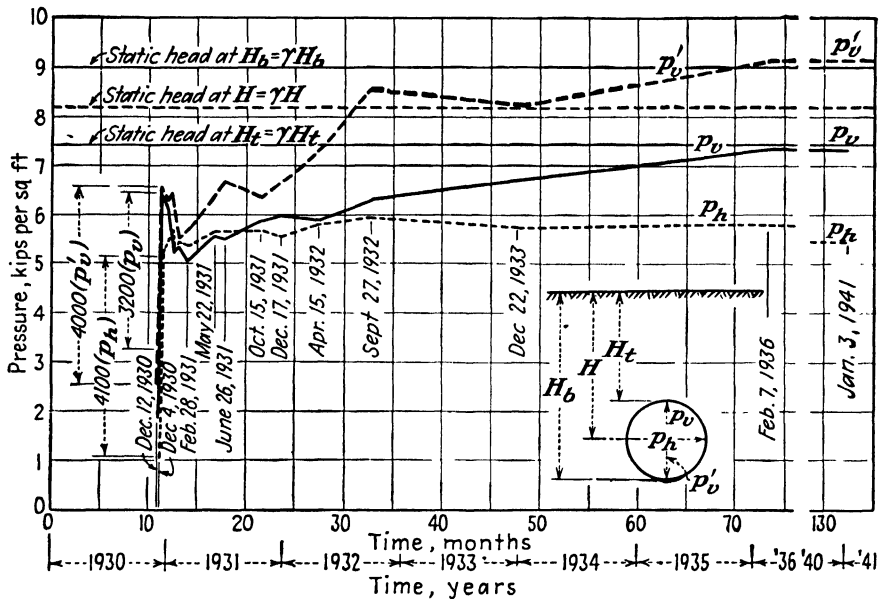
FIG. 10-46. Measured variations with time of the pressures exerted against sewer tunnels at Detroit. (After Housel, Ref. 178, 1943.)

ably reduces the weight of the overburden transmitted to the tunnel lining. A method of computation may be employed which is somewhat similar to that developed for underground conduits in trenches, described in Art. 10-25.

10-25. Pressures against Underground Conduits. The Marston Theory. Extensive studies of the problem were carried out between 1910 and 1920 at the Iowa Engineering Experiment Station by Anson Marston. A review of these and of other related studies was published recently by Spangler (Ref. 320, 1948). Figure 10-47 illustrates Marston's analysis of the case of a pipe conduit in a trench, where it is assumed that cohesion is inactive, and only frictional forces come into play. By equating the

vertical forces acting on an element of backfill, dh thick, within the trench, the following equation is obtained:

$$W + dW + 2K_A\left(\frac{W}{b}\right)\tan\delta\,dh = W + \gamma b\,dh \qquad (10\text{-}42)$$

The solution of this linear differential equation reads

$$W = \gamma b^2 C_d \qquad (10\text{-}43)$$

where

$$C_d = \frac{1 - e^{-\alpha h}}{2K_A\tan\delta} \qquad (10\text{-}44)$$

and

$$\alpha = \frac{2K_A\tan\delta}{b} \qquad (10\text{-}45)$$

In the above equations K_A is the coefficient of active earth pressure, as defined by Eq. (10-7), (10-8), or (10-9), δ is the angle of wall friction between the backfill and the walls of the trench, e is the base of natural logarithms, and γ is the unit weight of the backfill.
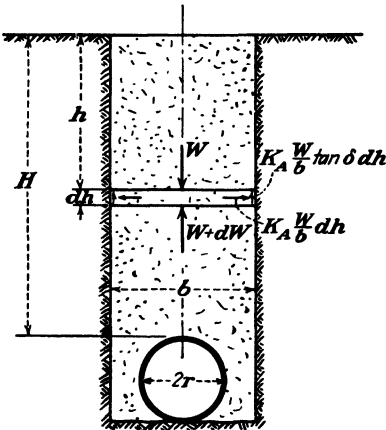
FIG. 10-47. Diagram illustrating A. Marston's (1913) analysis of vertical loads on pipe conduits in trenches. (After M. G. Spangler, Ref. 320, 1948.)
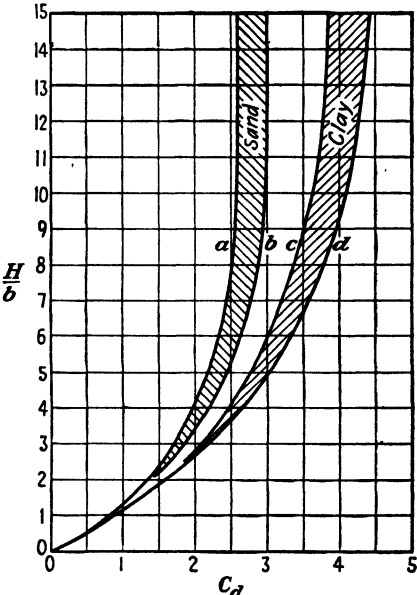
FIG. 10-48. Relationship between the depth-to-width ratio of a trench and the coefficient C_d governing the load transmitted to a pipe conduit. (After Spangler, Ref. 320, 1948.)

Figure 10-48 gives the variation of the coefficient C_d as a function of the depth/width ratio H/b of a trench. The angle of wall friction δ was set

equal to the angle of internal friction ϕ of the backfill. The four curves of Fig. 10-48 were computed for the following values of $K_A \tan \delta$:

Curve *a*.. . $K_A \tan \delta = 0.192$ (minimum for granular materials)
Curve *b*...... $K_A \tan \delta = 0.165$ (maximum for granular materials)
Curve *c*..... $K_A \tan \delta = 0.130$ (maximum for clay)
Curve *d*.. $K_A \tan \delta = 0.110$ (maximum for saturated clay)

In this connection it should be noted that if $\delta = \phi$,

$\phi = 30°$.. $K_A \tan \delta = 0.192$
$\phi = 25°$.. $K_A \tan \delta = 0.187$
$\phi = 20°$. $K_A \tan \delta = 0.178$
$\phi = 15°$. $K_A \tan \delta = 0.156$
$\phi = 10°$. $K_A \tan \delta = 0.124$
$\phi = 8°$. $K_A \tan \delta = 0.105$

Thus the reduction of the vertical load P due to friction along the walls of the trench theoretically is not very sensitive to changes in the frictional properties of the soil. The curves given in Fig. 10-48 are claimed to have been established by actual tests which corroborated the above theory.

It should be noted from Fig. 10-48 that curve *a* ($\phi = 30°$) indicates that no further increase of the pressure on the pipe conduit is to be expected if the depth of the trench exceeds nine times its width. This is in reasonable agreement with the results of measurements on silos, where an even greater reduction of vertical loads is to be expected and actually takes place owing to friction along all *four* walls of the silo. For instance, it will be noted from Fig. 10-17 that no further increase of vertical pressure was recorded after the depth of grain in the silo exceeded three times its average width.

A completely different and even reversed situation arises if the pipe conduit is covered by embankment fill. If the conduit is rigid, it may receive more load than the actual weight of the fill immediately above it. The stiffness of the pipe conduit itself, the type of its bedding, the compaction of the fill around it, all will influence the results. This point will be discussed further in Art. 16-18 in connection with design problems of conduits.

Practice Problems

10-1. At a depth of 33 ft below the surface of a cut in a fully saturated plastic clay with an average natural water content $w_n = 43$ per cent a lateral pressure $p_h = 1.05$ tons per ft² was measured. The cut was lined with wooden lagging between H piles. Free drainage was thus possible, but no seepage was visible. Determine the K_γ value of the earth pressure coefficient which will correspond to the above measurement.

Answer. This will be a K_s coefficient in the sense of Eq. (10-33), since the water appears to be held by the clay. Assuming a value of specific gravity $G = 2.70$, we

obtain from Eq. (4-5) the void ratio $e = (43 \times 2.70)/100 = 1.16$. The unit weight of the soil can then be computed from Eqs. (4-7) and (4-10):

$$\gamma = \frac{2.70 + 1.16}{1 + 1.16} \times 62.4 = 115.5 \text{ lb per ft}^3$$

The weight of the overburden will be $\gamma h = (115.5 \times 33)/2{,}000 = 1.90$ tons per ft². The earth pressure coefficient will be

$$K_\gamma = 1.05/1.90 = 0.554$$

10-2. To what values of the angle of internal friction ϕ and of the cohesion c may the coefficient of earth pressure $K_\gamma = 0.554$ correspond on the basis of conventional strength theories, so long as no pressure redistribution has taken place?

Answer. Any combination of the values ϕ and c given by the line in Fig. 10-49 will satisfy the value of $K_\gamma = 0.554$, according to Eq. (10-6). Thus, if we set $c = 0$ in that equation, we obtain

$$\begin{aligned} \tan^2 (45° - \phi/2) &= 0.554 \\ \tan (45° - \phi/2) &= 0.747 \\ 45° - \phi/2 &= 36.7° \\ \phi &= 16.6° \end{aligned}$$
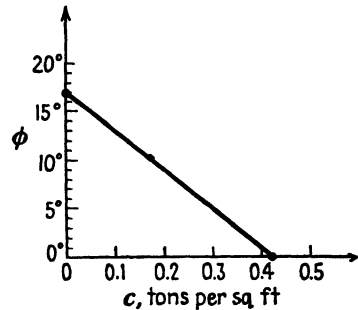
FIG. 10-49.

If we set $\phi = 0°$ in Eq. (10-6), we obtain

$$\begin{aligned} 1.00 - 2c/1.90 &= 0.554 \\ c = 0.446(1.90/2) &= 0.424 \text{ ton per ft}^2 \end{aligned}$$

By setting $\phi = 10°$ in Eq. (10-6), we obtain

$$\begin{aligned} \tan^2 40° - (2c/1.90) \tan 40° &= 0.554 \\ 0.708 - (2c/1.90)0.842 &= 0.554 \\ c &= 0.174 \text{ ton per ft}^2 \end{aligned}$$

Other points of the line shown in Fig. 10-49 can be obtained in a similar manner.

10-3. Check the maximum pressure values indicated by arrows and the letter P in Fig. 10-29(b) by means of Peck's equation for the pressures against the timbering of cuts in plastic clay.

Answer. According to Eq. (10-35), the coefficient K_a for an unconfined compressive strength $q_u = 0.50$ ton per ft² = 1,000 lb per ft² and an unbuoyed unit weight of $\gamma = 105$ lb per ft³ of the clay, for a depth of 42 ft of cut, will be

$$K_a = 1 - \frac{2 \times 1{,}000}{105 \times 42} = 1 - 0.454 = 0.546$$

and the corresponding pressure of the trapezoidal design diagram will be $p_h = 0.546 \times 42 \times 105 = 2{,}400$ lb per ft² = 1.20 tons per ft², as shown in Fig. 10-29(b) by the left-hand vertical arrow. The value corresponding to a depth of cut of 42 + 16 = 58 ft is obtained in a similar manner.

Note: See end of Chap. 16 for further problems connected with the subject matter of this chapter.

References Recommended for Further Study

Tables for the Calculation of Passive Pressure, Active Pressure, by Albert Caquot and Jean Kerisel, translated from the French by Maurice A. Bec, revised translation by Chief Scientific Adviser's Division, Ministry of Works, London, Gauthier Villars, 1948, 120 pp. Extensive tables of the type given in Tables 10-1 and 10-2 of this book, but covering a much wider range of values in much greater detail.

"Earth Pressure and Shearing Resistance of Plastic Clay," *Transactions of the American Society of Civil Engineers*, 1943, pp. 970–1109. A symposium including: Karl Terzaghi, "Liner-plate Tunnels on the Chicago (Ill.) Subway"; Ralph Peck, "Earth-pressure Measurements in Open Cuts, Chicago (Ill) Subway"; W. S. Housel, "Earth Pressure on Tunnels"; with discussions. Contains many valuable data on field observations and records; also some debatable attempts to relate measured values of earth pressure to the ultimate shearing strength of plastic clays.

"Underground Conduits—an Appraisal of Modern Research," by M. G. Spangler, *Transactions of the American Society of Civil Engineers*, 1948, pp. 316–374. Summary of experimental data and of design procedures of different types of pipe conduits in trenches and below embankments; with discussions.

"Lateral Earth Pressures on Flexible Retaining Walls," *Transactions of the American Society of Civil Engineers*, 1949, pp. 410–539. A symposium including: William H. Smith, "Introduction"; Gregory P. Tschebotarioff, "Large-scale Model Earth Pressure Tests on Flexible Bulkheads"; Edward R. Ward, John R. Bayliss, and Philip P. Brown, "Special Features on Large-scale Earth Pressure Tests"; Harris Epstein, "Application of Test Results to Quay Wall Design"; L. A. Palmer, "Experiences with Soil Types in Naval Construction"; J. C. Gebhard, "Cave-ins of Sandy Backfills"; L. C. Coxe, "Failure of Quay Wall at Mare Island, California"; with discussions. Summary of the experimental procedures and results of tests at Princeton University; comparison with existing theories and field observations; other field records.

Final Report. Large-scale Earth Pressure Tests with Model Flexible Bulkheads, by Gregory P. Tschebotarioff, submitted to Bureau of Yards and Docks, Department of the Navy, Jan. 31, 1949, Department of Civil Engineering, Princeton University, lithoprint, 272 pp. Contains descriptions of techniques of measurement, control, testing, and analysis of the results, with sample recordings and computations; summary of all findings made; comparison with existing theories and critical examination of the latter; design recommendations. (A list of libraries which have copies of the report may be obtained from the author.)

CHAPTER 11

THE COMPACTION AND THE STABILIZATION OF SOILS

11-1. Terminology. The term *compaction* shall be used in this book to designate the artificial increase of the density of a natural soil by mechanical means, that is, the *densification*. The natural soil may be compacted either in situ or, after transportation, in a new fill. By *consolidation* (Art. 6-1) is meant the gradual increase in the density of a soil under the natural action of forces of gravity, such as the weight of the soil itself or that of structures erected upon it. By *stabilization* will be meant any artificial method employed for the purpose of improving by suitable regrading or by special admixtures such properties of a soil as are important for the maintenance of the shearing strength and of the volume and shape of the soil. The loading and climatic conditions which the soil may encounter while serving as a foundation or construction material should be considered in this respect.

Thus reference will be made in this book to "acceleration of consolidation by means of sand drains" (Art. 6-10), to "compaction of a soil by means of sand piles" (Art. 11-4), and to "stabilization of sand by means of chemicals" (Art. 11-9). These distinctions are emphasized, since in the past all the above terms have been frequently and erratically interchanged in general usage. In addition, there are several schools of thought as to what the proper use of these terms should be. For instance, the term soil *solidification* is sometimes employed to designate soil stabilization, as defined above in a limited sense of the word. In its broadest interpretation, the term "stabilization" is sometimes used to cover any kind of action which improves the stability of a soil mass (Ref. 438).

11-2. The Effect on the Density of Fills of Variations in the Moisture and in the Compactive Effort Employed. The following experiments will demonstrate the relationship between the various factors involved. Let us take some silty sand, the general properties of which are indicated for soil 1 in Table 11-2, and let us compact it in the mold (Fig. 11-1) by

means of the type of hammer shown in Fig. 11-2, employing procedure *B* from Table 11-1. That is, the hammer will weigh 5.5 lb, and the guide cylinder around it will have such a height that the height of drop will be
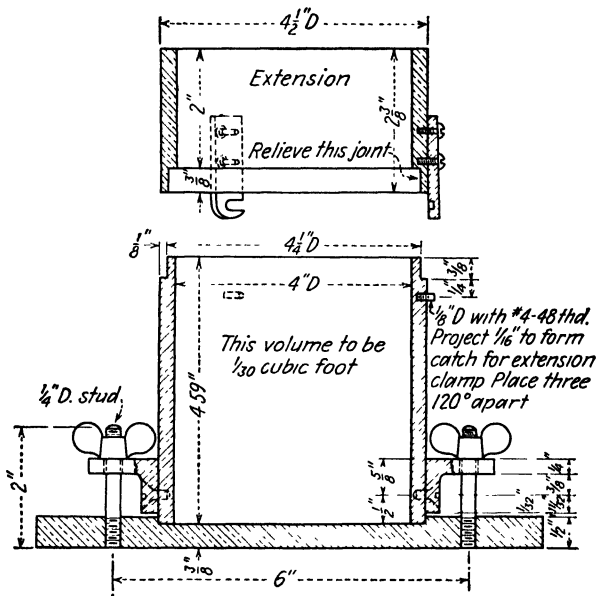
FIG. 11-1. Standard Proctor-type (also ASTM and AASHO) mold for soil compaction (see Ref. 10).

H = 12 in. To that end, the cylinder is set on the surface of the soil by one hand of the operator, the hammer is raised by the other hand as far as it will go and is then released. The soil will be filled into the mold in increments so selected that the compaction can take place in three layers;

TABLE 11-1. Data on Laboratory Compaction Procedures

Type	Weight of hammer, lb	Height of drop, in.	Number of blows per layer	Number of layers	Compaction energy, ft-lb per ft^3
(A) modified Proctor (or AASHO)*...	10.0	18	25	5	56,200
(B) standard Proctor (or AASHO)*...	5.5	12	25	3	12,300
(C) 15-blow Proctor...............	5.5	12	15	3	7,400

* American Association of State Highway Officials.

25 blows of the hammer will be applied to each layer. The extension piece shown in Fig. 11-1 is then removed, the soil along the surface of the lower mold (the volume of which is $\frac{1}{30}$ ft^3) is leveled off with a straight-

edge, the soil and mold are weighed, and the moist unit weight of the soil is computed. Let us assume that the value obtained was 124.5 lb per ft[3], and that the natural water content of that soil was found to be $w = 4.8$ per cent. This will give us point a in Fig. 11-3.

If we add some water to increase the water content to $w = 6.0$ per cent and repeat the same compaction procedure, point b in Fig. 11-3 will be obtained. By increasing the water content in small increments and repeating each time the same compaction procedure, points c, d, e, and f can be plotted. These points represent the moist density, that is, the unit weight of the soil solids plus the weight of the water in the voids. The dry density, that is, the unit weight of the soil solids only, can then be computed from Eqs. (4-8) and (4-6), giving the corresponding points a', b', c', d', e', and f' and curve B_1 (Table 11-1) applied to soil 1 (Table 11-2) at different moisture contents.

FIG. 11-2. Type of hammer employed for the field laboratory compaction of soil in the mold shown in Fig. 11-1.

By applying in the same manner the compaction procedures A and C to soil 1, curves A_1 and C_1 are obtained, as shown in Fig. 11-3. The three compaction procedures applied to soil 2 give curves A_2, B_2, and C_2, and applied to soil 3 give curves A_3, B_3, and C_3. It will be noted from Fig. 11-3 that in the case of soils 1 and 3 the *greatest dry density* $\gamma_{md\ max}$ is reached at a definite moisture content, which is termed the *optimum moisture content* w_{opt} (see Table 11-3).

The explanation of the recorded facts is as follows: At a low moisture content cohesive soils form lumps which cannot be broken up easily. They therefore hamper compaction. Addition of water at first helps to soften up and to break these lumps down, so that with the expenditure of the same compactive effort a greater density is obtained. The addition

TABLE 11-2. Characteristics of the Three Soils Referred to in Figure 11-3

Soil type	Specific gravity G	Consistency limits, per cent			Grain-size distribution, per cent		
		w_L	w_P	I_p	Sand	Silt	Clay
No. 1, silty sand....................	2.67	17	16	1	80	15	5
No. 2, sand..........................	2.67	Nonplastic		0	92	5	3
No. 3, clay..........................	2.73	68	21	47	10	28	62

of water is, however, beneficial up to a certain point only. Theoretically this point is reached when the amount of water present is sufficient to fill
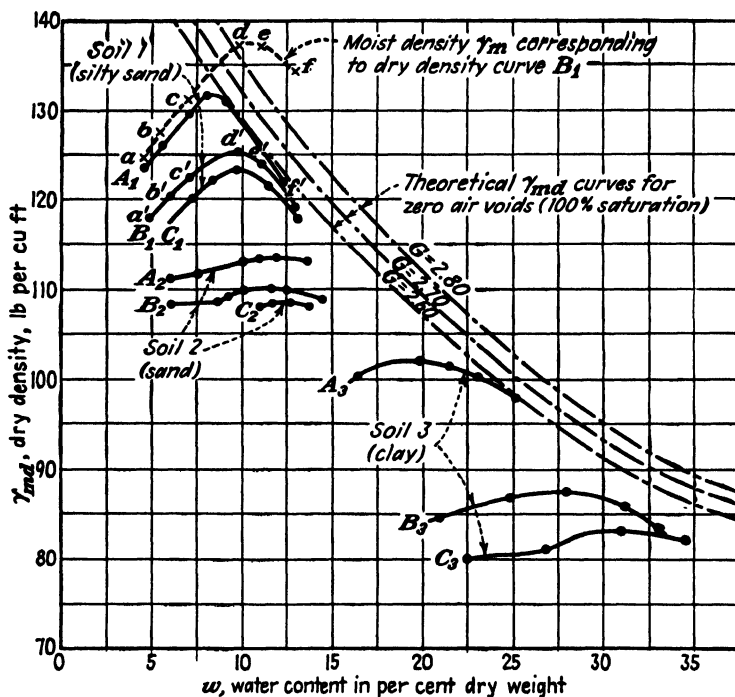
FIG. 11-3. The moisture-density relationship of three limit types of soils and the effect thereon of the energy expended on the compaction (see Tables 11-1 and 11-2). Compiled from data in Ref. 410.

all the voids of the soil, after having coated the individual particles, so that any further water added will only serve to keep the solid particles apart from each other and thereby will decrease the dry density. In

TABLE 11-3. Summary of Data Given in Figure 11-3

Soil type	Optimum moisture, per cent			Maximum dry density, lb per ft³		
	A	B	C	A	B	C
No. 1, silty sand	8	10	10	132	125	123
No. 2, sand	Indefinite			113	110	108
No. 3, clay	20	28	31	102	88	83

other words, the experimental curves should at the optimum moisture content reach the zero-air-voids curve, which corresponds to the value of

the specific gravity G of the soil tested, and follow that curve if any more water is added. Three such theoretical zero-air-voids (100 per cent saturation) curves have been plotted in Fig. 11-3 for values of $G = 2.8$, $G = 2.7$, and $G = 2.6$. Equations (4-7) and (4-5) were used for the computations (see also Prob. 4-3). It will be noted from Fig. 11-3 and Table 11-2 that at moisture contents greater than the optimum, the experimental curves do not quite reach their theoretical zero-air-voids curve but run parallel to it. This is an indication that saturation is not complete, but that some air is unavoidably entrapped in the voids of the soil during its compaction.

Other conditions being equal, an increase of the compactive effort produces an increased density of the soil, but only at moisture contents smaller than the optimum content which corresponds to the greater effort. At moisture contents higher than the optimum no further compaction can be produced by an increased effort, since instantaneous expulsion of the excess water entrapped in the voids is not possible. As a result, increased compactive efforts at water contents higher than the optimum only serve to set up excess pore pressures in the water filling the voids, which then facilitate shearing deformations of the entire soil mass. This fact has considerable practical importance for the selection of the water content at which field compaction should be undertaken and explains why it is usually preferable to make that selection "on the dry side" of the optimum (see Arts. 11-3 and 17-4).

The following additional important facts will be noted from Fig. 11-3 and Table 11-3. The water content of a relatively clean sand (2) has practically no influence on its dry density, as produced by the same compactive effort. A slight addition of silt or of clay to sand improves its grading and permits the development of a greater density for the same compactive effort. The effect of moisture during molding is then considerable. So long as the amount of silt and clay added is only small and no greater than is needed to partially fill the voids of the sand (see Fig. 4-4), producing an A-1 soil (Art. 12-11), the maximum density will increase, and the optimum moisture content will decrease, as compared with cleaner sand and the same compactive effort. A larger amount of clay reverses this trend; the maximum density decreases, and the optimum moisture content increases. Because of the greater surface area of fine particles, more water is required to coat them, and part of the water is adsorbed (see Art. 3-5).

Most of the above facts were first ascertained experimentally and reported by R. R. Proctor (Ref. 280, 1933) of Los Angeles. The method originally employed by him is listed as method (B) in Table 11-1 (for recent techniques, see Ref. 281). As the weight of the field compaction

equipment increased, it was found necessary to increase the compaction energy, if the laboratory results were to correspond to those obtained in the field. Method (A) of Table 11-1 was developed to meet this requirement. Method (C), which is seldom used, was designed for the purpose of duplicating conditions produced in the field by lightweight compaction equipment.

There are a number of devices used for the mechanical operation in the laboratory of the hammer illustrated in Fig. 11-2. Also, a different type of the so-called CBR mold, which is larger, 6-in. diameter, is frequently used (see Art. 19-5). As compared to Table 11-1, the number of hammer blows is then increased in proportion to the volumes of the molded specimens.

R. R. Proctor also employed an auxiliary device, known as the *plasticity needle*, to check the moisture content and density of a compacted soil. The device consists of a small plunger which is placed on the surface of the soil and is pressed a specified distance into it by manual pressure applied by means of a handle and a calibrated spring which can measure loads up to 100 lb. The compression of the spring indicates the resistance offered by the soil. Several interchangeable sizes of the plunger are available, varying from 1.0 to 0.05 in.^{2} in area. The device can be operated only on screened soil, since the presence of small gravel is liable to produce erratic results. Personal characteristics of the operator also appear to be of importance. For the above reasons this device is not used universally.

Proper compaction of fills is of the greatest importance, since upon it depends the shearing strength of the fill and hence the stability of earth dams, embankments, and road and airport base courses. It has been shown that the shearing strength of a fill increases with its density but, in addition, depends on the initial water content which was used for the molding of the specimen. For the same density the highest strengths were frequently obtained by the use of higher compactive efforts and of molding water contents somewhat below the optimum (see Turnbull and McRae, Ref. 403, 1950).

11-3. Soil Compaction in the Field by Rolling. This is the most effective compaction procedure when large masses of earth fill are to be handled. For the compaction of clay fills, a so-called *sheep's-foot roller* is usually employed, a close-up view of one of the existing models of which is given in Fig. 11-4. It is sometimes called a *tamping roller*. A steel drum has a number of steel studs welded to its surface, the shape of which resembles somewhat that of a sheep's foot; hence the name of the roller. The drum is empty for transportation but is filled with sand and water on the site where it is to be used. The entire weight of the drum comes to

bear on only a few of the sheep's-foot studs at the same time. So-called *footprint* pressures are thereby developed which are sufficient to crush and to compact any lumps of clay they come to bear on. Individual drums can then be attached side by side or tandem fashion and drawn all together by one caterpillar tractor (see Fig. 11-5).

The first known sheep's-foot roller was built in 1906 in California. In the 1920's this type of equipment came into general use in the United

FIG. 11-4. Close-up view of a sheep's-foot roller. (*Photo by Tschebotarioff, Ref. 375.*)
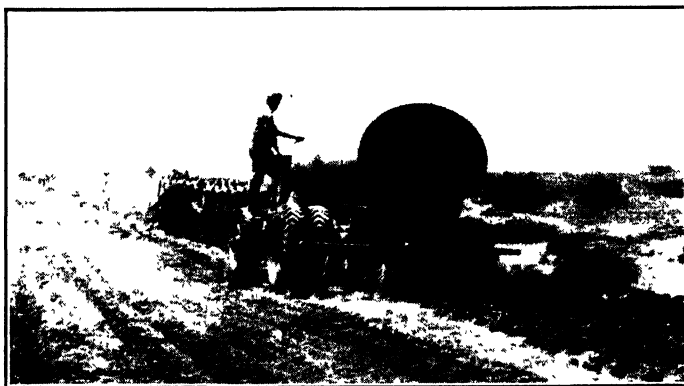
FIG. 11-5. A tractor-drawn tandem group of sheep's-foot-roller drums and a water-sprinkling truck during compaction of clay fill of an earth dam in Oklahoma. (*Photo by Tschebotarioff, Ref. 375.*)

States. According to O. J. Porter (Ref. 8), the present light standard sheep's-foot roller has a 43-in.-diameter drum, a loaded weight varying from 6,000 to 15,000 lb per 8-ft width of a drum, and footprint pressures varying from 60 to 300 psi. The heavy standard sheep's-foot roller has a 60-in.-diameter drum and footprint pressures from 300 to 600 psi. Some experimental giant sheep's-foot rollers have been built with 96-in.-diameter drums and 400- to 1,000-psi (that is, up to 72 tons per ft^2) foot-
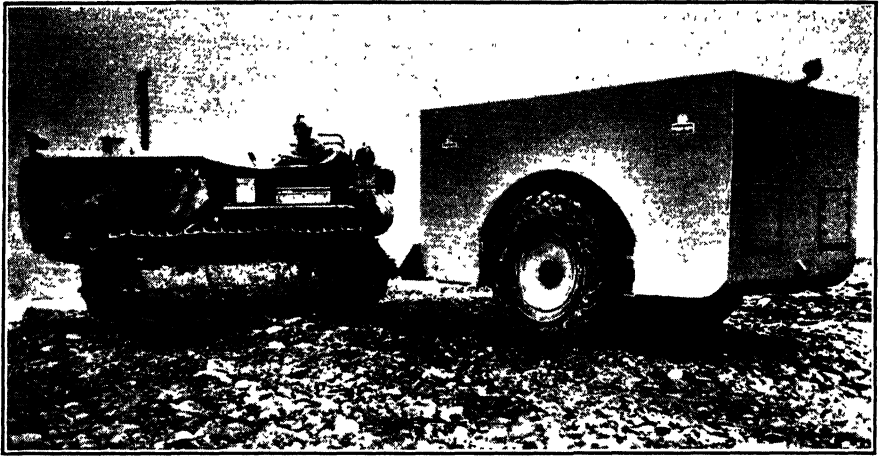
(a)
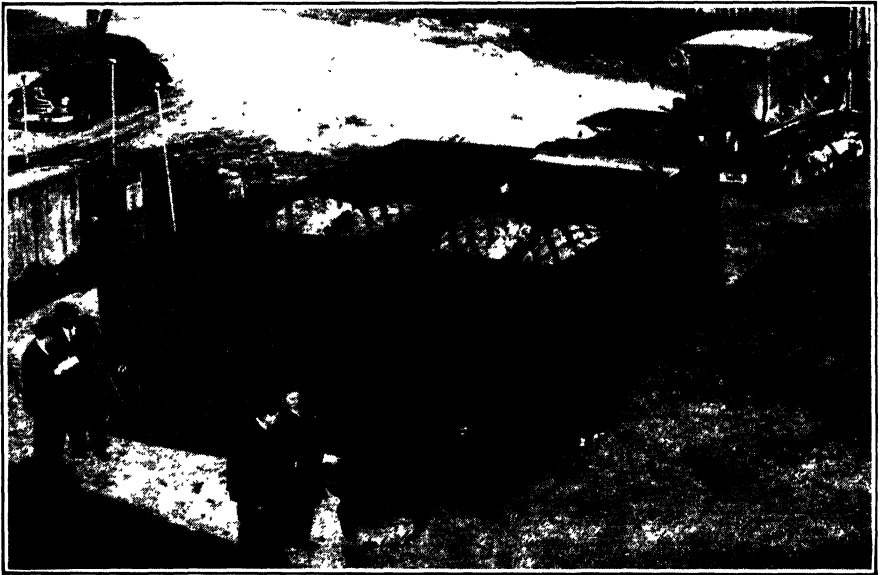
(b)

FIG. 11-6. (a) A 50-ton pneumatic-tire roller. (*Courtesy of Wm. Bros. Mfg. Co., Minneapolis, Minnesota.*) (b) The Porter "Super Compactor"; 60 tons when empty and 200 tons when fully ballasted. Hydraulic jack attachment at lower right permits field plate-bearing tests. (*Courtesy of O. J. Porter, Newark, New Jersey.*)

print pressures. These extra heavy rollers frequently are employed for a follow-up of the preliminary compaction of a layer by lighter rollers (Ref. 8).

In the case of sandy soils with little cohesion better results are obtained by means of pneumatic-tire rollers (see Fig. 11-6*a* for a model of this type). Pneumatic rollers are being employed more and more frequently for such soils, instead of the sheep's-foot type. Since no lumps requiring crushing by very high concentrated pressures are present in sandy soils, a pressure more uniformly distributed over a greater area avoids the danger of
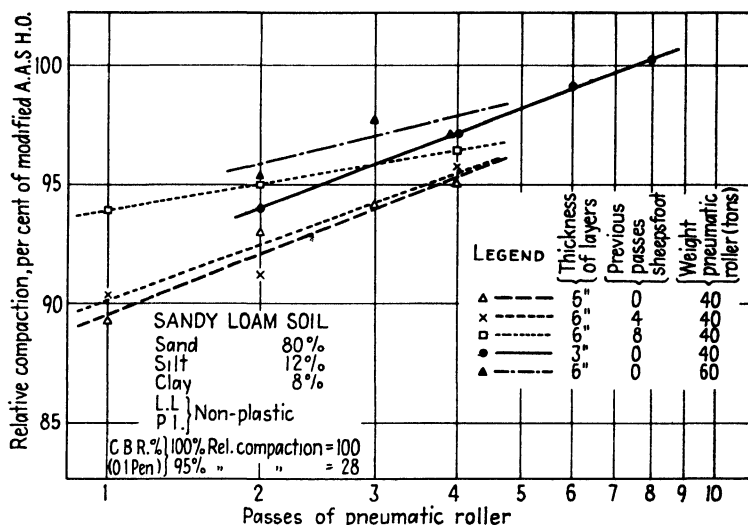
FIG. 11-7. Curves showing the results of compaction studies on the special test section constructed by the U.S. Engineers at Clover Field, Santa Monica, California. (After O. J. Porter, Ref. 8, 1946.)

localized shear failures or churning of the soil by the individual sheep's-foot studs. Rubber-tired rollers of this type have been built up to a total weight of 200 tons (see Fig. 11-6*b*) and produce efficient compaction. The air pressure of the tires can be used to regulate the area of their footprints. Heavy rubber-tired earth-moving equipment (Fig. 17-11) also can materially assist in the fill compaction during the deposition of the successive layers.

The thickness of layers to be compacted varies between 3 and 12 in; 6 in. is the customary value. The number of passes required by a roller to achieve a certain amount of compaction also varies. The rolling of experimental sections is sometimes advisable for important construction work, in order to decide on the thickness of fill layers and on the corresponding number of passes to be used in later work (see Fig. 11-7). The

density obtained is determined by means of the procedures outlined in Art. 11-5.

Moisture control during field compaction is very important. It is no accident that the methods of soil compaction in relation to proper moisture control were developed in the semiarid regions of the western United States. It is comparatively easy to add water to a fill (see Fig. 11-5), but it is very difficult rapidly to dry out soil which is too wet, for instance, as a result of rain. No rolling can be done during protracted rainy spells. This is one reason why hydraulic fills are sometimes selected instead of rolled fills for earth dams in regions with high precipitation (see Art. 17-3). Where compaction by rolling is essential, for instance, in the construction of highway and airport base courses, the sequence of the work should be so planned as to permit at all times the easy runoff of rain water from the surfaces where compaction is to be continued. Only a small depth of a few inches of soil will then get mushy on such surfaces after a heavy rainfall, and it can be quickly scraped off by a bulldozer before compaction is resumed.

FIG. 11-8. The BR-2 portable gasoline rammer in action. (*Courtesy of Barco Mfg. Co., Chicago, Illinois.*)

11-4. Soil Compaction by Impact. It has been attempted to compact soils by repeatedly dropping heavy steel plates on the soil surface. The plates, weighing 2 to 4 tons, were attached to a cable of a crane mounted on caterpillar tracks. According to Loos (Ref. 215, 1936), an increase of the weight without a corresponding increase of the area of the plate did not increase the effectiveness of the compaction, apparently because shear displacements with no decrease of volume were then induced. This procedure is not economical and is seldom used.

Another impact soil-compaction device was developed in Germany (Ref. 215), the so-called *frog*. An American modification of the device is shown in Fig. 11-8. A gasoline motor is incorporated in the head of the device, which has two inner pistons. An explosion of the mixture between the two pistons lifts the heavy head of the device into the air, past the

lower piston, which is attached to the foot of the device, thereby compressing a spring below that piston. This spring pulls up the foot of the device while the rest of it is still in the air. The entire rammer then falls to the soil surface before the next explosion in the gasoline motor occurs.

The original German devices weighed between 1,100 and 2,200 lb (Ref. 215). They appear to have been intended for use in groups for the compaction of large areas. Rolling (Art. 11-3) is much more economical for this purpose. The present American type, shown in Fig. 11-8, weighs 210 lb. The diameter of its foot is 9.5 in. ($A = 0.492\ ft^2$). The device rises approximately 14 in. into the air, and the compaction energy developed by it is thus 240 ft-lb per blow. The device is particularly well suited for the compaction of backfill in trenches dug for sewer or water pipes, or quite close to concrete structures, where there is no space for rollers to operate. In such cases it may have advantages over the smaller sized pneumatic tampers connected to jackhammer-type devices operated by compressed air. Tampers of the latter type have been conventionally used so far for compaction in cramped space, but to be effective, because of their small foot area, they appear to require the placing of the fill in very thin layers.
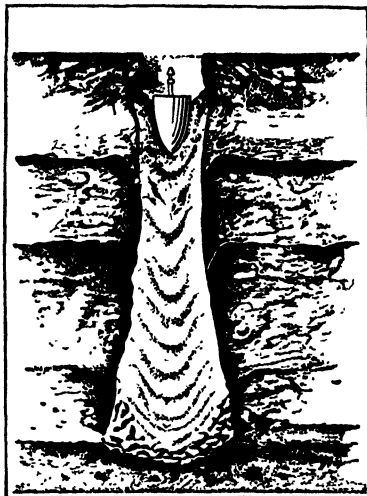
FIG. 11-9. Compaction of a slightly cohesive, granular soil layer by means of a Compressol type of sand pile.

The compaction of deep layers of natural soil can be successfully accomplished by means of sand piles, so long as the natural soil is of a fairly granular and permeable type. Figure 11-9 illustrates one such method which is based on a French cast-in-the-ground concrete pile of the Compressol type. It is now seldom used for its original purpose but can be successfully employed for the compaction of granular soils with some slight cohesion, as may be caused by capillary saturation and a slight silt or clay content. Only soils which will stand up when a heavy (2- to 3-ton) paraboloidal or conical steel weight is repeatedly dropped, so that it perforates a cylindrical hole to the desired depth, can be compacted in this manner. This has an over-all compactive effect, since much of the soil is displaced laterally. The hole is then backfilled in layers under continuous tamping.

In dry, clean sands, or below the ground-water table, casings have to be employed. The Franki type of cast-in-the-ground pile (see Fig. 15-9)

has been successfully tried out in such cases (Ref. 215). Sand instead of concrete is used, so that the objections raised against this type of concrete pile (see Art. 15-7) are no longer valid.

11-5. Soil Compaction by Vibrations. Experiments have shown that only noncohesive soils are strongly affected by vibrations (Art. 18-4) and can therefore be efficiently compacted in this manner. Field experience substantiates this.

The compaction of deep layers of sand can be accomplished by means of the *vibroflotation* procedure of Steuerman (Ref. 143). A device is employed which is somewhat similar to a gigantic spud vibrator of the type used for the vibratory compaction of mass concrete. It consists of a 15-in.-diameter and 82-in.-long cylinder, inside of which is located an electric 1,800-rpm motor which drives a smaller inner cylinder mounted slightly off center. This eccentricity produces the vibrations. Hoses attached to the outer cylinder permit the operation of water jets at its upper and lower ends. The entire device is lowered into the ground from a lead-carrying crane. As it sinks into the ground, the water jets loosen up the sand around the cylinder and the vibrations shake it down. The resulting compaction is evidenced by the formation of a crater at the ground surface. Sand is added to fill up this crater. This procedure is repeated as the "vibroflot" is withdrawn to the surface. A very dense sand core with dense sand all around it results. The satisfactory operation of this device has been checked in relatively clean sands (Refs. 215 and 143). It does not appear to be effective in silty sands, possibly because the reconsolidation by vibrations of the less permeable soil, after it is loosened up by the water jets, cannot occur rapidly enough. Better results can therefore be expected in silty sands from sand piles which are molded by impact (see Art. 11-4).

It is difficult in practice to combine advantageously the effects of vibrations and of rolling for the compaction of fills. Pneumatic-tire rollers are the most efficient type for the compaction of large masses of sand fills. Sand is the only type of soil which can be effectively compacted by vibrations. At the same time, the interposition of any type of springs between the vibrator and the soil, including pneumatic tires, is likely to dampen the vibrations. Most of the vibratory energy will then be dissipated by the springs, without contributing to the compaction of the soil (see Tschebotarioff, Ref. 8, 1946). This forecast was proved correct when a manufacturing concern unsuccessfully attempted to combine a vibrator with a heavy tire roller. Some successful experiments, however, have been made with vibrators attached to steel platforms, sometimes flat, but usually curved up at the edges, so that the platform would not bury itself in the sand as it is moved about. Small units of this type

with one-mass vibrators (Art. 18-3) were successfully employed in Michigan for the compaction of sand backfills behind retaining walls (Ref. 160, 1948). A somewhat larger unit was developed by the Vibro-Verken of Stockholm, Sweden, (1947). It weighs 3,300 lb and is provided with a two-mass vibrator (Art. 18-3) which can be inclined, permitting the self-propulsion of the entire platform-sled type of unit when desired.

Vibrators of this kind are likely to prove very useful for the compaction of sands in locations inaccessible to heavier equipment. Otherwise, for large areas and masses of sand fills, a small number of load repetitions (passes) by a heavy roller is likely to achieve the same result at a smaller cost (see Art. 18-4).

Some moderately successful attempts have been made to compact fully saturated deposits of natural sand by the detonation of explosives in boreholes (Ref. 219).

11-6. The Determination of the Soil Density in the Field. The usual procedure consists in removing the loose surface layer of a fill and then making a hole in the fill with a hand-operated auger. The soil extracted from the hole is carefully collected, sometimes in a special tray which is laid on the planed-off surface of the ground and which is provided with a hole in its center for the passage of the auger. The soil thus extracted is weighed both before and after drying in a field laboratory. The volume of the hole is measured to determine the volume which the soil originally occupied in the ground. From these data the dry density of the soil is computed (see Prob. 9-1).

There are three methods for the determination of the volume of the hole. One of them is illustrated in Fig. 11-10. Heavy oil is poured from a measuring cylinder into the hole. This procedure is quite simple but can be safely used only in fills with some clay content. In more pervious soils one has to use either a rubber balloon filled with water or uniform dry sand poured into the hole from a specified height from a calibrated receptacle, usually a gallon jar provided with a metal funnel (see Ref. 190).

11-7. Stabilization of Soil-fill Material by Mixing with Other Soils, Cement, Bitumen, or Chemicals. One way to improve the properties of a soil fill is to mix it with some other locally available soil, in order to obtain a desirable gradation. In the United States it is frequently desirable to obtain an A-1 or an A-2 type of soil (see Art. 12-11). In such a soil the skeleton is provided by the sand—addition of gravel is also beneficial—but there is just enough silt or clay to fill the voids and to bind the sand and gravel particles together. Swelling during wetting or shrinkage during drying are then reduced to a minimum. Soils of this type are of advantage for the construction of rammed-earth houses (Ref. 245).

In arid regions of the world conditions may be quite different. For instance, A. Mayer (Ref. 224, 1947) reported that in the French zones of the Sahara well-graded soil surfaces of desert roads were gradually worn down by traffic. The loosened particles of dry clay and silt were carried away by the wind, leaving only coarse sand and gravel at the surface, which then formed objectionable corrugations under continued traffic. Much better results were obtained by surfacing such low-cost roads with wetted-down and rolled silty clay.
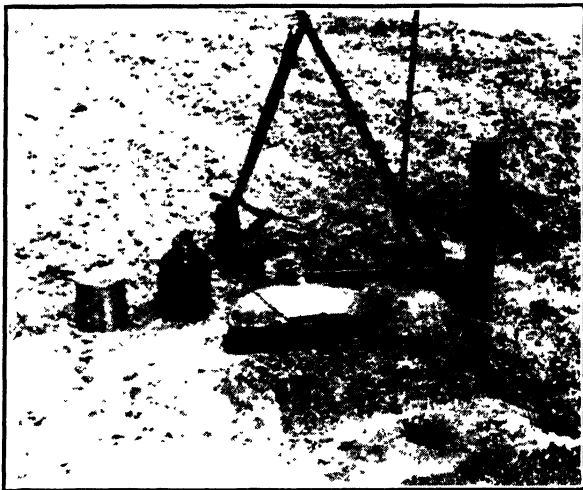
FIG. 11-10. The determination of the density of rolled-clay fill during the construction of the Inland Dam, Alabama. Equipment includes: syrup can with airtight top for carrying sample to the fire, gallon jug for No. 30 SAE motor oil, shovel with earth auger leaning against it, oil gun for salvaging some oil, rigid needle (handle above top of picture), beaker for measuring volume of oil poured into hole in the fill. (*After H. F. Peckworth, Ref. 264, 1939.*)

The mixing of clay soils with granular material requires the breaking down of the clay lumps, in order to permit the effective mixing of the two soils. The same requirement holds for all other forms of stabilization of fills by admixtures of any kind. Machines for the crushing and pulverizing of dry soils have been developed, but their effectiveness is limited to friable soil types.

Most soils can be effectively and economically stabilized by mixing them with cement. Thus soil-cement roads frequently have been constructed for light-duty service. The amounts of cement employed usually vary from 8 to 12 per cent of the soil by volume (Ref. 273). Preliminary tests are frequently needed to determine the amount of cement which should be added. These tests include the determination of the optimum moisture content and of the maximum density of the soil-cement mixture, as well as its compressive strength and durability.

Repetitional wetting-drying and freezing-thawing tests are employed in the laboratory to test the durability, in accordance with standards set up by the ASTM and the AASHO (see Refs. 273, 5, 10).

Cement stabilization is ineffective in soils with a high organic content or in soils containing substances, such as sulfur, which may produce a disintegration of concrete. Such substances may be strongly detrimental even when they are present only in the subgrade on which the soil-cement or concrete pavement is placed, since they can be accumulated in the pavement during dry seasons by the upward capillary movement of moisture from the subgrade and its subsequent evaporation near the pavement surface. The concrete pavement of an airport, built on a sulfur-containing subgrade, is known to have disintegrated (Ref. 442).

Bituminous-soil stabilization can be substituted under such conditions, since one of its effects is the waterproofing of the soil and the maintenance of the low water content essential for continued stability of cohesive soils. Cold-mixed asphalts in soils are, however, liable to be attacked by bacteria and, in time, may be completely eaten up. To prevent this, Winterkorn (Ref. 435, 1938) recommended the addition to bitumen of aniline furfural as a bactericidal agent. This admixture has been shown to have also a beneficial effect on the mechanical properties of submerged sand-bitumen mixtures (see Art. 18-4 and Ref. 383).

The stabilization of soils by the addition of artificial resins and other chemicals was intensively studied during the war, since it was found that very small amounts thereof could produce effective waterproofing of the soil particles, with a resulting improvement of the treated soil. Procedures of this type, by reducing the weight and hence the transportation costs of locally not available stabilization ingredients, therefore had special advantages in all remote and not easily accessible regions where roads or airports had to be constructed rapidly. The nature of the chemicals to be employed depends on the properties of the parent soil material and especially on the nature of the ions adsorbed on the surfaces of the soil particles (Art. 3-5). Preliminary treatment of the soil becomes necessary sometimes. In this entire field, which requires specialized knowledge of chemistry, the work of Winterkorn is particularly noteworthy (Refs. 443, 438, 435, 439, 444).

A general characteristic of modern chemical soil-stabilization methods is the need for partial drying of the chemically treated soil before the treatment becomes effective.

11-8. An Unusual Case of Accidental Underwater Stabilization of a Natural Clay Deposit and Its Implications

This case is illustrated in Figs. 11-11 and 11-12. During a laboratory study by Tschebotarioff (Ref. 395, 1948) of samples from the site of a proposed new dock, a large pocket of silty clay was encountered which had very unusual properties. The

pocket extended 600 ft in one direction and at least 300 ft at right angles to it. It was only some 17 ft deep. Within that layer the silty clay soil had a very high natural water content, which varied from w_n = 100 per cent to w_n = 169 per cent. The corresponding liquid-limit values were also quite high, varying from w_L = 140 per cent to w_L = 220 per cent. The plastic limits varied from w_P = 70 per cent to w_P = 170 per cent. The unusual features lay in the high shrinkage limits w_s = 60 per cent to w_s = 125 per cent, and in the very high values of the unconfined compressive strengths (Fig. 11-11). Thus a sample with w_n = 169 per cent and w_L = 174 per cent failed at 4.0 per cent strain (brittle failure, see Art. 7-10) under a unit pressure q_u =
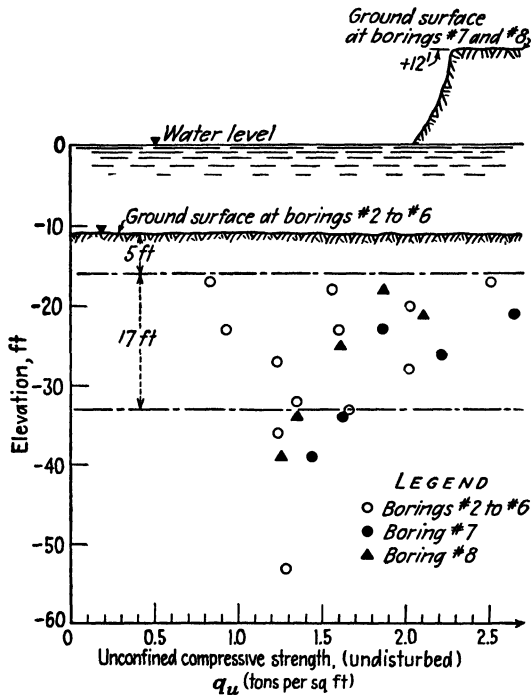
FIG. 11-11. Unusually high strength values within a 17-ft-thick layer of unpreconsolidated natural clay (see corresponding water contents, Fig. 11-12). (From Tschebotarioff, Ref. 395, 1948.)

2.65 tons per ft². The sensitivity to remolding was considerable S = 5.5 and S' = 17.7 (see Art. 7-22). The sample had only 30 per cent clay-size particles; 40 per cent were silt and 30 per cent sand. The time-compression curves in a consolidation test were almost straight lines.

It was noticed that all samples which exhibited these unusual properties contained small pockets of a white substance which within a few minutes after exposure to air changed its color to light blue. The material was tentatively identified by E. Sampson, Professor of Geology at Princeton University, as *vivianite* on the strength of visual inspection and X-ray analysis. This provided a clue for the further study of the case. Professor N. H. Furman found a considerable quantity of phosphates in the soil samples. This confirmed the identification, since vivianite contains up to 27 per cent phosphates (P_2O_5). It also contains up to 35 per cent iron oxides (Fe_2O_3) and FeO.

These substances were believed by Winterkorn to have caused the underwater cementation of the soil grains which produced the unusual combination of high strength and very loose structure. An attempt to reproduce such conditions artificially was then undertaken by E. Sampson, Jr., in Winterkorn's soil physics laboratory (Ref. 298, 1950). It is possible that further studies may lead to a practical method of underwater stabilization of hydraulic fills.

One more characteristic of this unusual natural soil should be mentioned. Although the overburden pressure of some samples had not exceeded 0.45 ton per ft² at any
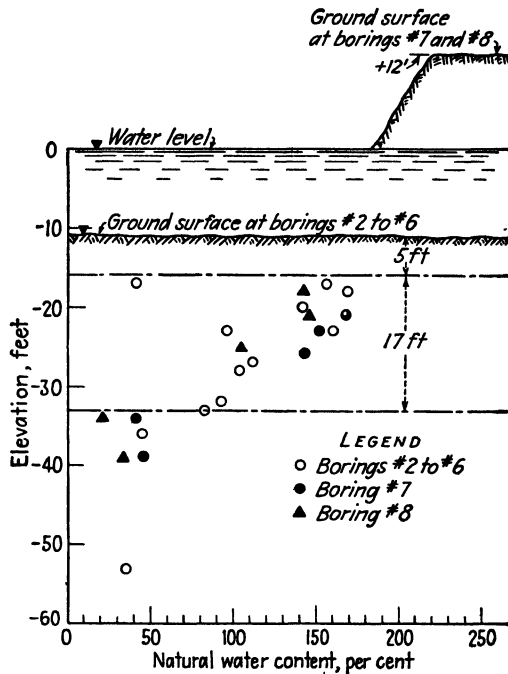
FIG. 11-12. Unusually high water content values within a 17-ft-thick layer of unpreconsolidated natural clay (see corresponding unconfined compressive strengths, Fig. 11-11). (From Tschebotarioff, Ref. 395, 1948.)

time of its past history, and the soil had never been exposed to drying, the preconsolidation load could be 12.5 times higher, as high as 5.7 tons per ft² (Ref. 395). This shows that the preconsolidation load, contrary to present conventional beliefs, may be strongly affected by factors other than forces produced by gravity or by capillarity during drying (see Art. 6-4).

11-9. Treatment of Natural Soils by Injections or Impregnation.

Cement or chemicals can be successfully injected into a soil only if the soil is sufficiently pervious to permit the easy passage of the solution or if it contains cracks which require filling.

An example of the injection of cement, known as *grouting*, is the treatment of railway roadbeds described in Ref. 35. Soft spots are sometimes

formed in the clay subsoil on which rests the crushed-rock or stone ballast of the roadbed proper. A slight depression in the subsoil surface is liable to become filled with water, which then produces a mushy condition at the contact surfaces between subsoil and ballast. The latter is pressed into the mushy subsoil by the repeated passage of trains, and the depression is thereby enlarged. An effective remedy is provided by the pressure grouting of these soft spots with cement slurries. These displace the soft mush and transform the ballast filling the depression in the subsoil into concrete.

Cracks may form during prolonged drought seasons in recent embankments for which rich clay was used. Cement injections into such cracks may prevent later instability resulting from the filling of such cracks with water during a subsequent rainy season. Proper initial compaction should, however, render such expensive remedial measures unnecessary in most cases.

Cement grouting of cracks to render them impervious to the passage of water is used as a matter of routine in the treatment of rock under and around the foundations of dams, especially when the rock is composed of limestone or dolomite and is therefore liable to have large open seams. Techniques of this kind have been successfully applied for the dams of the Tennessee Valley Authority (Refs. 334 and 335).

The injection of chemicals for the improvement of the mechanical properties of a soil can be successfully performed only in pervious soils, such as sands. Even so, a very close spacing of the injection pipes is required—approximately 12 in. on centers—if the entire mass of the soil is to be impregnated (Ref. 269). Otherwise the injected fluid is liable to follow the paths of least resistance to flow, that is, more pervious seams, which are not necessarily the least resistant parts of the soil mass in respect to compression or to shear. Such chemical treatment of a soil is therefore rather expensive and is seldom used on a large scale for routine construction purposes. It does, however, have advantages in some special cases where local treatment of sand seams is desired to simplify excavation operations or, in lieu of underpinning (Art. 15-13), for the widening of the bases of foundations. An example is provided by a case where a layer of completely dry sand was unexpectedly encountered during the driving of a tunnel. The dry sand trickled through the smallest openings in the timbering, thereby greatly increasing the pressures thereon, since the sand movements destroyed all relieving effects of arching (Art. 16-19). Stabilization of the dry sand by chemical injections through pipes driven ahead of the tunnel face was then successfully undertaken (Ref. 448).

Two types of chemical injections may be performed. In the first type,

of which the Joosten process (Ref. 194) is representative, two solutions of chemicals, usually sodium silicate and calcium chloride, which form a gel when brought into contact with each other, are employed. The first chemical is pressed into the ground as the injection pipe is driven in, and the second chemical while the pipe is pulled out. In the second type only one solution is employed, which is designed to begin hardening after a given period of time (Ref. 269).

Impregnation of a soil from its surface may be successfully resorted to when it is desired to improve the properties of a relatively thin upper layer. For instance, the 10-in.-thick lining of a calcium type of clay originally used in an artificial lagoon during the San Francisco International Exposition (1939) was found to permit seepage losses of the fresh water in the lagoon of 1.00 in. per day. By allowing salt water to percolate for a while through the lining, the calcium clay was changed into a sodium clay (Art. 3-5), and the seepage dropped to 0.10 in. per day. This happened because the thicker films of adsorbed water on sodium ions, as compared with calcium ions (Art. 3-5), filled the voids and blocked the passage of free water.

Recently Winterkorn (Ref. 444, 1950) improved the bearing properties of beach sands by impregnating them from the surface with suitable chemicals under simultaneous densification by vibratory "massage," using a platform-sled-type vibrator.

Practice Problems

11-1. During a field density test the volume of the hole made in a moist sand prior to its compaction was found by one of the methods outlined in Art. 11-6 to be $V = 0.072$ ft³. Prior to drying, the weight of the sand extracted was $W = 7.25$ lb, and after drying $W_s = 6.78$ lb. Determine the dry density γ_{md}, the water content w_n, the void ratio e (assume $G = 2.65$), and the porosity n.

Answer. The dry density is

$$\gamma_{md} = 6.78/0.072 = 94.2 \text{ lb per ft}^3$$

The weight of water is

$$W_w = 7.25 - 6.78 = 0.47 \text{ lb}$$

The water content is

$$w_n = (0.47/6.78) \times 100 = 6.9\%$$

From Eq. (4-6) and (4-10),

$$e = \frac{62.4 \times 2.65}{94.2} - 1 = 0.755$$

From Eq. (4-3),

$$n = \frac{0.755}{1 + 0.755} \times 100 = 43\%$$

(See Prob. 4-7 for the determination of the relative density of this sand.)

11-2. How many passes by a Barco-type portable gasoline rammer (Fig. 11-8) will be needed to develop an amount of compactive energy equal to that of a standard

Proctor test if the field compaction is to be performed in 6-in. layers and there will be 50 per cent overlap of the rammer imprints at each pass?

Answer. According to Art. 11-4, the energy developed by one drop of the rammer is 240 ft-lb, and the contact area of its foot with the soil is 0.492 ft². Hence, compactive energy for one pass will be

$$\frac{240 \times 12}{0.492 \times 0.50 \times 6} = 1{,}960 \text{ ft-lb per ft}^3$$

The compactive energy of a standard Proctor test, according to Table 11-1, is 12,300 ft-lb per ft³. Hence, the number of passes needed will be 12,300/1,960 = 6.3 passes.

References Recommended for Further Study

Technical Bulletin of the American Roadbuilders' Association, No. 109, 1946. (1) "The Use of Heavy Equipment for Obtaining Maximum Compaction of Soil," by O. J. Porter. Description of early and modern types of rollers; points of practical importance for effective compaction of rolled fills. (2) "Vibratory and Impact Compaction of Soils," by Gregory P. Tschebotarioff. Points of importance for the design and use of these special types of equipment.

"Soil Tests Shown Graphically," by W. J. Turnbull and J. L. McRae, *Engineering News-Record*, May 25, 1950, pp. 38–39. Methods of analysis of the results of compaction tests.

"Soil Stabilization," by Hans F. Winterkorn, *Proceedings of the 2d International Conference on Soil Mechanics and Foundation Engineering*, Rotterdam, Vol. V, pp. 209–215, 1948. Basic principles of the science and of the art of soil stabilization.

"Soil Cement Roads." Construction handbook published by the Portland Cement Association, Chicago, Illinois. Preliminary and control testing of soil-cement mixtures, both field and laboratory. Construction equipment and procedures.

"Current Road Problems." Series of pamphlets published by the Highway Research Board, Washington, D.C.: No. 5, "Granular Stabilized Roads"; No. 7, "Use of Soil-Cement Mixtures for Base Courses"; No. 12, "Soil-bituminous Roads."

CHAPTER 12

EXPLORATION AND CLASSIFICATION OF SOILS

12-1. Methods of Soil Exploration. There are two main subdivisions. *Surface surveys* form the first group. They include the study of geological maps and of available records of previous borings in the general vicinity of the proposed new construction site, from which a general idea can be formed about the subsurface conditions likely to be encountered. Airphotos can be of great help in selecting tentative locations for proposed new highways or airfields. Geophysical methods of soil exploration from the surface, namely, the seismic and the electric-resistivity methods, can give valuable data when it is important to ascertain the depth at which rock is located.

All surface surveys can give only approximate indications of the probable soil conditions at a site. Therefore they should be relied upon for preliminary investigations only, although it should be recognized that they provide very valuable data, especially for the rational planning of the necessarily slower and more expensive *subsurface exploration.* No important engineering structure should be designed without adequate data concerning the nature of the underlying soil. Such data can be obtained only by appropriate subsoil-sampling and -testing procedures. The samples can be obtained either from boreholes or from test pits; soundings provide additional, and sometimes essential, information.

These methods will be discussed in the subsequent articles of this chapter. The selection for a particular job of any one procedure should be based not only on the technical merits of the procedure itself, but also on the relative costs of the procedure as compared with the cost of the proposed structure. Thus an expensive method of subsoil exploration may be justified when used for the study of a site for a large new dam, both because its cost will form only a small fraction of the cost of the dam, and because the failure of a dam may have particularly disastrous consequences. The use of the same method may be unjustified, however, for some smaller and less vulnerable type of structure.
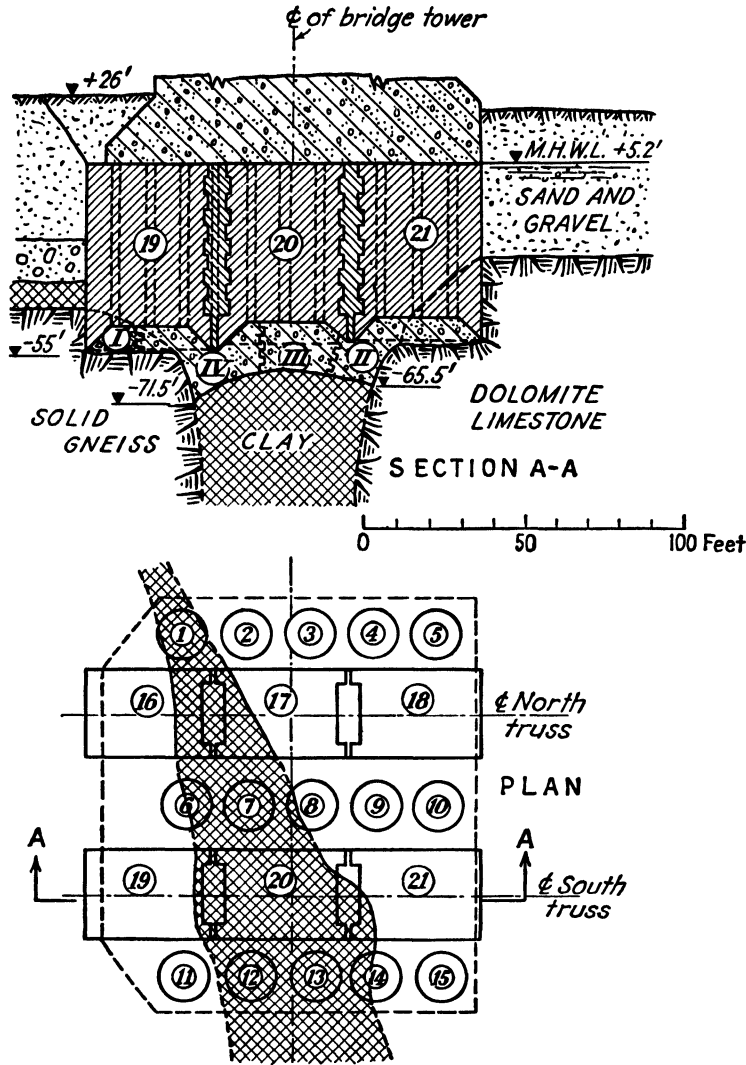
FIG. 12-1. An underground arch had to be concreted in the sequence (I), (II), (III), (IV) to bridge a clay-filled crevasse in rock beneath the compressed-air caissons of the Ward Island tower for the Hell Gate Bridge, New York. (*After O. H. Ammann, Ref.* 12, 1918.)

12-2. Study of the Geology of a Proposed Site. Such studies are always advisable; failure to undertake them at the right time may lead to considerable trouble later. Figure 12-1 illustrates such a case.

The foundation of the Ward Island tower of the Hell Gate Bridge in New York (Ref. 12, 1918) originally was to have consisted of a number of

separate caissons sunk by open dredging to rock. At the time the final location of the bridge was selected, the presence of a deep clay-filled fissure right under the bridge tower (see Fig. 12-1) had not been observed. Apparently it was missed by the preliminary borings. It therefore became necessary to sink the caissons with the help of compressed air (Art. 15-14) and to span the clay-filled fissure by means of an underground concrete arch on which the caissons then came to rest. The complicated sequence of the operations which thus became unavoidable is illustrated by Fig. 12-1. The bedding planes of the faulted rock were almost vertical at this location, and the fissure filled with clay had developed along the vertical plane of contact between two different types of rock—solid gneiss and dolomite limestone (Arts. 2-1 and 2-4). During the construction of the new Croton aqueduct in New York a similar fissured zone, filled with decayed rock, at a junction of schist and limestone was ascertained by means of an experimental tunnel and was then underpassed by means of an inverted siphon which carried the aqueduct tunnel some 300 ft below its original surface (Ref. 282).

Another case of serious trouble as a result of insufficient study of the geology of a site is illustrated by Figs. 12-2 and 12-3. The concrete dam could not be put into service because all the water in the reservoir behind it leaked out through sinkholes. Other similar cases are discussed in Art. 17-2. The way in which a *sinkhole* is formed is illustrated by Fig. 12-4. Water flowing through soil toward fissures in the underlying surface of cavernous limestone will gradually wash some of the soil through the rock fissures into the caverns below. An upper cavern will then gradually develop in the soil and will grow in size upward from the rock surface. When the roof of that second cavern becomes fairly thin, it will collapse under its own weight, forming a so-called sinkhole. A case where a footing of a factory shed over a newly formed sinkhole remained hanging by its column from the reinforced-concrete roof, which cracked and was deflected to form a catenary, as shown in Fig. 12-4, has actually occurred.

Seepage into the soil of industrial waste from defective, leaking sewers may accelerate the formation of sinkholes, especially if the underlying limestone is fissured by a fault. Carlton Proctor (Ref. 279, 1948) reports a case where an industrial plant in Tennessee was accidentally located right over such a faulted and fissured zone of limestone and suffered considerable and recurring damage because of the formation of sinkholes beneath it. Expensive cap grouting by a 1:1:8 mixture of cement, bentonite, and fine sand had to be resorted to, in order to seal off the surface of the fissured rock. A similar plant, located only a couple of miles away, did not have any sinkhole trouble. It was found that it lay out-
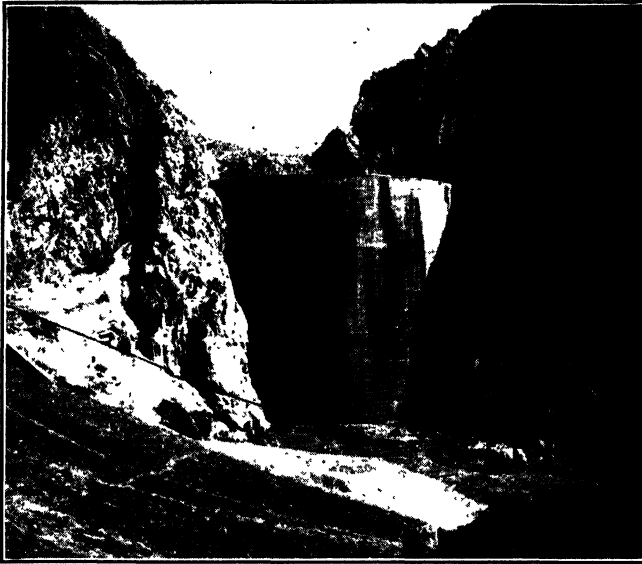
FIG. 12-2. An empty reservoir behind a concrete dam in Spain. The water leaked out through sinkholes of the type shown in Fig. 12-3. (*Courtesy of Professor Maurice Lugeon, Ref.* 218, 1933.)
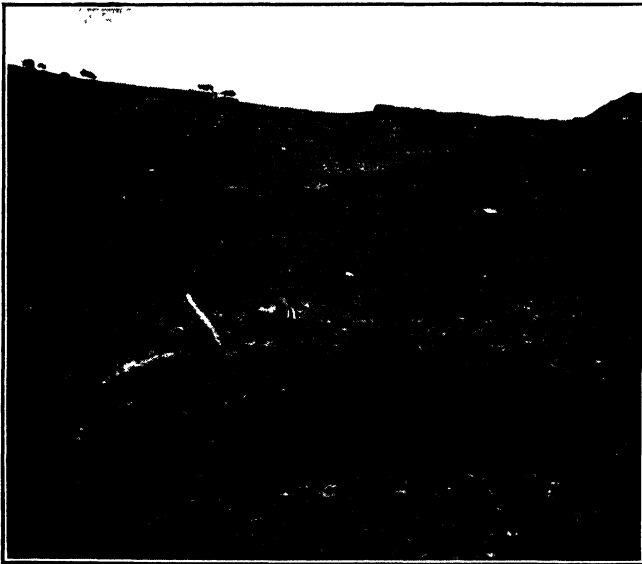
FIG. 12-3. A sinkhole in the bottom of the empty reservoir of the dam shown in Fig. 12-2. Cavernous limestone underlay the cohesive upper strata. (*Courtesy of Professor Maurice Lugeon, Ref.* 218, 1933.)

side of the fissured zone of the fault, and that an intact cover of shale protected the surface of the limestone there.

Geological advice can therefore be invaluable in the selection and exploration of sites of dams, tunnels, and other similar structures, and during their construtcion as well. Geological information, however, cannot be a substitute for soil tests. For instance, the geological age of a clay is not necessarily an indication of its probable stiffness. Clays of Devonian age, (Art. 2-1) may still be fairly compressible (Ref. 299).
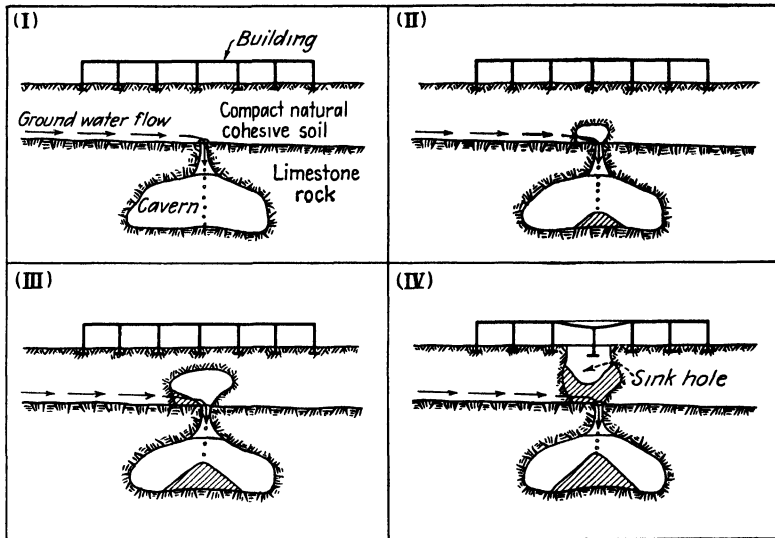
FIG. 12-4. Steps in the formation of sinkholes in cavernous limestone regions.

12-3. Airphoto Soil Surveys. A series of overlapping photographs taken from the air can be of considerable help in the preliminary selection of a route for a proposed highway or of the site for a new airport. The nature of eroded soil surfaces, the type of vegetation which grows on the soil, and many other features can be recognized from airphotos by a specially trained and experienced observer and can then be interpreted for identification of the underlying soil (see Ref. 189). A thorough knowledge of geology, geomorphology (the study of land forms), pedology (Art. 2-8), and soil engineering, and experience in the art of such identifications are needed to permit successful interpretations of this kind.

12-4. Electrical and Seismic Methods of Soil Exploration. The first of these two geophysical methods of exploration consists in the measurement of changes in the electrical resistance of the soil. These measurements are performed with the help of electrodes placed at the ground surface. Dense rock has a very high electrical resistivity. In other

rocks and soils the resistivity decreases with the amount of salts contained in solution. Therefore, when the general nature of the underlying soil is known, for instance, from a few borings, the limits of certain soil layers close to the surface can be rapidly and inexpensively established with the help of electrical resistivity measurements. Thus, according to Shepard (Ref. 308, 1949), the electrical method is best suited for shallow explorations to depths not exceeding 100 ft.

The seismic method of soil exploration is employed for the purpose of determining the limits of soils of different density and, especially, the limits between soil and rock. The method is based on the fact that the velocity of compression-wave propagation increases with the density of the material. In soils it can vary between 500 and 8,000 ft per sec, whereas in most unweathered and sound rocks it exceeds 6,000 ft per sec and may reach values of 25,000 ft per sec (see Hvorslev, Ref. 181, 1949). Since the velocity of wave propagation through water is 4,700 ft per sec, it follows that the seismic method can be successfully employed for the determination of the depth to sound rock even when the rock surface is located below the ground-water level. The waves are usually induced by the explosion of a dynamite cartridge at the ground surface. They are picked up by several detectors placed at varying distances from the point of the shot and are all simultaneously recorded on the same film of an oscillograph. Studies of this kind should be carried out only by men with special training. According to Shepard (Ref. 308, 1949), they have been successfully used by the U.S. Engineers for the selection of possibly suitable dam sites by determining the depth of overburden to sound rock and the extent of rock weathering. Of course, borings are invariably performed later on the sites selected.

Once the nature of a soil material has been established by borings, it is possible to check later appreciable changes in its over-all density by comparing the changed velocity of wave propagation to the one measured originally. This procedure was employed in Germany during the preliminary studies of different possible methods of compaction of a natural loose deposit of clean sand (see Loos, Ref. 215, 1936). Prior to compaction of the deposit the wave-propagation velocity was 490 ft per sec; after its compaction by Franki-type sand piles (see Arts. 11-4 and 15-7) it increased to 1,410 ft per sec. Compaction of the clean sand by the vibroflotation method (Art. 11-5) increased the wave-propagation velocity to 1,540 ft per sec. According to a later personal communication (1949) to Tschebotarioff from H. Lorenz, for the study of profiles less than 325 ft long the waves were induced by dropping a 45-lb weight to the ground surface from a height of 6 ft. Explosives were used only for the study of soil profiles exceeding 325 ft in length at the ground surface. It was

found possible to study very short distances, approximately 100 ft, by using very sensitive recording instruments and inducing the shock waves by means of sledge hammer blows on a 4- by 4-in. steel plate laid on the soil surface.

Sometimes waves are induced by continuous vibration (see Art. 18-7). Interpretation is somewhat more difficult in the case of such vibrogram records than it is in the case of single shocks.

12-5. Soil Exploration by Means of Test Pits. Exploration of this type usually is performed to shallow depths only—10 to 20 ft. In pervious soils it is necessarily limited by the elevation of the ground-water table. Wellpoints (Art. 14-9) have to be used in such soils to lower the ground-water table if a test pit is to be carried below its natural elevation. The use of wellpoints is an expensive procedure, which is justified for soil surveys only in special cases, for instance, for exploration problems of a semiresearch character in connection with the design of important structures.

FIG. 12-5. Method of obtaining a "chunk" sample. (*After G. E. Bertram, Ref. 28, 1946.*)

Shallow test pits, however, are frequently dug "in the dry" in connection with highway and airport work when it is desired to obtain a large "chunk" of undisturbed soil and, in general, when one wishes to get, by direct visual examination, a better idea of the exact soil profile than is possible from the study of borehole records.

A method of obtaining such a "chunk" sample of cohesive soil is illustrated by Fig. 12-5. A trench is first dug around the "chunk" at the bottom of the pit, and the "chunk" is trimmed down to the desired size with a knife, 8 to 12 in. length of sides of cube. It is then cut off with a large knife at the plane *ABC* and covered with $\frac{1}{8}$ in. of paraffin to prevent loss of moisture by evaporation, if it is to be tested in the field laboratory on the site. In the case that shipment of the sample is contemplated, a better protection is needed. This can be provided as follows: A solid wooden box, with its two ends removed, is placed over the sample after it has been trimmed down on its sides, but before it has been cut off at the plane *ABC*. The sample should be trimmed to provide approximately $\frac{1}{2}$ in. free space between the soil and the walls of the box. Hot paraffin is poured into that space and allowed to cool and harden before the sample is cut off at the plane *ABC* and removed together with the box. Some of the exposed soil at the two free ends is then scraped off. Paraffin is poured into the space thus formed, and the lids of the box are screwed

down. The entire box is then placed, with a layer of saw dust all around it, inside of a larger wooden box, to prevent damage to the sample from shocks during shipment. One may obtain a "chunk" sample from the wall of a test pit by digging a small cavern into the wall, large enough to permit trimming of the "chunk" on all four vertical faces.

In the case of clean sands it is seldom attempted to take "chunk" samples as described above. Instead one usually determines the natural density of the sand by one of the procedures described in Art. 11-6. The material removed is weighed on the spot and is then shipped in a disturbed state to the laboratory for the determination of its densest and loosest states, the knowledge of which is necessary for the computation of its relative density (see Art. 4-6).

12-6. Soil Exploration by Means of Wash and of Dry Sampling from Boreholes. Shallow borings for highway and airport work are frequently performed by means of hand-operated *screw-type augers.* Dry clean sands excepted, most soils above the water table will permit the advancement of boreholes to 15 or 20 ft depth without any casing to support the walls of the hole and to prevent their caving in. The screw auger is used both for the purpose of advancing the hole and to bring up to the surface for examination disturbed specimens of the soil layers encountered.*

For greater depths, or for work at any depth below the ground-water level, it is necessary to provide support for the walls of the hole. This is usually done by means of steel tubes—casings (see Fig. 12-6)—which are driven into the ground with the help of a tripod, motor winch, drive hammer, and other accessories. The casing comes in lengths varying from 5 to 10 ft. It is driven into the ground up to 3 ft at a time, whereupon the soil within the casing is cleaned out before driving is resumed or dry sampling is undertaken. In countries where manual labor is very cheap and mechanical appliances are scarce, the cleaning of the casing frequently is done by means of weighted screw-type augers which are manually rotated by a team of laborers. Similarly, a team of laborers is often substituted for a motor winch to pull the drill rods with their augers or attachments up to the surface and to operate the drive hammer.

In the United States the casings usually are washed out, as illustrated by Fig. 12-6. A pump continuously forces water through the hollow drill rods and the openings of the chopping bit, which at the same time is repeatedly raised and dropped with the help of the motor winch, thereby churning up the soil inside the casing. The water then rises in the space between the drill rods and the casing and flows out through a tee into a tank on the soil surface. Particles of the churned-up soil are carried

* Augers and all accessories can be obtained in a box suitable for transportation in a car, for instance, from the Acker Drill Co., Inc.
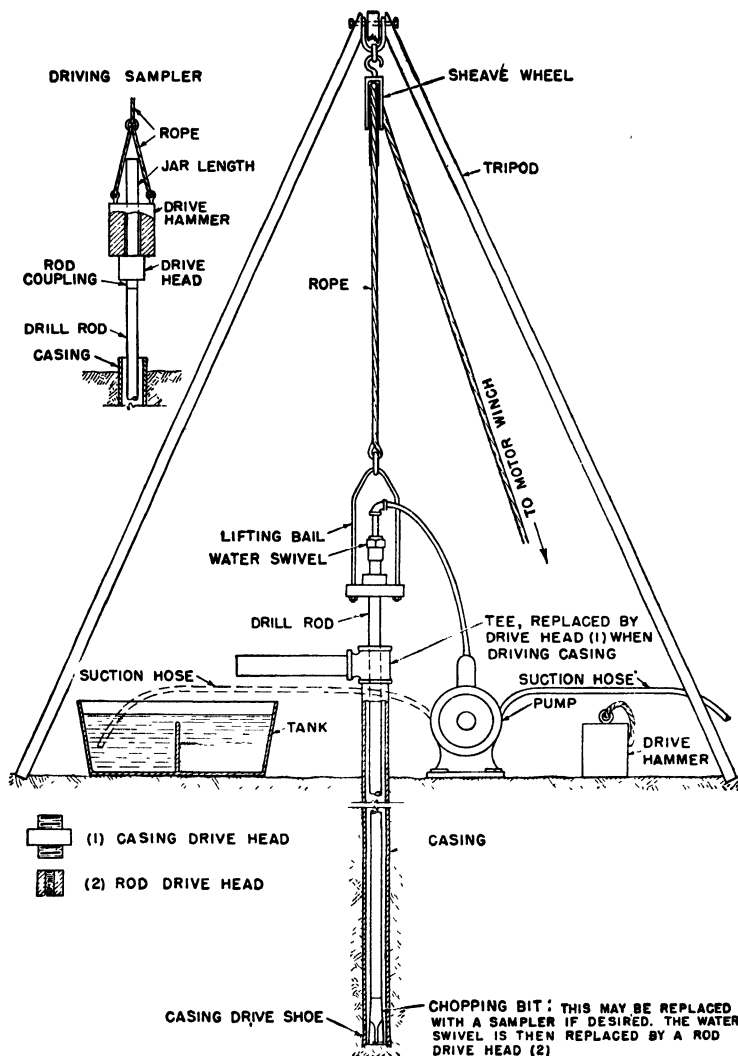
FIG. 12-6. The advancement of a cased hole by washing; the driving of split barrel samplers [Fig. 12-7(1)] for disturbed dry sampling. (*Courtesy of Sprague & Henwood, Inc.*)

upward with the water and are partially deposited in the tank. Careful observation of the wash water, as it comes up to the surface, can provide an experienced foreman with many useful indications concerning any changes in the soil layers which he is piercing. In the past, such observations of the wash water were sometimes extended to the preservation of soil samples periodically taken from the settling tank; this is known as *wash sampling*. Such samples can be extremely misleading, since most

of the fines are carried away from the tank with the water which overflows its rim, and since there occurs considerable mixing of soils from different layers before the wash water reaches the soil surface. The past practice of wash-sample borings, therefore, cannot be considered sound and should be abandoned entirely. Boreholes can and should be advanced with the help of wash water, where care should be exercised not to wash below the bottom of the casing, but soil samples should be taken by so-called dry-sampling or undisturbed-sampling procedures.

Dry sampling is somewhat of a misnomer, since the soil samples are taken from the ground approximately at their natural water content. The term is used to distinguish such samples from the samples taken from the wash water. A split-barrel sampler of the type shown in Fig. 12-7(1) is usually employed for the purpose. The flap valve is removed for all soils except cohesionless sands. This particular so-called S. & H. 1290S sampler (Ref. 324) is driven into the ground by means of a 300-lb drive hammer, dropped from a height of 12 in., and the number of blows per foot required to drive it into the soil is recorded. Such records provide useful indications concerning the soil density. There are other similar procedures (see Art. 12-9 and Table 12-1). After the sampler is pulled out of the soil and is brought up to the surface, the shoe and the head are unscrewed, and the barrel is split open along its seam. The soil it contains can then be examined and placed in properly labeled wide-mouthed glass jars with watertight and airtight screw tops, so that the sample will not dry out until it reaches the laboratory or the designing office for further examination and study. The jars should have a capacity of at least 8 oz. The samples obtained by this procedure give a good idea of the general nature and stratification of the soil layers penetrated. They permit general identification and classification tests (Art. 12-12), but their structure is much too disturbed to permit the determination of their strength or consolidation characteristics. If the knowledge of the latter properties is required, then so-called undisturbed sampling has to be undertaken.

The determination of the ground-water levels is a very important part of all soil investigations. The use of wash water for the purpose of advancing cased boreholes complicates the recording of the necessary data in cohesive soils. The casing is usually filled with water to its top, and it may take a long time until the excess water in the casing will seep out through its bottom and adjust itself to the natural water level in the surrounding soil. The same kind of difficulty will arise when drilling fluid is employed instead of a casing. Special standpipes should then be employed to observe the ground-water-level variations (see Art. 13-2).

12-7. Undisturbed Sampling from Boreholes. There is no such thing as a completely undisturbed soil sample extracted from a borehole. Some

deformations of the soil layers are unavoidable, even with the most carefully conducted sampling operations. The removal of a sample from the surrounding soil mass changes the stresses which had been originally acting at the boundaries of the sample, and this, in turn, may also cause its subsequent deformation, unless special precautions are taken. Therefore the term *undisturbed soil sample* is intended to mean a sample which has been disturbed so little that it can be used for the laboratory determination of the strength and consolidation characteristics of the natural soil in situ without any practically important errors.

The techniques of undisturbed sampling have undergone considerable modifications and improvements. During the 1930's emphasis was placed on the development of samplers which provided safeguards against the loss of the sample while it was being pulled up to the surface. To that end, the cutting edges of some samplers were provided with wire loops which could be pulled from the surface to cut off the bottom of the sample from the underlying soil mass. Other samplers permitted the pumping of air into the partial vacuum which was formed under the sampler as its upward withdrawal was begun (see Fig. 12-10); this relieved the suction at the bottom of the sample. Comparatively thick-walled samplers resulted. As a rule, they were driven into the soil in the way now used for dry samples only (Fig. 12-6).

An extensive 10-year study (1938 to 1948) of the problem of undisturbed sampling by M. G. Hvorslev (Ref. 181) led to the wide adoption of thin-walled samplers of the type shown in Fig. 12-7(2) and (3). Hvorslev's studies indicated that the best results were obtained when the samplers were pressed (Fig. 12-8) and not driven into the soil and when their so-called *area ratio* C_a, that is, the ratio of the area of the displaced soil to the area of soil sample, was reduced to a minimum (see Fig. 12-9).

$$C_a = \frac{D_w^2 - D_e^2}{D_e^2} \tag{12-1}$$

The thin-walled or *Shelby* tube samplers [Fig. 12-7(2)] were developed as a result of Hvorslev's studies.

These samplers usually come in three sizes of tubes: 2.0-in., 2.8-in., and 3.37-in. inside diameter, and in lengths varying from 18 to 30 in. The shorter length should be used with the smaller diameter tube; for the medium size a length of 24 in. appears ample. Attempts have been made to use tube lengths up to 54 in. in some soils, irrespective of the tube diameter (Ref. 232). The resulting economy of effort, when continuous sampling is required, does not appear always justified to the author, since

thin long tubes are likely to increase the disturbance of a sample because of the development of friction along the inner walls of the tube.

To decrease this friction the lower tip of the sampling tube is slightly bent in (Fig. 12-9). This relieves, during sampling, the friction along the outer cylindrical surface of the sample and the disturbance it causes,
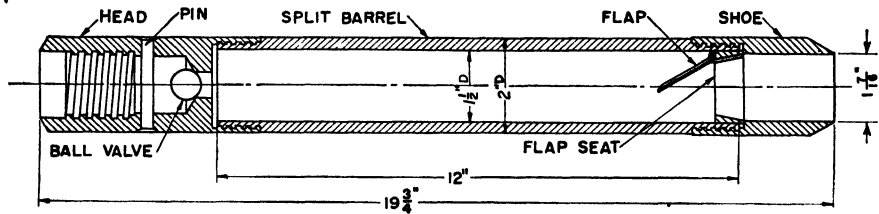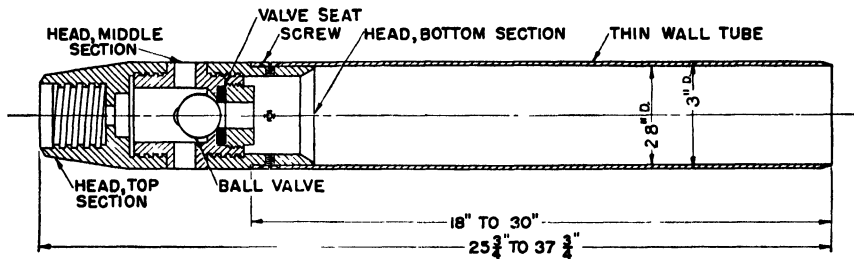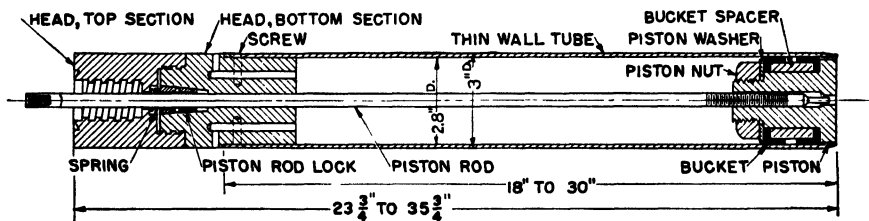
FIG. 12-7. Modern samplers (1) For disturbed dry sampling of all soils; (2) and (3) for undisturbed sampling of cohesive soils. (*Courtesy of Sprague & Henwood, Inc.*)

but also produces an opposite effect by permitting it to expand later, which is undesirable. Hvorslev recommends values of the *inside clearance ratio* C_i not exceeding 1.5 per cent for most soils and samplers, as producing the most desirable balance between these two opposite effects. (See Ref. 181 for further details and possible variations of this recommendation in different kinds of soil.)

$$C_i = \frac{D_s - D_e}{D_e} \tag{12-2}$$

The thin-walled tubes of the samplers are made of steel or of brass. Steel is less liable to buckle when pressed into stiff soils, but may corrode. Brass is easier to handle in the laboratory when it is necessary to cut off part of the tube and sample for testing while preserving the remainder.
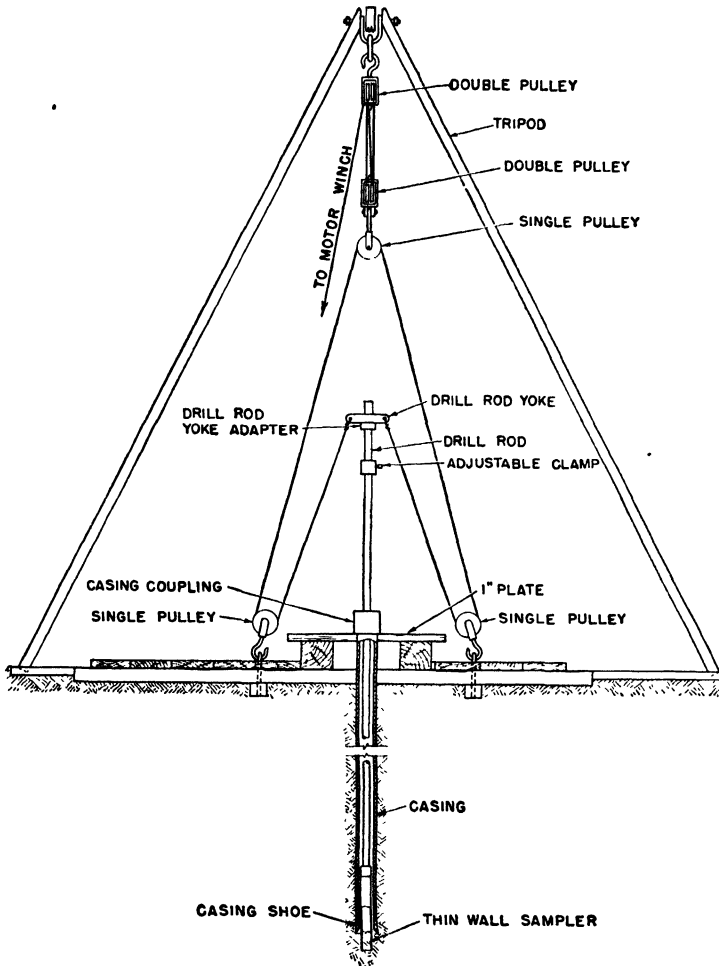
FIG. 12-8. For undisturbed sampling the samplers should be pressed, not driven, into the soil. (*Courtesy of Sprague & Henwood, Inc., Ref. 324.*)

As the sample tube is pushed a distance H into the ground, some of the soil may be displaced laterally and upward. As a result, the length L of soil in the sampler may be smaller than the distance H, (see Fig. 12-10). The ratio L/H is called the *recovery ratio* (Ref. 181).

A twist of the drill rod through 360° usually is sufficient to shear the

soil off at the lower tip of the sampler. The action of the ball valve at its top [Fig. 12-7(2)] will then help to prevent the sample from dropping out while it is raised to the surface. The samples almost invariably expand fairly rapidly, at least over part of their length, so that they adhere to the walls of the tube. This also helps to retain them in the tube during withdrawal.
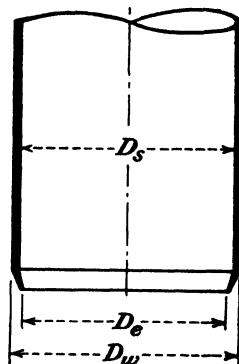
FIG. 12-9. Sketch illustrating the terms *area ratio* and *inside clearance ratio* of a sampler. (*After Hvorslev, Ref.* 181, 1949.)

In some cases this is not sufficient, and samplers of the *stationary-piston type* have to be resorted to [see Fig. 12-7(3), in which the piston is shown in the position it occupies before the start of the sampling]. After the assembly, as shown, is lowered to the bottom of the borehole and comes to rest on the soil, the piston rod is clamped at the soil surface, where it protrudes from the drill rod. The sampler tube is then pushed into the soil by means of the drill rod, past the piston, which remains stationary in space. During the withdrawal any relative movement of the piston and tube is prevented by a conical piston-rod lock.

Stationary-piston-type samplers were first used in Sweden. The clay there frequently is very soft, its shear strength ($q_u/2$) often varying between 0.1 and 0.2 ton per ft^2. The use of steel casing of the borehole is inadequate in such soft clays, since they are liable to be squeezed upward into the casing by the weight of the overlying soil. A stationary-piston-type sampler can, however, be pushed down from the surface through the soft clay to the elevation where one desires to take the sample. The clay is allowed to close over the sampler around the drill rod. The piston rod is then clamped at the soil surface, and the sampler tube is pushed past the piston into the soil to a depth sufficient to ensure that the lower half of the tube is filled with clay which had not been displaced and disturbed while the piston-tube assembly was being pushed down toward it. Long sampling tubes may be necessary in such cases.

FIG. 12-10. Sketch illustrating the term *recovery ratio* L/H of a soil sample and the cause of suction forces on the bottom of the sample. (*After Hvorslev, Ref.* 181, 1949.)

Irrespective of the type of sampler used, drilling fluid is frequently employed instead of steel casings in the south of the United States. The procedure is taken

over from the oil drilling industry. The composition of the heavy fluid is such that its lateral pressure is sufficient to prevent the walls of the borehole from collapsing or deforming excessively.

Hvorslev's studies of the effectiveness of different types of samplers frequently were performed on varved clays (Art. 2-7), photographs of which in a partially dried condition give a good record of the nature of the disturbance, if any, which they underwent during sampling. The photograph should be taken after the coarser grained silt varves have dried out sufficiently to change their original dark color to a light one (Art. 4-8), but before this has happened to the finer grained clay varves.
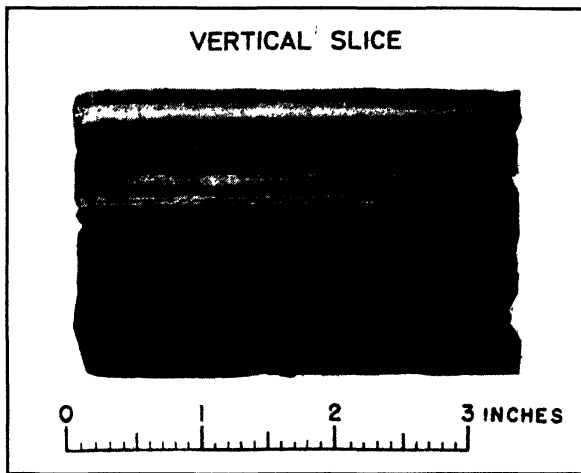
FIG. 12-11. Photograph of horizontally stratified, varved clay sample in perfect condition. *(From Tschebotarioff and Bayliss, Ref. 385, 1948.)*

This technique should be employed with all finely stratified soils as a routine laboratory control for the selection of suitable samples for strength and consolidation testing. It is fortunate that the varved clays, which are extremely sensitive to remolding, also photograph best (Art. 7-22).

Figure 12-11 shows a sample in perfect condition, which was taken with a thin-walled sampler. The stratification is horizontal, and a photograph of a vertical slice is therefore sufficient. Horizontal slices would all pass through the same varve and would therefore all be of the same color. A naturally inclined stratification would show up as parallel lines both on a vertical and on a horizontal slice of a really undisturbed sample. Figure 12-12 shows such a sample, which was extracted by a thin-walled sampler. On the other hand, any disturbance due to sampling operations will show up in the form of curved lines both on the vertical and on the horizontal slice (see Fig. 12-13 and compare with the data given by Prob. 12-1).

The method of partially drying and then photographing slices of soil samples, if anything of interest shows up, can frequently give valuable indications on points other than those related to the condition of the sample. For instance, the photograph shown in Fig. 12-14 indicated that the clay at a depth of 32 ft had been subjected to drying in the past.

The following precautions are advisable when taking undisturbed samples. Prior to sampling all loose and disturbed material should be
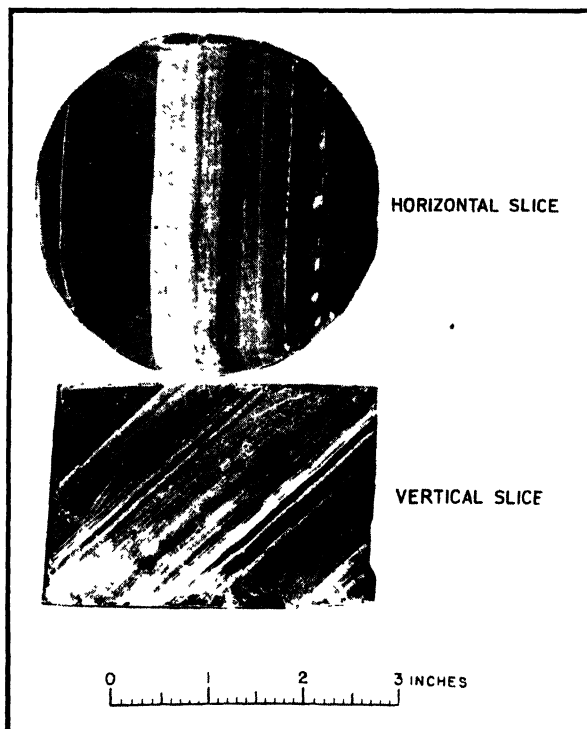
FIG. 12-12. Photograph showing the inclined natural stratification of a varved clay sample in perfect condition. (*From Tschebotarioff and Bayliss, Ref. 385, 1948.*)

removed from the casing down to the level of its cutting edge. A specially designed clean-out jet auger (Ref. 324) may be used for this purpose. Nevertheless, as an additional precaution, it is advisable to make laboratory strength and consolidation tests only on the lower half of the sample. After the sampler is brought up to the surface the soil-filled tube is disconnected from its head. The tube will serve as a container. All loose material should be removed from the upper end, and the soil at the lower end should be cut ¼ in. deep. The space between the ends of the sampling tube and the surface of the soil inside the tube is then filled

with hot paraffin. This is done first at the lower end of the tube. After the paraffin has cooled somewhat it will generally be found that a slight shrinkage crack has formed between the edge of the paraffin and the wall of the tube. A notch of triangular cross section, some 3⁄16 in. deep, is then cut all around the edge of the paraffin and is immediately resealed with hot paraffin to fill up the shrinkage crack. To that end, it is important to wipe away carefully any wet soil which may have adhered to the inside wall of the tube before the paraffining. The paraffin is to fill the entire
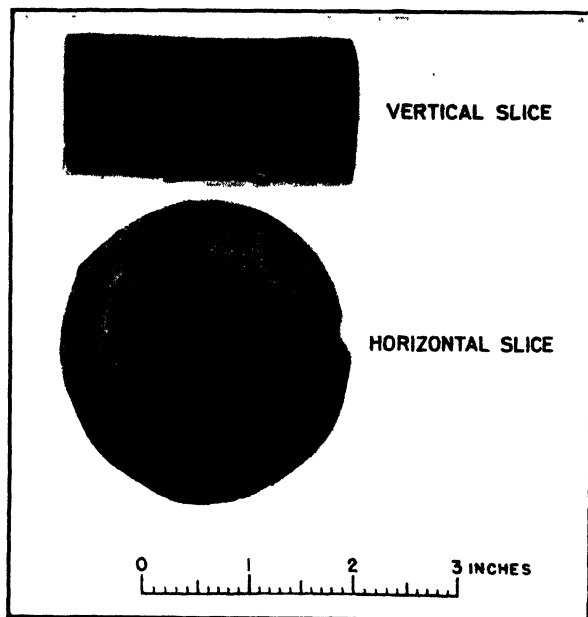
FIG. 12-13. Photograph showing the deflection of the natural horizontal stratification of a varved clay sample caused by the use of a sampler with somewhat too thick walls. (*From Tschebotarioff and Bayliss, Ref.* 385, 1948.)

upper end of the tube, down to ½ in. past the lowest of the screw holes by which the tube had been attached to the sampler head. Specially prepared, snugly fitting brass caps are then slipped over the ends of the tube. The joints between these caps and the tubes, as well as the screw holes, should be sealed by overlapping layers of friction tape. The tape should be brushed over with varnish or lacquer, extending over the surface of the adjoining metal. In this condition the clay sample can be expected not to lose any of its moisture for several weeks and even months.

The *sampling of sands* presents special problems. The provision of various types of valves at the bottom of the sampler has sometimes been undertaken for the purpose of retaining the sand sample in the tube during

the withdrawal of the latter through water to the surface; otherwise the sand would trickle out of the tube. All measures of this type increased the wall thickness of the tube and hence also the disturbance of the sand sample. Two recent developments have partially overcome this difficulty. The first originated at Vicksburg and is described by Hvorslev (Rev. 181, 1949). It was found that sand samples were retained in samplers of up to 5 in. diameter, provided the borehole was filled with
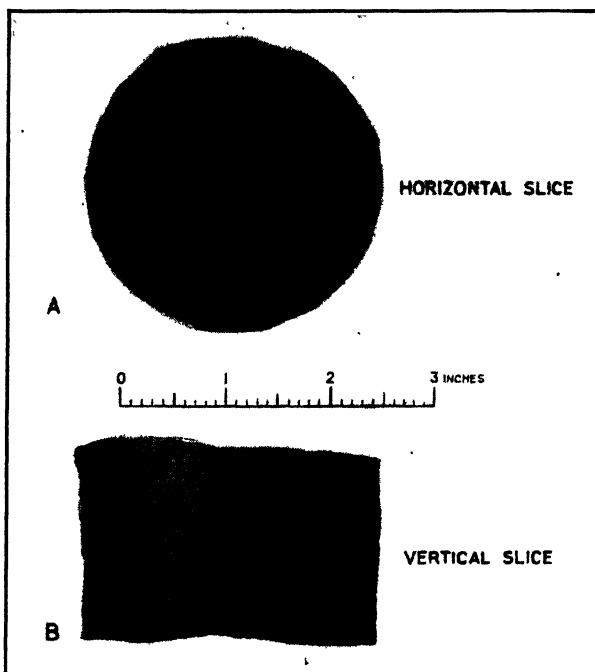
FIG. 12-14. Photograph of a Mississippi River clay sample extracted from a depth of 32 ft by means of a thin-walled sampler. Shows old shrinkage crack filled with sand in a subsequent flood. (*From an unpublished report by Tschebotarioff, 1946.*)

viscous drilling fluid. Apparently the fluid penetrated slightly into the sand surface and thereby provided a cohesive seal sufficient to prevent the trickling out of the individual sand grains. The remainder of the sand sample could then support itself in the tube by arch action (Art. 10-19). The second development occurred in England and is described by Bishop (Ref. 31, 1948). A special cylinder rests on the bottom of the borehole and surrounds the sampler tube. Compressed air is used to drive the water out of the cylinder, so that during the withdrawal of the filled sampler tube its lower face is no longer in water. The apparent cohesion (Art. 7-4) of the no longer fully saturated lower sand surface then helps

to seal off the rest of the sample. The natural stratification of the sand is preserved by these methods, but it is an open question whether its density is not changed by the pressing of the tube into the sand, especially if it was loose originally. The same objection applies to the method proposed by Fahlquist (Ref. 130, 1941) to retain sand samples by freezing the bottom of the tube. Since the freezing is done *after* the sampler is pushed into the sand, one "freezes" any disturbance one has created. Attempts to *first* freeze the sand ahead of the bottom of the casing and then to take a core (Art. 12-9) do not appear to have been made yet and would be complicated and expensive. For that reason penetration testing of sands (Art. 12-9) is still the most reliable method for the estimation of the natural density of sands in situ.

12-8. Core Borings. This type of boring is used when one wishes to penetrate into rock and to obtain a continuous core sample thereof. The type of equipment which is employed for this purpose is illustrated by Figs. 12-15 and 12-16. The machine operates on principles somewhat similar to those of the drill presses which can be seen in most machine shops. The engine A rotates the drill rod H by means of the bevel-gear drive E and the drill-rod chuck F. The outer core barrel K rotates with the drill rod. It is pressed down onto the rock surface by means of the hydraulic swivelhead D. A bit L, studded with industrial diamonds X, is mounted at the end of the core barrel and cuts a cylindrical ring into the rock leaving within that ring a cylindrical core of intact rock. As the bit cuts further into the rock, the rock core is free to move into the inner core-barrel head J, which is suspended on ball bearings and therefore does not have to follow the rotary motion of the outer core-barrel with its bit. Cooling water is circulated by the pump M through the hollow drill rod. A length of several feet of rock core can be obtained in this manner. As the withdrawal is begun, a split conical ring, the so-called core lifter V, wedges itself around the bottom of the rock core and thus permits it to be torn from the underlying rock. Cores as small as 1 in. in diameter can be obtained. Heavier machines than the ones shown in Figs. 12-15 and 12-16 have to be used if cores of more than a few inches in diameter are to be obtained. For the exploration of the sites of some important dams very large cores have been taken, leaving holes of 30 in. diameter into which geologists could be lowered for visual examination of the rock formation along the entire depth of the hole.

Attempts have been made to apply the procedures of core boring to the undisturbed sampling of clays (Ref. 181). The inevitable slight swaying of the rotating drill rod, when sampling at some depth, is, however, liable to disturb the clay core, unless it consists of stiff material not particularly susceptible to remolding.
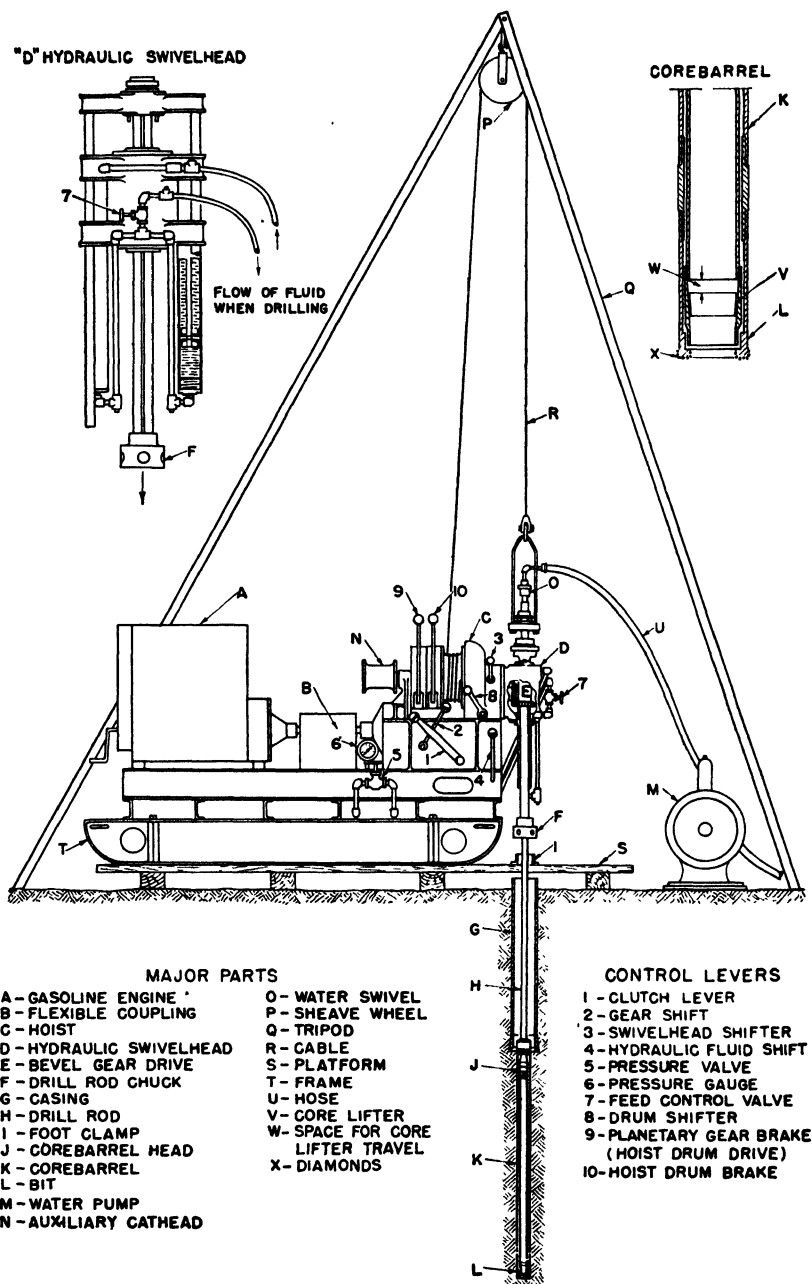
FIG. 12-15. Cross section of the core-boring machine shown in Fig. 12-16. (*Courtesy of Sprague & Henwood, Inc.*)

12-9. Soundings and Penetration Testing. The simplest type of sounding consists in driving a steel rod into the soil for the purpose of determining the elevation of the underlying rock surface. The results can, however, be very misleading, since individual boulders may be mistaken for solid rock. For this reason some city building codes in the United States require penetration into rock for depths varying between 5 and 10 ft by means of core borings (Art. 12-8).

Another type of sounding, the so-called drop-penetration testing, consists in driving a steel rod for a few feet into the soil at the elevation of the
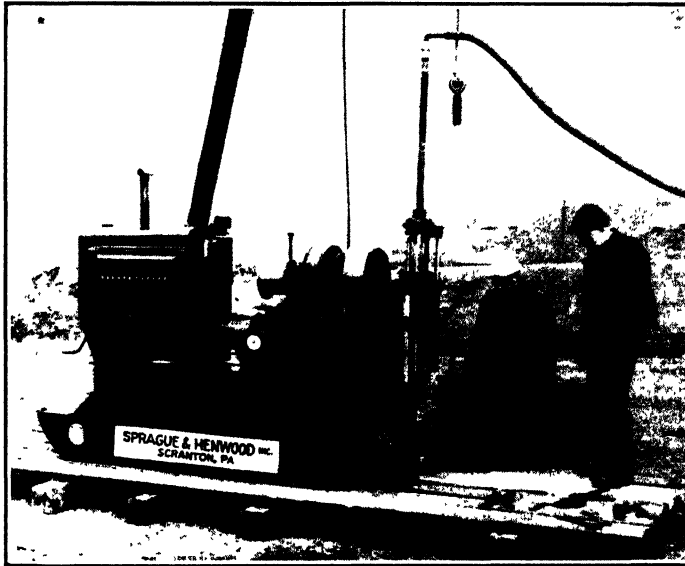
FIG. 12-16. Photograph of the core-boring machine shown in cross section in Fig. 12-15. (*Courtesy of Sprague & Henwood, Inc.*)

proposed foundation footing and judging the soil density from the number of blows which were required to drive the rod 1 ft. This type of test is not particularly reliable, since it provides information only concerning the few upper feet of the soil immediately beneath the footing. At greater depths, friction along the length of the rod tends to obscure the significance of the driving record in respect to the density of the consecutive soil layers penetrated by the rod. The method can, however, be of some use where light structures, such as factory sheds, are to be supported by small separate footings. It permits the rapid recording of the data obtained and their comparison with the later performance of the structure.

This was not the case in the quite recent past, when even more primitive procedures were in general use for foundation design. For instance,

G. W. Kirkland (1949) in a discussion of Ref. 268, reminisced on the point as follows: "His earliest experience of the science was to visit a site accompanied by a chief, who dug his umbrella into the soil and had said: '2-½ tons per sq. ft.'"

This kind of approach was more of a rule than an exception until quite recently. To keep a record of his experiences, the Philadelphia engineer Frank N. Kneas began testing granular soils down to a depth of 4 ft by means of a 1-in. solid steel rod which was driven into the soil by a 25-lb hammer dropped from a height of 36 in. The hammer had a hole in its center, so that it could slide on the rod until it hit a flange welded to the rod. The weight of only 25 lb permitted the lifting of the hammer by hand. Kneas' experiences are summarized in Table 12-1.

TABLE 12-1. Drop-penetration Records and the Soil-contact Pressures Structures Studied by F. N. Kneas*

Number of blows of 25-lb weight falling 36 in. on solid 1-in. rod

	Building on granular soil type:				
	A	*B*	*C*	*D*	*E*
Blows for 1st foot penetration	22	19	10	5	3
Blows for 2d foot penetration	30	34	24	9	10
Blows for 3d foot penetration	52	39	40	16	13
Blows for 4th foot penetration	62	28		26	16
Pressure p on the soil, tons per ft^2	6.0	6.0	4.5	3.0	2.0

Soils *A*, *B*, and *C* were compact sand and gravel soils at Philadelphia.
Soil *D* was a sandy soil at Atlantic City, New Jersey.
Soil *E* was loose glacial sand and gravel in the northern part of Pennsylvania.
* Ref. 199, 1937.

It should be emphasized that tests of this kind can be satisfactorily performed only to a shallow depth. Hence (Art. 9-8) they are of use only under conditions similar to those of the building shown in Fig. 12-19, that is, when the soil is granular and of approximately the same compressibility at the surface and at a greater depth. This last fact can be ascertained only by borings. Hence it is advisable to combine drop-penetration testing with the boring and sampling operations.

It therefore has now become customary to record the number of blows which are required to drive a dry-sampling spoon (Art. 12-6) 1 ft into the ground. There are, however, several procedures involving different types of spoons, weights, and heights of drop of the hammer. All these data should therefore always be reported on any spoon-driving records. Some of the existing procedures are summarized in Table 12-2. Special

TABLE 12-2. Some Proposed Correlations of Penetration Resistance and Soil Properties*

Extreme caution should be exercised in using any table of correlations outside the areas or for other conditions than those for which the correlations have been established; even then large deviations from such correlations have been reported. The penetration resistance depends not only on dimensions of the equipment and the consistency or relative density of the soil, but it may also vary with the method of operation, depth below ground surface, and other factors not yet fully investigated.

Author	H. A. Mohr		Terzaghi and Peck		New York City code		New England Div., C.E.	
Sampler	1-in. extra-heavy pipe 1.315-in. OD, 0.957-in. ID		Raymond 2.0-in. OD, 1.375-in. ID		2.50-in. OD		3.00-in. OD	
Hammer	140 lb ±, 30-in. ± fall		140 lb, 30-in. fall		300 lb, 18-in. fall		300 lb, 18-in. fall	
Soil	Designation	Blows per ft	Designation	Blows per ft	Designation	Blows per ft	Designation	Blows per ft
Sand and silt, relative density	Loose	Less 9	Very loose	Less 4	Loose	0–15	Very loose	Less 8
	Firm	9–13	Loose	4–10	Compact	16–50	Loose	8–16
	Hard	14–49	Medium	10–30	Very compact	Over 50	Medium	16–55
	Hardpan	Over 50	Dense	30–50			Compact	55–110
			Very dense	Over 50			Very compact	Over 110
Clay, consistency	Soft	Less 5	Very soft	Less 2	Very soft	0–2	Very soft	Less 8
	Medium	5–10	Soft	2–4	Soft	3–10	Soft	8–16
	Hard	11–30	Medium	4–8	Stiff	11–30	Medium stiff	16–55
			Stiff	8–15	Hard	Over 30	Stiff to medium hard	55–110
			Very stiff	15–30			Very hard	Over 110
			Hard	Over 30				

* From M. J. Hvorslev (Ref. 181, 1949).

Note: The S. & H. (Sprague & Henwood) procedure referred to in Figs. 12-18 and 12-19 is similar to the Raymond procedure described by Terzaghi and Peck. The dimensions of the S. & H. 1290S sampler [see Fig. 12-7(1)] are almost identical to those of the Raymond sampler; the hammer weighs 300 lb ±; a 12-in. ± fall is used; the energy is thus 86 per cent of that obtained by the Raymond method.

attention is drawn to Hvorslev's cautionary remarks, which form part of that table; they are fully justified. Particularly unreliable are the attempted correlations of the consistency and density of cohesive silts and clays and the driving record. Undisturbed sampling of such soils (Art. 12-6), followed by laboratory testing, should be resorted to in all cases where the knowledge of the shearing strength or of the consolidation characteristics of the cohesive soil is essential.

Driving records of the dry-sampling spoons nevertheless are extremely important, if only as an approximate indication, in all cases involving the density of granular noncohesive soils, that is, of sands and fine gravels. These records should always be obtained in such cases. They are much more important than the driving record of the casing, since the latter reflects the over-all average frictional resistance of all overlying layers already penetrated by the casing.

Dry samples are usually taken at 5-ft intervals of depth or at elevations where the wash water indicates a change in the soil material encountered. Attempts have been made to obtain an uninterrupted record of the resistance offered by the soil to penetration by a conical point pressed into the ground. Figure 12-17 illustrates several types of cones which have been developed for this purpose. Type I was developed by Terzaghi. A pressure gage registers at the soil surface the resistance P of the cone point (D = 2.75 in.). The stated purpose (Ref. 365) of the loosening of the sand by the water jet above the cone point was "to eliminate the influence of depth," since the resistance of sands to penetration by a cone is likely to depend on the depth below the soil surface, in addition to the density of the sand. It is, however, questionable whether the water-jet action can entirely eliminate the effect of depth, since the sand immediately below the cone is still stressed by the lateral pressures which originally existed in the deposit. A similar partial relief of the stresses which were originally present in the soil immediately above the cone point will also occur during the use of all the other cone points illustrated in Fig. 12-17.

The cone point of type II shown in Fig. 12-17 is most frequently used. For instance, its use was reported almost simultaneously (1936) for small-sized (D = 1.4 in.) static penetration soundings in Holland (Ref. 107), and for the driving of much larger sized test piles in England (Refs. 183, and 267), where this method of soil exploration has become known as *pre-piling*. In either case one can obtain either the resistance P of the cone point—by pressing the point or by driving it from the surface, by means of the inner shaft R, ahead of the outer pipe T—or the total resistance $(P + F)$, including the friction F along the pipe T, if that pipe is used to force the cone point into the soil. Usually one alternates the two above methods every foot or so.

The cone point of type III shown in Fig. 12-17 is a recent improvement of the Delft Soil Mechanics Laboratory, Holland, to minimize the danger that soil grains may wedge themselves between the shaft R and the tube T, when the latter is pushed down. In the position shown in Fig. 12-17(III) the shaft R has been pushed down the amount b ahead of the tube T. It can be pushed down only the distance a before the maximum distance L of its independent movement is reached.

The cone point of type IV shown in Fig. 12-17 was used by DeBeer in Belgium (Ref. 103). Only a short length H' of the tube T was of the
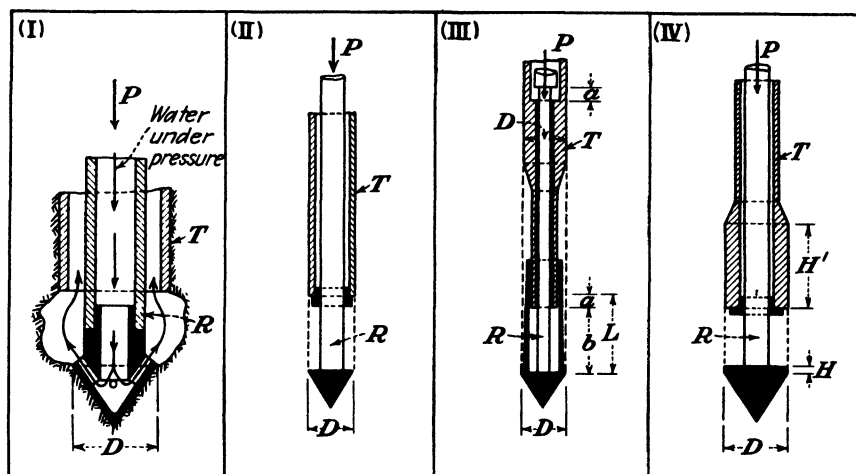
FIG. 12-17. Some cone points for deep soundings. (I) Terzaghi (1928) wash-point penetrometer (Ref. 365). (II) Conical point used both for drop-penetration testing (driving) (Ref. 183, 1936) and for static penetration testing (Ref. 107, 1936). (III) Delft type of point for static penetration testing (Ref. 414, 1948). (IV) Some modifications proposed by DeBeer (Ref. 103, 1945).

same diameter D as the cone point. This circumstance greatly decreased the friction on the tube, and therefore less effort was required to push the assembly down through the soil. Consideration was also given to an increase of the height of the point up to a value $H = 2D$, for the purpose of maintaining the *effect of depth*, that is, the effect of the overburden surcharge on the soil beneath the cone point. Otherwise some expansion of the soil into the space between the top of the cone point and the bottom of the tube would be inevitable.

Cone-penetration tests are performed as a matter of routine in Holland and in Belgium, where the soil conditions are particularly favorable for this type of investigation. Peat or soft clays frequently are found there down to depths of some 60 ft and are followed by sands of varying density. The cone points can then be easily pushed right down to and

into the sand, to determine in advance of construction the elevation to which pile points should reach. Correlations have been obtained between the resistance of the cone point and the bearing capacity of the end-bearing piles (Refs. 103 and 104). Attempts based on early work by Buisman (Ref. 48) have been made, to provide a rigorous analysis of the results of the cone-penetration tests. This was done by modifying the Prandtl equation (Art. 9-9) for noncohesive soils to take into account the weight of the soil, both in the sliding wedge and above it. This modified equation was then used to determine the angle of internal friction ϕ of the soil. Simultaneously the same cone-penetration-resistance data were sometimes used to determine from a modified Boussinesq equation (Art. 9-2) coefficients of compressibility of the soil (Refs. 103 and 48). No satisfactory explanation has yet been advanced which would justify the determination of compressibility coefficients from the resistance to what is essentially a shear failure. The above method of determining ϕ also is questionable for all soils, since the extent to which the weight of the overlying soil is actually effective in restraining the heaving of the soil can only be surmised. It cannot be fully effective around the cone, since some expansion of the overlying soil into the space which opens up between the cone point and the tube T does occur as the point is pushed down into the soil.

Thus such rigorous analyses of varied fundamental soil properties from cone-penetration-resistance data do not appear feasible, even though procedures for such analyses have been published. Nevertheless, cone-penetration data were expected to provide useful empirical correlations with the known performance of soil layers under structures, the behavior of which had been measured. It appeared likely to be most useful under conditions similar to those discussed in Prob. 12-4. For that reason comparative studies of the performance of the Delft type of cone point [Fig. 12-17(III)] and of the standard S. & H. drop-penetration test [Fig. 12-7(1) and Table 12-2] were undertaken in 1948 to 1949 by Sprague & Henwood, Inc., at Tschebotarioff's suggestion and under his supervision. The results are given in Figs. 12-18 and 12-19. The hydraulic swivelhead of a core-drilling machine of the type shown in Figs. 12-15 and 12-16 was adapted to press the cone points into the soil and to measure their resistance by gages which recorded the pressure in the oil of the swivelhead press.

The first study was made possible, by the cooperation of Spencer, White & Prentis, Inc., and of G. Lutz of the Turner Construction Co., on the site of a heavy structure founded on a deep bed of loose sand which was known to have settled approximately 3.5 in. (see Fig. 12-18). Other records referring to that structure are given in Fig. 13-9 and Prob. 9-1.
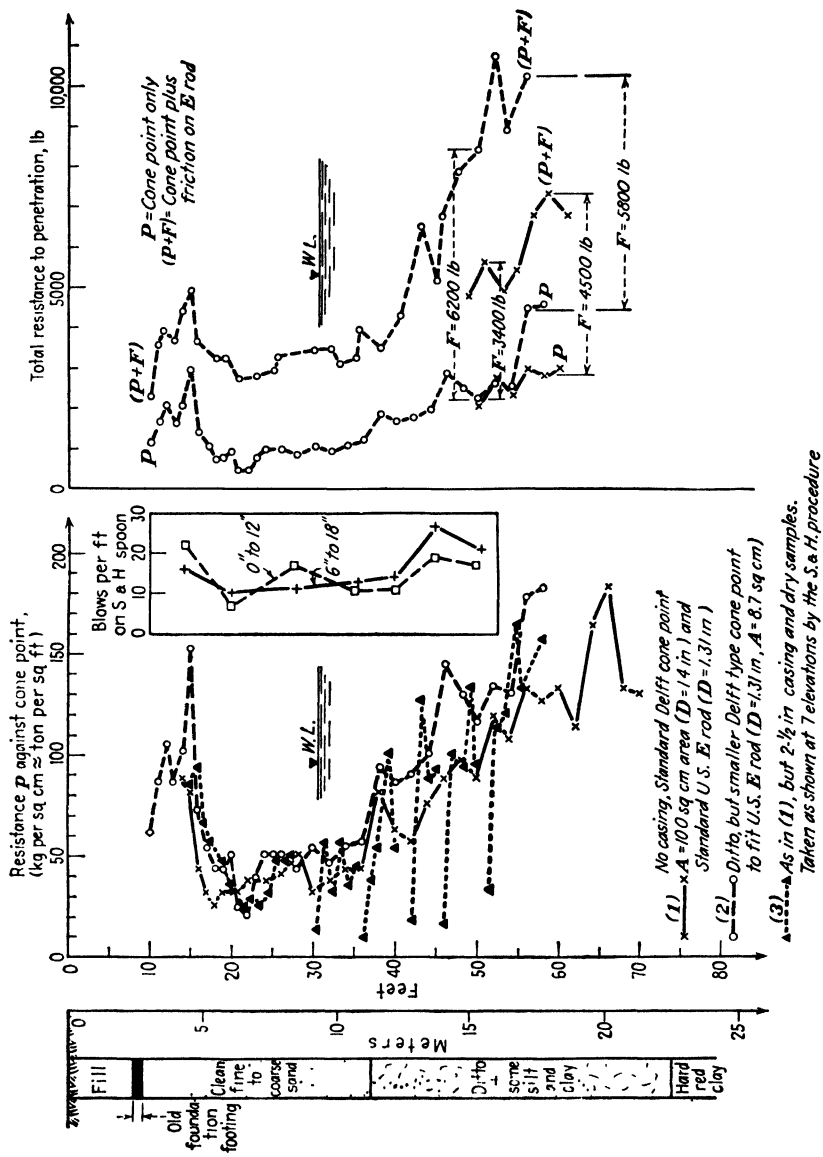
FIG. 12-18. Comparison between S. & H. dry-sampling spoon-driving record in loose sand and the penetration resistance of Delft-type cones. (Tests performed by Sprague & Henwood, Inc.; supervised by Tschebotarioff, 1948.)

Three cone-penetration soundings were performed at a distance of 4 ft from each other. It can be seen from Fig. 12-18 that they all gave results which agreed fairly closely with each other, as well as with the results of the S. & H. dry-sampling spoon-driving record. The static cone-point records appeared to be somewhat more sensitive to changes in soil density than the dynamic driving records of the spoon, but both showed the same trends. Immediately under the old footing foundation the sand was found to be somewhat compacted by the weight of the building which had rested on it in the past. Deeper down the sand was found to be of a loose to medium density (compare the spoon-driving record with Table 12-2). The sand gradually increased in density with depth. The spoon was driven 18 in. Note that the number of blows between 0- and 12-in. penetration is practically identical with the number recorded between 6- and 18-in. penetration. The loosening of the sand after the driving and the withdrawal of the S. & H. sampler every 5 ft or so is clearly shown by the cone-point record of the corresponding test 3 in Fig. 12-18. The disturbance, however, did not reach down more than a couple of feet. The use of a rod T for test 1, which had a diameter 0.1 in. smaller than the diameter of the cone, decreased the total friction F along the rod by some 25 to 45 per cent as compared with test 2 where the diameters of the rod and of the cone were identical.

The second study was made on the site of a building in Philadelphia which was founded on a layer of very compact sand and gravel (Fig. 12-19). The building had settled only between ⅛ and ¼ in. The settlement occurred very rapidly and ceased soon after application of the loads. A penetration test of the Kneas type (Table 12-1) at the elevation of the foundation footings gave 21 to 45 blows for the first foot and 36 to 100 blows for the second foot.* It can be seen from Fig. 12-19 that it proved possible to drive the S. & H. spoon at all elevations and to obtain a driving record, which indicated the very dense nature of the soil (compare with Table 12-2). On the other hand, it did not prove possible in many cases to press the Delft cone even a fraction of an inch into the soil at the bottom of the 2½-in. casing without bending the rod R, [see Fig. 12-17(3)]. This location is marked by the infinity sign (∞) in the resistance chart (Fig. 12-19). It can thus be concluded that the present Delft cone point cannot penetrate dense granular materials in which more than 50 to 70 blows per foot were required to drive an S. & H. sampler.

* The studies on the building illustrated by Fig. 12-19 were sponsored by the Foundation Committee of the Philadelphia Section, ASCE. Settlements were measured in 1938 (G. Tschebotarioff, committee chairman), and the cone-penetration versus spoon-driving comparisons were performed in 1949 (N. C. Courtney, committee chairman).

Therefore the cone-penetration test could not be expected to find general use in the United States as an independent means of investigation, that is, in the way it is employed in Holland, where it is sometimes used prior to the performance of borings. It is necessary to anchor the entire rig to the soil, in order to provide an effective reaction to the $(P + F)$ resistance of cone and tube, which may frequently exceed 11,000 lb (see Fig. 12-18). The rig has to be reanchored at each location of a sounding. This item is of no great importance in countries with low wage rates, but in the United States it may increase the total cost appreciably and offset economic advantages derived from the rapid performance of the sounding
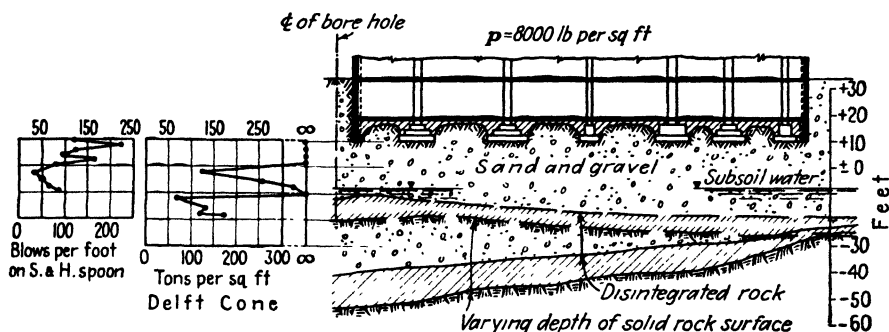
FIG. 12-19. Comparison between S. & H. dry-sampling spoon-driving record in dense sand and the penetration resistance of a Delft-type cone. (*Tests performed by Sprague & Henwood, Inc.; supervised by Tschebotarioff, 1949. Sponsored by Foundation Committee, Philadelphia Section, ASCE.*)

itself. These and other circumstances* delayed further studies of this type.

It is nevertheless believed that cone-penetration tests can be developed into a valuable *auxiliary* tool for use in conjunction with now customary procedures, that is, borings and laboratory tests (see Prob. 12-4). Some modifications of existing cone points and extensive research on the correlation of cone-test results to fundamental soil properties will, however, be needed first. Some promising but as yet unpublished studies have been made at the U.S. Waterways Experiment Station at Vicksburg.

12-10. Soil Load Tests. The settlement of a loaded area will increase with the size of the area, even if the unit load remains unchanged (see Art. 9-8). Thus load tests on small footings will give accurate settlement information only when the size of the test footings corresponds to the prototype size of the loaded area. This will be the case of wheel loads on highways or airports (Art. 19-6) but will hardly ever be the case of foundation footings of permanent structures (see Prob. 12-6). The size of the loaded area does not influence the ultimate bearing capacity of a clay

* See Tschebotarioff, *Engineering News-Record*, Nov. 23, 1950, p. 47.

(Art. 9-9). Therefore load tests may be used to determine the bearing capacity, but only if the clay has the same strength throughout the depth of the deposit (see Arts. 9-10 and 14-2).

Attempts to perform load tests in boreholes have been made (Ref. 201). Nevertheless, later correlations with the performance of actual structures indicated the complete unreliability of the results of such load tests, especially below ground-water level, since the soil of the bottom of the borehole or of its side walls has inevitably been disturbed or has expanded somewhat, so that its compressibility is much greater than in the natural state.

12-11. Classification of Soils. The earliest and simplest methods of classifying soils were based on the size of the individual grains. These methods have considerable limitations (see Art. 3-7).

There are several systems which classify soils for engineering purposes. Each system was developed for the purpose of coping with a specific engineering problem. Thus the PRA (Public Roads Administration) classification was originally developed in the 1920's to indicate the suitability of a given soil for the surfacing of low-cost secondary roads. The soils are divided into eight groups, designated by the symbols A-1 to A-8. The A-1 soils are sands with a slight amount of fines which is sufficient only to fill the voids around the sand grains partially and to cement the grains to each other but which is too slight to induce volume changes of the soil mass, that is, swelling or shrinkage, as a result of alternating wetting or drying. The A-2 soils are similar to the A-1 soils, except that they are less favorably graded, so that they either are less well cemented or are more susceptible to undergo volume changes with changes in their moisture content. A-3 soils are sands and gravels with no fines capable of cementing them. A-4 to A-7 soils are silts and clays of varying degrees of plasticity. A-8 soils are highly compressible peats and clays with a very high organic content. The PRA classification system has been recently amplified by the addition of subscripts (Ref. 5).

A more recent system, the so-called AC or airfield classification system, was developed by Arthur Casagrande (Ref. 66, 1942–1948) for the U.S. Army Engineers. It is summarized in Tables 12-3 and 12-4. Symbols referring to soil types and to some specific soil properties are used in different combinations to permit the classification of the soil in respect to its suitability as a foundation or a base-course material of airports. The same procedure can well be applied to highway work.

The significance of the symbols employed is as follows:

Type of soil:
G—gravel
S—sand

M—very fine sands and silts of the nonplastic rock-flour type (after the Swedish word *mo*)
C—clays, inorganic
O—clays and silts, organic
Pt—peat and highly compressible organic swamp soils

Grading (applies only to G and S soils):
W—well-graded clean material (Fig. 3-1)
P—poorly graded clean material
C—clay binder of well-graded G and S soils
F—presence of fines other than of the C type

Compressibility [refers only to M, C, and O soils and to the potential compressibility of the material as defined by the virgin compression curve (see Fig. 6-6)]:
L—low potential compressibility, such as is encountered with clays having a liquid limit $w_L < 50$
H—high potential compressibility, such as is encountered with clays having a liquid limit $w_L > 50$

See Prob. 12-5 for combinations of the above symbols. The Casagrande classification is particularly useful in connection with preliminary surveys based on rapid field examination and identification of soils (Art. 12-12).

There are other classification systems, for instance, the pedological system (Art. 2-8) or the one developed by the CAA (Civil Aeronautics Administration) in 1944 (see summary in Ref. 66). D. M. Burmister classified granular soils on the basis of the shape of their grain-size-distribution curves (Ref. 52, 1940) and applied this classification method to a study of their relative densities (Ref. 54, 1948) (see also Ref. 338). A modification of the PRA system is under study (Refs. 66 and 338).

The unconfined compressive-strength test can well serve classification purposes for natural clay deposits. The differentiation between brittle and plastic clays, based on the strain at failure, was discussed in Art. 7-10 and summarized in Table 7-1. The determination of the sensitivity of clays to remolding was discussed in Art. 7-22, and the proposed classification on that basis is given in Table 14-4. Table 12-5 suggests a classification of clays with respect to their natural stiffness on the basis of their unconfined compressive strength.

12-12. Methods of Field Identification of Soils. Visual inspection is, as a rule, sufficient to permit proper field identification of the gradation and of the shape and size of the grains of coarse-grained soils, that is, sands (S) and gravels (G). A pocket magnifying glass may be of help.

Differentiation among the M, the C, and the O type of fine-grained soils, and their L and H subdivisions, however, is not possible by visual inspection alone. A few simple auxiliary tests have to be employed.

In the *moist condition* one can differentiate between the silts (M) and

TABLE 12-3. The Soil Types of the Airfield Classification (Arthur Casagrande) System and Their Identification*

1		2	3	4		5	6
Major divisions		Soil groups and typical names	Group symbol*	General identification (on disturbed samples)		Observations and tests relating to material in place	Principal classification tests (on disturbed samples)
				Dry strength†	Other pertinent examinations		
Coarse-grained soils	Gravel and gravelly soils	Well-graded gravel and gravel-sand mixtures, little or no fines	GW	None	Gradation Grain shape Examination of binder wet and dry Durability of grains	Dry unit weight or void ratio Degree of compaction Cementation Stratification and drainage characteristics Ground-water conditions Traffic tests Large-scale load tests California bearing-ratio tests	Mechanical analysis
		Well-graded gravel-sand mixtures with excellent clay binder	GC	Medium			Mechanical analysis, liquid and plastic limits on binder
		Poorly graded gravel and gravel-sand mixtures, little or no fines	GP	None			Mechanical analysis
		Gravel with fines, silty gravel, clayey gravel, poorly graded gravel-sand-clay mixtures	GF	Very slight to high			Mechanical analysis, liquid and plastic limits on binder, if applicable
	Sands and sandy soils	Well-graded sands and gravelly sands, little or no fines	SW	None			Mechanical analysis
		Well-graded sand with excellent clay binder	SC	Medium to high			Mechanical analysis, liquid and plastic limits on binder
		Poorly graded sands, little or no fines	SP	None			Mechanical analysis
		Sand with fines, silty sands, clayey sands, poorly graded sand-clay mixtures	SF	Very slight to high			Mechanical analysis, liquid and plastic limits on binder, if applicable

Fine-grained soils containing little or no coarse-grained material	Fine-grained sands having low to medium compressibility; liquid limit < 50	Silts (inorganic) and very fine sands, mo, rock flour, silty or clayey fine sands with slight plasticity	ML	Very slight to medium	Shaking test and plasticity	Dry unit weight, water content, and void ratio	Mechanical analysis, liquid and plastic limits, if applicable
		Clays (inorganic) of low to medium plasticity, sandy clays, silty clays, lean clays	CL	Medium to high	Examination in plastic range	Consistency, undisturbed and remolded	Liquid and plastic limits
		Organic silts and organic silt-clays of low plasticity	OL	Slight to medium	Examination in plastic range, odor, color	Stratification, root holes, and fissures	Liquid and plastic limits from natural condition and after oven drying
	Fine-grained soils having high compressibility; liquid limit > 50	Micaceous or diatomaceous fine sandy and silty soils, elastic silts	MH	Very slight to medium	Shaking test and plasticity	Drainage and ground water conditions Traffic tests	Mechanical analysis, liquid and plastic limits, if applicable
		Clays (inorganic) of high plasticity, fat clays	CH	High to very high	Examination in plastic range	Large-scale load tests	Liquid and plastic limits
		Organic clays of medium to high plasticity	OH	Medium to high	Examination in plastic, range, odor, color	California bearing-ratio tests Compression tests	Liquid and plastic limits from natural condition and after oven drying
Fibrous organic soils with very high compressibility		Peat and other highly organic swamp soils	Pt	Readily identified		Consistency, texture, and natural water content	

* From Arthur Casagrande (Ref. 66, 1948). See also Table 12-4.

† For binder, fraction passing U.S. Standard mesh No. 40.

TABLE 12-4. The Engineering Characteristics of Soils According to the Airfield Classification (Arthur Casagrande) System*

3	7	8		9	10	11	12	13‡	14	15
Group symbols	Value as foundation when not subject to frost action	Value as wearing surface for stage or emergency construction		Potential frost action	Compressibility and expansion	Drainage characteristics†	Field compaction characteristics and equipment	Solids at optimum compaction, lb per ft^3, and void ratio, e	California bearing ratio for compacted and soaked specimen	Comparable groups in PRA classification
		With dust palliative	With bituminous surface treatment							
GW	Excellent	Fair to poor	Excellent	None to very slight	Almost none	Excellent	Excellent; crawler tractor, rubber-tired equipment	> 125 $e < 0.35$	> 50	A-3
GC	Excellent	Excellent	Excellent	Medium	Very slight	Practically impervious	Excellent; tamping roller,§ rubber-tired equipment	> 130 $e < 0.30$	> 40	A-1
GP	Excellent	Poor	Poor to fair	None to very slight	Almost none	Excellent	Good to excellent; crawler tractor, rubber-tired equipment	> 115 $e < 0.45$	25–60	A-3
GF	Good to excellent	Poor to good	Fair to good	Slight to medium	Almost none to slight	Fair to practically impervious	Good to excellent; crawler tractor, rubber-tired equipment, tamping roller§	> 120 $e < 0.40$	> 20	A-2
SW	Excellent	Poor	Good	None to very slight	Almost none	Excellent	Excellent; crawler tractor, rubber-tired equipment	> 120 $e < 0.40$	20–60	A-3
SC	Excellent	Excellent	Excellent	Medium	Very slight	Practically impervious	Excellent; tamping roller, rubber-tired equipment	> 125 $e < 0.35$	20–60	A-1
SP	Good	Poor	Poor	None to very slight	Almost none	Excellent	Good to excellent; crawler tractor, rubber-tired equipment	> 100 $e < 0.70$	10–30	A-3

SF	Fair to good	Poor to good	Poor to good	Slight to high	Almost none to medium	Fair to practically impervious	Good to excellent; crawler tractor, rubber-tired equipment, tamping roller§	> 105 $e < 0.60$	8–30	A-2
ML	Fair to poor	Poor		Medium to very high	Slight to medium	Fair to poor	Good to poor; close control essential; rubber-tired roller	> 100 $e < 0.70$	6–25	A-4
CL	Fair to poor	Poor		Medium to high	Medium	Practically impervious	Fair to good; tamping roller§	> 100 $e < 0.70$	4–15	A-4 A-6 A-7
OL	Poor	Very poor		Medium to high	Medium to high	Poor	Fair to poor; tamping roller§	> 90 $e < 0.90$	3–8	A-4 A-7
MH	Poor to very poor	Very poor		Medium to very high	High	Fair to poor	Poor to very poor	> 100 $e < 0.70$	< 7	A-5
CH	Poor to very poor	Very poor		Medium	High	Practically impervious	Fair to poor; tamping roller§	> 90 $e < 0.90$	< 6	A-6 A-7
OH	Very poor	Useless		Medium	High	Practically impervious	Poor to very poor	< 100 $e > 0.70$	< 4	A-7 A-8
Pt	Extremely poor	Useless		Slight	Very high	Fair to poor	Compaction not practical			A-8

* From Arthur Casagrande (Ref. 66, 1948). See also Table 12-3.

† These characteristics do not apply to undisturbed materials having fissures and root holes, such as most surface soils.

‡ These weights apply only to soils having specific gravities from 2.65 to 2.75.

§ Sheep's-foot roller.

the clays (C) with the help of the *shaking test* which gives a measure of the mobility of the water in the voids (see Rutledge, Ref. 294, 1940). A remolded pat of moist soil is placed in the palm of the hand or in a rubber cup formed by cutting a tennis ball in two. The surface of the soil is smoothed out with a knife, and the soil pat is shaken by tapping the palm of one hand on the palm of the other. If the soil is a silt, for instance, a loess or a soil of the rock-flour type, its surface will begin to glisten with the moisture which is pressed out of the voids of the soil as the soil grains with little cohesion slip past each other into a denser position as a result of the shaking. If one then squeezes the soil pat, the moisture will disappear from the surface, since the shearing stresses induced by the squeezing will cause the slightly cohesive or noncohesive soil to expand in very much the same manner as a saturated dense sand (see Fig. 7-23 and Art. 7-15). A highly cohesive clay soil will not exhibit such changes in the appearance of its surface when shaken or squeezed, since its grains will not slip past each other with the same ease.

TABLE 12-5. Relationship between the Consistency and the Unconfined Compressive Strength of Clays

Consistency	Unconfined compressive strength q_u, tons per ft^2	Shearing strength $c = \frac{q_u}{2}$
Very soft..........	0.3	0.15
Soft..............	0.3–0.6	0.15–0.30
Medium...........	0.6–1.2	0.30–0.60
Stiff..............	1.2–2.4	0.60–1.20
Very stiff..........	2.4	1.20

The sensitivity of a plastic clay soil to *remolding* can be estimated by taking a 1-in. cube of undisturbed material in its natural state and gently feeling its resistance to finger pressure before and after completely remolding it by hand.

The *plasticity* of a cohesive soil can be estimated by *rolling* it into *threads* in the manner that is used for the determination of the plastic limit (Art. 4-9). The feel of the threads after they start crumbling provides indications on the nature of the material (see Ref. 66).

In a *dry state* the strength of the soil is an indication of its cohesion and hence of its nature. It can be estimated by *crushing* some dried soil by finger pressure. A silt will crumble easily, whereas a rich clay will feel very hard. The surface of a rich dry clay, when rubbed with a knife, will appear shiny.

Some laboratory practice and training is, of course, necessary for proficiency in the identification of soils by field methods.

12-13. Graphical Soil Symbols. There is no generally accepted standard of such symbols, and a great number of systems are in existence. Figure 12-20 illustrates a compromise proposal by Hvorslev (Ref. 181, 1948). Most natural soils represent a mixture of several basic types. The symbols of the basic and special types of soils can then be combined
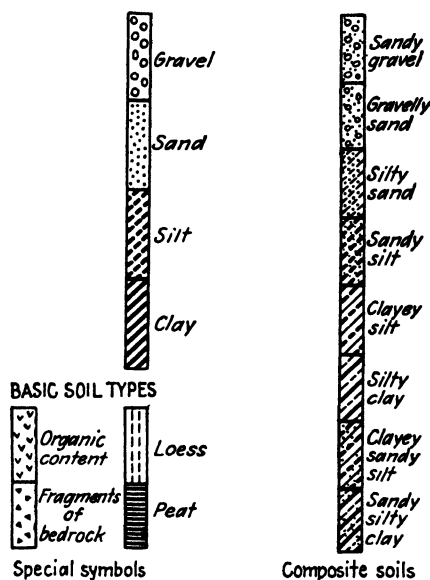
FIG. 12-20. Graphical soil symbols. Compromise suggested by Hvorslev (Ref. 181, 1948) between several existing systems.

in the manner shown in that diagram, where the symbol of the predominating type of soil is emphasized by being drawn in thicker lines.

Practice Problems

12-1. The sample illustrated in Fig. 12-11 is in perfect condition. It was extracted by a thin-walled sampler of the type shown in Fig. 12-7(II) with $D_w = 3.00$ in. and $D_e = 2.8$ in. (see Fig. 12-9). On the other hand, the strongly distorted sample shown in Fig. 12-13 was extracted by a sampler with an inner lining tube, outer split cylinder, and a somewhat thicker shoe to hold the assembly together, $D_w = 3.625$ in., and $D_e = 2.93$ in. What are the area ratios C_a of the two samplers?

Answer. According to Eq. (12-1), the thin-walled sampler will have a low value of the area ratio

$$C_a = \frac{3.00^2 - 2.80^2}{2.80^2} = 0.147$$

The second sampler, which had walls of medium thickness and produced unsatisfactory results, has a value more than four times higher,

$$C_a = \frac{3.625^2 - 2.930^2}{2.930^2} = 0.530$$

12-2. In view of the results of Prob. 12-1, would there be much point in performing strength tests on clay samples extracted by means of the dry-sampling technique and samplers of the type illustrated in Fig. 12-7(I)?

Answer. No; the area ratio of such samplers is much too high:

$$C_a = \frac{2.00^2 - 1.437^2}{1.437^2} = 0.94$$

If one is compelled for reasons of economy to use 2½-in.-diameter casing, then a 2-in. thin-walled Shelby tube sampler, of the type shown in Fig. 12-7(II), should be employed (D_w = 2.00 in.; D_e = 1.80 in.) for strength tests. It has

$$C_a = \frac{2.0^2 - 1.8^2}{1.8^2} = 0.23$$

This is satisfactory for strength tests of a preliminary nature but is too high for accurate consolidation testing.

12-3. A driving record through a sand layer indicated that from 8 to 17 blows per foot were necessary to drive an S. & H. 1290S dry sampler [see Fig. 12-7(I)] by means of a 300-lb hammer with a 12-in. height of drop. What is the density of that layer in your estimation?

Answer. With reference to Art. 12-9 and Table 12-2, the Terzaghi-Peck classification fits the driving procedure employed closest. Therefore the sand layer can be classified as being of loose to medium relative density.

12-4. A 4-in. casing was sunk on a river bank through a layer of clay and reached sand at a depth of 60 ft from the soil surface. The ground-water level, before the hole reached the sand, was at a depth of 15 ft below the soil surface but rose by 10 ft after the clay layer was pierced. The bottom of the casing was washed out by a chopping bit (Fig. 12-6), which was then withdrawn, and a dry sampler [Fig. 12-7(I)] was lowered to obtain a driving record for the purpose of estimating the density of the sand. It was, however, found that the sand had risen 2 ft into the casing. How would you meet the situation?

Answer. The rise of the water in the casing after the clay layer was pierced indicates some artesian pressure in the sand layer. It is therefore particularly important to keep the casing continuously filled with water to its top at all stages of the work. This includes the time during which the chopping bit is withdrawn. The volume of the bit and of 60 ft of drill rod above it is sufficient to cause a drop of several feet of the water level in the casing, unless water is continuously added to keep the casing full to the top. A drop of the water level in the casing, even if it occurred for a very short time only, may be sufficient to produce a quick condition (Art. 5-4) in the sand at its bottom and upward flow of the liquefied sand into the casing. Of course, the sand below the casing is also loosened thereby for a foot or two. If the artesian pressure is too great to prevent, by the measures just described, the sand from being forced upward into the casing, then another borehole should be sunk and its casing stopped in the clay layer some 5 to 10 ft above the top of the sand layer. A cone point of one of the types described in Fig. 12-17 can then be driven or, preferably, pressed toward and into the sand layer without any quick condition developing.

12-5. Two soil samples were described as CL-SC and SF-ML, respectively. What do these symbols mean?

Answer. According to the A. Casagrande classification (Art. 12-11), the first sample represents a border case between a low-potential-compressibility (lean) clay (CL) and a sand having some clay binder (SC). The second sample is also a border case, this time between sand with some fines (SF) and a nonplastic silt soil of low potential compressibility (ML).

12-6. The proposal was made to determine the permissible unit contact pressure with the soil (sand) of the footings for a new 200- by 300-ft four-story building from the results of two surface load tests on 1-ft-square test footings. Was the proposal reasonable?
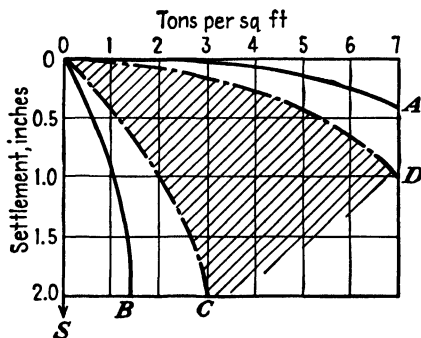
FIG. 12-21. Results of load tests on natural sand deposits with 1-ft² test footings. Curves *A* and *B* correspond to tests of the densest and of the loosest states of sands from different localities, reported by Terzaghi and Peck (Ref. 365, 1948). The shaded area between curves C and *D* gives the wide limits within which varied the curves of tests performed at a depth of *5* ft over the area of a single factory shed in Iowa, studied by Tschebotarioff.

Answer. No, it was not. As shown in Fig. 12-21, the density of sand may vary within wide limits over the area of a single structure. Two load tests of the type suggested would provide insufficient information concerning the density of the sand at the elevation where the tests were performed and no information at all concerning its density at depths in excess of 2 ft below that elevation (see Arts. 12-10 and 9-3). A larger number of penetration tests (Art. 12-9), in connection with a few borings, would give a much better idea of the limit and average values of the density of the entire soil mass which will have to support the new building.

References Recommended for Further Study

"Subsurface Exploration and Sampling of Soils for Civil Engineering Purposes," by M. Juul Hvorslev. Report on a research project of the ASCE sponsored by the Engineering Foundation, Harvard University, and the U.S. Waterways Experiment Station, 1948, 500 pp. Published by the Engineering Foundation, New York. An exceptionally thorough analysis of the problem and of the current procedures, with recommendations of advisable methods under varying conditions.

"Relation of Soil Mechanics and Geology in Foundation Exploration, Lower Mississippi Valley," by W. J. Turnbull and H. N. Fisk, *Proceedings of the 2d International Conference on Soil Mechanics and Foundation Engineering*, Rotterdam, Vol. III, pp. 3–5, 1948. A paper by an outstanding soil mechanics specialist and a leading

geologist which outlines organizational techniques essential for the successful coordination and teamwork of soil engineers and of geologists.

"Soil Tests for Military Construction," by G. E. Bertram, *Technical Bulletin of the American Roadbuilders' Association*, No. 107, 1946, 95 pp. Instructions for sampling and testing procedures in the field with improvised equipment. Covers exploration at shallow depths only.

"Subsurface Exploration by Geophysical Methods," by E. R. Shepard, *Proceedings of the American Society for Testing Materials*, 1949, pp. 993–1015. The applicability and the limitations of seismic and electric-resistivity methods of exploration under varying conditions.

"Classification and Identification of Soils," by Arthur Casagrande, *Transactions of the American Society of Civil Engineers*, 1949, pp. 901–991. Detailed discussion of the airfield classification and of other systems.

"The Influence of Geology on Soil Testing Methods in Western Europe," by H. Q. Golder, *Proceedings of the 2d International Conference on Soil Mechanics and Foundation Engineering*, Rotterdam, Vol. V, pp. 1–3, 1948. Relationships between the types of soil encountered in the small areas of the many countries studied and the local exploration and testing techniques.

Proceedings of the American Society for Testing Materials, 1950. Symposium of several papers on soil classification. Noteworthy suggestion by D. M. Burmister to express soil composition quantitatively by letters with subscripts, as is done in chemistry in respect to elements.

Geology and Engineering, by R. F. Legget, McGraw-Hill, 1939. Geological engineering aspects of site exploration.

Bodenuntersuchungen fuer Ingenieurbauten, by Edgar Schultze and Heinz Muhs, Springer, Berlin, 1950. German and other soil exploration procedures.

CHAPTER 13

THE SELECTION OF A SUITABLE TYPE OF FOUNDATION

13-1. Summary of Main Points to Be Considered. An adequate knowledge of the soil and of the ground-water conditions at the proposed site for a new structure is a prerequisite for any rational study of its foundation. In some cases it is even advisable to investigate the proposed construction site by means of a few borings before the land is purchased, since an excessive cost of the foundation might indicate the advisability of selecting a different location. The information which is to be obtained by a properly conducted soil investigation is outlined in Art. 13-2.

Simultaneously with the soil investigation a load plan for the proposed structure should be prepared. In the case of a building, the plan should indicate the concentrated loads of individual columns in tons or in kips, and the linearly distributed loads of bearing walls in tons per foot or in kips per foot. Each load plan should include sketches indicating the assumed nature, weight, and dimensions of all materials in the walls and in the floors, as well as the live loads which were used in the preparation of the load plan. This facilitates the necessary corrections and helps to prevent overloading of the foundation in case of later revisions of design.

With the data on the subsoil conditions and the load plan, the selection of a foundation type can be undertaken. The following main points have to be considered:

1. The loads of the structure have to be transferred to soil layers capable of supporting them without failing in shear (see Arts. 9-9, 9-10, 13-5, and 13-6).

2. The deformations of the soil layers underlying the foundation should be compatible with the deformations which the foundation itself and its superstructure, as well as adjoining structures, can safely undergo (see Arts. 13-3 and 13-4).

3. The construction operations should not endanger adjoining existing structures (see Arts. 13-4 and 13-9).

A study of the building codes and regulations of the city where the structure is to be built is essential, so that the foundation design and its execution will conform with any special local rules.

Several different safe solutions are often technically feasible for the design of a proposed foundation. Naturally, preference should then be given to the solution which achieves the desired objective at least cost. Sometimes a rough estimation will be sufficient to clarify this point, but frequently several alternative projects have to be worked out in some detail before their relative cost can be properly evaluated.

All estimates and plans should include provisions for adequate supervision of construction operations. The competence and integrity of field inspectors are of the utmost importance in all foundation work. Usually it is a simple matter to check at any later time the nature of the materials and the quality of the workmanship employed in the superstructure. It is, however, extremely expensive and sometimes impossible to do so in respect to a foundation unit once it is embedded in the ground.

Estimates and specifications should also include provisions for the control of the performance of the foundation, both during its construction, and after completion of the entire structure. It should be realized that the state of our present soil engineering knowledge is incomplete in many respects. Properly conducted measurements of the actual performance of a structure therefore provide at very little extra cost a necessary insurance against the unchecked development of an unforeseen situation and permit adequate countermeasures in time (see Art. 13-8).

13-2. Site Exploration. The various methods of soil exploration have been discussed in some detail in Chap. 12. The method to be employed should be the least expensive of the procedures which will provide the desired information. Thus there is no point in taking large-sized undisturbed samples of clay if the structure is so heavy that its foundation will obviously have to be carried down through the clay to sand or to rock. A decision as to the exploration procedure to be selected can frequently be made on the strength of data obtained during previous constructions in the immediate vicinity. When dealing with an entirely new location, however, it is advisable to make from the very start arrangements for a flexible program of exploration, which could be expanded or curtailed, depending on the nature of the first data obtained.

For instance, if one had to make a soil investigation for the building *ABCD* shown in plan in Fig. 13-1, on a site about which nothing whatsoever is known, then it would be advisable to start with five preliminary borings 1 to 5 of 2½ in. diameter at the four corners and at the center of the building, carried down to a depth equal to 1½ times the length of the building, unless rock is encountered first. Disturbed dry samples (Art.

12-6) and driving records of the dry-sampling spoon (Art. 12-9) would be taken in all soil layers; 2-in. undisturbed samples (Art. 12-7) would be taken in layers of soft to stiff clay (Table 12-5). All samples would be shipped to a soil-testing laboratory as they are extracted. The natural water contents w_n (Art. 4-3), the liquid limits w_L, the plastic limits w_P (Art. 4-7), the unconfined compressive strengths q_u in the undisturbed and in the remolded conditions, and the corresponding strains at failure (Arts. 7-10 and 7-22) would be determined and plotted for the cohesive samples of each borehole, in a manner similar to that shown in Fig. 13-2. The essential properties of all soil layers encountered can then be seen at a glance. If the weight of the building is such that there are doubts as
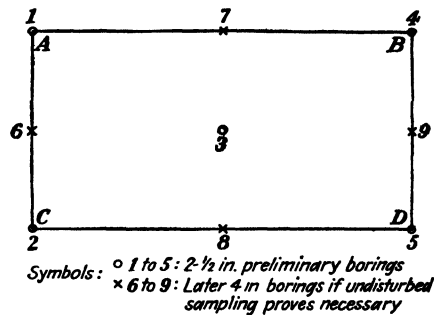
FIG. 13-1. Sketch showing location of boreholes at the start of the soil exploration for a future building ABCD.
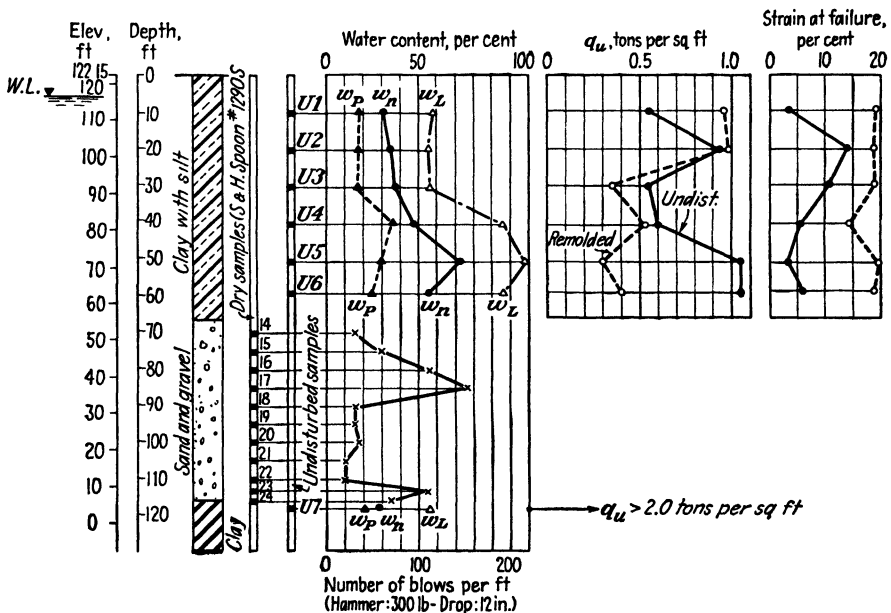
FIG. 13-2. Graphical presentation of the most essential properties of soil samples from one borehole.

to whether it is necessary to carry the foundation down to the sand layer at 65 ft depth, then a more careful study of the upper clay layer would be necessary, including a settlement analysis (Art. 13-7). Supplementary
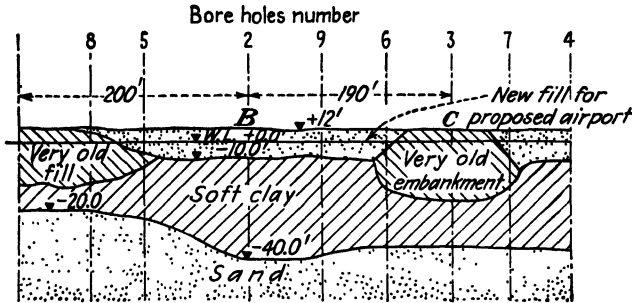
FIG. 13-3. Sketch illustrating the possible sequence of boreholes located so as to establish a comprehensive soil profile.
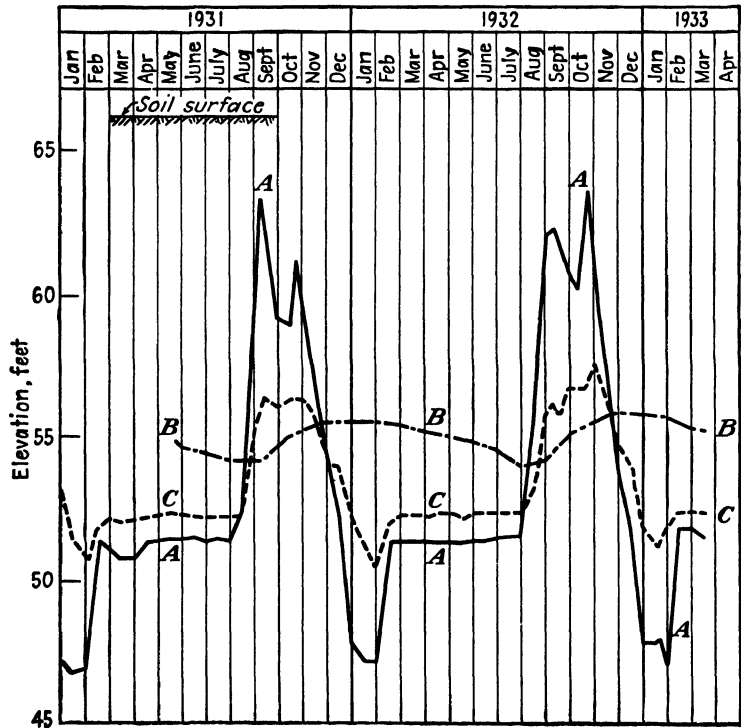
FIG. 13-4. Water-level variations. (A) In the river Nile. (B) In open pit 3,000 ft from river, dug 13 ft into 10 ft of fill and 25-ft-deep clay layer. (C) In 43-ft-deep observation pipe reaching through the clay into the underlying sand 4,000 ft from river.

boreholes of at least 4 in. diameter (holes 6 to 9) for undisturbed samples would then be required, as shown in Fig. 13-1.

Frequently, variations in soil conditions along horizontal planes make it necessary to locate borings in such a manner that a complete soil profile can be obtained. For instance, if preliminary borings 1 to 4, performed

as shown in Fig. 13-3 in connection with the proposed construction of an airport, disclosed the presence of a layer of soft clay of varying thickness, then the supplementary borings 5 to 9 would be needed to complete the profile and to permit a comprehensive settlement analysis (see Probs. 13-1 to 13-3).

When planning a program of water-level observations to permit the rational design of excavations, it should be remembered that these levels can vary with the time of the year and the soil layer in which the observations are made. Figure 13-4 illustrates this point. It will be noted that there is a lag in time and amplitude of the variations of the hydraulic head in the underlying sand layer, as compared with the free-water level in the river. This lag is particularly pronounced in the shallow open pit sunk through the fill into the clay layer which overlies the sand. Thus at low free-water levels in the river, the water in the open pit forms a so-called *perched water table* in respect to the underlying sand.

FIG. 13-5. Sketches showing possible manner of estimating the direction of differential settlements of a building from the inclination of cracks in its walls. (I) Cracks in a cross wall, caused by the settlement of one of its ends from $A'B'$ to AB. (II) Cracks caused by the deflection of the central part of a front wall.

A study of the condition of existing buildings near the proposed construction site, subject to the restrictive comments of Art. 13-3, can frequently provide valuable indications concerning the loading which the underlying soil layers can safely carry. The inclination of cracks provides clues regarding the differential settlements which produced them. Thus the cracks shown in Fig. 13-5(I) indicate that the wall AB must have moved downward in respect to CD from its original position $A'B'$. This elongated the diagonal CB' to CB, produced tension in the direction of that diagonal, and formed the cracks, as shown, at right angles to it. Of course, the same effect could be obtained if the wall $A'B'$ stayed in its original position and the wall CD moved upward, for instance, because dry clay under the foundation swelled most under the corner during a rainy season and lifted it (Ref. 447). Similarly, the pattern of cracks shown in Fig. 13-5(II) can be produced either by the greater settlement

of the center of a wall due to the natural compression of underlying soft clay layers (see Fig. 13-11) or by the greater swelling and lifting power of dry clay near the edges of a foundation, as will happen during rainy seasons in countries where such seasons occur periodically. This is the case, for instance, of some regions in Burma, as described by Wooltorton (Ref. 447, 1936). Thermo-osmosis (Art. 5-6) produces a reversed trend (Ref.

(I) (II)
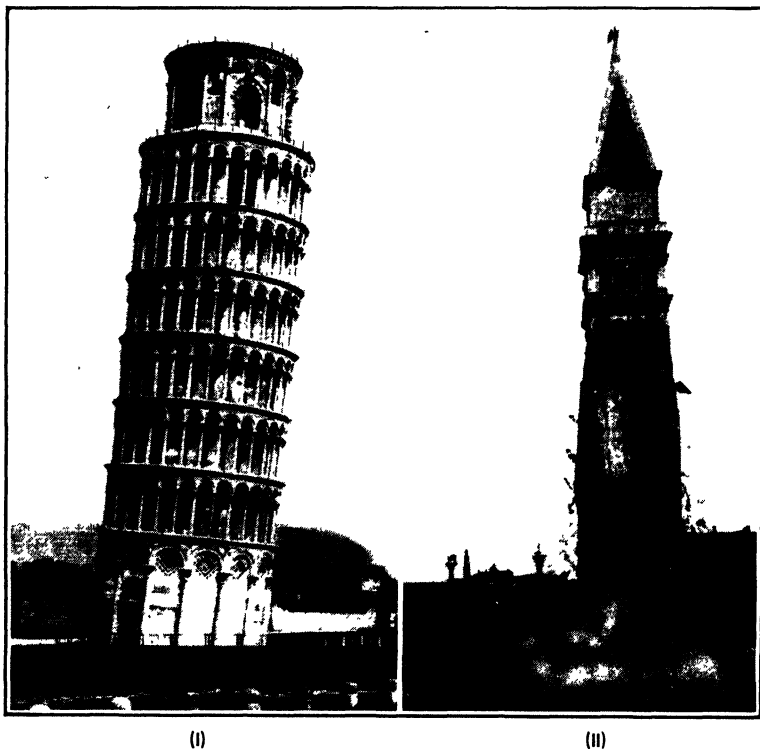
FIG. 13-6. Tilting of the foundation may or may not induce failure of the superstructure, depending on the design of the latter. (I) The campanile at Pisa still stands, although it is out of plumb by 9.7 per cent of its height. (II) The campanile at Venice collapsed (1902) as a result of being out of plumb by only 0.8 per cent of its height. [*Photo (II) from De Ingenieur, Ref.* 300.]

190*a*). Levels taken along parapets or cornices sometimes indicate the deformations which the building underwent (Fig. 9-3).

13-3. The Settlement Which a Structure Can Safely Undergo Depends on the Type of Its Superstructure. This point will be illustrated by some examples. The leaning tower of Pisa [Fig. 13-6(I)] began tilting from the very start of its construction; its foundation is underlain by alternating sand and clay layers (Ref. 314). The average unit contact pressure on

the soil is 5 tons per ft²; in high wind the pressure at the edge is 10 tons per ft². The tower is 150 ft high. An early tilting of the tower provided danger signals, and a carefully conducted strengthening of the masonry was undertaken, so that it has to date successfully withstood stresses induced by it being 14.7 ft out of plumb, that is, 9.7 per cent of its height. A completely different situation developed at Venice, where the 330-ft-high ancient Campanile (tower) collapsed in 1902, as shown in Fig. 13-6(II). The foundation was supported by closely spaced timber piles, the points of which were underlain by alternating layers of sand and clay (Ref. 314). The average unit contact pressure at foundation level was 6.4 tons per ft², and during wind pressures of 62.5 lb per ft² it reached a value of 8.6 tons per ft² at the edge of the foundation. The tower was 2.6 ft or 0.8 per cent of its height out of plumb. It was safe until some structural modifications weakened the superstructure and caused its sudden collapse. The new tower, still standing, was built to the exact architectural shape of the old one, but on a much larger foundation.

Most structures are to a certain extent flexible. It has been shown in Arts. 9-1 and 9-4 that a uniformly loaded soil surface will tend to settle more at its center than at its edges. A completely flexible superstructure can adjust itself to the settlement crater of the soil surface. A completely rigid superstructure, on the other hand, will tend to bridge the crater and to equalize the settlements of the soil surface beneath it by transmitting greater pressures to the edges. Incompletely rigid structures may be overstressed and cracked if they are not strong enough to equalize the settlements by bridging the crater and thereby increasing the pressures at its periphery and, at the same time, are not flexible enough to adjust themselves to the surface of the crater. The following equations, the derivation of which can be found in most textbooks on mechanics of materials, give the relationship between the curvature of a beam, as expressed by its radius of curvature r, and the bending moment M which is related to it:

$$M = \frac{EI}{r} \tag{13-1}$$

where M = bending moment
I = moment of inertia of beam
E = Young modulus of beam material
r = radius of curvature

For a beam of homogeneous material and thickness d the unit bending stress f is

$$f = \frac{Md/2}{I} = \frac{Ed}{2r} \tag{13-2}$$

By assuming that the elastic line is a circle, the radius of curvature r can be roughly estimated from the differential settlement y_d at the center of the span L:

$$r = \frac{L^2}{8y_d} \qquad (13\text{-}3)$$
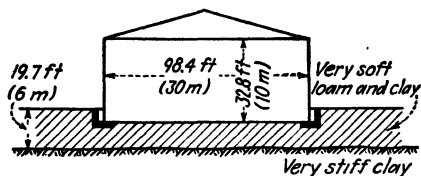
FIG. 13-7. A steel tank, when placed directly on the ground, safely underwent differential settlements, because of its flexible bottom. (From ASCE Foundation Committee report, Ref. 81, 1933.)

Substituting Eq. (13-3) into Eq. (13-2), we obtain

$$f = 4\frac{Edy_d}{L^2} \qquad (13\text{-}4)$$

These equations, as well as Fig. 13-8, illustrate the reasons why it is now customary to build storage steel tanks, of the type illustrated in Fig. 13-7, by placing the steel bottom of the tank directly on the soil surface, which is covered with only a thin layer of sand and asphalt to protect the steel from corrosion. Studies by Terzaghi (Ref. 81, 1933) indicated that this type of construction could be successfully employed under the same conditions where a steel storage tank founded on a 1-ft-thick reinforced-concrete inverted T-beam mat had failed. A mat of this type and thickness would not be strong enough to equalize a differential settlement y_d greater than some 2 or 3 in. (see Prob. 13-5). Once the mat failed, say, at the points A, B, C, and D, indicated in cross section in Fig. 13-8, the elastic line of the bottom of the steel tank would have to adapt itself to the surface of the concrete mat, that is, to the straight lines between these four points. The steel plate of the tank would be bent sharply, with very small resulting values r_2, r_3, r_4, and r_5 of the radius of curvature at these points, much smaller than indicated in the sketch, which is not drawn to scale. Failure of the steel plate would result, followed by leakage of the fluid stored in the tank. On the other hand, the thin steel plate of the bottom of the tank, when resting directly
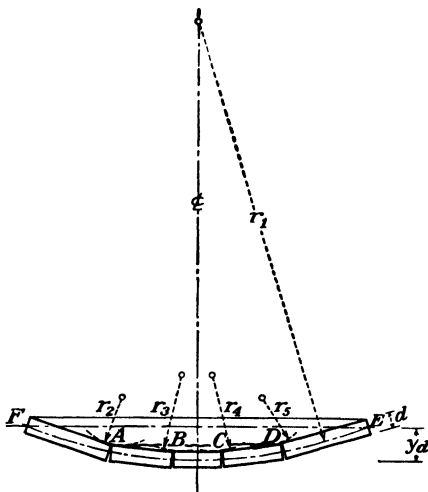
FIG. 13-8. Sketch illustrating the reason why a tank, such as is shown in Fig. 13-7, failed under similar soil conditions when it was founded on a 1-ft-thick reinforced-concrete mat of the inverted T-beam type.

on the ground, could safely adjust itself to the large radius of curvature r_1 without being in any way overstressed. Steel tanks of this type have been known to safely undergo differential settlements of as much as 1 ft (see Prob. 13-7). Of course, irrespective of the effects of differential settlements on the superstructure, the safety against a shear failure of the underlying soil, if it consists of clay, should be investigated (see Arts. 9-9, 9-10, 14-2, and 14-6).

The opposite extreme type of superstructure is illustrated in Fig. 13-9. A five-story storage building for a costly liquid was separated into small
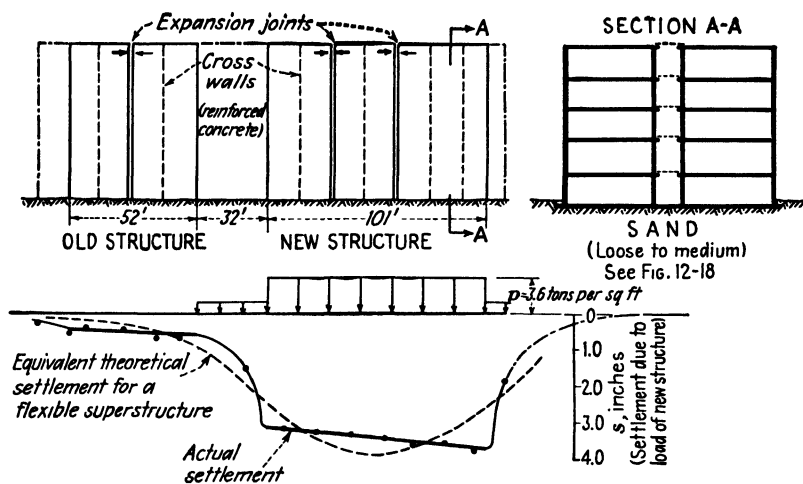
FIG. 13-9. Heavy structures can undergo differential settlements without damage when separated into small rigid units.

units which were perfectly rigid, since all the longitudinal and cross walls, as well as the slabs, were of reinforced concrete and formed a rigid monolith, capable of withstanding appreciable secondary stresses. The old structure, shown on the left of the diagram, is split up into four such units, and the new structure, shown at the center of the diagram, has six such units. The profile of the measured settlements in Fig. 13-9 shows that none of the units deflected at all, and that all units of each structure even settled to a slight uniform tilt. This indicates that the expansion joints (1 in. wide) functioned only partially, and that the combined action of tensile forces in the continuous foundation mat, plus compressive forces between adjoining units at the top of each joint, shown by arrows in Fig. 13-9, prevented any break in the uniformly inclined settlement surface, such as is sketched in Fig. 13-8. A slightly smaller settlement of the new structure occurred at the end closest to the old structure, presumably

because the soil (a loose sand, see Fig. 12-18) was already somewhat compacted there by pressures from the old structure.

The method of splitting up new buildings into small, very rigid, and strong units is frequently followed in mining areas where unforeseen but large motions of the soil surface may occur, with time, owing to the collapse of old shafts and tunnels, which often are at best only partially backfilled after completion of the mining. Such structural units are
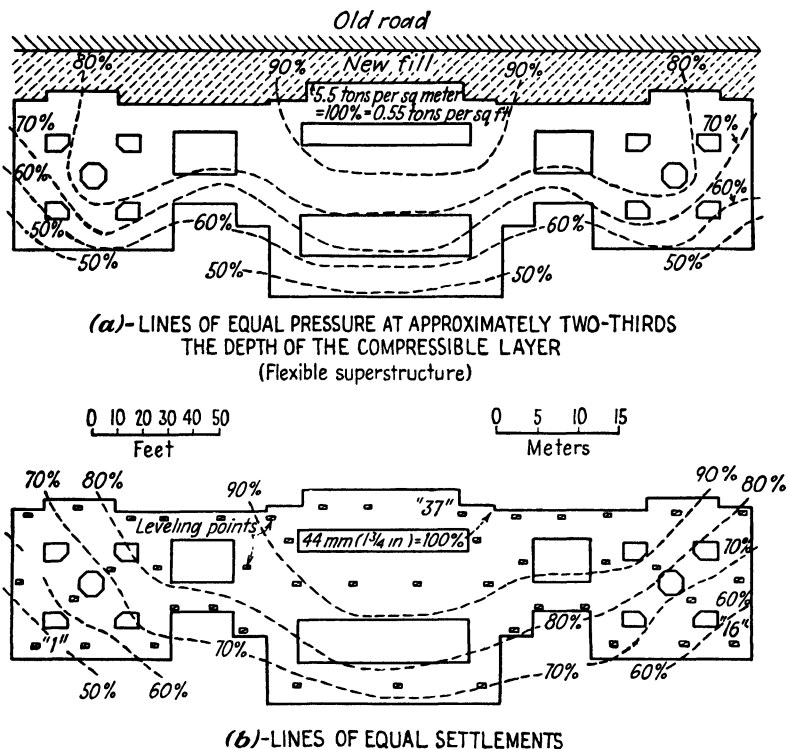
FIG. 13-10. The deflection of a long three-story masonry building indicates its great flexibility under the effect of small differential settlements (see Fig. 13-24). (*From Tschebotarioff, Ref. 370, 1936, and Ref. 377, 1940.*)

sometimes even given three-point support (see Legget, Ref. 210, 1939 and Mautner, Ref. 223, 1948).

The great majority of buildings are of a type which occupies an intermediate position between the two extremes which have just been discussed, that is, most buildings are of a semirigid type. A rigorous analysis of the amount of deflection which they can safely undergo is not possible, since very few numerical data are available concerning the strength and the elastic properties of entire masonry walls, especially

when they are weakened by windows or doors It therefore becomes necessary to base oneself on observations and measurements of full-scale structures in the field (Art. 13-8).

So long as the total settlement does not exceed 2 or 3 in., no damage is to be expected with most buildings. The differential settlement then does not exceed an inch or so, and it would appear that the masonry superstructure of most buildings can safely deflect by the necessary amount. Figure 13-10 illustrates this point. It will be noted that the lines of equal measured settlements follow the same pattern in respect to the magnitude and distribution of the settlements as do the lines of equal vertical pressure on the underlying clay layer. Since the vertical pressures were computed on the assumption of a perfectly flexible superstructure (see Art. 9-7), the similarity of their distribution to the settlement distribution indicates that the three-story (50-ft-high) 280-ft-long masonry building actually behaved up to that point as if it were almost perfectly flexible and that the clay layer was fairly homogeneous horizontally in respect to its compressibility. No cracks whatsoever could be noticed in the building. As time went by and the settlements increased, the equalizing effect of the semiflexible superstructure became more apparent (see W.S. Hanna, Ref. 165, 1950).

FIG. 13-11. Differential settlement and distribution of cracks over façade of a massive building. The location of the cracks is affected by the reinforced-concrete elements embedded in the masonry. *(From Tschebotarioff, Ref. 372, 1938, and Ref. 377, 1940.)*

A different case is illustrated by Fig. 13-11. The building was much heavier, higher (90 ft), but shorter (185 ft) along its main façade. Its total settlement was also larger and exceeded 12 in. because of the larger depth of compressible clay beneath its foundation and because of the characteristics of the latter. A leveling of the parapet indicated a differential settlement of 2 in. of the center of the façade in respect to its ends.

It will be noted that the 35-ft-high masonry wall between the parapet and the entrance columns of the façade deflected by that amount without cracking. This happened because the continuous reinforced-concrete lintel over the columns resisted the tension at the bottom of the wall, which acted as a 35-ft-high beam. The 13-ft-high masonry wall below the columns, however, cracked as shown. This can be attributed to the presence of an asphaltic and therefore slippery dampproof layer immediately above the reinforced-concrete pile-capping beam. The latter was intact, and the cracks, for instance, the one marked with a circle in Fig. 13-11, began in the masonry at the dampproof layer, where they were widest, and decreased in width higher up. The elevation of that layer
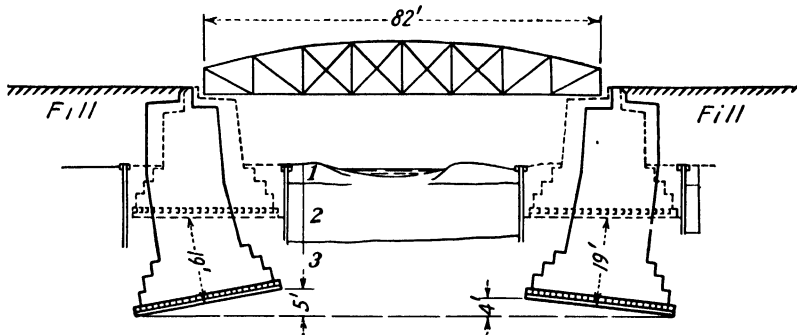
FIG. 13-12. Railroad service could be maintained over this simply supported girder bridge, in spite of a 19-ft settlement. (*From Wochenschrift d. Ost. Ing. u. Arch. Verein,* 1888, p. 342.)

therefore should have been staggered to key the masonry wall to the beam below (see Fig. 15-12). Other similar observations indicate that the cracking of masonry buildings supported by foundations which are likely to settle can be decreased to a minimum by providing within the walls continuous reinforced-concrete tie beams all around the building, of a height corresponding to one or two brick courses, immediately above and below window openings.

The amount of settlement which can be sustained without damage by a statically determined structure is illustrated in Fig. 13-12. The simply supported steel-girder bridge was continuously jacked up to keep it at its original elevation while the pier masonry and the approach fill were built up as their foundation settled to a total of 19 ft. Layer 1 was mud, layer 2 was clay, and layer 3 consisted of fine sand with many hollow shells, the crushing of which may have accounted for much of the settlement. Settlement was greatest on the embankment side, because of the added weight of the approach fill there.

The bridge illustrated in Fig. 13-13 could be kept in service, although it settled some 6½ ft and had a 5-ft differential settlement of its abut-

ments. The broken lines show, to scale, the original position of the bridge. The foundation had been apparently designed on the basis of the satisfactory driving record of individual piles, an unreliable procedure (see Art. 15-4). The driving of sheet piles on the river side did not slow down the rate of the continuously measured settlements. This provided an additional indication that they were caused primarily by a consolidation of the underlying layers and not by their lateral and upward flow. Part of the approach fill was removed and replaced by a light trestle; this decreased the rate of the settlements appreciably. A statically indeterminate structure, for instance, a two-hinged arch, would have failed
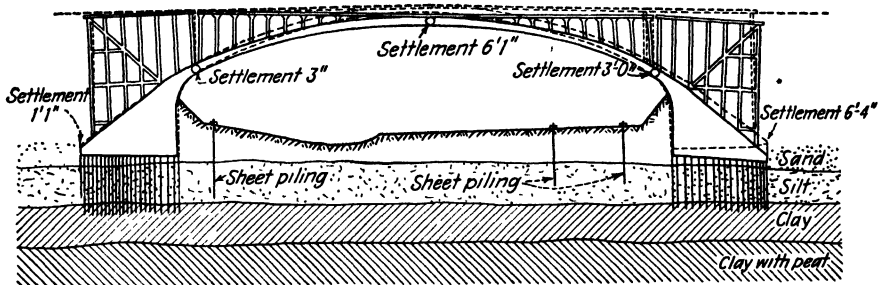
FIG. 13-13. A three-hinged arch bridge withstood the deformations caused by a 5-ft differential settlement of its foundations. (From Rybakoff, Ref. 297, 1937.)

inevitably at a fraction of the differential settlement which this three-hinged arch withstood.

13-4. The Presence and the Nature of Adjoining Structures Should Be Considered in Every Foundation Design. The damage that can be done by the settlements of a new building to an old building resting on compressible deposits is illustrated by Fig. 13-14. The severely damaged old four-story reinforced-concrete frame and brick building had been safely standing for a number of years until a new eight-story building was built next to it. The foundations of both buildings consisted of short 25-ft piles embedded in an upper stiff crust of clay below which softer clay was found. The settlement crater around the new building extended beneath the old one and caused a 6-in. differential settlement and cracking of its walls [compare with Fig. 13-5(I)].

The belief is frequently held that a structural expansion joint of an inch or so width between parts of buildings of different height and weight is sufficient to prevent damage of the lighter part by the settlements of the heavier part. This is a fallacy, since it is not possible to extend the structural expansion joint down through the soil between the two sections of the buildings. A so-called *settlement crater* will therefore be formed around the heavier part, as shown in Fig. 13-15, and will reach under the

lighter part, the settlement s_1 of which is much smaller than the settlement s_2 of the heavy part. The crater can extend to an appreciable distance around the new building (see Fig. 13-9). If the adjoining old building or the lighter part of the new building is designed to resist the stresses caused by part of it being cantilevered out over the settlement crater [see Fig. 13-15(II)], then no damage will be done to it. Otherwise it will have to adjust itself to the surface of the crater [Fig. 13-15(III)], and this may
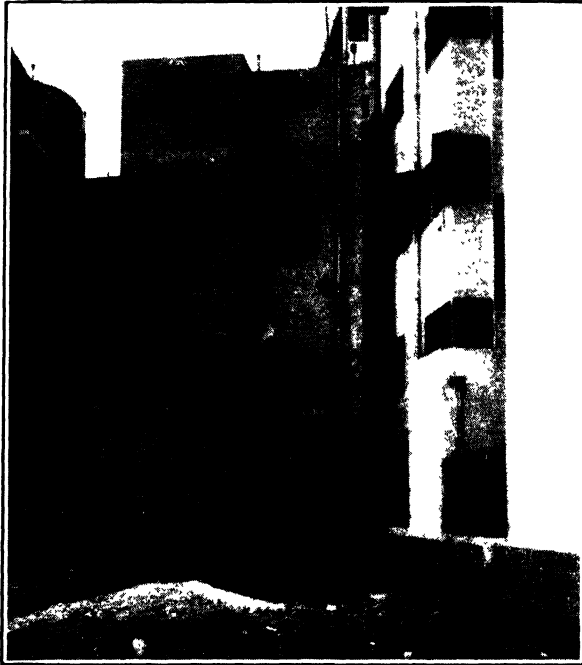
FIG. 13-14. Damage to the old four-story building on the left and in the center of the picture was caused by the settlement crater around the adjoining new eight-story building on the right. (*From Hanna and Tschebotarioff, Ref. 164, 1936.*)

produce damage of the type shown in Fig. 13-14. Expensive lawsuits may result. There are no generally accepted legal standards as to the responsibilities for damages of this kind when the two structures belong to different owners (see Ref. 276).

When building in localities with no firm soil layers within easy reach, the inevitability of differential settlements should be recognized in the architectural design. Considerable variations in the height of a structure, such as are shown in Fig. 13-15, should be avoided. If this is not possible, then at least arrangements should be made to build the low part of the structure somewhat later, when most of the settlements of the heavy part

have already taken place. This is frequently the case during the first year. At any rate, one should postpone the plaster work or the stone lining of the façade, since most of the visible and unsightly damages occur in such brittle surface materials. The structural framework usually can deform without being damaged. Settlement analyses (Art. 13-7) and settlement control observations (Art. 13-8) will help to decide the details of the structural design and the proper sequence of construction operations.

FIG. 13-15. Sketch illustrating discussion of measures necessary to prevent damage to light parts of a building by the settlement crater around adjoining heavy parts of the structure.

The relative elevation of the foundations of the new and of the old adjoining structures should always be given careful consideration. For instance, if building II shown in Fig. 13-16 is going to have two basements, so that its foundation will rest on rock, whereas the adjoining older and lighter building I had only one basement and was supported by overlying dense sand, then the wall *A* of building I will

FIG. 13-16. Wall *A* of building I has to be underpinned when building II is constructed; building III, when built later, has to be carried on piles of a type producing a minimum of soil displacement, or on caissons.

have to be underpinned (Art. 15-13) to transfer its load to the rock and to prevent the sand which supports the rest of the building I from yielding toward the deeper excavation of building II.

Similarly, if a later building III is to have only one basement, the presence of the two basements of the adjoining older building II will affect the choice of the foundation for building III. It will have to be carried down to rock, since otherwise excessive lateral pressures would be developed against the walls and the outer columns of building II along the line B. If piles are to be used to support building II, they should be of a type which will produce a minimum displacement of soil, for instance, the open-end steel-tube type (Art. 15-9), and which will hence produce a minimum increase of lateral pressure against the existing wall B. All of building III would then have to be supported on such piles, or on caissons carried down to rock, since otherwise it might tend to settle unevenly.

The possible effects of ground-water lowering should also be considered (see Art. 13-9).

13-5. The Depth to Which Foundations Should Reach. In all cases the foundation should be carried down below the depth h [see Fig.
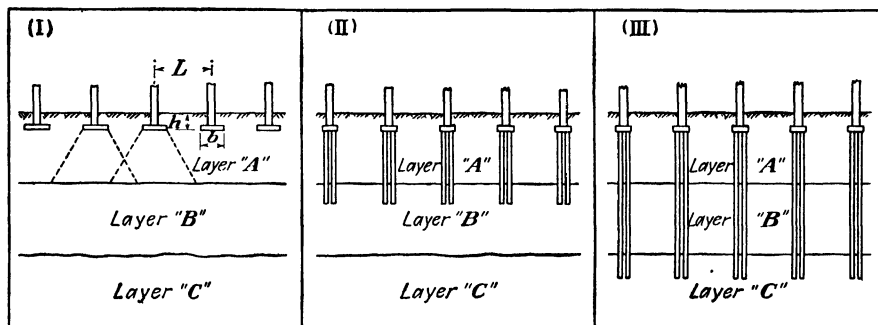
FIG. 13-17. Sketch illustrating the discussion of the depth to which foundations should reach.

13-17(I)] of seasonal variations in the upper soil layer, that is, through the so-called *active soil layer*, which may be affected by frost action and by other similar influences (see Art. 14-11).

Three hypothetical soil layers, A, B, and C, are shown in Fig. 13-17. The thickness of each layer may be assumed to vary from 10 to 40 ft, and the foundation may be supported by any of these three layers, depending on the following considerations. Whenever possible, deep foundations should be avoided, since their cost increases rapidly with depth. A foundation resting on the upper layer A, as shown in Fig. 13-17(I), will be acceptable for all types and weights of structures when all three layers A, B, and C have satisfactory supporting properties. If layer A is compact and stiff, whereas either or both of layers B and C are soft, then only

light structures can be supported on layer A. The limit permissible weight of the structure can be determined by means of settlement analyses (Art. 13-7), under consideration of the special points discussed in Arts. 13-1, 13-3, and 13-6.

If layer A is soft, whereas layer B is stiff, then the loads of the structure should be transferred to B by means of piles or caissons, as shown in Fig. 13-17(II). If the underlying layer C is soft to a great depth, then the limit weight of the structure which can be supported on B is to be determined in a manner similar to the one just outlined for layer A.
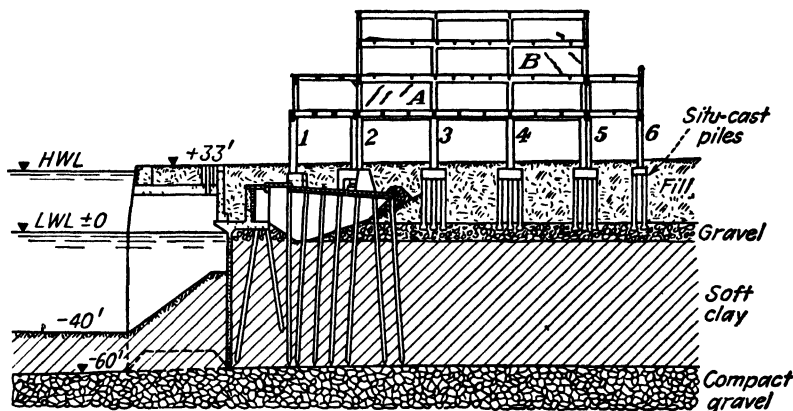
FIG. 13-18. Differential settlements and the resulting damage to the superstructure of the transatlantic pier in the harbor of Le Havre required the underpinning of rows 3, 4, 5, and 6 of columns, and the transfer of their loads to the layer of compact gravel at el. −60 ft. (*After Freyssinet, Ref. 139, 1939, and Rodio, Ref. 292, 1935.*)

When both layers A and B are too weak to support the loads of the proposed structure, whereas layer C is compact, then the foundation should be carried down to layer C.

In any case, it is advisable to avoid founding different parts of the same structure on different soil layers, even if the loads vary greatly, since otherwise differential settlements may be accentuated. This point is illustrated by Fig. 13-18. The quay wall was formed by caissons (Art. 16-16) sunk to compact gravel at el. −60 ft. The gaps between the individual caissons were bridged by reinforced-concrete slabs approximately at el. +20 ft. Column rows 1 and 2 of the pier building and some of the earth fill were supported by long precast reinforced-concrete piles, driven down to the same compact gravel layer at el. −60 ft. The remaining four column rows 3 to 6, however, were supported by short piles reaching down into an upper layer of gravel approximately at el. ±0.0. The inclination of the cracks at points A and B indicates that the consolidation of the soft clay below that gravel layer would have induced a greater settlement of

the center of the pier building, even if all its column rows were supported by the upper gravel layer [compare with Fig. 13-5(II)]. Column rows 3 to 6 therefore had to be underpinned by long piles reaching down to el. −60 ft. Nevertheless, the severe cracking at A was undoubtedly
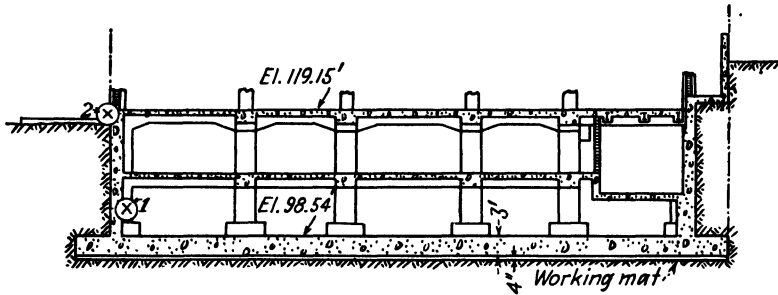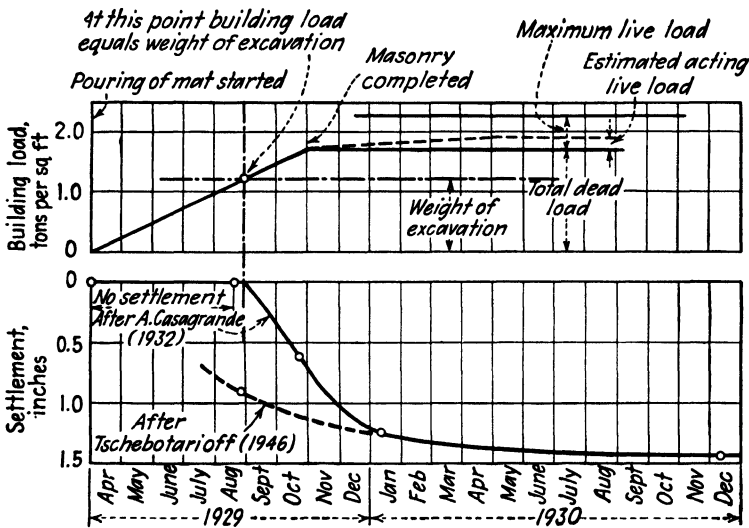
(B)

FIG. 13-19. Diagrams illustrating belief advanced in 1932 that settlements of a structure would not start until its weight equaled the weight of the excavation. Later studies (1946) showed this was based on incorrect data. (*From G. W. Glick, Ref.* 154, 1930, *A. Casagrande, Ref.* 61, 1932, *and Tschebotarioff, Ref.* 380, 1946.)

aggravated by the unyielding support originally provided to column rows 1 and 2.

The preceding discussion gives only a brief outline of the procedures which are to be followed under somewhat simplified limit conditions. It should be realized that in actual practice an innumerable number of com-

binations of other special conditions may arise in the field and that the selection of the solution best suited to meet all these conditions in the particular combination encountered is an *art* which can be developed only through experience in its practice, built up on a sound knowledge and understanding of the fundamentals involved.

13-6. The Decrease of Settlements by the Provision of Basements. The provision of a basement has a beneficial effect, in the sense that the excavation of the soil for the basement increases the ultimate load that the soil can carry by decreasing the danger of a shear failure under a mat covering the entire area (Prob. 14-1). However, the ultimate load
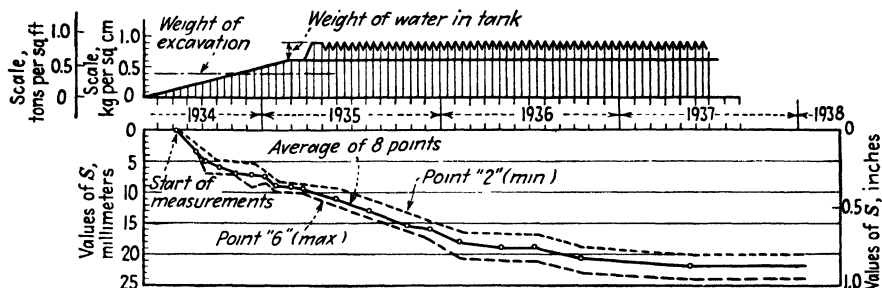
FIG. 13-20. Measurements on a water tank in Egypt showed that settlements began well before its weight equaled the weight of the excavation. (*After Hanna and Tschebotarioff, Ref.* 164, 1936, *and Tschebotarioff, Ref.* 377, 1940.)

on separate spread footings, when such are used, remains unaffected by basement excavation in a soil whose properties do not change with depth.

Subject to some important limitations, an excavation for a basement may serve to decrease the settlements of the building. These limitations were not realized at first. A. Casagrande published in 1932 (Ref. 61) the curve shown in Fig. 13-9(B), according to which the settlements of the Albany Telephone Building did not begin until the weight of the building exceeded the weight of the excavation. Observations made by Hanna and Tschebotarioff in Egypt, as shown in Fig. 13-20, however, indicated that settlements began well before that. At about the same time, Cuevas (Ref. 95, 1936) reported measurements in Mexico City excavations which recorded uneven heaving of the bottom of the pit up to values of 4 ft (Fig. 14-5). A reversal of such upward movements was therefore to be expected as soon as construction started. This type of movement was actually recorded during later measurements in Boston by A. Casagrande and R. E. Fadum (Ref. 65, 1944). Finally studies by Tschebotarioff (Ref. 380, 1946) showed that part of A. Casagrande's original 1932 data were based on some misunderstanding and that the actual settlements of the Albany Telephone Building were as given by the broken line in Fig.

13-19(*B*). This curve refers to the part of the building where no slide had occurred during the basement excavation (Art. 14-6).

Nevertheless, subject to some restrictions and limitations, basement excavations can be successfully employed for the purpose of decreasing settlements. The necessary precautions and a more detailed analysis of the problem are given in Art. 14-6.

13-7. Analysis of Settlements. By settlement analysis is meant the investigation and the detailed study of all factors which affect settlements. Of particular importance for foundation design is the knowledge of (*a*) the distribution in plan of settlements, (*b*) the final value of the settlements, and (*c*) the rate of the settlements.

The settlements themselves may be caused by the combined effects of vertical consolidation and lateral and upward displacement due to lateral pressures and to shearing stresses (see Figs. 9-5 and 9-8). The settlement component due to lateral and vertical displacement is of practical importance mainly in the case of soils with little shearing strength, such as very soft clays, which can be easily displaced, like a viscous fluid. This settlement component can be reduced in such soils by driving sheet piling around the perimeter of the foundation (see Prob. 15-4).

In all other soils the effects of the settlement component due to vertical consolidation usually predominate considerably. For that reason settlement analyses are, as a rule, limited to the study of this latter component.

The final value of the settlement of a certain point of the foundation is obtained as follows: The increment of vertical pressure caused by the foundation loads at several elevations of the underlying compressible layers is computed, as shown in Prob. 9-2. The corresponding values of the moduli of volume change m_v' are determined from laboratory consolidation tests on undisturbed samples, as shown in Prob. 6-2. The settlements for each layer are then computed and added up to give the final value of the surface settlement, as shown in Prob. 13-2. The soil layer within which originates 75 per cent of the surface settlement is termed the *seat of settlement.*

It should be realized that soil samples are subject to many types of disturbance and that the verification of settlement forecasts by systematic regional field observations on actual structures is essential, as outlined in Art. 13-8. Most observations carried out so far indicate that the observed settlements, as a rule, are somewhat smaller than the ones forecast on the strength of laboratory consolidation tests, in spite of the fact that the latter take into account only one of the two theoretically possible settlement components. An exception to this rule is presented by the measured settlements of some structures located close to the bank

of a river or of a lake, where lateral and upward squeezing of soft clay may have been facilitated in that direction.

Studies in Egypt (see Tschebotarioff, Ref. 369, 1936) have shown that settlements computed in the conventional manner from the first run of loading during a consolidation test were at least twice as large as those observed. This was attributed to the initial expansion during sampling and after flooding in the consolidometer of the swelling type of local clays. To counteract this effect, such samples were loaded up to the preconsolidation load (Art. 6-4), which was first determined on a separate sample from the same layer. Then the load was reduced to the value of the over-
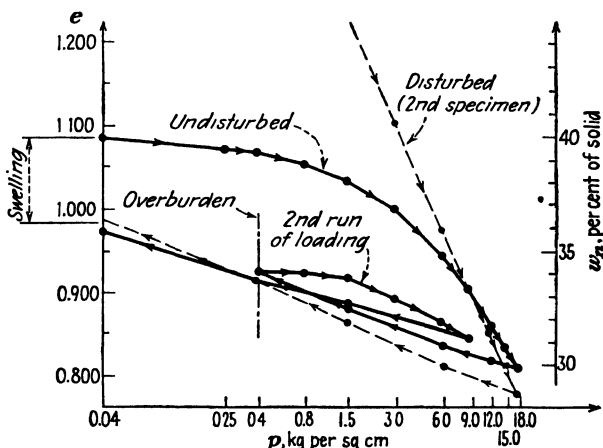
FIG. 13-21. The modulus of volume change m_v' of swelling clays tested in a submerged condition should be computed from the second run of loading in a consolidometer. (*From Tschebotarioff, Ref. 369, 1936.*)

burden at the elevation from which the sample was taken and was increased again. This second run of loading (see Fig. 13-21) was then used to compute the m_v' values, which were found to agree quite closely with the values computed from measurements of full-scale structures. Similar results were obtained through the application of the same procedure to compact varved clays at Albany, New York, by Tschebotarioff and Schuyler (Ref. 389, 1948), as shown in Fig. 13-22. This diagram brings out the various other factors which have to be considered when comparing the results of field settlement measurements and laboratory consolidation tests by means of the m_v' values. The m_v' laboratory values of that diagram refer to the range of pressure caused by an increment of 1 ton per ft^2 in excess of the overburden pressure at the depth from which the soil sample was extracted.

A somewhat different attempt was made by Hanna (Ref. 165, 1950) to

prevent swelling of Egyptian clays of the type to which Fig. 13-21 refers. A sampler with separate rings, which were then used as floating-ring consolidometers (Art. 6-2), was employed. The relatively thick walls of such ring samplers and the resulting high value of their area ratio (Art. 12-7) did not appear to cause harm in that type of clay, which is not sensitive to remolding (Art. 7-22). The same technique may be modified for use on more sensitive types of clay by sawing thin-walled Shelby tube samplers into rings, removing by means of a special tool the clay surfaces

FIG. 13-22. Comparison of values of the modulus of volume change m_v' computed from the average results of different laboratory consolidation-test procedures and from settlement observations of two buildings—A and B. (From Tschebotarioff and Schuyler, Ref. 389, 1948.)

remolded by the sawing, and then performing the consolidation test without removing the clay from the ring.

The compressibility of saturated clays can vary appreciably. Thus observations of structures show that naturally consolidated soft clays and silts may have m_v' values varying from 0.010 to 0.060 ft^2 per ton, whereas stiffer, overconsolidated clays (which acquired these characteristics, for instance, by past drying) will have m_v' values varying between 0.003 and 0.010 ft^2 per ton.

The rate of settlement of a structure resting on a clay layer can be determined as outlined in Probs. 6-3, 6-4, and 6-5, once the coefficients of permeability and the boundary conditions of drainage have been determined. Figure 13-23 illustrates the effect of variations in the value of the coefficient of permeability and of the layer thickness on the time which will elapse until 90 per cent of the final settlements will occur (see Probs.

13-1 and 13-3). This diagram refers to the simplest type of boundary conditions, as shown, and to an assumed value of its modulus of volume change $m_v' = 0.01$ ft^2 per ton. A higher value of m_v' will mean that more excess water will have to be expelled from the voids, so that settlements will take somewhat longer [Eq. (6-31)]. A method for the computation of settlements under boundary conditions permitting only partial drainage, that is, for the case of successive layers of varying permeability, has been given by Hamilton Gray (Ref. 159, 1945).
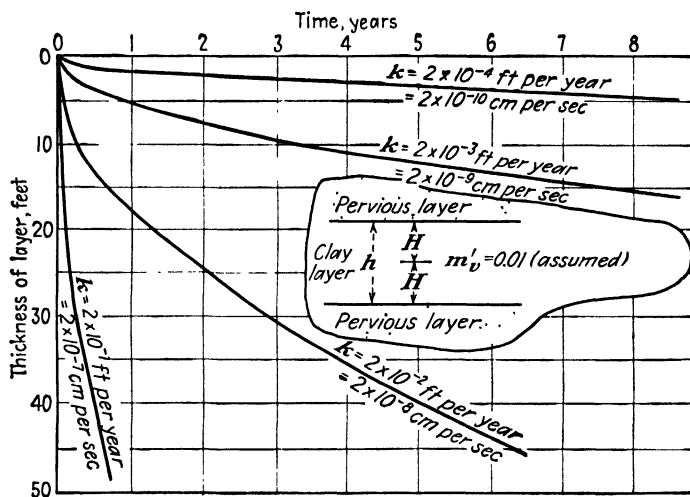
FIG. 13-23. Time required to reach 90 per cent consolidation (based on Terzaghi's theory of consolidation). (*From Tschebotarioff, Ref. 373, 1938.*)

13-8. Control Observations of Structures.

Measurements of the settlements of a structure, both during and after construction, serve as a control of its performance and as an insurance against unforeseen developments which might cause damages unless checked. Appropriate measures can then be taken in time. For instance, one of several piers which rested on pile foundations and supported the continuous main steel girders of the approach spans to a large bridge was found to develop a tendency for settlement. This was disclosed by repeated levelings. The girder was then repeatedly jacked up, and its bearing plates were shimmed up, so that the intended elevation of the girder support was maintained, without damage to the superstructure, until further settlements of the pier beneath had stopped. In another case continuous settlement measurements of a badly cracked building indicated that the rate of settlement had decreased to such an extent that the contemplated underpinning of its foundation was no longer necessary. The cost of such observations is

negligible by comparison with the importance and the value of the information which they supply.

Permanent bench marks should be provided for settlement observations; Terzaghi (Ref. 357, 1938) has developed a type of bench mark* which combines a satisfactory appearance with rugged construction. A large number of such bench marks should be installed if a clear picture of
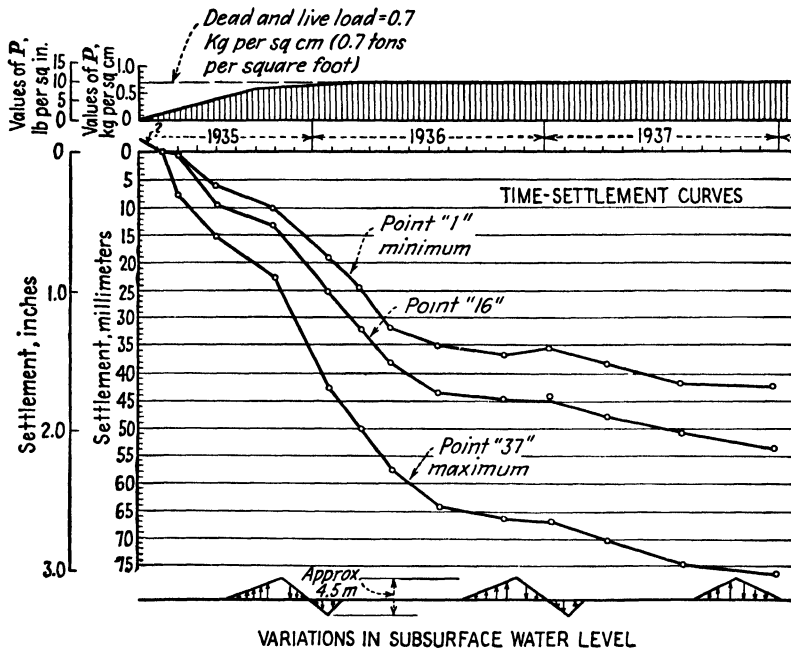
FIG. 13-24. Time-settlement curves reflect significant changes in the subsoil conditions, for instance, ground-water-level variations (compare with Fig. 13-10). (*From Tschebotarioff, Ref. 377, 1940.*)

the distribution of the settlements over the area of the structure is to be obtained. For instance, 45 such bench marks were used on the building illustrated in Fig. 13-10. A special type of water level (Ref. 357) may be advantageously substituted for optical leveling when working in a crowded basement or in a machine or factory shop (Ref. 371).

Levelings should be begun from the very start of construction. To that end, settlement bench marks should be installed in basement columns, for instance, at the elevation marked with a cross and the number 1 in Fig. 13-19(A). In the case of that particular building levelings were discontinued after its completion, since the lower basement bench marks no

*The Terzaghi bench mark is illustrated in Fig. 42 of Ref. 357. The dimensions are, however, erroneously indicated in inches—they should read mm—and the diameter of the bench mark is 32 mm and not 32 in.

longer could be easily related to outside monuments on the soil surface. This type of difficulty may be overcome by the early provision of several outside bench marks at the elevation marked by a cross and the number 2 in Fig. 13-19(A) in the same columns where there are bench marks at elevation 1. The compression of the column between elevations 1 and 2 can be neglected, as a rule, and the assumption made that the settlement of the bench marks at these two elevations of the same column is identical. The leveling circuit in the basement can then be easily related to the outside leveling circuit at any time.

Properly kept records of the performance of a structure should permit the presentation of their summary in graphical form. In addition to the distribution of settlements in plan, as shown in Fig. 13-10, time-settlement curves should be plotted, as shown in Fig. 13-24, in conjunction with any other relevant data, for instance, water-level variations (compare with Prob. 13-4). Loading, foundation, soil, and settlement profiles should also be drawn, for example as shown for a different building in Fig. 13-25.

There are three main types of time-settlement curves of actual structures. In the first type most of the settlement will occur during construction; this will be the case of foundations resting on compact pervious soils. In the case of structures supported by clay and silt soils the shape of the time-settlement curve may vary, depending on whether primary or secondary time effects predominate (Art. 6-9). If the soil follows the laws of Terzaghi's theory of consolidation, the settlements will decrease progressively and will stop entirely after a certain period of time, following the end of construction. The time-settlement curve will have a parabolic shape; this is the second type of curve. In the third type, the time-settlement curve may have the shape of a straight line, either from the very start or as a tangent to the initial parabola. This may indicate one of two things: either the settlements are caused by possible dangerous shearing deformations of the entire soil mass (see Art. 9-10), or the structure of the soil is such that the slippage of grain upon grain delays the consolidation. Such so-called secondary time effects will, however, also show up during a laboratory consolidation test (Art. 6-9). They may happen in peat and in some other soils (Art. 11-8). This point is of importance in connection with the use of sand drains (Art. 19-4).

The inclination of a factory chimney or of similar slender towers due to uneven foundation settlement can be determined by means of a transit. It should, however, be noted when measuring *changes* of such inclination that one-sided heating by the rays of the sun is liable to produce elastic lateral parabolic deflection of the chimney away from the sun. Tschebotarioff (1936) measured by means of Huggenberger clinometers (levels with micrometer screws to measure changes of inclination) the daily
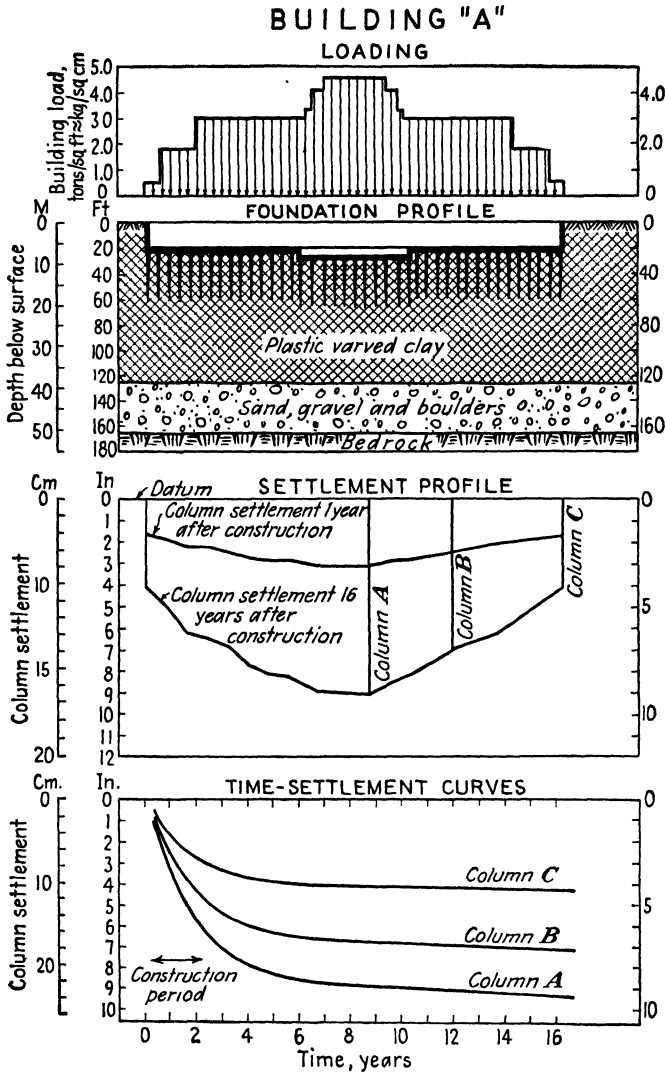
FIG. 13-25. Diagrammatic presentation of data summarizing the settlement records of a properly observed building. (*From Tschebotarioff and Schuyler, Ref. 389, 1948.*)

displacement of the top of a 130-ft-high and 12-ft-wide minaret, which was found to move laterally slightly over ½ in. (Ref. 329, Fig. 28). In plan the daily movement of the top of the minaret traced a loop. Any precise transit measurements of chimney inclinations should therefore be performed in cloudy weather or at night.

Lateral earth pressures in cuts (Art. 10-18) should be measured on

important constructions whenever possible. This can best be done by the measurement of strut forces. There are several techniques of such measurements. One method consists in measuring the strains in the struts, from which the loads can be computed when the Young modulus of the strut material and its cross-sectional area are known. Golder (Ref. 157, 1948) described a technique for the successful use of this method with seasoned timber struts. With metal struts the use of Carlson-type strain meters* (Ref. 59) is preferable. These meters utilize very thin prestressed wires mounted on porcelain spools and operate under remote control on the electric-resistivity principle, similar to the SR-4 strain gages (Art. 10-23). However, the Carlson meters are much more stable in their readings, since no cement capable of undergoing, with time, erratic volume changes is used. They can also be successfully employed for remote-control measurements of anchor pulls on sheet-pile bulkheads (Art. 16-14). A second method consists in the use of hydraulic jacks to measure the force required to relieve the existing stress in the struts, one by one (see Refs. 360 and 259).

Observations of this type, when begun at early stages of the construction, may permit important economies on sections of the excavation to be built later. A "design as you go" approach to the design of the sheeting and of the struts is fully justified when it is based on actual control measurements, in spite of administrative difficulties which it involves.

The use of earth and pore pressure measuring cells is outlined in Arts. 17-6 and 19-6.

13-9. Settlements Produced by the Lowering of the Ground-water Table. Excavations in sandy soils, or close to such pervious layers, frequently require the lowering of the ground-water table by means of wellpoints (Art. 14-9). This reduces the buoyancy and thereby increases the effective weight of the soil within the depth of the lowered ground-water table (see Prob. 13-4). As a result, that layer and the soil layers beneath it receive an additional load and undergo additional consolidation. Surface settlements will follow.

An example is provided by the very careful measurements performed during the construction of the Rotterdam tunnel. Some data concerning that project are given in Arts. 10-20 and 16-5, as well as in Figs. 10-29 and 16-13. Wellpoints relieved the uplift pressures in a sand layer which underlay soft clay and peat. As shown in Fig. 13-26, the ground-water level in observation wells, which reached to the sand, dropped at times up to 42 ft. The settlements of the ground surface were greatest close to the line of wellpoints and observation wells, 20 in. at a distance of 30 ft, but

* Designed and built by Professor Roy W. Carlson, University of California, Berkeley.

decreased with the distance, for instance, they equaled 3 in. some 360 ft away. The rate of settlement closely followed the variations in the water head of the sand layer.

In all similar work, careful studies should be made of the effect which differential settlements of the ground surface may have on existing structures in the vicinity. Such settlements will naturally increase with the
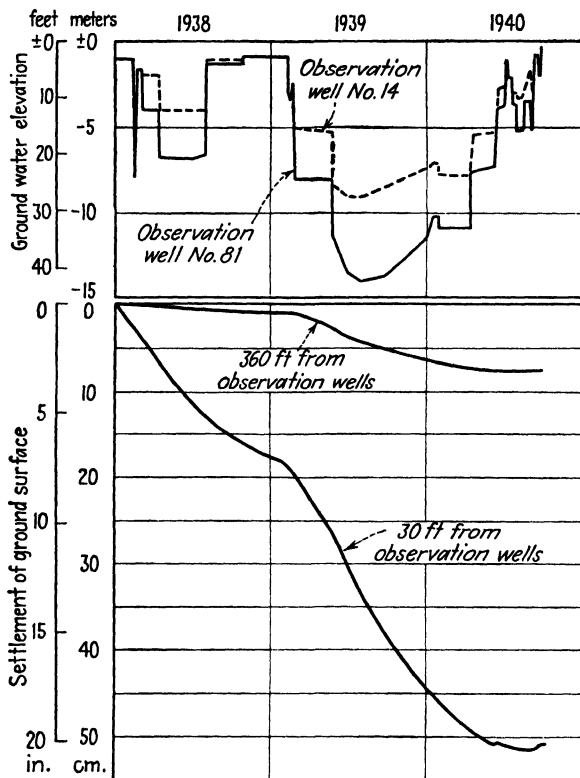
FIG. 13-26. Effect of the lowering of the ground-water table on surface settlements during the construction of the Rotterdam tunnel (see Figs. 10-29 and 16-13). (*After J. P. van Bruggen, Ref. 44, 1941.*)

depth to which ground water is lowered and with the duration of the pumping. The usual procedures of settlement analysis (Art. 13-7) are applied to the solution of the problem, where the loads which produce settlement are determined in a manner similar to that outlined in Prob. 13-4. The T_γ values from Fig. 6-11 should be used for the computation of the rate of settlement of layers, the effective weight of which has been increased by the lowering of the ground water.

The pumping of oil from deep strata can have similar effects. For

instance, serious problems have been created at Long Beach, California, where an area several miles wide along the coast has been sinking in recent years at a rate of 1.5 ft per year. The settlements have reached 11.0 ft and are estimated to reach 20 ft within a few years. Dikes and locks had to be built to keep high tides from flooding the city and harbor area; bridges over navigable channels had to be raised (Refs. 89 and 74).

Practice Problems

13-1. Check a point of one of the curves given in Fig. 13-23, say, for $h = 2H = 10$ ft and $k = 2 \times 10^{-9}$ cm per min $= 2 \times 10^{-3}$ ft per year. Note that $m_v' = 0.01$ ft² per ton and $T = 0.85$ for $U = 90$ per cent (see Fig. 6-11).

Answer. Eqs. (6-12), (6-27), and (6-29) can be transformed to read

$$t = \frac{H^2 T m_v' \gamma_w}{k}$$

Since H will be given in feet, m_v' in square feet per ton, and k in feet per year, the unit weight of the water must be given in the same units: $\gamma_w = 3.125 \times 10^{-2}$ ton per ft³. Hence

$$t = \frac{5.0^2 \times 0.85 \times 0.01 \times 3.125 \times 10^{-2}}{2 \times 10^{-3}} = 3.32 \text{ years}$$

This is the value which we read off Fig. 13-23 for $h = 10$ ft and $k = 2 \times 10^{-3}$ ft per year.

13-2. Estimate the final value of the settlement which will be caused by the consolidation under the weight of the new fill of the soft clay layer shown in Fig. 13-3. Assume for the first estimation that the full weight of the fill will be effective throughout the depth of the layer at the location of borehole 2, that the fill weighs 125 lb per ft³ above the water level (el. ± 0.0 ft) and 65 lb per ft³ below that level, and that the average value of the modulus of volume change of the soft clay is $m_v' = 0.060$ ft² per ton between the elevations -10 and -20 ft and $m_v' = 0.040$ ft² per ton between the elevations -20 and -40 ft.

Answer. The fill weighs

$$\begin{aligned} 12 \times 125 &= 1{,}500 \text{ lb per ft}^2 \\ 10 \times 65 &= \underline{650 \text{ lb per ft}^2} \\ & 2{,}150 \text{ lb per ft}^2 = 1.075 \text{ tons per ft}^2 \end{aligned}$$

With reference to Eq. (6-13), the final settlement is found to be

$$\begin{aligned} S_1 &= 10 \times 0.060 \times 1.075 \times 12 = 7.75 \text{ in.} \\ S_2 &= 20 \times 0.040 \times 1.075 \times 12 = \underline{10.35 \text{ in.}} \\ S &= 18.10 \text{ in.} \end{aligned}$$

13-3. What time is likely to elapse until 50 per cent of the settlement computed in Prob. 13-2 is reached? The average value of the coefficient of permeability of the 30-ft-thick soft clay layer was found to be $k = 8 \times 10^{-9}$ cm per sec $\approx 8 \times 10^{-3}$ ft per year; the average value of the modulus of volume change for the entire layer is $m_v' = 0.047$ ft² per ton.

Answer. From Fig. 13-23 we find $t = 2.9$ years for $U = 90$ per cent, $k = 2 \times 10^{-2}$ ft per year, $h = 30$ ft, and $m_v = 0.01$ ft² per ton. The value for $U = 50$ per cent

can be obtained by multiplication by the corresponding values of the time factor T [see Eq. (6-29) and Fig. 6-11]:

$$t_{50} = 2.9 \frac{0.20}{0.85} = 0.683 \text{ year}$$

The correction for values of k and of m_v' different from those employed in drawing Fig. 13-23 gives us the answer

$$t_{50} = 0.683 \times \frac{2 \times 10^{-2}}{8 \times 10^{-3}} \times \frac{0.047}{0.010} = 8.05 \text{ years}$$

13-4. With reference to Fig. 13-24, by what amount will the effective vertical pressures on the underlying layers be changed by a 4.5-m (14.7-ft) fluctuation of the ground-water level? Assume that the soil within the range of water-level variation remains fully saturated at all times, that its specific gravity is $G = 2.7$, and that its void ratio is $e = 1.00$.

Answer. With reference to Eqs. (4-7), (4-9), and (4-11), we find that, when saturated by capillarity, the soil weighs

$$\frac{2.7 + 1.0}{1 + 1.0} \times 62.4 = 115.5 \text{ lb per ft}^3$$

When buoyed, it weighs

$$\frac{2.7 - 1}{1 + 1.0} \times 62.4 = 53.1 \text{ lb per ft}^3$$

The difference per foot depth is $115.5 - 53.1 = 62.4$ lb per ft^3. Thus full buoyancy is effective, and a rise of the water level shown in Fig. 13-24 will decrease the effective pressures on the underlying layers by $62.4 \times 14.7 = 908$ lb per ft^2 = 0.45 ton per ft^2.

13-5. Estimate the compressive stresses in the concrete of a reinforced-concrete mat of an inverted T-beam type [Fig. 14-2(A)] with $b = 10$ in., $d = 12$ in., and $l = 8$ ft, provided as a foundation for a tank shown in Fig. 13-7; the differential settlement was $y_d = 3$ in. Assume 2,000-psi concrete, with $E_c = 2 \times 10^6$ psi.

Answer. If we neglect the double curvature of the settlement crater, as well as the fact that the neutral axis of a reinforced-concrete slab is not at its midheight, as was assumed in the derivation of Eqs. (13-2) and (13-4), we can use the latter equation for an approximate estimation of the compressive stresses at the top surface of a solid slab:

$$f_c = \frac{4 \times 2 \times 10^6 \times 12 \times 3}{(98.4 \times 12)^2} = 207 \text{ psi}$$

In the case of an inverted T beam, with reference to Fig. 14-2(A), this stress would be increased to

$$f_c = 207 \frac{l}{b} = 207 \frac{8 \times 12}{10} = 1{,}985 \text{ psi}$$

Crushing of the concrete in the webs and a failure of the type illustrated by Fig. 13-8 would therefore be likely to result, unless the concrete was of a particularly high quality.

13-6. What would be the approximate compressive stress in a solid reinforced-concrete mat of 4 in. thickness if it were substituted for the inverted T-beam mat analyzed in Prob. 13-5?

Answer:

$$f_c = 207 \times 4/12 = 69 \text{ psi}$$

This is a safe stress.

13-7. What would be the stress in the 1-in.-thick steel plate of the bottom of the tank shown in Fig. 13-7 that would result from a differential settlement $y_d = 12$ in. if the plate rested directly on the surface of the ground?

Answer:

$$f_c = \frac{4 \times 3 \times 10^7 \times 1 \times 12}{(98.4 \times 12)^2} = 1{,}030 \text{ psi}$$

This is a safe stress.

CHAPTER 14

SPREAD FOUNDATIONS. EXCAVATIONS

14-1. Permissible Values of Average Unit Contact Pressures with the Soil. So-called permissible or safe bearing values were established in the past on the basis of experience. Opinions as to the performance of different types of structures were apt to vary widely in different localities, since such opinions were usually based on the presence or on the absence of visible signs of damage to the local structures. Measurements were seldom made, so that the actual factor of safety in undamaged structures could only be guessed at. In addition, no methods had yet been developed to record numerically the relevant properties of soils, and such terms as "dense" and "loose" or "stiff" and "soft" easily lent themselves to wide differences in interpretation. Only average contact pressures between foundation and soil were given consideration in building codes, and as a rule, the safe pressures on deeper lying layers were not specified.

It is therefore not surprising that the building codes of cities with different geological and soil conditions varied considerably from each other as to the bearing values which were considered "safe" for soils designated by the same name. The impact of the new theoretical and experimental findings and of the new forms of synthesis of all available soil engineering knowledge, which are commonly referred to under the abbreviated name of *soil mechanics* (see Arts. 1-3 to 1-5), began to affect revisions of old building codes only in the late 1930's. A number of antiquated codes are therefore still in existence.

Some now customary approximate limits of safe bearing values are outlined in Table 14-1. These values refer not only to the average contact pressures between foundation and soil, but also to the pressures on softer layers at some depth below the foundation. Pressures on such layers can be computed for preliminary evaluation purposes as if they were uniformly distributed on areas of underlying layers limited by planes inclined at an angle of 30° with the vertical (see Fig. 9-1). The weight of soil excavated, for instance, for basements, may be subtracted from the weight of the structure.

It will be noted from Table 14-1 that there is considerable latitude for judgment in the determination of permissible pressures on *fissured* rock. It should be mentioned in this connection that some codes, for instance, the one of the Pacific Coast Building Officials, related the permissible bearing values p_0 of rock to its *crushing strength*, that is, to its unconfined compressive strength q_u, by specifying that $p_0 \leq q_u/5$. With

TABLE 14-1. Some Customary Permissible Bearing Values

Type of Rock or Soil (See Art. 2-1)	Permissible Bearing Value p_0, Tons per ft²
Igneous crystalline rocks* (granite, traprock, etc.)	100
Foliated metamorphic rocks* (schist, slate, etc.)	40
Sedimentary rocks* (sandstone, limestone, etc.)	15
Hard shales*	10
Hardpan (very compact cemented mixtures of gravel and sand)	10
Sands and gravels (depending on density, see Table 14-2)	0–6
Clays (depending on consistency, see Fig. 14-1 and Tables 14-3 and 14-4)	0–4

* Refers to sound condition; for broken rock the above values should be reduced. In some localities the above values may be greatly increased because of the high quality of the local deposits.

reference to Eqs. (9-20) and (7-17), it can be seen that this is equivalent to specifying a very high factor of safety $F_s = p_{max}/p_0 \geq 13.8$ for continuous footings. Even so, unconfined compression tests made by the author on core samples (Art. 12-8) of New Jersey shale, in combination with the above criterion, gave permissible pressures well above those of Table

TABLE 14-2. Approximate Limits of Permissible Bearing Values of Gravels and Sands

Relative density	Blows on S. & H. spoon (see Table 12-2)	Permissible bearing values, tons per ft² p_0
Dense	Over 30	3.0–6.0
Medium	10–30	1.0–3.0
Loose*	1–10	0.0–1.0

* The value of 0.0 ton per ft² refers to saturated loose sands under structures in the immediate vicinity of heavy machinery (such as compressors, forge hammers, etc.) or in regions of strong earthquakes. Such sands should be compacted (Arts. 11-4 and 11-5).

14-1. This indicates that these customary permissible bearing values are strongly influenced by the greater possibility of fissuration within a *large* mass of rock. These values may be increased when there is absolute certainty that the rock is quite sound (compare with Art. 15-9).

The permissible bearing values of sands and gravels are outlined in Table 14-2 as functions of the density determined by means of penetration

tests (Art. 12-9). Much further research is needed on this point (see Table 12-2), and here again much is left to individual judgment at present. Higher bearing values are usually assigned to coarser grained material, for instance, to gravel or to coarse sand, of the same density as fine sand. A reason for this is the greater likelihood of development of excess pore pressures in saturated fine sands and of their liquefaction due to shocks or vibrations (see Art. 7-16).

14-2. The Selection of Factors of Safety for Clay Soils. The problem of selection of an adequate factor of safety is particularly important when dealing with clay soils. The low shearing strengths of such soils do not permit excessive values of safety factors which would include our "factors of ignorance," since in many cases this would make it impossible to build the proposed structure on the location otherwise most suited for it. At the same time, the accurate determination of the actual shearing strength of clays is difficult.

Two main lines of approach to this problem have been developed. In the first and most generally accepted line, the permissible bearing value is based on the shearing strength at failure as determined by quick laboratory tests. For instance, Terzaghi and Peck (Ref. 365, 1948) suggest a normal value of the factor of safety $F_s = 3.00$ and a minimum value of $F_s = 2.00$, to be based on the results of unconfined compressive-strength tests carried to failure.

The second method of approach to the problem was developed by Housel at the University of Michigan and is based on the yield point of a clay, as determined by means of slow undrained double-transverse-shear direct-ring tests (Arts. 7-5 and 7-21 and Fig. 7-32). Very low values were obtained, and Housel introduced a correction factor, which he termed the *overload ratio*, by which the yield value of the clay was to be multiplied in order to obtain permissible values for use in design. Table 14-3 gives these values and is based on a letter of June 5, 1950, from W. S. Housel in reply to an inquiry by the author. The relationship between these overload-ratio values and the factors of safety based on the unconfined compressive strength q_u, as well as the values proposed by Terzaghi and Peck, is also given in Table 14-3. It will be noted that in the final analysis approximately the same permissible bearing values are obtained in some cases by both methods.

The overload-ratio value of unity is nevertheless somewhat too conservative, even for permanent structures. It appears to be based on the assumption that a progressive failure of a clay may develop under constant loading over a period of years. This assumption ignores the possibility of an increase of the shearing strength of a stressed clay over a period of years, caused by some additional consolidation when drainage

is possible, as is frequently the case (Art. 7-14). Additional consolidation under the action of stresses imposed by the foundation loads may be unimportant in the case of the compact type of clays of the Detroit region, studies of which appear to have formed the basis for the development of Housel's theories. Some of these clays are very soft ($q_u = 0.18$ ton per ft^2) at natural water contents of only 20 per cent. This is a rather unusual relationship, which does not seem to be frequently encountered elsewhere. In most clay deposits of other localities the favorable effect of additional consolidation over periods of years should not be ignored, since it is at least likely to counterbalance detrimental effects of gradual plastic flow.

TABLE 14-3. The Average Relationship between Housel's Overload Ratio and Factors of Safety F_s Based on the Unconfined Compressive Strength q_u of Clays

	Values suggested by Housel		Values suggested by Terzaghi and Peck (Ref. 365, 1948)
	Overload ratio	Factor of safety F_s	
Permanent structures	1.00 1.33	4.00 3.00	Normal
Temporary structures*	2.00 2.50	2.00 1.66	Minimum
Failure condition	4.00	1.00	Failure

* Refers to excavation and temporary loading conditions that will presumably not extend over a period of several months at the most.

The differentiation between factors of safety to be used for permanent and temporary loading suggested by Housel appears reasonable, since detrimental plastic flow effects cannot be neglected in large masses of clay (Art. 7-14), and since they are dependent on time. An essential point, however, has been so far disregarded in this connection, namely, the fact that the detrimental effect of plastic deformations of clay masses is dependent on the sensitivity of the clay to remolding (Art. 7-22). Table 14-4 attempts to take this into account by suggesting higher values of the factors of safety F_s for sensitive clays and for permanent structures. In practice the F_s values for temporary structures would be used mainly in connection with excavation problems (Art. 14-6). The permissible bearing value p_0 for a foundation would then be

$$p_0 = \frac{p_{max}}{F_s} \qquad (14\text{-}1)$$

The ultimate bearing capacity p_{max} of a footing is to be determined from Eq. (9-28), where it should be noted that p_{max} represents the unit load applied less the unit weight of the soil removed by the excavation (see Prob. 14-1). With reference to Eq. (7-17), for surface loading
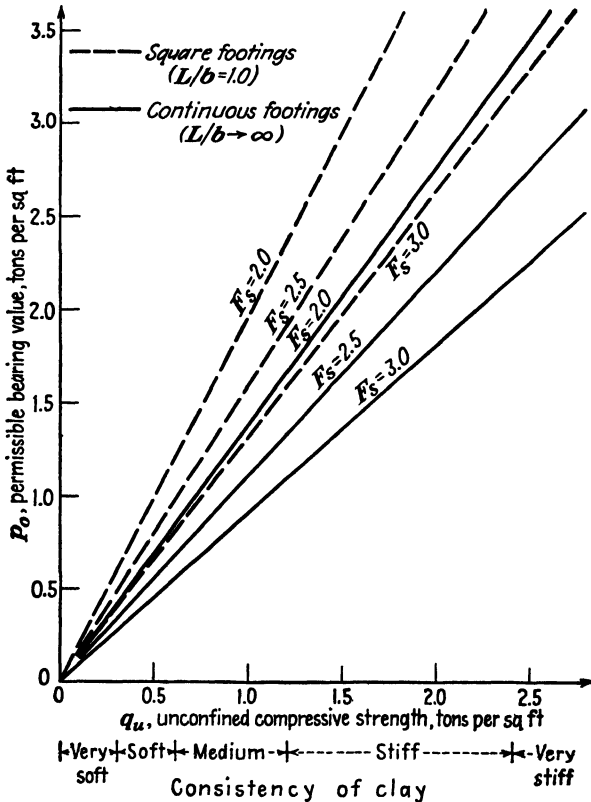
FIG. 14-1. The permissible bearing values of clays [based on Eqs. (9-28) and (14-1), for $h = 0$] (compare with Tables 14-3 and 14-4).

($h = 0$) and for a continuous footing ($L/b \rightarrow \infty$), we obtain

$$p_0 = \frac{5.52c}{F_s} = \frac{2.76q_u}{F_s} \tag{14-2}$$

Similarly, for a square footing ($L/b = 1.0$),

$$p_0 = \frac{7.95c}{F_s} = \frac{3.975q_u}{F_s} \tag{14-3}$$

Equations (14-2) and (14-3) are presented in graphical form in Fig. 14-1 for F_s values of 2.0, 2.5, and 3.0. The procedure for the selection of F_s

suggested in Table 14-4 should serve only as a general guide; other circumstances should also be considered before taking a decision, for instance, the degree of susceptibility of the clay to increasing its shearing strength by further consolidation (see Art. 7-14), and the possible rate of further consolidation depending on the thickness of the clay layer and on the nature of the available drainage boundaries (Art. 6-8). The unconfined compressive-strength test is recommended as a basis for the determination of the shearing strength of clays for reasons given and in the manner stated in Art. 7-25.

TABLE 14-4. The Selection of Factors of Safety on the Basis of the Average Sensitivity of a Clay to Remolding

Degree of sensitivity	Sensitivity ratio S	Suggested factors of safety F_s	
		Permanent structures	Temporary structures
High	≥ 4	3.0	2.5
Medium	2–4	2.7	2.0
Slight	1–2	2.5	1.8
Not sensitive	≤ 1	2.2	1.6

It is sometimes attempted to define the permissible bearing value p_0 of a clay as being equal to the unit pressure p_y at which the settlement-pressure curve ceases to be a straight line during a load test, that is, when the soil begins to yield (Ref. 83). This will happen when the maximum shearing stress τ_{max}' anywhere beneath the footing exceeds the shearing strength $s = c = q_u/2$. Therefore, with reference to Eq. (9-7),

$$p_y = \frac{\tau_{max}'}{0.29} = 1.67q_u = p_0 \tag{14-4}$$

With reference to Eq. (14-3), this procedure is therefore equivalent to the selection of a factor of safety for a square footing equal to

$$F_s = \frac{3.975q_u}{1.67q_u} = 2.38 \tag{14-5}$$

In practice it is often difficult, however, exactly to determine the value of p_y, since the settlement-pressure line often begins to show a curvature from the very start of the test (see Fig. 12-21). This type of expensive study therefore should not form the mainstay for the determination of permissible bearing values of buildings (for additional reasons see Art. 12-10 and Prob. 12-6).

The Proctor plasticity needle (Art. 11-2) can be employed for rough

field checks of the strength of plastic clays at the bottom of excavation pits for footings, in accordance with Eqs. (7-17), (14-1), and (14-3).

14-3. The Structural Design of Spread Foundations. It has been shown in Art. 9-4 that the distribution of soil reactions against a footing is not uniform. It will be noted, however, from Fig. 9-11 that in the case of isolated footings the nonuniform distribution of soil reactions changes the bending moments in the footing at the edge of the column only very slightly. If the column load is assumed concentrated at one-half the distance from the center line of the footing, as shown in Fig. 9-11, the difference between the distance of the center of gravity of a rectangular area to its edge will differ by approximately 25 per cent from the same distance for a parabolic area. The assumption of a uniform distribution of soil reactions for purposes of design of small individual footings is therefore entirely justified, since it will give bending moments which are at most approximately 25 per cent too large in the case of sands and approximately 25 per cent too small in the case of clays. This latter difference, however, can be well taken care of by the ample factors of safety of 2.0 customarily employed for flexural problems in structural reinforced-concrete design.

The effects on the superstructure of nonuniform distribution of soil reactions against a continuous mat, however, cannot be ignored if it is desired to prevent by a rigid design of the superstructure its otherwise inevitable deflection (see Arts. 13-3 and 13-7). This was, for instance, the case in the system of two-basement-deep Vierendeel-type girders shown in Fig. 13-19(A). The basis for the analysis was provided by model tests performed by the late Professor George E. Beggs at Princeton University on a bakelite model of the girder, using the Beggs deformeter method (see Ref. 207, pp. 265–270 and Glick, Ref. 155, 1936).

This method permits the determination of influence lines for the bending moments, the shears, and the thrusts of any section of the Vierendeel girder, as caused by the application of an upward load of unity along its base. It is then a comparatively simple matter to determine these values for any type of soil-reaction distribution. This is done by graphical procedures involving the multiplication of the influence-line values by the corresponding values of the soil reactions. For other computation procedures see Meyerhof (Ref. 226, 1947).

Individual footings are used so long as the side length b of the footing is appreciably smaller than the column spacing L [see Fig. 13-17(I)]. As the column loads increase, or if the soil in the layer A is found to have poorer bearing properties, it becomes necessary to increase the size of the individual footings. When b becomes almost as large as L the individual footings are merged to form a continuous *mat* or *raft*, the design of which

can be handled in the same manner as the reinforced-concrete floors of buildings. The main difference is that in the case of a foundation mat the floor is *inverted,* so that its dead weight can be subtracted from the soil reactions which the mat has to resist, whereas in an ordinary floor the dead and the live loads are added. Just as in the case of a building floor, there are three main types of reinforced-concrete foundation mats, individual panels of each of which are shown in Fig. 14-2. All three types are employed occasionally, although the first two, *A* and *B*, have some disadvantages. Both require expensive form work for the webs of the inverted T beams. They also require backfilling up to the level of the beams if the basement is to be used for storage or for any other purposes.
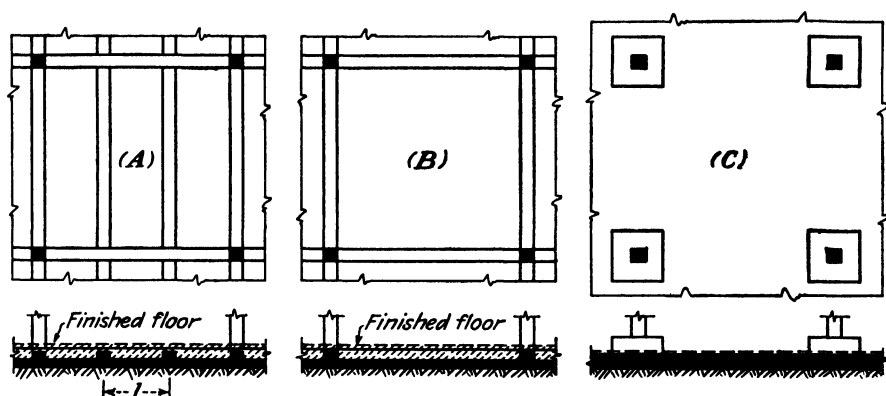
FIG. 14-2. Three types of continuous reinforced-concrete foundation mats. (*A*) Panel of inverted T beams—one-way slabs. (*B*) Panel of inverted T beams—two-way slabs. (*C*) Panel of inverted flat slabs.

In addition, this type of mat is not particularly suited to resist and to equalize tendencies for differential settlement which sometimes are unavoidable; the webs of the inverted T beams are sensitive to shear and to compressive stresses (see Prob. 13-5). The inverted flat slab-type of foundation mat [see Figs. 14-2(*C*) and 13-19(*A*)] is more satisfactory in this respect; it has a greater and more uniform resistance to bending and to shear, it requires much less formwork, no backfilling, and permits a better utilization of the full height of the basement for storage and for similar purposes.

The determination of the bending moments, the shears, and the cross sections of concrete and of steel is done in very much the same manner as in the case of an ordinary floor. The soil reactions are assumed uniformly distributed over the entire area of each panel. Further structural design details of foundation mats will not be taken up in this book, since they are very similar to the customary procedures employed for floor design,

which can be found in any textbook on reinforced concrete, for instance, Ref. 111. This is also true in the case of individual foundation footings.

14-4. Waterproofing. The basement of a small house will be used as an example of advisable waterproofing procedures (Fig. 14-3). If the footings, walls, and floor of a basement are made of solid monolithic concrete, this may keep the water from actually flowing into the basement, provided no cracks have developed anywhere. Nevertheless, the basement may be damp, since the permeability of concretes falls within approximately the same range as that of clays (Fig. 5-2). The inner surfaces of the walls and floors of a basement may therefore appear dry, whereas actually a steady slow flow of water may be occurring from the outside through the concrete toward a surface of evaporation within the concrete.

FIG. 14-3. Basement waterproofing of small house.

A continuous membrane of waterproofing material should therefore be applied to the outside of the walls and below the floor, as shown in Fig. 14-3. Cold asphalts should not be used, since they are susceptible to deterioration due to soil bacteria action. Asphalts placed hot are satisfactory but require very careful inspection, since they are apt to form bubbles which leave small openings in the membrane unless it is composed of alternating layers of asphalt and fabric. Bubbles are particularly liable to appear at the joints of cinder or cement blocks when they are used for the construction of the walls; quite a lot of water may then seep into the basement through a tiny hole. The practice of dumping the outside fill against the wall without compaction, and of leaving it to settle down over a period of years because of frost action, usually aggravates this condition. The fill gets sodden after the first heavy rain and then, after a dry spell, shrinks away from the wall, as shown by the broken line *BC* in Fig. 14-3. The crack between soil and wall may be very small; nevertheless, when filled with water, it may develop a head of several feet against a small gap in the membrane, forcing a lot of water into a hollow block. Proper compaction of the backfill (Arts. 11-2 and 11-4 and Fig. 11-8), is therefore advisable; it should form a slope *AF* immediately after the waterproofing of the walls.

A number of chemical compounds are now available which effectively seal the pores of the concrete and which can be substituted for hot asphalt when forming the outer waterproofing membrane. A so-called *vapor*

barrier should be formed by the use of such compounds on the inner face *DE* of a basement wall when it is built of hollow cement or cinder blocks. Otherwise condensation is likely to occur on humid hot summer days inside the hollow wall, followed by evaporation of the condensed water back into the basement during drier weather, so that the basement is constantly humid.

Drains should be placed along the outside of the footings whenever it is possible to provide an outlet for them somewhere along an adjoining
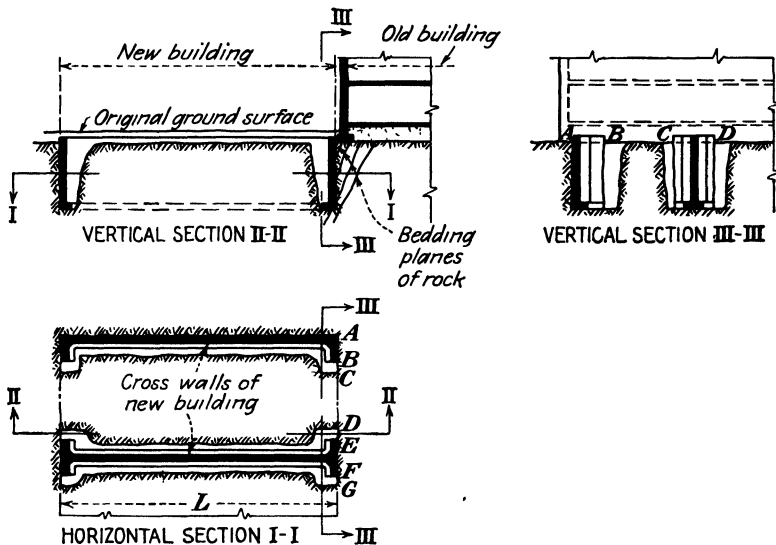
FIG. 14-4. Normal type of excavation for basement of new building damaged adjoining old wall, owing to sliding of underlying rock along inclined bedding planes. Alternating excavation and construction of cross walls in new basement, first step of which is shown in this sketch, solved the problem. (*From unpublished data of Spencer, White and Prentis, Inc.*)

slope. A sand blanket under the floor should then also be connected to such outlets to prevent the development of uplift against the floor. The filter drains should be graded, as discussed in Art. 17-7.

In heavy construction and deep excavations a protective outer *sand wall* is placed between the waterproofing and the soil (see Art. 15-13).

14-5. Open Excavations in Rocks and in Stiff Clays. As a rule, excavations of this type do not present any special problems for foundations of buildings. Vertical cuts can usually be made to the required depth without any lateral bracing or support (see Art. 8-2). There are, however, exceptions. One such case is illustrated by Fig. 14-4. Blasting of an open cut for the basement of a new building was begun in the usual manner at one of its corners, but an adjoining old building, which had no

basement, soon developed signs of distress. The origin of the trouble was traced to the inclined planes of the folded bedrock, slipping movement along which began to develop when they were deprived of lateral support by the excavation.

The following procedure solved the problem: Trenches were blasted with small charges and were dug out for the cross walls, leaving intact the rock blocks between these trenches. The individual rock seams under the outer footing of the adjoining old building were able to span the gaps AC, DG, etc., which were formed by the trenches. The cross walls of the new building and their footings were then concreted in their trenches.
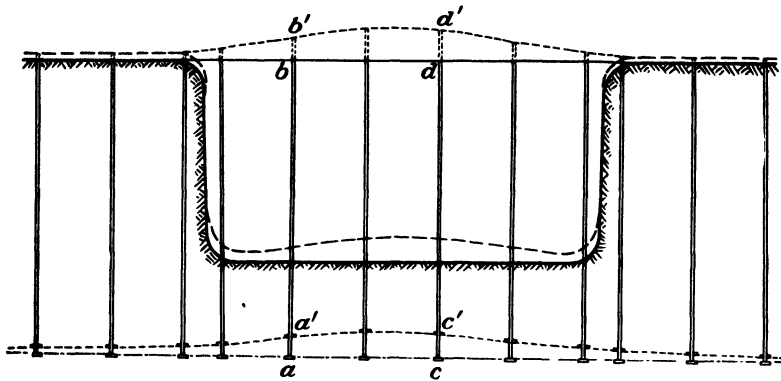
FIG. 14-5. The heave of the soft clay in and around an excavation pit in Mexico City. The heave of an underlying layer ac was measured by means of underground bench marks. (*After Cuevas, Ref.* 95, 1936.)

After the concrete of the cross walls hardened, the excavation of the rock was completed between the original cross trenches. The individual rock seams under the old building spanned the gaps BE, etc., between the cross walls, which were able to take up the entire thrust from the rock seams.

See Art. 18-7 for the estimation of the effect of blasting on adjoining buildings.

14-6. In Soft Clays the Depth of Excavation Is Limited by the Safety against Heaving of the Bottom of the Cut. The heaving of the bottom of cuts was briefly discussed in Art. 13-6. Figure 14-5 illustrates the nature of the heaving movement which was measured by Cuevas (Ref. 95, 1936) in Mexico City. The upward movement of soil layers at the center of the pit reached 4 ft. R. B. Peck (Ref. 260, 1943) measured lateral and upward movements of the underlying clay when the weight of the excavation in the Chicago subway cut shown in Fig. 10-25 reached the approximate value of the unconfined compressive strength $q_u = 0.67$ ton per ft^2 of the underlying clay of medium sensitivity—S varied from 3 to

4—(most of the movement occurred while the depth of excavation was increased from 10 to 13 ft, prior to the placing of the first brace). Model tests with gelatine, reported by Tschebotarioff and Schuyler (Ref. 389, 1948), demonstrated, as shown in Fig. 14-6, that a deep unbraced excavation induced not only displacements of the bottom and of the side walls of the pit, but also considerable deformations of the entire underlying and surrounding mass. The displacements were much larger than the ones induced by pile driving (see Art. 15-2) and could therefore cause appreciable remolding and weakening of a sensitive clay. These conclusions found further support in the full-scale observations reported in
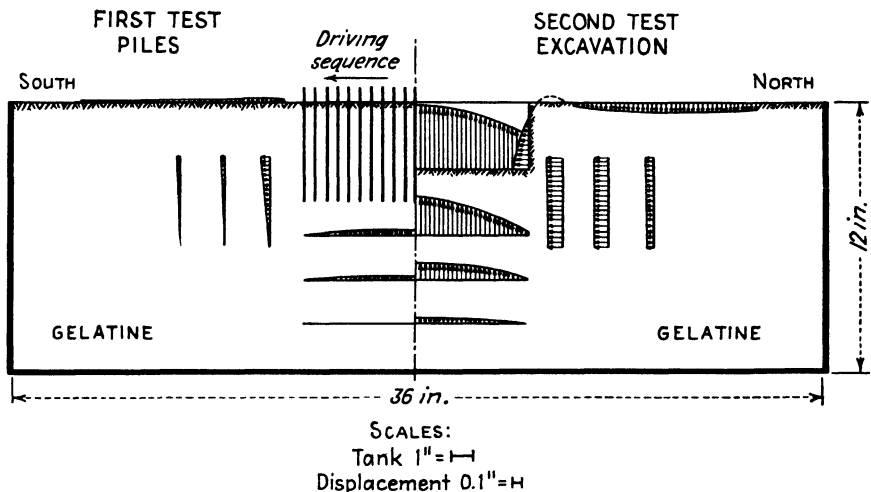
FIG. 14-6. Comparison of displacements by model tests. (*From Tschebotarioff and Schuyler, Ref. 389, 1948.*)

Fig. 31 of G. Freeman's (1944) discussion of Ref. 65. The distribution in plan of the settlements of the building (Fig. 13-19) showed that in the area of the slide illustrated in Fig. 8-4 the measured settlements were at least twice as large as in the part where no slide had taken place owing to more adequate precautions during the subsequent excavation. Thus unchecked excessive deformations of the clay during construction may have later detrimental consequences for the completed structure.

It should be noted that the bracing of the walls of the cut to resist the lateral pressures of the clay against them is not always sufficient to ensure a safe execution of the excavation. The possibility of heaving of the bottom of the pit should be taken into account, as shown by the following analysis, illustrated by Fig. 14-7. It represents a development of earlier work by Housel (Ref. 178, 1943) and by Terzaghi (Ref. 362, 1943). Two cases have to be considered:

In the first case [Fig. 14-7(I)] the depth D of the soft clay between the bottom of the pit and the upper surface of an underlying nonplastic layer (such as rock or sand) is smaller than the width b of the cut. With reference to Art. 9-9, failure of the clay is likely to occur along a cylindrical surface of an approximate radius $r = D$, as shown in Fig. 14-7(I). The failure will be caused by the weight of the overlying soil, namely, by the pressure p' which the soil will exert on the plane AB. Equation (9-28) can then be applied to the stability analysis of the clay beneath the plane
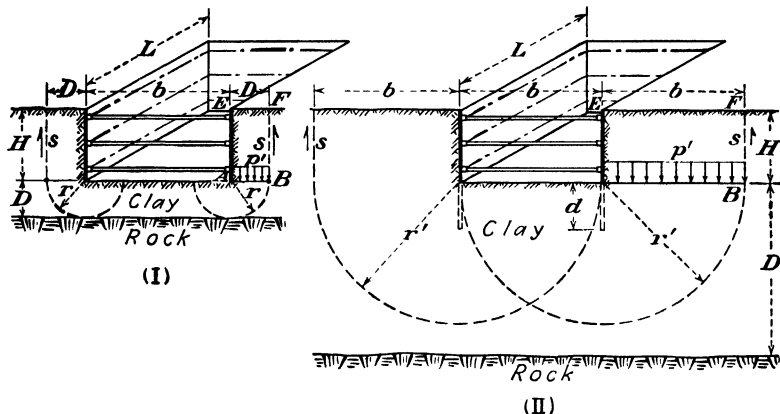
FIG. 14-7. Cuts in plastic clay. The sketch illustrates conditions governing safety against heaving of the bottom of the cut.

AB, with the following modifications: $h = 0$; D now stands for the symbol b of Eq. (9-28); the coefficient $5.52c$ should preferably be reduced to the original Prandtl value to read $5.14c = 2.57q_u$, since the radius r in Fig. 14-7 may actually be somewhat greater than D, and the reduction of p' by shearing stresses along vertical planes may be correspondingly smaller. The modified equation (9-28) will now read

$$p_{\max}' = 2.57q_u\left(1 + 0.44\frac{D}{L}\right) \tag{14-6}$$

The pressure p' on the plane AB of Fig. 14-7(I) can be taken to equal the unit weight of the soil above that plane, reduced by the shearing stresses $s = c = q_u/2$ along the vertical back and side faces of the block of clay overlying that plane, so that at limit equilibrium,

$$\begin{aligned} p_{\max}' &= \frac{1}{DL}[\gamma HDL - s(HL + 2HD)] \\ &= H\left[\gamma - q_u\left(\frac{1}{2D} + \frac{1}{L}\right)\right] \end{aligned} \tag{14-7}$$

Combining Eqs. (14-6) and (14-7), we obtain the limit depth of a braced cut which is compatible with equilibrium against heaving of the bottom:

$$H_{max} = \frac{2.57q_u\left(1 + 0.44\frac{D}{L}\right)}{\gamma - q_u\left(\frac{1}{2D} + \frac{1}{L}\right)} \tag{14-8}$$

If the length L of the cut is more than twice the depth D ($L \geq 2D$), local squeezing may occur in soft clays at the center of L; it is then advisable to ignore the restraining end effects and to transform Eq. (14-8) for that purpose as follows:

$$H_{max} = \frac{2.57q_u\left(1 + 0.44\frac{2D - L}{L}\right)}{\gamma - q_u\left(\frac{1}{2D} + \frac{2D - L}{DL}\right)} \tag{14-9}$$

valid for $D < L < 2D$ and $b > D$.

It will be noted that for $L = D$ Eq. (14-9) is identical with Eq. (14-8), whereas for $L = 2D$ it takes on the following simplified form which is equivalent to the omission of the restraining end effects:

$$H_{max} = \frac{2.57q_u}{\gamma - (q_u/2D)} \tag{14-10}$$

valid for $L \geq 2D$ and $b > D$.

In the second case [Fig. 14-7(II)], when the depth D of the clay is greater than the width b of the cut, a similar derivation gives equations which in all respects are identical with Eqs. (14-9) and (14-10), except that b should be substituted for D.

In order to obtain the permissible safe depth of braced excavations, the values of q_u should be divided by the factors of safety suggested in Table 14-4, and the q_u/F_s values substituted for q_u in Eqs. (14-9) and (14-10) (see Prob. 14-1).

Steel sheet piling extended to a distance d below the point A [see Fig. 14-7(II)] is beneficial, especially if stiffer clay is encountered below the depth d. Stability evaluations are then somewhat more elaborate than the ones just given, but follow the same general lines.

An examination of Eqs (14-8) to (14-10) shows that the value of H_{max} will increase with a decreasing value of L. This circumstance can be utilized in the case of long cuts with a large value of L. The excavation is then carried out in successive stages, as shown in Fig. 14-8. As soon as the excavation of each narrow section of cut is completed, the corre-

sponding section of the foundation mat is concreted and is weighted down still further, if necessary, by temporarily placing over the mat some of the clay that is removed from the next adjoining section of the cut, or by concreting parts of the cross walls.

The procedure of excavation in sections can be employed when undercutting a high bank of clay, as was done by Spencer, White and Prentis, Inc., in the case of the building shown in Fig. 14-9. The completed portions of the foundation mat served a double purpose in this case. First, they loaded by their weight the surface of the clay and thereby prevented excessive heaving. Second, they served as abutment to the steel braces which shored the sheeted vertical soldier H beams. Thus they resisted the lateral earth pressure which the bank exerted against these supports of the cut. The safety against horizontal sliding of the mat should be determined. The total lateral earth pressure E_A (Art. 16-5), multiplied by a factor of safety F_s (Table 14-4), should not exceed the product of the horizontal area of the mat which is in contact with the clay and the shearing strength $s = c = q_u/2$ of the clay. Since the surface clay layer immediately under the foundation mat is likely to have been somewhat remolded and weakened by construction operations, it is advisable to provide keys, A in Fig. 14-9, which anchor the mat in undisturbed zones of the clay. Such keys were not necessary in this particular case, since the mat received sufficient passive earth support at the other end of the excavation.

FIG. 14-8. Excavation and concreting of the bottom slab in small sections increases the safety against heaving of the bottom of a cut in clay.

A similar procedure can be applied to the case where a cut for a new foundation is so wide that it is not economical to strut the walls of one side of the cut against the walls of the other side. The center of the excavation is then dug out first, the sides being cut on a slope, and parts of the concrete foundation mat are poured immediately. The cut is then extended from the center outward, and its supports are shored against
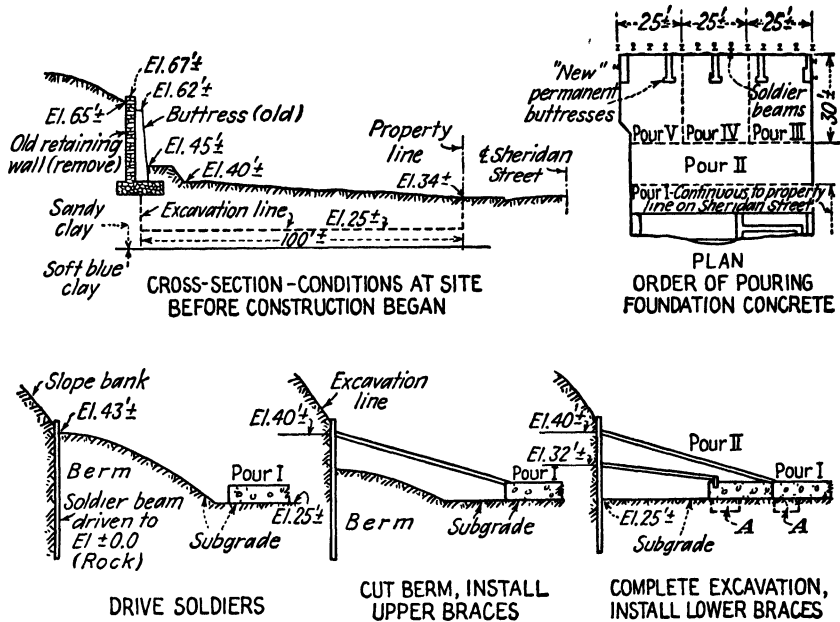
FIG. 14-9. The sequence of excavation, of concreting, and of bracing which was necessary to ensure stability of bank and safety against heaving of bottom of cut for a new building at Albany, New York. (*After Charles B. Spencer*, Ref. 322, 1950.)

the completed sections of the mat (see Casagrande and Fadum, Ref. 65, 1944).

14-7. Measures to Decrease and to Equalize Settlements. Removal of earth, for instance, for basements, is an effective measure, so long as no heave and therefore no weakening of the underlying layers is caused thereby. The analysis of the safety against such detrimental heaving has been given in the preceding articles. The essential criteria will be summarized in Art. 14-8. The time during which an excavation pit is left open should be reduced to a minimum. Otherwise the underlying clay may expand by absorption of water. This will increase its compressibility and decrease its shearing strength. As soon as the excavation reaches the desired depth, a working mat should be immediately placed on its surface to prevent churning up of the clay by moving men and equipment. For instance, a 4-in.-thick working mat of concrete was used in the case illustrated by Fig. 13-19(A).

The removal of earth after completed construction may sometimes have a beneficial effect on settlements. For instance, this was the case when the approach fill to the bridge shown in Fig. 13-13 was removed (see Art.

13-3). Similar measures may have also helped to slow down the settlements of the National Theater at Mexico City; it was necessary to excavate ramps around it to permit access to what was originally a ground floor but became almost a subbasement after 6 ft settlement (Fig. 14-10).
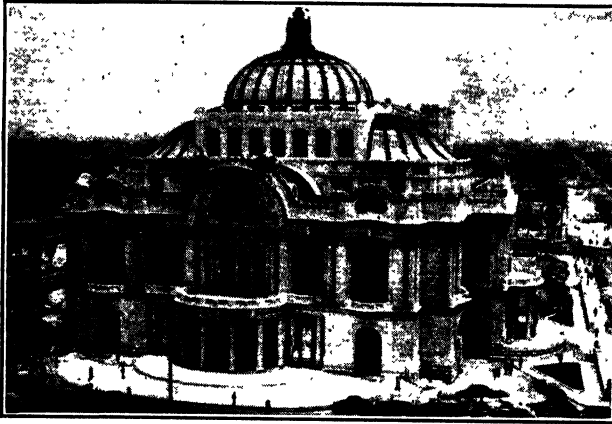
(A)

(B)

FIG. 14-10. The National Theater at Mexico City, which has settled over 6 ft since its construction in 1909 (Ref. 81). (A) General View. (B) Approach ramp excavated to permit access to stage entrance from street level. Drive-in was originally at elevation where lined-up busses are shown. (*Photos by Boris Ashurkoff.*)

The magnitude of the settlements was considerable, even for the soft clay of Mexico City (Fig. 2-6 and Refs. 94 and 95). It was in part caused by the excessive weight of the 8-ft-thick massive reinforced-concrete foundation mat, which alone weighed almost as much as the entire superstruc-

ture. A cellular type of raft of a greater depth could have achieved the same degree of strength with much less weight. Recent investigations in Mexico City have shown that the clay is somewhat more resistant at a depth of some 60 ft. Pile foundations reaching to that firmer layer are therefore used sometimes; but an additional unpleasant problem was then found to arise, since the surrounding soil, including sidewalks, settled down around the building (see Albin, Ref. 4, 1949).

A second type of measure for the equalization of settlements consists in the increase of the unit contact pressures on the soil at the outer periphery of the building, especially at its corners. This measure is feasible only so long as it is not essential to have a continuous mat under the entire building. Then, by having somewhat narrower footings along the center of the outer walls than in the interior of the building and still narrower ones at the corners (check for shear failure, Art. 9-9), greater settlements will be induced there than at the center of the building in the upper soil layers. Thus these differential shallow-seated settlements will tend to offset somewhat the dishlike or crater effect of the deep-seated settlements. This measure was applied to a Boston building (see Casagrande and Fadum, Ref. 65, 1944).

A third type of measure consists in the design of walls, for buildings several stories high, as solid reinforced-concrete girders, strong enough to enforce uniform settlements by bridging the otherwise inevitable settlement crater. Separation of the structure into units is helpful in this connection (see Fig. 13-9).

Finally, a work sequence involving the later construction of lower and lighter parts of a building, (see Fig. 13-15 and discussion thereof in Art. 13-4), can be resorted to for the purpose of decreasing differential settlements.

14-8. Summary of Essential Steps in the Design of a Spread Foundation on Clay

1. Determine relevant properties of the soil at the site (Art. 13-2) and the proposed loads of the structure (Art. 13-1).
2. Check safety of the proposed foundation mat, or of individual footings, against the danger of a shear failure of the underlying clay (Arts. 9-9, 13-6, 7-25, and 14-2).
3. Perform a settlement analysis (Art. 13-7) to correlate the superstructure design with the differential settlements to be expected (Arts. 13-3 and 14-7).
4. Check whether an unsupported cut can be safely made in the excavation for the foundation mat (Arts. 8-5 and 8-8). If not:
5. Check the safety against heaving of the bottom of a braced cut, if

such a cut has to be made (Art. 14-6), and determine the lateral pressures against the bracing thereof (Arts. 16-4 to 16-6).

For examples of possible procedures along the above lines see Prob. 14-1.

14-9. The Unwatering of Excavations in Sand. Wellpoints. The bottom of excavations in sand is not susceptible to heave due to excessive shearing stresses, as is the case with excavations in clays. Such heaving involved shear failures of the clay at considerable depths below the bottom of the cut. This type of failure is possible in clays because they frequently have a constant shearing strength which is independent of the
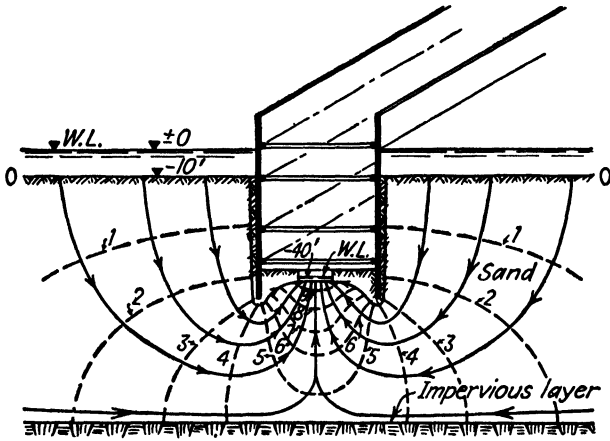
FIG. 14-11. Unwatering of excavations in sand by pumping from sump pits may create a dangerous quick condition, as illustrated by this example.

weight of the overburden (Art. 7-23), but it is unlikely in most types of granular soils, such as sands. The shearing strength of sands depends on frictional and not on cohesive properties and therefore increases with depth below the soil surface.

Sands, when fully saturated, may however cause a different type of trouble in excavations, namely, they are liable to become quick (Art. 5-4) unless special precautions are taken for the unwatering. This is illustrated by Fig. 14-11, which gives a vertical section through a sheet-pile cofferdam (Art. 16-17) driven through shallow water for the purpose of construction of a bridge pier within that cofferdam. The base of the pier was to rest on sand at elevation −40 ft. If the unwatering of the excavation is attempted by pumping from a sump pit, the flow of water toward the sump pit would follow the pattern and would form the flow net shown in Fig. 14-11 (see art. 5-3). According to Prob. 14-2, a quick condition would then result in and around the sump pit. In other words, the sand at the bottom of the excavation would start to "boil" and would be par-

tially liquefied and pushed upward into the excavation. In addition, since in a quick condition sand has no supporting power for lateral as well as for vertical loads, the sheet piles of the cofferdams would lose the support they previously had at their lower ends in the sand. Excessive load would then be thrown onto the lower struts of the cofferdam bracing, so that a progressive collapse of the bracing and an inward displacement of the sheet piling might become imminent.

A partial preventive remedy may be obtained by placing a temporary clay blanket on the sand surface OO around the cofferdam. Fully effective measures require the use of *wellpoints*.

FIG. 14-12. Vertical cross section through a wellpoint in operation. (Courtesy of Moretrench Corp., Ref. 237.)

The principle of operation of a wellpoint is illustrated by Fig. 14-12. A steel pipe of approximately 1½ in. diameter, with perforated side walls at its lower end, covered with a wire-mesh filter screen, that is, the so-called *wellpoint*, is jetted into the ground by pumping water through it. The water rises to the surface past the outer walls of the pipe and forms a cylindrical hole around the wellpoint, which can be gradually filled with sand while the velocity of the jetting water is decreased. Water from all pervious layers above the tip of the wellpoint can then reach it, irrespective of the presence or of the absence of any horizontal impervious seams which might otherwise cut off the flow from some of the intermediate pervious layers. Wellpoints are jetted in rows, where each wellpoint is connected at the soil surface to a header pipe which, in turn, connects with a pump [see Fig. 14-13(B)].

A quick condition is prevented by the use of wellpoints, since the seepage forces (Art. 5-4) are directed down or horizontally toward the metal filter mesh of the point, which can resist them, and which does not permit the movement of any sand particles through the filter. By driving the wellpoints below the elevation of the bottom of a sheeted excavation (see Fig. 16-10) the seepage forces are diverted from their upward direction

(*A*)

(*B*)

FIG. 14-13. Dewatering by means of wellpoints of the excavation through sand for part of the cutoff trench of the Coralville Dam, Iowa. (*A*) General view. (*B*) Close-up view. (*Courtesy of* Moretrench Corp.)
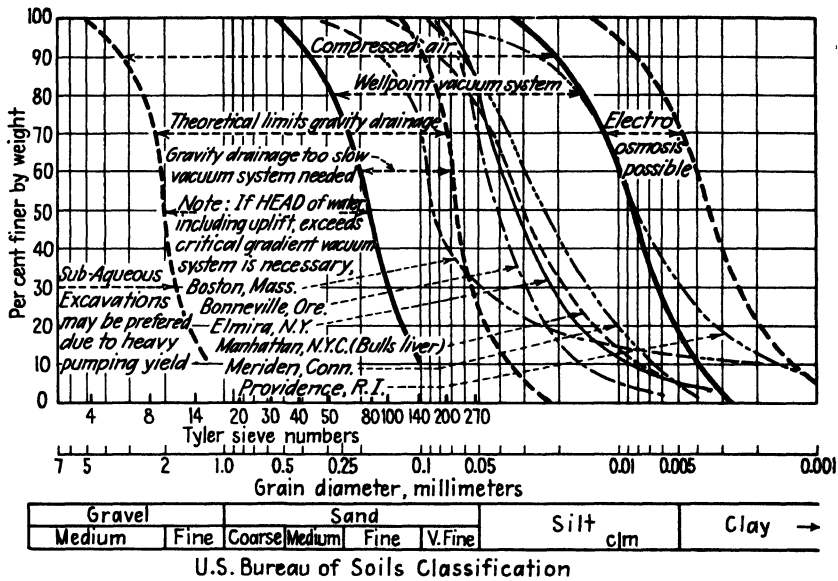
FIG. 14-14. Delineating limits of soil-dewatering methods. Successful wellpoint-drainage installations in fine-grained soils. (*Courtesy of Moretrench Corp.*)

toward the excavation. The bottom of the pit is thereby ensured against the development of a quick condition.

The stability of slopes can also be greatly improved by the use of properly placed wellpoints (Fig. 14-15), since it is then possible to reverse the natural direction of the flow of water toward the face of the cut. The reversed seepage forces then contribute to the stability of the cut, instead of undermining it. Figure 14-13 illustrates the application of this principle which permitted an excavation of a cutoff trench for a dam in the dry on fairly steep slopes through sand down to rock at a depth of 41 ft below the water level in the adjoining river (see Art. 17-4).

FIG. 14-15. Electro-osmosis causes flow of water through fine silt and rock-flour types of soil toward wellpoint electrodes. Proper location of wellpoints permits open cuts on slopes which otherwise would not be stable. (*After Leo Casagrande, Ref. 72, 1949.*)

In very fine sands with some silt and clay admixtures a very close spacing of ordinary wellpoints may become necessary in order to lower the

ground-water table around them adequately. The so-called vacuum method can then be employed to increase the normal gravitational head under whose action water will flow through these layers toward the well-point. An airtight clay plug is provided at the soil surface over the top of the cylindrical sand filter around the wellpoint (see Fig. 14-12). Unwatering creates a partial vacuum in the cylindrical sand filter around the wellpoint; the gravitational head under whose action water will flow toward the wellpoint is then increased by the difference between the atmospheric pressure and the partial vacuum pressure in the voids of the sand filter.

Electro-osmosis (Art. 5-6), when used in connection with wellpoints (Fig. 14-15), may create an additional head which will force the movement of water even through relatively impervious silt and rock-flour types of soils. Leo Casagrande (1947) reported a number of cases where excavations in such soils became possible through the use of electro-osmosis. Rows of well electrodes acted in combination with adjoining rows of rod electrodes. One of the examples given is that of a U-boat pen at Trondhjem, Norway, where all ordinary measures failed for a 46-ft-deep excavation next to the ocean. The unsuccessful measures included sloping of the sides of the excavation and their protection by 60-ft-long sheet piles embedded 50 ft in the ground. Before the cut could be completed, deep-seated slides occurred, distorted the piling, and moved it a considerable distance toward the excavation. However, after an electro-osmotic drainage installation was put into operation, the construction was completed without any further difficulty (Ref. 71).

The grain-size curves of soils in which wellpoint drainage of different types can be successfully employed are shown in Fig. 14-14. It is based on the experiences of the Moretrench Corporation.

14-10. Underwater Excavations and Concreting. The Tremie Method. The difficulties of unwatering deep excavations without creating quick conditions in sand layers sometimes make it advisable to resort to underwater excavation and to the underwater concreting of at least part of the foundation. An example of this kind of work is provided by Fig. 14-16 which illustrates a 65-ft-deep excavation for a U.S. Navy drydock and the underwater concreting of its floor. The general principles of placing concrete underwater will be discussed first.

Segregation will occur if concrete is dumped through any appreciable depth of water. The original constituents will become separated; the gravel will sink to the bottom first, and the sand will settle over it, followed by some cement. A certain proportion of the cement will remain in suspension in the water. The general picture will be similar to that obtained in a measuring cylinder during a laboratory sedimentation test for purposes of grain-size determination (Art. 3-6). It is therefore essen-

tial to prevent entirely, or to reduce to an insignificant minimum, the distance that concrete has to move through water.

Where small quantities are involved, for instance, for the concreting of bore piles (Art. 15-7) or of small caissons, the concrete can be placed
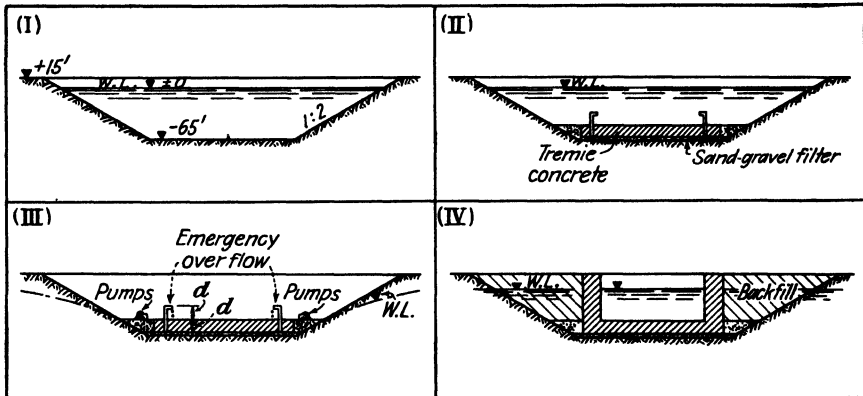
FIG. 14-16. Steps in the construction of a large U.S. Navy drydock. (I) Excavation by dredging. (II) Underwater concreting of floor by the tremie method. (III) Unwatering (note overflow standpipes, an emergency safety device against displacement of floor by hydrostatic uplift). (IV) Backfilling after walls were concreted in the dry.
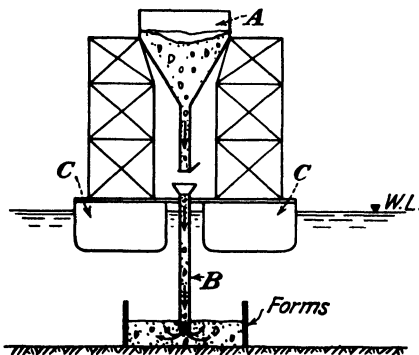
FIG. 14-17. Sketch illustrating the tremie method of placing large quantities of concrete underwater.
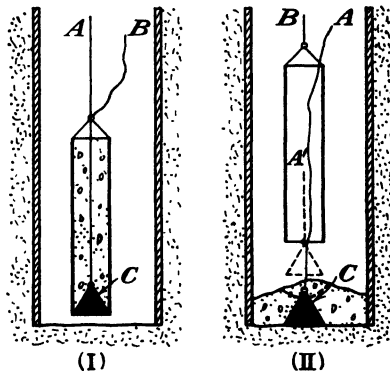
FIG. 14-18. Special buckets are used for the placing of small quantities of concrete underwater.

underwater by means of special buckets of the type illustrated in Fig. 14-18. Two cables are provided; the first, A, is attached to the bottom C of the bucket and is used to lower the entire concrete-filled bucket through the water. When the bucket touches the bottom of the excavation cable A is released, and the walls of the bucket are pulled up by the cable B, allowing the concrete to slide into place over the sloped sides

of the bottom C, which is then also pulled up by cable A, as shown by the broken line A' in Fig. 14-18(II).

This method is too slow where large quantities of concrete are involved; the so-called *tremie* method is then resorted to (see Fig. 14-17). Steel hoppers A are mounted on barges C and are kept filled with concrete by means of belt conveyors or pumps from mixing plants usually mounted on other barges nearby. The bottom of the hopper A is connected to a retractable funnel B which can reach to the bottom of the excavation and can be opened or closed at its lower end by remote control. Funnel B is kept continuously filled with plastic concrete, which slides down under the action of gravity. The bottom end of funnel B is *kept below the surface of the concrete*, so that the plastic mix is pressed outward and upward from within the already deposited mass, as shown by the arrows in Fig. 14-17. No segregation is then possible.

Suction dredges mounted on barges are employed for underwater excavations of the type shown in Fig. 14-16(I). A rotating tool is used to cut up and to loosen the soil in front of the suction pipe which is lowered to the soil surface from the dredge. The soil-water mixture is then pumped away in very much the same manner used for hydraulic fills (see Art. 17-3). This type of excavation permits the rapid handling of large volumes of soil and is relatively inexpensive.

In the second stage [Fig. 14-16(II)], steel trusses are lowered into place by floating cranes to serve as reinforcement of the concrete floor; this is also done for the forms. Divers check the adjustments. Concreting of the floor is then carried out by the tremie method (Fig. 14-17, see Ref. 121). In some cases the forms and the concrete of the side walls of the dock are also placed underwater, where the tremie method is used. In others, they are concreted in the dry. The latter procedure requires unwatering, as shown in Fig. 14-16(III), after building a temporary cofferdam (Art. 16-17) across the end of the excavation next to the free water. Wellpoints may be used on the slopes to take care of seepage through any sand layers intersected by the slope and to pump water away from beneath the floor. To that end, a gravel filter may be placed beneath the floor before the latter is concreted; the filter should be graded (Art. 17-7). Emergency overflow standpipes are then provided in the floor to prevent excessive uplift pressures from developing against the completed concrete floor in case the filter ceases to function properly in the vicinity of the pumps or the latter break down. These uplift pressures would be relieved by means of the overflow pipes before there was danger of displacement of the floor. The height of the overflow pipes is designed accordingly (see Prob. 14-3).

Overflow standpipes can be used to reduce uplift against floors of

permanent structures. Full hydrostatic uplift pressures will be developed against such a floor if no seepage through it is possible. For instance, if the cofferdam of Fig. 14-11 were excavated and lightly braced underwater, and if a tremie concrete seal were provided, the weight of that seal would have to be sufficiently large to counterbalance after unwatering of the excavation the full head of 40 ft of water, that is, for limit equilibrium the seal would have to be $40 \times 62.5/140 = 18$ ft thick (see also Prob. 16-3). On the other hand, a seal of only 5 ft thickness would provide an ample factor of safety against uplift, if the sump pit shown in Fig. 14-11 were filled with graded filter material prior to the placing of the concrete seal and were kept pumped out later through a pipe embedded in the seal (see Prob. 14-4). No continuous pumping would be necessary to create this favorable condition if the surrounding and underlying soil were silt or clay. A slight trickle through standpipes connected to a filter layer would be sufficient to dissipate the larger part of the hydrostatic head along the length of the flow lines drawn in Fig. 14-11, in the same manner as is shown for a sand soil in Probs. 14-2 and 14-4. If the trickle were stopped, full uplift pressure would develop with time.

An alternative method of coping with uplift pressures consists in anchoring the floor of the dock to the underlying soil by means of closely spaced piles. This method is of advantage when the soil is soft so that piles would be needed anyway to support the weight of the floor when the dock is filled with water. The same piles can then serve to resist tension when the dock is empty and to increase the weight of the floor which resists uplift by the weight of the soil around the piles (Ref. 121). The piles should then be spaced sufficiently close, so that negative friction of the soil against the pile, as determined by pulling tests, would be greater than the volume of the soil around each pile.

14-11. Foundations of Buildings in Regions of Permafrost and of Seasonal Rainfall: Foundations of Refrigerator Plants and of Furnaces. A basic rule of construction in temperate climates is never to found structures on frozen ground. This means in effect that foundations should be carried down below the depth of frost penetration, since volume changes of the ground during freezing and thawing (Art. 5-7) would otherwise produce uncontrollable motions of the foundations. The depth of frost penetration, and hence the minimum depth of the foundations, varies in different localities.

The principle that foundations should rest on soil layers not subject to seasonal volume changes, that is, *not* on the so-called *active layèrs*, is valid everywhere. The methods for the implementation of this principle, however, are reversed in the so-called *permafrost* regions of the far north. In a large part of Siberia and in certain areas of Alaska and of Canada the

ground remains eternally frozen below a certain depth. Above this layer of permanent frost, *permafrost*, the active layer thaws out in the summer and freezes again in the winter. This poses numerous problems in highway design and construction (Art. 19-7). As in temperate zones, the depth of the active layer varies with the locality and with its climate. Buildings founded on the active layer of the permafrost zones invariably suffer heavy damage. Structures are therefore founded on the eternally frozen ground which is not subject to volume changes so long as it *stays* frozen. Properly designed foundations should therefore prevent the transmission of heat to the ground from the building, since this might lower the elevation of the permafrost surface under the building. Some measures to that effect, as employed for small structures in Siberia, are illustrated by Fig. 14-19. A timber grillage is interposed between the concrete or masonry footing and the permanently frozen ground; timber is a fairly good thermic insulator and will not decay when frozen. The faces of footings within the active layer are sloped as shown in the sketch and are coated with smooth cement-plaster finish and asphalt. These measures are intended to facilitate the separation of the soil from the footing when the active layer freezes and heaves in the winter. The lower floor of the building is thoroughly insulated, but an air space connected to the outside is left between the floor and the ground. Piles jetted into the permafrost zone by means of a steam jet are sometimes used in Alaska instead of footings. Fiberglass is used for insulation (Ref. 291).

FIG. 14-19. Insulation of the wall footings of a building in the permafrost zone of Siberia. (After *B. D. Vassilieff, Ref.* 411, 1937.)

In regions of seasonal rainfall, for instance Burma (Ref. 447), some clay soils expand during the rainy season. This occurs mainly around the periphery of the building, so that the outer walls are frequently raised somewhat, mainly at the corners, with severe cracking resulting. Unit bearing pressures on the ground are therefore increased under such walls to the limit consistent with safety against shear failure. This is, however, only a partial remedy, since swelling pressures of some clays are extremely high. Proper drainage of the water away from the outer walls of a building by suitable slopes and by impervious coating of the soil surface is therefore necessary, as well as other similar measures. In cases of heavy buildings caissons are sometimes (Art. 15-12) carried down through the

active (swelling) layer of clay, belled out in the inactive zone for anchorage, and suitably reinforced to resist tension.

Loess soils on their original site of deposition (Art. 2-6) are liable to cause trouble during the first rainy season following a new construction. The thin vertical channels left in the loess by decayed grass roots are then likely to collapse under the combined action of the foundation loads and of percolating moisture. Considerable settlements of new structures are apt to result. Load tests, with and without flooding of the soil surface, can be used to detect in advance of construction possible danger of this kind. Sand piles (Art. 11-4) have been successfully used in southern
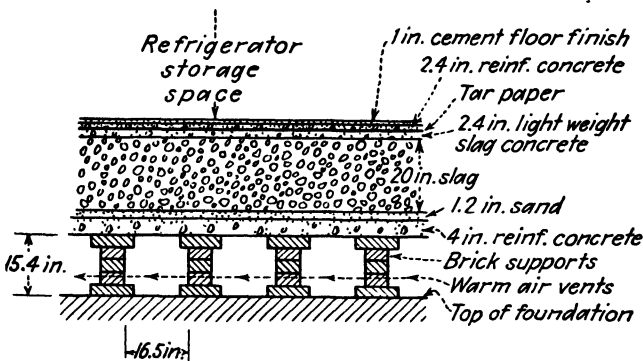
FIG. 14-20. Warm-air vents installed under an insulated basement floor of a U.S.S.R. refrigerator warehouse prevented the freezing and heaving of the soil under the foundation. (After M. Steuerman, Ref. 326, 1936.)

Siberia to compact the loess in advance of construction and to close its open channels. This eliminated later trouble to new buildings founded in this manner (see Refs. 1 and 371).

Refrigerator plants have been frequently damaged by uneven heaving of the ground which froze beneath them. Apparently the most elaborate insulation could not prevent such freezing over a long period of time. These conclusions were substantiated by British measurements, reported by L. F. Cooling and W. H. Ward (Ref. 84, 1944). The provision of warm air vents between a thoroughly insulated floor of the refrigerator and the top of the foundation mat, as illustrated by Fig. 14-20, was tried out in the U.S.S.R and was reported by M. Steuerman (Ref. 326, 1936) to have been successful. A similar method of air-vent insulation is proposed by W. H. Ward and E. C. Sewell (Ref. 422, 1950) for the insulation of furnaces. Numerical solutions of the effect of different insulation thicknesses are given in that paper. Several cases are on record when, in the absence of such precautions, the heat transmitted from furnaces

through their foundation to underlying plastic clay caused uneven drying and shrinking. Serious damage to the whole structure resulted.

Practice Problems

14-1. The construction of a building of width $b = 70$ ft and length $L = 100$ ft is contemplated on a site where the soil consists of clay with fairly uniform properties down to a depth of 100 ft. The unit weight of the clay is $\gamma = 120$ lb per ft^3 = 0.06 tons per ft^3, its unconfined compressive strength $q_u = 0.7$ ton per ft^2, and its sensitivity is medium ($S = 2.3$). These values were established as averages from some 30 samples throughout the depth of the deposit. Determine (*a*) the safe depth to which a vertical unsupported cut could be made for the excavation, (*b*) the safe depth to which a vertical, laterally braced cut could be made for the excavation, (*c*) the permissible bearing pressure for a continuous mat if no basement is provided and the foundation mat is carried to a depth of 5 ft below the soil surface, (*d*) the permissible bearing pressure for a continuous mat if a basement is provided and the foundation mat is carried to a depth of 20 ft below the soil surface.

Answer. With reference to Table 14-4, the following factors of safety will be used: $F_s = 2.0$ for the temporary excavation and $F_s = 2.7$ for the building itself.

(*a*) The critical height of an unsupported vertical bank in this clay will be (see Eq. 9-10)

$$h_{cr}' = \frac{1.29 q_u}{\gamma} = \frac{1.29 \times 0.7}{0.06} = 15.1 \text{ ft}$$

The safe height will be

$$h_0 = h_{cr}'/F_s = 15.1/2.0 = 7.5 \text{ ft}$$

(*b*) With reference to Eq. (14-9), for H_{max} and $F_s = 2.0$, noting that $b < D$, so that the values of b should be used instead of D in Eq. (14-9), the safe depth of simultaneous excavation of the entire area will be

$$H_0 = \frac{2.57 \dfrac{0.7}{2.0}\left(1 + 0.44 \dfrac{2 \times 70 - 100}{100}\right)}{0.06 - \dfrac{0.7}{2.0}\left(\dfrac{1}{140} + \dfrac{2 \times 70 - 100}{70 \times 100}\right)} = 22.5 \text{ ft}$$

The limit depth H_{max} is obtained by using in the above equation $q_u = 0.7$ instead of 0.7/2.0

$$H_{max} = 36 \text{ ft}$$

(*c*) The 5 ft of excavated soil will be almost entirely replaced by the foundation mat. No load reduction will therefore be possible. With reference to Eq. (9-28),

$$p_{max} = 2.76 \times 0.7(1 + 0.38 \tfrac{5}{70} + 0.44 \tfrac{70}{100}) = 2.60 \text{ tons per ft}^2$$

$$p_0 = \frac{p_{max}}{F_s} = \frac{2.60}{2.70} = 0.97 \text{ ton per ft}^2$$

(*d*) The additional 15 ft of excavated soil will be replaced in part by columns, walls, and floors. Therefore only some 85 per cent of the weight of the soil removed can be taken to represent an effective reduction of load as compared with case (*c*). Without that reduction,

$$p_{max} = 2.76 \times 0.7(1 + 0.38 \tfrac{20}{70} + 0.44 \tfrac{70}{100}) = 2.74 \text{ tons per ft}^2$$

and, with that reduction, the safe load is

$$p_0 = \frac{p_{max}}{F_s} + 0.06 \times 15 \times 0.85 = 1.01 + 0.76 = 1.77 \text{ tons per ft}^2$$

The provision of a 15-ft basement has thus increased the permissible load by 80 per cent. A greater increase might be achieved by the provision of two basements, but the deeper excavation would only be possible if carried out in narrow sections (see Fig. 14-8; also Art. 13-6).

14-2. With reference to the flow net drawn in Fig. 14-11, what is the danger of a quick condition developing in the sump pit?

Answer. The total head lost is $h = 40$ ft. Ten equipotential lines have been drawn in Fig. 14-11, so that the head lost between each pair of adjacent lines is $\Delta h = 4.0$ ft. When drawn to a larger scale, the distance between the last two equipotential lines, that is, between the one marked "9" in Fig. 14-11 and the bottom of the sump pit, can be measured: $L = 1.9$ ft. According to Eq. (5-18), the hydraulic gradient below the bottom of the sump pit will be

$$S = \Delta h/L = 4.0/1.9 = 2.1$$

Failure due to the development of a quick condition will be inevitable, since the highest possible value of the critical hydraulic gradient for very dense sand (see Art. 5-4) is $S_{cr} = 1.05$. Thus the factor of safety is much smaller than unity: $F_s = S_{cr}/S = 1.05/2.1 = 0.50$.

14-3. What is the factor of safety against displacement of the floor mat of the dock shown in Fig. 14-16(III), after unwatering, if the overflow standpipe extends to a distance $d/2$ above the top of the floor of thickness d?

Answer. The maximum uplift pressure which can then develop against the bottom of the floor is $p_w = 1.5d \times 62.4 = 93.7d$. It will be resisted by the weight of the concrete floor $p_\gamma = d \times 140$. The factor of safety is

$$F_s = (140d)/(93.7d) = 1.49$$

14-4. Prior to unwatering the cofferdam shown in Fig. 14-11, the surface of the excavation was covered by a graded filter, and a 5-ft-thick seal of concrete was placed over it. Several overflow standpipes reaching into the filter layer were left embedded in the concrete. Estimate the factor of safety against uplift of the concrete seal.

Answer. It has been shown in Prob. 14-2 that within the upper 1.9 ft of soil a head of 4.0 ft of water was dissipated. The flow net which corresponds to the conditions of the present problem will differ somewhat from the one drawn in Fig. 14-11, but not much. If we make the unfavorable assumption that only the weight of the seal will resist a head of 4.0 ft of water, the factor of safety against uplift will still be adequate: $F_s = (5 \times 140)(4 \times 62.5) = 2.81$.

References Recommended for Further Study

The Theory and Practice of Reinforced Concrete, by Clarence W. Dunham, McGraw-Hill, 1944, pp. 258–281. Determination of the depth and of the reinforcement of foundation footings.

Soil Mechanics in Engineering Practice, by K. Terzaghi and R. B. Peck, Wiley, 1948, pp. 413–453. Summary of permissible bearing values of different building codes in the United States and other data related to the design of foundation footings.

"Working in the Dry with the Moretrench Wellpoint System." Published by the Moretrench Corporation, New York. Illustrated description of a number of dewatering jobs; other relevant data.

Underpinning, by E. A. Prentis and Lazarus White, Columbia University Press, 2d ed., 1950. Appendix outlining the legal problems involved in determining responsibilities for the support of adjoining properties during excavations.

Permafrost and Related Engineering Problems, by Siemon W. Muller, Edwards Bros., Inc., Ann Arbor, Michigan, 1947. Soil investigations and design and construction problems in permafrost regions.

"Blasters' Handbook." Published by the du Pont Co., 339 pp. Practical information of importance when blasting rock for excavation purposes.

Foundations of Structures, by Clarence W. Dunham, McGraw-Hill, 1950, Chap. 5, Spread Footings, pp. 90–134; Chap. 6, Foundation Walls, pp. 135–170; Chap. 7, Mats, pp. 171–201. Much useful information for structural designing and detailing.

"Foundations for Buildings in the Orange Free State Goldfields," by J. E. Jennings, *Journal of the South African Institution of Engineers*, Pretoria, November 1950–March 1951. Examples of structural damage due to nongravitational water migration under buildings founded on swelling fissured clays. Description of special foundation designs to meet the problem, including Texas-type tension piles or caissons anchored by underreaming in the underlying unshattered clay.

CHAPTER 15

PILE AND CAISSON FOUNDATIONS. SHEET PILING. UNDERPINNING

15-1. Types of Piles and of Pile-driving Equipment. Piles are intended to transmit foundation loads to deeper soil layers and may be made of timber, of concrete, or of steel. Combinations of the three materials are also employed. Concrete piles may be either of the precast type, or may be situ-cast, that is, cast or molded in the ground. Steel piles may be either of the so-called H-pile type, that is, consist of wide-flanged rolled-steel sections, or of the pipe-pile type.

Depending on the nature of support provided at the selected site by the surrounding soil, the piles may be defined either as *end-bearing* or as *frictional.* The term *floating* is sometimes used instead of *frictional.* Most piles are driven into the ground, but a few of the situ-cast concrete type are bored into the ground in very much the same way as boreholes made for soil exploration. The majority of piles are vertical, but, when it is necessary to offer resistance to horizontal forces (Prob. 16-7), they can be driven at an angle—the so-called batter piles. The maximum possible inclination, or *batter,* of the piles depends on the design of the pile-driving equipment available and may reach 45° (Ref. 29).

There are three main types of pile-driving hammers: the drop hammer, the single-acting steam hammer, and the double-acting steam hammer. The *drop hammer* consists of a solid piece of metal which is lifted by means of a cable operated by a winch, and which is then released from the desired height by some automatic device. It is comparatively slow in operation and is seldom employed in modern heavy construction work. In the *single-acting hammer* the energy of the steam is used only to lift the ram to the desired height. The driving energy is therefore provided only by the weight of the dropping ram. In the *double-acting hammer* the steam is first used to lift the ram, which moves inside of a solid casing, and then the direction of the steam pressure applied to the ram is reversed, so that it accelerates the ram on its downward path and increases thereby its energy at impact. The effectiveness of different types of hammers is

usually compared in terms of foot-pounds of energy per blow. A wide variety of types and sizes is available, up to 5-ton rams delivering 90 strokes per minute with 55,000 ft-lb energy per blow (see Ref. 75). Most double-acting types of hammer may be easily adapted for special jobs, such as the pulling of sheet piling, where the direction of the hammer action has to be reversed (Fig. 16-24), or for driving under water. Timber piles for temporary supporting platforms on construction jobs, or in military engineering, can be quickly driven by lightweight gasoline-operated hammers, somewhat similar to the soil compactors shown in Fig. 11-8. Such hammers do not require heavy driving rigs.

To avoid damage to the head of the pile, special anvils, cushions, and caps have to be employed during driving. This is particularly important in the case of timber and of precast reinforced-concrete piles.

The maneuverability of the pile-driving rig can save much time on a job while the rig is moved from the location of the pile it has driven to a new one. Figure 15-10 shows the base of an old-fashioned type of rig mounted on skid pipe rollers. A lot of time can be wasted while changing the direction of movement of such a rig. This is not true in the case of modern types of rig, mounted on caterpillar tracks (see Fig. 15-11). The leads of the rig have to be sufficiently rugged to guide the pile and the hammer in their downward movement. In addition, they have to be specially designed to withstand appreciable compressive forces when the casing of situ-cast piles (Fig. 15-9) has to be pulled up from the ground as the pile is molded (see Figs. 19-6 and 19-8, which illustrate rigs built along these lines for sand drains).

15-2. The Remolding of Clays by Pile Driving. The interaction between piles and the surrounding soil is one of the first points to be considered when designing a pile foundation, especially when clay layers are to be penetrated. The clay in the immediate vicinity of the piles is strongly distorted, as shown in Fig. 15-1. The general displacement of soil layers may not be as considerable as in the case of an excessively deep excavation (Fig. 14-6); nevertheless, it is usually sufficient to cause detrimental settlements of sensitive clays. This was the case of the building to which Fig. 15-1 refers. Steel-pipe piles had been driven closed end to hardpan through over 100 ft of varved clay. The displaced clay heaved around the building; trenches were closed thereby. The sensitivity of such clays is considerable, with average values of $S \geq 5.0$ (see Art. 7-22 and Table 14-4). A subbasement was provided in that building, and its floors and partitions were placed directly on the ground, apparently on the assumption that this should be safe, since the weight of some 6 ft of the original soil had been removed in the excavation for the subbasement. Nevertheless, signs of distress soon appeared there in the form of cracks,

both in the floors and in the partitions. The location of the cracks indicated that the central portion of the floors was settling with the ground beneath it, whereas the edges of the floors were prevented from doing so by the pile-capping beams on which they rested. Accurate measurements showed that the reconsolidation of the remolded clay under its own weight, as evidenced by the settlements of special bench marks which were embedded in it, continued for several years. Mudjacking (Art. 19-6) was used to keep the floors level.
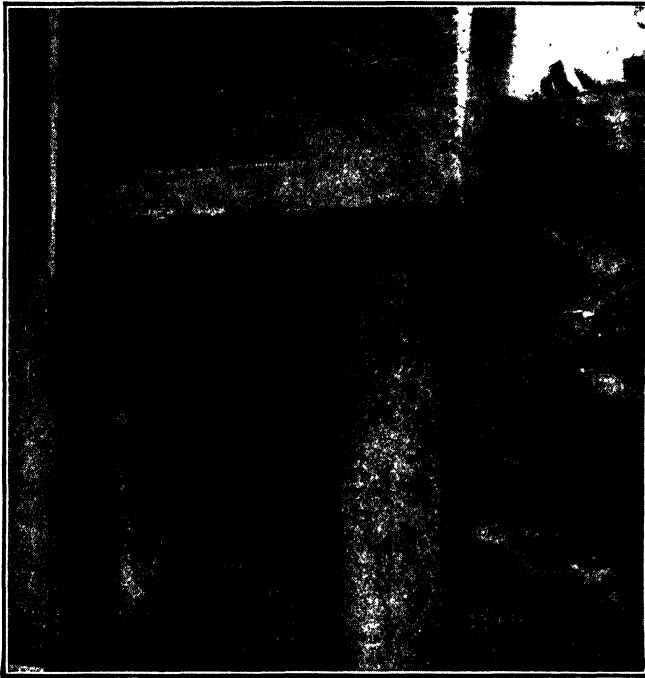
FIG. 15-1. The distortion of clay layers in the vicinity of a group of steel-pipe piles which had been driven closed-end. (*From G. Freeman and J. Parsons, Ref.* 138, 1950.)

Incompletely consolidated and/or remolded clay layers can overload end-bearing piles, owing to the effects of the so-called *negative friction.* This term is employed to designate frictional forces which are applied in a downward direction to the pile surface, as opposed to the usual condition where the surrounding soil provides at least some frictional support to the piles by means of frictional forces acting in an upward direction. A particularly dangerous condition may arise when piles are driven through a newly placed fill, for instance, slag or gravel, and through underlying soft clay to a deeper lying hard layer. As the clay consolidates the entire weight of the fill may then be transmitted through negative friction to the

piles and, in some instances, may crush them. Pile foundations should be avoided under such conditions, especially if any of the piles have to be driven on a batter.

The attitudes of engineers toward the use of piles in clay have fluctuated appreciably during the past quarter of a century. The slogan "when in doubt, drive piles" was popular at first. A. Casagrande (Ref. 61, 1932) drew attention to the harmful effects which pile driving has on clays, but it was shown later that not all of his original generalizations are valid. For instance, not all clays are weakened by any form of remolding (see Art. 7-22). Some types of clay are at first weakened by remolding but then regain their strength with time as a result of *natural hardening* (see Art. 4-1 and Ref. 238). The removal of soil by excavation for deep cellular foundations is not always a beneficial alternative to pile driving (see Art. 14-6). The pendulum swung back to the other extreme in 1949 when A. E. Cummings, G. D. Kerkhoff, and R. B. Peck (Ref. 98) attempted to show that pile driving into clay not only was not harmful but was even beneficial. Their conclusions were based on indirect reasoning. No measurements of soil-surface settlements had been made in the tests to which they referred in support of their claims. This and other flaws were brought out by most of those who discussed their paper and supplied definite data contradicting the generalizations which they had advanced (see, for instance, Refs. 398 and 138).

On the strength of the evidence available at present, the following recommendations can be made: The sensitivity of a clay to remolding should be determined by means of unconfined compression tests (Art. 7-22 and Refs. 164 and 377). If the clay is found to be of a nonsensitive or of a slightly sensitive type (see Table 14-4), the driving of piles should not cause any concern in respect to a possible weakening of the clay. On the other hand, if the clay is of a highly sensitive type, it should not be relied upon for the support of frictional piles, floors, or other structural elements, if the clay has been remolded by the driving of end-bearing piles to an underlying firmer stratum. Clays of a medium sensitivity are in an intermediate group, concerning which insufficient data are available to permit definite recommendations. Load tests of piles may provide some useful indications.

15-3. Bearing Capacity of Piles. Load Tests. When interpreting the results of load tests on single piles, it should always be remembered that they provide data only concerning the bearing power of the one pile tested. Such tests therefore bring out the properties of the pile type in relation to the surrounding soil, but only in respect to the number of piles which were tested simultaneously. A careful study of the entire soil profile at the site should be made before conclusions can be drawn con-

cerning the probable behavior of larger pile groups than the ones tested or of the entire building. The reasons for this are similar to those which limit the usefulness of load tests on small spread footings (see Arts. 9-1, 9-8, and 12-10). This point is illustrated by Fig. 15-2. During a load test on a single pile only a small volume of soil immediately around the test pile is stressed by the applied load. Stresses of equal intensity will reach to a much greater depth under the building itself. Should it happen that a weaker layer is located at a greater depth, as shown in Fig. 15-2, it will receive only negligible stresses from a single test pile, because of the load-distributing action of the overlying sand. However, in the
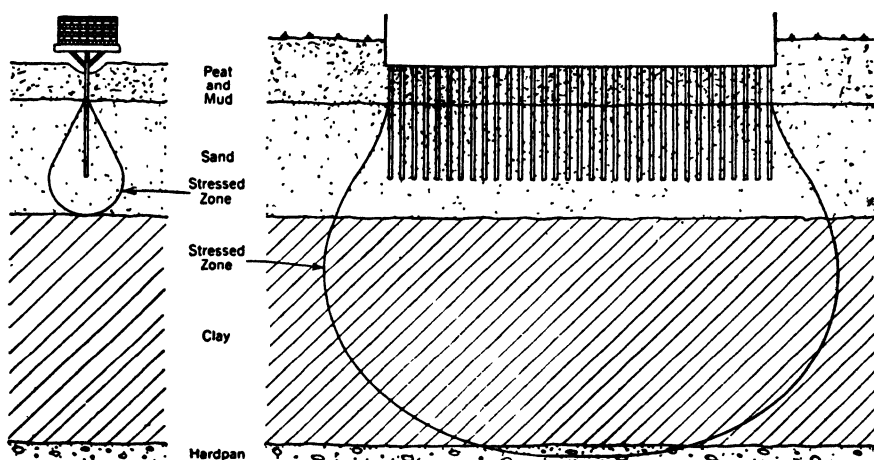
FIG. 15-2. Sketch showing why the results of load tests on single piles cannot be used to forecast the behavior of the entire structure. (*From Gilboy, Ref.* 152, 1937.)

case of the structure itself, the stresses transmitted to the underlying clay layer will be considerable (compare with Probs. 15-2 and 15-3; also see discussion of Fig. 13-13 in Arts. 13-3 and 15-4.

The point is illustrated further by the case of the Mixed Law Courts Building at Cairo, Egypt, the façade of which is shown in Fig. 13-11. The structure was supported by 28-ft-long situ-cast concrete piles of the Simplex type (see Art. 15-7). The piles were embedded in a stiff upper crust of brown-colored clay, not sensitive to remolding. Load tests on single piles, of which the curve, pile II, in Fig. 15-3 is representative, gave only small settlements, varying from $\frac{1}{16}$ to $\frac{1}{4}$ in. under 40- to 60-ton loads, which was the maximum any pile of the building had to carry. This is less than 0.01 in. settlement per ton load, which value is frequently used as one of the criteria for the satisfactory behavior of a test pile (Ref. 366). Nevertheless, the building itself settled some 50 times more than

the test pile, that is, it settled over a foot, much of it differentially (see diagrams of building *T*, Tschebotarioff, Ref. 377, 1940). This happened because a softer layer of darker colored clay underlay the upper oxidized stiff brown-colored clay in which the piles were embedded. The seat of the settlements of the building was located in that deeper lying clay layer.

Something very similar to the record of this building on the Nile River happened in the Mississippi Delta to the new (1938) Charity Hospital at New Orleans, which sustained a maximum settlement of 21 in. and differential settlements of 7.5 in. (see R. F. Bland, Ref. 32, 1950). Other such instances have been recorded in many other localities.

FIG. 15-3. Results of load tests on two situ-cast piles of the Simplex type under different soil conditions.

The test pile I in Fig. 15-3 was a 35-ft-long end-bearing Simplex-type pile at another location, which reached into a thick sand layer. Its test diagram is similar to that of pile II, but the building which was erected at the site of pile I settled less than an inch, that is, only some five times more than the test pile under the same loading per pile. Part of the settlement of an end-bearing pile may be attributed to the elastic compression of the concrete (see Fig. 15-3).

The need for a careful study of the properties of *all* underlying soil layers is therefore obvious. With these reservations in mind, however, load tests can serve a useful purpose in determining the supporting power of different types of piles, especially when they are end-bearing. Thus the new New York City building code, as reported by J. H. Thornley (Ref. 366, 1949), permits loads per pile, when substantiated by load tests, which are almost twice the limit values set for the same types of piles when no load tests were performed.

Because of the considerable forces involved, load tests are seldom carried out on more than one pile at a time. There are two ways of performing such load tests. The first is illustrated by Fig. 15-2. A specially designed platform is placed over the head of the pile and weights

are laid on the platform. Settlement readings are taken on the head of the pile by means of an optical level in respect to a bench mark set at least 15 to 20 ft away from the test pile. The second load-test procedure consists in placing a hydraulic jack on the pile and a heavy steel girder over it. The girder is anchored down to two or more adjoining piles. This procedure is somewhat simpler in operation and less expensive than the one provided by platform loading. However, the exact nature of the interaction between the loaded test pile and the adjoining piles which are stressed in tension is somewhat uncertain. For further details concerning pile-test loading techniques see Ref. 11 and Prob. 15-5.
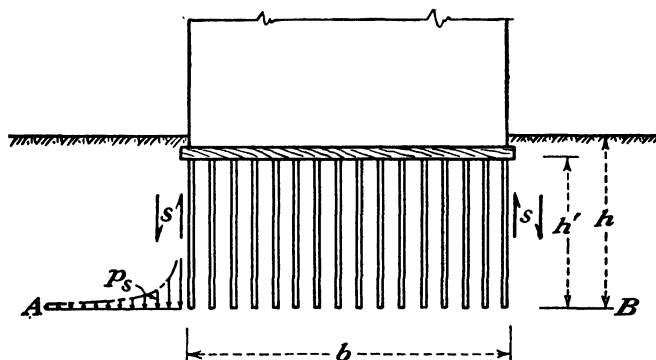
FIG. 15-4. Sketch illustrating the determination of bearing capacity of floating pile foundation embedded in a nonsensitive clay.

The bearing capacity of frictional piles embedded in clay is approximately equal to the outer *skin* surface of the pile times the shearing strength of the clay $s = c = q_u/2$ (see Ref. 388 and Prob. 15-1). According to the results of load test on pile groups reported by Frank A. Masters (Ref. 222, 1943), shear failure of clay starts along the surface of corner piles. The causes of this are somewhat similar to the causes of smaller settlements of corners of spread footings and of the greater concentration of reaction pressures at the edges and corners of spread footings on clay (see Art. 9-4). In other words, failure starts along the outer skin of the corner piles, because this is where shearing stresses reach their limit value first.

The ultimate bearing capacity of a pile foundation embedded in clay can be computed from Eq. (9-28), where the value of p_{max} obtained for the plane AB from that equation (see Fig. 15-4) can be reduced by the sum of the shearing stresses s along the outer perimeter of the entire pile group (see Prob. 15-3).

So-called "static pile bearing formulas" have been based on values

of the angle of internal friction ϕ and of lateral pressures (Art. 10-1) based on ϕ. Such formulas are most unreliable in use.

Sometimes it is important to determine the purely end-bearing properties of a pile. This can be done by performing first a load test of the ordinary kind, which would give the end-bearing plus the frictional resistance, followed by a pull-out test, which would provide a measure of the frictional resistance alone. The difference between the values obtained by the first and by the second test would indicate the end-bearing resistance of a single pile. For a time there were some doubts whether the frictional pull-out resistance of a pile in sand was the same as the frictional resistance of a normally loaded pile. Small-scale model tests performed in several laboratories of different countries with model piles constructed along the lines of Fig. 12-17(II) had all indicated a much smaller frictional resistance when the outer cylinder T was pulled up than when it was pushed down (see Ref. 388).

However, this seems to be an effect which is limited to the upper few inches or feet of sand, close to its surface. At any rate, Tschebotarioff (1949) obtained exactly the same frictional resistance F for upward and for downward movement of the outer cylinder T of a Delft-type cone [see Fig. 12-17(III)], which cylinder reached all the way to the sand surface, at four different total depths varying from 20 to 50 ft. These tests were performed during the part (2) of the study illustrated by Fig. 12-18 and marked by circles and broken lines in that diagram.

Experience shows that there is no danger of buckling of centrally loaded vertical end-bearing piles below ground level, and that even the softest types of clay provide enough lateral support to the piles to prevent any such buckling. Of course, this does not apply to the upper portions of piles which protrude from the ground into air or water, as is the case with piles supporting harbor piers or jetties or piles forming part of unbraced bents of bridge trestles. Such piles should be treated as ordinary columns down to a depth of 5 ft below the surface of the ground in which they are embedded. Below that depth they will be usually supported laterally by the ground. However, the reverse is true if the ground tends to move or to slide at an angle to the axis of the piles; end-bearing piles could offer very little resistance to such movement and would be strongly affected thereby.

15-4. Pile-driving Formulas and Records. For over a century attempts have been made to determine the bearing capacity of a pile from its driving record. One group of engineers equated the energy of the falling hammer to the work expended in driving the pile, that is,

$$WH = RS + Z \tag{15-1}$$

where W = weight of the falling hammer (or ram)
H = height of drop of W
R = ultimate resistance of the soil to penetration by the pile
S = penetration of the pile into the soil per blow (*set*)
Z = sum of all energy losses due to any cause whatever

The practical difficulty centers on the determination of the value of Z, since there are a great number of sources of energy losses during pile driving. To mention some: temporary compression of the ground; temporary compression in the pile; temporary compression in the driving head, including its packing; bouncing of the hammer on the pile; and elastic deformations of the hammer itself.

Another group of scientists, for instance Eytelwein (1820), based their formulas on the Newtonian theory of impact, although, as shown later by A. E. Cummings (Ref. 96, 1940), Newton correctly qualified his laws of impact by reservations which precluded their use for problems similar to those of pile driving.

The fundamental difference between the two approaches was not always realized. For instance, many formulas represent modifications of the so-called *complete* pile-driving formula which, according to A. E. Cummings (Ref. 96), originated with Redtenbacher (1859) and reads

$$R = \frac{AE}{L}\left[-S \pm \sqrt{S^2 + WH\,\frac{(W + Pn^2)2L}{(W + P)AE}}\right] \qquad (15\text{-}2)$$

where W, H, R, and S have the same significance as in Eq. (15-1)
E = modulus of elasticity of pile
A = cross-sectional area of pile
P = weight of pile
L = length of pile
n = coefficient of restitution

The above Redtenbacher formula ignores the frequently very important losses from temporary compression of the ground and considers mainly energy expended on the compression of the pile. At the same time, as shown by A. E. Cummings (Ref. 96), it subtracts some energy losses twice, since they are already included in Newton's coefficient of restitution n. This is only one example of the confusion which exists on this subject.

Two different trends are still in evidence among engineers concerning pile formulas. Thus the Committee on the Bearing Value of Pile Foundations of the ASCE was unable to reach agreement on the subject and published (Ref. 82, 1943) two versions of its report. Report (A) recognizes the many limitations of pile-driving formulas but implies encouragement of the hope that rational use of such formulas is neverthe-

less possible in practice if proper judgment is exercised. Report (B) carries to its logical conclusion the recognition of these limitations by stating:

All dynamic pile-driving formulas are subject to definite limitations and any dynamic pile-driving formula is nothing more than a yardstick to help the engineer secure reasonably safe and uniform results over the entire job. The use of a complicated formula is not recommended since such formulas have no greater claim to accuracy than the more simple ones.

The author of this book endorses the above views of Report (B).

A simple formula based on field experience and frequently used in the United States is the so-called *Engineering News* formula, developed by Wellington (1888).

$$R = \frac{12WH}{S + c} \tag{15-3}$$

where c is a coefficient and the other terms have the same significance as in Eq. (15-1). The factor 12 is introduced because H is taken in feet and S in inches. With a factor of safety $F_s = 6.0$, the safe load R_s on the pile, for drop hammers and for single-acting steam hammers, is

$$R_s = \frac{R}{6} = \frac{2WH}{S + c} \tag{15-4}$$

and for double-acting steam hammers,

$$R_s = \frac{2(W + Ap)H}{S + c} \tag{15-5}$$

where A = area of the piston of the ram
p = steam pressure on the piston

The coefficient c is given the following values:

c = 1.0 for drop hammers
= 0.1 for steam hammers
= $0.1(P/W)$ for steam hammers, if the inertia and weight of the pile are to be considered

It should be noted that the above formula is fairly satisfactory in granular soils but does not take into account possible bouncing of the pile in saturated cohesive soils, that is, the considerable amount of energy which may be dissipated on the temporary compression of some of these soils. This point can be quite important. The interest in soil mechanics of the author of this book was first aroused some 23 years ago when he worked as a reinforced-concrete designer for a European construction company in Egypt and had to design new continuous foundation mats for

three government buildings in the Nile Delta over floating pile foundations which had been condemned. The static load tests showed that the piles could carry less than one-third of the load they were supposed to carry, both according to the specifications and to a dynamic pile formula employed to check the driving. An investigation showed that the saturated clay at that site behaved somewhat like rubber, so that the piles had little final penetration per blow, but bounced considerably. This possibility had not been taken into account by the formula and therefore had not been reported by the men on the job. The faith in pile-driving formulas of the director of the construction company was severely
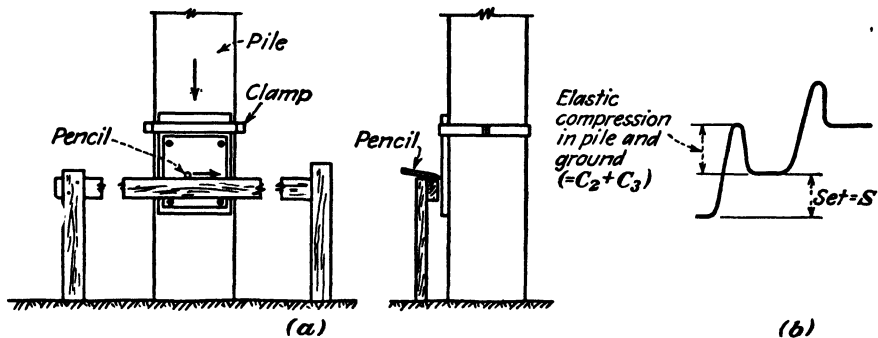
FIG. 15-5. Experimental method of determining the elastic compression in pile and ground during driving.

shaken by the incident, but the lesson had cost his firm a considerable amount of money.

A comparatively simple and yet rational formula which permits the evaluation in the field of the energy losses by means of actual measurements is the Hiley formula (Ref. 174, 1930), which is much used in Great Britain. It reads

$$R = \frac{kWH}{S + C/2} \tag{15-6}$$

The terms R, W, H, and S have the same significance as in Eq. (15-1); H is taken in inches; k is a coefficient, always smaller than unity, which denotes the efficiency of the hammer blow, that is, the fraction of its original energy (WH) actually transmitted to the pile; $C = C_1 + C_2 + C_3$ represents energy losses due to temporary compression of the driving head and packing (C_1), the pile (C_2), and the ground (C_3).

The values of S, C_2, and C_3 can be measured on any job by means of the arrangement shown in Fig. 15-5. A pencil is moved by hand along a guiding board at constant speed from left to right, as shown in diagram (a). Since at the same time the pile moves downward under the hammer

blow and then moves back (upward) as it recovers partially, a record, as shown in diagram (*b*), is obtained on a sheet of paper clamped to the pile.

According to Ref. 272, the value of k may vary between the limits of $k = 0.15$ for a heavy pile, light hammer, and fresh wood cushion, and $k = 0.68$ for a light pile, heavy hammer, and well-compacted old cushion; these values include corrections for equipment efficiency. C_1 also is based on empirical data (see Ref. 272). Since the Hiley formula permits a fairly close check on all energy losses, a lower factor of safety than in the case of the *Engineering News* formula can be used, namely, $F_s = 2.0$, so that the permissible safe load on a pile will be $R_s = R/2$, where R is the value obtained from Eq. (15-6).
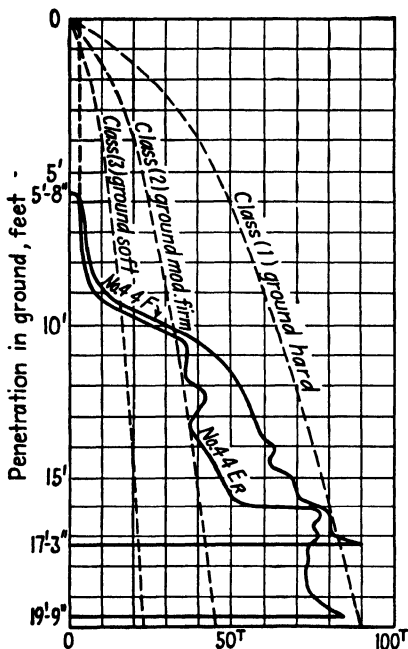
FIG. 15-6. A graphical method of recording the driving resistance of piles which facilitates the comparative evaluation of the supporting properties of the soil strata penetrated. (*Courtesy of British Steel Piling Co., Ltd.*)

In some types of cohesive soils piles may "freeze" after a pause in the driving, that is, they will offer more resistance to the driving when it is resumed than they did before the stoppage. This phenomenon has not yet been fully clarified, especially in respect to the physical characteristics of the soils where it may occur.

Summing up, considerable caution and judgment is necessary when estimating the actual bearing capacity of a pile by means of driving formulas. Nevertheless, driving records are very useful, since it is possible to make expensive static load tests only, at best, on a very small fraction of the total number of piles driven, but it is a simple matter to keep a driving record of *every* pile driven on a job, and thereby to relate their performance to the results of the few static load tests made on that site. A good way to keep such records is illustrated by Fig. 15-6. A supply of graphs is printed on tracing paper, including three curves which designate the limits of the driving resistance which is to be expected at different depths with the type of pile and hammer used on the job in class 1 ground—hard, class 2 ground—medium firm, and class 3 ground—soft. The particular three limit curves in the diagram were established on the strength of experience with the Hiley formula and different equipment in

different soils. A single-acting hammer was used in the case of Fig. 15-6, with $W = 2.0$ tons, and a stroke $H = 48$ in. for the pile No. $44E_R$ and $H = 36$ in. for the pile No. 44F. Both were 50-ft-long 14- by 14-in. timber piles. The final set was $S = 0.29$ in. for the first of the above two piles, and $S = 0.23$ in. for the second. With these data and other equipment coefficients of the Hiley formula the actual driving record of each pile on a job can be quickly plotted on separate graph sheets, and any number of blueprints thereof can be obtained, if so desired. The driving performance of each pile on a job can be compared with the others by a glance at the file record. Any soft spots missed by the necessarily not too closely spaced borings during the soil investigation made in advance of construction are immediately revealed by a graphical record of the type shown in Fig. 15-6, which serves as a yardstick for the comparison of the performance of the piles over the entire job. The depth of penetration of individual piles can then be quickly adjusted when necessary to the actual soil condition encountered beneath each pile. However, this remark refers only to the few feet of soil around the tip of that particular pile which provides its support. All the restrictive comments of Art. 15-3 concerning the validity in respect to the entire pile foundation of load-test results on single piles apply to an equal extent to the results of pile-driving records. In other words, borings should ascertain the nature and the properties of soil layers well beneath the elevation to which the tips of the piles will reach. This is essential since otherwise detrimental settlements of the entire structure may result, as illustrated by Fig. 13-13. The piles of the bridge which is shown there were all driven to a satisfactory resistance, according to dynamic formulas and to the actual pile-driving records, into a fairly stiff layer of clay. Deep borings were performed only later and disclosed the presence of much softer underlying layers of clay and of peat, in which layers the seat of the considerable surface settlements was located; these settlements reached a maximum of 6 ft 4 in.

It is not always possible to drive piles, especially if they are made of timber, through a compact layer of sand without serious damage to the piles. At the same time it is often necessary to have the piles reach to a deeper elevation, for instance, when there is a danger of scour or of later erosion by water currents. *Jetting* of the piles has to be used then, that is, a water jet churns up the sand along the tip of the pile, which sinks into the sand as a result. When the desired elevation is almost reached, the jet is withdrawn, and the pile is driven to *refusal*, that is, to the minimum penetration per blow desired.

15-5. Timber Piles. Timber piles represent the oldest type of piling in existence. They have been employed by the human race since prehistoric days, for instance, for the so-called lake dwellings.

When fully submerged, timber piles will not decay and are likely to last for centuries. For instance, after the collapse of the Campanile at Venice [see Fig. 13-6(II)], excavation revealed that the timber piles which had been driven for the tower foundation over a thousand years before the collapse were still in such good condition that they were left in place for the foundation of the new tower, and only additional piles were driven all around the old ones to increase the total area of the foundation.

Timber piles will deteriorate rapidly if subjected to alternate drying and wetting. Creosoting and other forms of impregnation treatment of the entire mass of the pile timber by various chemical preservatives will delay the process of decay, but cannot prevent it entirely. For that reason, foundations of permanent structures supported by timber piles should be carried down to an elevation where the tops of the timber piles will remain permanently below the lowest ground-water-level elevation. The probability of the ground-water table dropping progressively in urban areas because of the diversion of normal replenishment, subsurface drainage, and the use of ground water should be considered, since expensive underpinning measures and litigation as to responsibilities might become necessary if the timber piles started to rot.

The portions of timber piles which protrude from the soil into free water are liable to be attacked by various types of *marine borers*. Most of them occur in salt water. The *molluscan* group of borers, which includes the teredos and other shipworms, grows inside of timbers, whereas borers of the *crustacean* group, for instance, the limnoria, usually eat the wood from its surface. Timber piles of piers and jetties have been rapidly destroyed by such borers in some instances. Pollution of the water usually decreases the danger of the appearance of borers, but there are a great number of other factors, which vary in different localities, on which their existence depends (see Ref. 75). Expert advice should be sought on the matter prior to deciding whether to use timber piles in contact with free water or not. The borers do not penetrate through the voids of soils, even of sands, so that timber piles embedded in soil under relieving platforms with steel or reinforced-concrete sheet piling on the water side are safe from attack by borers (see Figs. 16-31 and 16-33).

Bark provides some natural protection against borer attack, but it should be removed from those portions of the pile skin which are relied upon to receive some frictional support from the soil.

There usually is no difficulty in obtaining timber piles in lengths up to 60 ft. Greater lengths have been employed, up to 135 ft, but they are difficult to obtain, especially on the eastern and southern coasts of the United States; west coast timber is frequently available in greater lengths.

Great care should be exercised not to *overdrive* timber piles, that is,

not to damage them when trying to pierce a stiff layer. This can easily happen in compact sand. The slight permanent set S which is recorded per blow at the soil surface may then mean not that the pile penetrates the sand as one body, but that it has been crushed and that its fibers are telescoped or forced past each other at the zone of failure. If there is any suspicion that something of the kind is occurring, then it is advisable to pull out one or more piles for examination. If the piles actually have been damaged, one should either change the specification and stop the driving at a higher elevation than originally intended, or one should resort to jetting.

Timber piles usually are not permitted to carry loads in excess of 12 to 18 tons per pile.

15-6. Precast Reinforced-concrete Piles. Piles of this type can carry much heavier loads, up to 50 tons per pile, depending on the dimensions, and can take fairly heavy punishment during driving. Since the casting of the piles is done at the soil surface, close control and inspection of their manufacture is possible.

However, this type of pile has some disadvantages. The required length of the pile has to be accurately determined in advance of construction. This is not always possible. Changes of length after the pile has been driven are time-consuming and therefore expensive.

If the pile is too long, the following steps are necessary to cut it off: First, the surface concrete has to be chipped off to expose the steel reinforcement. The steel has to be burned off with a torch, and only then can the excess length be knocked off. An increase of length of the pile is also complicated. Additional steel reinforcement has to be cut to the required length and spliced with the reinforcement of the pile proper. Often this requires chipping off the concrete of the pile to a length of 3 ft or so, in order to expose the steel bars and permit their splicing. Vertical forms have then to be built over the original head of the pile and removed after the extension has been cast. Driving can be resumed only after the new concrete has hardened sufficiently.

Sometimes steel bars are allowed to protrude from the head of the pile in order to permit their splicing with the reinforcement of the pile-capping beams (Fig. 15-12). Special perforated templets are then used, both during the casting of the pile, to hold the bars in their exact positions, and during the later driving, to form an anvil over the concrete of the pile.

The casting and storage of reinforced-concrete piles requires appreciable space on the site of the job itself.

The greatest stresses to which the precast piles are subjected are produced during their handling and lifting prior to the driving proper. For instance, as shown in Fig. 15-7, the pile which is being lifted into position

for driving by a cable from the top of the pile-driver leads will act as a beam on two supports, stressed by its own weight. The reinforcement has to be designed accordingly. Precast reinforced-concrete piles have been made in lengths exceeding 100 ft. Too great bending stresses would be caused in such long piles if they were handled in the manner shown in Fig. 15-7. Support at several points should then be provided by means of a system of cables and pulleys at all stages of their handling (see Ref. 272).
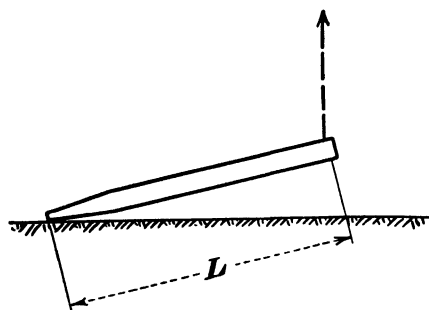
FIG. 15-7. Precast reinforced-concrete piles have to be designed to resist stresses caused by their own weight during transportation prior to driving. (*From Ref. 272.*)

Sometimes the piles are cast with an enlarged base in order to increase the point resistance (see Fig. 15-8, which shows four such piles cast in each tier). This type is of advantage for purely end-bearing piles with very soft layers above the layer in which the piles are to receive their support. They are frequently used in Holland where some 50 to 60 ft of soft clay and peat are usually followed by sand (see Fig. 16-13).
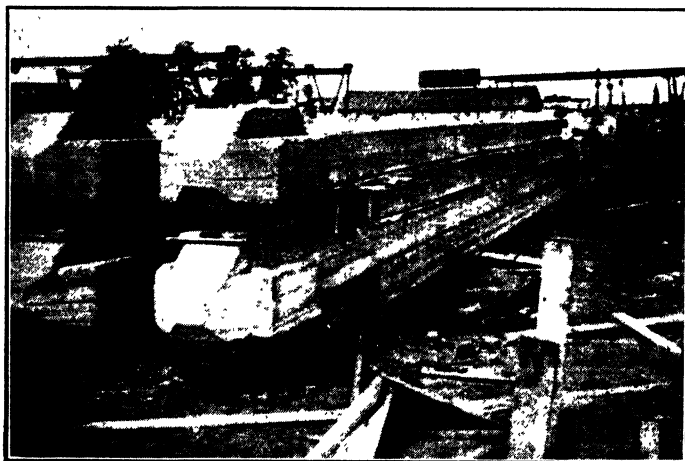
FIG. 15-8. Tiers of precast reinforced-concrete piles after removal of the side forms in a casting yard in Holland. The pile points are enlarged to provide greater bearing area and to minimize effects of "negative friction" along pile stem. (*Photo by Tschebotarioff, 1948.*)

15-7. Cast-in-place Concrete Piles with and without Steel Casing. The oldest type of cast-in-the-ground, or *situ-cast*, piles was obtained by filling a borehole of large diameter or a well with concrete. Such *bore*

piles are still used in Europe, where the casing is sunk into the ground by usual boring procedures, that is, by augers or by washing (Art. 12-6), and is then filled with concrete. A special cap is fitted onto the casing. Air or water pressure is applied to compress the concrete in the casing and, at the same time, to lift the casing out of the ground. The procedure is somewhat similar to that used for sand-drain construction (see Art. 19-4). Very high pressures are sometimes needed when the upper part of the casing is gripped by compact clays of a swelling type. A danger exists then that the cement grout may be pressed out of the concrete into underlying
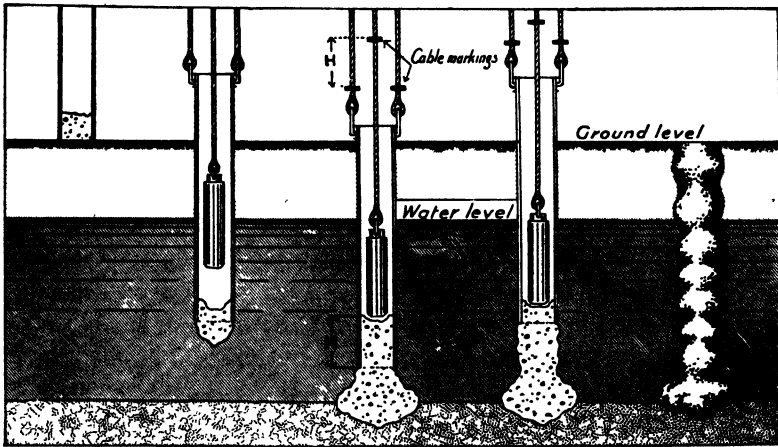
FIG. 15-9. Steps in the formation of a cast-in-the-ground (situ-cast) concrete pile of the Franki type. (*From a catalogue of the Franki Pile Co.*)

sand layers, if such are present. There are other similar practical difficulties which have to be overcome in order to have a guaranteed good execution of the job. This type of pile is seldom used in the United States.

The most customary way of forming a situ-cast pile is to *drive* the casing and then to pull it up as it is filled with concrete. In some types of piles, for instance, in the old *Simplex* type, the driving was done by means of conventional-type hammers, hitting on the top of the casing, which acted as a hollow pile, since it was provided with a metal or pre-cast concrete shoe. The shoe was left in the ground as the casing was withdrawn. A somewhat different method, the *Franki-pile* method, of driving a casing by a hammer which is later utilized as a concrete tamper is illustrated by Fig. 15-9. This method saves the cost of the shoe. The arching of the dry concrete plug (Art. 10-19), and its friction along the inner walls of the casing were found sufficient to drive the entire casing into the ground if only light blows were delivered by the hammer-tamper,

which, to that end, was lifted only slightly before each blow. When the desired elevation was reached, the 2-ton hammer-tamper was lifted as far as possible and dropped, so that the concrete plug was at least partially knocked out through the bottom of the casing. From then on the molding of the piles of the Franki, Simplex, and other similar types proceeds essentially along the lines illustrated by the third, fourth, and fifth steps in Fig. 15-9. The following essential precautions have to be observed:

The distance H cannot be greater than two or, at the utmost, three times the inner diameter of the casing, since otherwise there will be serious danger that the blow of the tamper will not be sufficient to push the concrete down out of the casing, which is lifted slightly by means of cables simultaneously with each blow. This distance H is checked at the soil surface by the pile driver operator, who has to watch the relative positions of the markings on the cables attached to the casing and to the tamper constantly. At the same time, it is dangerous to have too little concrete in the casing or to tamp it below the bottom of the casing, since soil might then get mixed with the concrete or even separate the concrete shaft of the pile into disconnected sections with only soil layers between them. This means that the proper execution of piles of this type depends to a very large extent on the unrelenting vigilance of the pile driver operator. There is no way to check later, except by pile load tests which, because of their cost, can be made only on a very small number of piles (Art. 15-3). This type of concrete piling is therefore very far from being foolproof.

In addition, such piles cannot be driven through very soft sandy clays or silts or through sand lenses under a high head of water, since the lateral water pressure would then squeeze the concrete into the casing and some of the soil after it as well. In other words, this procedure simply would not function under such conditions. Another kind of pile of the same type can then be successfully employed, namely, the *Vibro* pile. The casing is provided with a shoe and is driven to the desired elevation by a hammer hitting on its top, whereupon it is filled over its whole depth with concrete of a fairly fluid consistency. A special type of hammer, the direction of action of which can be reversed, is used with these piles. The casing is pulled up as the upward-acting hammer hits an attachment of the pile casing. The vibrations induced thereby in the casing, as well as the considerable static head of the fluid concrete, prevent its adherence to the walls of the casing and ensure a continuous shaft of the finished pile, even when the pile pierces layers of soft clay or water-bearing sand under a considerable head. The Vibro pile is therefore essentially an end-bearing pile. It does not have the many corrugations along the length of its shaft which are present in Simplex or in Franki piles (see Fig. 15-9),

and which increase the frictional resistance along the skin of these latter types of piles. However, this is not always a disadvantage (compare with Fig. 15-8) and frequently is of little importance one way or another. Vibro piles have been driven in lengths up to 65 ft.

All three types of situ-cast piles so far discussed, the Simplex, Franki, and Vibro, as well as other similar piles, have one further disadvantage. Piles, especially end-bearing ones, are usually driven within a few feet of each other in clusters, so that the whole group would support a column load. A pile driver can drive several piles a day. The piles are driven successively next to each other. Therefore the concrete of a pile does not have time to harden or, sometimes, even to set before the adjoining pile is driven next to it. The moving about of pile drivers is a time-consuming and expensive proposition. Therefore it is not practicable to move the pile driver to operate at another location until the concrete hardens in the first pile of a cluster, and then to bring the pile driver back to mold the second pile. It may therefore happen in localities where boulders are present that the first piles of a cluster would miss a boulder. One of the following pile casings would hit the boulder on its edge and, as it was driven in farther, would force it sideways against the still green concrete of the first piles; this would crush and destroy their shafts. For this reason many building codes of different cities in the United States forbid the use of such cast-in-the-ground concrete piles unless the concrete is protected by a steel casing which is permanently left in the ground (compare with Art. 15-10).

It should be noted that the above objection applies only to *concrete piles* but cannot possibly be valid in the case of *sand piles* (Art. 11-4), so that the Franki type of pile represents a very efficient way to compact a deep layer of loose sand, especially when the sand is silty.

One of the better known types of American situ-cast concrete piles with permanent protective casing is the Raymond pile. Three steps in the driving of a standard tapered type of Raymond pile are given in Fig. 15-10. The first step is shown on the left of the sketch and refers to the stage when the outer shell has been driven into the ground by means of the inner *mandrel* or *pile core*. The shell is made of sheet metal in sections of 4-ft and 8-ft lengths. It is reinforced and stiffened with a spiral wire on a 3-in. pitch. The point diameter is 8 in., and the diameter increases at the rate of 0.4 in. per foot of pile length. The core is employed to stiffen the shell and to prevent its buckling during driving. It is collapsible, that is, by being made of three separate parts along its entire length it can be easily separated from the shell and withdrawn after completed driving. During driving the three parts of the core are wedged apart by a special mechanism and are thus temporarily pressed against

the inner wall of the shell. The second step in Fig. 15-10 shows the construction stage after the core has been withdrawn. The inside of the shell is inspected to ascertain that it has not been damaged. In the last stage the shell is filled with concrete.

Raymond standard-type piles are made in lengths of 15 to 37 ft. For greater lengths, up to 100 ft, a heavier type, the so-called step-tapered
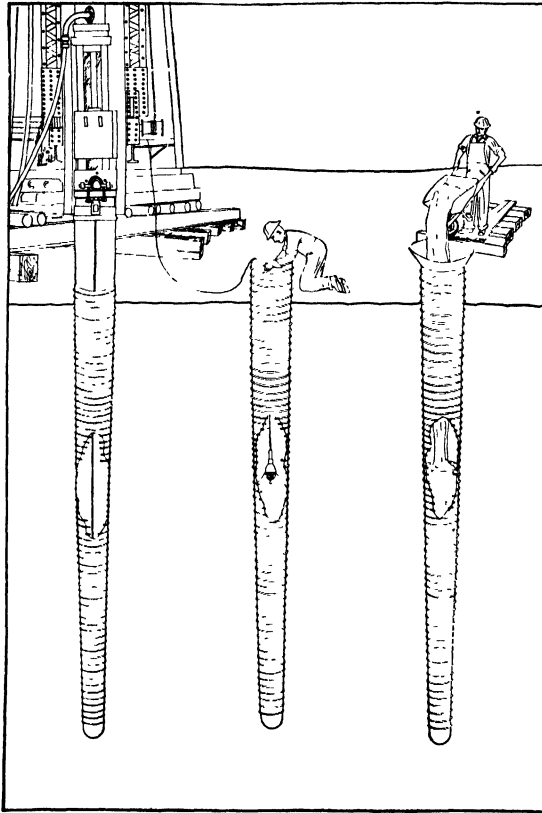
FIG. 15-10. Steps in the construction of a standard Raymond concrete pile. Old type of pile driver on skid rollers. (*Courtesy of Raymond Concrete Pile Co.*)

Raymond pile is employed. Figure 15-11 illustrates a Raymond pile of the composite type, which permits some economy of steel. The lower part of the pile is made of timber. Naturally, this part of the pile must remain permanently submerged. The upper part is of the step-tapered type. Both parts are driven simultaneously.

For other types of situ-cast piles see Ref. 75. Depending on their nature, on the soil conditions encountered, and on the provisions of local
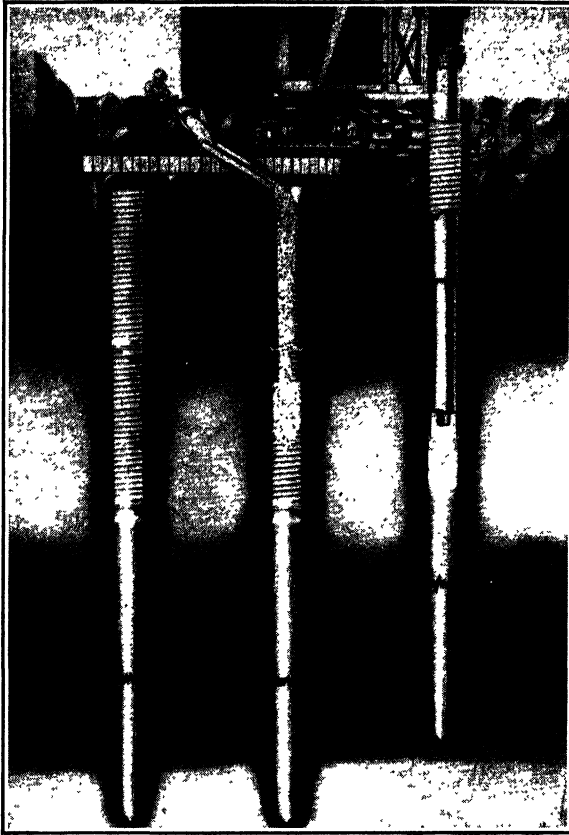
FIG. 15-11. Steps in the construction of a composite concrete and timber Raymond pile. Modern type of pile driver on caterpillar tracks. (*Courtesy of Raymond Concrete Pile Co.*)

building codes, situ-cast concrete piles may be assigned loads varying from 30 to 60 tons per pile.

15-8. Design of Pile-capping Beams. The procedures for the determination of the depth and the steel reinforcement of pile-foundation footings under concentrated column loads can be found in any textbook on reinforced-concrete design, for instance, in Ref. 111. Some special points, however, should be considered when designing continuous pile-capping beams under masonry walls of buildings.

In plan, as shown in Fig. 15-12, the piles should be staggered somewhat, in order to improve their resistance to any lateral loads that may be transmitted by the wall. The capping beams are designed as continuous girders, but in the case of solid masonry walls, they do not have to resist the weight of the entire height of the masonry above a span, which can be

taken as extending from center to center of the adjoining piles. The masonry wall, as a rule, would itself be in a position to span the distance between two adjoining piles, or even greater lengths. Therefore, if no windows or other openings occur over the span, it is usually sufficient to design the capping beams to support the load of a triangle of masonry *ABC*, as shown in Fig. 15-12, which is formed by intersecting lines inclined at an angle of 30° with the vertical. Greater loads should be taken into account, however, if the continuity of the masonry wall is broken by openings, so that its beam action is impaired. The concrete capping
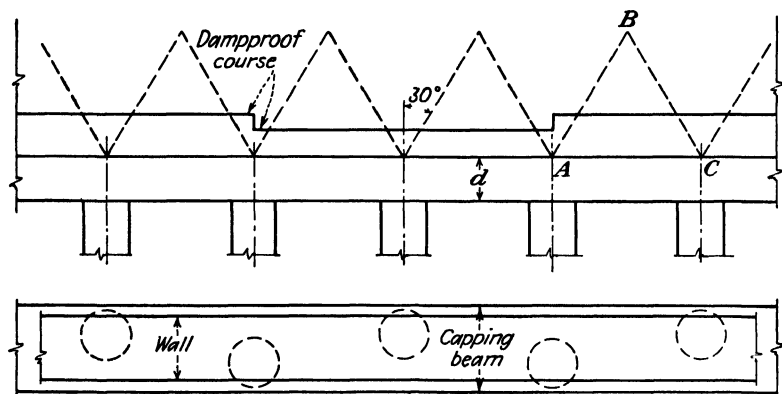
FIG. 15-12. Sketch illustrating discussion of the design of a pile-capping beam and of the measures to ensure proper interaction between the capping beam and the wall above it.

beams should have continuous equal top and bottom reinforcement; diagonal tension can be best taken care of by stirrups.

If the pile foundation is of a floating type, that is, if the piles are supported by friction in cohesive types of soil, it is advisable to ensure the monolithic action of the pile-capping beams and of the masonry above it in order to span the settlement crater. To that end, sliding along any dampproof courses should be prevented if one wishes to avoid damages to a structure of the type illustrated by Fig. 13-11 and discussed in Art. 13-3. This can be done by staggering the elevation of the dampproof course, as shown in Fig. 15-12, since this would key the masonry above the dampproof course to the one below it. The entire masonry wall would then act as one gigantic composite beam, with the concrete capping beam providing its tensile reinforcement.

15-9. Steel Piles and Drilled-in Caissons. One of the most frequently used types of steel piles is made of heavy wide-flanged I beams. Such piles are usually referred to as *H-beam piles*. For available sections, see Steel Handbook (Ref. 7). The H piles have been in use since 1908, according to Ref. 29. They have been picked up and driven in single

pieces exceeding 200 ft in length. As compared with precast reinforced-concrete piles, they have the advantage of being easier to handle on a job. They do not have to be of an exactly predetermined length before driving, since an excess length can be quickly cut off by a torch or an extra length added by welding. Depending on the section used, under favorable soil conditions H piles can be assigned *maximum* loads not to exceed 48 to 120 tons per end-bearing pile, or 48 to 70 tons per friction pile (Ref. 29). When the H piles are embedded in the ground, as a rule, there is no danger of progressive rusting and deterioration of the steel, unless the soil is pervious, and a current of water through its voids continuously brings fresh deleterious solutions into contact with the skin of the pile. The unprotected portions of the pile exposed to free air or water may or may not be endangered by rusting, depending on local conditions (see steel sheet piles, Art. 15-11). Protection at the water line by a concrete cover may become necessary.

Some engineers are apt to question the performance of end-bearing H piles driven down to hard rock, since the rock surface may be uneven. It appears possible that an H pile may rest on rock only at its edge and, as a result, may be subjected to appreciable bending stresses at its tip, where this condition may not be detected from the soil surface without a load test. Excavations have occasionally revealed that H piles could be overdriven and split when the edge of a pile hit the edge of a boulder.

The steel-pipe piles do not have the above disadvantages, since they can be inspected along their entire length prior to concreting in very much the same way as is shown in Fig. 15-10 for a Raymond concrete pile. However, the steel shell is made of sufficient thickness to permit its driving without a temporary stiffening inner core; this increases the cost of such piles. Pipe piles can be driven either closed-end or open-end. A conical steel point is welded to the tip of the *closed-end* pipes. The resulting connection is so rugged that piles of this kind can be driven through many feet of rock riprap and underlying materials which are sometimes found over soft clay at the edge of rivers or lakes where the riprap was dumped from past rock excavations in the vicinity, creating a difficult foundation problem for later construction. The steel point centers the reaction to the pile load when bedrock is reached. Closed-end pipe piles displace an amount of soil equal to their volume and therefore should not be used under conditions where this may be harmful (see Figs. 15-1 and 13-16, and discussions thereof). *Open-end* pipe piles should then be used; they are driven in a few feet at a time and the soil within the pipe is cleaned out before driving is resumed. This slows down the work and makes it more expensive than driving piles closed-end. The removal of the soil from an open-end pipe can best be done by washing, in the

same manner as in the case of borehole casings (Art. 12-6). This is not always possible in cities, since it is usually forbidden to discharge such soil-laden water into sewers, where the silt and clay particles might settle out and clog the sewers. Compressed air may then be used to blow the soil out of the pipe. An air jet pipe is driven a few feet into the soil within the pipe and a few inches of water are poured over the top of the soil. Maximum pressure is built up in the compressor tank and is suddenly released. The resulting blast of air shoots the soil out of the pipe (see H. T. Immerman, Ref. 182, 1943).

FIG. 15-13. Drilled-in caisson for heavy column loads; connection to ground floor of building. (From *Charles B. Spencer, Ref.* 321, 1941.)

End-bearing pipe piles on rock with a wall thickness of ½ in. and a diameter of 20 in. have been allowed to carry up to 150 tons per pile.

The usual seamless type of pipe employed for piling work in the United States can be obtained in Europe only with difficulty. Sheet piles of the Larsen type, similar to the American DP-1 and DP-2 sections (Fig. 15-15), welded longitudinally in pairs and provided with a welded-on point, have been successfully employed instead in Stockholm Harbor, according to a communication from Dr. Paul Leimdoerfer to the author.

A combination of a large steel-pipe pile with an inner steel H-pile reinforcement has been developed in the United States for heavy concentrated column loads (Fig. 15-13) and is known under the name of *drilled-in caissons* (see Charles B. Spencer, Ref. 321, 1941 and Robert E. White, Ref. 430, 1943). A 30-in.-diameter and ½-in.-thick caisson shell is driven down to rock through sometimes as much as 100 ft of clays and sands. A heavy star drill is then repeatedly dropped onto the rock surface in the caisson until a socket 5 to 9 ft deep is formed within it. The caisson shell can then be driven in a little further to form a watertight

seal with the rock. It is usually possible to bail all the water out from the caisson and to lower an engineer in a bosun's chair into the caisson to inspect the nature of the rock. After the H-pile core is lowered into the caisson, the whole is concreted. When bailing of the water is not possible, tremie concreting has to be resorted to (Art. 14-10). Because of the drilled-in socket in the rock, part of the caisson load is distributed through the sides of the socket to a much greater rock area than would be the case if the caisson merely rested on the rock surface. Very high loads, varying on different jobs from 220 to 1,420 tons per caisson, have therefore been used in actual construction.

15-10. The Selection of a Suitable Type of Pile. No single type of pile can be best suited to meet all of the great variety of conditions likely to be encountered in foundation work. It has been shown by the preceding articles that each type of pile has its merits and its disadvantages. Frequently more than one type of pile may meet the technical requirements of a given job. The availability of material at the given time and place and its cost will prove the deciding factor.

The types of piles which provide the greatest safety against improper execution and which permit constant good inspection and control on the job usually cost more than less foolproof types. As a rule, they also require a larger amount of steel. This circumstance is of no particular importance in peacetime in a country like the United States which produces large quantities of steel; but it may prove prohibitive for such pile types in countries which find it difficult to import all the steel they need, even for more essential items. Local engineers are then compelled to sacrifice some of the safeguards against improper execution in favor of economic expediency, especially when the local soil conditions permit doing so without much risk. For instance, the city of Cairo in the Nile Delta of Egypt has many reinforced-concrete buildings up to 10 to 14 stories high; practically all of the pile foundations are of the situ-cast type, Simplex, Franki, Vibro, and other similar systems (Art. 15-7). On the whole, they have a satisfactory record of performance, although none of them use permanent outer protective steel casings, as are required for situ-cast piles by the building codes of New York and of many other cities in the United States. Thus a great number of factors may influence the choice of pile types, including the general economic structure and the past engineering experiences and tradition of a given country.

15-11. Sheet Piling. As their name implies, piles of this type are driven very closely next to each other so that they form a continuous wall or *sheet*. The purpose of such a wall of sheet piling may be either to cut off the flow of water through the soil or to keep the water and the soil out of an excavation which requires vertical cuts too deep to stand without

support. Sheet piles may be made of steel, of reinforced concrete, or of wood. Steel sheet piles will be discussed first. Figure 15-14 shows a few typical sections and Table 15-1 some of the more essential properties of some of these.

TABLE 15-1. Essential Properties of Some American Steel Sheet Piles

Section No.		Area, in.²	Width, in.	Weight, lb per ft² of wall	Section modulus, in.³ per linear ft of wall	Interlock* strength, lb per in.
U.S. Steel	Bethlehem Steel					
MZ 38	ZP-38	16.77	18	38.0	46.8	8,000
MZ 32	ZP-32	16.47	21	32.0	38.3	8,000
MZ 27		11.91	18	27.0	30.2	8,000
MZ 22		11.86	22	22.0	19.0	8,000
M 110	DP-1	12.56	16	32.0	15.3	8,000
M 116	DP-2	10.59	16	27.0	10.7	8,000
M 115	AP-3	10.59	19⅝	22.0	5.4	8,000
M 112	SP-4	8.99	16	23.0	2.4	12,000
M 113	SP-5	10.98	16	28.0	2.5	12,000
	SP-6a	10.29	15	28.0	2.4	16,000
	SP-7a	11.76	15	32.0	2.4	16,000
M 117	AP-8	11.41	15	31.0	7.1	10,000
	SP-9	4.38	8½	21.0	1.4	8,000

* See catalogues of respective companies for additional information.

When steel sheet piles have to resist lateral pressures of water or of soil by serving as vertical beams supported by wales and struts (see Figs. 14-11 and 16-13), their resistance to bending, as governed by their section modulus, is of paramount importance. Sheet piles with deep webs, for instance, the ZP or the DP types shown in Fig. 15-14, are then employed. The DP or the U sheet-pile type is the older type and corresponds to the one known under the name of *Larssen* sheet piles in Europe. It will be noted that the interlocks of this type of sheet pile coincide with the neutral axis of the wall. It will also be recalled from conventional mechanics of materials that shearing stresses reach their maximum value at the neutral axis of a beam. Therefore the DP type of sheet piles does not permit the full utilization of the entire depth of the wall section and acts in a manner similar to the way rectangular beams act when they are laid on top of each other. Unless sliding at the plane of contact of the two beams is prevented, the section modulus of the system will equal only the sum of the section moduli of the two beams, that is $2bh^2/6 = bh^2/3$. However, if sliding along the plane of contact is prevented by rivets or by other measures, the two beams will act as one

beam of the height $2h$ which will have a two times greater section modulus, namely $b(2h)^2/6 = 2bh^2/3$.

Therefore the efficiency of the *DP* type of piling, that is, the ratio of the section modulus per foot width of wall to its weight per square foot of wall, is quite low, as indicated by the line connecting points marked by
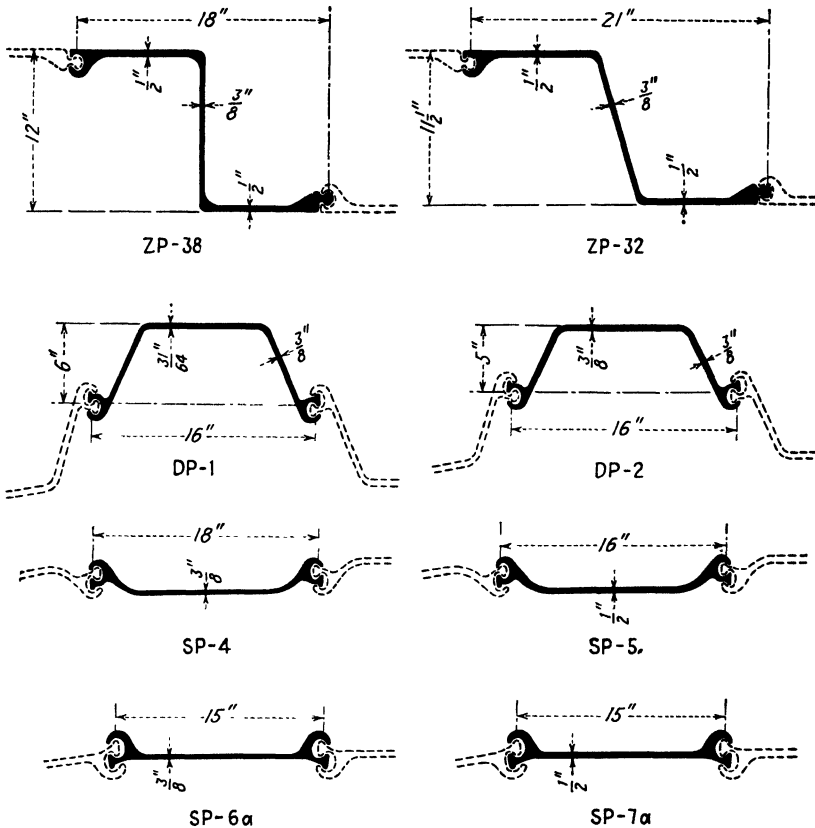
FIG. 15-14. Some types and dimensions of American steel sheet piles. (*From catalogue of the Bethlehem Steel Co.*)

crosses in Fig. 15-15. It can be doubled, as shown by the line connecting points marked by crosses within circles, if sliding at the interlocks is prevented. This has sometimes been done with the tightly fitting interlocks of some European sheet piles. After rolling they were pressed together in pairs all along their length to form what was essentially a large Z pile. To avoid a cumulative twisting effect peculiar to all unsymmetrical sections, ten such "left-handed" double U-sheet piles were followed by a single U pile and then by ten "right-handed" double U-sheet

piles. But, even so, their efficiency is lower than that of the European types of Z piles, for instance, the Krupp piles, marked by the letter *K* in Fig. 15-15, or the United States sheet piles, marked by the symbols ZP or MZ in Fig. 15-15. The twisting effect of Z piles is canceled by the action of each pair of such piles. For other points related to the selection of steel sheet piles see Leimdorfer (Ref. 212, 1949).

The shallow webbed steel sheet-pile sections, such as the SP sections of Fig. 15-14, are useful mainly when they have to resist interlock tension
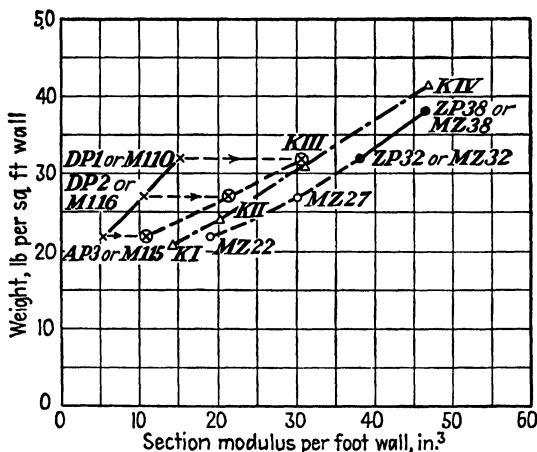
FIG. 15-15. Efficiency comparison of some types of steel sheet piling. (From Tschebotarioff, Ref. 397, 1949.)

(horizontal) with little or no bending in a vertical direction, as would be the case with the sheeting of cellular cofferdams (see Fig. 16-37).

The corrosion of steel sheet piles varies with the locality. It develops most easily in the "spray zone" above the lowest water level, where drying alternates with wetting. In England the loss of thickness in sheet piles has been found to average 0.003 in. per year in sea water and 0.002 in. per year in fresh water. These figures may vary considerably elsewhere. In some places where the sandblast action of dune sand combines with the corrosive action of salt water, much more rapid deterioration has been observed.

Underground and underwater corrosion of metals induces an electric current. It has been found that corrosion can be prevented in such cases by generating an external current of greater intensity and opposite direction to the corrosion current. This procedure is known as *cathodic protection.**

* See "The Cathodic Protection of Steel Piling in Sea Water," by H. A. Humble, *Corrosion*, September, 1949.

Table 15-2 gives the properties of some lightweight corrugated steel sheeting which can be used for shallow excavation trenches and similar purposes. There is also a noninterlocking type of such sheeting which is somewhat lighter.

TABLE 15-2. Properties of Lightweight ARMCO Corrugated Steel Sheeting (Interlocking)

Type		Weight, lb per ft² of wall	Section modulus, in.³ per linear ft of wall
Gage	In.		
8	0.1719	11.7	1.28
10	0.1406	9.7	1.04
12	0.1094	7.5	0.82

Both timber and reinforced-concrete sheet piles cannot be satisfactorily designed to resist any appreciable interlock tension and have to act as separate vertical beams. For that reason they are unsuited for use in cellular cofferdams (Fig. 16-37) and in similar structures. It is always a problem to ensure close contact between adjoining timber or concrete sheet piles. At the soil surface the leads of the pile driver guide
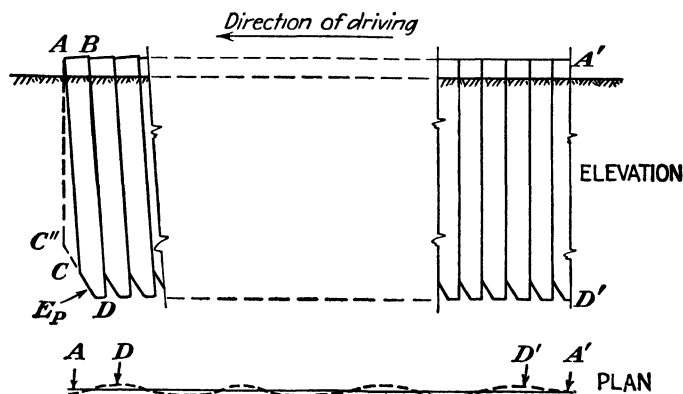
FIG. 15-16. Sketch illustrating causes of some of the difficulties encountered when driving long, continuous walls of sheeting, especially when timber or reinforced-concrete sheet piles are used.

the individual piles; below the surface this can be somewhat facilitated by tapering off one side of each pile, as shown in Fig. 15-16, so that the passive earth pressure E_p would press each successive pile against the ones previously driven. This method is not always effective. The piles are provided with tongues and grooves, and, in the case of reinforced-concrete sheet piles, the grooves are usually grouted later with cement in situ

(see Fig. 16-31). The discussion of that diagram in Art. 16-15, however, shows that special precautions are often necessary to prevent escape of submerged sand through gaps which may have been left between the individual sheet piles.

A special problem arises when driving long continuous walls of sheet piling. As shown in Fig. 15-16, the top of the wall can be made to form a straight line at the soil surface by proper guiding of the individual piles there. However, all types of sheet piles inevitably deviate somewhat from a vertical plane as they are driven and encounter small stones or other obstacles which deflect them from their original direction. Excavations frequently indicate that the lower portion of a sheet-pile wall follows an undulating line, as shown in plan by the broken line DD' in Fig. 15-16. Since a straight line $A'B$ between two points is shorter than an undulating line $D'D$, the lower edge D of a pile does not reach a vertical line through its upper edge B, and after a while the piles begin to get more and more inclined, as shown by the pile $ABCD$ in Fig. 15-16. The insertion of a specially made trapezoidal sheet pile $ABC''D$ may then become necessary to permit further driving. When sheet piling is to form a closed circuit it is advisable not to drive the first piles all the way, but to embed them partially in the ground and then drive the successive piles in the same manner, until closure between the first and the last pile has been obtained. Then the driving can be resumed and completed in the same sequence in one or more stages.

15-12. Small Caissons or Wells for Land Piers. Steel sheet piling can be used to form small caissons under conditions similar to those illustrated by Fig. 15-17, that is, when the sheeting can reach down to rock and thereby cut off flow of water toward the later excavation without any or much pumping being necessary. A caisson of this kind is essentially a small cofferdam (Art. 16-17), but only light bracing and shallow-web steel sheet piling was needed in the case of Fig. 15-17, mainly because of the small dimensions and depth of the caisson.

Figure 15-18 illustrates two other types of light caissons or wells which are used in clay soils. The *Chicago caisson* is used in clays of at least medium stiffness, so that the wall of the cylindrical excavation shaft will stand up vertically to a distance L, which is usually made equal to 5 or 6 ft. The caisson is made of sufficient width to permit a man to work in it. The walls of the shaft section are then lined with vertical planks, a few inches shorter than L, and are supported laterally by two pairs of steel half rings wedged apart and thus pressed against the timber lining. In this manner the caisson can be carried down step by step to hardpan or to rock. Some *loss of ground* is bound to occur, that is, more clay is taken out than originally occupied the volume of the excavated shaft. This is
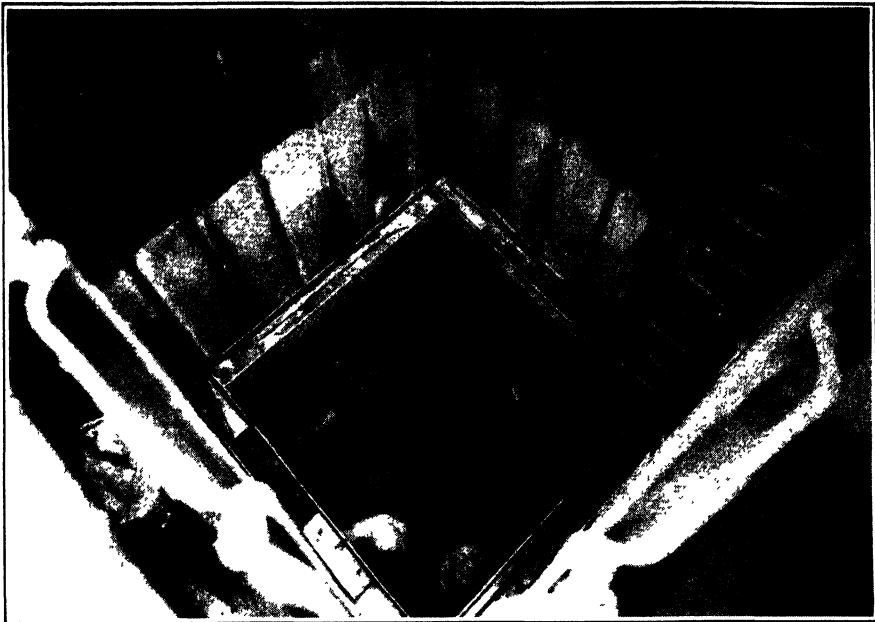
FIG. 15-17. Looking down into excavation for a pier within a caisson formed by steel sheet piling driven down to rock. (*Courtesy of Spencer, White and Prentis, Inc.*)
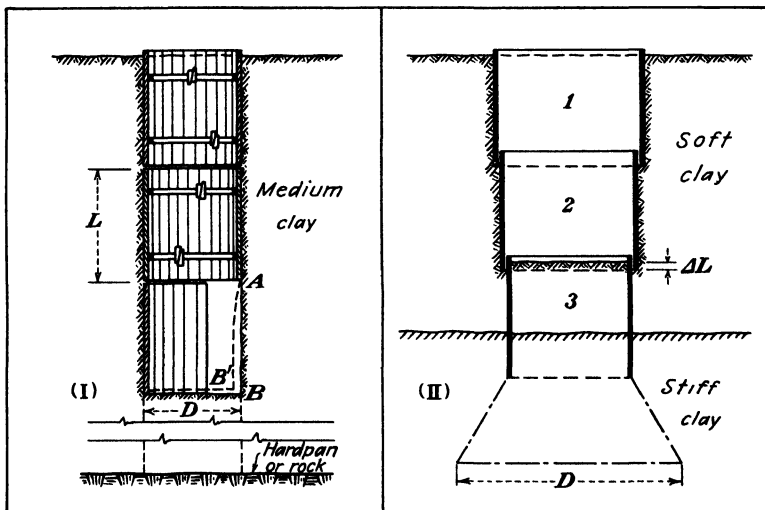
FIG. 15-18. Construction procedures. (I) Chicago-type caisson through medium clay to hardpan. (II) Gow-type caisson through soft clay, belled out in stiff clay.

caused during excavation by some squeezing of the clay toward the as yet unbraced shaft, as shown by the broken line AB' in Fig. 15-18(I). This may lead to some surface settlements (compare with Fig. 16-45 and discussion thereof).

In softer types of clay the loss of ground may become too large for the safety of adjoining structures, and in very soft clays the unbraced shaft section may close entirely. A different construction procedure is then employed, as shown in Fig. 15-18(II). It is known as the *Gow or Boston type of caisson.* Short but wide sections of steel cylinders are driven into the soft clay and are excavated to within a distance ΔL of the lower edge of the cylinder. The distance ΔL depends on the stiffness of the clay and
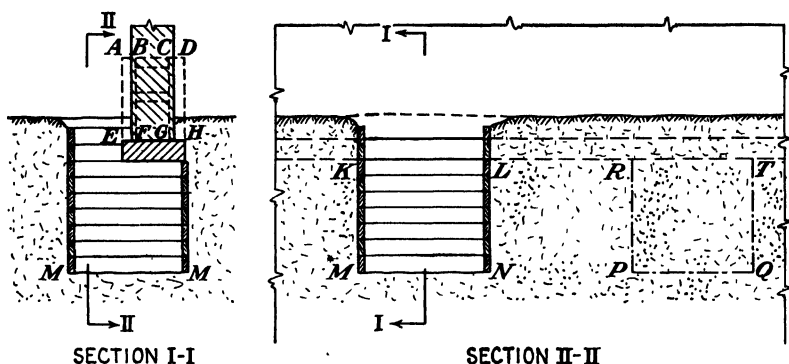
FIG. 15-19. Sketch illustrating discussion of underpinning procedures (see Fig. 15-21) and the box-sheeting of pits in sand.

has to be made sufficiently large to prevent excessive amounts thereof from being squeezed up into the steel cylinder. Another cylinder section, of a slightly smaller diameter than the preceding one, is then lowered into the shaft and driven down. A telescopic shaft is thereby obtained. When a stiffer, non-water-bearing stratum is reached, the base of the caisson can be *belled out,* that is, increased conically by hand excavation, or *underreamed* to give a larger diameter D of horizontal contact area with the soil.

The procedure illustrated by Fig. 15-19 is used in digging pits through moist clean sand, close to the soil surface. Such sand usually will not stand up vertically for more than a few inches. Horizontal wooden planks are then placed and nailed to form a box, which is frequently sufficiently strong to resist the lateral pressures of the sand around the shaft (Art. 10-16) without any additional bracing. Spaces are left between successive planks to permit packing with soil of the spaces between the planks and the natural ground (see Fig. 15-20 and Ref. 276). After packing is completed, a few tufts of hay stuck into the openings, will be sufficient to prevent the driest of sands from running out.

15-13. Underpinning. It is sometimes necessary to carry an existing foundation to a greater depth, for instance, when a deeper basement (Fig. 13-16) or a subway (Fig. 15-20) is dug nearby. The process is known as *underpinning.* Either piers or piles may be used for this purpose.

In both cases a series of pits are dug under the old foundation. A new pit is not dug until the underpinning of an already excavated

FIG. 15-20. Subway excavation showing concrete underpinning piers for columns of old adjoining building. (*Courtesy of Spencer, White and Prentis, Inc.*)

adjoining pit is completed. Usually the existing footing and the wall above it are sufficiently strong to span at first the width of the underpinning pit while it is dug, and later the distance from pier to pier. If not, the wall can be strengthened, as shown by broken lines in Fig. 15-19, section I-I, by casting reinforced-concrete beams *ABEF* and *CDGH* on both sides of the wall and tying them together through openings in the wall.

Figure 15-20 illustrates one of the underpinning jobs during the construction of the Sixth Avenue Subway in New York. Three- by 4-ft open pits, 10 ft on centers, were sunk under the buildings to the top of rock, in

a manner somewhat similar to that shown in Fig. 15-19. Before the pits were concreted, vertical steel angles were installed at their outer corners. These angles were utilized later to support the horizontal timber sheeting of the subway excavation (see Fig. 15-20). The building loads were transferred from the old footings to the concreted underpinning pits by means of steel struts and wedges.

As the subway excavation progressed, steel struts 10 ft on centers braced the cut. The struts were prestressed by means of steel plates and wedges. A steel waler was used on the upper set of struts to act as a horizontal stabilizing element. A 4-in.-thick concrete *sand wall* was
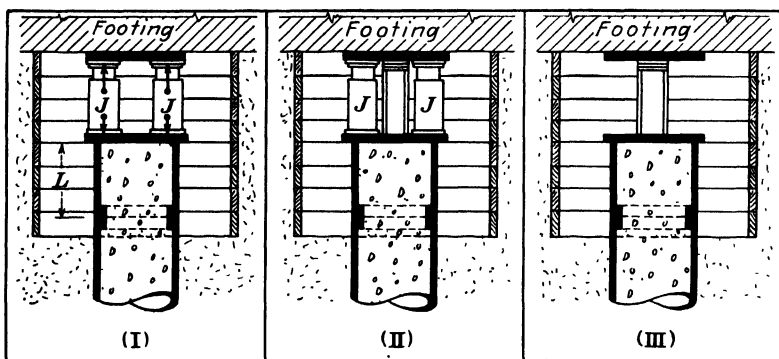
FIG. 15-21. The ***pretest*** **method (patented) of wedging underpinning piles.** ***(After Prentis and White, Ref. 276, 1950.)***

poured later right against the horizontal sheeting and against the concrete underpinning piers. The horizontal sheets remained in place and were never removed. The purpose of the sand wall is to provide protection to the subway waterproofing and to permit placing it against a smooth surface. The so-called *three-ply-membrane type of waterproofing* was used, a coat of hot asphalt alternated three times with a coat of impregnated linen fabric. The walls of the subway were then concreted against the waterproofing membrane.

When rock is at a considerable depth, underpinning piles have to be used instead of piers. In order to prevent later unequal settlements of the underpinned building, especially if the new piles reach only to sand or gravel, it is often essential to *pretest* each pile to the full load that it will have to carry. First a shallow pit is dug under the old footing, as shown in Fig. 15-19. Then a steel-pipe pile is pressed open-end in short sections of length L down into the soil by means of jacks supported by the old footing. Each length of pipe L is mucked out by means of specially designed tools, for instance, by the orange-peel bucket, which is similar in operation to the clamshell bucket, but has four moving sections, instead

of two. When the underpinning pile reaches the desired elevation it is filled with concrete, which is allowed to harden. The pile is capped with a steel plate, and another steel plate is placed and grouted against the old footing. Two hydraulic jacks are then inserted between the two plates, as shown in Fig. 15-21(I). The jacks apply to the pile the part of the building load which the pile will have to carry later. The load is maintained for a short while until all settlement of the pile ceases (see Prob. 15-6). A steel strut is then wedged in between the pile and the old footing. As shown in Fig. 15-21(II), this should be done *before* the jacks are removed, since otherwise the pile will rebound, as shown by line *CD* for pile I in Fig. 15-3, and settle again when reloaded (dotted line *DE* in Fig. 15-3). After removal of the jacks [Fig. 15-21(III)] and completion of the pretesting of the other piles the excavation pit can be concreted. In this manner it is possible to transfer the entire load of a heavy structure to a new foundation without any measurable settlement. For further details see Prentis and White (Ref. 276).

15-14. Bridge Foundations. Compressed-air and Open Caissons. The piers of a bridge in deep water often have to be carried down through a greater depth of soil than is the case with land piers (see Fig. 15-22). The land-side bridge spans are comparatively short, and the pier loads are therefore small. The danger of scour in rivers is also smaller there, since the velocity of the flowing water is smaller at shallow depths than in the main river channel. For that reason the land-side piers can usually be built within sheet-pile cofferdams of the type illustrated by Figs. 14-11 and 16-35(I), where piles are sometimes driven within the cofferdam excavation when it is necessary to extend the depth of the foundation still further.

For the deep-water piers large caissons have to be used. There are two main types, the *compressed-air caissons* (Fig. 15-23) and the *open caissons* (Fig. 15-24). Special problems are presented by the flotation of a caisson until it comes to rest on the soil and by the later excavation of the soil below the caisson so as to sink it to the desired elevation. A great variety of procedures have been developed to that end, only a few of which will now be outlined.

The oldest procedure consisted in building up the caisson right over its final location on a platform which was suspended on steel rods either from a temporary pile trestle or from anchored barges. As the caisson was built up, the platform was lowered by means of the suspension rods. Compressed-air locks were built into the shafts left for this purpose in the caisson, and compressed air could be used to decrease the load on the suspension rods after the caisson platform was lowered below water level. Timber and masonry were used in past construction of caissons, but in

modern work they have been replaced to a large extent by steel and reinforced-concrete cellular construction. It is now customary to build the cutting edge of the caisson on shore, to float it out to its location, to
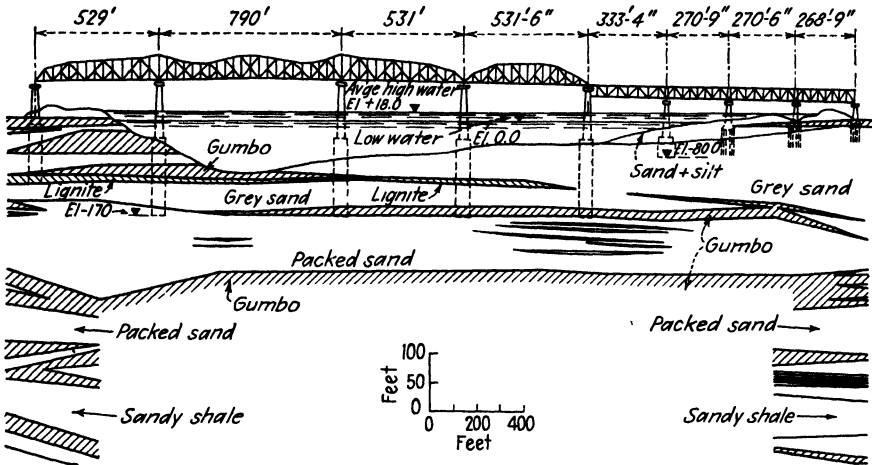
FIG. 15-22. The geological profile, Mississippi River bridge, New Orleans, Louisiana. (From Carlton S. Proctor, Ref. 278, 1938.)
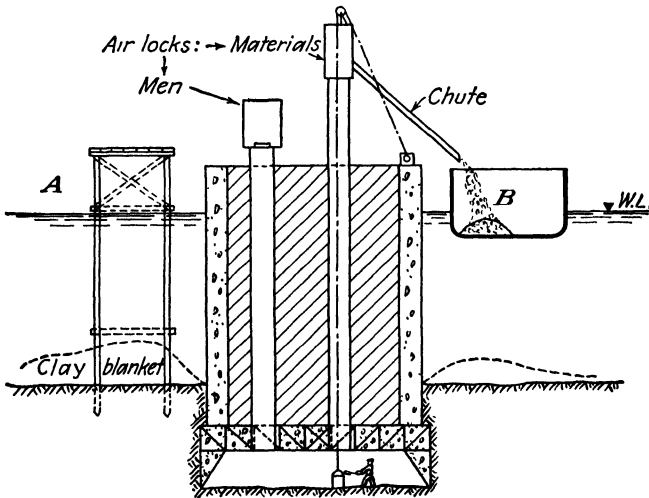
FIG. 15-23. Sketch illustrating operation of a compressed-air caisson.

anchor it there, and to build it up, as shown in Fig. 15-24, until it reaches soil firm enough to support its dead weight.

Several methods have been in use to keep the caisson afloat up to that point. The false-bottom method consisted in providing a temporary timber bottom for each of the caisson cells, which could then be kept

partially pumped out to float the caisson until it came to rest on firm soil. The false bottom was then removed to permit further excavation within each cell. This was not always easy, since the timbers swelled and jammed under high uplift pressures to such an extent that sometimes they had to be hammered out piece by piece by means of long H piles. The false-bottom method is therefore suitable for shallow depths only.

The greatest depth of water through which a caisson of any kind has been floated is 120 ft [see Carlton S. Proctors' (Refs. 277 and 278, 1936) description of the sinking of the *Moran caisson* for one of the piers of
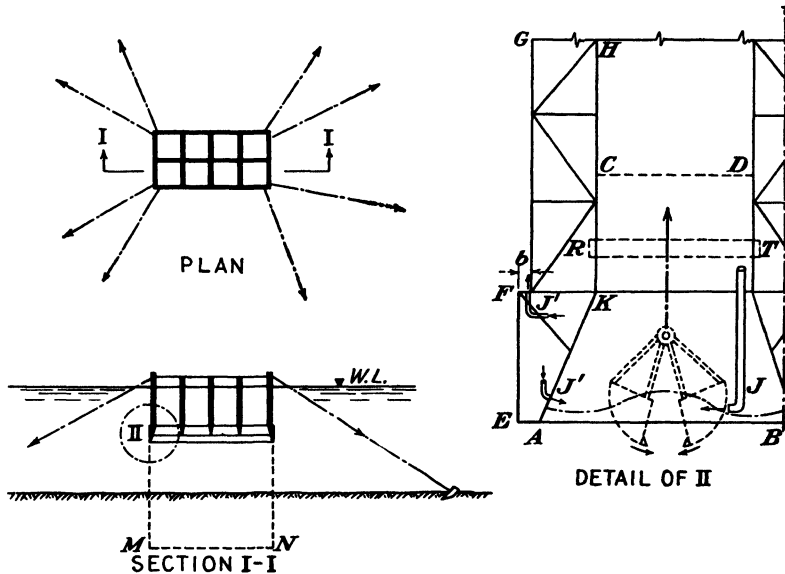
FIG. 15-24. Sketch illustrating methods of flotation and excavation of open caissons for bridge piers.

the San Francisco–Oakland Bay Bridge]. Compressed air was used to provide its flotation. Each cell of the caisson was of a cylindrical shape, was steel-lined, and was provided with a steel half dome. Compressed air could be applied within each cell to press the water level in it down to the desired elevation. Only part of the cells had to be put under air pressure in order to provide flotation; the remaining cells could be extended upward, provided with half domes, and, in turn, put under air pressure. The half domes could then be cut off by torches from the cells which had provided flotation up to that time, and their upward extension could be undertaken. The process of staggered extension of the cells was continued until the caisson reached firm ground. Then all the half domes were removed, and underwater excavation was started in each cell. That caisson was sunk to a total depth of 240 ft.

In some bridge caissons the walls of the individual cells, that is, the space marked *GHFKEA* in Fig. 15-24, are made hollow for purposes of flotation. Temporary platforms on timber piles or on barges are still often employed to provide auxiliary surfaces for construction equipment for all modern types of caissons, as shown in Fig. 15-23, and sometimes for their anchorage, but only seldom for purposes of flotation.

In very rapidly flowing water the type of flotation and of anchorage shown in Fig. 15-24 is not always possible. The so-called *sand-island* method has been employed in some such cases, for instance, for the caissons of the Mississippi River bridge at New Orleans, shown in Fig. 15-22, and for the caissons of a later bridge of the same type at Baton Rouge (Ref. 127). A 110-ft-diameter steel cylinder was lowered to the river

TABLE 15-3. Excerpt from Rules Regulating Work under Compressed Air*

Maximum gage pressure, lb	Corresponding head of water, ft	Time per shift, hr	Total time, hr	Rest interval, hr	Time of decompression, min
18	41	4	8	0.5	9
26	60	3	6	1	18
33	76	2	4	2	33
43	99	1	2	4	43
50	115	0.5	1	6	50

* Ref. 206.

bottom from a temporary platform supported by timber piles onto board mattresses and was then filled with sand, forming a huge cell or a small island, on the surface of which the cutting edge of the reinforced-concrete open caisson could be cast in the dry, and the caisson then gradually built up and sunk by dredging the cells down through the sand of the island and the underlying soil. Later the island could be removed.

Excavation under compressed air, as shown in Fig. 15-23, is now seldom employed. The reasons for this will become apparent from an examination of Table 15-3. Under air pressure corresponding to 115 ft of water head a workman working for only one hour would have to be paid for a full day. No human work is at all physically possible under any appreciably higher pressures. However, it should be noted that the heads of water indicated in Table 15-3 as corresponding to certain values of gage pressure in the caisson working chamber apply only to work in pervious sandy soils. In such cases clay blankets may even be necessary around the caisson, as shown in Fig. 15-23, to prevent blowouts or excessive losses of air bubbling up through the voids of sand or gravel. But when working in impervious clay soils, gage pressures smaller than the actual head of

water may be sufficient. For instance, when caisson 1 (see Fig. 12-1) reached a depth of 100 ft below free-water level, a gage pressure of only 18 lb was necessary to permit manual excavation in the working chamber. In clay soils very little water will actually seep through into the working chamber of a caisson, once it has penetrated sufficiently deep into the clay, and that water can be easily pumped away. Even the slightest motion of the water will dissipate part of the hydraulic head along the paths of its flow, which will be somewhat similar to those shown in Fig. 14-11. The air pressure in the working chamber can then be comparatively low, but it should be maintained at a value sufficient to prevent the plastic squeezing of the clay up into the chamber; the problem is somewhat similar to that in open cuts (Art. 14-6). Compressed-air caissons can be very useful under unusually difficult subsoil conditions, such as are illustrated by Fig. 12-1.

Underwater dredging of the individual cells of open caissons by means of clamshell buckets, as shown in Fig. 15-24, is most frequently resorted to. Jet pipes J which may be moved to any desired position are most frequently used to loosen the soil around the cutting edge, as shown in that diagram. Jet pipes and nozzles, J' in Fig. 15-24, may be built into the walls of the caisson for the same purpose and also for the purpose of decreasing friction along the outer skin of the caisson. This friction sometimes becomes so great that the caisson "freezes" and stops moving. This is particularly likely to happen with compressed-air caissons (see Prob. 15-7). An offset just above the cutting-edge frame will help to decrease somewhat the friction along the skin of the caisson above it. Experience indicates that the width b of the offset (Fig. 15-24) should not exceed a few inches; otherwise it does not appear to be effective.

After completed excavation the bottom of each cell of the caisson is sealed by tremie concrete (Art. 14-10). Grooves RT (Fig. 15-24) are left in the walls of each cell during its construction to permit better keying in of the tremie seals. Usually the concrete seal does not fill the entire depth of the cell but extends only up to some line CD, the space above being left filled with water to decrease the pressures on the soil at the base of the caisson. The entire caisson is then capped by a heavy concrete plate above the water level.

The depth to which caissons should reach depends on several considerations. First of all, it should be sufficient to prevent *scour* from undermining the caisson or decreasing the overburden surcharge weight around it to a dangerous extent. The bridge piers and their caissons represent an obstruction to the flow of water, so that the streamlines are crowded closer together near the piers, in a manner similar to that illustrated by Fig. 16-36 for the outer corners of cofferdams. A greater velocity of flow

right next to the skin of the pier will be the result, especially during floods, when some scour of the river bottom may occur because of the increased velocity in the main channel, even when it is not obstructed in any way. Streamlining the caissons and the piers may help to a certain extent, as may various types of protection of the river bottom around the pier, such as heavy stone riprap or mattresses woven of brush, weighted down by rocks and sunk to the river bottom prior to the caisson construction. In spite of such precautions, scour in excess of 20 to 30 ft has been known to occur around some bridge piers in the main channel (see Refs. 327 and 127).

The second consideration is that the caissons should rest on the stiffest layer available, so that this layer could be utilized to distribute the pressures to any weaker underlying layers. In the case of the Mississippi River bridge shown in Fig. 15-22, the caissons rested on the surface of a layer of compact sand, almost 100 ft thick, beneath which was gumbo, a highly colloidal clay. The use of theory for the practical determination of the maximum safe loads on sand layers at that depth is greatly limited by a number of as yet uncertain factors (see Terzaghi, Ref. 362, pp. 133–135, 1943). The loads employed are therefore largely based on the experience of previous successful constructions. They are frequently higher than the ones indicated in Table 14-1. For instance, in the case of the Baton Rouge Mississippi bridge, reported by Erickson (Ref. 127), after deduction of all buoyancy effects, deduction of the weight of excavated soil, and consideration of wind and of all other forces, unit contact pressures up to 10 tons per ft^2 were obtained.

There is a great variety of possible combinations of the different construction procedures outlined in this chapter. For instance, as shown in Fig. 15-25, hollow precast reinforced-concrete (or timber) piles driven underwater from a barge may be capped by a reinforced-concrete caisson which was constructed on land, faced, while floating, with granite ashlar in its upper part, floated out to the site, sunk, and concreted under the use of compressed air. A trench was dredged out prior to the driving of the piles, partly to remove the upper soft mud and partly to provide room for the sand cushion which was needed as a support (see Art. 16-16) for the later rock riprap which was to serve as scour protection.

There are many special types of bridge foundations, for instance, see Bretting (Ref. 39, 1936). Two should be mentioned. The *trestle* type consists of a large number of precast reinforced-concrete or steel piles (timber for a temporary structure) which extend above the water level and are braced to each other in so-called *bents* upon which rest the short beam-type and therefore light, spans of the bridge. Such pile trestles are of particular advantage over long stretches of nonnavigable shallow water,

the flow of which it is not desired to cut off by the fill of an embankment, and on poor underlying foundation material. The bridge load is then distributed over a very large area, so that deep foundations of large spans and their heavy unit loads can be avoided.

Another, but rather unusual, type of permanent structures is the *pontoon* bridge, which is sometimes employed to advantage over long
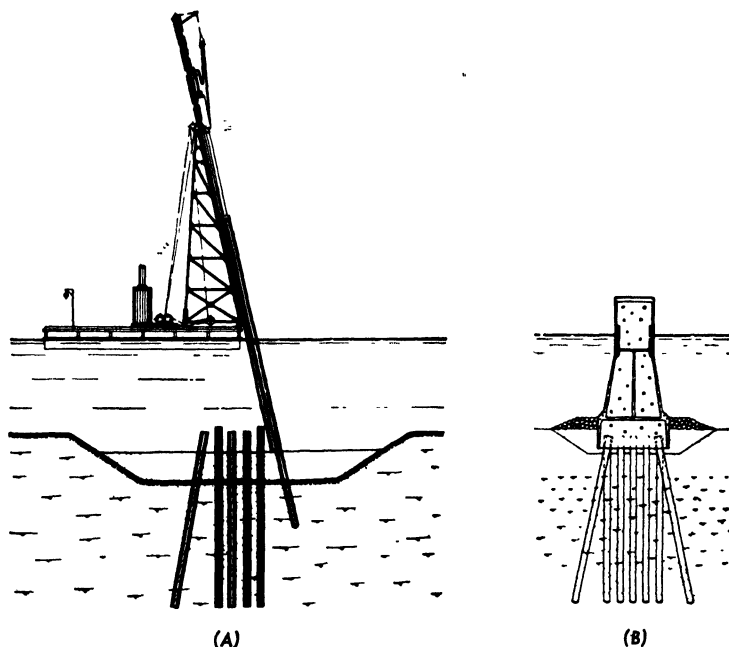
FIG. 15-25. Steps in the construction of a special type of bridge pier in Denmark. (A) Piles are driven by means of a follower. (B) The caisson was floated and sunk over the piles; compressed air was used in the working chamber to permit its concreting in the dry. (*From A. Engelund, Ref.* 117, 1936.)

stretches of relatively deep but calm water underlain to a great depth by poor foundation material. A notable example of such a bridge is that which was built near Seattle (see Charles E. Andrew, Ref. 14, 1939). The cellular reinforced-concrete pontoons were cast in drydocks and were then towed out and anchored at the site; they were connected to each other by specially designed elastic couplings.

Practice Problems

15-1. Pile II in Fig. 15-3 began to show considerable settlement under a load of 70 tons (metric) or 70(2,205/2,000) = 77 U.S. tons. The pile diameter was 50 cm = 1.635 ft. It was 8.5 m = 27.8 ft long. Since the pile was embedded in a stiff clay layer which was underlain by softer clay, its resistance depended almost exclu-

sively upon the shear along its outer surface. Evaluate the magnitude of the unit shear along its skin.

Answer. The area of the cylindrical outer surface of the pile is

$$A = \pi \times 1.635 \times 27.8 = 143 \text{ ft}^2$$

and the shear $s = 77/143 = 0.54$ ton per ft². The corresponding unconfined compressive strength would be $q_u = 2c = 2s = 1.08$ tons per ft². This actually is the approximate value of the lower limit of the strength of samples from this clay formation.

15-2. Compare the reduction in the average unit pressure on a horizontal plane immediately beneath the tips of 30-ft-long and 1.5-ft-diameter (d) frictional piles embedded in clay, which will be caused by the shearing resistance $s = c$ along the outer perimeter of a single pile and of a nine-pile footing, as shown in Fig. 15-26, with that of a 4 times larger footing of 36 piles. The spacing of the piles is $L = 4$ ft on centers.
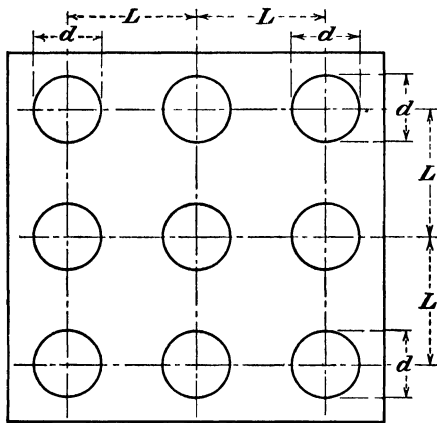
FIG. 15-26. Sketch illustrating Prob. 15-1 on the spacing of piles.

Answer. In the case of a single pile the shearing resistance along the skin surface is $\pi \times 1.5 \times 30 \times c = 143c$; the corresponding base area of the pile is $\pi \times 0.75^2 = 1.76 \text{ ft}^2$; the pressure reduction per square foot of base area is then $143c/1.76 = 80.5c$. In the case of the nine-pile footing shown in Fig. 15-26 the corresponding values will be: $4(4 + 4 + 1.5)30c = 1{,}140c$ for the entire group of nine piles or $126c$ per pile; the average base area per pile will be $9.5^2/9 = 10.0 \text{ ft}^2$ and the pressure reduction will be $12.6c$ per square foot of base area. In the case of the 36-pile footing we obtain

$$4[(5 \times 4.0) + 1.5]30c = 2{,}580c$$

for the entire group of 36 piles, or $72c$ per pile; the corresponding base area is $(21.5)^2/36 = 12.8 \text{ ft}^2$ per pile, and the unit reduction is $72c/12.8 = 5.6c$ per square foot of base area.

It will be noted therefore that the influence of shear along the outside surface of pile groups on the reduction of pressures below the pile points decreases rapidly with the number of piles in a group, especially if the piles are closely spaced. This explains why groups of piles will settle more than a single pile under the same unit load per pile. The increase of the total base area of the pile group at the pile points has the same effect on settlements as an increase in the size of any footing (Art. 9-1) but, in addition, the unit pressures at the elevation of the pile points become larger with an increase in the number of piles.

15-3. Compare the increase in the permissible unit load on a clay soil which is made possible by an excavation with the corresponding effect of a floating pile foundation.

Answer. Let us consider for comparison the case of the 70-ft-wide and 100-ft-long building analyzed in Prob. 14-1. If the clay was of a medium sensitivity with $S = 2.3$, only a load test could determine the loss, if any, in the shearing strength of the clay due to remolding by the driving of the piles. However, if the clay had a low sensi-

tivity, say, $S = 1.2$, then the full value of $s = c = q_u/2 = 0.7/2 = 0.35$ ton per ft² could be used in estimating the decrease of pressure on the plane AB at the pile points (see Fig. 15-4). Let us assume that the pile length is $h' = 25$ ft and that the distance from the soil surface to the points is $h = 30$ ft. Then the total shear which can be developed along the outer surface of the mass of piles under the building will be $[2(100 + 70)25]\ 0.35 = 2{,}980$ tons, and the corresponding average pressure reduction on the plane AB will be $2{,}980/7{,}000 = 0.425$ ton per ft².

With reference to Eq. (9-28) and Fig. 15-4, the ultimate pressure on the plane AB in excess of the weight of the soil above it, plus the total outer perimeter shear or, in other words, the ultimate unit weight of the building, becomes

$$\begin{aligned} p_{max} &= [2.76 \times 0.7(1 + 0.38\,{}^{30}\!/_{70} + 0.44\,{}^{70}\!/_{100})] + 0.425 \\ &= 2.77 + 0.425 = 3.195 \text{ tons per ft}^2 \end{aligned}$$

In a slightly sensitive clay a factor of safety $F_s = 2.5$ could be used (see Table 14-4) but for purposes of comparison with the case of Prob. 14-1(*d*) the value of $F_s = 2.7$ will be maintained. The pressures p_s (see Fig. 15-4) may be neglected to compensate for slight remolding. Accordingly, the permissible unit pressure on the pile foundation will be

$$p_0 = p_{max}/F_s = 3.195/2.7 = 1.18 \text{ tons per ft}^2$$

This value is smaller than the 1.77 tons per ft² obtained by a 15-ft excavation [see Prob. 14-1(*d*)]. It should further be noted that the safe load on a mat 5 ft below the soil surface was $p_0 = 0.97$ ton per ft²; therefore the use of the 25-ft piles permitted an increase in the safe loading of 0.21 ton per ft², whereas the 15-ft excavation permitted an increase of 0.80 ton per ft². Thus the latter procedure is of more advantage when ground-water conditions permit it.

15-4. Examine the nine sketches of different soil conditions given in Fig. 15-27 and state whether the use of piles was justified by the circumstances.
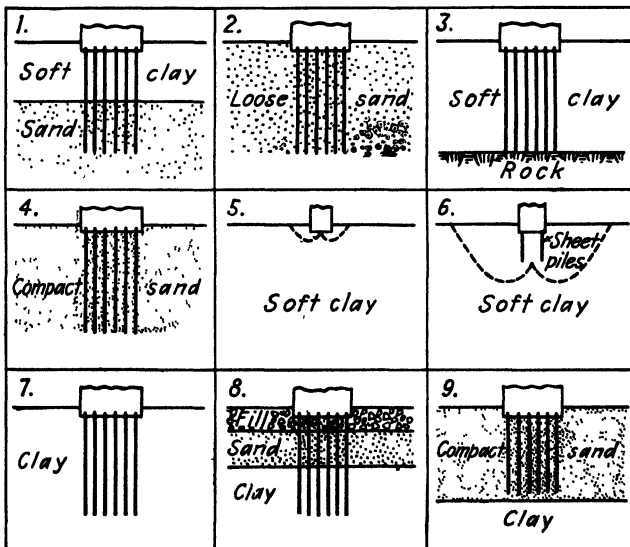
FIG. 15-27. Diagrams illustrating the discussion in Prob. 15-4 of instances of beneficial and detrimental uses of piling. (After W. P. Kimball, Ref. 196, 1939.)

Answer. The use of piles was certainly beneficial in the cases 1, 2, and 3. In case 4 there would have been no need for piles, unless there was danger of later surface scour or erosion of the compact sand, for instance, close to an ocean beach. The piles would then have to be jetted. The use of sheet piles in case 6, as compared with case 5, was slightly beneficial because of the increased area of the possible surface of failure. In case 7 the question cannot be answered without more information on the degree of sensitivity of the clay to remolding. In a sensitive clay, the use of piles would be harmful, in a clay of medium sensitivity indifferent, except for the waste of money, and in a nonsensitive clay somewhat beneficial (compare with Prob. 15-3). The use of piles in the manner shown in Fig. 15-27 for cases 8 and 9 was definitely harmful. The piles should not have been driven that far and allowed to pierce the sand layer. In case 8 they should have been stopped in the upper portion of the sand layer, so that it would assist in distributing the pressures on the underlying clay. This also holds true in case 9, except that there may be no need for piles there at all, unless there is danger of scour (compare with discussion of case 4).

15-5. A certain museum exhibited a model which had been presented to it and which purported to show the proper manner to perform a pile load test. The settlement of the pile was to ba measured to 1/1,000 in. by a dial gage. The point of the gage rested against a metal strap attached to the pile, and the gage itself was supported by a stand which stood on the soil at a distance from the skin of the pipe which, in the original, would equal 4 in. Should you approve this arrangement on a job for which you were responsible?

Answer. No. The soil close to the test pile would also move down, forming a crater around it. Therefore the support of the gage would move down too, and the gage would register only a small fraction of the actual settlement of the pile. The gage should be attached to a horizontal beam on two supports, each of which should be several feet from the skin of the pile (see Ref. 11).

15-6. A small caisson of the type shown in Fig. 15-18 was carried down for underpinning purposes to a layer of very stiff but fully saturated clay. Pretesting of the caisson (see Fig. 15-20) was proposed. What would be your comments?

Answer. There would be not much point in doing this, unless the load on the pretesting jacks were maintained for days, until measurements showed that all downward movement of the caisson had stopped. Pretesting is most efficient in granular soils, where the compression occurs very rapidly.

15-7. A compressed-air caisson for a river pier of a bridge was to have been sunk through clay down to a certain elevation in a sand layer which was fixed by the specifications. Within 5 ft of that goal the caisson, which had already penetrated the sand, "froze," presumably because of the lateral pressures exerted against its skin by the overlying compact clay, which was of a swelling type. Piling all available weight on top of the caisson and jetting along its sides did not help. The contractor appealed for permission to stop the caisson at the elevation reached, but this was denied by the resident supervising engineer. The contractor then ordered all men from the working chamber of the caisson and suddenly released the air pressure. This action was equivalent to removing the uplift of the air pressure from the caisson, which immediately sank down some 7 ft. When air pressure was reapplied, the working chamber was found to be full of sand, which was excavated, whereupon the caisson was concreted. What are your comments concerning this procedure?

Answer. The sudden removal of the air pressure created a momentary quick condition in the sand under the caisson (Arts. 5-4 and 14-9). The increased effective weight of the caisson made it move downward to, and even past, the required elevation,

but, simultaneously, the mass of quick sand rushed upward into the 12-ft-high working chamber of the caisson. The loosening effect of such a movement must have extended into the sand layer to a considerable depth below the final elevation of the bottom of the concrete-filled working chamber. Thus the letter of the specification had been complied with, but a very unsatisfactory final condition of support was created for the completed caisson. It would have been much more sensible to get permission to approve the original request of the contractor, even if it meant having to change the specifications.

References Recommended for Further Study

Pile-driving Handbook, by Robert D. Chellis, Pitman, 276 pp. Description of numerous pile and pile-driver types and much useful practical information.

"Concrete Piles—Design, Manufacture, Driving." Published by the Portland Cement Association, Chicago, 80 pp.

Underpinning, by E. A. Prentis and Lazarus White, Columbia University Press, 2d ed., 1950, 318 pp. Description of many cases of successful underpinning work and of the techniques employed.

"Dynamic Pile Driving Formulas," by A. E. Cummings, *Journal of the Boston Society of Civil Engineers*, January, 1940. Also *Contributions to Soil Mechanics*, Boston Society of Civil Engineers, 1925–40, pp. 392–413. Discussion of the many fallacies and limitations of pile driving formulas.

Foundations of Structures, by Clarence W. Dunham, McGraw-Hill, 1950, Chap. 9, Piles, pp. 283–327; Chap. 10, Pile Foundations, pp. 326–418; Chap. 12, Caissons, pp. 470–509; Chap. 13, Bridge Piers, pp. 510–580; Chap. 14, Bridge Abutments, pp. 587–626. Much useful information for structural designing and detailing.

CHAPTER 16

EARTH-RETAINING STRUCTURES. COFFERDAMS. TUNNELS AND CONDUITS

16-1. General Considerations. It has been shown in Chap. 10 that the so-called *classical* earth pressure theories (Coulomb, Rankine) give results closely corresponding to field observations only in the case of granular backfills of retaining walls capable of tilting outward around their base. This is because these classical theories are based on the assumptions that complete rupture by shear has taken place in the backfill, that the maximum possible value of the shearing strength is simultaneously active along the entire surface of failure, and that the distribution and the magnitude of lateral pressures is not affected by the nature of the deformations of the supporting structure. These assumptions are correct only for the simplest case.

Especially in the case of cuts through plastic clay soils, considerable discrepancies exist between lateral-pressure design values computed from the ultimate strength of the soil and the actual observed pressure values.

The design recommendations of the present chapter will therefore be based primarily on data obtained from measurements and observations of full-scale structures. Other design procedures advanced elsewhere will be given for comparison. Specific values of lateral pressures will be recommended for all cases where sufficient evidence has been accumulated to permit precise numerical recommendations. Otherwise likely limit values will be indicated, together with observation procedures during construction which may narrow down the gap of uncertainty. Lateral pressures in their distribution diagrams will be expressed as fractions of the weight of the overburden γh at each elevation.

16-2. The Design of Backfilled Retaining Walls. The great majority of backfilled retaining walls will tilt slightly outward around their base, as illustrated by Fig. 10-15. A purely horizontal displacement of the type illustrated by Fig. 10-1(III) is an exception. Therefore such retaining walls may be designed for a hydrostatic pressure distribution, as illustrated by Fig. 16-1 for a *gravity retaining wall*. The value of the coeffi-

cient K_A may be taken from Tables 10-1 and 10-2 if the soil is granular and cohesionless. For a horizontal surface of the soil and a vertical wall surface:

Loose sand: $K_A = 0.30$
Dense sand: $K_A = 0.25$

The above value for dense sand holds if the wall will yield slightly during or after compaction of the sand; this seems to be the case in all retaining walls of the gravity type.

If the backfill is composed of clay soil, the pressure distribution will be essentially triangular, as indicated in Fig. 16-1. The magnitude of the lateral pressure, however, may vary within a very wide range, depending on the degree of saturation of the clay, which may vary with the time of the year. In view of the uncertainty attached to this point, some authors, for instance, Terzaghi and Peck (Ref. 365, 1948), recommend designing walls backfilled with clay for lateral pressures corresponding to fluid soil weights ranging from 100 to 120 lb per ft³ so long as no water enters the clay during floods. This is equivalent to assuming that K_A will range between 0.8 and 1.0. Actually, at present, there is no reason to assume that K_A will exceed the value of 0.5 if the clay is fully consolidated, even when it is saturated by receding floods, so long as the clay is not of a strongly swelling type. If the clay is liable to swell, then the swelling pressures which it will exert against a retaining wall may be well in excess of values corresponding to $K_A = 1.0$. As a result the wall may be damaged or will *creep*, that is, it will be pushed slightly outward by the swelling clay during wet seasons. During dry seasons the clay will shrink, but the cracks formed at the surface (Art. 8-2) may be filled by surface debris washed down into them before the new swelling of clay closes the cracks. Thus the full swelling pressures may be again exerted against the wall and will push it out slightly again. This process of outward *creep* may continue for many years. Frost action (Art. 5-7) may have a similar effect.

FIG. 16-1. Assumptions for the design of a gravity retaining wall.

The entire problem of pressures exerted by clay backfills represents a suitable subject for systematic regional research. Until more experi-

mental data become available, walls backfilled with mixtures of sand and clay should be designed, according to Fig. 16-1, for a value of $K_A = 0.5$, which should take care of unfavorable conditions of saturation of the backfill (see Art. 10-17). Weep holes should be provided in the walls or continuous graded gravel drains (Art. 17-7) installed behind the walls to allow for drainage and to prevent the building up of full water pressures against the wall (Art. 10-11). They should be protected from freezing. Gutters should be provided to carry the water away before it seeps into the soil near the wall. The use of clay backfills likely to swell should be avoided. Drainage arrangements illustrated in Fig. 16-2 have been suggested by A. Casagrande (Ref. 333, 1936) to facilitate backfill drain-
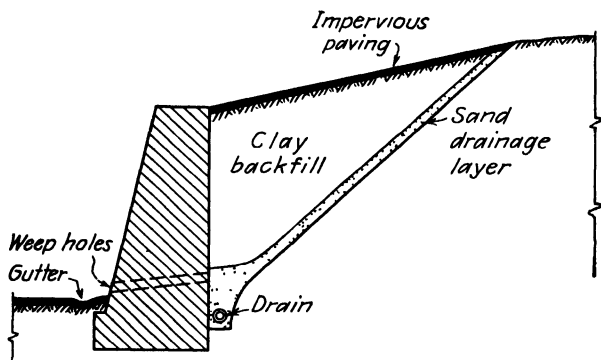
FIG. 16-2. Special measures are needed to divert water from clay backfills. (*After A. Casagrande, Ref.* 333, 1936.)

age and to decrease any tendency of the backfill to increase its volume owing to swelling or frost heaving. However, insufficient field information is yet available to judge the degree of effectiveness of such measures in different climates.

The dimensions of a gravity retaining wall are determined as follows: the width b at the base must be such that the stabilizing moment of the weight W of the wall around edge 1 is greater than the overturning moment of the earth pressure E around the same edge; the resultant R must fall within the middle third of the base, so that edge 2 will still be pressed against the ground; the pressure p_1 beneath edge 1 should not exceed the permissible pressure on the ground (Art. 14-1); the shearing resistance along plane 1-2 of the base should be greater than the earth pressure E, since sliding would otherwise result. Passive earth pressure against the toe is usually neglected (see Prob. 16-1). The right dimension is arrived at by trial. For the first attempt one may take $b = 0.4h$.

In the case of clay soils the shearing resistance along plane 1-2 of the base can be taken to equal one-half of the unconfined compressive strength

q_u of the clay. If this value is low, piling (including batter piles) may have to be resorted to. Graphical procedures, similar to those illustrated by Fig. 16-51(IV), can be conveniently used to determine the loads to be carried by the piles.

Reinforced-concrete retaining walls are frequently used instead of massive gravity walls. Figure 16-3 illustrates two of the more current types. The lateral pressure distribution against plane 0-2 and the over-all dimensions of the wall are determined in the same way as indicated above for gravity walls. The weight of the soil above the heel of the wall is to be included in the over-all stability computations. The weight of the soil above the toe may be included if no danger exists of its later
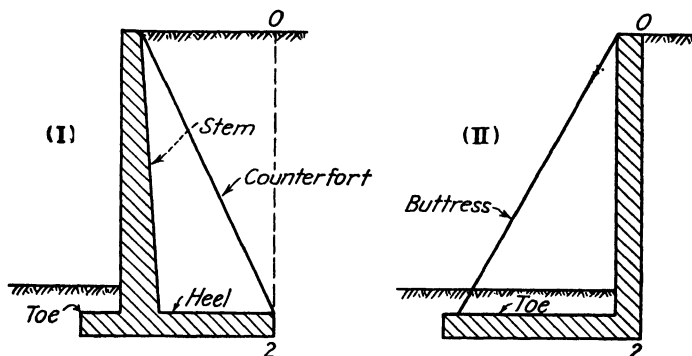
FIG. 16-3. Reinforced-concrete retaining walls.

removal. Once the lateral pressures and the soil reactions are determined, the detailed design of the component parts of the wall is undertaken in the same manner as is done for any other structural elements of reinforced concrete subject to bending (see any handbook for examples of computations, for instance, Dunham, Ref. 111).

Gravity retaining walls in the form of a *crib* are sometimes employed, as shown in Fig. 16-5. They are modeled after timber-crib cofferdams (Art. 16-17), but are usually built of interlocking prefabricated reinforced-concrete units of two types, *A* and *B* (Fig. 16-4). The spaces between these units are filled with soil. The width b of the crib is determined in the same way as has been indicated above for an ordinary gravity wall. The dimensions of the prefabricated units should be chosen so that $f \geq 2e$; otherwise dry granular fill would not be retained within the crib. The prefabricated units of type *B* are designed to resist in bending, as beams of span a on two supports, a maximum total lateral pressure equal to $(d + e)a \times 0.5\gamma b$, where γ is the unit weight of the soil. The *B* units should also resist one-half of the total vertical pressure indicated below for the *A* units. This lateral pressure will correspond to that in a silo
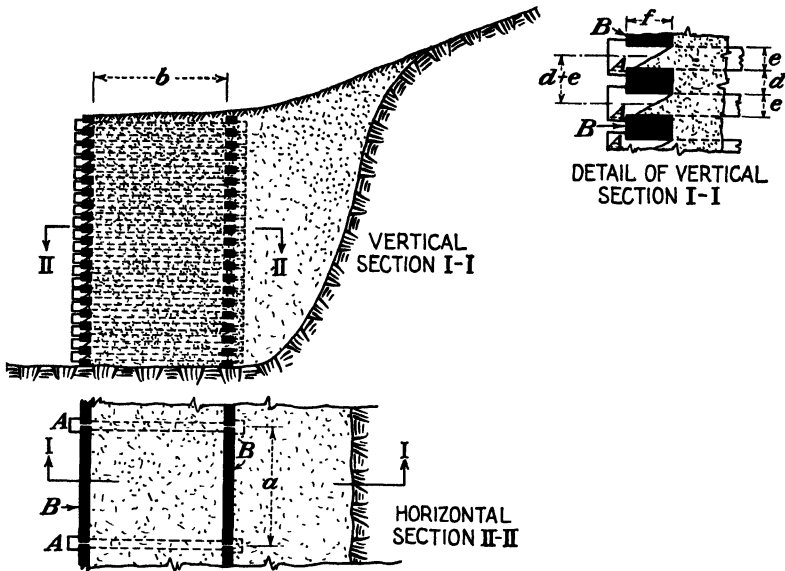
FIG. 16-4. Design of crib retaining wall. Precast reinforced-concrete units (see Fig. 16-5).
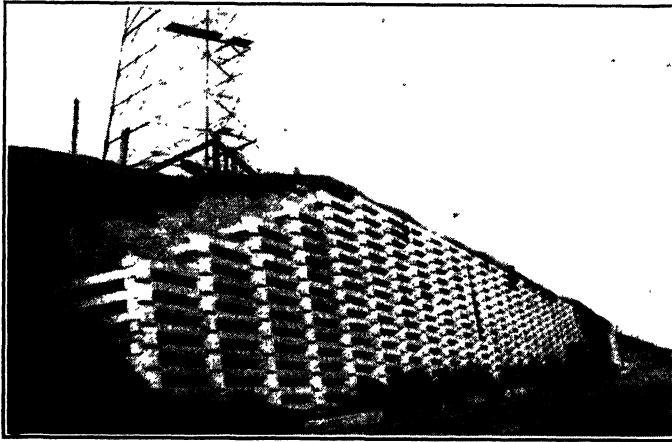
FIG. 16-5. Face of reinforced-concrete crib retaining wall. (*Photo by Tschebotarioff, Ref.* 375, 1939.)

(Art. 10-15) and will be developed if the crib is filled with soil prior to backfilling. The active pressures after backfilling should not create any greater bending moments. Symmetrical tensile and compressive reinforcement should be used for both types of units. The A units should be reinforced to take up in tension the total lateral force exerted against a B unit; the head of the A units should be designed to take up that force in shear. In addition, the A units should be designed to resist in bending, as

beams of span b on two supports, a total vertical force assumed transmitted to it by friction from both sides and equal to $(d + e)b \times 0.5\gamma a \times 0.58$, where the first part of the equation represents the total lateral pressure ($K_n = 0.5$), and the coefficient of wall friction is taken to equal $\tan \delta = 0.58$ ($\delta = 30°$).

Crib walls of this type permit some economy of concrete and can be quickly erected if a stockpile of prefabricated units is available. They permit excellent drainage of the backfill.

If the retaining structure is such that the surface of the wall in contact with the soil is *rigid* and *unyielding*, then the lateral earth pressures
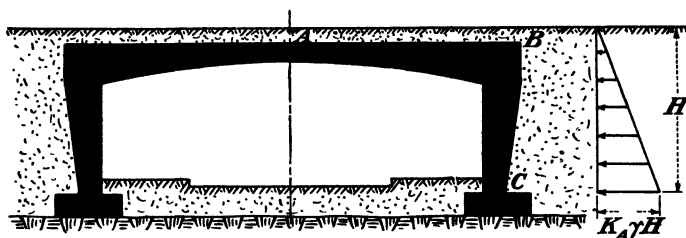
FIG. 16-6. Lateral backfill pressures against rigid unyielding walls.

exerted against it may be expected to increase considerably and approach the at-rest values (see Art. 10-17). The wall panels of a building with several basements [Fig. 13-16(II)] or the legs of a rigid frame bridge (Fig. 16-6) may be taken to be rigid and unyielding in this sense. The pressure distribution will still be essentially hydrostatic, as in Fig. 16-1, but the corresponding K_A value should be taken as follows:

Loose sand: $K_A = 0.50$
Dense sand: $K_A = 0.70$ or higher, depending on degree of compaction of the backfill

Precise data relating the compactive effort expended on the densification of a sand backfill to its lateral pressures are not yet available.

In the case of *rolled-clay backfills* there is little reason to assume that compaction of the clay would increase its lateral pressures beyond values corresponding to $K_A = 0.5$. Since during dry spells the lateral pressures may be appreciably smaller, the effect of lateral pressures should not be considered at all when determining the bending moments in the center A of the deck of a frame bridge, as shown in Fig. 16-6. Their maximum value should be used for the design of the legs BC and of the knee B of the frame.

The pressures exerted by a *hydraulic fill*, if composed of clean sand, may be taken to correspond to those of a normally deposited loose sand, as

given above. If the backfill has a high clay content, then the lateral pressures exerted by it will follow Fig. 16-1 but may range between values corresponding to $K_A = 1.0$ and $K_A = 0.5$, depending on the rate of deposition of the fill and on its consolidation characteristics (Art. 6-8 and Fig. 10-8). The estimation of the exact intermediate value of K_A to be used in such a case for design is complicated and should be undertaken only by professional soil engineers.

16-3. The Bracing of Open Cuts. General Methods. Figure 16-7 illustrates some of the methods employed for the bracing of open cuts. Each *brace* or *strut* b should be installed as soon as the excavation reaches its elevation. This is less important in shallow cuts (10 to 12 ft) through compact cohesive soil [Fig. 16-7(IV)], but it is essential in shallow cuts through softer soils and for all soils in the case of deep cuts if accidents of the type illustrated by Fig. 8-4 are to be avoided.

There are two main types of wall lining in deep cuts, illustrated in Fig. 16-7(II) and (III). In the first type wide-flange steel *H piles* a are driven from the surface into the ground, 5 to 6 ft on centers, before the excavation is begun. *Horizontal timber sheeting*, or *lagging*, c, is then inserted, board by board, behind the flanges of the H piles as excavation progresses. Sometimes gaps of ½ to 1.0 in. height are left between adjacent boards to facilitate drainage. The gaps are stuffed with hay if the soil is sandy, to prevent the soil from trickling out through the gaps after drying. When the elevation of a row of struts b is reached, a horizontal *wale* e is placed against the H piles, and the struts or braces b are tightly wedged against it. The horizontal spacing of the braces usually is a multiple of the spacing of the H piles. It may vary from row to row and frequently is made smaller in the upper rows than in the lower ones. Both the wales and the braces can be made of heavy timbers, up to 12 to 14 in. square, or of steel H beams.

In the second type of cut lining [Fig. 16-7(III)] a continuous row f of steel sheet piles (Art. 15-11) is driven into the ground instead of H piles. No horizontal timber lagging is then needed, but a much greater quantity of steel is used in this type of lining, which, as a result, is comparatively more expensive than that shown in Fig. 16-7(II). The use of continuous steel sheet piling becomes necessary in the case of soft clay soil, especially if it alternates with thin water-bearing layers which are difficult to unwater. In the latter case sheet piling will keep the water out of the excavation, but the bracing may have to be designed to resist full water pressure (Art. 10-20). Continuous sheet piling has the further advantage of strongly reducing, or even preventing entirely, the lateral and upward squeezing of the soft clay toward the bottom of the excavation, that is, the so-called *loss of ground*. By this term is meant the removal of a greater

amount of soil than corresponds to the volume of the excavated space. Any inward yield of the bracing causes a settlement of the adjoining soil surface (see Fig. 10-25), with possible damage to buildings resting thereon. That is why braces should be well wedged in and, in special cases, even *prestressed* (Art. 15-13). The loss of ground may have a similar undesirable effect. Sheet piling, especially when reaching to a stiffer stratum (Fig. 16-13), may serve to prevent it.

Both the H piles and the sheet piling walls act as continuous beams on several elastic supports provided by the braces. The bending moments
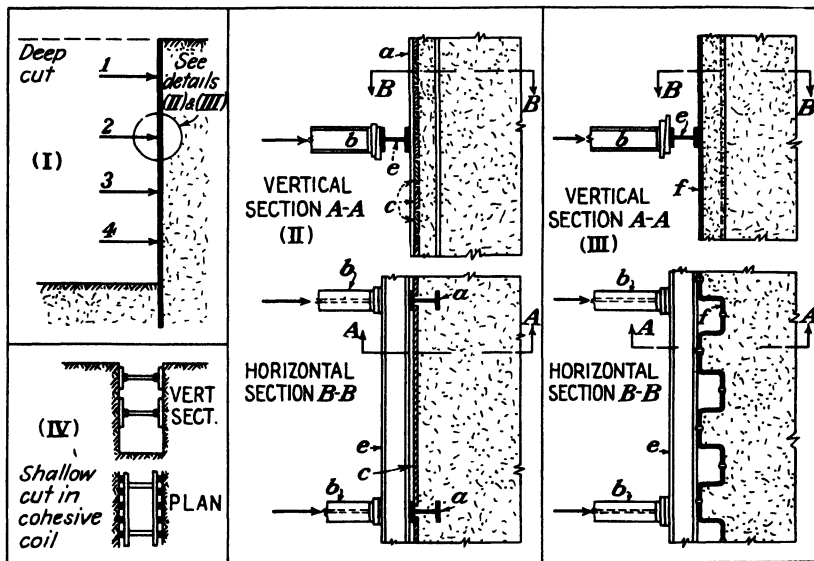
FIG. 16-7. Some types of bracing in open cuts.

of a continuous beam on several supports, as well as the reaction pressures against these supports, are strongly affected by any unequal yielding of the supports. When the amount of yielding of each support is known, its effects on the above values may be computed by conventional procedures of structural theory. However, it is not possible in practice when dealing with the bracing of open cuts to determine numerically the amount of yield of the supports in advance of construction, since it will primarily depend on the manner in which each brace has been wedged in, that is, on an unpredictable factor involving the personalities of laborers and supervisors on the job. There is therefore no point in making theoretical assumptions concerning the probable amount of this yield for the purpose of using it in the time-consuming computations of continuous beams on elastic supports. The simplified procedure proposed by Terzaghi (Ref.

360, 1941), illustrated by Fig. 16-8, should be used instead. Essentially it consists in neglecting the load-redistributing effects of pile continuity and, to that end, assuming hinges at all of the supports, except the upper one. As shown in Fig. 16-8, the problem is thus rendered statically determinate, and the pressures against the braces may be computed from
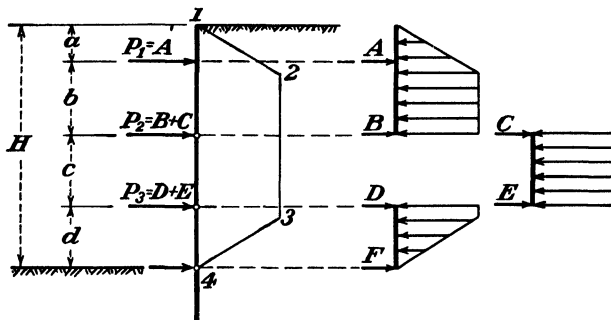
FIG. 16-8. Simplifying assumptions for the computation of strut forces *P* in a braced cut from a given lateral-earth-pressure diagram 1-2-3-4. (*After Terzaghi, Ref.* 360, 1941.)

the reactions of several independent beams on two supports. See Prob. 16-2 for an example of such computations.

16-4. Lateral Pressures to Be Used for the Design of the Bracing of Cuts in Sand. Figure 16-9 gives the diagram of lateral pressures *oabc* which should be used in the design of the bracing of cuts in sand. It is
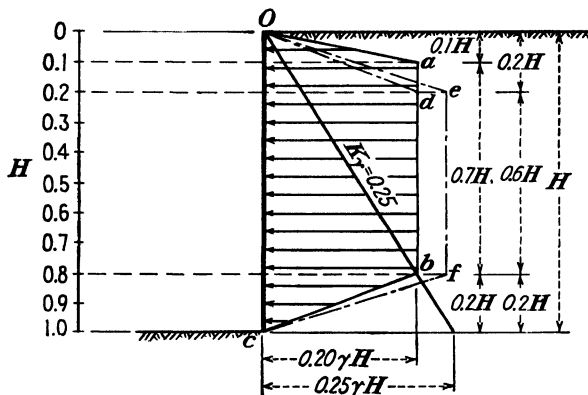
FIG. 16-9. Lateral-earth-pressure diagram *oabc* suggested for use when designing braced open cuts in sand.

based primarily on the results of full-scale field measurements (see Figs. 10-13, 10-21, and 10-22) and represents a simplification of Terzaghi's method (Art. 10-18 and Fig. 10-21). Terzaghi's diagram related the lateral pressures of the sand to its internal friction. The trapezoid *odbc*

in Fig. 16-9 represents the Terzaghi-Peck recommendation for dense sand and the trapezoid *oefc* their recommendation (Ref. 365) for loose sand, both expressed in terms of the *same* unit weight γ of the sand for which Fig. 16-9 is drawn. A smaller unit weight would have to be used for sand in a loose state, approximately 100 lb per ft^3, as compared with approximately 120 lb per ft^3 for dense sand. Thus the actual lateral pressures of loose and of dense sand, according to the Terzaghi-Peck recommenda-
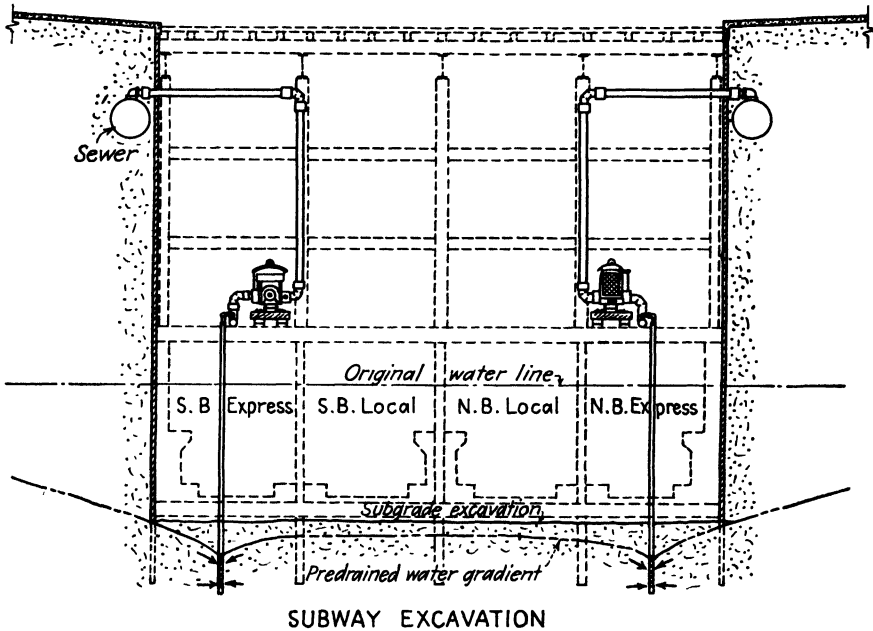
FIG. 16-10. Lowering of the ground-water table by means of wellpoints during subway construction in New York. (*After Moretrench Corp., Ref. 237.*)

tions, would be almost identical, the decrease of the K_A value for dense sand being compensated for by its increased unit weight. The suggested diagram *oabc* in Fig. 16-9, however, would give higher pressure values for dense sand in the upper zone of the cut. This is in accordance with general considerations concerning arching (Art. 10-19), the effectiveness of which, together with the higher pressures in the upper zone of the cut is likely to increase with sand density (see Fig. 10-22, and the observed decrease of pressures after rupture in bank which permitted expansion of dense sand).

All these different methods give pressure values which do not differ from each other by more than 20 per cent. Thus the factors of safety customary in structural design are quite ample to take care of the still

existing slight margin of uncertainty where cuts in sand are concerned. See Prob. 16-2 for an example of relevant computations.

When the bottom of the cut in sand reaches below the ground-water level, wellpoints (Art. 14-9) provide the most convenient means of lowering that level, as illustrated by Fig. 16-10 for a section of a subway cut in New York. In some cases the intermediate rows of vertical H piles are omitted. This increases the unstiffened length of the struts, which then have to be made heavier, but more free space is gained at the bottom of the excavation, so that bulldozers, power shovels, and trucks can perform the excavation and removal of the soil more quickly and conveniently.

16-5. Lateral Pressures to Be Used for the Design of the Bracing of Cuts in Plastic Clay. The Terzaghi-Peck lateral-earth-pressure diagram of Fig. 16-11 is based, in part, on the results of full-scale measurements on the Chicago subways (Art. 10-20), but mainly on the following general considerations. The maximum possible shearing strength of the soil, equal to one-half of its unconfined compressive strength q_u, is assumed to be active at its full value along possible surfaces of failure, in accordance with the Rankine-Résal equation (10-3), the angle of internal friction ϕ being taken to equal zero. Then, in accordance with Terzaghi's general wedge theory (Art. 10-19), a redistribution of lateral pressures is assumed to take place along the depth of the cut in such a manner that the pressures at the bottom of the cut are strongly decreased and that the theoretical Rankine tensile zone at the top of the cut not only disappears entirely but is even replaced by compressive stresses higher than the residual pressures in the lower zone. At the same time, the possible transfer by shearing stresses of part of the lateral pressures to the clay beneath the elevation of the bottom of the cut is ignored entirely, since the total lateral pressure is still assumed to correspond to the same Rankine-Résal value.

FIG. 16-11. The Terzaghi-Peck lateral-earth-pressure diagram for the design of braced open cuts in plastic clay, based on the ultimate strength of the clay. (*After R. B. Peck, Ref. 260, 1943.*)

The above reasoning involves quite a number of questionable and contradictory assumptions. It has been demonstrated in Art. 10-20 that the agreement claimed between computations based on the above procedure and values measured on full-scale structures actually existed only at cer-

tain depths of the cut, but that at smaller depths the procedure illustrated by Fig. 16-11 produced unsafe design values and at greater depths gave uneconomical design values.

For that reason the lateral-earth-pressure diagram illustrated by Fig. 16-12 is proposed instead. It is suggested for clays which are plastic in their natural state as well as for clays which are originally brittle (Table 7-1). Plastic clays in a state of *consolidated equilibrium* have been found to have an approximate value of $K_n = 0.50$ under a variety of conditions (see Arts. 10-9 and 10-20). The state of *consolidated equilibrium* of a plastic material was considered by Tschebotarioff (Ref. 384, 1949) to represent a condition of incipient failure to which strength theories of elastic materials could not be applied. A brittle clay, on the other hand,
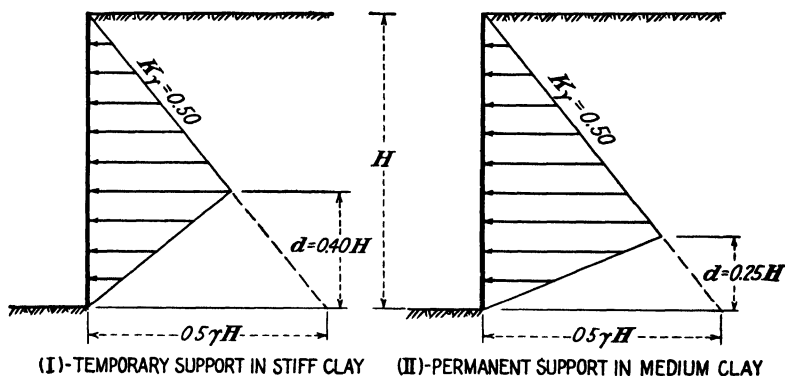
FIG. 16-12. Neutral-earth-pressure-ratio method. Lateral-earth-pressure diagram proposed for the design of braced open cuts in plastic clay. *Note:* For soft clays, $d = 0$ in all cases. (*After Tschebotarioff, Ref.* 397, 1949.)

would at first behave like an elastic material but, as a result of deformations during construction operations, would be remolded and become plastic. For such brittle clays the values proposed by the *neutral-earth-pressure-ratio method of design* represent maximum limits. Field measurements have as yet failed to provide evidence that true arching, in the sense of Fig. 10-23 and the discussion thereof, can occur in plastic clays and increase pressures against the top of a cut, as happens in sand (compare Figs. 10-26, 10-29, and 10-30 with Figs. 10-13, 10-21, and 10-22). For that reason the recommendations presented in Fig. 16-12 are based on a constant value of the coefficient of lateral earth pressure at rest, taken to equal $K_\gamma = K_n = 0.50$ (these are K_s values, Art. 10-13), and on a partial transfer of lateral pressures by shearing stresses to the soil beneath the elevation of the bottom of the cut. The durability of this effect is somewhat uncertain in soft clays (Art. 7-21 and Ref. 240)—hence the restrictions given in the diagrams of Fig. 16-12. The full effect may
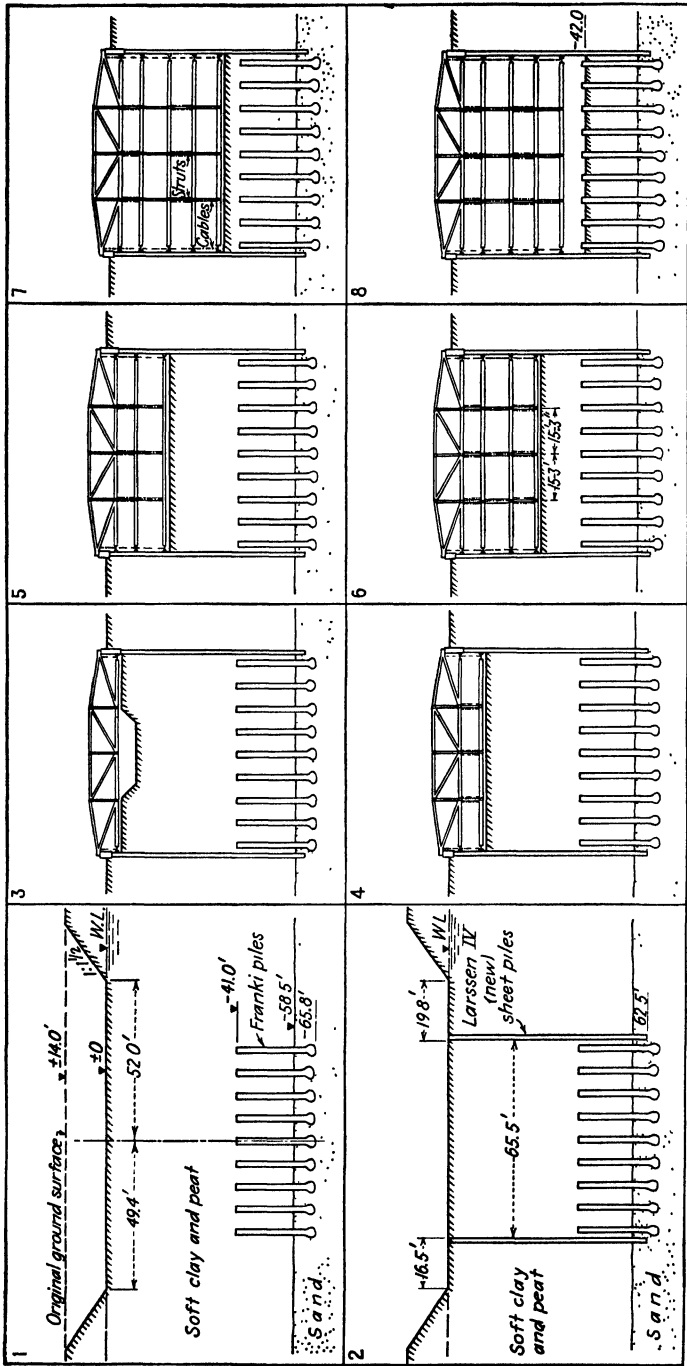
FIG. 16-13. Construction sequence during excavation of open cut on the approaches to the Maas River Tunnel at Rotterdam, Holland [see Fig. 10-29(b)]. (After J. P. van Bruggen, Ref. 46.)

be assumed when only temporary support has to be provided in stiff clays; it should be reduced somewhat for permanent support in medium clays; in soft clays it should be neglected entirely ($d = 0$), as was done, after van Bruggen (Ref. 44), by the Dutch engineers for the Rotterdam tunnel. The permissible stresses in the structural members should not be any greater than the values customary for permanent structural work.

Figure 16-13 illustrates the construction sequence on the Rotterdam tunnel approaches. First a wide trench was excavated down to the water level by power shovels. This reduced expenses by facilitating this part of the excavation and by decreasing the amount of sheet piling required. Then situ-cast concrete Franki piles (Art. 15-7) were driven down to sand to support the concrete tunnel (stage 1). The pile cylinders above el. −41 ft were filled with sand (they are not shown in the diagram). Steel sheet piling of the Larssen IV new profile was then driven down to sand (stage 2). The excavation was then begun, and each row of braces was lowered into position and cross-stiffened after its elevation was reached (stages 3 to 8). Meanwhile wellpoints (Art. 14-9) (not shown in the diagram) had been driven along the river side of the sheet piling into the sand, and pumping was started to relieve the uplift pressures against the clay plug between the two rows of sheet piling (see Prob. 16-3 and Art. 14-10). Subsequent to completion of stage 8, the concreting of the rectangular tunnel body was begun, and the rows of braces were removed one by one as the concrete reached their elevation. See Art. 10-20 and Fig. 10-29 for further data about this job.

16-6. Cuts in Other Types of Soil. A comparison of the two lateral-earth-pressure computation methods outlined in Art. 16-5 is given in Fig. 16-14 (compare with Fig. 10-27). Both methods give approximately the same value of the total lateral pressure at a certain depth of excavation H, which increases with the strength of the clay—approximately 25 ft for $q_u = 0.5$ ton per ft^2; 30 ft for $q_u = 0.7$ ton per ft^2; 40 ft for $q_u = 1.0$ ton per ft^2. At smaller depths the *neutral-earth-pressure-ratio method* is more conservative than the *strength method;* the reverse is true at greater depths.

It should be noted that good agreement between values based on the neutral-earth-pressure-ratio method and actually measured field values has been obtained at all depths in the case of soft clay at Rotterdam which had been remolded by pile driving (Art. 10-20 and Figs. 10-29 and 16-13). In the case of the medium undisturbed Chicago clay measured values of lateral pressures prior to the completion of excavation were found to be in complete disagreement with the strength theory. However, the slope of the measured lateral pressures corresponded to $K_\gamma = 0.10$ at the start of the excavation and gradually increased to $K_\gamma = 0.45$ when the biggest

depth for that job was reached (Fig. 10-26). Thus the neutral-earth-pressure-ratio method, based on a value of $K_n = 0.50$, was somewhat conservative for the Chicago conditions at small depths. At greater depths the strength method was too conservative (Art. 10-20).

It is probable that the same trend will be accentuated in the case of soils of greater strength and, especially, if these soils have an undisturbed brittle structure due to natural cementation or to other causes. The building up of lateral pressures against the bracing of a cut may then be somewhat similar to the performance of the loam soils tested in a cell apparatus, shown in Fig. 7-20. Very small lateral pressures will be
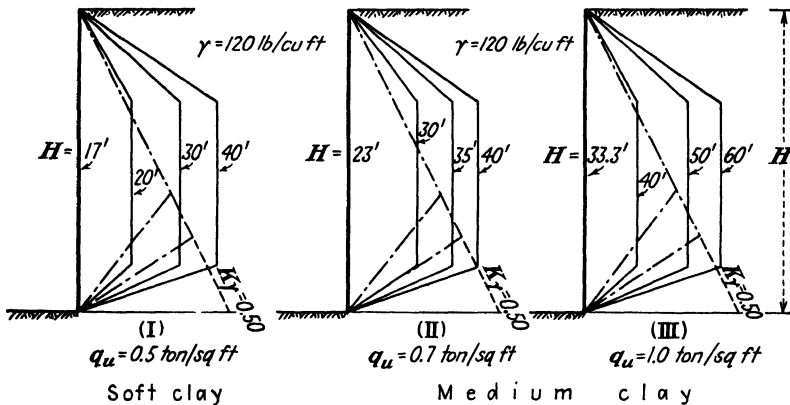
FIG. 16-14. Comparison of lateral-earth-pressure diagrams for the design of braced open cuts in plastic clay. Full lines—based on the ultimate strength of the clay; dash-dotted lines—based on limit values of the neutral lateral-earth-pressure ratio.

registered until the deformations associated with the progress of the excavation will become large enough to break down the structure of the soil, whereupon the lateral pressures will gradually increase to their active value, which in the case of cemented granular soils may be smaller than the neutral value of $K_n = 0.50$. Thus in such stiff soils (fissured clays excluded) the strength theory may prove satisfactory at smaller depths. There is much room for valuable further experimental study in this entire field.

When planning a large new cut, the likely limits of lateral-earth-pressure variation should be determined on the basis of the preceding theories, and flexible specifications should be set up to permit the adaptation of the design of the bracing of the cut to the results of measurements performed on the first sections of the cut to be built. The bracing for these first sections should be designed on the basis of the most unfavorable assumptions. Because of the remaining limitations in our knowledge, only an

experimental approach of this kind will ensure a design which is both safe and economical, difficulties of administering such a *design-as-you-go* procedure notwithstanding.

16-7. Surcharge Effects. It is convenient to express a uniformly distributed surcharge p_s in terms of a layer of soil having the same density γ as the underlying soil and a weight equal to p_s. The height of this soil
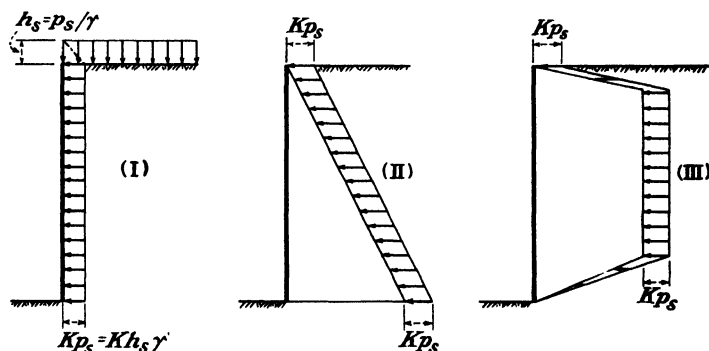
FIG. 16-15. Lateral-pressure distribution produced by surcharges uniformly distributed over the soil surface.

layer will then be $h_s = p_s/\gamma$, and the lateral pressures exerted by it from the surface of the soil downward will equal, as shown in Fig. 16-15(I),

$$p_{hs} = h_s\gamma K = p_sK \tag{16-1}$$

The coefficient K in Eq. (16-1) should have the same value as was assigned to it for the determination of the lateral pressures exerted by the underlying soil. The rectangular lateral-pressure diagram of the surcharge, shown in Fig. 16-15(I), should be added to the corresponding lateral-earth-pressure diagrams of the triangular or of the trapezoidal types, as the case may be, in the manner illustrated by Fig. 16-15(II) and (III).

Lateral pressures exerted by concentrated loads may be computed from Eq. (10-38) and Fig. 10-32, as explained in Art. 10-21. That is, the Boussinesq equation for lateral pressures can be applied under the assumption of a Poisson ratio $\nu = 0.5$, where the lateral-pressure values obtained from that equation, or by the use of the Newmark charts (Art. 9-6), should be doubled, in order to take into account the effect of maximum possible restraint of lateral displacements imposed on the soil by the interposition of a rigid wall. The suggested procedure should give somewhat conservative and safe values.

16-8. Effect of Tidal Variations. At low tide the free-water level drops faster than the level of the water in the backfill behind the sheet-

pile bulkhead. Appreciable lateral pressures may be exerted against the sheet piling as a result of such a *tidal lag* (see Fig. 16-16). The effect is somewhat similar to that of a surcharge; it should be considered in designs. The amount of lag varies with the magnitude of the local tidal variation and with the nature of the backfill. It should be determined experimentally in advance of construction, for instance, by observing the water-level variations in perforated pipes sunk into the soil near existing waterfront structures.
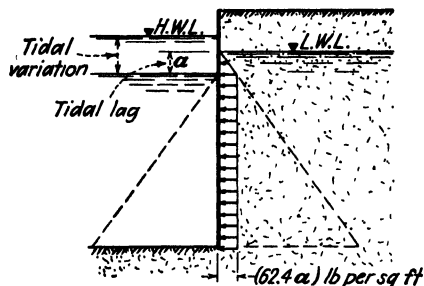
FIG. 16-16. Lateral pressures exerted against a row of sheet piling as a result of a lag in the tidal variation of the water level in the backfill.

16-9. The Free-earth-support Method of Designing Anchored Flexible Sheet-pile Bulkheads. Noncohesive Soil.

This method is based on the assumption that the soil into which the lower end of the sheet piling is driven is incapable of producing effective restraint of the sheet piling to the extent necessary to induce negative bending moments. The pressure distribution in a granular soil which corresponds to this assumption is shown in Fig. 16-17 for a minimum depth of embedment D' compatible with equilibrium, that is, when the factor of safety in respect
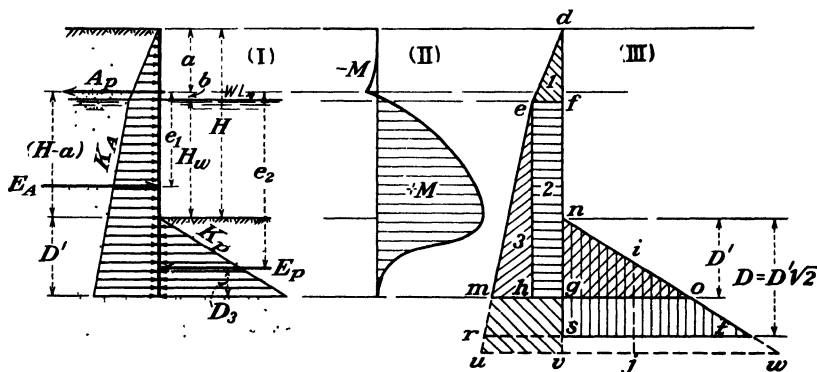
FIG. 16-17. The free-earth-support method of anchored-bulkhead design in sand. (I) Equilibrium of forces for depth of embedment giving a factor of safety of unity. (II) Shape of bending moment diagram. (III) Pressure diagrams for other depths of embedment.

to the limit value of the passive resistance of the soil in front of the bulkhead is equal to unity ($F_s = 1.00$).

Figure 16-17(I) refers to a condition where the depth of embedment is just sufficient for limit equilibrium, assuming that the maximum possible

passive resistance is fully mobilized. The anchor pull can then be determined from the condition that the sum of the horizontal forces is equal to zero:

$$A_P = E_A - E_P \tag{16-2}$$

where

$$E_A = [\tfrac{1}{2}(a+b)^2\gamma K_A] + [\gamma'(a+b)K_A(H_w+D')] + [\tfrac{1}{2}\gamma'(H_w+D')^2K_A] \tag{16-3}$$

and

$$E_P = \tfrac{1}{2}\gamma' D'^2 K_P \tag{16-4}$$

In the above equations γ refers to the unbuoyed and γ' to the buoyed unit weight of the granular soil [Eqs. (4-7) to (4-11)]; all the other symbols are as shown in Fig. 16-17(I). The first bracketed expression in Eq. (16-3) represents the area *def* of the lateral-earth-pressure diagram [Fig. 16-17(III)], the second represents the area *efgh*, and the third represents the area *emh*. Equation (16-4) represents the area *ngo*. The depth of embedment D', which will correspond to the limit equilibrium, can be determined from the condition that the sum of the moments around the point where the anchor connects with the bulkhead must equal zero:

$$E_A e_1 = E_P e_2 \tag{16-5}$$

where

$$E_A e_1 = -\left[\frac{1}{2}(a+b)^2\gamma K_A\left(\frac{a+b}{3}-b\right)\right] + \left[\gamma'(a+b)K_A(H_w+D')\left(\frac{H_w+D'}{2}+b\right)\right] + \frac{1}{2}\gamma'(H_w+D')^2K_A\left[\frac{2}{3}(H_w+D')+b\right] \tag{16-6}$$

and

$$E_P e_2 = \tfrac{1}{2}\gamma' D'^2 K_P(H_w + b + \tfrac{2}{3}D') \tag{16-7}$$

In actual design all values contained in Eqs. (16-6) and (16-7) are selected and are numerically known, with the one exception of the depth of embedment D'. Thus after insertion of the corresponding figures into these equations, Eq. (16-5) may be given the form

$$C_1D'^3 + C_2D'^2 - C_3D' - C_4 = 0 \tag{16-8}$$

where C_1, C_2, C_3, and C_4 are numerical coefficients, so that the value of D' can be determined. Substitution of trial values is one of the simplest ways to solve the cubic equation (16-8). For instance, if after consideration of all relevant points we select $K_A = 0.30$, $K_P = 3.00$, $\gamma = 115$ lb per ft^3, $\gamma' = 69$ lb per ft^3, $H_w = 28$ ft, $a = 15$ ft, and $b = 2$ ft, and substitute

these values into Eqs. (16-6) and (16-7), they can be transformed into a cubic equation of the above type, from which, by trial, a value of $D' = 18$ ft, corresponding to a ratio $D/H = 18/(28 + 2 + 15) = 18/45 = 0.40$, is obtained.

Once D' is known, E_A and E_P are determined from Eqs. (16-3) and (16-4) and the anchor pull A_P from Eq. (16-2). The numerical values of all forces acting upon the bulkhead are then known. The bending moments induced by these forces can be determined in accordance with the customary procedures of mechanics of materials. Figure 16-17(II) indicates the shape of the bending moment curve which will result from such computations.

The actual depth of embedment D is made greater than D' to obtain the desired factor of safety against rupture of the soil in front of the bulkhead and against failure of the entire structure. A factor of safety of two ($F_s = 2.00$) is sometimes chosen to that end. One of the frequently used methods of computation assumes that the effectively mobilized portion of the passive earth pressure has the shape of a trapezoid *nvji*, the area of which is equal to one-half of the maximum theoretically possible triangular resistance area *nwv*, as shown in Fig. 16-17(III). This assumption complicates the relevant computations to an extent which does not appear justified, since so many other approximations are involved in the basic assumptions of this design method. For that reason the Danish rules (see Art. 16-12) permit the determination of the actual depth of embedment D from

$$D = \sqrt{2}\, D' = 1.42D' \tag{16-9}$$

This relationship appears to be based on the fact that, as shown in Fig. 16-17(III), the area of the triangle *ngo* will be one-half of the area of the triangle *nst* if *ng* is made equal to D' and *ns* to D, as indicated by Eq. (16-9). This leaves out of consideration the theoretical increase of the total active pressure by the area *mgsr*. Therefore Eq. (16-9) would provide an approximate factor of safety $F_s = 1.7$, and not 2.0, as assumed. If $F_s = 2.0$ is desired, then D should be made equal to

$$D = 1.7D' \tag{16-10}$$

The free-earth-support method provides very conservative values, as shown in Table 16-1 and Art. 16-13.

16-10. The Free-earth-support Method of Designing Anchored Flexible Sheet-pile Bulkheads. Cohesive Soil. The conventional application of the free-earth-support method to bulkhead design in clay soils is illustrated by Fig. 16-18. In accordance with Eq. (10-10), the active pressures are obtained from the fluid pressure ($K_\gamma = 1.00$) by subtracting

from it $2s$, taken to equal $2c$. Below the dredge line *fda* the areas of the active-pressure triangles *abc* and *def* are equal and cancel the area of the passive-fluid-pressure triangle *fgh*. The residual unit passive pressure *hj* is then equal to

$$p'' = p_P - p_A = 4s - \gamma H \tag{16-11}$$

Equation (10-15) forms the basis for the determination of p_P. A prerequisite for equilibrium is the condition that

$$s = c \geq \frac{\gamma H}{4} \tag{16-12}$$

or

$$q_u \geq 0.5\gamma H \tag{16-13}$$

Otherwise, in accordance with Eq. (16-11), no positive value of the residual unit passive pressure can be obtained in front of the bulkhead at any depth of embedment. In other words, there exists a critical height:

$$H_{cr} = \frac{2q_u}{\gamma} \tag{16-14}$$

FIG. 16-18. The free-earth-support method of anchored-bulkhead design in clay when based on the ultimate strength of the soil. (*After Skempton, Ref. 310, 1946.*)

This is a familiar relationship [Art. 8-1 and Eq. (8-4)].

The preceding procedure appears to be entirely rational insofar as the determination of the maximum possible passive resistance is concerned, since it is quite logical to base the theoretical maximum resistance to rupture on the ultimate strength of the soil. As regards the active pressures, however, the same inconsistencies of this method are possible as have been established for cuts in clay soils (Art. 16-5, also see Art. 10-20 in this connection). Once a depth of embedment has been established which is safe against rupture, no rupture can occur above the dredge line either, and the bulkhead deformations and not the ultimate strength of the clay will govern the active pressures.

The method illustrated by Fig. 16-18 leads to the following procedure of design: Once the lateral-pressure diagram has been determined as shown in that sketch, the minimum depth of embedment D' compatible with equilibrium is established by taking moments around the point of application of the anchor pull A_P, in a manner similar to that described

in Art. 16-9 for sands. The actual depth of embedment D, however, is now made equal to $D'F_s$. If the factor of safety is to be $F_s = 2.0$, then $D = 2D'$.

16-11. The Fixed-earth-support Method of Designing Flexible Anchored Sheet-pile Bulkheads. Noncohesive Soils. This method is based on the assumption that the bulkhead deflections y are such that the elastic line of the bulkhead shall take the shape indicated by the broken line in Fig. 16-19(I). This line reverses its curvature at the point of contraflexure c. This is equivalent to assuming that the soil beneath the
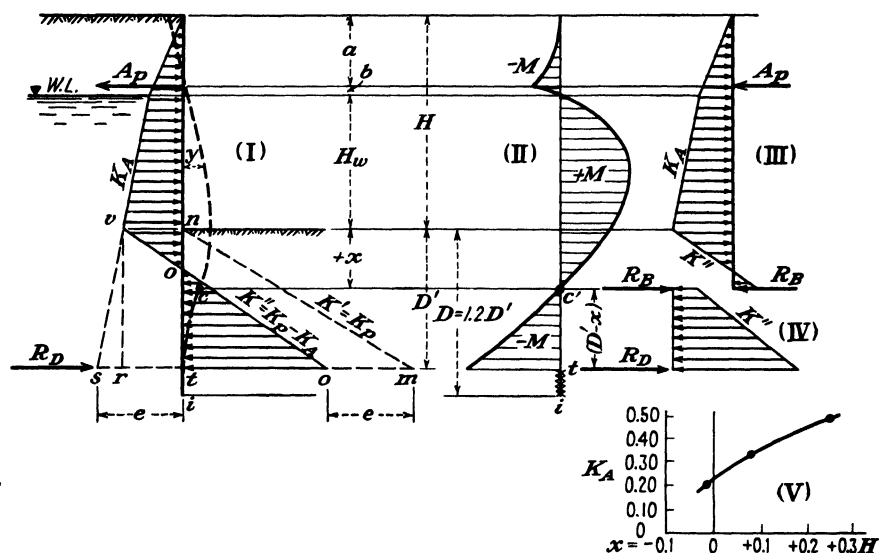
FIG. 16-19. The fixed-earth-support method of anchored-bulkhead design in sand.

dredge line exercises effective restraint on the bulkhead deformations. As a result, the bulkhead acts like a partially built-in beam subjected to bending moments, the diagram of which has the shape indicated by Fig. 16-19(II).

The classical method of computation involves a number of arbitrary simplifying assumptions. The passive resistance of the soil behind the bulkhead at its lowest tip is replaced by a concentrated force R_D at a distance ti above that tip equal to $0.2D'$. The elastic line of the bulkhead is assumed to be tangent to the vertical at the point t.

The residual line of passive pressures is then drawn, as shown in Fig. 16-19(I), by subtracting the active from the passive pressures. To that end, the distance st is made equal to om, and a line is drawn to connect the points v and o. An arbitrary value is selected for D', and a deflection line, otherwise termed the elastic line, of the bulkhead is determined for the

known loading and made tangent to the vertical through t. Graphical methods (Ref. 362) are preferable in this connection. If the elastic line thus determined does not intersect the vertical at anchor-level elevation (assumption: lateral displacement there is $y = 0$), then the depth D' has been estimated incorrectly and is not compatible with the conditions of equilibrium imposed. A new value has then to be selected for D', and the entire procedure of determining the elastic line has to be repeated for the new depth until a value of D' is found at which the elastic line will intersect the vertical at anchor level. This is the so-called *elastic-line method.* It is extremely time-consuming and, for that reason, is seldom used in practice. It will therefore not be elaborated upon further in this book.

The use of the elastic-line method, however, permitted the development by H. Blum (Ref. 34, 1931) of a much simpler procedure, which is known as the *equivalent-beam method.* By repeated trial computations involving different values of ϕ, where K_A was based on Eq. (10-7) and K_P was taken to equal $2/K_A$, Blum succeeded in establishing a theoretical relationship between ϕ and the distance x from the dredge line to the point of contraflexure c. Figure 16-19(V) gives this relationship, where ϕ is expressed in terms of K_A. It should be noted in this connection that the doubling of the K_P value, as compared with the value obtained from Eq. (10-7), was undertaken by Blum not because he considered the beneficial effect of wall friction (Art. 10-5), but because of the results of previous tests by Franzius (Ref. 136, 1927) at Hannover. During these tests Franzius obtained very high values of passive resistance and recommended doubling the values of passive resistance obtained by the use of the heretofore customary equation (10-14a). The direction of the wall friction (Art. 10-5) was not given any consideration by this recommendation, which should therefore not be used indiscriminately. The test box used by Franzius was 3.3 ft wide and 4.9 ft high. Therefore side-wall friction may have had a very great influence on the increase of the passive resistance of the soil in the box when the front wall was pushed in. It is questionable whether his test data can be applied to a normally long wall under field conditions.

Blum's equivalent-beam method consists in assuming a hinge at the point of contraflexure c, where the bending moment is zero. The part of the bulkhead above the hinge can then be treated as a separate, freely supported beam with an overhanging end, as shown in Fig. 16-19(III), and its reactions (the anchor pull A_P and the shear R_B at the point of contraflexure) and bending moments can be determined in the customary manner. After that, the lower portion of the bulkhead below the point of contraflexure c is treated as a separate, freely supported beam on two

supports. All the loads acting on that beam are known, since K'' is given, except the reaction R_D. The span $(D' - x)$ of that beam, compatible with equilibrium, is also not yet known. This span, however, can easily be determined by equating the moments of the loads shown in Fig. 16-19(IV) around the point of application of R_D. Once $(D' - x)$ is computed, the final depth of embedment is determined from

$$D = 1.2(D' - x + x) = 1.2D' \qquad (16\text{-}14a)$$

The fixed-earth-support method has sometimes been criticized (Refs. 43 and 101) because of some of its allegedly doubtful assumptions. More elaborate experimental investigations (Ref. 397), however, have shown that it comes very close to reality where backfilled bulkheads are concerned (see the design recommendations made in Art. 16-14).

16-12. The Danish Regulations for Bulkhead Design

These regulations (Ref. 99, 1926 and Ref. 100, 1937) have a purely empirical character. Their origin appears to be as follows: Up to some 50 years ago timber piles and sheet piles were used almost exclusively in the construction of quay walls. In the course of decades of experience with such walls, according to the Danish engineer J. Brinch Hansen (Ref. 166, 1946) "certain empirical rules were developed which led to dimensions that proved reasonable." In 1898 the Danish professor Teller (Ref. 166) made the flat statement that "quay walls are never calculated in practice, but are made in accordance with established rules." Check computations by the Coulomb theory of existing old structures showed that the actual stresses were "3 to 4 times as great as the ordinary allowable stresses in timber structures," (Ref. 166). This was attributed to actual bending moments in the sheet wall smaller than the calculated moments "owing to the actual earth pressure and its distribution deviating from the assumptions made" (Ref. 166). The possibility that the observations made could be explained by smaller than usual factors of safety, which were nevertheless sufficient for limit stability, does not appear to have been formally considered. Nevertheless, this possibility cannot be dismissed, since factors of safety equal to five or six are frequently used in establishing allowable stresses for timber structures, so that a three to four times higher than usual working stress would still leave a small margin of safety varying between 1.25 and 2.00. This factor of safety could nevertheless be adequate for stability, since failure of individual timber sheet piles could not occur in such structures, their average strength counted.

When reinforced concrete was introduced at the beginning of the present century, according to J. Brinch Hansen (Ref. 166), conditions corresponding to those of timber quay walls were "assumed to exist, so that reasonable dimensions can be obtained by calculating the wall corresponding to the earth pressure found by Coulomb's theory but with allowable stresses of 3–4 times the stresses applying to ordinary reinforced concrete structures." Such an analogy between timber and reinforced concrete appears somewhat risky, since factors of safety smaller than for timber are used when establishing permissible stresses for concrete and for steel. Nevertheless, a reinforced-concrete pier at Aalborg, Denmark, was built in 1906 by the Danish firm Christiani & Nielsen on the basis of this analogy (Ref. 166). This was a daring experiment and, in the light of our present knowledge, a considerable gamble. Nevertheless, it

succeeded; the pier still stands after more than 40 years of satisfactory service (Ref. 166). A check computation of this pier is given in Prob. 16-4 by means of the procedure outlined in Art. 16-14 and based on the results of the Princeton model experiments (Art. 10-23). It will be noted from Prob. 16-4 that the stresses in the row of sheet piles shown on the left of Fig. 16-20 (8.3 in. thick) are very high but, nevertheless, do not preclude stability. The stresses in the row of sheet piles on the right of Fig. 16-20, however, are so high that the absence of failure can be explained only by several additional factors which decreased the stresses and which are as follows: first, the relieving effect of the timber piles supporting the anchors; second, a possible slight
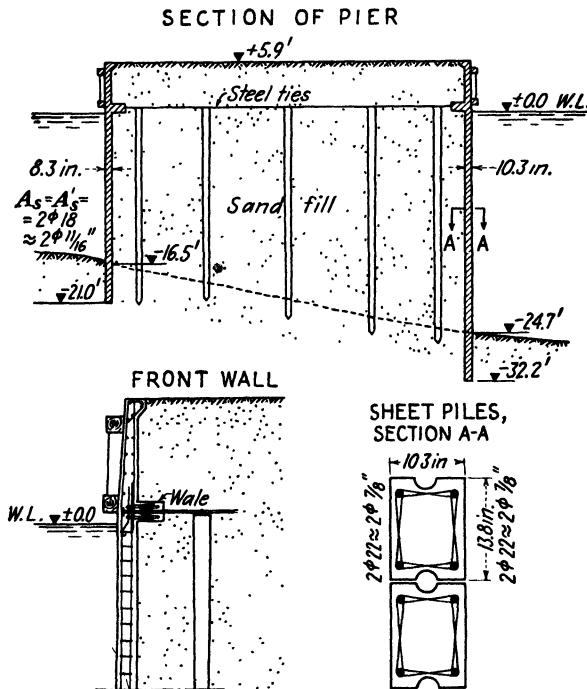
FIG. 16-20. Details of pier at Aalborg, Denmark. (*After J. Brinch Hansen, Refs.* 166 *and* 168, 1946.

"bin" action (Art. 10-15) in a horizontal direction, that is, horizontal arching, especially under surcharge effects (compare with Fig. 16-26 and discussion thereof); third, the relieving effect of the sloping natural compact ground behind the sheet piling.

It should be noted that the Aalborg pier is underdesigned (Ref. 166), even according to the later official Danish rules for such structures (Ref. 99, 1926 and Ref. 100, 1937). These rules were developed on the strength of considerations of the type illustrated by Fig. 16-21. When checking the stability of some old existing piers at Hamburg, Germany, it was found by Ehlers (Ref. 112, 1910) that the stresses in the timber sheet piling AB behind old existing massive relieving platforms, if computed on the basis of the Coulomb distribution of lateral earth pressures, reached values of 6,000 psi (Ref. 331). Ehlers explained this by the formation of two planes of shear failure, AC and BD, instead of the one plane of failure BD assumed by the Coulomb theory.

As a result, sand arches may be formed between these two planes of failure, and part of the Coulomb pressure is thereby transferred from the sheet piling *AB* to the relieving platform above it. In the light of our present knowledge (Art 10-23) this concept appears sound, since the sheet piling of the type illustrated by Fig. 16-21 has practically immovable supports, and a large part of the backfill soil above the upper abutment *A* would be in place before the full load comes to bear on it. Ehlers did not attempt to evaluate the change of lateral-earth-pressure distribution induced by this arching but suggested using higher design stresses in such cases.

Such an attempt was made later in the official rules of the Danish Society of Engineers, (Ref. 99, 1926 and Ref. 100, 1937) and led to the pressure-distribution diagram illustrated in Fig. 10-39(a). It should be definitely understood that it was not based on any actual measurements. Judging from statements made by one of the authors of the Danish rules, Professor Bretting (Ref. 40, 1948), this attempt was carried out by applying to anchored bulkheads conclusions concerning arching reached from observations of tunnels, of shafts, and of cuts with rigid unyielding supports, both in the field and in the laboratory. As shown by Tschebotarioff (Refs. 391 and 396, 1948), this procedure is fallacious, since anchored sheet-pile bulkheads do *not* have unyielding supports, unless they are connected to relieving platforms (see Art. 16-15). The Danish rules do not limit their application to sheet piles of relieving platforms of the type studied by Ehlers and illustrated by Fig. 16-21. In fact, no structural or construction limitations of any kind are imposed, although a number are essential (Art. 10-23).

FIG. 16-21. The concept of arching was used by Ehlers (Ref. 112, 1910) to explain the stability of old overstressed timber sheet piles behind relieving platforms in Hamburg Harbor.

With reference to Fig. 10-39(A), the main values for the design of a bulkhead according to the Danish rules are determined empirically as follows:

First, the ordinate q of the pressure diagram shown in Fig. 10-39(A) is computed from the equation

$$q = \frac{k[4 + (10h/L)]}{5 + (10h/L)} p_m \tag{16-15}$$

where q = distance MM' in Fig. 10-39(A)
L = distance AB in Fig. 10-39(A)
h = height of surcharge and of the soil above the anchor level, transformed to correspond to the unit weight of the soil above the anchor level
p_m = uniformly distributed unit load which will produce the same bending moment in the sheeting as the load trapezoid $ADFB$

and

$$k = \frac{1}{1 + \dfrac{0.01}{\sin \phi}\sqrt{\dfrac{(1 + n)Ea}{L\sigma}}} \tag{16-16}$$

where n = ratio of the negative bending moment at anchor level to the positive bending moment of the span below it
E = Young modulus for sheet-pile material
a = wall thickness or, for steel sheeting, distance between extreme fibers
σ = permissible bending stress
ϕ = angle of repose

The theoretical minimum depth of penetration t_0 is estimated (Ref. 290) as being equal to 0.30 or 0.35 of the depth H_w from water level to the dredge line. The actual depth of penetration D for a factor of safety $F_s = 2.0$ is made $D = \sqrt{2}\, t_0$.

Once the pressure-distribution diagram has been established as indicated above, the bending moments and the anchor pull A_P are determined for estimation purposes from the following approximate relationships:

$$+M_2 = M_0 - \frac{M_1}{2} - \frac{17}{192} qL^2 \tag{16-17}$$

$$A_P = A_0 + A_1 - \tfrac{1}{12} qL \tag{16-18}$$

$$B = E_p = B_0 - \frac{M_1}{L} - \frac{1}{3} qL \tag{16-19}$$

where $+M_2$ = maximum positive bending moment to be used for design of sheet piling
M_0, A_0, B_0 = bending moment and the two reactions of a beam of span L freely supported at A and B and loaded with the trapezoid $ADFB$
M_1 = negative bending moment at anchor level
A_1 = reaction component equal to the area enclosed by pressure curve above anchor level
q = pressure-reduction ordinate computed from Eq. (16-15)

In a publication of the Danish Society of Engineers by I. A. Rimstad (Ref. 290, 1940) the following statement is made concerning the entire procedure defined by Eqs. (16-15) to (16-19): ". . . this method, although rather complicated, is to be considered only as a rule of thumb."

A rigorous solution of the redistribution of pressures due to sheet-pile deflections was obtained by Ohde (Ref. 252, 1938). The resulting pressure-distribution curve is illustrated in Fig. 10-39(C). As shown by the Princeton bulkhead tests (Art. 10-23), this distribution is valid only for a completely unyielding anchor support. Such a condition is not likely to arise in the field, except for sheet-pile bulkheads on the land side of relieving platforms (Fig. 16-21). In addition, the method is valid only for minimum embedment D producing a condition on the verge of failure. It involves very complicated computations (Ref. 290) and will not be described further.

16-13. Comparison of the Preceding Methods of Bulkhead Design.

Table 16-1 gives a comparison of the depths of embedment D, of the corresponding ratios D/H, of the anchor pulls A_P, and of the maximum positive bending moments M_{max} in the sheet piling, as obtained by the five methods of bulkhead design discussed in the preceding articles. This comparison was made by Rimstad (Ref. 290, 1940) for a hypothetical bulkhead, for which the dimensions, the values of the surcharge and of the tidal lag, as well as the relevant backfill-soil properties, are given in Fig. 16-22.

TABLE 16-1. Comparison of Design Values Obtained by Different Computation Procedures for the Anchored Bulkhead Shown in Fig. 16-22*

No.	Designation		Statical system	Factor of safety for depth of embedment	Friction angles						Depth of embedment D, ft	$\frac{D}{H}$	Anchor pull A_p, lb per ft	Maximum positive bending moment M_{max}, ft-lb per ft
					Passive		Active							
					ϕ	δ	ϕ for layer A	ϕ for layer B	ϕ for layer C	δ				
						0				0	21.3	0.92	6,400	39,100
I.	Fixed earth support. Elastic line		Effective fixation of embedded portion D of bulkhead	2.0	35°	17.5°	35°	30°	35°	$\phi/2$	14.5	0.63	5,000	27,600
						35°				ϕ	11.3	0.49	4,140	21,200
						0				0	23.6	1.02	5,700	31,800
II.	Fixed earth support. Equivalent beam $x = 0.1H$			2.0	35°	17.5°	35°	30°	35°	$\phi/2$	14.6	0.64	5,070	28,200
						35°				ϕ	10.7	0.46	4,480	24,700
						0				0	16.7	0.73	7,380	51,600
III.	Free earth support		Noneffective fixation of embedded portion D of bulkhead	2.0	35°	17.5°	35°	30°	35°	$\phi/2$	10.3	0.45	5,880	37,100
						35°				ϕ	7.6	0.33	4,960	30,000
	Danish regulations	Reinforced concrete									6.5	0.28	5,220	18,400
IV.		Structural steel		2.0	30°	22.5°	35°	30°	35°	0	6.5	0.28	5,200	17,800
		High-strength steel									6.5	0.28	5,160	16,950
V.	After J. Ohde			2.0	35°	19.5°	35°	30°	35°	$\phi/2$	9.3	0.41	8,320	19,500

* From Rimstad (Ref. 290, 1940).

The computations were performed for three different values of the angle of wall friction: $\delta = 0$, $\delta = \phi/2$, and $\delta = \phi$, where ϕ is the angle of internal friction. It will be noted from Table 16-1 that variations in the assumed value of the angle of wall friction δ have a very considerable effect on all essential design dimensions and values. As explained in Art. 10-5, this is not caused by a decrease of the active pressures, but by an increase of the passive resistance pressures with high values of δ. Wide and overlapping ranges of essential design values, D, A_P, and M_{max}, may be obtained by varying assumptions concerning the value of δ for each of the five computation methods.
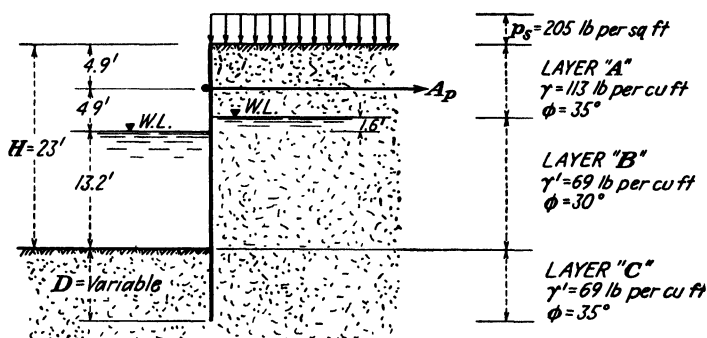
FIG. 16-22. Bulkhead dimensions, soil properties, and loads for which the comparative computations of Table 16-1 have been performed.

Considerable differences of opinion have existed as to which of the possible combinations of assumptions given in Table 16-1 should be used in actual design. The Princeton bulkhead tests (Art. 10-23) have provided definite data to settle many of the uncertainties which had existed in this respect heretofore.

16-14. Recommended Procedure of Bulkhead Design, Based on the Results of the Princeton Tests and of Full-scale Observations in the Field. Figure 16-23(I) illustrates the lateral-earth-pressure diagram which is proposed for the design of flexible anchored bulkheads in sand (Tschebotarioff, Ref. 397, 1949). It corresponds to the results of the model tests with flexible anchored bulkheads at Princeton University, which showed (Ref. 397) that full restraint of the lower portion of the bulkhead was effective when the ratio D/H equaled 0.43, where the point of contraflexure approximately corresponded to the dredge-line elevation ($x = 0$) for normal backfilling operations. According to Art. 16-9, this depth of embedment D provides a factor of safety of at least $F_s = 2.0$, since tests performed with a ratio $D/H = 0.27$ still showed full stability of the bulkhead.

The proposed procedure represents a simplification of Blum's equivalent-beam method (Art. 16-11). A depth of embedment $D = 0.43H$ is selected, and a hinge is assumed at dredge-line elevation. The active pressures p_h above dredge-line elevation are computed with the help of the equations

$$K_A = \left(1 - \frac{a}{f'H}\right) 0.33f''' \tag{16-20}$$

$$p_h = K_A \gamma h \tag{16-21}$$

In the above equations h is measured from the top of the backfill downward. γ is the unit weight of the backfill, and the product γh represents
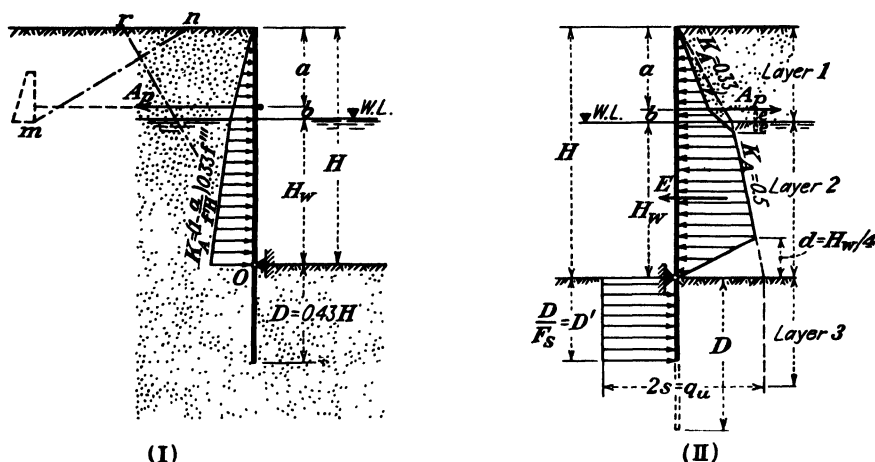
FIG. 16-23. The simplified equivalent-beam method for the design of anchored bulkheads. (I) In clean sand. (II) In clay. (*After Tschebotarioff, Ref 397, 1949.*)

the weight of the overburden at the depth h. The coefficient f''' is intended to express the effect of wall friction on the reduction of the active earth pressure. It can be taken to equal $f''' = 0.9$. The coefficient f' is intended to take into account the uncertainty concerning the relative importance of the passive earth pressures above anchor level and the tensile strength of the sand layer saturated by capillarity above the water level. This coefficient may vary between the values $f' = 1.5$ and $f' = 3.5$. It is recommended that until further studies and observations are made, the value of this coefficient be taken for design purposes at $f' = 3.5$ (Ref. 397).

The maximum positive bending moment computed with the help of Fig. 16-23(I) and Eq. (16-20) can be used for design purposes in conjunction with a 33 per cent increase in the permissible unit stresses in the steel from 18,000 psi to 24,000 psi. The factor of safety of $F_s = 1.4$ which is

thus obtained in respect to the yield point of the steel is believed to be sufficient to take care of vibration and of other possible unfavorable effects where sheet piling is used in *clean sand*, in view of the ductility of the piling material and of the observed decrease of the active lateral pressures which takes place with an increased flexibility of the bulkhead (Ref. 397). Many earth structures, including dams and embankments, often do not have a factor of safety against rupture of the soil higher than $F_s = 1.5$. On the other hand, the permissible stresses in steel are based on the yield point but in respect to the ultimate strength provide a factor of safety of at least $F_s = 3.0$. To equalize the strength of these parts of the structure, some designers (Epstein, Ref. 125) have suggested an increase of the permissible unit stress in the sheet piling to the elastic limit. Danish designers appear to have actually done so in practice (see problems at the end of this chapter).

No corresponding decrease of factors of safety is permissible in the design of the anchors and of their supports and connections, especially if there is some uncertainty concerning the properties of the soil beneath the dredge line. Any excessive yielding of the soil in front of the bulkhead may be counteracted, in part, by an increased resistance of the anchor (Ref. 397). For that reason it is recommended to increase, in all cases, the anchor-pull values computed from the diagram of Fig. 16-23(I) by dividing them by the expression

$$\left(1 - \frac{a}{f'H}\right) f'' \qquad (16\text{-}22)$$

The coefficient f'' can be taken to equal unity in cases where reliable granular material is located beneath the dredge line. Any uncertainty concerning the nature of this material and, hence, concerning the safe depth of embedment, may be partially compensated for by decreasing the value of f''.

However, there is no advantage in providing excessively rigid supports for the anchors, especially if the wall is of the "sunk" type, since otherwise pressure conditions similar to those of Fig. 16-9 would be created in sandy soil, as illustrated by Fig. 16-24. The anchors in that case were short (some 20 ft long), and were unyieldingly tied back into a concrete highway slab. The slab did not yield; the anchors were overstressed, as a result, and failure occurred. The hooks on the anchor turnbuckles proved to be the weakest link of the system and gave way. On the other side of the same highway cut the otherwise identical anchors stood up satisfactorily. They were longer and were tied back to so-called *deadmen*, that is, to anchor plates buried in the ground, which provided yielding supports, of the type shown by broken lines in Fig. 16-23(I). In addition.

better support at the bottom of the cut had been provided at the side where no failure took place.

Deadmen should be placed back far enough to receive sufficient passive support from the soil above the probable failure plane *mn*, shown by dash-dotted line in Fig. 16-23(I), outside of the plane *ro* beyond which the soil may slide in the active wedge behind the bulkhead (see Art. 10-2).

Figure 16-23(II) suggests a lateral pressure diagram for the design of anchored bulkheads in *clay soils*. The proposed depth of embedment D is based on the ultimate strength of the clay below the dredge line and a factor of safety $F_s = 2.0$. Therefore $D = 2D'$, where D' is established by

FIG. 16-24. Collapse of sheet-pile wall due to failure of turnbuckle hooks on short anchors which were rigidly tied into a concrete roadway. (*Photo by Tschebotarioff, 1949.*)

taking moments around the point of application of the anchor pull A_P (see Art. 16-10). The active-pressure diagram is based on the maximum neutral values of clay soils and on considerations identical to those of Art. 16-5. If both the layers 2 and 3 are composed of soft clay, the distance d in Fig. 16-23(II) should be made equal to zero, and the clay of both layers in front and behind the bulkhead may be strengthened by means of sand piles or drains (Refs. 166 and 88, see Arts. 6-10 and 19-4).

Some uncertainties still exist concerning the performance of *sand-clay* mixtures in backfills. During the Princeton bulkhead tests it was found that a hydraulically placed backfill after consolidation behaved essentially like a clay when its granular composition consisted of 70 per cent sand, 20 per cent silt, and 10 per cent clay. When it consisted of 85 per cent sand, 10 per cent silt, and 5 per cent clay, it behaved essentially like a sand when normal backfilling was done, but it developed very high lateral pressures when subjected to severe vibrations (Ref. 397). In this respect

the admixture of clay to sand without the mixture being compacted had a reverse effect as compared with the behavior of thoroughly compacted sand-clay mixtures. The latter were found during the Princeton vibration subgrade tests to become less sensitive to vibration if a slight amount of clay was added to the sand (see Art. 18-4).

No precise recommendations can yet be made concerning the design of bulkheads where the natural soil and the backfill are composed of sand-clay mixtures. Until further research is performed all such design computations should include "factors of ignorance" (see Tschebotarioff, Ref.
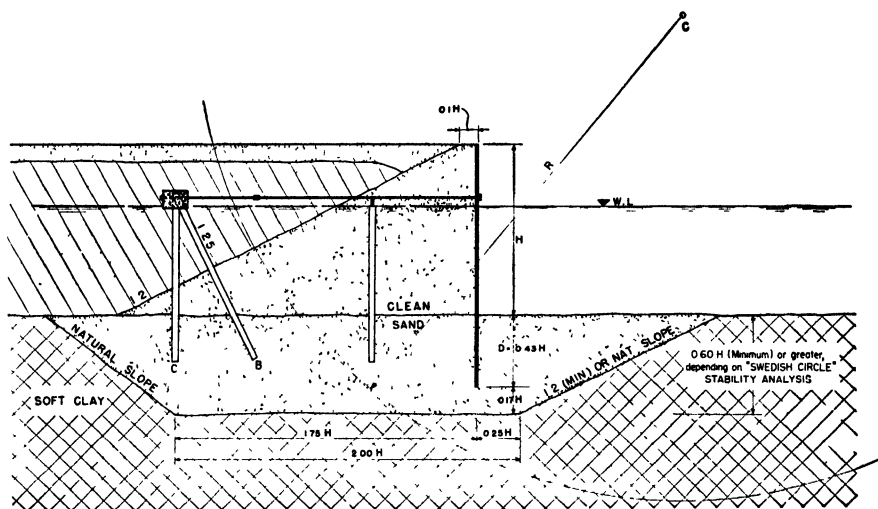
FIG. 16-25. Suggested construction of quay wall, consisting of anchored bulkhead without relieving platform, on soft clay and with a limited amount of clean sand available for backfilling. (*After Tschebotarioff, Ref. 397, 1949.*)

399, 1950). In any case, no increase of usually permissible stresses should then be allowed for the structural members of the bulkhead if the design is made according to Fig. 16-23(I). The coefficient f'' in Eq. (16-22) should be set at 0.7 or even, in extreme cases, such as in soft bottom soils, at 0.5. As an alternative, a construction of the type illustrated by Fig. 16-25 may be considered. A trench is first dredged in the natural soft soil and is then filled with selected clean sand, preferably above the final dredge level. The sheet piling and the anchor piles are driven into the sand, and a sand dike is formed behind the bulkhead at the natural angle of repose by dredging the sand from in front of the bulkhead and placing it at the back. After this is done, the rest of the backfilling may be performed hydraulically with whatever material is available, except for the upper bearing layer, which should be made of selected material compacted

by rolling (Art. 11-3). The use of the sand dike will permit the design of the sheet piling, for pressures corresponding to Fig. 16-23(I), as if the entire backfill were composed of clean sand (Refs. 125 and 126 and Art. 10-23). The stability of the entire structure should be investigated by means of the Swedish circle method—only one of the several necessary trial circles is shown in Fig. 16-25—to prevent deep slide failure of the type illustrated by Fig. 8-6. See Prob. 16-7 for anchor-pile design.

Layered soil systems, that is, alternating layers of sand and of clay, can create considerable difficulties, especially if soft clay underlies sand or rock fills. An example of what this condition may mean is provided by
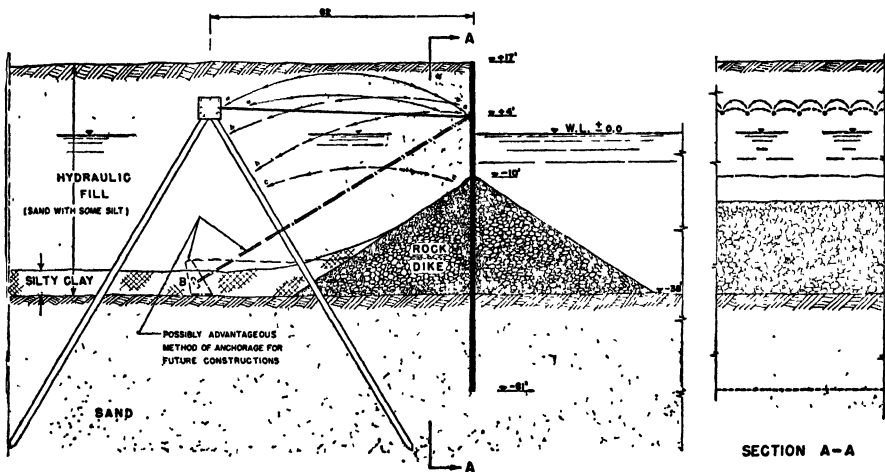
FIG. 16-26. Probable types of arching which developed at Long Beach Pier C bulkhead after consolidation of the hydraulic fill. (*From Tschebotarioff, Ref. 399, 1950.*)

the careful measurements on full-sized anchored bulkheads at Pier C in Long Beach Harbor in California, which were performed and reported by Professor C. Martin Duke (Ref. 110, 1950) and discussed by Tschebotarioff (Ref. 399, 1950). The general dimensions of the bulkhead are shown in cross section in Fig. 16-26. The surface of the hydraulic fill (Art. 17-3) settled over a foot as the fill consolidated. A large part of this settlement could be attributed to the 5- to 6-ft-thick layer of silty clay deposited ahead of the sand fill proper from the fill water which was allowed to flow all along the length of the 2,365-ft-long pier before reaching an overflow. Such conditions should be avoided in this kind of work, and overflows should be provided only a short distance from the orifice of the pipe which discharges the fill. The settlement of the overlying sand fill followed the consolidation of the soft clay and loaded by its weight the anchor tie rods and the batter piles, as shown in Fig. 16-26. It should be

noted that the 3-in.-diameter tie rods were spaced 6 ft apart, and the timber batter piles only 3.0 ft center on center.

Lateral-earth-pressure measurements were performed by means of Carlson pressure cells, marked by the letters P and a reference number in Fig. 16-27 (stage 1). The measured earth pressure values are given in kips (1,000 lb) per square foot. The anchor pull values were determined by means of Carlson strain meters (Art. 13-8). Their measured values are given in Fig. 16-27 in kips per foot.

It will be noted from Fig. 16-27 (stage 2), that after completion of backfilling the pressure distribution was essentially hydrostatic and that no evidence of vertical arching [Art. 10-14 and Fig. 10-16(III)] was obtained. This confirmed the findings of the Princeton model tests (Art. 10-23) on that point. Above the anchor level at stage 2 the lateral pressures approximately corresponded to the ones obtained at Princeton during a model test (No. 59) with a sand-silt mixture of a grading similar to that of the Long Beach backfill, that is, to an average value of $K_\gamma = 0.44$ (Ref. 397). However, below the anchor level the lateral pressures were much higher and corresponded on the average to $K_\gamma = 0.70$. The readings of cell P8 were probably too high, since this cell was found to have been dislodged from its original position flush with the inner face of the bulkhead, so that it protruded somewhat into the fill; but there is no reason to doubt the over-all accuracy of the other readings. There are two possible explanations for the 60 per cent higher values of the lateral pressures at stage 2 below the anchor level of the Long Beach pier, as compared with those of the corresponding Princeton model test 59. First, slight continuous vibrations produced by wave action may have caused the 60 per cent increase, since strong vibrations of the completed backfill of this type during Princeton test 59 had demonstrated its considerable susceptibility to vibrations and produced an almost four times greater increase of 227 per cent, as compared with static lateral pressures. Second, horizontal arching along the lines *cc*, as shown in Fig. 16-26, may have caused this increase (see Fig. 10-23 and its discussion). However, there can be no doubt as to the causes of the subsequent redistribution of pressures and of overloading of anchors which occurred as the consolidation of the fill and of the underlying clay progressed (see stages 3, 4, and 5, Fig. 16-27).

Two other examples of more extreme conditions of this type will be given. Figure 16-28 illustrates the first case. A concrete relieving platform on piles, built in 1929 to 1930, was anchored back to pile clusters over a distance of 375 ft by means of 2-in.-diameter steel anchor tie rods spaced 5 ft apart. At their other end the anchors connected to the outer pier leg of the craneway. A layer of soft clay was located at some depth
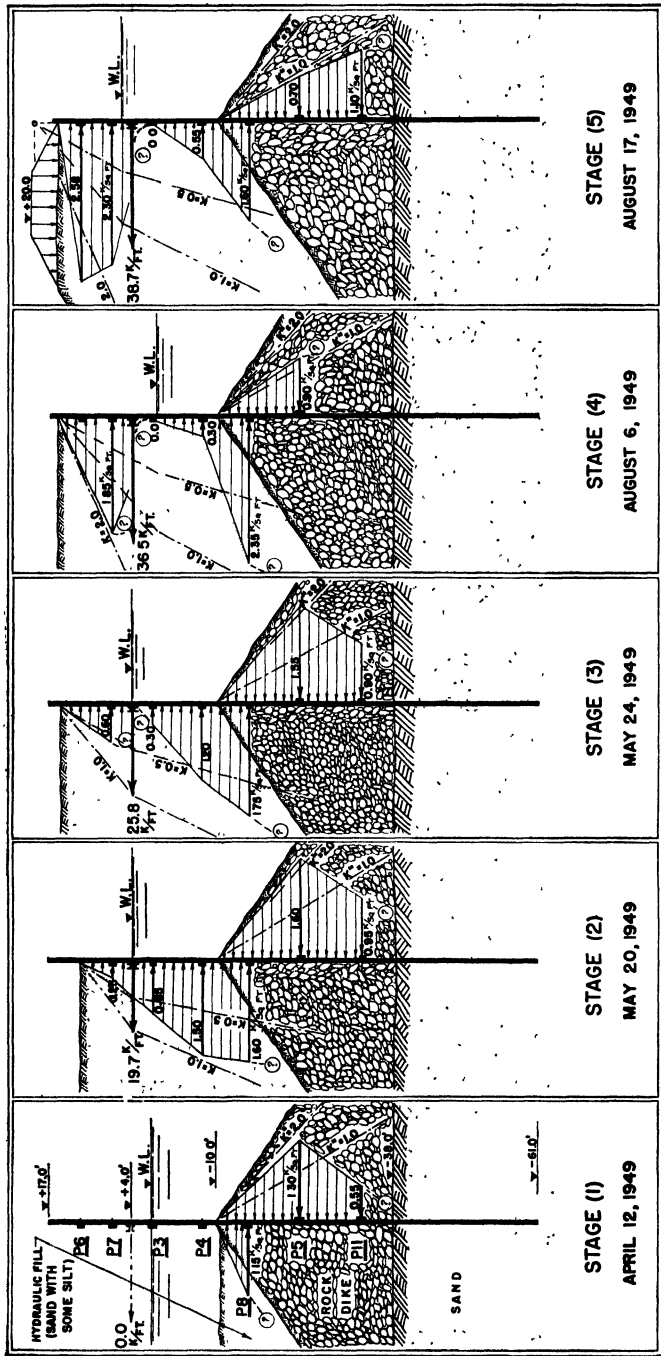
FIG. 16-27. Analysis of the Long Beach Pier C bulkhead-test data. The observed redistribution of lateral pressures after consolidation of the hydraulic fill is attributed to overloading of the anchors, which produces a tendency of the wale to move inward, with resulting accentuation of horizontal arching above the anchor level, of the type illustrated by Fig. 16-26. (*From Tschebotarioff, Ref.* 399, 1950—*discussion of C. Martin Duke's Ref.* 110, 1950.)

below the anchors. Hydraulic fill was placed up to the level of the anchors, granulated slag was placed around, and cold slag above the anchors. Stock piles of iron ore were placed on the completed fill, loading its surface to three tons per square foot. The first indication of trouble was that the outer pier leg of the craneway was found to have moved inward almost 6 in. ($5\frac{7}{16}$ in.). When the ore stock piles were removed, it was found that the fill surface had formed craters with a maximum settlement of about 3 ft at their centers. An excavation revealed that
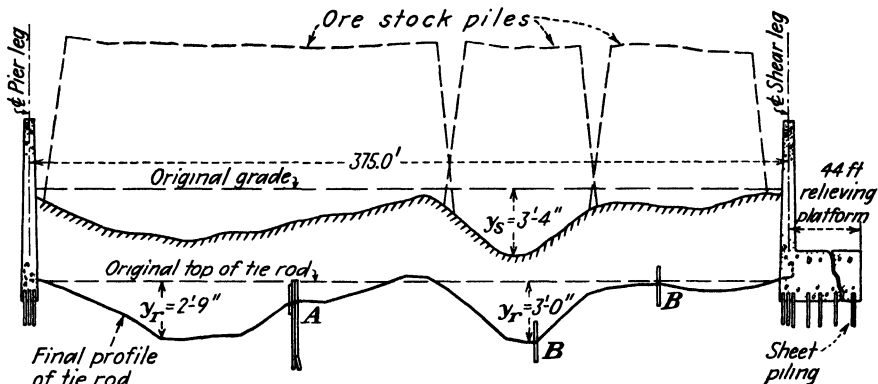
FIG. 16-28. The 3 ft differential settlement of the soil surface and of the 375-ft-long anchor tie rods of a relieving platform due to consolidation of underlying clay by the surcharge weight of ore piles. The pier leg of the overhead craneway was pulled $5\frac{7}{16}$ in. toward the shear leg which formed part of the relieving platform. (Courtesy of M. D. Ayers, Steel Company of Canada, Ltd.)

the anchors had been deflected by the same amount and in the same manner from their original elevation (see Fig. 16-28).

Something similar must have occurred at a greatly reduced scale at Long Beach Pier C. The anchors were loaded by part of the weight of the fill. This would have made them deflect somewhat and pull the wale and the bulkhead inward. Even a slight inward motion of wale and bulkhead, not exceeding a fraction of an inch, as the fill continued to consolidate, should be sufficient to induce horizontal arching of the type shown in Fig. 16-26 by the curved lines *aa*, *bb*, and *cc*. The resulting distribution of lateral pressures has a shape which only superficially resembles the shape which is assumed to correspond to conventional types of *vertical* arching (see Fig. 10-39). It will be noted from Fig. 16-27, stages 3, 4, and 5, that the pressure was zero below the anchor level. The previously customary assumptions concerning vertical arching (Fig. 10-39), by contrast, included appreciably increased pressures immediately below the anchor level, since the arching was supposed to be a product of the primary deflection of the sheet piling. However, no additional deflection

of the bulkhead was measured at Long Beach Pier C after stage 2 (Fig. 16-27) was reached. It should further be noted from Fig. 16-27 that a progressive decrease of the passive resistance pressures of the outer rock dike against cell P5 was observed during stages 2 to 5. This observation excludes any possibility of vertical arching, since the outer dike would then have to act as an outer abutment to any such vertical arches and to provide an increased resistance to their load. The observed *decrease* of the passive resistance, however, is entirely consistent with the explanation offered in Fig. 16-26, since horizontal arching above the anchor level loaded and pulled in the anchor, and through it the bulkhead, and thereby decreased the passive resistance pressures at the top of the outer dike. Finally (see Table 16-1), the conventional assumptions concerning vertical arching, as presented by the Danish rules, do not lead to any increase of the anchor pulls, as compared with the free- or fixed-earth-support methods. The Ohde method is more reasonable and leads to an increase of some 60 per cent in the anchor-pull values. However, there was an increase of 85 per cent in the anchor pull at Long Beach Pier C between stages 2 and 4, or of over 140 per cent as compared with normal assumptions. The anchors were stressed almost up to the elastic limit, and some bolts and other minor connections actually failed in places. The need to avoid overloading of the anchors by the weight of the fill is therefore apparent.

This need was recognized in Sweden, according to a communication to the author from Dr. Paul Leimdorfer, head of the Department of Quays and Docks of the Harbor Board of Stockholm. Figure 16-29 shows the special precautions which had to be taken to protect some anchors in Stockholm Harbor from overloading by the weight of the rock fill, which in some places was underlain by clay pockets. Hollow concrete boxes were placed around the anchors in a manner similar to that illustrated by Fig. 16-30. Where these precautions had not been taken, failure of some anchors had resulted. Arrangements similar to those of Fig. 16-30 were used when necessary to protect the anchors during the Princeton model tests, for instance, during the test illustrated by Fig. 10-42.

In another case, in the harbor at Dunkirk, France (see Ref. 211, 1949), recently a 200-ft-long section of a bulkhead-type quay wall suddenly slid out to sea. It was found that the anchors had failed. They were made of rolled-steel channels which showed signs of cracks, possibly caused in the first place by the impact of wartime explosions, from which rusting had spread and weakened the section further. The use of steel cables for the anchorage of bulkheads has been considered in Europe instead of more rigid profiles. Of course, the cables would have to be well protected against rusting too.

Even with these improvements, there would still remain the possibility that horizontal arching, as shown in Fig. 16-26, would develop along the lines *cc* and would greatly overload the outer row of batter piles of the anchorage. Excavations in other localities have sometimes revealed serious damage to timber piles of this type either (see A. Agatz and E. Schultze, Ref. 2, 1936) because the piles were overdriven (Art. 15-5) into the underlying sand, or because they were broken by the weight of the overlying and settling soft clay. It is therefore advisable to consider possible alternatives to the conventional type of anchorage of pile clusters
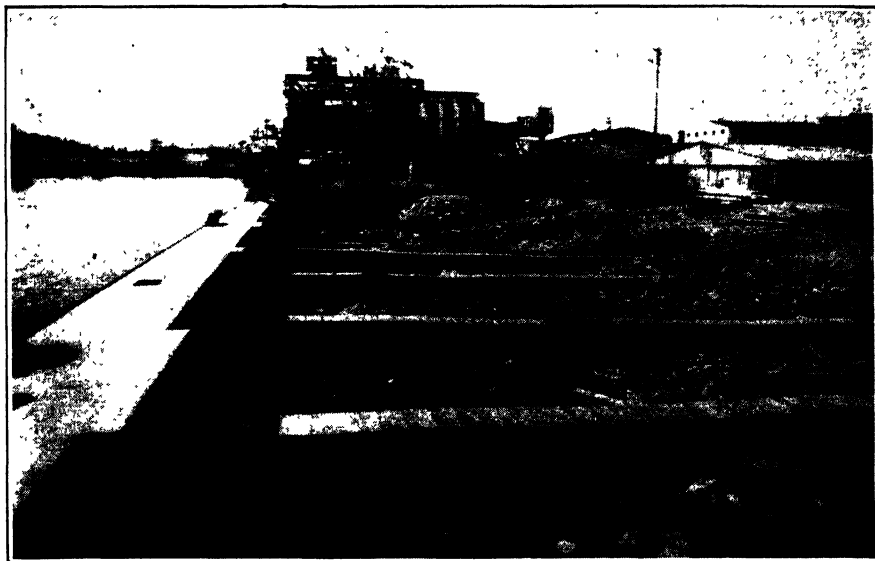
FIG. 16-29. The anchors of a bulkhead in the harbor of Stockholm, Sweden, are encased in hollow concrete boxes to protect them from overloading by the weight of the rock fill above them. *(Courtesy of Dr. Paul Leimdoerfer, Stockholm Harbor Board.)*

shown in Figs. 16-25 and 16-26. One such alternative solution would consist in anchoring the wale to the point *B* on the original harbor bottom, as shown in Fig. 16-26 by broken lines. Short batter piles, not extending above that point, could provide support there at a great economy in length of piles employed; they could be driven in as shown in Fig. 15-25(*A*). This type of support, however, would be somewhat *too* unyielding, and it has been shown, with reference to Fig. 16-24, how undesirable that is. A better solution would therefore consist in providing anchor blocks at the point *B*, either by precasting them and lowering them by a crane from barges, or by dredging a trench and filling it with tremie concrete. Precast anchor blocks were used for a different purpose in the harbor of Rio

de Janeiro (Ref. 331) and were combined with precast reinforced-concrete tie rods. The latter feature does not have any apparent advantages, but a combination of precast anchor blocks at point B in Fig. 16-26, of an inclined steel tie rod between point B and the wale, as shown by broken lines in that diagram, and of a rock or clean sand-gravel dike right up to the level and slope of the inclined tie rod might provide a rational solution in many cases of doubtful backfills. The outer dike could be dispensed with, if necessary, if the dredging and backfilling arrangement at the toe of the bulkhead shown in Fig. 16-25 is used.
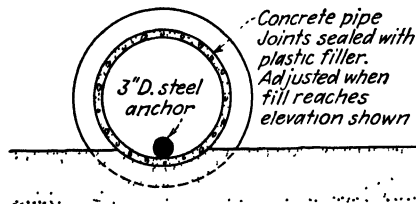
FIG. 16-30. Possible way of protecting anchors against overloading by later settlements of fill.

A result completely different from that at Long Beach Pier C was obtained on a Pacific island (Ref. 255, 1949) under different soil conditions. Measurements were performed by means of Carlson strain meters of anchor pulls on a steel sheet-pile bulkhead of the "sunk" type, that is, the sheeting was driven in and anchored first, whereupon the soil was dredged out on the harbor side of the sheeting. The soil was compact coral sand which probably was somewhat cemented, although this did not show up on any of the disturbed samples extracted. The anchor pulls were found to be stressed only from 5,900 psi to a maximum of 8,100 psi, that is, to less than 48 per cent of the stresses anticipated on the strength of computations of the conventional type. A surcharge of 0.6 ton per ft² over a 200-ft² area increased the anchor pulls by only 4 per cent.

The need for further systematic regional studies of different possible combinations of soil types is therefore apparent, in spite of the considerable progress already achieved.

16-15. Bulkheads Combined with Relieving Platforms. This type of quay-wall construction is employed to deal with heavy surcharges which would otherwise produce excessive lateral pressures against the sheet piling. A massive platform is supported by timber or reinforced-concrete piles and relieves the sheet piling of the bulkhead from the lateral-pressure effects of loads above the level of the platform. Hence its name.

Figure 16-21 illustrates the type of massive concrete blocks on timber piles which were used before the advent of reinforced concrete half a century ago. The sheet piling, placed on the land side of the platform in Fig. 16-21, sometimes is placed in the same manner in modern structures, since the soil may then be left to slope from dredge level upward under the relieving platform. In sand the point of contraflexure may be taken at

one-half of the height h_l of the slope (Ref. 397) for design in connection with Fig. 16-23(I). The depth of embedment beneath that point, however, should be then determined without making any allowance for the beneficial effects of wall friction, since the outward tilting of the platform may slightly tend to pull the sheeting out of the ground (see Art. 10-5).

If timber piles are used to support the relieving platform in waters infested with marine borers (Art. 15-5), then the sheet-pile bulkhead should be made of reinforced concrete or of steel, should be placed on
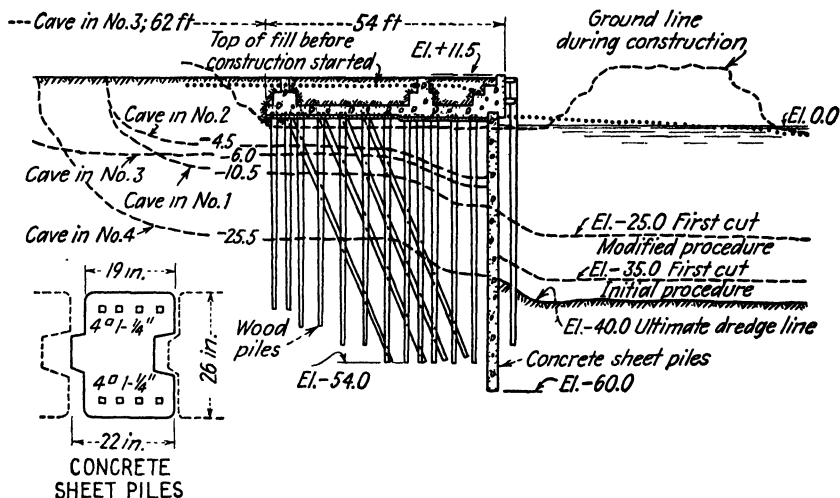
FIG. 16-31. Heavy relieving platform on wood piles with reinforced-concrete sheet-pile bulkhead of the sunk-wall type. Fine sand leaked through gaps between sheet piles, causing cave-ins, until repairs were made. (*After J. C. Gebhard, Ref.* 145, 1948.)

the water side of the platform, and should be backfilled, since the borers do not penetrate into the voids of sand.

Figure 16-31 is an example of such construction. It is a heavy relieving platform of the *sunk-wall* type, that is, the piling was not backfilled but was driven (sunk) into existing soil, which was then dredged out on the water side. In the case illustrated by Fig. 16-31 a 3,000-ft-long quay wall had to be built across an indentation in the harbor shore line and backfilled to provide a wharf and increase the land area behind it (Ref. 145). To that end, a wide sand dike was first constructed on the line of the quay wall to el. +11 ft, as shown in Fig. 16-31. The average depth of the original sandy bottom was at el. −20 ft. The dike material (fine uniform sand) was placed hydraulically by dredging and pumping from the bottom of the bay. The untreated wood piles and the reinforced-concrete sheet piles were then jetted and driven into the sand to the desired elevation, and the reinforced-concrete relieving platform was

built over them. All joints between the sheet piles were cleared of sand by a water jet and were pumped full of cement grout. The portion of the sand dike on the outer (water) side of the sheet piling was then dredged away by a suction dredge.

During the first stage of construction the dredging was advanced almost to the full depth desired. This, however, appeared to induce excessive deflections of the exposed sheet piling relative to the adjoining units still fully embedded in the sand. The grout in the joints between the sheet piles was damaged thereby, so that the fine sand trickled out through the openings (see Fig. 5-10). The resultant cave-ins behind the relieving platform, shown in Fig. 16-31, extended well beyond the usual natural 1:2 slope of such sand. This may be attributed to the action of seepage forces induced by the suction of the dredge. During the second stage of construction the procedure was changed. Dredging was done in steps, and joints were inspected by divers and regrouted if necessary. The suction cutter head of the dredge was kept at least 25 ft away from the sheet piling. No further trouble was encountered. The sheet piling was somewhat overdesigned (see Prob. 16-6 and compare with Prob. 16-7).

FIG. 16-32. Section of C. & N. wharf at Copenhagen (see Fig. 16-51). (After J. Brinch Hansen, Refs. 166 and 168, 1946.)

A light type of reinforced-concrete wharf developed by the Danish firm Christiani & Nielsen, the C. & N. wharf, is illustrated in Fig. 16-32. The lateral pressures against the sheet piling were computed in accordance with the Danish rules (Art. 16-12). This type of wharf design has the advantage that the reinforced-concrete sheet piling supports part of the relieving platform. The resulting axial load decreases the tension in the reinforcing steel caused by bending stresses due to lateral earth pressure. Another advantage is provided by the load of the relieving platform on the rear anchor piles, which reduces the tension in pile T of Fig. 16-32. A large number of similar wharves have been built (Ref. 166).

Problem 16-7 gives an example of check computations of the wharf illustrated in Fig. 16-32 for lateral pressures determined in accordance with the results of the Princeton bulkhead tests and the corresponding

design recommendations of Art. 16-14. The resulting stresses are only slightly higher than customary and are entirely sufficient for stability and safety. A comparison with the results of a similar computation (Prob. 16-6) applied to the heavy conventional type of wharf (Fig. 16-31) illustrates the possibility of appreciable economies in this field of design and of construction with full assurance of safety, as a result of latest research. It should be noted that the C. & N. type of light wharf, of which Fig. 16-32 is representative, has a number of advantages, apparent from the study of Prob. 16-7. It was originally patented in Denmark, Norway, Sweden, Germany, and Russia, but the validity of the patents appears to have expired long ago.
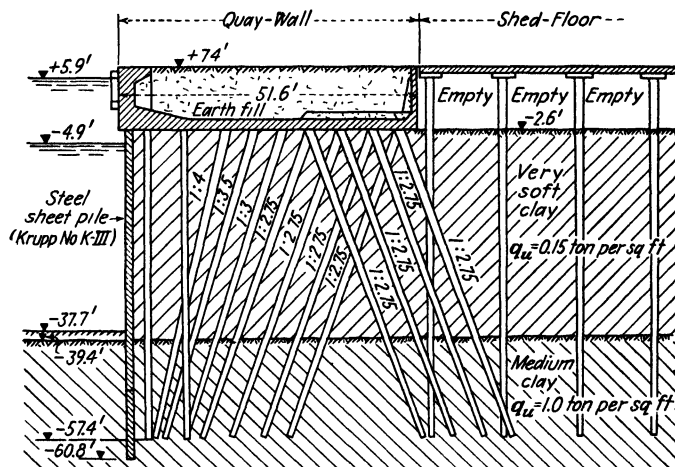
FIG. 16-33. Section of quay wall and shed floor at Bangkok, Siam. (After J. Brinch Hansen, Refs. 166 and 167, 1946.)

Figure 16-33 illustrates a heavy cellular reinforced-concrete relieving platform on timber piles driven into medium clay (q_u = 1.0 ton per ft^2) through very soft clay (q_u = 0.15 ton per ft^2); steel sheet piling was used. The cells of the relieving platform were filled with earth to weigh down the tension timber piles with reversed batter, but the space beneath the floor of the adjoining shed was left empty, so as to relieve the lateral pressure of the soft clay against these piles. The lateral pressures exerted by the soft clay were assumed to be resisted partly by the steel sheet piling and partly by the timber piles beneath the platform. The computed bending moment was distributed between them in proportion to their relative flexibility, as expressed by the EI values of the steel sheet piles and of the timber piles; E is the Young modulus of the material, and I the moment of inertia of the cross section of the piles. The length of the piles, which is a third factor affecting their flexibility, is the same for both

types of piles and could therefore be disregarded. The above appears reasonable and can be used in other similar cases in clay soils as a first approximation, in view of the lack of more precise data.

The method which was used by A. E. Bretting on this job to determine the value of the lateral pressures (Ref. 167), however, is questionable. It consisted in assuming that the sliding surfaces form angles of 45° with the horizontal. Equations of equilibrium for each such inclined soil element were established by considering its deformations in relation to the deflection of the wall. A system of simultaneous equations is thus obtained which involves the use of the ultimate shearing strength of the clay and of its modulus of elasticity in shear. A reasonably accurate evaluation of this latter soil coefficient, however, does not appear practicable (Ref. 397). It is difficult enough to determine in the laboratory the correct strength at failure of a clay, but it is much more difficult to obtain reliable values of the modulus of elasticity in shear which would actually correspond to the condition of the soil in situ. It should be remembered in this connection that the driving of numerous piles for the relieving platform (Fig. 16-33) would remold the clay to an unknown extent. Problem 16-8, however, shows that an analysis of the sheet piling in accordance with the recommendations of Art. 16-14 indicates high stresses which nevertheless are sufficient for stability if the relieving action of the timber piles is taken into account.

Several methods have been developed for the estimation of the axial load distribution in a pile group among individual batter piles of different or of identical batter. Most of these methods are graphical (see Ref. 415). In the case of a relieving platform all the pile loads should be axial, since no lateral support can be provided by the soil surrounding the piles.

A somewhat similar problem is presented by the anchorage of a suspension bridge when the anchor block is supported by piles. The front row of batter piles will receive some lateral support from the soil before it, up to the limit of the resistance to bending of that pile row or of the shear strength of the soil. The extent to which the subsequent inner rows of piles will receive lateral support will depend on the nature of the soil. If the soil is clay, its support of the inner rows of piles may be insignificant, as compared with the outer row, and should be neglected, since the clay around the piles is likely to be weakened by remolding due to pile driving and by the swelling and expansion which would follow the excavation for the anchor block above it. In any case, it is just as fallacious and dangerous to compute the total resistance of a pile foundation to lateral bending, or its displacements, by adding the resistances, or displacements, of single test piles or of small groups of test piles, as this is in the case of vertical loading (see Art. 15-3).

16-16. Caisson Types of Earth-retaining Structures. This type of construction has considerable advantages in marine and waterfront work. A reinforced-concrete caisson of cellular design is built at a convenient location, floated, towed to the place of the new structure, and then filled with water to make it sink over the exact spot designated for it. Other caissons are then placed in the same manner next to it to form a continuous wall or to act as piers for intermediate cellular-type girders (Fig. 13-18).

Frequently part of the soft natural bottom is dredged away and the trench filled with sand, as shown in Fig. 16-34, forming a mattress *efgi* to distribute the load of the caisson on the underlying soil. When the latter consists of soft mud, the mattress has in some cases been made 20 ft thick. In addition, a temporary sand dike of a height reaching above the final ground level at the wharf has been used sometimes to consolidate by its weight the soft mud beneath the future wharf and to increase thereby the shearing strength of the soil.
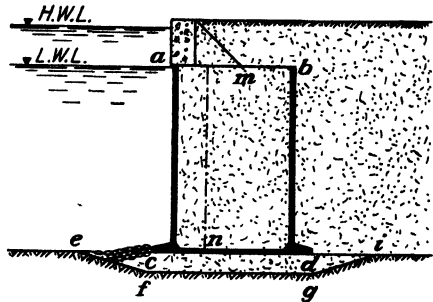
FIG. 16-34. Cellular reinforced-concrete caisson type of quay wall.

This was successfully done at Rotterdam, Holland, and at Sourabaya, Belawan, and Samarang in the Dutch Indies (Ref. 331).

The use of a thin *sand mattress* is frequently advisable even over a bed of stiffer clay if it is sensitive to remolding (Art. 7-22). An edge of the caisson usually comes first into contact with the bottom and is liable to create there a momentary concentration of pressures sufficient to remold and to thereby weaken the clay. Such local but progressively spreading remolding may also develop in the case of rocks dumped on the bottom for a sea wall. A sand mattress distributes over the clay all pressure concentrations at the sand surface and preserves thereby the natural structure of the underlying clay.

The caissons are usually built of reinforced concrete on land and are launched from slipways in the same manner as are ships. They must be designed to have floating stability at all stages, and the walls of the caissons are designed to resist the stresses during launching and floating. In a few cases the caissons are built in drydocks and are floated out after completion. In the case of the harbor at Gdynia, Poland (Ref. 331), economies were achieved by building caissons directly on the ground along the edge of a sand bar which had to be dredged away as part of the harbor development. Expensive launching arrangements could be dispensed

with, as a result, and the caissons were floated simply by pumping the sand away from around and beneath them by means of the suction heads of hydraulic dredges.

The walls of the caisson cells vary from 6 to 12 in. in thickness. Apart from launching and floating stresses, they should resist lateral pressures of the sand with which the cells are filled once the caisson is in place. On the water side they should, in addition, resist pressures engendered by the impact of waves and of ships. Wave pressures vary considerably at different locations. Thus in the British Isles (Ref. 331) measurements showed a maximum wave pressure of 3.5 tons per ft^2 at Dunbar and a low of 1.0 ton per ft^2 at the comparatively sheltered Penzance. On the Great Lakes of North America the maximum intensity of wave pressure seldom exceeds 1.0 ton per ft^2. A method for the estimation of the intensity and of the distribution of wave pressures has been given by Molitor (Ref. 233, 1935).

The need for a thicker wall of the caisson on the water side, *ac* in Fig. 16-34, is sometimes met by providing a second thin wall *mn* and then filling the space between it and the outer wall *ac* with concrete, once the caisson is in place. A considerable variety of designs of the caisson itself and of its superstructure is possible (see Stroyer, Ref. 331).

Once the caisson is in place, is filled with sand and/or concrete, and is backfilled, it acts essentially as a massive gravity retaining wall.

16-17. Cofferdams. The name *cofferdam* is given to a wide variety of temporary structures employed for the purpose of keeping water and earth out of excavations necessary for the construction of permanent structures.

One of the simplest types of cofferdam is illustrated in Fig. 16-35(I). It consists of a single wall of sheet piling driven in the form of a box within which the foundation can be constructed in the dry once the water is pumped out from the interior of the cofferdam. This particular illustration refers to a river pier of a bridge in shallow water, up to 30 or 35 ft. The rows of struts and their wales are designed to resist the full lateral water pressure. The lower row (3) is sometimes made of reinforced concrete and is left embedded in the pier foundation. The sheet piling is usually steel of the deep web type (Art. 15-11), of a section chosen to resist bending as a beam spanning vertically the distance between the wales of adjacent rows of struts. After the pier is completed the sheet piling is removed either by pulling it from the ground or by cutting it at the level *AA* of the bottom. Pulling the full length of the piling for the purpose of re-using it is seldom possible if the concrete adheres to it over part of its length. Divers and special torches are used for underwater cutting.

The depth d to which the sheet piling is driven into the ground below the level CC of the excavation inside of the cofferdam should be sufficient to ensure stability of the bottom of that excavation. If the soil is sand to a considerable depth, the greatest danger will be that of a quick condition (Art. 14-9) as a result of the unwatering of the cofferdam. This danger will be decreased by a greater length d of the sheet piles, since this will increase the length of the paths of percolating water. The exact length of d can be determined by trial, where a flow net (Art. 5-3) is constructed for each trial value of the depth d selected. Seepage into the cofferdam may be strongly reduced if a slightly less pervious layer is located at the elevation BB of the pile points. If the entire soil to a considerable depth is composed of plastic clay, then the stability of the bottom of the excavation against shear failure and upward heaving should be investigated (see Art. 14-6). In some cases it may prove advisable to place the pier on piles if a stiffer layer is available deeper down. In such an event the sheet piles of the cofferdam are driven first, and then the piles are driven with the help of followers (Art. 15-14) inside of the cofferdam, prior to its unwatering, down to the desired elevation, which is usually chosen somewhat below the mud line. The struts and wales of the inner bracing of the cofferdam are then placed, the cofferdam is unwatered and excavated somewhat below the pile heads, and the pier is concreted. If the water is deep, the use of such cofferdams may become uneconomical. The piers are then founded on caissons of various types (see Art. 15-14).

Frequently the width of the excavation is such that it is not practicable to brace one wall of the cofferdam against the wall on the other side of the excavation. It is then necessary to resort to self-supporting cofferdam walls, some types of which are shown in Fig. 16-35(II), (III), and (IV). If the new structure is a dam across a river, then the procedure illustrated by Fig. 16-36 is employed, unless it is possible to temporarily divert the whole river into a new channel, which is only practicable with some small rivers. In the case of large rivers construction in stages becomes necessary. A cofferdam is built next to one of the river banks, as shown in Fig. 16-36(I). The enclosed space is unwatered, so that excavation may proceed to the desired level. A section of the dam is then built in the dry within the enclosure, whereupon the cofferdam is removed and transferred to the other bank [Fig. 16-36(II)], where the whole operation is repeated. Sometimes more than two construction stages are necessary in order to keep a sufficiently large section of the river channel open before the dam is completed [Fig. 16-36(III)].

The cofferdams temporarily block off part of the river channel, so that the velocity of the flow of water is increased in the open part, especially next to the cofferdam, where the flow lines squeeze themselves together,

as sketched in Fig. 16-36. Scouring of the river bottom is then possible, especially near the corners A, B, F, and G of the cofferdams, as shown in Fig. 16-36, which should therefore be given a streamlined shape (Ref. 429).

The type of cofferdam cross section indicated in Fig. 16-35(II) is essentially a small dam and is designed along the same general lines (see Art. 17-5). This cofferdam section is not suitable for use in rivers with rapid currents or with floods which may top the cofferdam, since it is susceptible to destruction by scour.
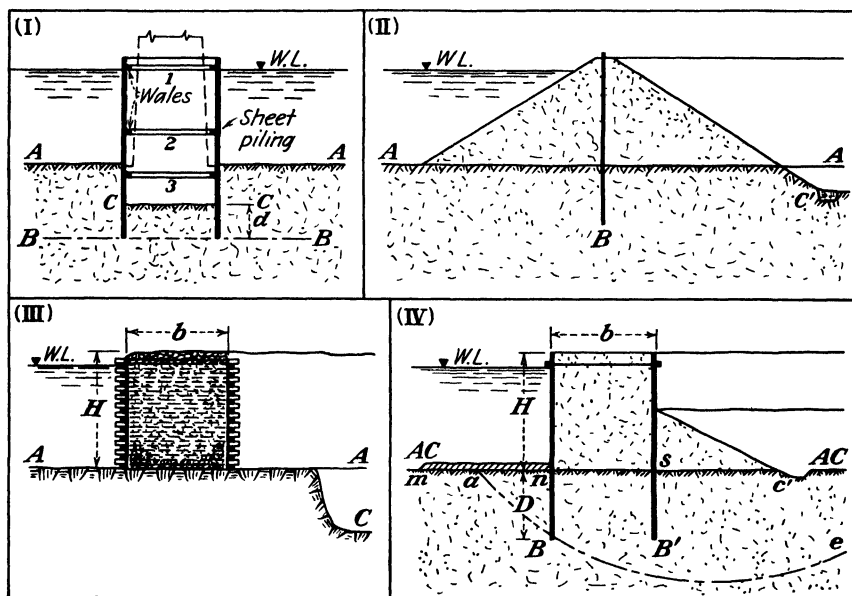
FIG. 16-35. Some types of cofferdams.

The *timber-crib* type of cofferdam section illustrated in Fig. 16-35(III), on the other hand, may be well used in rivers with rapid current and is particularly suited to rivers with rocky bottoms. The lower part of the timber frame is made on land and may be "tailored" to fit the contours of the rock surface. After launching, the timber-frame cells are built up to their full height, are towed out to the position they are to occupy in the completed cofferdam, and are sunk by filling with rock ballast and with soil to decrease seepage; sometimes additional sheeting is used. The completed block acts as a gravity dam, and its resistance to overturning and sliding is analyzed in the same manner as is done for gravity retaining walls (Art. 16-2). In the case of large cofferdams the cribs are composed of more than one cell. The timbering of each cell is designed to resist the lateral pressures of its fill. These pressures are estimated in the same way

as the pressures in bins (Ref. 429 and Art. 10-15). In the case of the Bonneville Dam (Ref. 429) the individual crib pockets or cells had a maximum size of 12 by 12 ft. The maximum height H of the Bonneville cofferdam was 65 ft, its maximum width b was 60 ft = $0.9H$. This appears to be the highest cofferdam of this type.

Figure 16-35(IV) gives a section of the so-called *double-walled sheet-pile cofferdam* type. It is used when the river bottom is composed of sand or of clay. Two rows of steel sheet piles are driven parallel to each other and are tied by anchors and wales. Each row acts similarly to single-walled anchored sheet-pile bulkheads. But the anchored sheet piles now have to resist not only the active lateral earth pressures exerted by the fill placed between the two rows of piling, but also the overturning forces of
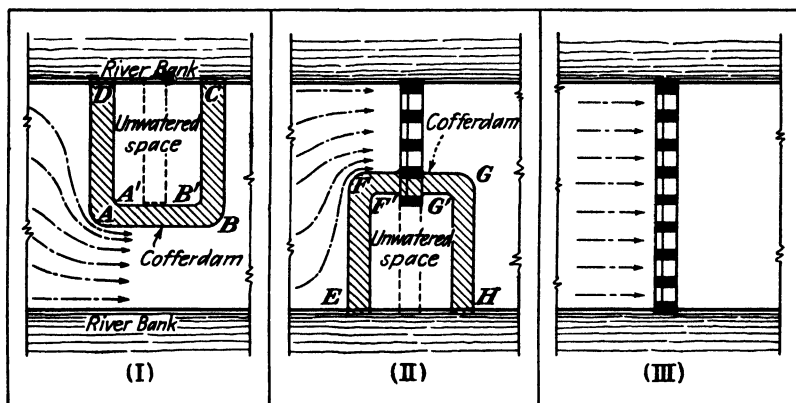
FIG. 16-36. The use of cofferdams for the construction in stages of a permanent dam across a large river.

the water after unwatering of the cofferdam. If the soil is sand, seepage forces may strongly affect the stability of a cofferdam (Ref. 429), and a complete flow-net analysis is advisable. A horizontal clay blanket mn placed on the outer (water) side on the river bottom may strongly reduce seepage while active, but it is not reliable if any scour is likely to occur. Inner berms with adjoining drainage ditch C, as shown in Fig. 16-35(IV), are helpful in reducing the danger of a quick condition and are used whenever there is space for their construction. Otherwise the width b of the double-walled cofferdam has to be made almost equal to its height H, and the depth of penetration D of the sheet piling may have to equal $0.65H$ (Ref. 364). If the soil is clay, the stability analysis should include a study of the safety against shearing rupture of the clay along various possible curved surfaces of sliding, such as ae.

The conventional type of analysis of the forces acting on the sheet pil-

ing, as used in Europe, is given by Packshaw (Ref. 364, 1945). Model tests have been made by Rimstad (Ref. 290, 1940), but much remains to be learned yet about the actual performance of such cofferdams which are still designed largely upon the empirical basis of previous experience. The same holds true for a type of double-walled cofferdam, the *cellular cofferdam*, which has been developed in the United States. Figure 16-37 illustrates the circular type of cells used for the cellular cofferdam which enclosed during its construction the Kentucky Dam of the Tennessee
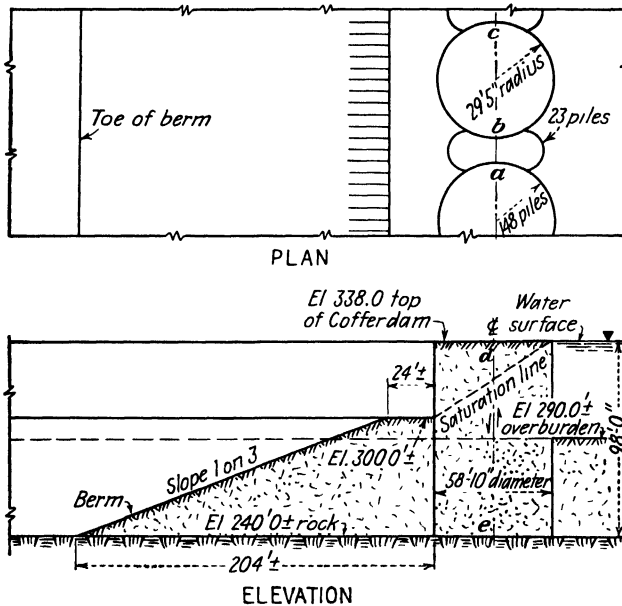
FIG. 16-37. Cellular cofferdam used for the construction of the Kentucky Dam, Tennessee Valley Authority. (After Colburn, Ref. 77, 1945.)

Valley Authority. With a total height of 98 ft this is the highest cofferdam built so far. The use of an inner berm permitted a small diameter of the cells equal to $0.59H$. Freely supported cofferdams usually have a width of the cells equal to $0.85H$ or $1.00H$.

The first cellular cofferdam was constructed in 1910 for the raising of the battleship *Maine* from the bottom of Havana Harbor in 35 ft of water. The underlying soil and the fill in the cells was clay, so that the cofferdam began to tilt dangerously when the water level was lowered by 15 ft. It had to be braced against the hull of the ship before unwatering could be successfully completed (Ref. 364).

The vast majority of the cellular cofferdams constructed so far either reach down to rock or are embedded in sand. The fill usually is selected

to be of a granular and noncohesive character. The radial lateral outward pressures of the fill in the cells induce tensile stresses in the sheet piling. Accordingly, straight-web sections with high interlock strength such as M112 (see Art. 15-11) are employed in cellular cofferdams, whereas in double-wall cofferdams [Fig. 16-35(IV)] the sheet piles have to resist bending, so that arch-web sections with high values of their section moduli have to be employed.

It has been customary to analyze a cellular cofferdam resting on rock as a gravity retaining wall, specifically with respect to its resistance against sliding along its base and against overturning. TVA engineers and Terzaghi (Ref. 364, 1945) have shown that, in addition, the possibility of shear failure of the fill along vertical planes should be studied, since in some cases it may prove to be the governing factor. The resistance to sliding of sheet piles along their interlocks *a*, *b*, and *c* (Fig. 16-37) should be added to the shearing resistance of the soil along the vertical plane *de*. The interlock friction is a function of the interlock tension; according to Terzaghi's analysis (Ref. 364, 1945), it may increase the total shearing resistance along vertical planes by some 50 per cent, so that the presence of transversal sheet-pile wall sections should constitute an important advantage of the cellular type of cofferdam as compared with the plain double-wall type. Lubrication of the locks should be avoided, even though it facilitates pulling of the sheet piles for re-use. Since the use of berms may decrease somewhat the interlock tension along the plane *de* and, hence, the interlock friction and resistance to sliding along that plane, differences of opinion exist (Ref. 364) concerning the advantages of using such berms in connection with cellular cofferdams.

When the sheet piles of the cofferdam are driven into sand, the upward seepage pressures of the percolating water may decrease the passive resistance of the sand along the inner face sB' [Fig. 16-35(IV) and Art. 14-9] of the inner row of sheet piling, unless berms with drainage ditches C' to lengthen and flatten the paths of percolation, or similar measures, are used for cellular cofferdams as well as for double-wall cofferdams, to which Fig. 16-35(IV) refers. White and Prentis (Ref. 429, 1940) report some cofferdam failures on the Mississippi River which were caused by the absence of measures to counteract the detrimental effects of seepage forces. Inner corners are particularly dangerous in this respect, since flow lines converging on the corner from two directions at right angles to each other squeeze themselves closely together there, with a resulting increase in the velocity of flow (Art. 5-4).

The preceding discussion gives only an outline of the most essential points to be considered when designing cellular cofferdams. For further details see Terzaghi's paper (Ref. 364, 1945) and discussions thereof (Ref.

77). Much further useful experimental research can be performed in this field.

Design modifications, such as supplementary berms, riprap blankets, or cable anchorages sometimes have to be introduced as construction proceeds and observations reveal weak points. Careful continuous field-control measurements are therefore essential. The circular cells of cellular cofferdams usually act as individual self-supporting units. This has many practical advantages during construction and in the case of local failures due to interlocks being damaged by faulty driving or to other causes.
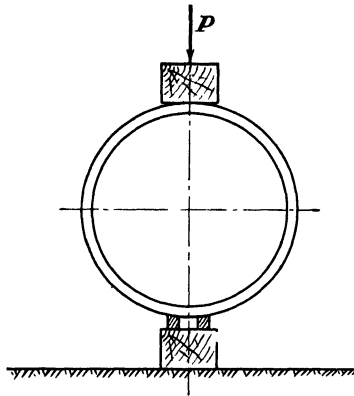
FIG. 16-38. The three-edge bearing method for laboratory tests of pipes. (*After Spangler, Ref.* 320, 1948.)

16-18. Underground Conduits. The most unfavorable loading of a conduit pipe is produced by two concentrated and opposite forces acting along a pipe diameter; the bending moments in the walls of the pipe are then at a maximum. On the other hand, radially acting pressures when distributed uniformly all around the pipe produce the most favorable type of loading, since bending moments are then equal to zero and only compressive stresses are engendered in the walls of the pipe.

The so-called three-edge bearing method of laboratory test illustrated by Fig. 16-38 represents a loading condition very closely approaching the
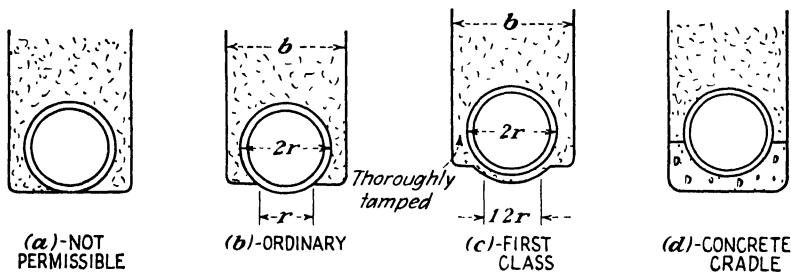
FIG. 16-39. Types of bedding for sewers and other ditch conduits. (*After Spangler, Ref.* 320, 1948.)

most unfavorable one and is likely to produce greater stresses in the pipe than any of the four types of bedding illustrated by Fig. 16-39. The increase of the bearing area in bedding type *b* decreases the bending moments somewhat; this is even more true in type *c* where thorough compaction of the backfill tends to increase lateral pressures. The reason for

this is as follows: Under the weight of the fill the pipe is compressed in the vertical direction, and its originally circular cross section acquires an elliptical shape, as illustrated by section AA of Fig. 16-40. The vertical diameter is shortened, whereas the horizontal diameter is lengthened, because of the tendency of the pipe to bulge out laterally. The lateral displacement of the adjoining soil induced by this deformation increases the lateral pressures against the pipe beyond the active and the neutral
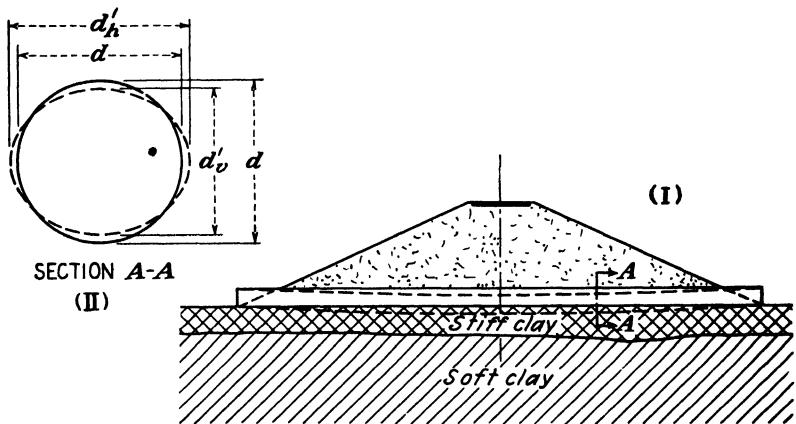
FIG. 16-40. The transversal and the longitudinal deformations of a conduit.

values. A condition of passive resistance is thus created (see Art. 10-1). No precise numerical relationship between the lateral yield of pipes and the increase of the passive resistance of different types of soils has yet been established. On the strength of tests carried out at the Iowa State College, Spangler (Ref. 320, 1948) recommends the increase of the ultimate load that a pipe may carry, as compared with the value deter-

TABLE 16-2. Load Factors for Different Types of Conduit Supports

Bearing Type as in Fig. 16-38	Load Factor L_f
a	1.1
b	1.5
c	1.9
d	2.2–3.4

mined by the three-edge bearing test, by multiplying the latter with the so-called *load factor* values shown in Table 16-2.

In the case of *trench conduits* and bedding of types a and b Eq. (10-43) should be used to determine the vertical load W which the pipe has to carry. If the soil has been well tamped on both sides of the pipe, then the trench width b can be replaced in Eq. (10-43) by the outer diameter

$2r$ of the pipe to give

$$W = \gamma(2r)^2C_d \tag{16-23}$$

To resist this loading a pipe should be selected with an ultimate failure strength P under a three-edge bearing test equal to

$$P = \frac{WF_s}{L_f} \tag{16-24}$$

where F_s = factor of safety selected
L_f = load factor, from Table 16-2
C_d = a coefficient, defined in Art. 10-21 and Fig. 10-48

The above theoretical analysis, as developed by Dean Marston and Spangler, appears to be well substantiated by actual observations and experimental data in so far as the performance of thick-walled conduits in trenches is concerned. The numerical accuracy of the analysis of thick-walled conduits below embankments, as developed by these authors (Ref. 320), however, appears to be much less certain.

If the embankment fill around and above a conduit is loose, then the compression of a layer of thickness $2r$ may be greater than the decrease of the vertical diameter of the conduit under the same load. In that case the picture of load redistribution given in Fig. 10-47 for a trench may be reversed, and not only will the conduit have to carry the full weight of the overburden above it, but some of the weight of the surrounding soil may be transferred to it by what is sometimes called *negative friction*. The term is used in a similar problem of end-bearing piles driven through soft soil which consolidates further under its own weight (Art. 15-2). This problem of frictional load transfer along vertical planes between two materials of different compressibilities does not yet lend itself to practically usable numerical evaluations. It is therefore advisable to prevent the development of such undesirable increases of load on the conduit by suitable construction operations along the lines indicated in Fig. 16-41. The pipe is laid in a prepared bed of compacted soil partly below the level of the natural soil. Selected granular material A is thoroughly rolled and compacted on both sides of the pipe to an elevation reaching somewhat above the top of the pipe. The space B immediately next to the pipe is compacted by mechanical tamping (Art. 11-4). The space C is filled by loosely dumped soil, and the space D is subjected to normal embankment-compaction procedure. A condition partially resembling the trench bedding is thereby created.

Flexible pipes appear to bear up particularly well under heavy loading if the surrounding fill is granular. O. K. Peck and R. B. Peck (Ref. 261, 1948) have reported the results of a survey of the performance of 18

flexible corrugated steel-pipe culverts under railway embankments with depths of overburden (selected granular fill) reaching up to 50 ft. The satisfactory performance of these culverts indicated that a state of approximately equal all-around pressures must have been reached as a result of deformations similar to those illustrated by section AA of Fig. 16-40. Some of the compaction measures suggested in Fig. 16-41 were used in a few cases. The measured shortening of the vertical diameter of these culverts varied considerably but did not exceed 7.1 per cent.

When the depth of the overburden is 50 ft (Ref. 261), its weight can be assumed to equal $50 \times 120 = 6{,}000$ lb per ft². Assuming a uniform all-around pressure distribution of the above intensity against the 10-ft-
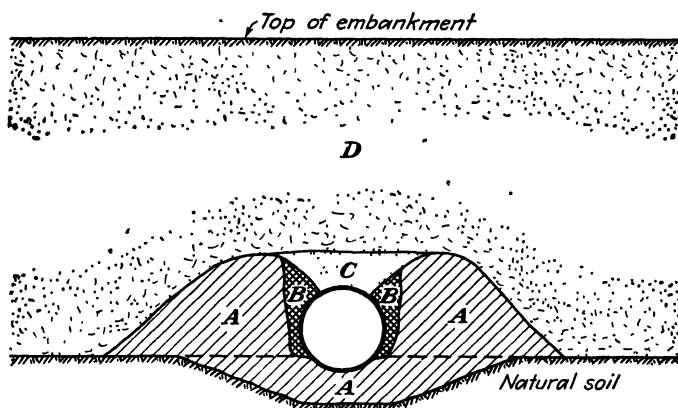
FIG. 16-41. Recommended procedure for the construction of embankments over conduits. (After O. K. Peck and R. B. Peck, Ref. 261, 1948.)

diameter culvert, we obtain a value of $6{,}000 \times {}^{10}\!/_2 = 30{,}000$ lb compressive force per foot length of each of the two walls of the culvert. The method of computation is identical with that employed for the determination of tensile stresses in the walls of a boiler. The metal-wall thickness of this culvert was 0.2813 in., giving a cross-sectional area of 3.37 in.² and a unit compressive stress in the steel of $30{,}000/3.37 = 8{,}800$ psi. This is, of course, only a very rough estimation for a hypothetical load distribution, and much more work, including more precise field measurements, will be needed before the design of such culverts can be placed on a fully reliable and rational basis.

When the soil beneath the embankment is composed of soft clay, settlements of the original ground surface may be induced by the consolidation of the clay under the weight of the embankment. As a result, the conduit will be deformed longitudinally, as shown in Fig. 16-40, since the settlements will be greatest beneath the center of the embankment. In some

such cases it is advisable to provide flexible joints between the longitudinal sections of pipe.

When pipe conduits are laid just beneath the ground surface over mud or very soft clay, their support on piles may become necessary (Ref. 13).

16-19. Tunnels. The methods of tunneling depend on the nature of the rock or of the soil which the tunnel has to pierce. Preliminary geological studies are essential (Ref. 416), in addition to soil engineering investigations. If the rock is entirely sound no special supports may be required to carry the weight of the tunnel roof during construction. On the other hand, elaborate precautions and a special sequence of construction operations may be necessary if preliminary geological advice indicates that the rock is shattered or that other hazards are to be expected. Figure 16-42 illustrates the construction procedure which was employed for the short (540 ft) but record-width (79 ft at the springline) tunnel through the shattered interbedded sandstones and shales of Yerba Buena Island, connecting the two parts of the San Francisco–Oakland Bay Bridge. Similar procedures are employed when tunneling through other weakened types of rocks.

First of all, as shown in Fig. 16-42(*A*), a small pilot tunnel ("monkey drift") is advanced at the crown. This has the advantage of permitting the consulting geologists, who should always be present on important jobs of this type, to verify, as the work progresses, the preliminary evaluations of the state of the rock which they had made from core-drill borings and surface examination of the geology of the site. Necessary changes of construction procedure can then be made in time. Side-wall drifts are advanced shortly after.

During the next stage, illustrated by Fig. 16-42(*B*), the concrete side walls are built, and the roof is excavated in shallow sections which are temporarily braced against the central rock core left intact for that purpose.

Finally, as shown in Fig. 16-42(*C*), the concrete of the roof arch is placed either by gravity from the center "monkey drift" or by forced pumping. Additional grouting of spaces between the lining and the rock and of the rock seams is sometimes resorted to.

As a last step, the rock core is removed. Many modifications in the details of the above procedure are possible, of course, depending on local conditions.

The estimation of the rock pressures exerted against the tunnel lining is still largely a question of guesswork based on previous experience with the satisfactory, or otherwise, performance of linings in similar rock formations, although attempts at numerical analysis of stress conditions around a tunnel shaft have been made (Ref. 184).

When tunneling through stiff clay, procedures similar to those in rock, as illustrated by Fig. 16-42, have frequently been employed. They are usually referred to as the *liner-plate method*, since light liner plates, strengthened by steel arch ribs, are installed to support the clay prior to the concreting of the permanent lining. The two factors on which the success of this method depends are the shearing strength of the clay and the width of the tunnel. The unit pressure over the width b of the continuous footing for the temporary lining (see Fig. 16-42, where this value
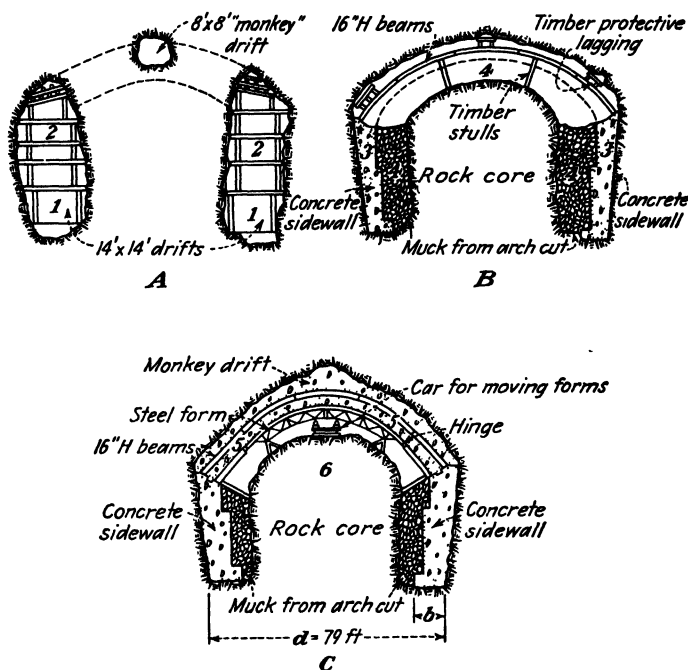
FIG. 16-42. The sequence of the construction operations, Yerba Buena Tunnel. (After Carlton S. Proctor, Ref. 278, 1938.)

refers to the permanent lining) increases with the value of the diameter d of the tunnel. If this unit pressure of the footing becomes excessive, as compared with the shearing strength of the clay (Art. 9-9), excessive settlements of the footing will follow and may even lead to a shear failure and upward squeezing of the underlying clay when the central clay core of the tunnel is removed. Considerable loss of ground would then result, that is, more clay would be removed than corresponds to the volume of the tunnel. This would be accompanied by uneven settlements of the ground surface and by damage to structures erected thereon.

The use of compressed air during construction may partially relieve

the clay pressures transmitted to the temporary footing and permit the installation of a permanent lining, which in such cases is given a base over the full width of the tunnel, so that it forms a monolith with the side walls and roof.

Chicago experience has shown (Ref. 361) that the liner-plate method could be successfully employed there for the tunneling under compressed air of small sewer tunnels, but that for the wider subway tunnels the much more expensive shield method had to be resorted to in the sections where softer clay was located. Terzaghi (Ref. 361, 1943) has given a method for the numerical estimation of the limit conditions under which the liner-plate method may still be safely used.
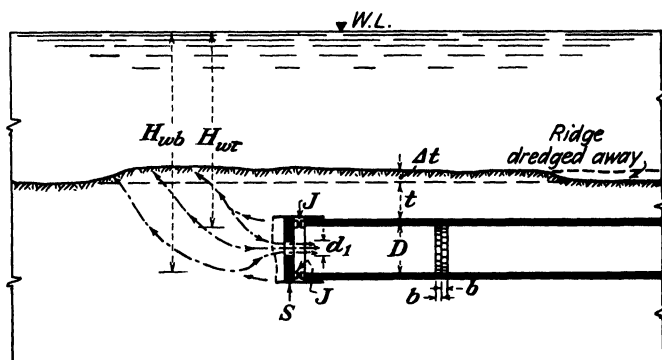
FIG. 16-43. Longitudinal section of subaqueous tunnel, showing principle of shield method of construction through mud or soft clay.

The principle of the *shield method* of tunneling is illustrated by Fig. 16-43 as applied to the construction of a subaqueous tunnel. A specially constructed metal shield S is pressed forward into the ground by a battery of some 20 or 30 hydraulic jacks J placed around the circumference of the shield in such a way that the completed cylindrical body of the tunnel lining may be used by the jacks as a support. The stroke of the jacks is made to correspond to the width b of each ring of the steel lining, and the number of jacks corresponds to the number of the steel-segment units of the ring. Thus, after completing a forward thrust, it is possible to relieve the pressure on the jacks, one by one, and to replace them by the steel segments of the lining, which can then again serve as a support for the next thrust.

No loss of ground can then occur in a radial direction, since the shield overlaps the completed lining at all stages. Neither will any loss of ground occur at the face of a shield in the case of a subaqueous tunnel, where it is even advantageous to push some of the soil ahead of the shield. This can be done, as shown in Fig. 16-43, by having only a very small

opening in the shield through which the soil is squeezed into the interior of the tunnel. The amount of expensive removal of soil through the tunnel is then decreased to a minimum. A ridge Δt high is formed by the soil which is pushed up over the tunnel; it can be subsequently dredged away. This type of procedure can be successfully used only in plastic clay or mud of low shearing strength; examples are the Holland Tunnel and the Lincoln Tunnel tubes under the Hudson River at New York (Ref. 198). Compressed air is employed in all cases during construction to minimize the amount of water seeping into the tunnel at its face.
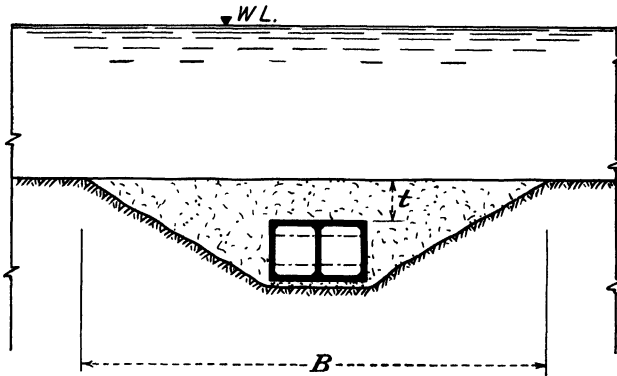
FIG. 16-44. Cross section of subaqueous tunnel, showing principle of the trench method of construction.

When doing subaqueous tunneling through sand or other pervious strata with high frictional resistance, it is no longer possible to push some of the soil out of the way of the tunnel, and it becomes necessary to remove all of it through openings in the shield, a procedure which requires considerable skill and experience. Care has to be taken to prevent blowouts at the tunnel face due to escape of compressed air to the surface through the shield and the overlying pervious strata. To that end, temporary clay blankets have to be sometimes placed over the sandy bottom, as had to be done during the construction of the Queens Tunnel under the East River at New York (Ref. 315).

The shield method of subaqueous tunneling is advantageous in harbors where the waterfront is crowded with structures which might be damaged by the extensive dredging necessary in connection with the *trench method* of subaqueous tunneling, the principle of which is illustrated by Fig. 16-44. A trench is dredged to the required depth. The slopes depend not only on the properties of the soil material (Art. 8-8) but may be strongly affected by the prevailing velocities of the current in the overlying body of water. The tunnel shell is built of reinforced concrete and

steel in sections, the ends of which are closed by temporary bulkheads to permit flotation. The sections are towed one by one to their locations, are filled with water, and are sunk to a prepared bed of sand. Underwater connection of the suitably designed ends of the separate sections is then made either with the help of divers and tremie concreting (Art. 14-10), or with compressed-air diving bells lowered from the surface of the water. The underlying bed of sand is pressure-grouted to eliminate cavities between it and the tunnel body and to ensure uniform distribution of the load on the soil. Divers remove the end partitions of the tunnel sections from its interior, from which water is then pumped out (Refs. 119 and 122). The trench is backfilled.

The minimum depth t of soil over the top of both types of subaqueous tunnels is selected to ensure a safe distribution of the load of an accidentally sunken ship which would not crush the tunnel shell. This depth t usually varies between 15 and 20 ft.

The connection of both types of subaqueous tunnels to the land approaches is usually made at the ventilating towers placed on each shore. Figure 10-29(II) shows one of the Rotterdam tunnel towers which was founded on a compressed-air caisson at a suitably greater depth than the adjoining tunnel sections of the trench type, subaqueous on one side and braced open cut on the other. Shield tunnels are frequently started through an opening in the side walls of the caisson of a ventilation tower.

The use of the shield method in land tunneling also minimizes radial loss of ground toward the tunnel shaft; it is, however, not possible to push any soil out of the way of the advancing tunnel, as can be done sometimes in subaqueous work (see Fig. 16-43). The ground heave might cause as much, or more, damage to buildings on the surface as would a loss of ground. Therefore most of the shield face has to be left open. The amount of the resulting loss of ground may be estimated by the method illustrated in Fig. 16-45. A loosely fitting point P is attached to a 2-in. pipe of known length l and is pressed horizontally into the clay ahead of the face of the tunnel. The distance r from the rear end of the pipe to a reference mark R on the completed tunnel lining is measured and recorded. The pipe is then withdrawn, leaving the point P in the clay. When the excavation reaches that point, the distance L_2 between the point P and the reference R is remeasured; $s = r + l - L_2$ will then represent the linear dimension of the excess ground excavated ("lost") at that elevation. If this amount is excessive and this fact is confirmed by surface settlements, which should always be measured, the air pressure may be increased to reduce it.

As explained in Art. 10-24, the full weight of the overburden is likely to come to rest on the tunnel lining some time after construction if the soil is

plastic clay. For that reason the permanent lining should be designed to carry that full weight. The lateral pressures to be expected have not yet been fully determined, especially the passive resistance which a plastic clay can be relied upon to maintain permanently in the case of flexible ring-shaped tunnel linings and deformations of the type illustrated by Fig. 16-40(II). Therefore the range of variation from $K = 1/3$ to $K = 2/3$, as used for the design of the Chicago subway tubes, without surcharge, appears reasonable until more data become available on this
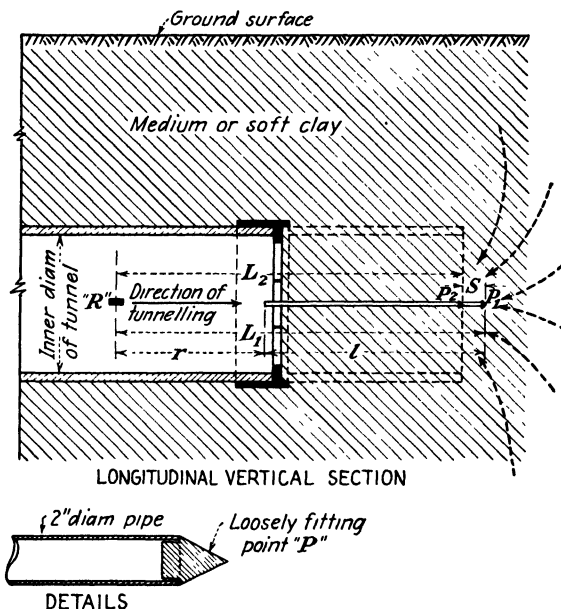
FIG. 16-45. Method of estimating amount of loss of ground due to squeezing of medium or soft clay into face of tunnel. (*After Terzaghi, Ref.* 361, 1943.)

subject [see reports by Nicolet and by Gunlock on the design and the construction of the tubes and stations (Ref. 249, 1944)]. Heavy wall sections are the consequence of such assumptions; further experimental studies may permit their reduction in future structures.

When tunneling through sand, only part of the weight of the overburden will come to rest on the tunnel lining at any time if adequate precautions are taken. The relief will be due to the transfer of the soil weight immediately above the tunnel to the adjoining soil mass by shearing stresses along vertical planes. The effect is similar to the load relief on conduits in trenches, as illustrated by Fig. 10-47. Equation (16-23) may be used for the estimation of the total load which the tunnel lining may have to carry, where the coefficient C_d may be determined from Fig.

10-48 by the substitution of the ratio $H/2r$ for the ratio H/b of that diagram, r being the tunnel radius.

Great care must be taken to prevent any escape of sand into the tunnel during its construction. Moist sand will usually arch over small openings and will not cause trouble in this respect; but entirely dry sand, which is sometimes encountered, is liable to trickle into the tunnel through the smallest gaps in the temporary lining. Sand movements of this kind destroy most if not all of the arching around the tunnel, with a resulting strong increase of both vertical and horizontal pressures on the supports of the lining. Such cases have been recorded and cause considerable difficulties. An efficient countermeasure was provided by chemical grouting and solidification (see Art. 11-9) from the tunnel face of the sand ahead of it, prior to tunneling through troublesome sections where the sand was completely dry (Ref. 448).

Practice Problems

16-1. Determine the safety against overturning and against sliding along its base of the gravity retaining wall illustrated in Fig. 10-30.

Answer. Prior to the reinforcement of the wall, its weight W is estimated to be

$$\frac{12 + 10}{2} \times 42 \times 140 = 64{,}800 \text{ lb per ft}$$

$$16 \times 5 \times 150 = \underline{13{,}500}$$

$$W = 78{,}300 \text{ lb per ft} = 39.15 \text{ tons per ft}$$

The moment resisting overturning around the outer edge of the footing is $M_r = 39.15 \times 10 = 391.5$ ft-tons per ft.

The maximum lateral pressure shown in Fig. 10-30 is redrawn in Fig. 16-46 in a simplified form to correspond to the conditions which may be assumed to have existed before the reinforcement of the wall (see also Fig. 16-12). The total lateral earth pressure E is then

FIG. 16-46.

$$E = 0.7 \times \tfrac{1}{2}(26 + 19) = 15.8 \text{ tons per ft}$$

The overturning moment is

$$M_o = 15.8 \times 21.3 = 336.0 \text{ ft-tons per ft}$$

and the factor of safety against overturning is

$$M_r/M_o = 391.5/336.0 = 1.16$$

The shearing stress along the 15-ft-wide base is

$$\tau = \frac{15.8}{16.0 \times 1.0} = 0.99 \text{ ton per ft}^2$$
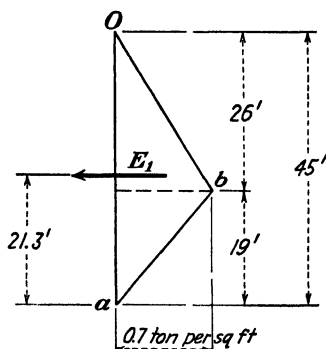
The factor of safety against sliding due to shear failure of the underlying gray London clay with a shear strength $s = 2.2$ tons per ft² is $s/\tau = 2.20/0.99 = 2.22$. Thus it is almost twice as large as the factor of safety against overturning even if the passive resistance at the toe is neglected. Nevertheless, the wall failed by slow outward

sliding and had to be reinforced. This shows again that in stiff-fissured clays the strength at the contact surfaces of the fissures governs the behavior of the clay mass, and not the strength s of the intermediate intact lumps of clay.

16-2. Select steel sections for the wale and the strut of the middle braces of the cut in sand illustrated in Fig. 10-22 in accordance with the design recommendations of Figs. 16-8 and 16-9.

Answer. The relevant portion of the lateral-pressure diagram is drawn in Fig. 16-47. The unit lateral earth pressure is

$$0.20\gamma H = 0.20 \times 120 \times 28.2 = 676 \text{ lb per ft}^2$$

The pressure against the wale is

$$676(8.4 + 6.3)\tfrac{1}{2} = 4{,}940 \text{ lb per ft}$$

Assuming that the wale does not extend for more than two spans of 20 ft between the individual middle braces, the maximum bending moment that it will have to resist is

FIG. 16-47.

$$M = \frac{4{,}940 \times 20^2 \times 12}{8} = 2{,}960{,}000 \text{ in.-lb}$$

With a permissible stress $f = 20{,}000$ psi in the steel, the required section modulus will be

$$S = \frac{2{,}960{,}000}{20{,}000} = 148 \text{ in.}^3$$

Select a 106-lb 12- by 12-in. wide-flange section with $S = 144.5$ in.^{3} (Ref. 7).

The axial compressive load on the brace will be

$$P = 4{,}940 \times 20 = 99{,}880 \text{ lb}$$

If we select a 49-lb 10- by 10-in. wide-flange section with 14.4 in.^{2} cross-sectional area and a radius of gyration $r = 2.54$ in., the unit compressive stress will be

$$f = \frac{99{,}880}{14.4} = 6{,}900 \text{ psi}$$

By providing cross bracing at 25-ft intervals, the slenderness ratio of the free length l will be

$$\frac{l}{r} = \frac{25 \times 12}{2.54} = 120$$

and the permissible unit compressive stress (Ref. 7),

$$17{,}000 - 0.485(120)^2 = 10{,}000 \text{ psi}$$

which is more than the actual value and therefore satisfactory.

16-3. With reference to Fig. 16-13, showing the excavation sequence on the approaches to the Rotterdam tunnel, determine the critical depth of excavation h_x below the water-level elevation (± 0.00) prior to setting the wellpoint system into operation. Neglect the extra weight of the Franki piles and the tensile strength at the elevation of sand (-58.5) of the unreinforced concrete of these piles.
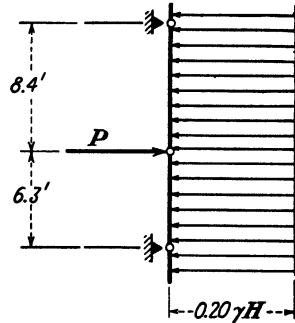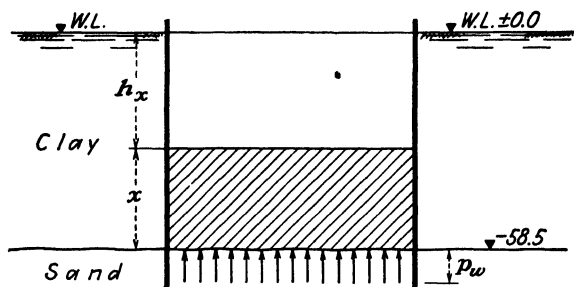
FIG. 16-48.

Answer. As shown in Fig. 16-48, an uplift pressure p_w will be exerted by the water in the undrained sand layer against the bottom of the overlying clay layer between the two rows of steel sheet piles.

$$p_w = 58.5 \times 62.4 = 3{,}650 \text{ lb per ft}^2$$

This uplift pressure is resisted only by the weight of the saturated, unbuoyed, remaining x-feet-thick plug of clay. The plug will be in danger of being pushed upward when

$$x = \frac{3{,}650}{105} = 34.8 \text{ ft}$$

The critical depth of excavation is

$$h_x = 58.5 - 34.8 = 23.7 \text{ ft}$$

It was therefore necessary to relieve the uplift pressure shortly after the start of the excavation by using a system of wellpoints (Art. 14-9) and to unwater the underlying sand layer during the time of the tunnel construction. This was actually done (Arts. 10-20 and 13-9).

16-4. With reference to Fig. 16-20, check the bending stresses expected in the reinforced-concrete sheet piling of the Aalborg pier according to the lateral-pressure diagram of Fig. 16-49(II).
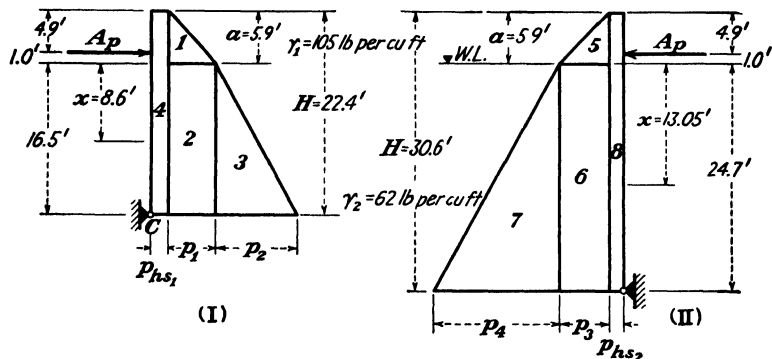
FIG. 16-49.

Answer. From Eq. (16-20),

$$K_A = \left(1 - \frac{5.9}{3.5 \times 30.6}\right) 0.33 \times 0.9 = 0.280$$

From Eq. (16-21),

$$p_3 = 105 \times 5.9 \times 0.280 = 173 \text{ lb per ft}^2$$
$$p_4 = 62 \times 24.7 \times 0.280 = 428 \text{ lb per ft}^2$$

With a surcharge of p_s = 210 lb per ft² we get from Eq. (16-1),

$$p_{hs_2} = 210 \times 0.280 = 59 \text{ lb per ft}^2$$

Area 5: 173 × ½ × 5.9 = 510 lb per ft width of bulkhead
Area 6: 172 × 24.7 = 4,270 lb per ft width of bulkhead
Area 7: 428 × ½ × 24.7 = 5,280 lb per ft width of bulkhead
Area 8: 59 × 30.6 = 1,780 lb per ft width of bulkhead
The anchor pull is

$$A_p = \frac{1}{25.7}\left[510\left(\frac{5.9}{3} + 24.7\right) + 4{,}270\,\frac{24.7}{2} + 5{,}280\,\frac{24.7}{3} + 1{,}780\,\frac{30.6}{2}\right]$$
$$= 5{,}330 \text{ lb per ft width}$$

The maximum positive bending moment M will be located at the distance x below the water level where the shear V is equal to zero.

$$V = 5{,}330 - 510 - 173x - 428\,\frac{x}{24.7}\,\frac{x}{2} - 59(5.9 + x) = 0$$
$$8.7x^2 + 231x - 4{,}480 = 0 \qquad x = 13.05 \text{ ft}$$

The value of M is found to be

$$+5{,}330 \times 14.05 = +74{,}800 \text{ ft-lb}$$
$$-510\left(\frac{5.9}{3} + 13.05\right) = -7{,}650 \text{ ft-lb}$$
$$-173\,\frac{(13.05)^2}{2} = -14{,}750 \text{ ft-lb}$$
$$-428\,\frac{(13.05)^3}{24.7 \times 6} = -6{,}420 \text{ ft-lb}$$
$$-58\,\frac{(13.05 + 5.9)^2}{2} = -10{,}450 \text{ ft-lb}$$
$$M = +35{,}530 \text{ ft-lb}$$
$$= 426{,}000 \text{ in.-lb per ft}$$

The area of tensile (A_s) and of compressive (A_s') steel is

$$A_s = A_s' = 2\,\frac{(22/25.4)^2}{4} = 1.18 \text{ in.}^2 \text{ per pile of 13.8 in. width}$$
$$= 1.18(12.0/13.8) = 1.02 \text{ in.}^2 \text{ per ft}$$

Assume the distance from the extreme fibers of concrete to the center of the adjoining steel to be d' = 1.3 in. Then d = 10.3 − 1.3 = 9.0 in., and d'/d = 0.144. The ratio of reinforcement is

$$p = p' = \frac{1.02}{12 \times 9} = 0.0094$$

Assuming that the ratio of the modulus of elasticity of steel to that of concrete is $n = 15$, $pn = p'n = 0.141$.

From diagram 5, Ref. 406 (d'/d = 0.15), we obtain

$$k = 0.352 \qquad j = 0.846$$

The unit tensile stress in the steel will be

$$f_s = \frac{M}{A_s jd} = \frac{426,000}{1.02 \times 0.846 \times 9.0} = 54,000 \text{ psi}$$

and the unit compressive stress in the concrete

$$f_c = \frac{f_s k}{n(1-k)} = \frac{54,800 \times 0.352}{15 \times 0.648} = 2,000 \text{ psi}$$

If the surcharge effects are neglected (area 8 in Fig. 16-49) the following values are obtained in a similar manner:

$$f_s = 45,500 \text{ psi} \qquad f_c = 1,750 \text{ psi}$$

Thus the tensile stress in the steel is found to exceed the yield point; the sheet piling is underdesigned (Ref. 166), even according to the Danish Rules. The fact that it has not failed may be explained by special favorable circumstances outlined in Art. 16-12.

A similar check of the opposite wall of the pier according to the active pressures in the diagram in Fig. 16-49(I) gives us $A_p = 3,410$ lb per ft, $f_s = 38,300$ psi, and $f_c = 1,375$ psi. If the surcharge effects (area 4 in Fig. 16-49) are neglected we obtain $f_s = 30,000$ psi and $f_c = 1,100$ psi. The actual values are likely to be somewhat higher, since the anchor pull of the longer sheet piles in the deeper water (right-hand side of Fig. 16-20) has been shown to be $A_p = 5,330$ lb per ft. It will therefore induce some passive pressures against the shorter piles near the anchor level.

If we select for the anchors 1¾-in.-diameter bars with upset screw ends and $A_s = 2.405$ in.^{2} (Ref. 7) and space them 8 ft center on center, the unit stress in the anchors will be

$$f_s = \frac{5,330 \times 8}{2,405} = 17,700 \text{ psi}$$

16-5. Check the values reported in Table 16-1 for the loading given in Fig. 16-22 in accordance with the various computation methods referred to in that table.

16-6. With reference to Fig. 16-31, check the stresses in the concrete sheet piles in accordance with the design recommendations of Art. 16-14.
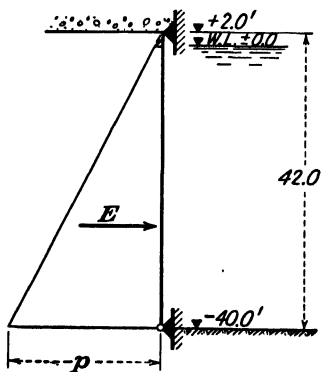
FIG. 16-50.

Answer. The timber piles under the relieving platform take up all the vertical loads and the horizontal thrust at the level of the platform. They cannot be fully relied upon to relieve the lateral pressures against the sheet piling, since any escape of the sand between the individual concrete sheet piles is likely to produce sand movements between the timber piles and possibly build up full active lateral pressures against the sheeting. The pressure diagram of Fig. 16-50 will therefore be used for the analysis, even though it represents an unfavorable assumption. According to Eq. (16-20), with $a = 0$

$$K_A = 0.33 \times 0.9 = 0.30$$

and from Eq. (16-21)

$$p = 62 \times 42.0 \times 0.30 = 782 \text{ lb per ft}^2$$

The total lateral pressure

$$E = \tfrac{1}{2}(782 \times 42.0)$$
$$= 16{,}400 \text{ lb}$$

The maximum positive bending moment for triangular loading of the type indicated is

$$M = 0.128 \times 16{,}400 \times 42.0 = 88{,}200 \text{ ft-lb}$$
$$= 1{,}058{,}000 \text{ in.-lb per ft actual width of bulkhead}$$
$$= 1{,}058{,}000(^{22}\!/_{19}) = 1{,}225{,}000 \text{ in.-lb per ft effective width of sheet piles}$$

Assuming $d' = 2.5$ in., $d = 26.0 - 2.5 = 23.5$ in. and $d'/d = 0.106$.

$$A_s = A_s' = 4 \times 1.25^2 \times {}^{19}\!/_{22} = 3.41 \text{ in.}^2 \text{ per ft effective width}$$

$$p = p' = \frac{3.41}{12 \times 23.5} = 0.0121$$

If $n = 15$, $pn = p'n = 0.181$.

From diagram 4, Ref. 406 ($d'/d = 0.100$), we find

$$k = 0.365 \qquad j = 0.888$$

$$f_s = \frac{1{,}225{,}000}{3.41 \times 0.888 \times 23.5} = 17{,}200 \text{ psi}$$

$$f_c = \frac{17{,}200 \times 0.365}{15 \times 0.635} = 660 \text{ psi}$$

The concrete sheet piles are therefore overdesigned in respect to the recommendations of Art. 16-14.

16-7. With reference to Fig. 16-32, check the stresses expected in the reinforced-concrete sheet piling according to the lateral-earth-pressure diagram of Fig. 16-51(I). Determine the loads to be carried by the piling under the relieving platform in accordance with the diagrams of Fig. 16-51(II) and (III).
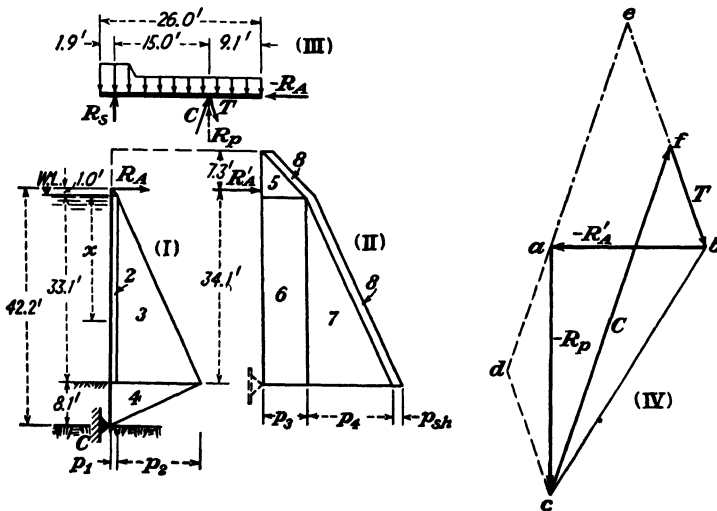
FIG. 16-51.

Answer. Assuming the unit weight of the backfill above the platform to be 120 lb per ft³, and that of the reinforced concrete of the relieving platform to be 150 lb per ft³, we obtain for the vertical load on the sheet piling R_s = 7,050 lb per ft width of bulkhead, and for that on the two anchor piles R_p = 17,700 lb per ft. By considering a surcharge of 200 lb per ft² these values are increased to 8,500 lb per ft and 21,500 lb per ft, respectively.

From Eq. (16-20), for $a = 0$, $K_A = 0.30$; and from Eq. (16-21),

$$p_1 = 0.30 \times 115 \times 1.0 = 35 \text{ lb per ft}^2$$
$$p_2 = 0.30 \times 62 \times 33.1 = 615 \text{ lb per ft}^2$$

The properties of the firm-clay layer below el. −33.1 ft have not been determined numerically. The unfavorable assumptions are therefore made that the point of contraflexure C will be located at the surface of the limestone rock, and that the clay will transmit some active lateral pressure to the sheet piling, as shown in Fig. 16-51(I). With these assumptions, the anchor pull is found to be R_A = 5,530 lb per ft, the distance below water level to the point where the shear is zero and the bending moment a maximum x = 22.7 ft, and the bending moment of a freely supported beam at that point M = 1,050,000 in.-lb per ft. Since the sheet piling forms a monolith with the relieving platform, it is permissible to assume partial restraint at the upper end and to reduce the above value of the bending moment by multiplication by the ratio of moment coefficients $\frac{8}{12}$, giving M = 700,000 in.-lb per ft width of the bulkhead for use in the computations. With the axial force N on the sheet piling being equal to R_s, the eccentricity is $e = M/N$ = 700,000/7,050 = 99.4 in. Assuming d' = 1.7 in., $d = D - d'$ = 15.7 − 1.7 = 14.0 in. The compressive reinforcement per foot width is A_s' = 1.39 in.², and the tensile reinforcement A_s = 2.11 in.².

Using the above values and Eq. (7-23a) of Ref. 111, we obtain kd = 5.9 in. Substituting this value in Eqs. (7-21) and (7-20) of Ref. 111, we obtain for the tensile stress in the steel f_s = 25,000 psi and for the compressive stress in the concrete f_c = 1,215 psi. Both are reasonable values (see Art. 16-14).

The diagram of Fig. 16-51(II) is to be used for the determination of the thrust against the relieving platform. The effect of surcharge on the soil surface outside the relieving platform is represented by area 8. With K_A = 0.30, we obtain p_3 = 300 lb per ft², $p_4 = p_2$ = 615 lb per ft², p_{sh} = 0.30 × 200 = 60 lb per ft², and R_A' = 10,950 lb per ft.

The full value of the thrust R_A' will be used for the analysis of the batter piles. However, no surcharge on the platform will be considered simultaneously, and the value of the vertical load will be R_p = 17,700 lb per ft. Graphical procedures of analysis will be used, as shown in Fig. 16-51(IV). Should we assume that only the vertical load R_p were acting, then both batter piles would receive the same compressive loads, equal to the scale values of the lines *ad* and *dc*, each equal to 9,200 lb per ft width of the bulkhead. Similarly, if only the lateral thrust R_A' were acting against the platform, then both piles would receive the same loads of 17,000 lb per ft, but of opposite signs, *ae* compression and *eb* tension. The simultaneous action of R_p and R_A' results in the addition of their effects, as shown in Fig. 16-51(IV). The compressive load on the pile is increased to C = 17,000 + 9,200 = 26,200 lb per ft, and the tensile load is decreased to T = 17,000 − 9,200 = 7,800 lb per ft, or to 30 per cent of the corresponding compressive load. This is also a reasonable proportion, since piles can carry in tension only a fraction of the load they can resist in compression (Art. 15-3). It should be noted in this connection that the elevation of the relieving plat-

form can be changed to achieve the desired relationship between the loads on the compression and tension piles.

If the precast reinforced-concrete piles are to be allowed to carry 40 tons per pile in compression (Art. 15-6), then their spacing becomes 80,000/26,200 = 3.05 ft. Since the piles would be at least 16 in. square, only 20 in. free space would be left between them. Part of the difference between the lateral-pressure-diagram areas of Fig. 16-51(I) and Fig. 16-51(II) would be transmitted by shear to the firm clay and rock at the lower boundary. However, part of it would have to be resisted in bending by the closely spaced tension batter piles. No reliable method has yet been developed for the estimation of the relative magnitude of this second load component; it is frequently ignored in the hope that the usual high factors of safety in structural members will suffice to prevent failure. Heavy reinforcement of the T pile is therefore advisable.

16-8. With reference to Fig. 16-33, check the stresses expected in the steel sheet piling according to the lateral-earth-pressure diagram of Fig. 16-52.

Answer. According to Art. 16-14 and Fig. 16-23, we assume $K_A = 0.50$ and $d = 0$. The buoyed unit weight of the soft clay is taken at 50 lb per ft³. Then

$$p_1 = 0.50 \times 50.0 \times 36.8 = 920 \text{ lb per ft}^2$$

The effects of the tidal lag (Art. 16-8) are considered by drawing the pressure-diagram areas 2 and 3 in Fig. 16-52 with

$$p_2 = 1.0 \times 2.3 \times 62.4 = 143 \text{ lb per ft}^2$$

FIG. 16-52.

Taking moments around the point C, we obtain the lateral thrust on the relieving platform R_A = 8,180 lb per ft width of bulkhead. In the sheet piling the shear will be zero at a distance x = 20.8 ft from the upper support. The maximum bending moment will be located there and will equal

$$M = 1{,}255{,}000 \text{ in.-lb per ft width of bulkhead}$$

The Krupp No. III section of steel sheet piling used on that job has a section modulus of 30.9 in.³ per ft of wall. Therefore, if the entire lateral pressure of the clay were to be resisted by the steel sheet piling alone, excessively high bending stresses would be engendered.

$$f_s = 1{,}255{,}000/30.9 = 40{,}600 \text{ psi}$$

Some of the timber piles under the relieving platform will undoubtedly participate, together with the steel sheet piling, in resisting the lateral pressures of the soft clay. It is therefore admissible to distribute the total maximum bending moment between these structural units in proportion to their relative flexibility, as expressed by their EI values, since their length L is identical.

With the Young modulus of steel E_s = 29,500,000 psi and the moment of inertia of the sheet piling I_s = 147 in.⁴, the corresponding product is $E_sI_s = 4.34 \times 10^9$ lb in.² For wood we can assume E_w = 1,000,000 psi. At least four timber piles in each row are located within the possible sliding wedge of clay and therefore represent the minimum number which will participate in resisting the lateral pressures of the clay. Assuming the average diameter of the piles to be 12 in., and assuming a 3-ft spacing
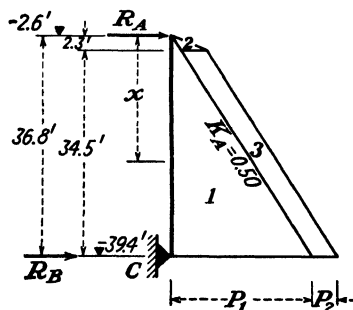
between the pile rows, we obtain the following average value for the moment of inertia of the active piles per foot width of bulkhead:

$$I_w = \pi \frac{12^4}{64} \times \frac{4}{3} = 1{,}010 \text{ in.}^4$$

and

$$E_w I_w = 1.35 \times 10^9 \text{ lb-in.}^2$$

The sheet piling can then be expected to receive the following fraction of the total lateral load:

$$\frac{4.34}{4.34 + 1.35} = 0.765$$

The unit bending stress in the sheet piling therefore should be reduced to 31,000 psi. This is high, but compatible with equilibrium.

16-9. What factor of safety against failure of the underlying stiff clay is provided by the depth of embedment of the sheet piling shown in Fig. 16-33?

Answer. With reference to Fig. 16-23, the total active lateral earth pressure E, equal to the sum of the areas 1, 2, and 3 of the pressure diagram shown in Fig. 16-52, is E = 22,060 lb per ft width of bulkhead. The load transmitted to the stiff clay beneath the dredge line is $R_b = E - R_A$ = 13,800 lb per ft.

The total depth of embedment is D = 60.8 − 39.4 = 21.4 ft. The unconfined compressive strength of the clay is q_u = 1.0 ton per ft^2 = 2,000 lb per ft^2, and the residual limit passive resistance of the clay is $q_u - p_1 - p_2$ = 2,000 − 920 − 143 = 937 lb per ft^2. The total limit resistance of the clay is 937 × 21.4 = 20,100 lb per ft. The factor of safety is F_s = 20,100/13,880 = 1.45.

References Recommended for Further Study

Theory and Practice of Reinforced Concrete, by C. W. Dunham, McGraw-Hill, 2d. ed., 1944, Chap. 8, Retaining Walls, pp. 212–254. Numerical examples of determination of over-all dimensions and steel reinforcement of reinforced-concrete retaining walls; illustrations of construction details.

Concrete Structures in Marine Work, by R. Stroyer, Knapp, Drewett & Sons, Ltd., London, 1937. Many good illustrations and descriptions of existing reinforced-concrete wharves, piers, and docks of various types in different parts of the world. Some of the recommendations concerning lateral-earth-pressure determinations are, however, outdated. Contains English translation of the 1926 Danish rules (Ref. 99) for sheet-pile bulkhead design.

Cofferdams, by Lazarus White and Edmund A. Prentis, Columbia University Press, 2d. ed., 1950. Contains a valuable illustrated description of experiences with the design and construction of cofferdams on the Mississippi River and in other localities.

"Stability and Stiffness of Cellular Cofferdams," by Karl Terzaghi, *Transactions o the American Society of Civil Engineers*, 1945, pp. 1083–1210. Critical review of existing design methods and new suggestions. Discussion by a number of engineers.

"Rock Tunneling with Steel Supports," by R. V. Proctor and Thomas White. Published by Commercial Shearing & Stamping Co., Youngstown, Ohio, 1946. Contains five chapters (95 pp.) by Karl Terzaghi on "Rock Defects and Loads on Tunnel Supports."

"Concrete Pipe Handbook," by Howard F. Peckworth. Published by the American Concrete Pipe Association, Chicago.

CHAPTER 17

SOME SOIL ENGINEERING ASPECTS OF DAM CONSTRUCTION

17-1. Types of Dams and the Principles Which Govern Their Choice. Dams may be made of timber, steel, concrete, or rock and earth fill. To fulfill its purpose a dam must be designed to prevent at a minimum cost excessive or dangerous seepage both through the dam itself and through the soil or rock beneath and around the dam. The pressures transmitted by the dam to the underlying soil should not create a danger of shear failures in that soil, nor of excessive settlements and deformations thereof which might damage the dam itself and thereby endanger its stability.

It follows that concrete dams are best fitted for erection on sites where they can be founded on stiff and impervious material, that is, preferably on sound rock. Earth dams are not limited by this restriction; because of their large dimensions, the pressures which they transmit to the underlying soil are distributed over considerable areas. For the same reason seepage losses and the danger of a quick condition are decreased, since the length of the paths of percolation under the dam is increased considerably. The earth dam itself can deform without much difficulty to adjust itself to deformations of the underlying soil which would have destroyed the much more brittle concrete.

Timber dams are seldom used and then only for small and temporary structures. Steel is employed in dams mainly as an accessory material of construction.

The nature of the material available at the site is an important consideration in the choice of the type of dam to be built. Thus rock-fill dams (Ref. 144) are of advantage in distant mountain valleys where there is little or no soil suitable for the construction of the dam. The rock fill ensures the structural stability of the dam, and it is rendered watertight by a membrane covering its upstream face. A blanket of rolled-clay fill is best suited for this purpose (Ref. 264). However, in some cases where no suitable soil at all was available within easy reach, thin reinforced-concrete, steel, or timber blankets have been used.

The factors affecting the choice between an earth dam of rolled fill and one of hydraulic fill are outlined in Arts. 17-3 and 17-4.

17-2. Some Causes of Dam Failures. To quote from H. V. Hinckley's analysis (Ref. 176, 1911) of some early dam failures: "What good is there in the mistakes of others if we do not profit by them?"

Much can be learned from past failures that will be of value for future designs. This is true in all soil engineering work and especially in the field of dam construction.

The first requirement for the satisfactory performance of any dam is that it should be built on a site with geological features permitting the storage of water in the reservoir behind the dam. That this is not necessarily the case of all sites in regions of cavernous limestone was illustrated by Figs. 12-2 and 12-3 and by the discussion thereof in Art. 12-2. Intensive grouting as a possible remedial measure in such locations, as successfully employed by the Tennessee Valley Authority, is described in Refs. 334 and 335. For general procedures of grouting foundations of dams see Ref. 313.

Trouble of this kind, however, is not limited to limestone regions, as shown by the following quotation from a letter to the author by Edwin B. Eckel, Chief of the Engineering Geology Branch of the U.S. Geological Survey:

> The Lone Pine Dam, on Show Low Creek, Navajo County, Arizona, is a fine example of a project that failed because of unexpected leakage through the reservoir floor. The dam, of rolled-earth and rock-fill construction, is 700 ft long, 100 ft high, and was supposed to store 11,000 acre-ft in a 330-acre reservoir.* It was built with Public Works Administration funds in 1935–36. Shortly after the reservoir began to fill, numerous leaks appeared in the reservoir floor and walls. All efforts to stop them were ineffective and they were so large that no water was ever made available for irrigation.
>
> Geologic investigation, after the failure, showed that leakage occurred through open tension cracks in the massive sandstone bedrock. These cracks characterize parts of a very large area in northeastern Arizona and are described in general fashion in Water Supply Paper 836-B, pp. 56–57. At the reservoir site the bedrock cracks, which doubtless extend downward several hundred feet, were completely hidden by soil or other overburden. The head of water in the reservoir was sufficient to wash this material out, so that all the reservoir water entered the cracks and presumably became part of the ground water body at depth.
>
> After my geologic investigation of the reservoir in 1939, I came to the conclusion that an ordinary examination for a small dam such as this, if confined to the dam and reservoir sites, would probably have overlooked the cracks or missed their significance. The loss of this reservoir, however, is an excellent case in favor of regional geologic mapping before construction activities begin; had

* One acre = 43,560 ft^2.
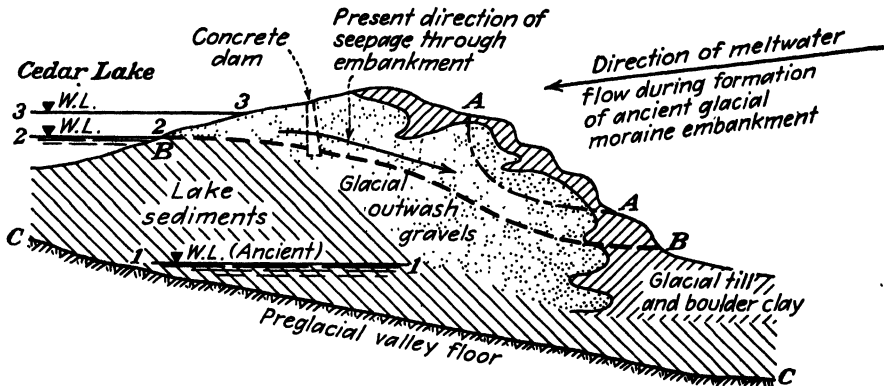
FIG. 17-1. Sketch showing geological profile 6,000 ft away from the concrete Cedar Creek Dam through natural embankment in the failure zone AA illustrated by Fig. 17-2. (*From J. Hoover Mackin, Ref. 221, 1941.*)

FIG. 17-2. Photograph of the 1918 failure of natural embankment which adjoined the concrete dam at Cedar Creek (see Fig. 17-1). (*From J. Hoover Mackin, Ref. 221, 1941.*)

adequate geologic maps of this region been available the danger of encountering open tension cracks would almost certainly have been foreseen.

Thus systematic regional studies are just as important in geological engineering as they are in soil engineering.

Geological and soil engineering studies should be extended well beyond

the site of the dam proper and should cover not only the floor, but also any natural embankment walls of the reservoir. Disregard of this circumstance may lead to trouble, as illustrated by Figs. 17-1 and 17-2, which in addition provide further evidence of the freak soil formations which may occur in regions of former glaciation (see Art. 2-7). The glacial ice had moved *up* a valley, forming a moraine embankment across it. As the embankment grew, the level of Cedar Lake above the glacier was raised with it from 1-1 in ancient times to the level 2-2. This latter level was maintained prior to the construction of a concrete dam across the

FIG. 17-3. The St. Francis Dam, as it appeared in 1926, prior to its failure. (*Photo by E. A. Bayley.*)

postglacial valley marked by the broken line *BB* in Fig. 17-1. This valley was cut through the natural embankment by the postglacial Cedar Creek which provided an overflow for the waters of Cedar Lake.

The construction of the concrete dam raised the water in the lake to the level 3-3 and saturated well above the line *BB* the glacial outwash gravels which formed the core of the natural embankment adjoining the dam. The water in the gravel could not escape, since the outer face of the moraine embankment was covered by a layer of varying thickness of glacial till and boulder clay. This is a tentative explanation of the failure, as given by J. Hoover Mackin in Ref. 221. As the water pressure grew against the outer impervious layer, it finally gave way at one of the weaker zones, with the consequences illustrated by Fig. 17-2. Within

approximately an hour over a million cubic yards of detritus was washed out from the embankment, forming an amphitheater-shaped crater (marked *AA* in Fig. 17-1) in its face. Its walls were found to be formed of bedded gravels, whereas the narrow throat with steep walls seen in Fig. 17-2 was cut through till. The flood waters which rushed down the valley

FIG. 17-4. The St. Francis Dam after its failure. (From Ref. 79, 1928.)

through that amphitheater destroyed railroad tracks, a saw mill, and a small village. The discharge through the amphitheater decreased very quickly and continued at a slow rate for several months until the water level in Cedar Lake dropped appreciably.

Thin horizontal water-bearing seams represent another important geological feature, since, if overlooked, the uplift pressures at the toe of dams in such seams may reduce frictional shearing resistance along these seams and produce failure. Geologists can detect such features better than engineers. According to Ref. 176, neglect of uplift was the cause of

the 1911 failure of the concrete dam at Austin, Pennsylvania, with a loss of over 100 lives. Relief wells (Art. 17-7) can prevent such disasters. The dam was built on sandstone and shale, and uplift had not been anticipated.

Geological studies without engineering strength testing of rocks and soils, however, may be inadequate. The disastrous consequences of weak foundation material under a concrete dam are illustrated by the "before" and "after" photographs in Figs. 17-3 and 17-4. According to the official report (Ref. 79) on the failure of the 205-ft-high St. Francis Dam, the cause thereof lay in defective foundations. At the east end the dam rested on mica schist and at the west end on reddish conglomerate which became soft when wet. This latter property was apparently ascertained only after the failure. Both end portions of the dam failed suddenly. Huge chunks of concrete, measuring 50 to 100 ft side length, were carried half a mile from the original site by the suddenly released torrent, which caused much damage downstream of the dam. There were 236 known dead and 200 missing.

Failures of earth dams due to weak underlying soil strata have occurred sometimes. Usually the failure took place during construction and was evidenced by a slumping of one of the slopes in a manner indicating a rotational type of slide (Art. 8-7). As a rule, an underlying saturated clay layer was found to be responsible for the failure. This was true in the case of the Chingford Dam in England (Ref. 310) and the Marshall Creek Dam in the United States (Ref. 118). Reconstruction of that dam at flatter slopes proved to be an effective remedy (see Art. 8-12).

A failure of a hydraulic-fill dam due to what appeared to be the combined action of sliding along a weak stratum in the natural soil and a flow slide in the loose hydraulic fill was illustrated by Fig. 8-11 and discussed in Arts. 8-10 and 8-11.

The most frequent cause of earth-dam failures is provided by inadequate spillways. Careful hydrological studies of maximum precipitation and runoff toward all tributary streams are therefore of greatest importance. An earth dam cannot resist erosion by water flowing rapidly over its crest; therefore if an earth dam is *topped*, it is certain to be destroyed. Spillways must therefore be designed to take care with an ample margin of safety of the greatest possible flood that may ever occur. They are built of concrete and are usually placed in a cut through natural ground at one of the ends of the dam (see Fig. 17-6). The most disastrous known failure of a dam was caused by an inadequate spillway and the topping of the earth fill at South Fork Dam in Pennsylvania (see Ref. 80, 1891). The released mass of water swept down the valley, causing what is often referred to as the Johnstown Flood, since Johnstown was the locality
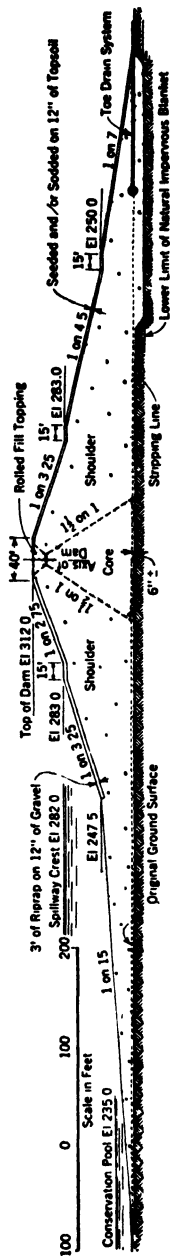
FIG. 17-5. Cross section of the Sardis Dam (hydraulic fill). (*From N. R. Moore, Ref. 235, 1939.*)
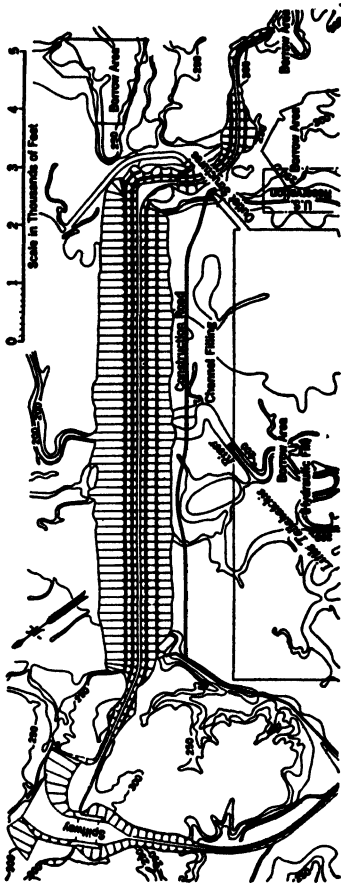
FIG. 17-6. Plan of the Sardis Dam. (*From N. R. Moore, Ref. 235, 1939.*)

which suffered most. In all, 2,280 lives were lost and 1,675 bodies were recovered. The material damage was enormous.

The silting up of a reservoir may increase lateral pressures against a dam, as compared with usual design assumptions which consider only water pressure. The increase in pressure may become dangerous in the case of an underdesigned concrete dam, and at least one failure was

FIG. 17-7. Cross section showing construction procedure for a hydraulic-fill dam at stage illustrated by photograph of Fig. 17-8.
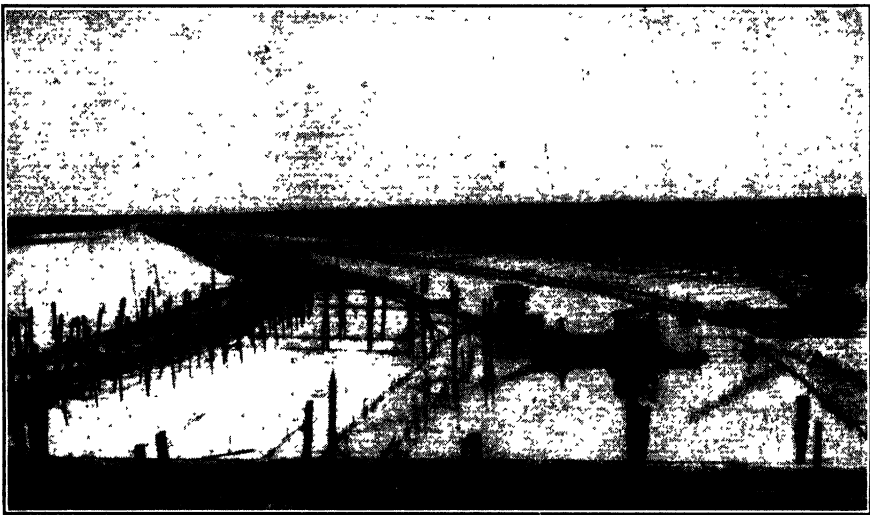
FIG. 17-8. The Sardis Dam under construction by the U.S. Engineer Department. General layout of the hydraulic-fill pipelines. (*Photograph by Tschebotarioff, Ref. 375, 1939.*)

attributed to this cause (see Ref. 176). The increase in lateral pressure may be estimated to equal 0.5 of the buoyed weight of the silt (see Art. 16-2).

Descriptions of other dam failures may be found in Ref. 47. A case of construction difficulties due to inadequate preliminary geological studies is outlined in Ref. 317. The engineer who had neglected to make these studies was sued by the owners.

17-3. Construction of Hydraulic-fill Dams. The 95-ft-high Sardis Dam, built by the U.S. Engineers across a tributary of the Mississippi River, will be used for the discussion of hydraulic-fill dam-construction
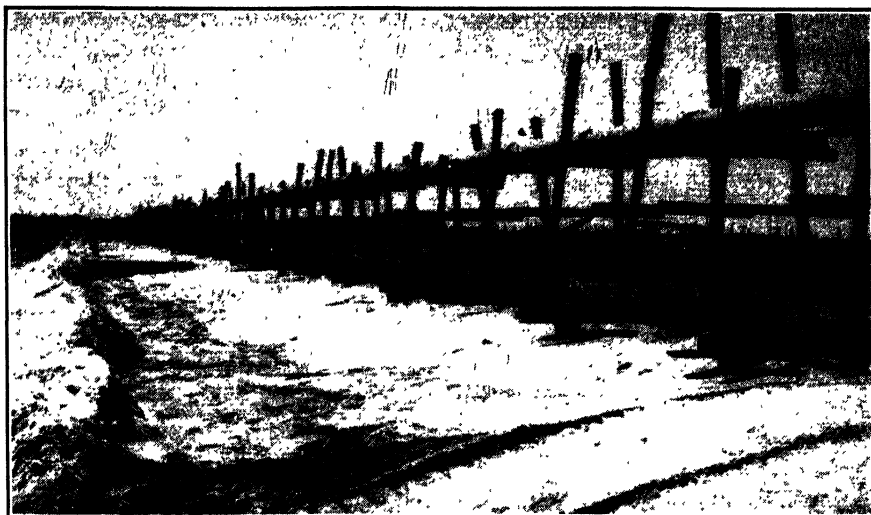
FIG. 17-9. A close-up view of the hydraulic-fill pipeline and of the outer slope of the dam shown in Fig. 17-8. (*Photograph by Tschebotarioff, Ref. 375, 1939.*)
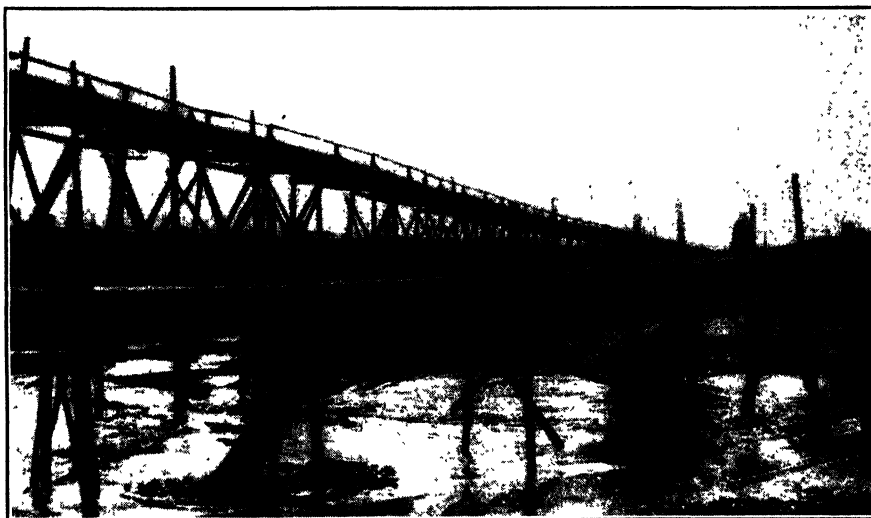
FIG. 17-10. View of a discharge point along a hydraulic-fill pipeline employed by the U.S. Engineer Department for repairs of the Fort Peck Dam slide (*Photograph by Tschebotarioff, Ref. 375, 1939*)

procedures. A cross section of that dam is shown in Fig. 17-5, and its plan in Fig. 17-6. The methods used for the placing of the hydraulic fill are illustrated by Figs. 17-7 to 17-10.

A dredge, of a type similar to those employed for underwater excavations (Art. 14-10), cuts its way from the river to the borrow area. The

mixture of soil and water cut up by the suction head of the dredge is pumped, sometimes over a distance of several miles, to the site of the dam. The pipe line is laid along both edges of the dam, as shown in Fig. 17-8. Each length of 10 ft or so of the pipe is provided with a slot on its lower face which can be opened or closed manually by means of a sliding metal plate. Usually the soil-water mixture is discharged through not more than three or four slots opened at one time (see Fig. 17-10). The discharge can thus be located at any point of the pipeline around the dam. The pipeline is so placed that the water it discharges will flow toward the center line of the dam. The sand is deposited first, close to the pipe, and forms the pervious outer *shell* or *shoulder*, whereas silt and clay flow toward the inner core *pool*, where they settle out and form an impervious *core* for the dam. The fine colloidal clay remains in suspension for a considerable time and in modern construction work is usually pumped away by a small pump floating on a raft on the core pool (Fig. 17-8). The permeability of the silty clay core is so low that the discharge through the dam will be insignificant, even without the finer colloidal-sized particles, whereas the rate of consolidation, and therefore the rate of increase in the shearing strength, of the core will be greatly improved by the removal of colloids. A clamshell (Fig. 17-8) is used to stir up the sediment of the core pool in order to prevent the deposition of streaks of sand which might form undesirable and even dangerous pervious channels through the core.

When the sand reaches the level of the pipe, a new temporary supporting timber trestle is provided. The pipeline is disconnected and is raised to the new trestle; this stage is illustrated in Fig. 17-9, just before the old trestle was pulled out. In this manner the pipeline is successively raised, as shown in Fig. 17-7, from the position 1-1 to 5-5, and further on until the dam is completed. A bulldozer is used to provide the first small embankment at 1-1. For methods of constructing upstream slope protection see Fig. 8-23.

Hydraulic-fill dams can be constructed in any weather, and in this respect they have a considerable advantage over rolled-fill earth dams. However, the very nature of the hydraulic-fill process, as described above, limits its application in earth-dam construction to sites where the soil in the local borrow areas consists of mixtures of sand, silt, and clay. Where such soils are available, the hydraulic-fill method provides a comparatively inexpensive method for the transportation and the deposition of very large masses of soil. The Fort Peck Dam was built by hydraulic-fill methods which involved the moving of some 100 million cubic yards of soil; it is thus the largest man-made structure in existence. A considerable disadvantage of the hydraulic-fill method is that the sand is deposited

in a comparatively loose condition and may be therefore susceptible to flow slides (see Arts. 8-10 and 8-11). Some compaction may be obtained by letting a caterpillar tractor roll back and forth over the newly deposited sand.

17-4. Construction of Rolled-fill Dams. The compaction of the fill has to be performed in accordance with the general principles discussed in Arts. 11-2 and 11-3. Soil of any composition can be dug up by shovels in borrow pits (Fig. 17-11) and transported to any designated section of the dam by heavy rubber-tired equipment, which can materially assist the special rollers (Figs. 11-4 to 11-6) in the compaction of the fill. The cost
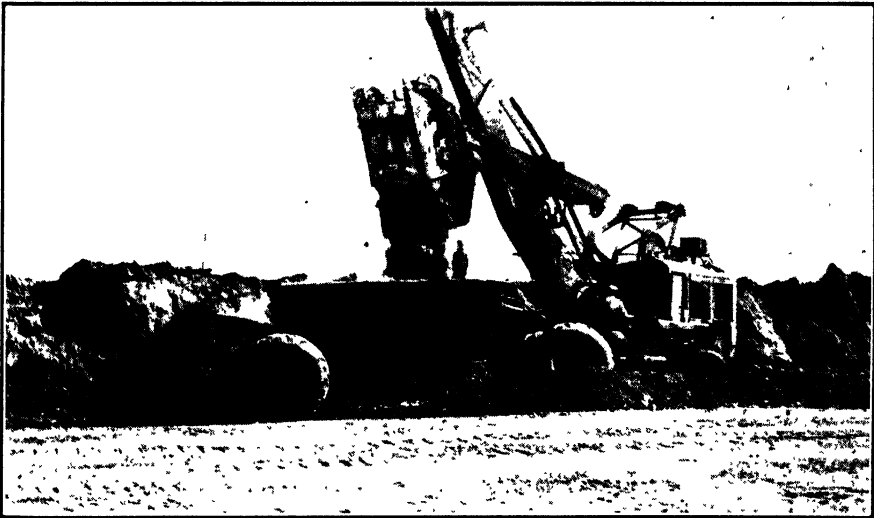
FIG. 17-11. A borrow pit for a rolled-fill earth dam. (*Photograph by Tschebotarioff, Ref. 375, 1939.*)

per unit of volume of rolled fill is appreciably higher than that of hydraulic fill.

The fill should be rolled on the "dry side," that is, at water contents at least 2 per cent below the optimum, for reasons explained in Art. 17-6. The water may be added either at the site of the dam (Fig. 11-5) or by sprinklers in the borrow pit area when the soil there is very dry. A combination of both methods may be employed. Work has to be interrupted during protracted periods of rain.

Care should be taken not to have less pervious material placed on the downstream face of the dam if one wishes to avoid disasters of the type illustrated by Figs. 17-1 and 17-2. Impervious material (clay) is usually placed in the center of the dam; sometimes an upstream blanket is employed. The latter method has the disadvantage that small animals may bore holes into it. Also, sloughing of the blanket or cylindrical sur-
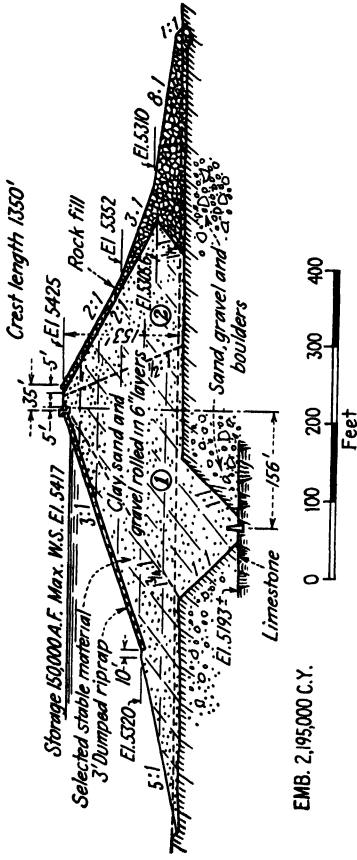
FIG. 17-12. Cross section through the rolled-fill Deer Creek Dam, built in 1937 by the U.S. Bureau of Reclamation. The cutoff trench reached to rock. (Courtesy of the U.S Bureau of Reclamation.)
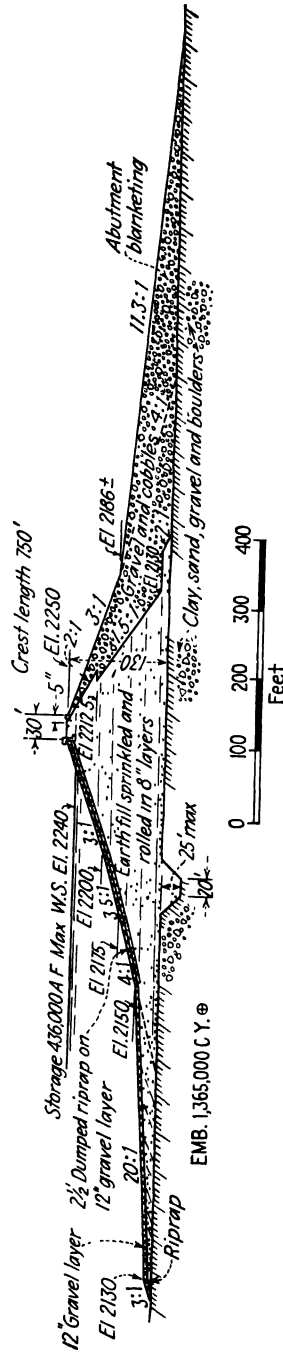
FIG. 17-13. Cross section through the rolled-fill Cle Elum Dam, built in 1931 by the U.S. Bureau of Reclamation on a deep bed of sedimentary deposits. (Courtesy of the U.S. Bureau of Reclamation.)

face slides thereof may occur in case of a sudden drawdown, that is, of a rapid drop in the upstream water elevation (see Art. 8-10). Somewhat flatter upstream slopes may be required to prevent such slides. Continuous field control of the density and water content of the fill is essential in all cases; the methods of such control are outlined in Art. 11-6.

Figures 17-12 and 17-13 give the cross sections of two rolled-fill earth dams built by the U.S. Bureau of Reclamation. The Deer Creek Dam (Fig. 17-12) is of a somewhat later construction (1939), when careful selection of soils and field control were already employed as a matter of routine. Relatively impervious soil was placed in zone 1. Granular material was placed in the outer zone 2. The impervious core was extended down to rock by means of a *cutoff trench*. A concrete *cutoff wall* reaching into rock was placed along the bottom of the cutoff trench and extended upward along the walls of the canyon. The purpose of such cutoff walls is to decrease the danger of seepage along the plane of contact between natural soil or rock and the rolled fill, since such a contact plane always represents a zone of weakness. The purpose of the cutoff trench, as implied by its name, is to prevent seepage under the dam. Wellpoints may have to be employed for the excavation of the cutoff trench in water-bearing sandy soils (see Fig. 14-13), where the trench may have to be built in sections (compare to cofferdam construction, Fig. 16-36) and the river temporarily diverted through specially built tunnels or other types of outlet structures (Fig. 17-6).

Steel sheet piling is sometimes used to provide a cutoff under a dam when digging a deep trench is not practicable. This was done under the Fort Peck Dam, but did not prove fully effective (Art. 17-7). On sites where boulders prevent the driving of sheet piling, the use of compressed-air caissons (Art. 15-14) has been tried successfully. This was the case at the Quabbin Dam (Ref. 109, 1934). Small reinforced-concrete caissons were successively sunk side by side to rock at depths up to 100 ft. The individual caissons were then connected, also under compressed air, to form a continuous core wall under the dam.

In some cases the rock is at such considerable depth under a dam that it is not possible to reach it by any type of cutoff wall or trench. It then becomes necessary to design the dam so that its stability will not be affected by uplift pressures created by water seeping through the soil under the dam. Figure 17-13 illustrates a 1931 design of a rolled-fill dam under such conditions.

17-5. Stability of Earth Dams. The failure of any type of dam after its completion is more disastrous in its consequences than the failure of any other type of structure (see Art. 17-2). The stability of a dam should therefore be the subject of particularly careful studies. The examples

cited in Art. 17-2 show that the study of both geological and engineering features is necessary to ensure a stable dam. Close cooperation and understanding between geologists and soil engineers is therefore even more important for the design of all types of dams than it is for other foundation studies (see Art. 12-2).

Soil engineers are mainly concerned with earth dams and have to study two principal factors on which their stability depends. First of all, the strength of the soil in the dam itself and in the foundation beneath it should be sufficient to resist the shearing stresses which are induced under any sloping earth surface. In other words, the slopes selected for the dam should be related to the shearing properties of the soil. The second problem is to control the seepage forces through the dam and its foundation in such a manner that there is no possibility for a quick condition developing anywhere and that the general stability of the dam is not endangered in any way.

The stability of the slopes of a dam is usually studied in accordance with the procedures discussed in Arts. 8-8 and 8-9, that is, by the Swedish cylindrical-failure-surface (circular-arc) method. In some cases the intensity of shearing stresses is estimated by means of the theory of elasticity (see Juergenson, Ref. 195, 1934). Flatter slopes are required on weaker types of soils. It will be noted from Figs. 17-5, 17-12, and 17-13 that, as a rule, the slope is varied along the height of a dam. It is made steeper near the top and is flattened out toward the base.

Some compaction of sand fills, especially in earthquake regions, is essential to prevent flow slides (Art. 8-11). On the other hand, there is some question whether excessive compaction of any type of fill is necessary when the underlying soil is comparatively weak. It appears possible that such overcompaction may even be detrimental, since it will provide a comparatively rigid superstructure which may be overstressed while adapting itself to the deformations of the underlying weaker material.

Rolled-fill material should be compacted on the "dry side" (Arts. 11-2 and 11-3), since otherwise excessive pore pressures may be developed in the fill. Control observations (Art. 17-6) are therefore essential and may indicate the need for changes of the original design. (According to Ref. 418, 1948, the "design as you go" method of construction, based on control observations, is part of the regular practice of the U.S. Bureau of Reclamation.) The development of excessive pore pressures u decreases the frictional component of the shearing strength of a granular rolled fill, in accordance with Eq. (7-14). The estimation of that component in a semicohesive fill requires extensive triaxial tests (see Arts. 7-25 and 7-26). In cohesive soils high pore pressures indicate that no further consolidation

and no further corresponding increase of density and of shearing strength of the fill (Art. 7-23) are taking place.

The stability of a hydraulic-fill dam presents special problems during the period of its construction (Art. 17-3). The outer shell, or "shoulder," which is composed of granular material, has to resist lateral outward fluid pressures of the slowly consolidating inner clay core. An analytical treatment of this stability problem has been given by Gilboy (Ref. 151, 1934). Measures to accelerate consolidation of the clay core are sometimes employed (Art. 17-3).

The control of seepage forces in earth dams is effected by placing the less pervious soil at the center or on the upstream face of the dam (see Art. 5-3). The seepage forces will then be dissipated within that less pervious material [see Fig. 5-6(*D*)] at a safe distance from the downstream face. This is intended to prevent the development of a quick condition there (Art. 5-4) and to ensure stability by having a sufficient thickness of soil between the zone where the seepage forces are absorbed and the downstream face. It will be noted that this procedure was employed in the case of the two dams illustrated in Figs. 17-12 and 17-13, where the outward grading of the soil types was done in several steps, with cobbles and rock fill following the gravel. The slopes were flattened out considerably near the base of the dam shown in Fig. 17-13, thereby appreciably lengthening the path of the water percolating under the dam and decreasing the hydraulic gradient (Arts. 5-3 and 5-4). It will be noted that the cutoff trench of that dam did not reach down to rock.

The flat slopes of a hydraulic-fill dam are therefore well suited to conditions where the underlying soil is pervious to a considerable depth. Additional precautionary measures may be possible and necessary, as illustrated by Fig. 17-5. In that case a thin layer of loam covered a deep bed of sand, thus forming a natural impervious blanket over it. This blanket was not disturbed under most of the dam and upstream thereof, except for the stripping of the upper 6 in. of soil, which were weakened by a considerable amount of grass roots. The dam was built directly on top of this blanket, except for the portion under the downstream toe where the top soil was removed all the way down to the sand, as shown in Fig. 17-5, and drain pipes were installed. This ensured the relief of possible excessive uplift pressures near the toe of the dam in a manner similar to, but somewhat more effective than, that of the shorter drain at the toe of the model dam shown in Fig. 5-6(*D*). No special grading of the filter material appears to have been undertaken in this case, since any clogging of the filter with time would be compensated for by the favorable effect of the increased thickness of the impervious upstream blanket due to the

deposition of silt from the usually muddy waters of the particular river behind that dam.

Very little or no pervious material (sand or gravel) is available at some dam sites. Toe drains are then sometimes used, but they require careful grading of the filter material if they are not to become rapidly clogged (see Art. 17-7).

Thus, as in other soil and foundation work, efficient designs of dams require the selection from a large number of possible solutions of the ones best suited to the general geology and to the types, stratification, and properties of soils in the area of the proposed site for the dam.

17-6. Control Observations in the Field. The field measurement of pore pressures (Art. 6-1) in different sections of a dam provides essential information which cannot be obtained by any other means. Purely theoretical analyses cannot take fully into account the great complexity and accidental variations in the composition of the soil in different parts of a large dam.

A number of devices have been developed for the purpose of measuring pore pressures. Figure 17-14 illustrates the type of device which is employed by the U.S. Bureau of Reclamation (1948) in foundation material. Prior to the construction of the dam a hole is drilled (Art. 12-6) down to the elevation in the natural soil where it is later desired to measure the pore pressure. A plastic pipe is inserted into the hole. Metal pipes are not advisable, since their interaction with some soils may develop gases which will increase the pressure in the water of the pipe to values well in excess of the actual pressure in the voids of the soil around the lower end of the pipe. This end is perforated, as shown, and the space between the pipe and the walls of the hole is backfilled with granular material for a distance of 12 in. from the bottom. Higher up that space is filled with a clay slurry. It is essential that the slurry be of a highly impervious type, since otherwise the device will register the highest pore pressure in any one of the soil layers intersected by the pipe, instead of the pressure at its lower end.

The top end of the plastic pipe, above the natural soil surface, is covered by a cemented plastic piezometer tip, as shown in Fig. 17-14. The lower end of the tip is protected by a porous disk, and a double line of plastic tubing is connected to the upper end of the tip. Both branches of the tubing are then carried through specially dug and backfilled (tamped) trenches to a terminal well on the downstream face of the dam. Some 14 pipes of this type can be placed in a 2-ft-wide trench. The purpose of the double line of tubing is to permit the periodical control flushing of any air or gas bubbles from the tubing and the piezometer tip.

A similar but somewhat simplified installation is used within the rolled

fill. No vertical pipe is needed, and the piezometer tip is laid at the selected location in a 1-ft³ pocket of granular material. Such piezometer tips of the "embankment" type are similar to the "foundation" type
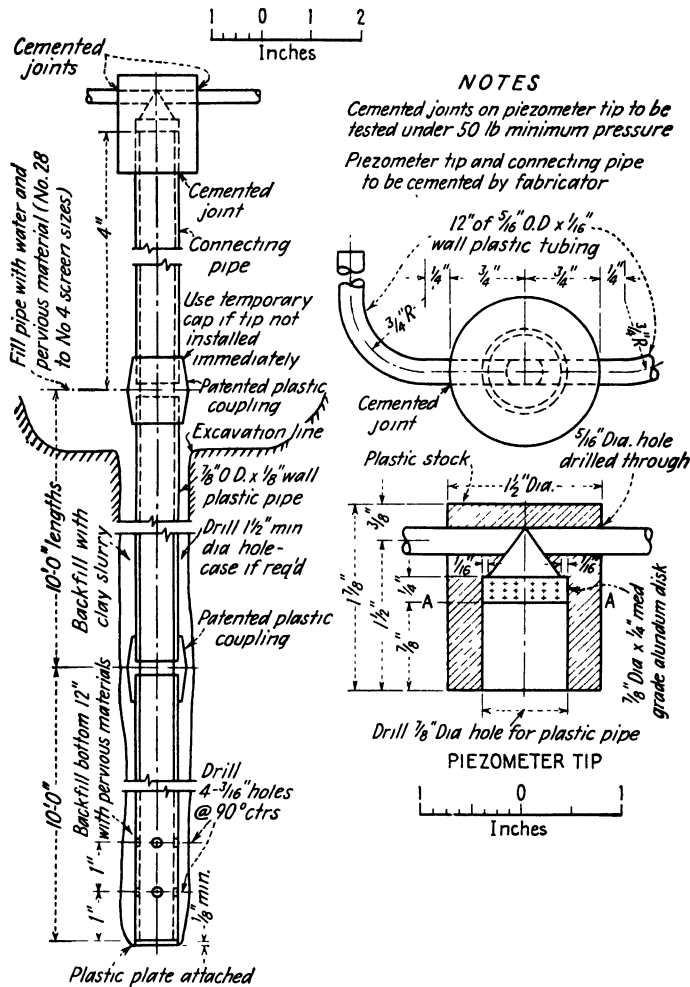
FIG. 17-14. Part of the pore-pressure measuring equipment used by the U.S. Bureau of Reclamation.

shown in Fig. 17-14 but are made shorter along the dotted line AA of that diagram.

A large number of such devices are installed on new dams for control purposes. For instance, pore pressures were measured at 40 points by as many separate piezometer tips on the Boysen Dam (1948). All tips were connected by tubing to one terminal well, where a system of brass

pipes and valves permitted their connection to two bourdon-tube-type altitude pressure gages which were used for the measurement of the pore pressures (see Ref. 419).

Other types of pore-pressure measuring devices are discussed in Art. 19-4.

The great practical value of pore pressure control measurements is demonstrated by the following facts. According to F. C. Walker and
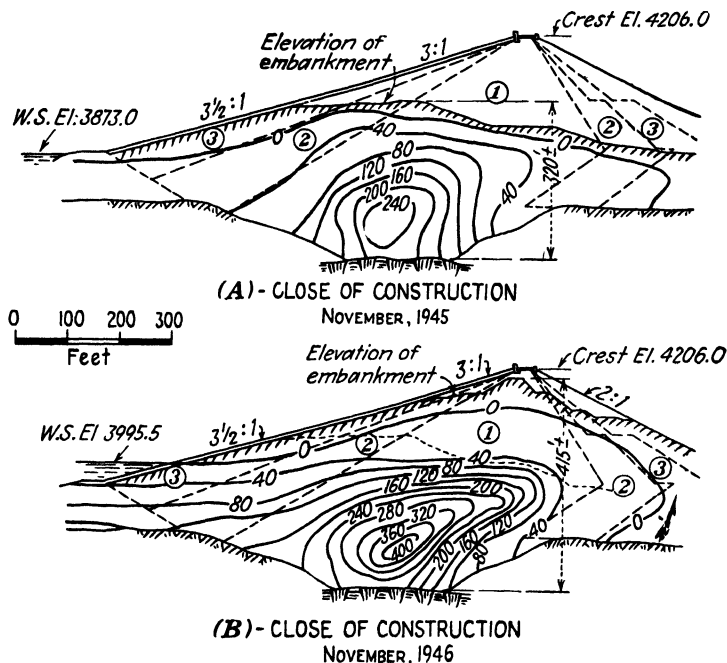
FIG. 17-15. Results of pore-pressure measurements performed by the U.S. Bureau of Reclamation during the construction of the rolled-fill Anderson Ranch Dam. All pressures are given in feet of water. ***(After F. C. Walker and W. G. Holtz, Ref. 419, 1950.)***

W. G. Holtz (Ref. 419, 1950), pore pressures amounting to 65 per cent of the superimposed fill were measured in 1940 during the construction of the 300-ft-high Green Mountain Dam, in spite of extremely high dry densities of the fill, which reached 150 lb per ft^3 and had an average of 136 lb per ft^3 (compare with Fig. 11-3). The compaction had been performed at the optimum moisture content. In spite of the high density, the great weight of the superimposed fill nevertheless induced some additional consolidation. Since the excess water could not escape rapidly from the large mass of the fill, considerable excess pore pressures were inevitably developed. That this is detrimental to the shearing strength of the fill was shown in Art. 7-9. Compacting on the "dry side" of the optimum, that

is, at a water content smaller by some 2 per cent than the optimum, proved an effective remedy. This point is illustrated by Fig. 17-15.

Up to the close of construction for the winter in November, 1945, on the Anderson Ranch Dam, compaction of the rolled fill of the impervious core (zone 1) had been performed at the optimum moisture content, in accordance with the views of many authorities at that time. However, considerable pore pressures were measured, as shown in Fig. 17-15(*A*). During the following season the fill was rolled at moisture contents smaller than the optimum, and the pore pressures developed within the drier soil mass were found to be insignificant, whereas they increased still further in the underlying wetter fill of the previous season [Fig. 17-15(*B*)]. Similar results were obtained on other dams (see Ref. 417), so that rolling on the "dry side," in accordance with special laboratory control procedures (Refs. 419 and 175), is now generally employed by the U.S. Bureau of Reclamation.

Measurements of earth pressures in earth dams are now seldom made, because of the uncertainties connected with the performance of earth-pressure cells when they are embedded in soil. This point will be discussed further in Art. 19-6; techniques for the measurement of settlement of individual soil layers will also be outlined in that article.

17-7. Graded Horizontal Filters and Relief Wells. In some localities very little pervious soil material is available. Excessive uplift pressures at the toe of the dam will then require relief. Attempts have sometimes been made to achieve this by placing there graded filters, as shown in Fig. 17-16. A perforated pipe is laid under the downstream slope of the dam in a trench parallel to the toe of that slope. The pipe is surrounded on all sides by gravel, then by coarse sand, followed by finer sand, and then by the regular fill material of the dam. Graded filters of this type are very expensive, since the fairly large quantities of granular material employed have to be first sieved out mechanically to obtain separate stock piles of the desired gradations. The sequence of successively reduced grain sizes in each following soil layer of the filter around the drain pipe, where the pipe is sometimes referred to as a *French drain*, is essential if clogging of the filter with time is to be prevented.

The following general principles apply to the design of any type of drain. If a coarse-gravel drain is laid in a trench dug through clay soil, seepage and other pressures will gradually squeeze the clay into the gravel until all its voids are filled with clay, are "clogged," and the drain ceases to function. Studies by G. E. Bertram (1940) and others (Refs. 27 and 343) indicate that a satisfactory performance of the filter can be expected if the following conditions are observed: The grain-size curves of soils for the proposed filter layers are determined and are plotted as shown in Fig.

3-1. The grain sizes of each soil corresponding to 15 per cent of the total (D_{15}) and to 85 per cent of the total (D_{85}) are read off from the grain-size curves. There will be no danger of the finer soil being squeezed into the voids of the coarser soil if the D_{85} of the finer soil is not smaller than one-fourth to one-fifth of the D_{15} of the coarser soil; this is the requirement needed to prevent clogging.

Graded horizontal filters may be employed for the purpose of preventing a quick condition (Art. 5-4) by loading with their weight the under-

FIG. 17-16. The placing of a graded filter around the perforated toe drain pipe of a rolled-fill earth dam built by the U.S. Engineer Department in Oklahoma. (*Photograph by Tschebotarioff, Ref. 375, 1939.*)

lying surface of the soil within which *all* of the seepage forces are to be dissipated; these are the so-called *weighted* or *reversed* filters. The D_{15} of the coarser layers of such filters should be at least four to five times greater than the D_{15} of the underlying finer layers.

Later pore pressure measurements appear to indicate that horizontal drains of the type shown in Fig. 17-16 may not always be fully effective (Ref. 230). Dangerous uplift pressures may be reduced, even at any time after construction, by drilling a row of relief wells along the toe of a dam or of a levee. (A *levee* is an embankment built along the shores of a river to contain its flood waters from inundating adjoining lands; it is essentially a small dam.)

An example of the beneficial effect of relief wells is provided in Fig. 17-17. Uplift pressures corresponding to some 40 ft of water head were

measured after completion of the Fort Peck Dam in the sand and gravel layers underlying the toe of that dam. The steel sheet piling which was used as a cutoff wall apparently was not fully effective. The drilling of a row of relief wells, however, decreased the uplift pressures at the toe of the dam to insignificant values. Similar measures were used at other dams with reported success (see Refs. 230 and 409).
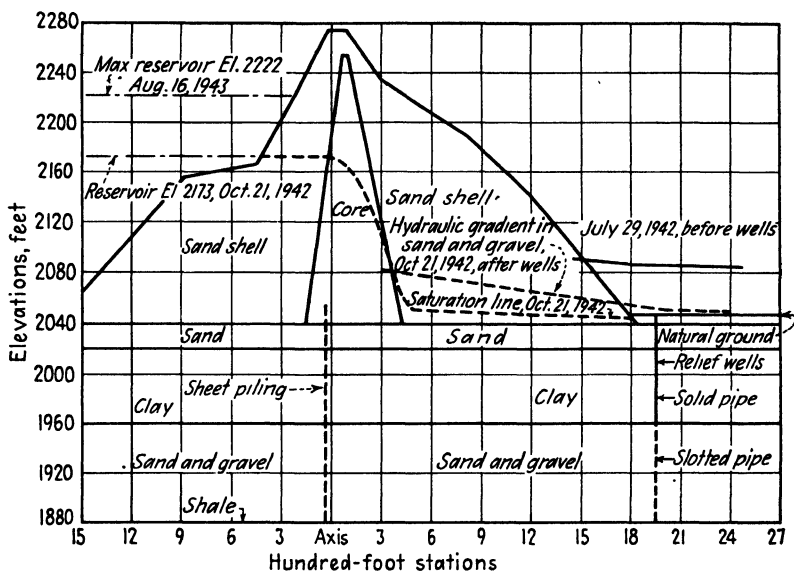
FIG. 17-17. The decrease of dangerous uplift pressures at the toe of the Fort Peck Dam subsequent to the installation of relief wells. (*After T A Middlebrooks and William H. Jervis, Ref. 230, 1947.*)

Borrow areas for the fill of a dam can sometimes be utilized for the relief of uplift pressure. It is therefore often advisable to locate such borrow areas on the downstream side of the dam. They should not be located on the upstream side if this would perforate a natural impervious blanket.

References Recommended for Further Study

Engineering for Dams, by William P. Creager, Joel D. Justin, and Julian Hinds, Wiley, 1945, Vol. I, General Design, 246 pp.; Vol. II, Concrete Dams, 372 pp.; Vol. III, Earth, Rock-fill, Steel, and Timber Dams, 251 pp.

"Progress Report of the Subcommittee on Consolidation of Materials in Earth Dams and Their Foundations," R. R. Philippe, chairman, *Proceedings of the American Society of Civil Engineers*, separate No. 48, December, 1950.

CHAPTER 18

EFFECTS OF VIBRATORY AND OF SLOW REPETITIONAL LOADING OF SOILS. MACHINERY FOUNDATIONS

18-1. Problems to Be Studied. Vibratory or slow repetitional loads, depending on their direction and on the point of their application to a rigid body, can produce six types of motion thereof, in accordance with the six *degrees of freedom* of such a body in space. There can be three types of *translations*, that is, displacements, namely, in the vertical direction and in two horizontal directions at right angles to each other. Also, there can be three types of *rotations*, namely, around a vertical axis and around two horizontal axes at right angles to each other. The great majority of combined theoretical and experimental studies in this field have been so far restricted by the complexities of the problem to the simplest type of motion, namely, to a vibrational or slow repetitional displacement (translation) in the vertical direction. In order to arrive at the proper evaluation of the advisable practical procedures of design and construction it is well to emphasize the fact that much more complicated types of foundation motion are possible and actually do occur in a great variety of combinations.

The determination of the *natural frequency* of a machine foundation is of considerable practical importance, since *resonance* will occur when the operational speed of a machine happens to coincide with the natural frequency of the foundation-soil system. Both the amplitude of motion of the foundation and the values of the unbalanced forces which excite the vibrations are greatly amplified at resonance to an objectionable extent and can lead to structural damage. The study of measures which can prevent such dangerous situations is therefore an important part of the design of machine foundations.

The resistance to vibratory and repetitional loading of soils of different type, density, and degree of saturation, as compared with their resistance to static loading, is another factor which has to be studied, since it is of

practical importance for the design of machine foundations and of highway and airport pavements.

The knowledge of the effect of blasting on adjoining structures and of the corresponding protective methods is of importance for civil engineering contractors. These problems will be briefly examined in this chapter.

Closely related to the above problems, in the sense of a common theoretical basis, are questions of wave-propagation velocities through different types of soils and of their application to site exploration (Art. 12-4) and problems of soil compaction (Arts. 11-4 and 11-5).

FIG. 18-1. Sketch illustrating the terms of Eq. (18-1).

18-2. The Phenomena of Resonance. Let us consider the behavior of a solid block resting on a spring, as shown in Fig. 18-1. If we give the block a sudden downward push in the direction of its vertical axis and then release the pressure, the block will start vibrating up and down in a vertical direction. Assuming that no forces whatsoever oppose this *free vibration*, its theoretical *frequency*, that is, the number of cycles of motion per unit of time, will be

$$f_n = \frac{1}{2\pi}\sqrt{\frac{k}{M}} = \frac{1}{2\pi}\sqrt{\frac{kg}{W}} \tag{18-1}$$

where f_n = natural frequency of block-spring system
k = linear spring coefficient, in units of load required to compress the spring by a unit of length, for instance, lb per in.
M = mass of block
W = weight of block
g = acceleration of gravity

For the derivation of Eq. (18-1) see any textbook on mechanical vibrations, for instance, Den Hartog (Ref. 106). The theoretical undamped vibrations, as expressed by Eq. (18-1), are supposed to continue indefinitely. This, in reality, is never the case, and the vibrations are found to gradually decrease in amplitude (that is, in the distance of their oscillatory motion) and to stop entirely after a while, unless the push which excited the vibrations in the first place is repeated periodically, that is, unless we deal with *forced vibrations*. The frequency of such vibrations of decreasing amplitude, that is, of *damped vibrations*, is

$$f_{nd} = \frac{1}{2\pi}\sqrt{\frac{k}{M} - \frac{c^2}{4M^2}} \tag{18-2}$$

where f_{nd} = natural frequency of damped vibration
c = damping constant

The other symbols have the same significance as in Eq. (18-1). It will be noted from a comparison of Eqs. (18-1) and (18-2) that the presence of damping decreases somewhat the natural frequency of a vibrating body. To this day no reliable and practicable methods have been developed which would permit the numerical determination of the damping constant c of soils. For that reason damping is usually neglected in the analysis of field experiments involving the determination of the natural frequency of foundation-soil systems. These analyses use Eq. (18-1) as a starting point.
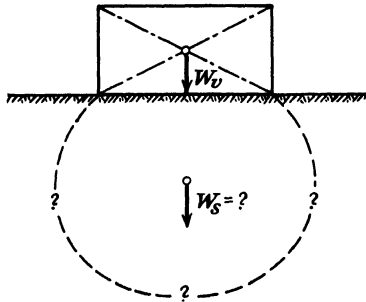
FIG. 18-2. Sketch illustrating the terms of Eq. (18-3).

It is not possible to place heavy foundations on springs, although this is sometimes done in the case of light machinery (Art. 18-6). Foundations of heavy machines are therefore placed directly on the ground, so that the conditions of their support correspond to Fig. 18-2, rather than to Fig. 18-1, on which Eq. (18-1) was based. In the case of an actual foundation, shown in Fig. 18-2, it is no longer possible to neglect the weight of the soil spring, as was done in the derivation of Eq. (18-1), where
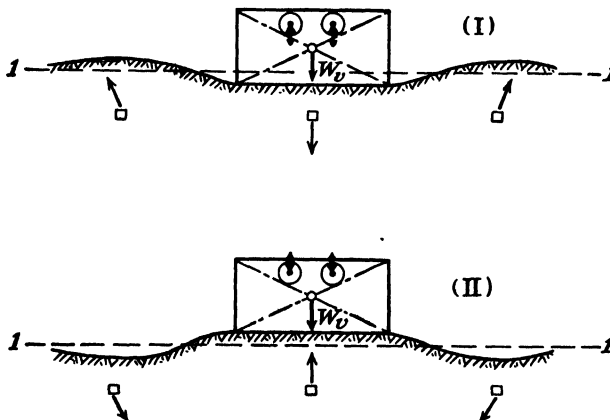
FIG. 18-3. The probable nature of the soil-surface deformations around a two-mass vibrator inducing vertical oscillations. (*After Crockett and Hammond, Ref. 92, 1947.*)

it was assumed that the weight of the spring is negligible in respect to the weight W of the block. The soil acts as a spring for the foundation and vibrates together with it, as shown in Fig. 18-3. Lorenz (Ref. 217, 1934) attempted to assign a definite value to the mass of the vibrating soil and, to that end, transformed Eq. (18-1) to read

$$f_n = \frac{1}{2\pi}\sqrt{\frac{k'Ag}{W_s + W_v}} \tag{18-3}$$

where A = contact area between base of foundation and soil
$k' = k/A$ = dynamic modulus of soil reaction, or volume spring coefficient
W_v = weight of machine and of its foundation
W_s = weight of vibrating soil

Equation (18-3) is often quoted without any reservations, and Lorenz even attempted to use it to determine experimentally the actual value of W_s. However, it will be shown in Art. 18-3 that the procedure employed for this purpose was based on assumptions proved later to be incorrect. It should also be realized that there cannot be a clearly defined limit for the vibrating soil mass W_s, such as is indicated by broken lines in Fig. 18-2. A glance at Fig. 18-3 will show that the motions of the soil are more complex than the motion of the machine and foundation. The term W_s in Eq. (18-3) should therefore be considered as referring to what might be called an *equivalent weight* of soil, with no clearly defined physical boundaries.

18-3. Experimental Determination of the Natural Frequencies of Vibrator-soil Systems. Experiments with forced vibrations are usually performed by means of a machine the action of which is illustrated by Fig. 18-4. This type of machine was first employed by E. Schmidt (Ref. 304, 1921) to study damping characteristics of different insulation materials under foundations. It was then extensively used by R. Bernhard and W. Spaeth (Ref. 25, 1929) for the study of natural frequencies of steel bridges. A. Hertwig, G. Fruh, and H. Lorenz (Ref. 171, 1933) of the German Research Society for Soil Mechanics (abbreviated name: DEGEBO) adapted this type of machine to the study of the effect of forced vibrations on soils.

The machine is sometimes referred to as a *two-mass oscillator*. It has two shafts which are geared together and which rotate in opposite directions. Each shaft has an eccentric weight, shown black in Fig. 18-4, which is so mounted that the horizontal component of its centrifugal force cancels out the corresponding component of the eccentric weight on the other shaft of the machine, and vice versa. Only the vertical component of the centrifugal forces remains; it varies according to a sinusoidal curve, as shown in Fig. 18-4, reaching a maximum downward value at stage *b* and a maximum upward value at stage *d*. For constant values of the eccentric weights, their centrifugal forces increase with the square of the speed of rotation of the shafts. In some modern oscillator machines the unbalanced eccentric weight can be varied while the machine is in operation.

One of the original broad objectives of the DEGEBO studies aimed at determining the dynamic properties of different types of soils, in the hope that practically usable relationships could be established between these dynamic properties and the resistance of such soils to static loading by foundations. If successful, this procedure would have had the advantage of permitting the nondestructive testing of the soil in situ and the determination of the average over-all properties of a large mass thereof, instead of the at present unavoidable extrapolation to the entire mass of the properties of small samples extracted from boreholes under great difficul-
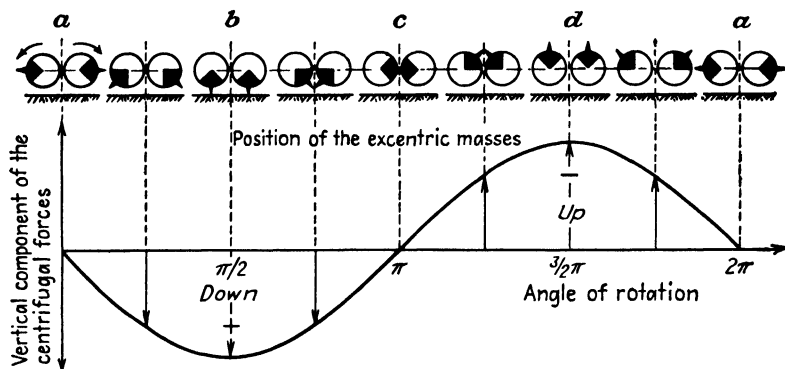
FIG. 18-4. Variation of the vertical component of the centrifugal force during one shaft revolution of the two-mass oscillator. (*After Hertwig, Fruh, and Lorenz, Ref.* 171, 1933.)

ties and tested in a laboratory. The attempt was worth while, and much useful information was obtained, although the original broad practical objective proved impossible to attain, for reasons which will be now outlined.

One of the essential dynamic properties of soils is the velocity of wave propagation through the soil. Continuous forced vibrations produced by machines of the type shown in Fig. 18-4 presented very few advantages for the study of wave-propagation velocities and had a number of operational drawbacks, as compared with the conventional hammer-impact or dynamite-blast techniques. The limited applicability of such methods of wave-propagation-velocity determination was discussed in Art. 12-4.

The second dynamic property of soils emphasized in the DEGEBO studies was the natural frequency of different soil-vibrator systems. Table 18-1 summarizes the results obtained prior to 1933 by the DEGEBO with their standard-type vibrator which weighed 2,700 kg (6,000 lb) and had a contact area with the soil of 1.0 m^2 (10.7 ft^2), giving a contact pressure of 0.28 ton per ft^2. Soft soils, similarly to soft springs, have a low value of k and k' and, hence, a low natural frequency f_{nd} [Eqs. (18-1) to

(18-3)]. The effect of the size of the contact area A with the soil and of a number of other factors on the natural frequency of a soil-vibrator system was not fully realized at first. The results of the early DEGEBO tests were reprinted in some English-language publications without any indications as to the limits of their validity. A consequence of this has been a widespread erroneous belief that the value of the natural frequency of a soil is a clearly defined basic physical property of a soil type, which can be numerically related to its strength and to other similar relevant engineering properties.

Later studies of the DEGEBO indicated the following limitations of their procedure: All other factors remaining constant, an increase in the

TABLE 18-1. Natural Frequencies of a DEGEBO Standard-type Vibrator on Different Kinds of Soils

Nature of soil	Natural frequencies, f_{nd}	
	Cycles per sec	Cycles per min
6 ft of peat, overlying sand	12.5	750
6-ft-thick old fill consisting of medium sand with remnants of peat	19.1	1,145
Gravelly sand with clay lenses	19.4	1,165
Old, well compacted by traffic slag fill	21.3	1,280
Very old, well compacted fill of loamy sand	21.7	1,300
Tertiary clay, moist	21.8	1,310
Lias clay, moist	23.8	1,430
Very uniform yellow medium sand	24.1	1,445
Fine sand with 30 per cent medium sand	24.2	1,455
Uniform coarse sand	26.2	1,570
Nonuniform compacted sand	26.7	1,600
Quite dry tertiary clay	27.5	1,650
Compact clay	28.1	1,685
Limestone, undisturbed rock	30.0	1,800
Sandstone, undisturbed	34.0	2,040

centrifugal force of a vibrator brought about a decrease in its natural frequency. Thus a standard-type DEGEBO vibrator (see preceding paragraph) at a low centrifugal-force setting was found to have on a certain sand a natural frequency f_{nd} = 1,600 cycles per min. A progressive increase in the centrifugal force progressively decreased this value on the same soil down to a minimum of f_{nd} = 1,320 cycles per min, that is, by 17 per cent. Presumably greater exciting forces cause a larger equivalent weight of soil W_s to participate in the oscillations; according to Eq. (18-3),

this would decrease the value of f_n (see Lorenz, Ref. 217, 1934, and Ref 382). Similarly, a decrease in the weight of the standard DEGEBO vibrator from 6,000 to 4,500 lb on the same soil, all other factors remaining unchanged, had a reverse effect. At a low value of the centrifugal force the natural frequency was raised from $f_{nd} = 1{,}600$ cycles per min to $f_{nd} = 1{,}740$ cycles per min and at a high centrifugal-force value from $f_{nd} = 1{,}320$ cycles per min to $f_{nd} = 1{,}380$ cycles per min.

Lorenz then attempted to determine the value W_s from vibrator tests performed with three different sizes of contact areas with the soil, $A = 10.7 \text{ ft}^2$, $A = 5.3 \text{ ft}^2$, and $A = 2.7 \text{ ft}^2$ (Ref. 217). The value of W_v was kept constant in all three tests; this left for each test two unknowns in Eq. (18-3), W_s and k'. Lorenz eliminated k' by assuming that it is a constant; this permitted the solution of the three equations for W_s. However, this procedure was erroneous, as pointed out by Tschebotarioff and Ward (Ref. 386, 1948).

A series of tests performed by Barkan (Ref. 19, 1934) in the U.S.S.R., simultaneously with, but independently of, the work of Lorenz, had shown that k' could not be a constant. This coefficient is equal to

$$k' = \frac{p_d}{S_d} \tag{18-4}$$

where k' = dynamic modulus of soil reaction
p_d = alternating component of average vertical contact pressure with soil due to repetitional (dynamic) forces
S_d = soil compression caused by p_d ($\approx$ one-half of the amplitude of vibration)

Barkan assumed that S_d could be taken as approximately equal to the elastic rebound S_e of a static load test. The coefficient k' could then be determined, as shown in Fig. 18-5, from

$$k' = \frac{p_d}{S_e} \tag{18-5}$$

It would appear somewhat more logical to determine this modulus from the hysteresis loop formed by the pressure-settlement curve after reloading, as shown in Fig. 18-5, that is, to take

$$k' = \tan \beta \tag{18-6}$$

However, this is an unimportant detail, since a series of tests performed by Barkan demonstrated that for the same intensity of the static load p_d the value of the elastic rebound S_e increased with the size of the loaded area (see Fig. 18-6). This result is in agreement with the known facts about the relationship between settlements and the size of a footing

(see Arts. 9-1 and 9-8). It therefore follows that the coefficient k' cannot be a constant, as had been assumed by Lorenz, but that its value will decrease with the size of the loaded area. Barkan's tests emphasized several other factors which make it impossible to determine the true value of the dynamic modulus k' from static load tests. For instance, he found that the value of the rebound S_e and therefore of k' was strongly affected by the rate at which the unloading was performed; a slow rate of unloading increased S_e, especially on clay soils.
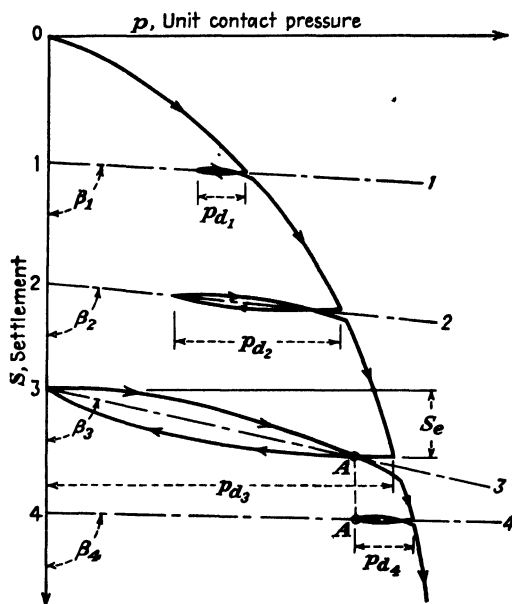
FIG. 18-5. Sketch illustrating discussion of the reasons why the dynamic modulus of soil reaction $k' = p_d/S_d$ (volume spring coefficient) cannot be determined from static load tests.

The exact degree of magnification of the dynamic forces at resonance depends on damping factors which can only be guessed at. Hence this degree of magnification is not known, although it will be noted from Fig. 18-5 that the value of $k' = \tan \beta$ will change considerably, depending on the extent of this magnification, as expressed by the values of p_d.

The preceding discussion has led to a negative result, in the sense that it has demonstrated the impracticability of some of the design techniques which are still sometimes advocated at present (compare Refs. 246 and 400, 1951). The determination of soil coefficients which are needed for the rigorous analysis and forecast of natural frequencies of soil-vibrator systems has been shown to be a problem of a highly indeterminate character. The understanding of this point is essential to the appreciation of

the importance of possible alternative semiempirical procedures of machinery-foundation design which are outlined in Arts. 18-5 and 18-6.

It should further be noted that an attempt was made to relate permissible bearing properties of soils to their natural frequencies, as established by a standard DEGEBO-type vibrator. It will be seen from Table 18-1 that, if we leave out such extreme types of supporting material as peat and rock, the natural frequencies of all types of sands and clays were found to vary within comparatively narrow limits, from 1,145 to 1,685 cycles per min, that is, by some 50 per cent at the utmost. At the same time, it will be seen from Table 14-2 that the range of possible variations in the permissible bearing values on medium to dense sands, and of corresponding penetration resistances, is ten times greater, from 1.0 to 6.0 tons per ft². The same holds true for clays. Thus there is little chance that the natural frequencies of vibrator-soil systems can ever be rationally utilized practically for the determination of permissible bearing values p_0 of new foundations. Such p_0 values have been published sometimes alongside f_n values in tables similar to Table 18-1, but their selection appears to have been entirely arbitrary, without consideration of the numerous other factors involved (Arts. 14-1 and 14-2).

FIG. 18-6. Static load tests showed that the elastic rebound S_e (see Fig. 18-5) increased with the intensity of pressure p and with the size of the loaded area A. (*After Barkan, Ref. 19, 1934.*)

It has been shown in the preceding discussion that there is no such thing as a definite value for the natural frequency of a certain type of soil. There are, however, certain *ranges* for such frequencies. Thus natural frequency values published by Crockett and Hammond (Ref. 93, 1948), which were obtained by striking the ground with a heavy hammer and measuring ground vibrations by means of an oscillograph, fell within the same ranges as the values obtained by forced vibration and reported in Table 18-1. Rocks had values exceeding 30 cycles per sec (1,800 cycles

per min); peats and soft clays from 15 cycles per sec (900 cycles per min) down to 7.5 cycles per sec (450 cycles per min); sands and medium to stiff clays had intermediate values between these two extreme types of materials. However, even if one employs the impact method to determine the natural frequency of a soil, one will find that different values may be obtained on the same site, depending on whether a new structure has been added or an old one removed close to the place of the test.

Therefore, instead of speaking about the natural frequency of a soil or of the ground, it is more rational to refer to the *natural frequency of a site*, or of a *soil-foundation system*, where the terms "site" or "system" cover all characteristics which may affect the value of the natural frequency of a new foundation. These are the nature of the soil and rock stratification and the depth and the properties of the successive layers; the presence next to the site of surcharges, such as buildings, other machines and foundations thereof, embankments, or cuts; the weight of the machine itself and of its foundations; the size of the contact area of the new foundation with the soil; the characteristics of the exciting forces; and other factors outlined in Arts. 18-5 and 18-6.

18-4. The Resistance of Different Types of Soils to Vibratory and to Slow Repetitional Loading. A by-product of the DEGEBO tests was the finding that sands, especially when they were of uniform grading, were more susceptible to deformation by vibratory loading than were clays. No general numerical relationships, however, were established. In order to obtain such relationships a series of tests was performed at Princeton University in 1943 to 1946 under the sponsorship of the Technical Development Service of the Civil Aeronautics Administration (CAA). The results were reported by Tschebotarioff and McAlpin in Refs. 378, 381, and 382.

Equipment of the CBR type (Art. 19-5 and Fig. 19-10) was employed for the tests. However, since vibratory tests cannot be combined with controlled-strain loading equipment because of the great inertia of the head through which the load is applied, the CBR equipment was modified, so that tests of the controlled-stress type could be performed (Art. 7-13). Actual weights were applied to the plunger, and the settlement (penetration) of the plunger was recorded as a function of the load (see Fig. 18-10). A vibrator of the type shown in Fig. 18-4 was attached to the loading frame and was started after the entire static load had been applied. The centrifugal force of the vibrator was varied between 1 and 25 per cent of the static load on the plunger. The ratio of the dynamic penetration, that is, of the additional plunger penetration under the action of the vibrator, and the static penetration was used as a measure of the sensitivity of a soil to vibratory loading. The static penetration used for the

computation of such ratios was taken from the end section of the static load–penetration curve corresponding to the magnitude of the centrifugal force employed.

It was essential to avoid any magnification of the centrifugal-force values by resonance. Preliminary experiments were therefore performed to determine the resonance ranges of the vibrator-soil-container systems, so that these ranges could be avoided. To that end, the vibrator speed was gradually increased from its minimum of 900 rpm to its maximum of 3,200 rpm. Plunger penetrations and amplitudes of vibration were measured and plotted against the vibrator velocity, as shown in Fig. 18-7. It will be noted that for that particular test the increment of plunger penetration, as well as the amplitude of vibration, reached a pronounced peak at 2,100 rpm. This was the natural frequency of the system. All other tests of this kind indicated that the natural frequencies of the systems in all cases appreciably exceeded the 1,000- to 1,500-rpm range employed for the main series of tests; thus all danger of full or partial resonance was excluded. A surcharge of 0.5 psi was applied in all tests to the soil surface around the plunger.
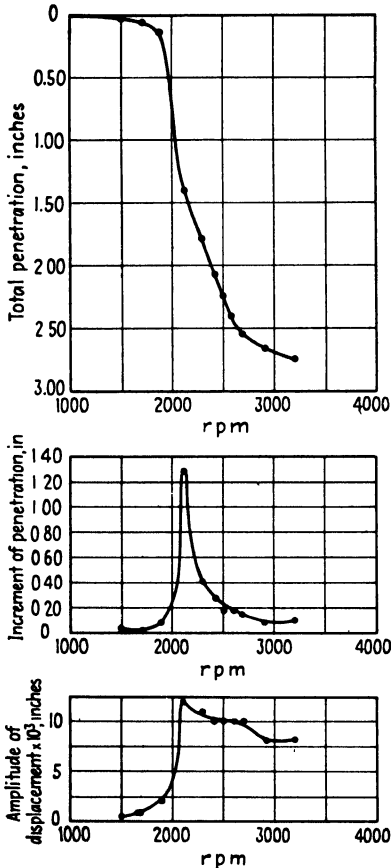
FIG. 18-7. Determination of resonance range of loaded 2-in.-diameter plunger on dense, dry, well-graded sand from the increment of penetration vs. velocity curve. (*After Tschebotarioff and McAlpin, Ref. 382, 1947.*)

Two sands were used for the tests. One was well-graded, the other was uniform (see Fig. 3-9 for a microphotograph of the latter). Tests were performed at different densities and degrees of saturation. A summary of the results of static penetration tests for the well-graded sand is given in Fig. 18-8. It will be noted from that diagram that for values of the void ratio e smaller than $e = 0.65$, that is, for medium to loose states of relative density D_d (see Art. 4-6), the plunger penetrations were quite large under all conditions of saturation. It will further be seen from Fig. 18-8 that a
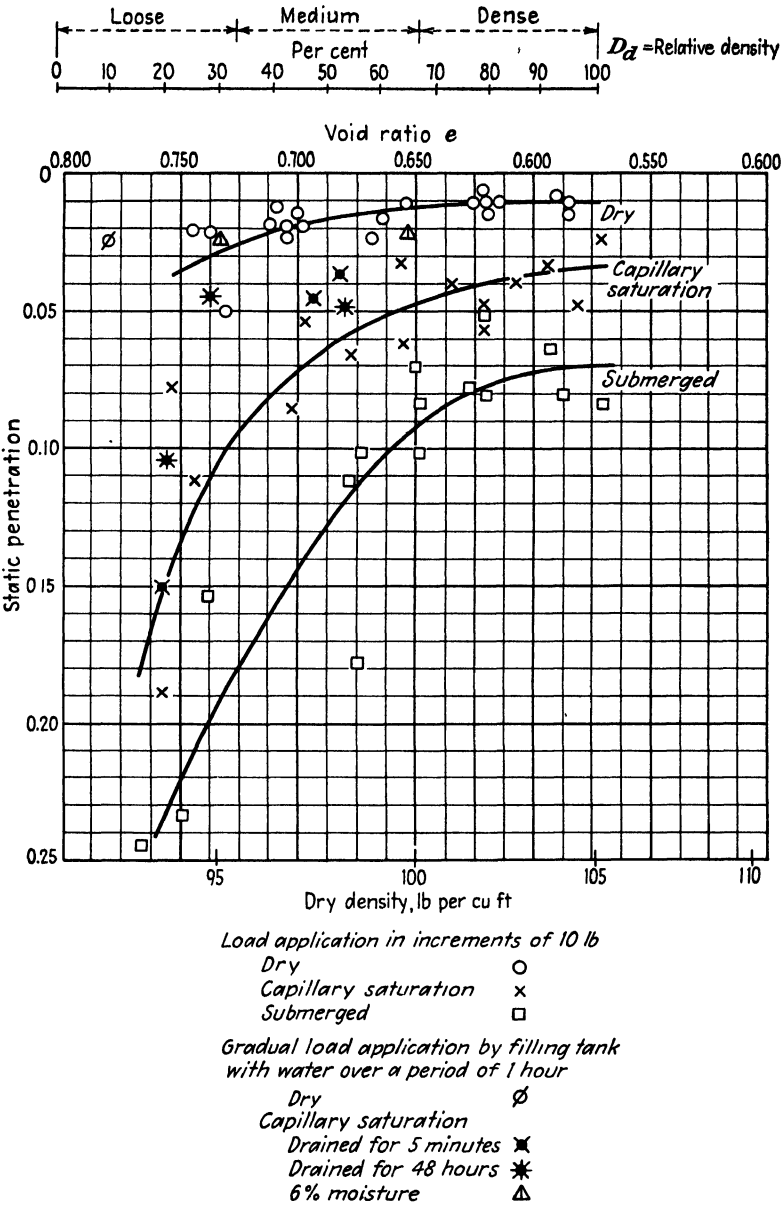
FIG. 18-8. Effect of density and of state of saturation on the static plunger penetrations into well-graded sand. (After Tschebotarioff and McAlpin, Ref. 382, 1947.)

dry density $\gamma_{md} = 100$ lb per ft^3 corresponds to $e = 0.65$; this is equal to (100.0/105.2)100 = 95 per cent of the maximum dry density of 105.2 lb per ft^3 for that sand. This point will be of importance in connection with the discussion in Art. 19-6 of specifications for the field compaction of fills and of base courses.

Submerged and partially saturated sand offered less resistance to plunger penetration than did dry sand of the same density. This might possibly be attributed to the composition of that natural sand, 95 per cent of which was quartz grains and 5 per cent limonite (iron oxide), which softens when moist. However, it is also possible that the very fact of submergence or of partial saturation produced full or local buoyancy conditions which decreased the effective stresses between the sand grains and, hence, also decreased the shearing strength below the sand surface and the resistance to loading of the whole sand mass.

Capillary saturation is known to improve the *trafficability* of a sand surface. For instance, the sand at Daytona Beach, Florida, from which location came the uniform sand used in these tests, is known to provide an excellent surface for the world-famous automobile racecourse. It should be noted in this connection that these good properties of the sand race track are primarily due not to its low compressibility, but to the resistance of a thin top layer of sand to tangential forces applied to its surface by the revolving wheels and tires of the moving car (see Art. 19-8 for further discussion of this point).

The dynamic plunger penetrations in the well-graded sand, that is, the plunger settlements produced by the centrifugal forces of the vibrator, followed the same general trends as the static penetrations shown in Fig. 18-8. For a vibratory force equal to 25 per cent of the maximum static load 10 min of vibration at 1,000 rpm, that is, 10,000 load repetitions, produced plunger penetrations at least 2 to 15 times larger than the penetrations produced by a static load of equivalent magnitude. Even greater ratios of dynamic and static penetrations, up to 45, were obtained in some cases.

Neither the static nor the dynamic plunger penetrations in the *uniform* Daytona Beach sand (pure quartz) followed clearly defined trends insofar as the effects of saturation were concerned. A dense state of the sand could be obtained only by combining static pressure with strong tapping of the container; small plunger penetrations were then recorded (Refs. 381 and 382). Static pressure alone (up to 2,000 psi = 144 tons per ft^2) produced only a loose to medium state. The plunger penetrations were then erratic, as well as their ratios (Fig. 18-9), depending apparently on the accidental structural arrangement of the grains. An exception was provided by the series of tests performed on uniformly sized moist sand,

marked by triangles in Fig. 18-9, where the figures next to the triangles indicate the static pressure, in pounds per square inch, which was used for compaction. Owing to bulking (Art. 3-5), very low densities were obtained in proportion to the compaction pressure applied.
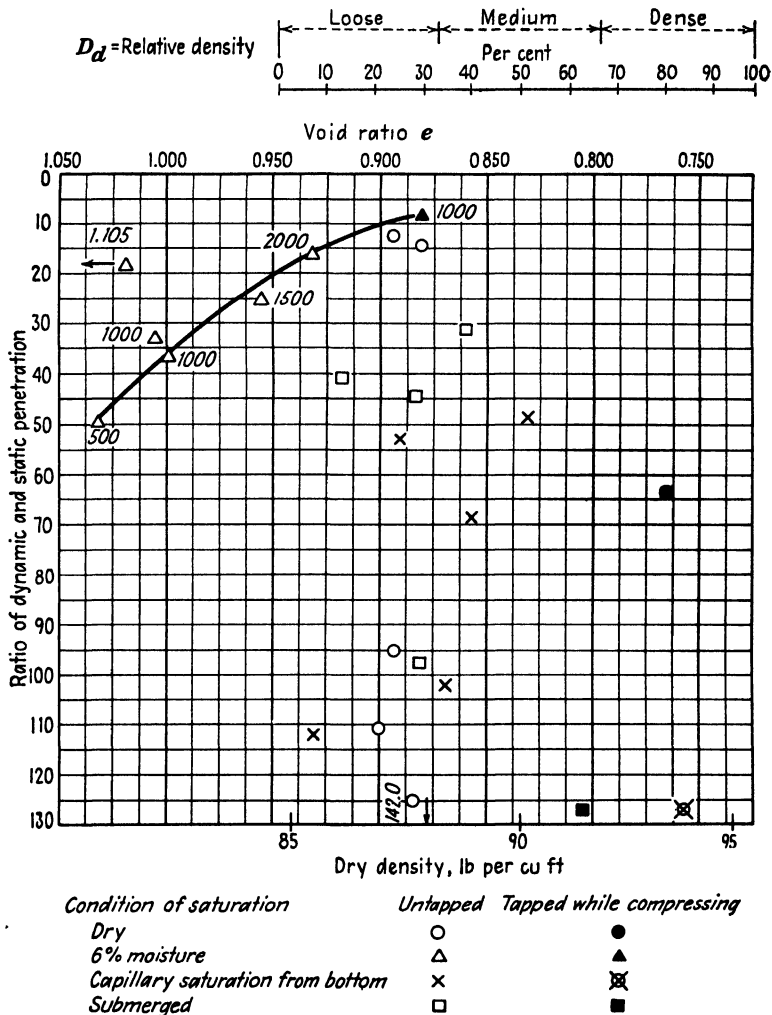
FIG. 18-9. As compared with static loading, the response to vibratory loading of a uniform sand is considerable, but erratic. (After Tschebotarioff and McAlpin, Ref. 382, 1947.)

It will be noted from Fig. 18-9 that this uniform sand was highly susceptible to vibrations. The dynamic plunger penetrations were at least 15 to 70 times higher than the corresponding static penetrations, and in one case they were 142 times higher.

The dynamic plunger penetrations appeared to be proportional to the intensity of dynamic stresses, which were a function of the centrifugal force. It will be noted from Fig. 18-10 that even a slight vibratory force equal to only 1 per cent of the original static load produced after 10 min of vibration on the uniform sand a plunger penetration equal to 25 per cent of the total static penetration.
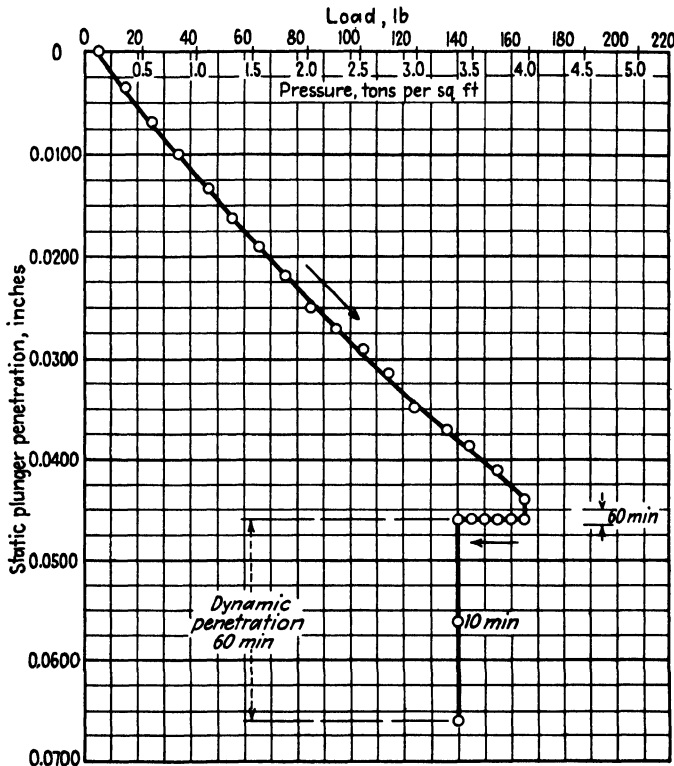
FIG. 18-10. A vibratory force equal to only 1.05 per cent of the original static load produces after 10 min of vibration on uniform dry sand of medium density a plunger penetration equal to 27 per cent of the total static penetration. (*After Tschebotarioff and McAlpin, Ref.* 382, 1947.)

Tests were performed with two types of clays. The first was a silty clay (w_L = 31 per cent, w_P = 24 per cent, I_P = 7 per cent); the second was somewhat richer (w_L = 43 per cent, w_P = 25 per cent, I_P = 18 per cent). The clays were tested in their semisolid range of consistency (Art. 4-7), that is, at water contents below their plastic limits. All were thoroughly compacted by static pressure in accordance with the procedure for the preparation of CBR specimens (Art. 19-5) but without any soaking after the compaction.

In contrast to the sands, the clays, when compacted to the above density and consistency, were found to be unaffected by vibrations. Their dynamic plunger penetrations after 10 min vibration were on an average equal to the static plunger penetrations under a load equal to the centrifugal force of the vibrator. The difference in the behavior of sands and of clays may be explained as follows: Vibratory forces repeatedly increase and then decrease the contact pressures between the soil grains.
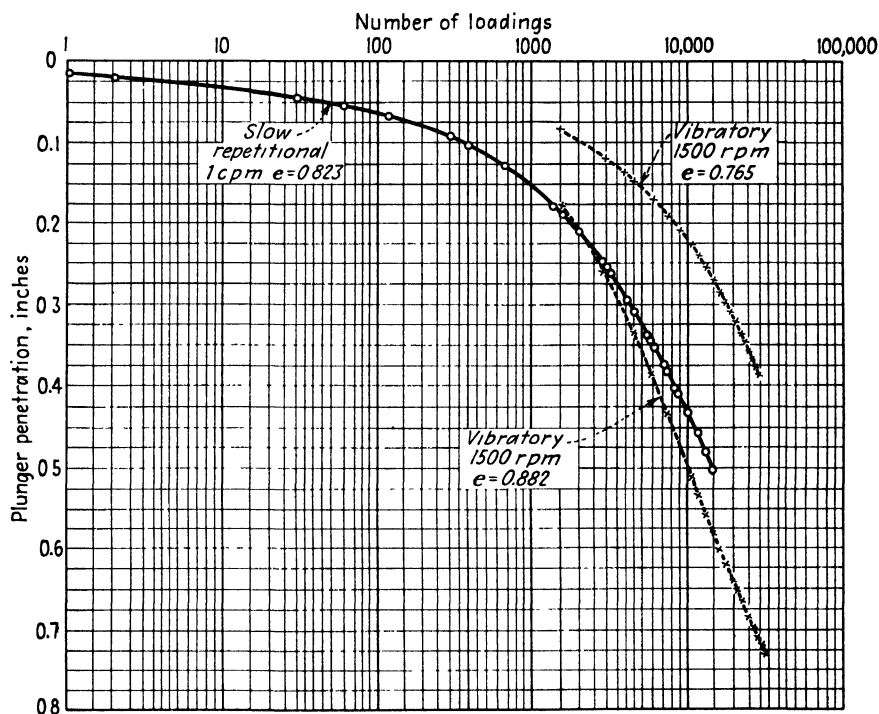
FIG. 18-11. Comparison of plunger penetrations into sand under the effect of vibratory and of slow repetitional loading. (*After Tschebotarioff and McAlpin, Ref.* 382, 1947.)

In the case of clays this does not break the cohesive bond between the particles, which is independent of the external pressures (Art. 7-23). However, in the case of sands, the shearing strength of which *is* dependent on external pressures (Arts. 7-15 and 7-24), repeated variations of such external pressures apparently causes progressive slippage of the sand grains on each other.

Sand-clay mixtures, when thoroughly compacted in the same manner, behaved essentially like a clay and were unaffected by vibrations. This is exactly the reverse of the behavior of uncompacted, fully saturated sand-clay mixtures (see Art. 16-14).

Slow repetitional tests were performed at 1 cycle per min in order to determine the effect, if any, of the frequency of load repetition outside of the resonance range. As shown in Fig. 18-11, the *number* of load repetitions was found to be the governing factor under such conditions, irrespective of the frequency. The plunger penetrations in sand of the same density increased in an almost identical manner with the number of load repetitions, irrespective of whether the load reversals occurred at 1 cycle per min or at 1,500 rpm.

The vibrations induced by heavy truck traffic along a highway some 150 ft from the building on the ground floor of which the tests were performed were found to have approximately the same effect on the continued penetrations into sand of a loaded plunger, as would be produced by a repetitional variation of 1 per cent of the static load at 1 cycle per min.

FIG. 18-12. The typical shapes of plunger penetration vs. load repetition curves (a) on clays; (b) on sands. (*After Tschebotarioff and McAlpin, Ref. 382, 1947.*)

The same results were obtained with clays, except that the *shape* of the curves giving the number of load repetitions versus plunger penetrations was different from that of sands. As shown by curve *a* of Fig. 18-12, the plunger penetrations in clay tended to stop entirely with time, usually after some 10,000 load repetitions; in the case of sands (curve *b*) they still continued.

As compared with the plunger penetration under static loading, the effect of 10,000 load repetitions increased with the intensity of the repetitional load, which was expressed as a fraction of the original static load (Fig. 18-13). See also Arts. 19-5 and 19-6 for the significance of this fact for airport and highway design.

Unconfined and triaxial compression tests were performed in 1946 to 1948 at Harvard University to determine the effects of transient loading, that is, of loading of short duration, on the shearing strength of soils. The results were reported by A. Casagrande and W. L. Shannon (Ref. 68). To produce failure in clays during 0.02-sec load application, a 1.4 to 2.6 times higher load was required than in the case of the customary 10-min duration of this type of test. This is in agreement with the known behavior of other materials under sudden temporary loading and with the results of previous tests concerning the effect of the rate of load applica-
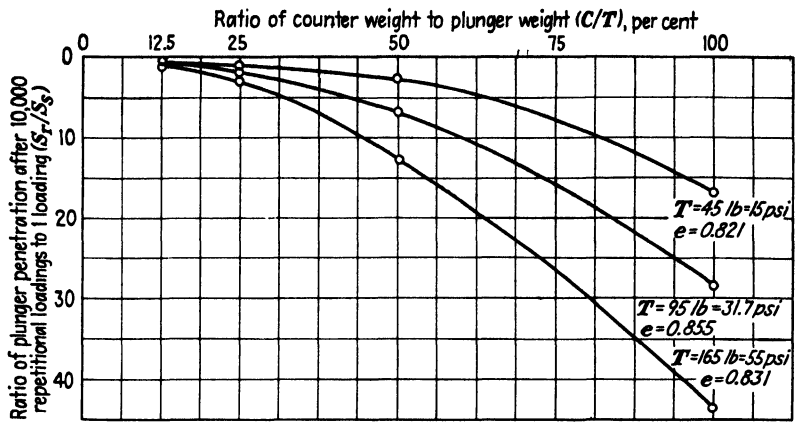
FIG. 18-13. The effect on plunger penetrations of slow repetitional loading increases with the intensities of the repetitional load and of the original static load. (*After Tschebotarioff and McAlpin, Ref. 382, 1947.*)
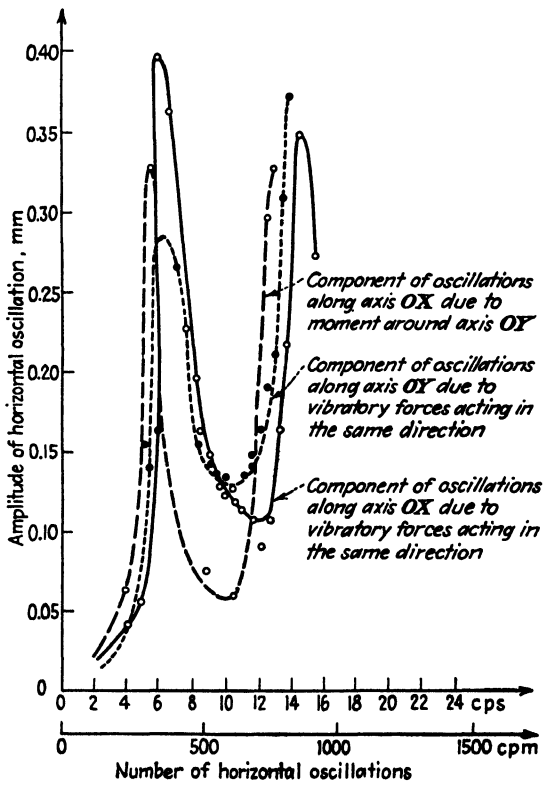
FIG. 18-14. Resonance curves of a model footing ($A = 2.0m^2 = 21.5\ ft^2$) under the action of horizontal vibratory forces and moments. (*After Barkan, Ref. 19, 1934.*)

tion on the shearing strength of undrained clay specimens (Art. 7-21). The attempted application of the results of these tests to slope-stability problems in earthquake regions, however, is open to some questions (see discussion of Ref. 68 by Tschebotarioff).

18-5. Analysis of Resonance Records of Machine Foundations. Very little precise information has been published concerning such cases. Tschebotarioff and Ward (Ref. 386, 1948) attempted to correlate the few
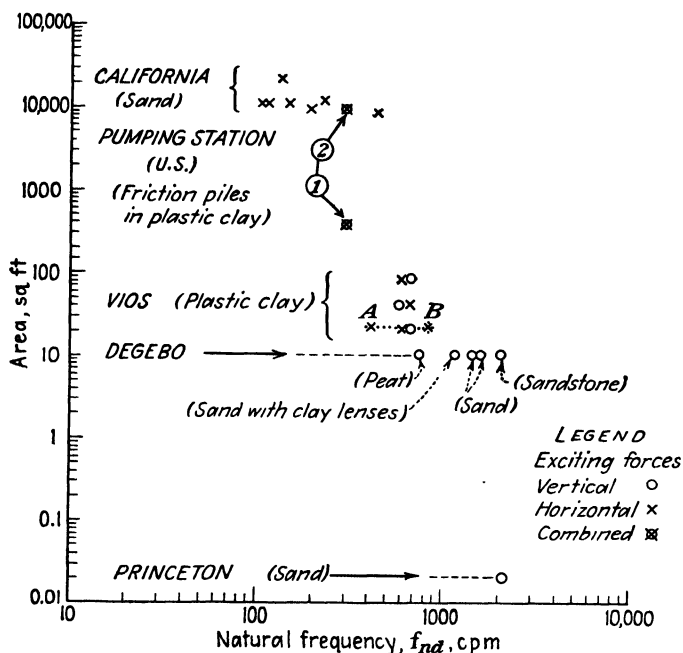
FIG. 18-15. Recorded natural frequencies plotted against the area of the foundation. (After Tschebotarioff and Ward, Ref. 386, 1948.)

data that were available by plotting the recorded natural frequencies f_{nd} against the contact area A of the foundation with the soil (see Fig. 18-15). The results showed considerable scattering, which could be attributed, in part, to different intensities of contact pressure p with the ground. To eliminate this variable, Eq. (18-3) was transformed to read

$$f_n = \sqrt{\frac{A}{W_v}}\frac{1}{2\pi}\sqrt{\frac{k'g}{1 + W_s/W_v}} = \frac{1}{\sqrt{p}} f_{nr} \qquad (18\text{-}7)$$

where p = unit average contact pressure between the foundation and the soil

f_{nr} = reduced natural frequency = natural frequency at an average unit pressure p on the ground equal to unity

The other symbols have the same significance as in Eqs. (18-3) and (18-1).

Values of the reduced natural frequencies f_{nr} were then computed with the help of Eq. (18-7) from the f_{nd} values of Fig. 18-15 (where the simplifying assumption was made that $f_n = f_{nd}$), and were plotted against the contact-area values A, as shown in Fig. 18-16. The point marked "Princeton" was obtained during the 2-in.-diameter plunger tests (Art.
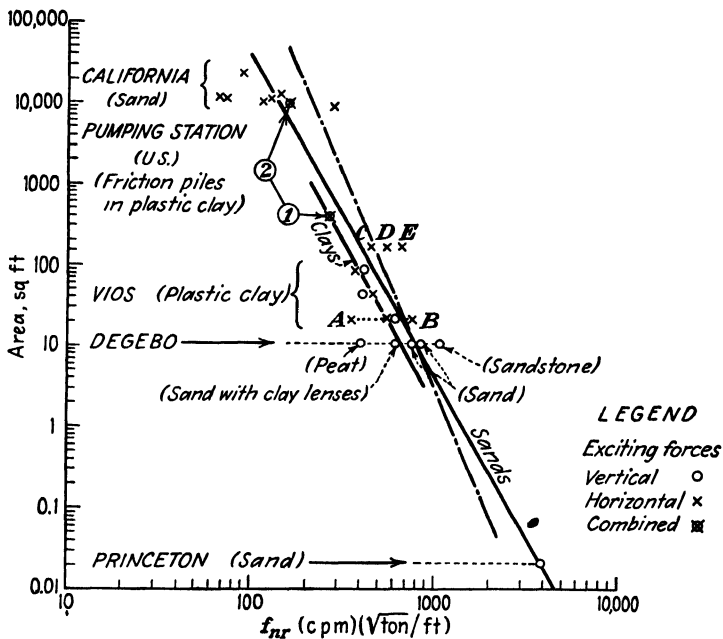
FIG. 18-16. Reduced natural frequencies f_{nr}, computed from Fig. 18-15, plotted against the area of the foundation. (*After Tschebotarioff and Ward, Ref. 386, 1948.*)

18-4) when the plunger was placed on a large mass of sand. The points marked "DEGEBO" refer to tests on different types of soils in Germany with a standard-type vibrator of that society, described in Art. 18-3.

The points marked "VIOS" refer to Barkan's (1934) tests in the U.S.S.R. on saturated clay (Ref. 19). Most of the VIOS natural frequency values were obtained from vibrograms of oscillations of large model foundations induced by the impact of a swinging pendulum. In the case of the smaller of the three model foundations (A = 2.0 m² = 21.5 ft²) forced horizontal vibrations were induced by means of a vibrator operating in the manner illustrated by Fig. 18-4, except that the vibrator was rotated 90°, so that the two shafts were one above the other and not

side by side. It will be noted from Fig. 18-14 that two amplitude peaks were obtained, indicating at least two values, at 420 and at 840 cycles per min, for the natural frequencies of the foundation-soil system. These two values are marked by crosses and by the letters A and B in Figs. 18-15 and 18-16. The natural frequency of the same foundation under the action of impact had an intermediate value of 660 cycles per min.

The points marked "pumping station" refer to a case in the Mississippi Valley. Point 1 corresponds to the area A of a single compressor foundation and point 2 to the area occupied by the entire group of compressor foundations.

The points marked "California" refer to low buildings founded on sand studied by the U.S. Coast and Geodetic Survey (Ref. 408, 1936) in connection with earthquake investigations. Higher and more slender buildings had much lower values of natural frequency.

With the data available when Ref. 386 was written (1948), it appeared that certain patterns were emerging. As shown in Fig. 18-16, the reduced natural frequency values f_{nr} for the same types of soils, when plotted to a log-log scale versus area A, were located along straight lines. It did not then appear likely that when more data became available differences greater than indicated by the full and dash-dotted lines in Fig. 18-16 would be established. These conclusions of Ref. 386 may have been too optimistic. W. K. Newcomb reported in 1951 (Ref. 246) data which corresponded to the points C, D, and E in Fig. 18-16. Point E represented the natural frequency of a foundation resting on dry clay and gravel. This point is in approximate agreement with the rest of the data in Fig. 18-16, since such dry material would not differ much in its dynamic properties from the sandstone of the DEGEBO tests. However, point D represented the primary and point C a secondary natural frequency of a foundation resting on saturated clay and sand; these points might be brought into agreement with point B, but they certainly do not fit the rest of the original data.

It therefore appears possible that not clearly defined lines, such as are shown in Fig. 18-16, but parallel bands will define the relationship between f_{nr} and A. Bands for primary and for secondary frequencies may overlap. The practical implications of this conclusion are outlined in the next article.

18-6. The Design of Machine Foundations. A properly designed foundation for a machine must first of all meet the general requirements for all foundations (Art. 13-1). Considerable rigidity of the machine foundation is essential, since a slight deflection of a few thousandths of an inch may cause bearing trouble, especially when several bearing supports are required. The possibility of warping of concrete slabs should be con-

sidered in this connection. Such warping may occur when the top surface of the slab dries out, whereas the lower surface remains moist. Massive block-type construction is the best measure against warping of this type.

An adequate mass of the foundation is also necessary in order to absorb vibrations and to prevent resonance between the machine and the soil-foundation system. There is a great variety of contradictory opinions as to how this is to be achieved.

Some authors recommend increasing the weight of the foundation in proportion to the operational speed of the machines which it has to support. This suggestion is apparently based on the assumption that the unbalanced forces are likely to increase with the speed of the engines. This proposition ignores the fact that all cases of troublesome vibrations so far reported were due to resonance, occurred at operational speeds smaller than 1,000 cycles per min, and were caused in most cases by compressor reciprocating engines working at 300 to 400 cycles per min.

Other authors suggest increasing the foundation weight in proportion to the power of the engines. This appears reasonable, but the figures suggested differ widely. Thus F. T. Morse (Ref. 239, 1942) suggest that for each brake horsepower of multicylinder engines a minimum of 1,600 lb weight of the foundation should be provided for gas engines, 1,250 lb for diesel engines, and 500 lb for steam engines. For single-cylinder engines the above values should be increased by some 40 to 60 per cent. On the other hand, G. C. Boyer (Ref. 38, 1943) gives the following average values tabulated from records of engines running at 400 rpm or less: for three-cylinder engines 550 lb of foundation weight per brake horsepower, decreasing with an increasing number of cylinders to 355 lb per brake horsepower for eight-cylinder engines. Still smaller foundation-weight values appear to be often used for high-powered engines operating at and above 1,000 cycles per min. Thus there are no generally accepted definite rules on the matter as yet, and the entire subject presents good opportunities for further fruitful research.

Objectionable vibrations of existing installations can usually be traced to resonance, that is, to the coincidence of the operational speed of the machines with the natural frequency of the soil-foundation system. Usually it is not possible to change the operational speed of a machine, and it therefore becomes necessary to change the natural frequency f_n of its support. This can be done by changing the weight W_v of the foundation [Eq. (18-3)]. Cases are on record where this was successfully accomplished. In the case of the pumping station referred to in Figs. 18-15 and 18-16 the effective weight W_v of the foundation was increased by some 7 per cent by lowering the free-water table 2 to 3 ft along the depth of the mat. This was accomplished by providing a system of

drains around the foundation mat by connecting them to a specially designed sump pit and by continuous pumping; originally the free-water table was just below the ground surface. Objectionable vibrations stopped as a result of this measure which decreased f_n, according to Eq. (18-3), below the value at which resonance had been occurring. No trouble is to be expected when the operational speed of machines is higher than the natural frequency of their support, since the dangerous resonance range is passed within a fraction of a second when the engines are started.

In another case of a compressor foundation objectionable rocking vibrations of the type illustrated by Fig. 18-17 interfered with operation;
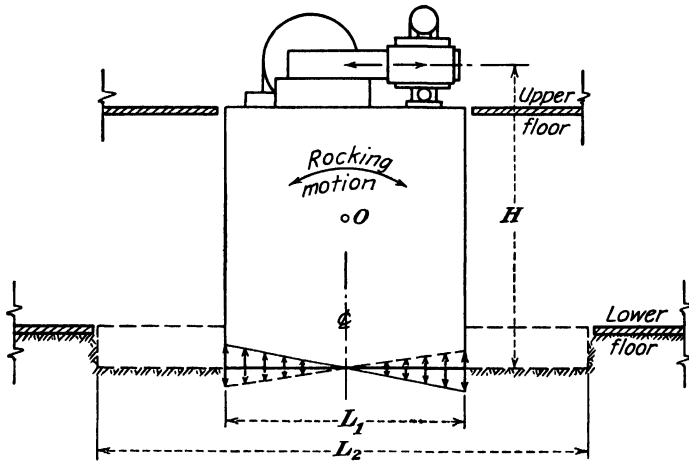
FIG. 18-17. The ratio H/L of compressor foundations should be reduced to a minimum to decrease danger of a rocking type of motion in resonance with the natural frequency of the foundation-soil system. (*After Wallace K. Newcomb, Ref. 246, 1951.*)

resonance was indicated. Part of the floor was resting on the foundation block. The floor was then provided with independent cantilevered supports and was separated from the engine foundation. This decreased the weight W_v of the latter and, according to Eq. (18-3), must have increased the natural frequency f_n to values exceeding the 300-rpm operational speed of the machine at which resonance had been occurring. This measure proved fully effective.

The almost unsurmountable difficulties in making rigorous and yet accurate forecasts of the natural frequencies of foundation-soil systems have been outlined in Art. 18-3. Further studies along the lines of Art. 18-5, with time, may possibly provide sufficient experimental data to permit such forecasts on a semiempirical basis, but at present it appears advisable to recognize the danger that the speed of a machine, especially when it operates below 500 cycles per min, may coincide with one of the possible

(Fig. 18-14) peaks of the natural frequency ranges of its supports. To meet this situation, Tschebotarioff (Ref. 400, 1951) suggested for future designs the provision of cavities near the four corners of machine foundation blocks which could be filled, or emptied, to change the weight of the block by some 15 to 20 per cent if any excessive vibrations due to resonance should occur later.

W. K. Newcomb correctly suggested the maximum possible decrease of the ratio H/L (Fig. 18-17) of compressor foundations to prevent rocking in resonance. An increase of the base length from L_1 to L_2 obviously increases the general stability of the foundation block. In addition, the natural frequency of the foundation-soil system will be increased (see Prob. 18-2). As compared with foundations subjected to static loading (Table 14-1), two to three times lower unit pressures p_0 should be used for the foundations of machinery.

The effect of the presence or of the absence of purely frictional piles on the natural frequency of a floating foundation is somewhat uncertain. The pumping station referred to in Figs. 18-15 and 18-16 was supported by such piles.

Foundations of machinery should be separated from the foundations and floors of the building itself. Small foundations can be supported by springs. According to Crockett and Hammond (Ref. 92, 1947), a machine weighing 110 tons was successfully mounted on compressed-air springs; laminated and helical springs have also been used for lighter machines. This is an effective method of preventing the transmission of vibrations to adjoining structures through the ground. Spring pads have been employed for the same purpose for heavier machines up to 700 tons, but they appear to be somewhat less effective. Cork is a satisfactory spring-pad material only so long as it does not get wet and start rotting. Asbestos fiber appears to be the most enduring of similar materials (see Ref. 92).

FIG. 18-18. A forge-hammer foundation. (After Andrews and Crockett, Ref. 16, 1945.)

A special problem is presented by forge-hammer foundations (Fig. 18-18). According to Andrews and Crockett (Ref. 16, 1945), the largest

unit in operation at that time had a 25-ton hammer B (*tup*), and its foundation G weighed 3,000 tons. This gives a 1:120 ratio between the weights of the hammer itself and of its foundation. The frame A is usually connected to the steel anvil D on which rest the dies C. Oak-timber or plywood pads E support the anvil and are underlain by a grillage of steel I beams F, which are concreted together with the foundation block G; zones r in Fig. 18-18 are heavily reinforced. Spring pads fg are placed between the anvil D and the foundation block G. A number of design variations are possible (see Ref. 16).

18-7. Effect of Blasting on Structures. Foundations in Earthquake Regions. Blasting is frequently resorted to in all types of construction work involving excavations. The safe amount of explosives which can be used without damage to adjoining structures represents a problem of considerable interest both to construction contractors and to insurance companies. A comprehensive study of the matter was carried out by the Liberty Mutual Insurance Co. (see F. J. Crandell, Ref. 90, 1949).

Experiments were performed over a number of years with charges of between 1 and 100 lb of dynamite, fired at distances of between 25 to 250 ft from adjoining buildings. An accelerograph was used to measure the frequencies f and the accelerations a of the vibrations induced in the ground by the blasting. Seismographs were used to measure frequencies f and displacements D_1 of the vibrations. It was found that damages to buildings could be related to the kinetic energy (KE) of the oscillating ground.

$$\text{KE} = \frac{MV^2}{2} = \frac{W}{2g \times 4\pi^2}\frac{a^2}{f^2} \tag{18-8}$$

$$\text{KE} = \frac{W}{2g \times 4\pi^2} 16\pi^4 f^2 D_1^2 \tag{18-9}$$

where KE = kinetic energy
M = mass of the vibrating soil
W = weight of the vibrating soil
g = acceleration of gravity, ft per sec^2
a = measured acceleration, ft per sec^2
f = measured frequency of vibration, cycles per sec
D_1 = measured vibratory displacement of ground

There was no way of determining either the mass M or the weight W of the vibrating soil. Therefore all observations were correlated with the so-called *energy ratio* (ER) of the vibrating ground.

$$\text{ER} = \frac{a^2}{f^2} \tag{18-10}$$

$$\text{ER} = 16\pi^4 f^2 D_1^2 \tag{18-11}$$

The energy ratio ER could be determined experimentally from Eq. (18-10) if an accelerograph was employed for the field measurements, and from Eq. (18-11) if a seismograph was used.

The results of the studies are summarized in Fig. 18-19. Normally built structures, not prestressed as a result of differential settlements, were not damaged if the energy ratio ER of the vibrations induced by the blast was smaller than three; there was a considerable probability of
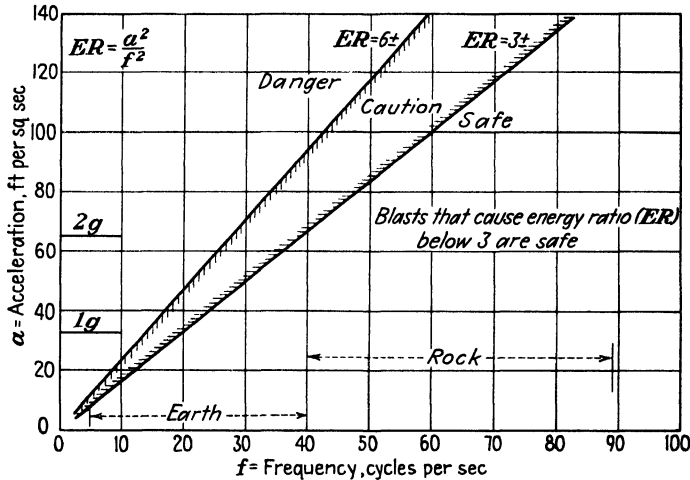
FIG. 18-19. Relationships between frequency and acceleration of shock waves through the ground, as caused by blasting, and established by field studies, which may be dangerous, doubtful, or safe to adjoining buildings. (*After F. J. Crandell, Ref. 90, 1949.*)

damage if the energy ratio ER was greater than six. The following relationship was established experimentally:

$$\mathrm{ER} = \left(\frac{50}{D}\right)^2 C^2K \qquad (18\text{-}12)$$

where ER = energy ratio [see Eqs. (18-10) and (18-11)]
D = distance from the center of the detonation, ft
C = amount of dynamite detonated at any instant, lb
K = constant depending on the ground conditions at the site

The results of the above investigation (Ref. 90) can be applied in practice as follows: A few experimental blasts are made at the new site with small charges of known weight, and vibration measurements are performed. The energy ratio ER is computed from Eq. (18-10) or (18-11), depending on the type of instrument employed for the measurements. The value of ER is inserted in Eq. (18-12). Since C and D are known,

the constant K characterizing the soil conditions of the site can be computed from Eq. (18-12). The same equation (18-12) can then be used to determine the weight of the maximum safe charge C, by setting ER = 3.

F. J. Crandell's paper (Ref. 90) mentions the following additional important facts: By exploding charges with millisecond delays, instead of instantaneously, the detrimentally effective energy transmitted through the ground was greatly reduced. Human beings are much more sensitive to blasts than are buildings, and an ER value of 0.6 had a severe effect on persons; advance warning of the coming blast decreased the severity of its effect.

Studies of earthquake damage show that structures founded on rock are less apt to be severely damaged than are structures erected on softer types of soil deposits. F. J. Crandell (Ref. 90) quotes the U.S. Coast and Geodetic Survey measurements during the destructive 1933 earthquake at Long Beach, California. In the basement of buildings measurements were taken giving on an average $a = 3$ ft per sec^2 and $f = 1$ cycle per sec; according to Eq. (18-10) this gives a very high energy ratio of ER = 9. Thus accelerations which are a fraction of gravity g can cause severe damage on soft ground, where the frequency is extremely low, but this will not be the case on rocks which transmit vibrations at high frequencies (see Fig. 18-19).

Attempts have been made to provide flexible foundation connections between the superstructure and the ground, the idea being that the ground could then oscillate under the superstructure, which would remain stationary in space and would therefore be unaffected by the earthquake. A small experimental one-story reinforced-concrete house was built on a system of rollers which were placed in two layers at right angles to each other. This method can be applied only to very small and light structures, and even then it is so expensive that it is not likely to be adopted for general use.

Plans were also made to build multistoried houses as a rigid unit from the second story upward and to provide long unstiffened slender columns in the first story; only the partitioning of the first floor was then expected to be damaged by an earthquake. However, the consequences of a failure of this type of experiment would have been too disastrous, and the plans never materialized. The present general practice is to stiffen structures at all elevations.

Very few data are available on the actual performance of pile foundations in earthquake regions. However, it is believed that mat or raft foundations are generally safer in such localities (Ref. 92). If spread footings are used instead of a mat in an earthquake region, then the individual footings should be connected to each other by reinforced-concrete struts and thus stiffened.

Practice Problems

18-1. What is the probable length of wave in (*a*) rock, (*b*) sand?

Answer. (*a*) According to Art. 12-4, the velocity of wave propagation in rock is at least $v = 6{,}000$ ft per sec. According to Table 18-1 and Art. 18-3, the frequency is at least $f = 30$ cycles per sec. Therefore the probable wave length is $L = v/f = 6{,}000/30 = 200$ ft. (*b*) Similarly, in loose sand $L = {}^{500}\!/_{20} = 25$ ft.

18-2. A compressor foundation loaded the soil over an area of 15 by 20 ft, or 300 ft², to an intensity of $p = 2.0$ tons per ft². What will be the effect on the natural frequency of the foundation-soil system if the area of the foundation mat is increased to $20 \times 30 = 600$ ft²?

Answer. According to Fig. 18-16 (assuming that the relationship expressed by the dash-dotted line holds) and Eq. (18-7), the natural frequency of the 300-ft² foundation would be

$$f_n = f_{nr}/\sqrt{p} = 420/\sqrt{2.0} = 298 \text{ cycles per sec}$$

For the 600-ft² foundation,

$$f_n = 370/\sqrt{1.0} = 370 \text{ cycles per sec}$$

Thus the increase of the area, by decreasing the pressure p on the soil, raises the natural frequency of the system.

18-3. During the construction of some German superhighways the spacing of the transverse joints in the concrete pavement (Art. 19-6) was alternated between 17 and 20 m for the purpose of preventing vibratory resonance in cars traveling at high speeds. The natural frequency of a car on rubber tires at normal air pressure varies between 2 and 3 cycles per sec. At what speed would a car with $f = 2$ cycles per sec have to travel in order to vibrate in resonance with bumps produced at every transverse joint uniformly spaced at $L = 19$ m?

Answer. $L = 19/0.305 = 62.5$ ft. The period of vibration of the car is $T = 1/f = \frac{1}{2} = 0.5$ sec. To be in resonance, the car would have to travel at a speed

$$v = \frac{L}{T} = \frac{62.5}{0.5} = 125 \text{ ft per sec} = 125\,\frac{60 \times 60}{5{,}280} = 85 \text{ mph}$$
$$= 85 \times \tfrac{8}{5} = 135 \text{ km per hr}$$

References Recommended for Further Study

Mechanical Vibrations, by J. P. Den Hartog, McGraw-Hill, 3d ed, 1947. General theory of vibrations.

"Large Hammers and Their Foundations," by W. C. Andrews and J. H. A. Crockett, *The Structural Engineer*, London, October, 1945, pp. 453–492. Numerous examples of hammer foundations, successful and otherwise.

"Reduction of Ground Vibrations into Structures," by J. H. A. Crockett and R. E. R. Hammond, *Institution of Civil Engineers Structural Paper No.* 18, London, 1947. Discussion of the theory and practice followed in dealing with the problem.

"The Effect of Vibratory and Slow Repetitional Forces on the Bearing Properties of Soils," by Gregory P. Tschebotarioff and George W. McAlpin, *Civil Aeronautics Administration Technical Development Report No.* 57. Results of laboratory experiments and discussion of their practical implications.

"Ground Vibration Due to Blasting and Its Effect upon Structures," by F. J. Crandell, *Journal of the Boston Society of Civil Engineers*, April, 1949 (summary in *Engineering News-Record*, May 4, 1950). Results of field experiments and practical recommendations based on these results.

CHAPTER 19

SOME SOIL ENGINEERING ASPECTS OF HIGHWAY AND AIRPORT CONSTRUCTION

19-1. Failures of Embankment Foundations. Shear failures and slides of highway embankments built on soft clay or on mud are liable to occur in the same manner as may happen on any other slope under such conditions (see Fig. 8-6). A case of a rotational slide (Arts. 8-7 to 8-9) is

FIG. 19-1. View of road after rotational slide of embankment and of underlying peaty silt. (Courtesy of *D. W. Taylor, Ref.* 341, 1938.)

illustrated by Fig. 19-1. A 15-ft-high highway embankment was built over a pocket of peaty silt which had been missed by wash-sample borings (Art. 12-6). The fill and the pavement were completed when the underlying peaty silt yielded laterally and heaved, creating a small island in an adjoining pond (not shown in the picture but located on the right-hand side of it). The rotational nature of the slide, however, is apparent from the appearance in Fig. 19-1 of the paved surface of the embankment fill.

The reconstruction was carried out by driving short piles through the pocket of peaty silt and thereby providing support for the pavement (see Taylor, Ref. 341, 1938).

The consequences of an outward sloughing of the end slope of a 55-ft-high embankment next to a bridge across a river are illustrated by Fig. 19-2. Horizontal sliding occurred along the base of the embankment where a clay layer was located and was overlain by some submerged uncompacted sand fill which had been dumped through the water to replace the excavated very soft mud. The lateral pressures developed
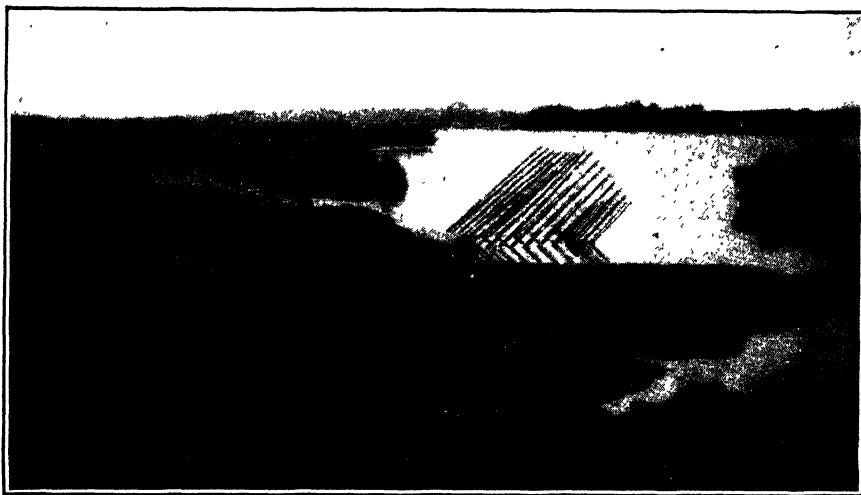
FIG. 19-2. A bridge pier, while under construction, is pushed over by the pressure developed as a result of the sloughing out of the end slope of the adjoining 55-ft-high embankment. (*Photograph by Tschebotarioff*, 1950.)

by the fill of the embankment as it slid outward overturned the two partially completed adjoining bridge piers, one of which is seen in the photograph.

In order to provide an adequate foundation for an embankment, soft underlying natural soil either has to be excavated or displaced (Arts. 19-2 and 19-3), or its strength has to be increased by appropriate measures (Art. 19-4).

Some special problems concerning the stability of slopes in highway cuts were outlined in Arts. 8-14 to 8-16.

19-2. Removal of Soft Natural Soils by Excavation and by Surcharge Displacement. Peat and other soft soils with a high organic content are liable to continue settling for a long time when loaded by the weight of the fill, even if no outright shear failure occurs through the embankment and the underlying soil. Such settlements may be due only in part to con-

solidation; gradual lateral plastic yielding may also be a contributing factor, as well as the decay of organic matter. Drainage of adjoining areas for agricultural purposes may increase such settlements. According to Ref. 253, peat soils in Louisiana, when dried, shrink to 40 per cent of their original volume. In the fenland districts of England drainage of the peat soils caused continuous surface settlements measured over periods of 60 years and more; the settlements exceeded 40 per cent of the original thickness of the soft layer.

The replacement of soft mud and peat by granular material is therefore often advisable in order to provide a proper foundation for an embankment. When the depth of the soft layer of peat or mud does not exceed
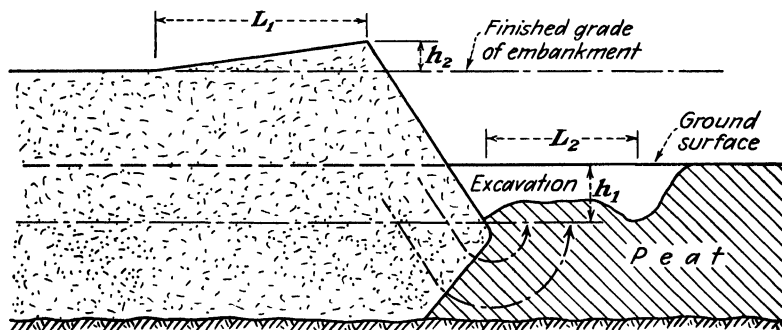
FIG. 19-3. Longitudinal section of embankment under construction shows how excavation of upper 10 ft of swamp can be combined with a backfilling procedure to displace the underlying peat by temporary surcharge. (*After Field Manual of Michigan State Highway Department, Ref. 228, 1946.*)

10 ft, complete excavation of the soft material can be performed without difficulty. Usually this is done by means of clamshell buckets or draglines operated by cranes from the end of the fill embankment. In some cases, when the proposed embankment approaches the edge of a waterway, it is possible to remove entirely even a greater depth of soft soil by underwater excavation of a wide trench from a floating dredge (Art. 14-10). The trench is then backfilled hydraulically (Art. 17-3) with granular material.

For depths greater than 10 ft, a procedure illustrated by Fig. 19-3 is usually employed. It consists in the excavation of the upper part of the swamp to a depth h_1 = 10 ft and to a distance L_2 corresponding to the reach of the crane operated from the top of the fill, which is dumped without compaction to a height h_2 above the finished grade of the embankment. This is done to increase the height of the end slope of the embankment and to facilitate its outward sliding and the displacement of the soft peat, as indicated by dash-dotted lines in Fig. 19-3 (compare with Art.

8-12). Only clean uncompacted granular material should be used for the fill. Excavation of the peat ahead of the fill should be combined with saturation of the fill by jetting in order to destroy any apparent cohesion (Art. 7-4) which might give it some temporary strength. The fill of the embankment is frequently advanced first along the center line of the embankment, so that it takes on, in plan, the shape of a wedge. The excavating is then done on both sides of the wedge, and most of the peat is displaced laterally.

The temporary fill is then removed down to the water line and is re-used for further surcharge and mud displacement by end-dumping operations off the advancing embankment head, as illustrated by Fig. 19-3. The permanent body of the embankment is built up in layers and is compacted above the water level by rolling (Art. 11-3).

19-3. Displacement of Soft Natural Soils by Blasting. The usual procedure is illustrated by Fig. 19-4. The sand fill is dumped on the surface of the swamp, sinks somewhat into it, and displaces some of the underlying mud or peat laterally. It is essential to remove the vegetation cover not only under the fill itself, but also to some distance around it. Otherwise this cover, which has some tensile strength, would restrain the displacement of the mud in the zones A of Fig. 19-4. One to three rows of cartridges are then placed under the fill by jetting from its surface, and the central rows are detonated one second later than the outer rows. The mud is shot out laterally by the force of the explosion, and the sand fill sinks into the space thus formed between it and the deeper, more resisting layers. The detonation of a single central row of cartridges usually does not produce sufficient displacement of the mud under the toe of the embankment (Fig. 19-5), and supplementary shots become then necessary if a condition of this kind is revealed by check borings.

FIG. 19-4. Underfill method of swamp-mud and peat displacement under an embankment by blasting. (*After Leo Casagrande and T. A. Wheeler, Ref. 333, 1936.*)

Operations of this type were frequently performed in the lake districts of Michigan and Minnesota during the early 1920's. They were also used in harbor work in Scandinavian countries and for German highways in the 1930's. Observations of the later performance of highways and of harbor retaining-wall backfills provided with a foundation by such

"swamp-shooting" methods, however, often disclosed uneven surface settlements which were traced to individual pockets of undisplaced mud. The settlements of the rock fill, which overloaded bulkhead anchors and necessitated their protection, as illustrated by Fig. 16-29, were due to pockets of soft clay and mud. The risk of the formation of such pockets is always considerable, since the force of the explosion does not appear to be distributed uniformly but is frequently channeled in an unpredictable manner. The displacement of soft muds and clays by blasting, therefore, does not represent a fully reliable foundation embankment-construction procedure.

Sometimes blasting is used as an accessory to the displacement procedure illustrated by Fig. 19-3. Cartridges are detonated below the
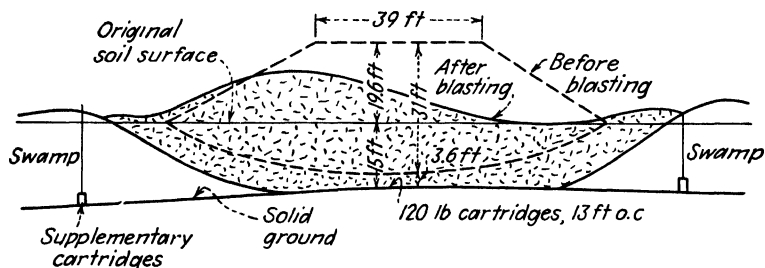
FIG. 19-5. Example of the results of blasting peat by the underfill method. (*After Leo Casagrande and Peter Siedek, Ref.* 333, 1936.)

bottom of the excavated trench in order to liquefy the mud there (Ref. 228).

19-4. Use of Sand Drains to Increase the Shearing Strength and to Accelerate the Consolidation of Deep Natural Beds of Soft Clay. Displacement of very soft clays and muds can hardly ever be successfully performed if the troublesome layer exceeds 50 to 60 ft in depth; it is not always possible even at shallower depths when the clay is of a low to medium strength. Special measures become then necessary to improve the properties of the clay.

During the construction of the 1939 World's Fair at New York on a 70-ft-deep layer of soft organic silt (Ref. 137), so-called mud waves were apt to occur when the fill was placed in layers exceeding 4 ft in height. A *mud wave* is essentially a slide along a cylindrical surface (see Fig. 8-6) which produces lateral and upward displacements of the underlying soft clay. Such displacements are liable to remold the clay and to lower its shearing strength still further (Art. 7-22), thus facilitating further slides during continued filling. It therefore proved necessary to place the fill in layers extending over the entire area, not exceeding 4 ft in depth, and at a

maximum grade of 3 per cent. This ensured stability (Art. 8-8) by preventing shear failures of the mud-wave type. However, settlements continuing for many years, owing to consolidation (Art. 6-1) of the clay under the weight of the fill, could not be prevented by such measures.

Continued settlements of the soil under an embankment fill may damage concrete pavements and create undesirable dips in airport runways, especially when the depth of soft underlying soil varies (see Fig. 13-3). It then becomes necessary to accelerate the consolidation of the clay, so that it is largely completed before the concrete pavement is laid. *Sand drains* are used for this purpose; the theory on which their use is based was given in Art. 6-10. The construction procedures employed for the installation of the sand drains are illustrated by Figs. 19-6 to 19-8.

A hollow mandrel, a heavy 16- to 20-in.-diameter steel pipe, is driven into the clay in very much the same manner as is done for cast-in-the-ground concrete piles of the Simplex type (Art. 15-7). A metal plug closes the bottom of the pipe and, in some types of mandrel, is left in the ground when the mandrel is pulled out. Prior to pulling, the mandrel is filled with clean sand [not more than 3 per cent passing the 200-mesh sieve (Ref. 247)]. One of the several possible techniques (Refs. 123 and 124) employs compressed-air pressure (up to 7 tons per ft^2 $\approx$ 97 psi) to force the sand down and to ensure the essential continuity of the sand shaft. The air pressure against the top lid of the mandrel also helps somewhat to reduce the effort necessary to pull the mandrel out of the ground. In some mandrels a permanent hinged plate is used to provide a plug at its bottom; this was done for the rigs shown in Figs. 19-6 to 19-8, built by Kiernan-Terry Corp. to O. J. Porter's specifications.

Temporary surcharges in the form of excess height of fill are sometimes employed, under the assumption that the settlement due to, say, 60 per cent consolidation under a high temporary overload may be greater than the settlement corresponding to 90 or 95 per cent consolidation under the final smaller load of the permanent embankment. This procedure, however, does not take into account the possibility of secondary consolidation (Art. 6-9), whose effects may be important in peat and some other soils.

When time permits, it is advisable to construct some test sections with different spacing of the sand drains and different heights of surcharge fill in order to decide on the procedure to be followed during later construction. Careful settlement, pore-pressure, and lateral-displacement control measurements should be performed both during such preliminary studies and during all actual construction.

Displacement measurements are made on stakes or on other firmly fixed bench marks around the surcharge fill to make sure that no shear failure of the mud-wave type is about to develop owing to excessive weight of the
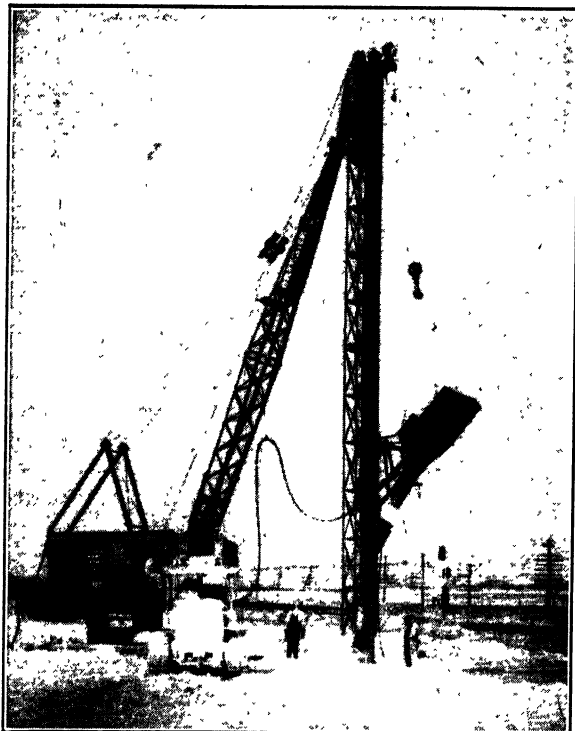
FIG. 19-6. 25-ft-long sand-drain hollow mandrel about to be filled with sand from the loading skip. (*Courtesy of O. J. Porter.*)
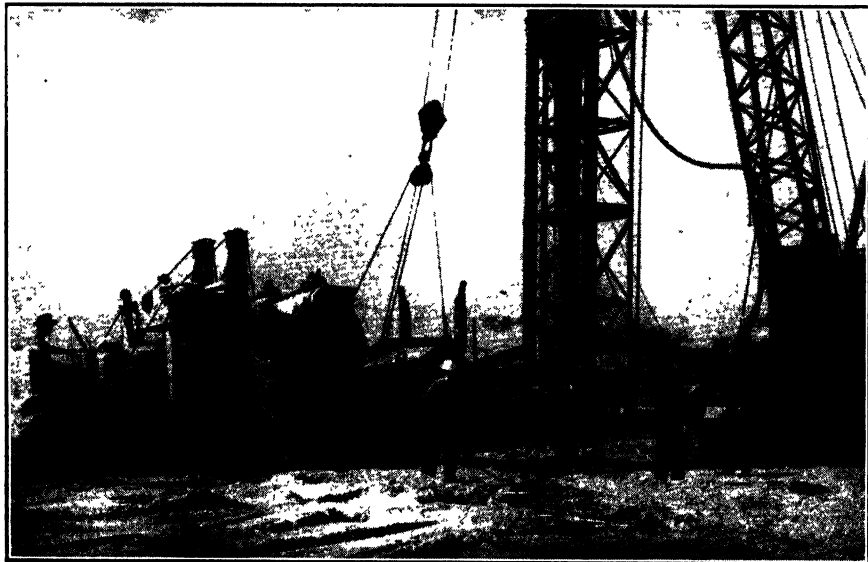
FIG. 19-7. Filling with sand the loading skip of the sand-drain driving rig shown in Fig. 19-6. (*Courtesy of O. J. Porter.*)

surcharge. Such mud waves would be liable to sever the continuity of the individual sand drains and thereby render them useless.

Pore-pressure measurements serve a similar purpose; they are performed with the help of devices of the type illustrated by Fig. 19-9. The bourdon gage should be in a position to read vacuum pressures when the free-water level is well below the elevation of the surface of the fill and of the gage (see Prob. 19-4). This type of gage pipe and point can be placed

FIG. 19-8. Driving rig and hollow plugged mandrel for 102-ft-long sand drains. (*Courtesy of O. J. Porter.*)

and sealed off in the clay in a manner similar to that shown in Fig. 17-14. Pore-pressure measuring devices of the open-standpipe type are not to be recommended, although they are used sometimes. The water level in the standpipes takes a comparatively long time to adjust itself. Further, the open standpipe may act as a drain in respect to the clay around its tip and may thereby accelerate its consolidation locally, so that the reading will not be representative of the state of the entire clay layer at that elevation.

The usual spacing of sand drains in the United States varies from 8 to 12 ft on centers. A special "wick" type of vertical cardboard drain has

been developed in Sweden for closer spacing in some highly impervious local clays (see discussion by Kjellman of Ref. 20).

Sand drains can be used for purposes other than the acceleration of settlements. Thus they were employed in California to relieve lateral pressures of an unconsolidated clay layer against a harbor earth-retaining structure (Ref. 88) by accelerating the consolidation of the clay. In New York they were used to permit the construction of a levee around La Guardia Airport (Ref. 124); first attempts to build such a levee failed
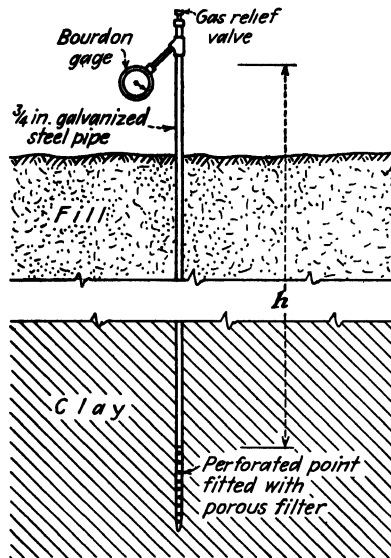
FIG. 19-9. Type of pore-pressure measuring equipment frequently employed to check the effectiveness of sand-drain action in the field.

because of slides toward the adjoining bay. The use of sand drains permitted the rapid increase of the shearing strength of the underlying soft clay as the levee was built up. The levee was required to prevent high tides from flooding the airport, which had settled 3 to 6 ft as a result of the consolidation of the clay.

19-5. The Design of Base Courses for Flexible Pavements. The CBR Method. In a so-called flexible pavement a thin upper layer of asphalt provides the wearing surface. An underlying layer of selected and compacted soil, the *base course*, distributes the wheel loads over the underlying natural soil, the subgrade. Base-course thicknesses for highway pavements were until recently determined largely on the strength of experience with their performance, satisfactory or otherwise, in different localities. The continued increase in the weight of airplanes and the need

for some simple criterion which would permit the rapid and safe construction of new airports in any part of the world led during the Second World War to the development of the so-called CBR method of design.

This method is based on a purely empirical procedure with which experiments were begun in 1929 by the California State Highway Department; the letters CBR stand for "California bearing ratio." The design procedure is based on the results of the CBR test, which is performed with equipment of the type illustrated in Fig. 19-10. A soil specimen is compacted in a 6-in.-diameter cylindrical mold by any one of the compaction
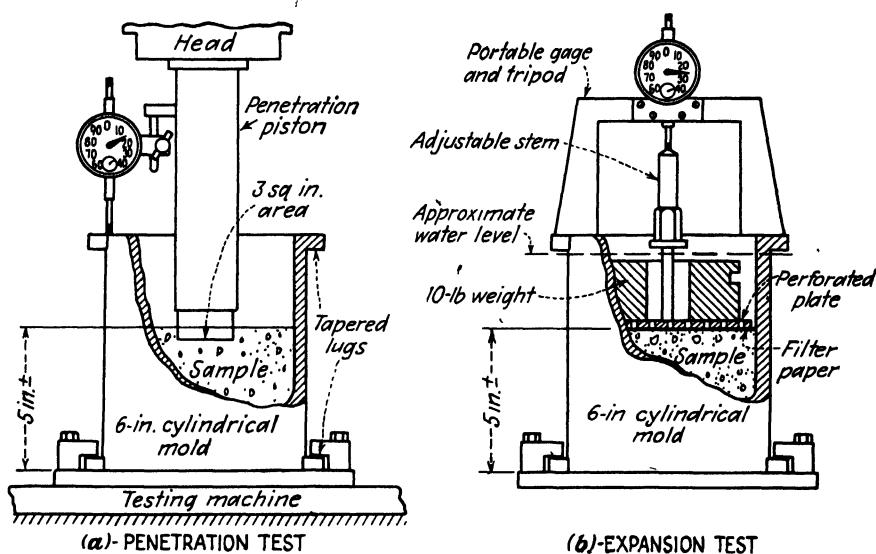
FIG. 19-10. Original equipment for the CBR test. (After O. J. Porter, Ref. 271, 1950.)

procedures listed in Table 11-1 for 4-in.-diameter standard molds. The number of blows, however, is increased in proportion to the larger volume of the 6-in.-diameter mold. In the original California procedure 2,000 psi static pressure was used for compaction; it is frequently referred to as the Porter static-compaction method. After compaction a surcharge weight is placed on the soil surface, and the mold is submerged for four days. The swelling of the soil is recorded as shown in Fig. 19-10. Accord- to O. J. Porter (Ref. 271):

> Subgrades which have proved satisfactory usually show an expansion of less than 3% of the initial height of the specimen during the 4 day soaking period whereas good base and subgrade materials show less than 1%. Many of the poorer clay and adobe soils often show an expansion ranging from 7% to 20%.

After completed soaking the mold is placed in a testing machine or in a controlled-strain (Art. 7-13) type of press. A plunger of 3 in.^{2} area (1.91 in. diameter) is forced 0.1 in. into the soil, and the resistance encountered at that penetration is recorded. The ratio of that resistance to the resistance of crushed rock at the same penetration is taken to represent the CBR value (see Prob. 19-1).

A CBR value of 100 indicates excellent material with supporting properties as good as those of crushed rock. Low CBR values indicate poor material (see Fig. 19-11).

Molds with a detachable collar, similar to the smaller standard molds of Fig. 11-1, are frequently employed instead of the model shown in Fig. 19-10 (see Ref. 337).

Observations were made on California highways having different base-course thicknesses and traveled by trucks of either 7,000- or 12,000-lb wheel loads. Correlation of the field data thus obtained to base-course and subgrade CBR values led to the development of design charts for these wheel loads (Fig. 19-11). Special test sections with varying base-course thicknesses were then built during the Second World War by the U.S. Engineer Department in several localities (Ref. 337) over which heavily loaded dump and carry-all trucks with wheel loads reaching 70,000 lb traveled continuously. The design curves shown in Fig. 19-11 were developed from such *accelerated traffic tests;* they have since been extended to wheel loads of 150,000 lb (see Prob. 19-2 for examples of the use of these curves). Base-course material should be frost-resistant in cold regions (Art. 19-6).

The CBR pavement-design procedure is safe and even appears to be too conservative. Criticisms of the procedure for leading to over-designed pavements are based on the following: As pointed out by Palmer (Ref. 256, 1944) and by Tyrrell and Palmer (Ref. 405, 1949), accelerated traffic tests are performed so that the wheels pass repeatedly over the same spots, causing formation of ruts. Actual traffic is more distributed and produces, as a result, some additional compaction of the base courses. Experience with airfields of the Bureau of Yards and Docks of the U.S. Navy is stated to be in full agreement with the following quotation from McLeod (Ref. 220, 1947):

> . . . Canadian experience indicates that an airplane wheel load of any given magnitude can be carried by a pavement and base course which have only a fraction of the thickness specified by U.S.E.D. (United States Engineer Department) design.

Objections are also raised against the excessive softening of some soils by the four-day soaking which precedes the CBR test. It is claimed that

this produces much more unfavorable conditions than are actually encountered in the field, even during the spring breakup when the frost leaves the ground. In spite of all these shortcomings in the present applications of the CBR test to design problems, it remains a valuable
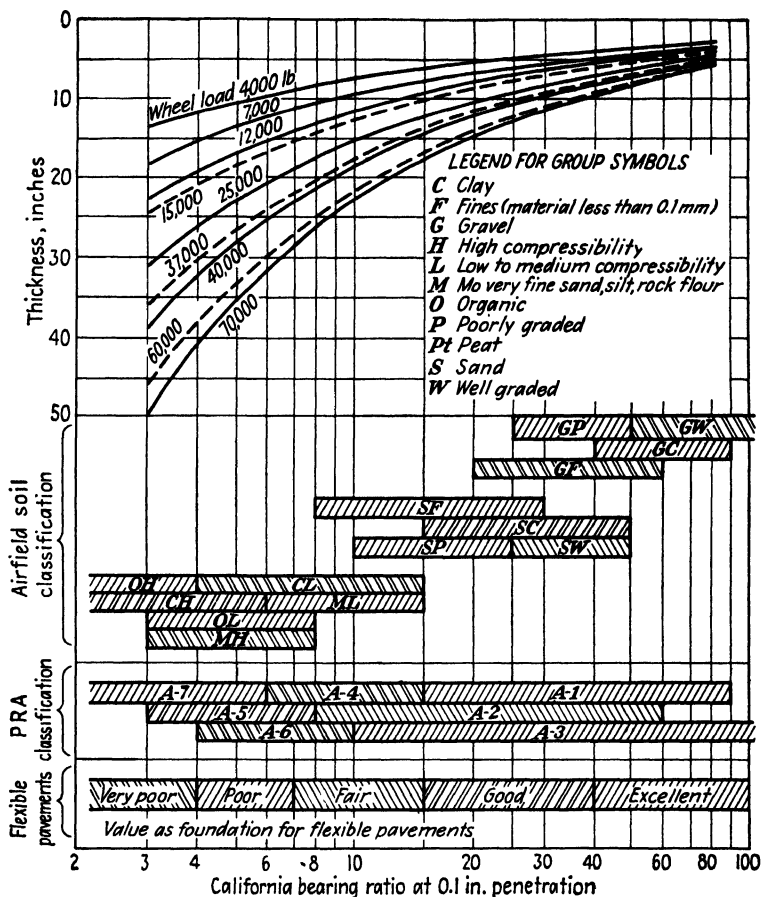
FIG. 19-11. Chart for the design of flexible pavements, giving combined thickness of pavement and base in respect to the CBR values of the underlying material. *(After J. H. Stratton, discussion of Ref. 66, 1948.)*

index type of test, by means of which a rough evaluation of the strength characteristics of a soil can be made.

The CBR test can be performed on undisturbed subgrade soils. The subgrade surface is usually compacted by rolling in the same manner as is done for base-course fills. There are, however, some exceptional types of soils where this is not always advisable. For instance, Fruhauf

(Ref. 142, 1946) pointed out that some lateritic soils in the tropics (Art. 2-8) have good drainage properties in their undisturbed natural condition, which are lost if the soil structure is broken down by compaction. The final over-all effect is detrimental to pavement stability.

It will be noted from the answers to Prob. 19-2 that the CBR procedure for the design of flexible pavements does not take into account possible *slab action* of the upper base-course layers, that is, their flexural resistance, in distributing loads over the weaker underlying layers. An attempt to take this into account by a rigorous solution of stress distribution in layered systems was made by Burmister (Ref. 53, 1943). Related strength studies by means of triaxial tests have also been made. For the present, incompletely developed status of this approach to design problems, see Wilson and Williams (Ref. 432, 1950).

19-6. The Modulus of Subgrade Reaction and the Design of Rigid Pavements. Early attempts to establish a procedure for the design of
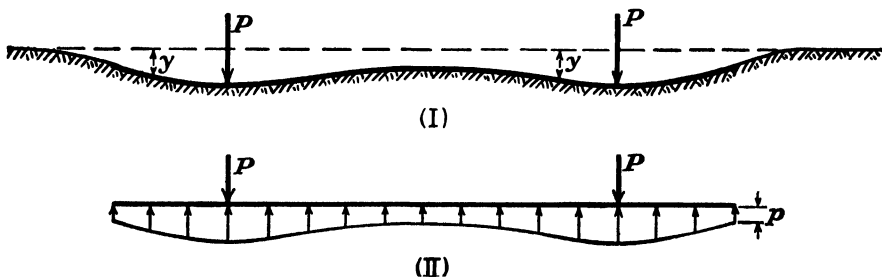
FIG. 19-12. Sketch illustrating discussion of the physical significance of the term *modulus of subgrade reaction* $k_s = p/y$ and of the limits of its validity.

concrete pavements, which are frequently referred to as "rigid" by comparison with the "flexible" bituminous pavements, were based on the assumption that the reaction pressures p of the soil under any point of the pavement were proportional to the deflection, or settlement, y of the soil surface.

$$p = k_s y \tag{19-1}$$

where k_s is taken to represent a constant for a given type of soil. This constant is called the *modulus of subgrade reaction*. The assumption expressed by Eq. (19-1) can be valid only for an imaginary soil with no shearing strength, such as would be simulated by a viscous liquid or by a bed of helical springs set side by side. In an actual soil Eq. (19-1) approximately corresponds to reality only in the case of a fairly flexible structural element acted upon by concentrated loads, for instance, a railroad tie, shown in Fig. 19-12. Another similar condition is presented by the portion of a steel sheet-pile bulkhead embedded in the ground [see

Fig. 10-37(*a*) to (*d*)], where the function of a concentrated load is performed by the shear which is transmitted at dredge level to the soil beneath it through the sheet piling. Equation (19-1) can be applied for the analysis of such and other similar problems, as was done by Palmer and Thompson (Ref. 258, 1948).

However, an examination of Fig. 9-11 reveals that Eq. (19-1) is in direct disagreement with known facts concerning the distribution of reaction pressures exerted by cohesive soils against uniformly loaded flexible footings; the soil reactions are smallest at the center of the loaded footing where the settlements are greatest. The relationship $p = k_s y$ should therefore never be applied to problems involving uniformly distributed loads. It is rather doubtful whether one should apply it to borderline cases, as has sometimes been attempted, for instance, to drydocks of the type shown in Fig. 14-16(IV).

It is also questionable whether Eq. (19-1) should be used for the analysis of concrete pavement slabs loaded by rubber-tired wheels which distribute pressures over a certain area of the concrete surface. Early analyses by Westergaard were based on Eq. (19-1), but inconsistencies between the results of such analyses and field observations compelled various empirical corrections of the original assumption of a "liquid subgrade" expressed by Eq. (19-1). The present trend is to approach the analysis of the problem from the point of view of the theory of elasticity (see Refs. 427, 213, and 266). Ref. 266 gives influence charts for pavement design, which are used similarly to the Newmark charts (Art. 9-6) for the computation of stress distribution in soils.

Much further useful research can be carried out on this subject. Measurements of soil-reaction pressures against concrete pavement slabs should contribute to the clarification of the problem. The embedment of individual *earth-pressure cells* within subgrade or base-course soil layers cannot lead to fully reliable results because of differences in the compressibility of the pressure cells and of the surrounding soil (see Art. 9-3 and Ref. 24). But this difficulty does not arise when the surface of the cells is placed flush with a rigid surface, for instance, with a smooth lower surface of a concrete pavement slab. Carlson earth-pressure cells, which utilize the Carlson strain meter (Art. 13-8), are well suited for measurements of this type, under both transient and sustained loading. The WES cells, which utilize a small number of SR-4 gages (Art. 10-23), are not as well suited for measurements other than for short periods of time. The Goldbeck cells (Arts. 10-17 and 10-24) utilize air pressure to break an electric contact in the cell and were frequently used in the past; they are seldom employed now because the electric contact point in the cell is liable to be worn down with time and to lose its sensitivity. Any

of the above earth-pressure cells can be adapted for the measurement of pore pressures within soil layers. To that end, their pressure-measuring flexible diaphragm has to be protected by a porous cover.

Load tests on plates up to 30 in. in diameter are frequently performed on subgrades, base courses, and pavement surfaces. They are fully justified in airport and highway work, since it is always possible to make the test plate of a size equal to the tire imprint of the heaviest plane (Art. 12-10). The tests are usually of a controlled-strain type (Art. 7-13). A jack placed between the test plate and a heavy truck (Ref. 336), or special attachments to compaction equipment, such as are provided on the 100-ton roller in Fig. 11-6(*b*) (lower right-hand corner on photograph), are sometimes used for that purpose.

It is often necessary to measure not only the surface settlement of a pavement, but also the *settlement* of the subgrade surface. To that end, a *plate* is laid on the surface of the subgrade and is provided with a rod which reaches almost to the pavement surface (Refs. 336 and 337). A pipe protects the rod from friction with the surrounding base course. The arrangement is somewhat similar to that shown in Fig. 12-17 for cone-penetration measurements. Levelings are made on the top of the rod after removing a protecting cap which covers the pipe; the top of the cap is flush with the pavement surface. The settlements can be measured electrically by remote control. Similar techniques can be applied to the measurement of settlements of different layers in earth-fill dams (Art. 17-6).

Suddenly applied loads, such as are produced by a landing airplane, have been found to affect pavements less than repeated slowly moving or stationary loads, especially when vibrations are transmitted to the pavement (compare with Art. 18-4). For that reason the pavements of taxiway, hardstand, and warmup areas of airports usually are made some 20 per cent stronger than runway pavements. Special precautions are indicated on airports where the subgrade consists of not too dense sand of uniform grading (Prob. 19-3) and where a considerable rise of the ground-water table is possible (Refs. 381 and 382). Drainage of all airports should be given particular attention (Ref. 192).

Numerous repetitions of heavy loads may cause damage to highway pavements. It happens frequently on four-lane pavements that the concrete slabs of the right-hand lane, which are subjected to particularly heavy truck traffic, settle down somewhat more than the adjoining lighter-traveled lane, especially when the concrete is laid directly on the subgrade or on insufficiently compacted base-course or embankment fill material. A laborious procedure known as "mudjacking" is then employed to provide partial remedy to such conditions. Holes are

drilled through the concrete slabs and are connected by hoses to a *mud-jack;* this is the name given to a vehicle combining a mixer for a water-soil-cement slurry and a pump which forces the "mud" slurry under the pavement and lifts ("jacks") it up to the desired elevation.

Another difficulty which may arise when concrete pavements are laid directly on clay subgrades is the so-called *pumping.* Water penetrates into the joints between the slabs and forms a liquid clay slurry. When a heavy truck passes over an expansion joint first one and then the other edge of the slab deflects somewhat and ejects ("pumps") some water with clay particles upward through the joint. In this manner a small cavity is formed under the edges of the concrete slab, which looses part of its support. A crack will then usually appear in the concrete a short distance from the joint and parallel to it. Drainage and the use of granular base courses are possible preventive measures; "mudjacking" can be employed for repairs (Refs. 445 and 446).

It has been indicated (Art. 18-4) that a small addition of silt and clay improves the resistance of granular soils to vibratory and to slow repetitional loading. However, the same addition may render such soils susceptible to frost heaving (Art. 5-7). This will not be true in the case of bituminous additions (Ref. 383), but these are expensive.

In all regions with a cold winter, base courses have to be built of thoroughly compacted *frost-resistant material.* There are some variations in the definition of such material. The New Jersey Turnpike Authority (Ref. 247) defines the grading requirements of frost-resisting material as follows: "not more than 10% shall pass a 200 mesh sieve and not more than 5% of its particles shall be less than 0.02 millimeters in size."

The same specifications require that material of the highest quality shall be placed to a depth of 1 ft 4 in. beneath the concrete pavement. This material, grade A, shall be pervious well-graded free-draining frost-resistant A-3 soil according to PRA classification (Art. 12-11) with not more than 6 per cent passing a 200-mesh sieve, a plasticity index $I_p \leq 3$ per cent (Art. 4-7), and a CBR $\geq$ 20 per cent when compacted at 100 per cent of the maximum density obtained by the modified AASHO procedure (Table 11-1 and Art. 19-5). The following 1 ft is to be of grade B material, which is defined as frost-resistant, graded so that not more than 10 per cent passes a 200-mesh sieve, with a plasticity index $I_p \leq 6$ per cent and a CBR $\geq$ 15 per cent when compacted at 100 per cent maximum density.

Both A and B materials, as well as 1 ft of regular embankment material, are to be compacted to 95 per cent of their maximum density. Thus a total depth of 3 ft 4 in. below the concrete pavement slab is to be com-

pacted to 95 per cent. The remainder of embankment fill is to be compacted to 90 per cent of its maximum density, as defined above for grade A material.*

Compaction requirements are less stringent when fills are placed over large areas at very flat slopes, as is done for many airports. An extreme case is the Logan Airport at Boston (see A. Casagrande, Ref. 67, 1949). Some 25 ft of hydraulic clay fill was placed over a 100-ft bed of natural clay; no other suitable fill material was available in the area. The hydraulically deposited clay fill consisted "of balls of clay varying from pebble to head size, which are laid down in a matrix of semifluid clay." This fill did not stand on slopes steeper than 1:50. Careful studies were performed, including observations on experimental test sections and extensive pore-pressure measurements in the field during construction. The increase with time of the strength of the upper clay-fill layers was taken into account, and a design thickness for pavement and base of 5 ft for the runways and $5\frac{1}{2}$ ft for the ends of the runways and the taxiways was adopted. This included 6 in. of bituminous pavement, followed first by 6 to 12 in. of crusher-run stone, and then by gravel and sand.

19-7. Some Special Problems in Permafrost Regions. The nature of permafrost and its effect on local foundation practice has been outlined in Art. 14-11. One of the special problems confronting highway construction in permafrost regions of the far north is illustrated by Fig. 19-13(I). In early winter the active layer starts freezing from the surface. The frozen zone of the active layer reaches the permanently frozen soil first of all under an embankment. Elsewhere the cover of vegetation and of snow, which acts as an insulation, delays freezing somewhat, but all vegetation was removed from under an embankment during its construction, and the roadway has to be kept cleared of snow to permit traffic. When an embankment is located on the side of a hill, ground water may continue flowing through the as yet unfrozen lower part of the active soil layer until it encounters the completely frozen active layer under the embankment, which then acts as a dam. If a sufficient head is built up, the water may break out to the surface through the upper frozen part of the active layer and freeze there, forming large masses of *surface ice* (other names are *nalyed* or *icing*) along the embankment. In some extreme cases it may even overflow and cover the roadway. In the spring this ice will provide large quantities of melt water, which will soften the soil and thereby endanger the stability of the embankment and of the roadbed.

* See *Engineering News-Record*, Nov. 23, 1950, pp. 35–38, for details of alternative designs of Portland cement concrete and of asphaltic concrete. The latter was adopted, the bids having been lowest for this type.

A preventive measure worked out by Soviet engineers in Siberia is illustrated by Fig. 19-13(II). It aims at intercepting the ground water and forcing the inevitable development of surface ice at locations where it cannot harm the highway. To that end, the vegetation and turf cover is removed, and a shallow excavation is made along a so-called *freeze belt*, some distance uphill from the highway and parallel to it. The belt is cleared of snow during the first month or so of the winter. As a result of these measures the active layer freezes through under the belt before it
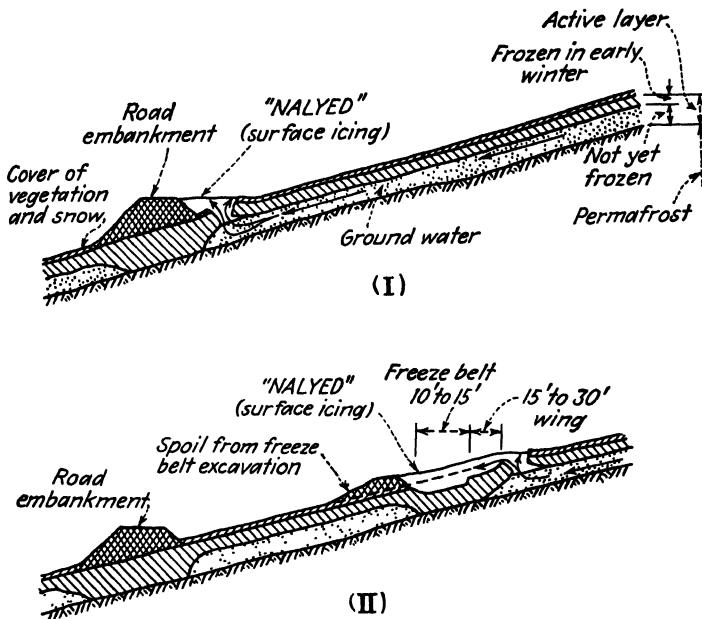
FIG. 19-13. The formation of large quantities of surface ice (*nalyed*) in permafrost regions. (I) Detrimental when occurring next to unprotected embankment. (II) Not dangerous when controlled by excavation of suitably located "freeze belt." (*After V. G. Petrov and S. W. Muller, Ref. 242, 1947, and A. Tchekotillo, Ref. 344, 1946.*)

freezes under the road embankment, and the surface ice will be formed in the belt, where it will do no harm. Drainage ditches are provided to carry away from the belt part of the surface water and the melt water in the spring. Several consecutive belts of this type have to be provided in some locations (Ref. 344).

Drainage ditches have to be protected from freezing by special *warmth-retention* measures, as shown in Fig. 19-14. Similar measures have to be taken under small bridges, since otherwise the ice under the bridge will be covered with less snow than on open stretches, and the river channel will be liable to freeze under the bridge right down to the bottom before it

does so elsewhere. Surface ice may then be formed in front of the bridge and may destroy it. Freeze belts, cut into the ice during early winter at shallow spots upstream of the bridge, may be used in some cases (see Tchekotillo, Ref. 344, 1946).
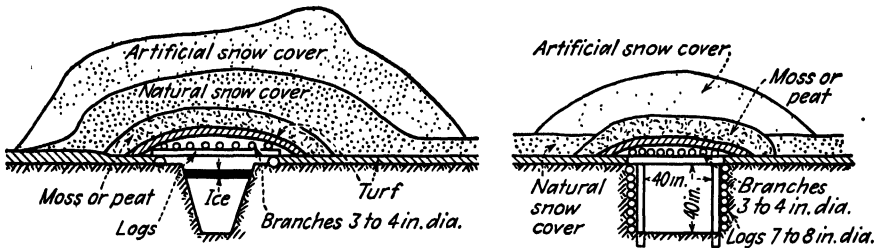
FIG. 19-14. Two methods of warmth retention in drainage ditches to prevent their freezing and forming *nalyed* (surface icing) at undesirable points. Such protected ditches are used to carry water away from a roadway fill or a "freeze belt" (see Fig. 19-13). (*After A. Tchekotillo, Ref. 344, 1946.*)

19-8. Effects of Horizontal Forces Applied to the Pavement Surface.

Airplane engines are warmed up while the main wheels are locked. The propeller thrust H is then transmitted by the locked wheels to the pavement surface, as shown in Fig. 19-15. A redistribution of vertical loads takes place between the wheels (see Prob. 19-3). The question arises what the effect of the force H on the shearing stresses in the pavement and base course will be. This point was investigated by Frank Baron (Ref. 18, 1947). To simplify the rigorous analysis of the problem, the elliptical tire imprint was replaced by a rectangle (Fig. 19-16). It was further estimated that engines warming up at approximately 2,200 rpm will
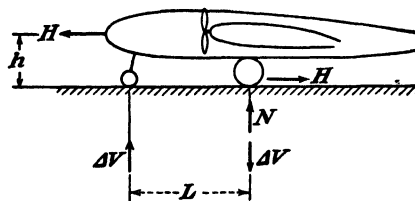
FIG. 19-15. The warmup of airplane engines with blocked wheels causes a redistribution of the loads between the front and the main wheels.

develop a horizontal thrust H equal to one-third of the original normal load N on the main tires $H = N/3$. Curve 1 in Fig. 19-16 was then obtained for $H = 0$ (airplane motors not running) and curve 3 for the original value of N plus $H = N/3$. A horizontal thrust H brings about a reduction ΔV in the value of N (see Fig. 19-15). For the case studied, $\Delta V = 0.15N$. If this reduction is taken into account, curves 2 and 4 will be obtained in Fig. 19-16 instead of curves 1 and 3. It will be noted

that curve 4 (which indicates the shear developed during engine warmup), intersects curve 1 (engines not running) at a depth $z = 0.34a = 0.17(2a)$. Therefore (see Tschebotarioff and McAlpin, Ref. 382, 1947) the thrust caused by the warmup of engines increases shearing stresses in a flexible pavement only at shallow depths not exceeding 17 per cent of the largest diameter of the tire imprint; at a depth equal to 10 per cent of the large
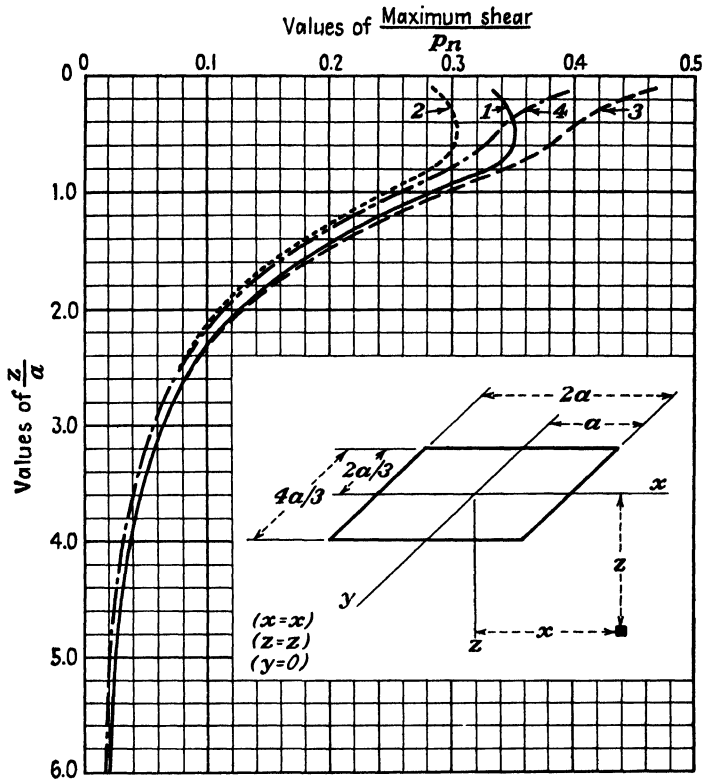
FIG. 19-16. Theoretical variation of maximum shearing stresses with depth below the center line of an area loaded by a vertical and by a horizontal force. (*After Frank Baron, Ref. 18, 1947, and Tschebotarioff and McAlpin, Ref. 382, 1947.*)

diameter the shearing stress is increased only by some 12 per cent. The increase is therefore negligible, except for its effect on the wearing surface of the pavement.

Where no improved wearing surface is present, for instance, on dirt or on desert roads, horizontal forces transmitted to the soil surface by accelerating or decelerating vehicles may cause so-called *corrugations* or *washboard waves* (see A. Mayer, 1947, and discussion by Tschebotarioff, Ref. 224). F. E. Relton (Ref. 284, 1938) explained washboard formation by

the action of horizontal forces applied to the soil surface and pointed out that the effect can be visualized by passing one's finger along the back of the other hand; the surface tends to heap up in front of the advancing point of application, ridges alternating with depressions. Washboards can develop in any climate and may even be aggravated in humid climates by the softening of the dirt-road surface due to accumulation of water in the depressions (Ref. 224). The remedy lies in the provision of more resisting surfacing.

Practice Problems

19-1. A CBR test (Art. 19-5) was performed on a certain soil, and a resistance of 340 lb was recorded for 0.1 in. penetration. What is the CBR value of that soil?

Answer. The resistance of crushed rock at 0.1 in. penetration is taken to equal 1,000 lb. Therefore the CBR value of the soil tested is $(340/1{,}000)100 = 34$ per cent.

19-2. Design a base course for a flexible pavement to support 25,000-lb wheel loads over a subgrade with a CBR value of 5 per cent. Two types of material are available for the construction of the base course: the first has a CBR value of 80 per cent and the second a CBR value of 15 per cent.

Answer. According to Fig. 19-11, a total pavement plus base thickness of 23 in. will be required for a 25,000-lb wheel load over a subgrade with a CBR value of 5 per cent. A total pavement plus base thickness of 12 in. will be needed over a base course with a CBR value of 15 per cent, and a minimum 4-in. thickness of pavement will be needed over a base course with a CBR value of 80 per cent. We thus have two alternatives: (*a*) 4 in. of pavement followed by 19 in. of base course with a CBR value of 80 per cent. (*b*) 4 in. of pavement followed by 8 in. of base course with a CBR value of 80 per cent and 11 in. of base course with a CBR value of 15 per cent (see discussion of this point in Art. 19-5).

19-3. Measurements made on an airplane showed that during the warmup of its engines the vertical load N on the main wheels (Fig. 19-15) was decreased by some 15 per cent. The magnitude of the vertical vibratory forces induced by the engines was measured simultaneously and was found to equal only 3 per cent of N. The authors of a certain 1945 report therefore decided that no attention need be given to vibratory forces. Is this generalized conclusion correct?

Answer. No. Vibratory forces can be entirely disregarded under the above conditions only on well-compacted cohesive soils. However, as outlined in Art. 18-4, granular soils, especially if they are of uniform grading, are very strongly affected by vibratory forces, so that a vibratory force equal to $0.03\ N$ might be equivalent in its effect on the deformations of the soil to a 100 times greater static force, that is, to $3.00\ N$. In addition, any improper adjustment of the engines of an airplane may greatly amplify the above usual low value of the vibratory forces (see Refs. 26 and 382).

19-4. A pore-pressure measuring device of the type shown in Fig. 19-9 has been installed 15 ft below the surface of a clay bed, which surface coincides with the free-water level. A 55-ft-high embankment has been placed over the clay, so that the distance h of Fig. 19-9 is $h = 15 + 55 = 70$ ft. What is the percentage of consolidation U_z (Arts. 6-7 and 6-8) of the clay layer at that elevation if the bourdon gage indicates (*a*) a pressure of 7 psi? (*b*) a vacuum of 9 psi?

Answer. (*a*) Assuming that the fill weighs 120 lb per ft^3, the surcharge applied to the clay by the weight of the fill is $55 \times 120 = 6{,}600$ lb per ft^2. This would be the

pressure in the pore water of the clay so long as no consolidation whatsoever has occurred ($U_z = 0$). The actual excess pressure in the pores of the clay at that elevation, however, is equal to the weight of the 55-ft-high column of water in the pipe leading to the gage above the free-water level plus the reading of the bourdon gage itself, that is, $(55 \times 62.4) + (7 \times 144) = 4{,}450$ lb per ft². Thus the water still carries $(4{,}450/6{,}600)100 = 67.5$ per cent of the surcharge, and the percentage of consolidation $U_z = 100 - 67.5 = 32.5$ per cent.

(*b*) Similarly, the pressure in the water is $(55 \times 62.4) - (9 \times 144) = 2{,}200$ lb per ft² and $U_z = [1 - (2{,}200/6{,}600)]\,100 = 66.6$ per cent.

To measure pressures corresponding to greater percentages of consolidation U_z an arrangement similar to that shown in Fig. 17-14 should be employed on an embankment of this height. The vertical pipe should be stopped at some distance below the top of the embankment and should be connected by flexible horizontal pipes to suitably protected gages on the face of the embankment slope.

References Recommended for Further Study

Field Manual of Soil Engineering, Michigan State Highway Department, Lansing, Michigan, revised, 1946, 304 pp. Surveys and construction procedures; extensive treatment of problems presented by embankment construction on swamps.

"Development of CBR Flexible Pavement Design Methods for Airfields," *Proceedings of the American Society of Civil Engineers*, January, 1949. A symposium. Discussion in May, June, and September, 1949, issues.

"Load Tests of Bearing Capacity of Soils," *American Society for Testing Materials Technical Publication No.* 79, 1947. A symposium. Techniques of testing and application of the results to design problems of highway pavements.

"Influence Charts for Concrete Pavements," by Gerald Pickett and G. K. Ray, *Proceedings of the American Society of Civil Engineers*, Vol. 76, Separate No. 12, April, 1950. Design charts.

Permafrost and Related Engineering Problems, by Siemon W. Muller, Edwards Bros., Inc., Ann Arbor, Michigan, 1947, 230 pp.

Laboratory Manual in Soil Mechanics, by Raymond F. Dawson, Pitman, 1949, pp. 168–177. Techniques of the CBR test with examples.

REFERENCES

Abbreviations

AASHO	American Association of State Highway Officials, Washington, D.C.
ARBA Tech. Bull.	American Roadbuilders' Association Technical Bulletin, Washington, D.C.
CAA Tech. Dev.	Civil Aeronautics Administration Technical Development, Indianapolis, Indiana.
Civil Eng.	Civil Engineering, published by ASCE, New York.
Colloid Chem.	Colloid Chemistry, published by Reinhold, New York.
Contrib. S.M., Boston Soc. Civil Engrs.	Volume of 1925–1940 Contributions to Soil Mechanics of the Boston Society of Civil Engineers, 413 pp.
ENR	Engineering News-Record, published by McGraw-Hill, New York.
1*st Int. Conf. S.M. & F.E.*	Proceedings of the International Conference on Soil Mechanics and Foundation Engineering, 1936, Harvard University, Cambridge, Massachusetts.
2*d Int. Conf. S.M. & F.E.*	Proceedings of the 2d International Conference on Soil Mechanics and Foundation Engineering, 1948, Rotterdam.
Iowa State Coll. Agr. Mech. Arts Eng. Expt. Sta. Bull.	Bulletin of the Engineering Experiment Station, Iowa State College of Agriculture and Mechanical Arts, Ames, Iowa.
J. Boston Soc. Civil Engrs.	Journal of the Boston Society of Civil Engineers.
J. Franklin Inst.	Journal of the Franklin Institute, Philadelphia, Pennsylvania.
J. Inst. Civil Engrs.	Journal of the Institution of Civil Engineers, London.
J. Western Soc. Engrs.	Journal of the Western Society of Engineers, Chicago.
Mich. State Coll. Agr. Eng. Expt. Sta. Bull.	Bulletin of the Engineering Experiment Station, Michigan State College of Agriculture and Applied Science, East Lansing, Michigan.
Phil. Mag.	The Philosophical Magazine, published by Taylor and Francis, Ltd., London.
Proc. ASCE	Proceedings of the American Society of Civil Engineers, New York.
Proc. ASTM	Proceedings of the American Society for Testing Materials, Philadelphia.
Proc. HRB	Proceedings of the Highway Research Board, Washington, D.C.
Proc. Purdue Conf. S.M.	Proceedings of the Conference on Soil Mechanics and Its Application, 1940, Purdue University, Lafayette, Indiana.
Struc. Engr.	The Structural Engineer, published by the Institution of Structural Engineers, London.
Trans. ASCE	Transactions of the American Society of Civil Engineers, New York.

Trans. ASME	Transactions of the American Society of Mechanical Engineers, New York.
Trans. Electrochem. Soc.	Transactions of the Electrochemical Society, New York.
Univ. Illinois Eng. Expt. Sta. Bull. Ser.	Bulletin of the Engineering Experiment Station, University of Illinois, Urbana, Illinois.
Univ. Wash. Eng. Expt. Sta. Ser. Bull.	Bulletin of the Engineering Experiment Station, University of Washington, Seattle.
U.S. Bur. Recl.	United States Bureau of Reclamation, Denver, Colorado.
U.S. Engr. Dept.	United States Engineer Department, Department of the Army, Washington, D.C.
U.S. Geol. Survey WSP	United States Geological Survey, Water Supply Paper, Washington, D.C.
U.S. Pub. Roads Admin.	United States Public Roads Administration, Washington D.C.
U.S. Waterways Expt. Sta.	United States Waterways Experimental Station, Vicksburg, Mississippi.

1. Abeleff, I. M., *Construction Practice on Loess Soils* (in Russian), Moscow, 1934.
2. Agatz, A., and E. Schultze, *Der Kampf des Ingenieurs gegen Erde und Wasser im Grundbau*, Springer, 1936.
3. Aichhorn, W., *Ueber die Zusammendrueckung des Bodens infolge oertlicher Belastung*, dissertation, Freiberg, Saxony, 1931.
4. Albin, Pedro Jr., Special Foundations Support Mexico City's Buildings on Highly Compressible Clay, *Civil Eng.*, August, 1949, pp. 25–28.
5. American Association of State Highway Officials, *Standard Specifications*, 1950. Part I. Specifications. Part II. Methods of Sampling and Testing.
6. American Colloid Co., *Bentonite; Technology and Industrial Uses*, data sheets, Chicago.
7. American Institute of Steel Construction, *Steel Construction Handbook*, New York.
8. *ARBA Tech. Bull.* 109, (1) The Use of Heavy Equipment for Obtaining Maximum Compaction of Soils, by O. J. Porter. (2) Vibratory and Impact Compaction of Soils, by Gregory P. Tschebotarioff. 1946.
9. *ASCE Manual of Engineering Practice* 22, Soil Mechanics Nomenclature, 1941.
10. *ASTM Procedures for Testing Soils*, 1950.
11. *ASTM Tentative Standard for Load Tests on Piles*, (in preparation).
12. Ammann, O. H., The Hell-Gate Bridge and Approaches of the New York Connecting Railroad over the East River in New York City, *Trans. ASCE*, 1918, pp. 852–1039.
13. Amsterdam Department of Public Works, Earth Pressure on Horizontal Circular Conduits, 2d *Int. Conf. S.M. & F.E.*, vol. IV, pp. 312–320, 1948.
14. Andrew, Charles E., The Lake Washington Pontoon Bridge, *Civil Eng.*, December, 1939, pp. 703–706.
15. ———, Building the World's Largest Floating Bridge, *Civil Eng.*, January, 1940.
16. Andrews, Walter C., and J. H. A. Crockett, Large Hammers and Their Foundations. *Struc. Engr.*, October, 1945, pp. 453–492.
17. Ayres, Q. C., *Soil Erosion and Its Control*, McGraw-Hill, 1936, 365 pp.
18. Baron, Frank, A Mathematical Study of Shearing Stresses Produced in a Pavement by the Locked Wheels of an Airplane during the Warm-up of Its Engines, *CAA Tech. Dev., Note* 47, 1947.

19. BARKAN, D. D., Vibrations of Foundations (in Russian), symposium: Experimental Study of Vibrations of Mat Foundations Resting on Cohesive Saturated Soils, *Trans. Vios*, 1934.

20. BARRON, REGINALD A., Consolidation of Fine-grained Soils by Drain Wells. *Trans. ASCE*, Vol. 113, pp. 718–754, 1948.

21. BAYLISS, JOHN R., *Design, Calibration and Use of the Lateral Earth Pressure Meter*, master's thesis, Princeton University, January, 1948.

22. BELCHER, D. J., L. E. GREGG, and K. B. WOODS, The Formation, Distribution and Engineering Characteristics of Soils, *Highway Research Bulletin* 10, Purdue University, 1943, 389 pp.

23. BESKOW, GUNNAR, *Soil Freezing and Frost Heaving* (translated from Swedish by J. O. Osterberg), Northwestern University, Evanston, Illinois, 1947, 145 pp.

24. BENKELMAN, A. C., and R. J. LANCASTER, Important Considerations in the Design and Use of Soil Pressure Cells, *Proc. HRB* 1940, pp. 299–313.

25. BERNHARD, R., and W. SPAETH, Rein dynamische Verfahren zur Untersuchung der Beanspruchungen von Bauwerken, *Stahlbau*, 1929.

26. ———, Study on Vibrations Transmitted to Pavements During Warm-up Periods of Airplanes. *CAA Tech. Dev., Note* 48, 1947.

27. BERTRAM, G. E., An Experimental Investigation of Protective Filters, *Harvard University Graduate School of Engineering Pub.* 267, S.M. Series 7, 1940.

28. ———, Soil Tests for Military Construction. *ARBA Tech. Bull.* 107, 1946, 95 pp.

29. *Bethlehem H-Piles*, Catalogue 223, 1949.

30. BINGER, WILSON V., and THOMAS F. THOMPSON, Excavation Slopes—Panama Canal, *Trans. ASCE*, 1949, pp. 734–755.

31. BISHOP, A. W., A New Sampling Tool for Use in Cohesionless Sands below Ground Water Level. *Geotechnique*, London, Vol. 1, No. 2, December, 1948.

32. BLAND, ROBERT F., *Settlement of the Charity Hospital of Louisiana*, paper presented at meeting of ASCE, Los Angeles, April, 1950.

33. *Blasters' Handbook*, du Pont Co., Wilmington, Delaware, 399 pp.

34. BLUM, H., *Einspannungsverhaeltnisse bei Bohlwerken*, W. Ernst und Sohn, Berlin, 1931.

35. BOASE, ARTHUR J., Railway Roadbeds Stabilized with Portland Cement Grout, *Civil Eng.*, October, 1945, pp. 447–449.

36. BOUSSINESQ, J., *Applications des potentiels a l'etude de l'equilibre et du mouvement des solides elastiques*, Gauthier-Villars, 1885.

37. BOUYOUCOS, G. J., *Mich. State Coll. Agr. Eng. Expt. Sta. Tech. Bull.* 22, 1915.

38. BOYER, GLENN C., *Diesel and Gas Engine Power Plants*, McGraw-Hill, 1943.

39. BRETTING, AAGE E., Foundations of Modern Bridges in Denmark, *1st Int. Conf. S.M. & F.E.*, Vol. III, pp. 193–201, 1936.

40. ———, General Report—Section V; Earth Pressure: Stability and Displacements of Retaining Constructions, *2d Int. Conf., S.M. & F.E.*, Vol. VI, p. 100, 1948.

41. BRIDGMAN, PERCY W., *Proc. Am. Academy*, Vol. 47, pp. 441–458, 1912.

42. BROWN, PHILIP P., *A Critical Study of Existing Lateral Earth Pressure Theories, Including the Design of a Model Flexible Anchored Bulkhead for the Investigation of these Theories*, master's thesis, Princeton University, January, 1948.

43. BROWZIN, BORIS S., Upon the Deflection and Strength of Anchored Bulkheads, *2d Int. Conf. S.M. & F.E.*, Vol. III, pp. 302–308, 1948.

44. BRUGGEN, J. P. VAN, De Maastunnel te Rotterdam, *De Ingenieur*, 1941.

45. ———, The Construction of the Maas Tunnel at Rotterdam, *2d Int. Conf. S.M. & F.E.*, Vol. VI, pp. 37–42, 1948.
46. ———, Letter to G. P. Tschebotarioff, May 19, 1949.
47. BRYAN, KIRK, Geology of Reservoir and Dam Sites, *U.S. Geol. Survey WSP* 597.
48. BUISMAN, A. KEVERLING, *Grondmechanica* 2e. druk, Delft, 1943, 281 pp.
49. BULL, ANDERS, Side Pressure on Retaining Walls, *ENR*, 1934, pp. 514–515.
50. BURGGRAF, FRED, Portable Machine for Making Surface Tests. *Proc. HRB*, Vol. 18, Part II, pp. 249, 426–428, 1938.
51. BURMISTER, D. M., Some Investigations of the Shearing Resistance of Cohesionless and Cohesive Materials, *Proc. ASTM*, Vol. 39, pp. 1071 to 1083, 1939.
52. ———, Practical Methods for the Classification of Soils, *Proc. Purdue Conf. S.M.*, pp. 129–139, 1940.
53. ———, The Theory of Stresses and Displacements in Layered Systems and Applications to Design of Airport Runways, *Proc. HRB.* 1943, pp. 126–148.
54. ———, The Importance and Practical Use of Relative Density in Soil Mechanics, *Proc. ASTM*, Vol. 48, 1948.
55. CADLING, LYMAN, and STEN ODENSTAD, The Vane Borer. *Proc.* 2, *Royal Swedish Geotechnical Inst.* Stockholm, 1950.
56. CAIN, W., *Earth Pressure, Retaining Walls and Bins*, Wiley, 1916.
57. CAQUOT, ALBERT, and JEAN KERISEL, *Tables for the Calculation of Passive Pressure, Active Pressure and Bearing Capacity of Foundations* (translated from French by Maurice A. Bec; revised translation by Chief Scientific Advisers' Division, Ministry of Works, London), Gauthier-Villars, 1948, 120 pp.
58. CARLSON (CADLING), LYMAN, Determination in-situ of the Shear Strength of Undisturbed Clay by Means of a Rotating Auger, *2d Int. Conf. S.M. & F.E.*, Vol. I, pp. 265–270, 1948.
59. CARLSON, ROY W., Five Years Improvement of the Elastic Wire Strain Meter, *ENR*, May 16, 1935, pp. 696–697.
60. CASAGRANDE, ARTHUR, Research on the Atterberg Limits of Soils, *Public Roads*, October, 1932.
61. ———, The Structure of Clay and Its Importance in Foundation Engineering, *Contrib. S.M. Boston Soc. Civil Engrs.*, pp. 72–126, 1940 (also *J. Boston Soc. Civil Engrs.*, April, 1932).
62. ———, Characteristics of Cohesionless Soils Affecting the Stability of Slopes and Earth Fills, *Contrib. S.M. Boston Soc. Civil Engrs.*, pp. 257–276, 1940 (also *J. Boston Soc. Civil Engrs.*, January, 1936).
63. ———, Seepage through Dams, *Contrib. S.M. Boston Soc. Civil Engrs.*, pp. 295–337, 1940 (also *J. Boston Soc. Civil Engrs.*, January, 1937).
64. ———, and R. E. FADUM, Notes on Soil Testing for Engineering Purposes, *Harvard University Graduate School of Engineering Pub.* 268, January, 1940, 74 pp.
65. ———, and R. E. FADUM, Application of Soil Mechanics in Designing Building Foundations, *Trans. ASCE*, 1944, pp. 383–490.
66. ———, Classification and Identification of Soils, *Trans. ASCE*, 1948, pp. 901–992.
67. ———, Soil Mechanics in the Design and the Construction of the Logan Airport, *J. Boston Soc. Civil Engrs.*, April, 1949, pp. 192–222.
68. ——— and W. L. SHANNON, Strength of Soils under Dynamic Loads, *Trans. ASCE*, 1949, pp. 755–773.
69. CASAGRANDE, LEO, Naeherungsverfahren zur Ermittlung der Sickerung in

geschuetteten Daemmen auf undurchlaessiger Sohle, *Bautechnik*, Berlin, No. 15, 1934.

70. ———, Structures Produced in Clays by Electric Potentials and Their Relation to Natural Structures, *Nature*, London, Vol. 160, p. 470, 1947.
71. ———, The Application of Electro-osmosis to Practical Problems in Foundations and Earthworks, *Department of Scientific and Industrial Research*, London, 1947, 16 pp.
72. ———, Electro-osmosis in Soils, *Geotechnique*, London, Vol. 1, No. 3, pp. 159–177, June, 1949.
73. Cassel, F. L., Slips in Fissured Clay, 2*d Int. Conf. S.M. & F.E.*, Vol. II, pp. 46–50, 1948.
74. Chadwick, W. L., and R. Howard Annin, Subsidence in Long Beach Harbor Area Requires Special Engineering Construction, *Civil Eng.*, June, 1950, pp. 17–22.
75. Chellis, Robert D., *Pile-driving Handbook*, Pitman, 1944, pp. 276.
76. ———, The Relationship between Pile Formulas and Load Tests, *Trans. ASCE*, 1949, pp. 290–321.
77. Colburn, R. T., Discussion of Ref. 364, *Trans. ASCE*, 1945, pp. 1135–1145.
78. Commission for the Investigation of the Causes of the Collapse of the Campanile di San Marco, Report, *bollettino ufficiale del ministero dell'instruzione pubblice*, Jan. 29, 1903, p. 177.
79. Commission Appointed by Governor C. C. Young to Investigate the Causes Leading to the Failure of the St. Francis Dam Near Saugus, California, Report, California State Printing Office, Sacramento, 1928.
80. Committee on the Cause of the Failure of the South Fork Dam, Report, *Trans. ASCE*, Vol. 24, pp. 431–460, 1891.
81. Special Committee on Earths and Foundations, Lazarus White, Chairman, Report, *Proc. ASCE*, May, 1933.
82. Committee on the Bearing Value of Pile Foundations, Pile-driving Formulas—Progress Report, *Proc. ASCE*, May, 1941, pp. 853–866.
83. Converse, F. J., *The Practical Use of Shear Test Data*, paper presented to 36th Annual Convention ARBA, San Francisco, 1939.
84. Cooling, L. E. and W. H. Ward, Damage to Cold Stores Due to Heaving, *Proc. Inst. Refrig.*, London, 1944. pp. 31–47.
85. ———, Development and Scope of Soil Mechanics, *The Principles and Applications of Soil Mechanics*, Inst. Civil Engrs., London, 1944, pp. 1–30.
86. Corps of Engineers, U.S. Army, *Report on the Slide of a Portion of the Upstream Face of the Fort Peck Dam*, July, 1939.
87. Coulomb, Charles Augustin, Essai sur une application des règles de maximis et minimis à quelques problêmes de statique relatifs à l'architecture, *Mem. Div. Sav., Academie des Sciences*, Paris, Vol. 7, 1776.
88. Coxe, L. C., Failure of Quay Wall at Mare Island, California, *Proc. ASCE*, January, 1948, pp. 93–100. Also *Trans. ASCE*, 1949, pp. 499–507.
89. ———, Long Beach Naval Shipyard Endangered by Subsidence. *Civil Eng.*, November, 1949, pp. 766–769.
90. Crandell, F. J., Ground Vibration Due to Blasting and Its Effect upon Structures, *J. Boston Soc. Civil Engrs.*, April, 1949 (summary in *ENR*, May 4, 1950).
91. Creager, William P., Joel D. Justin, and Julian Hinds, *Engineering for Dams*, Wiley, 1945. Vol. I, General Design, 246 pp. Vol. II, Concrete Dams, 372 pp. Vol. III, Earth, Rock-fill, Steel, and Timber Dams, 311 pp.

92. CROCKETT, J. H. A., and R. E. R. HAMMOND, Reduction of Ground Vibrations into Structures, *Inst. Civil Engrs. Structural Paper* 18, London, 1947.
93. ———, and R. E. R. HAMMOND, The Dynamic Principles of Machine Foundations and Ground, *Institute Mech. Engrs*, London, 1949.
94. CUEVAS, JOSE A., Foundation Conditions in Mexico City, *1st Int. Conf. S.M. & F.E.*, Vol. III, pp. 233–237, 1936.
95. ———, LAZARUS WHITE, and KARL TERZAGHI, Discussion on the Movements within Foundation Pits during Excavation, *1st Int. Conf. S.M. & F.E.*, Vol. III, pp. 228–331, 1936.
96. CUMMINGS, A. E., Dynamic Pile Driving Formulas, *Contrib. S.M., Boston Soc. Civil Engrs.* Also *J. Boston Soc. Civil Engrs.*, January, 1940.
97. ———, Discussion of Symposium on Earth Pressure and Shearing Resistance of Plastic Clay, *Trans. ASCE*, 1943, pp. 1067–1072.
98. ———, G. O. KERKHOFF, and R. B. PECK, Effect of Driving Piles into Soft Clay, *Proc. ASCE*, December, 1948.
99. DANSK INGENIØRFORENING, *Foreløbige Regler for Beregning og Udførelse af Jernbetonkonstruktioner i Vandbugning*, Copenhagen, 1926.
100. ———, *Normer for Vandbygnings Konstruktioner* (*Danish* 1937 *Bulkhead Regulations*), Copenhagen, 1937.
101. DAVIDENKOFF, R. N., About the Calculation of Anchored Bulkheads with Fixed Earth Support, *2d. Int. Conf. S.M. & F.E.*, Vol. V, pp. 122–124, 1948.
102. DAWSON, RAYMOND F., *Laboratory Manual in Soil Mechanics*, Pitman, 1949, 177 pp. plus data sheets.
103. DE BEER, E., Etude des fondations sur pilotis et des fondations directes par l'appareil de penetration en profondeur, *Annales des Travaux Publics de Belgique*, Avril, Juin, Aout, 1945.
104. ———, and M. WALLAYS, Limitation of the Validity of Application of the Formulas from Prandtl-Buisman and from Andersen for the Ultimate Bearing Capacity of the Soil underneath Footings, *2d Int. Conf. S.M. & F.E.*, Vol. I, pp. 63–68, 1948.
105. ———, and M. WALLAYS, Correlation between the Results of Cell Tests and Compression Tests, *2d Int. Conf. S.M. & F.E.*, Vol. I, pp. 173–184, 1948.
106. DEN HARTOG, J. P., *Mechanical Vibrations*, McGraw-Hill, 3d ed., 1947, 378 pp.
107. DELFT SOIL MECHANICS LABORATORY, The Predetermination of the Required Length and the Prediction of the Toe Resistance of Piles, *1st. Int. Conf. S.M. & F.E.*, 1936, Vol. I, p. 181.
108. DONATH, A. D., Untersuchungen ueber den Erddruck auf Stuetzwaende, *Zeitschrift fuer Bauwesen*, Berlin, 1891.
109. DORE, STANLEY M., Foundations and Embankments of Quabbin Dams, *1st Int. Conf. S.M. & F.E.*, Vol. II, pp. 300–307, 1936.
110. DUKE, C. MARTIN, *Field Study of a Sheetpile Bulkhead*, paper presented at ASCE meeting, Los Angeles, April, 1950.
111. DUNHAM, CLARENCE W., *The Theory and Practice of Reinforced Concrete*, McGraw-Hill, 1944, 558 pp.
111*a*. ———, *Foundations of Structures*, McGraw-Hill, 1950, 679 pp.
112. EHLERS, H., *Beitrag zur statischen Berechnung von Spundwaenden*, Hamburg, 1910.
113. ———, Beitrag zur statischen Berechnung von Spundwaenden unter Beruecksichtigung besond. oertlicher Verhaeltnisse, *Zeitschrift fuer Architektur und Ingenieurwesen*, 1919, p. 1.

114. EHRENBERG, J., Das Ausfliessen einer Sandkippe in einer Braunkohlengrube. *Bautechnik*, No. 19, Berlin, 1933.
115. EMMONS, W. H., G. A. THIEL, C. R. STAUFFER, and I. S. ALLISON, *Geology*, McGraw-Hill, 1939, 451 pp.
116. ENDELL, K., and U. HOFFMAN, The Chemical Nature of Clays, 1st *Int. Conf. S.M. & F.E.*, Vol. I, pp. 51–54, 1936.
117. ENGELUND, AUKER, A Special Foundation Method for Bridge Piers Adopted in Danish Fjords, 1st *Int. Conf. S.M. & F.E.*, Vol. I, pp. 291–294, 1936.
118. Rebuilding Marshall Creek Dam, *ENR*, 1939, pp. 23–25.
119. Mobile Builds a Vehicle Tunnel for Gulf Coast Highway Traffic, *ENR*, April, 1940, pp. 572–576.
120. Iowa Road Carved through Loess Bluffs, *ENR*, Apr. 29, 1940, pp. 277–279.
121. Twin Drydocks Construction Underwater, *ENR*, Nov. 19, 1942, pp. 702–703.
122. Precision Control in Sinking Prefabricated Sections for Maas Tunnel, *ENR*, March, 1946, pp. 336–340.
123. Making Sand Drains Stick in the Mud, *ENR*, July 21, 1949.
124. Saving LaGuardia Airport, *ENR*, December 15, 1949, p. 35. Also *ENR*, Aug. 28, 1947, p. 291.
125. EPSTEIN, HARRIS, Application of Test Results to Quay Wall Design, *Proc. ASCE*, January, 1948, pp. 58–72. Also *Trans. ASCE*, 1949, pp. 464–478.
126. ———, Reduction of Lateral Cohesive Soil Pressure on Quaywalls by Use of Sand Dykes, 2d. *Int. Conf. S.M. & F.E.*, Vol. III, pp. 291–296, 1948.
127. ERICKSON, E. L., Foundations of Mississippi River Bridge at Baton Rouge, Louisiana, *Proc. HRB*, 1940, pp. 757–786.
128. Es, L. S. C. VAN, Das Untersuchungsverfahren ueber die Eignung von Bodenarten fuer den Bau von Staudaemmen mit Hilfe der Konsistenzwerte von Atterberg, *Proc.* 1st *Congress on Large Dams*, Stockholm, 1933, pp. 125–131.
129. FABER, OSCAR, Pressure Distribution under Bases and Stability of Foundations, *Struc. Engr.*, 1933.
130. FAHLQUIST, F. E., New Methods and Techniques in Subsurface Explorations, *J. Boston Soc. Civil Engrs.*, 1941, pp. 144–160.
131. FELD, JACOB, Review of Pioneer Work in Earth Pressure Determination, *Proc. HRB*, 1940.
132. ———, Early History and Bibliography of Soil Mechanics, 2d *Int. Conf. S.M. & F.E.*, Vol. I, pp. 1–7, 1948.
133. FELLENIUS, W., *Erdstatische Berechnungen*, W. Ernst und Sohn, Berlin, 1927. 4th ed., 1948.
134. FIDLER, HAROLD A., A Machine for Determining the Shearing Strength of Soils, *Proc. Conf. on Soils and Foundations, Corps of Engineers, U.S. Army*, 1938, Boston, pp. D-1–D-6.
135. FORCHHEIMER, PHILIP, Zur Grundwasserbewegung nach isothermischen Kurvenscharen, *Sitzungsberichte der K.K. Akademie der Wissenschaften*, Vienna, Vol. 126, No. 4, pp. 409–440, 1917.
136. FRANZIUS, O., Versuche mit passivem Druck, *Bauingenieur*, Berlin, 1924, pp. 314–320.
137. FREEMAN, GEORGE L., GEORGE W. GLICK, and HAMILTON GRAY, The Application of Soil Mechanics in Building the New York World's Fair, *Civil Eng.*, October, 1940.
138. FREEMAN, GEORGE, and J. PARSONS, Discussion of Ref. 98, *Proc. ASCE*, October, 1949.

139. FREYSSINET, E., *Une revolution dans les techniques du beton*, Paris, 1939.
140. FROCHT, M. M., *Photoelasticity*, Wiley, 1941.
141. FROEHLICH, O. K., *Druckverteilung im Baugrunde*, Springer, 1934, 183 pp.
142. FRUHAUF, BEDRICH, A Study of Lateritic Soils, *Proc. HRB*, 1946, pp. 579–594.
143. ———, Wet Vibration Puts Strength in Sand, *ENR*, June 23, 1949, pp. 60–62.
144. GALLOWAY, J. D., The Design of Rock-fill Dams, *Trans. ASCE*, 1939, pp. 1–93.
145. GEBHARD, J. C., Cave-ins of Sandy Backfills, *Proc. ASCE*, January, 1948, pp. 84–93. Also *Trans. ASCE*, pp. 490–499.
146. GERBER, EMIL, *Untersuchungen ueber die Druckverteilung im oertlich belasteten Sand*, dissertation, Technische Hochschule, Zurich, 1929.
147. GERSEVANOFF, N., Improved Methods of Consolidation Test and of the Determination of Capillary Pressure in Soils, 1*st Int. Conf. S.M. & F.E.*, Vol. I, pp 47–50, 1936.
148. GEUZE, E. C. W. A., Résultats d'essais avec l'appareil à pression triaxiale, *Congrès de l'Urbanisme du Sous-Sol*, Paris, 1936.
149. ———, Critical Density of Some Dutch Sands, 2*d Int. Conf. S.M. & F.E.*, Vol. III, 1948.
150. ———, Horizontal Earth Pressure against a Row of Piles, 2*d Int. Conf. S.M. & F.E.*, Vol. IV, pp. 135–140, 1948.
151. GILBOY, GLENNON, Mechanics of Hydraulic Fill Dams, *Contrib. S.M., Boston Soc. Civil Engrs.*, pp. 127–147. Also *J. Boston Soc. Civil Engrs.*, July, 1934.
152. ———, The Scientific Method in Earthwork, *Civil Engr.*, December, 1937, pp. 822–830.
153. ———, Discussion of Ref. 229, *Trans. ASCE*, 1942, pp. 752–755.
154. GLICK, GEORGE W., Rigid Rectangular Frame Foundation for Albany Telephone Building, *ENR*, Nov. 27, 1930.
155. ———, Foundations of the New Telephone Building, Albany, N.Y., 1*st Int. Conf. S.M. & F.E.*, Vol. I, pp. 279–284, 1936.
156. GOLDBECK, A. T., The Measurement of Earth Pressure on Retaining Walls, *Proc. HRB*, 1938, pp. 66–80.
157. GOLDER, HUGH Q., Measurement of Pressure in Timbering of a Trench in Clay, 2*d. Int. Conf. S.M. & F.E.*, Vol. II, pp. 76–81, 1948.
158. ———, The Influence of Geology on Soil Testing Methods in Western Europe, 2*d. Int. Conf. S.M. & F.E.*, Vol. V, pp. 1–3, 1948.
159. GRAY, HAMILTON, Simultaneous Consolidation of Contiguous Layers of Unlike Compressible Soils, *Trans. ASCE*, 1945, pp. 1327–1357.
160. GREENMAN, ROY L., The Use and Treatment of Granular Backfill, *Mich. State Coll. Agr. Eng. Expt. Sta. Bull.* 107, 1948.
161. GRIM, R. E., The Clay Minerals in Soils and Their Significance, *Proc. Purdue Conf. S.M.*, 1940, pp. 216–223.
162. ———, Some Fundamental Factors Influencing the Properties of Soil Materials, 2*d Int. Conf. S.M. & F.E.*, Vol. III, pp. 8–12, 1948.
163. ———, Mineralogical Composition in Relation to the Properties of Certain Soils, *Geotechnique*, London, Vol. I, No. 3, June, 1949.
164. HANNA, W. S., and GREGORY TSCHEBOTARIOFF, Settlement Observations of Buildings in Egypt, 1*st Int. Conf. S.M. & F.E.*, Vol. I, pp. 71–77, 1936.
165. ———, Settlement Studies in Egypt, *Geotechnique*, London, Vol. III, No. 1, pp. 33–45, June, 1950.
166. HANSEN, J. BRINCH, Development of the C. & N. Wharf Type, *Christiani & Nielsen Bulletin* 56, Copenhagen, 1946.

167. ———, Reinforced Concrete Wharf, Bangkok, Siam, *Indian Concrete Journal*, Apr. 15, 1948, pp. 78–79.
168. ———, Letter to G. Tschebotarioff, Dec. 3, 1948.
169. HARDY, W. B. and T. V. HARDY, Note on Static Friction and on the Lubricating Properties of Certain Chemical Substances, *Phil. Mag.*, Vol. 39, No. 223, pp. 32–35, July, 1919.
170. HARROUN, D. T., Stability of Cohesive Earth Masses in Vertical Embankments, *Proc. HRB*, 1940, pp. 751–756.
171. HERTWIG, A., G. FRUH, and H. LORENZ, Determination by Means of Forced Vibrations of Soil Properties of Particular Importance for Construction Work (in German), *DEGEBO pub.* 1, Berlin, 1933.
172. ———, Bemerkungen ueber neuere Erddruckuntersuchungen, *DEGEBO pub.* 7, Berlin, 1939.
173. HIGHWAY RESEARCH BOARD, *Current Road Problems* (series of pamphlets), 1946, No. 5, Granular Stabilized Roads; No. 7, Use of Soil-Cement Mixtures for Base Courses; No. 12, Soil-bituminous Roads.
174. HILEY, A., Pile Driving Calculations with Notes on Driving Forces and Ground Resistance, *Struc. Engr.*, Vol. 3, pp. 246–259 and 278–288, 1930.
175. HILF, J. W., Estimating Construction Pore Pressures in Rolled Earth Dams, *2d Int. Conf. S.M. & F.E.*, Vol. III, pp. 234–240, 1948.
176. HINCKLEY, H. V., *Lessons from the Austin Dam Failures*, Oklahoma Engineering Society, 1911. (On file at United Engineering Societies Library, New York.)
177. HOGENTOGLER, C. A., *Engineering Properties of Soil*, McGraw-Hill, 1937, 434 pp.
178. HOUSEL, W. S., Earth Pressure on Tunnels, *Trans. ASCE*, 1943, pp. 1037–1058.
179. HUGI, *Untersuchungen ueber die Druckverteilung im oertlich belastetem Sand*, dissertation, Zurich, 1927.
180. HVORSLEV, M. JUUL, *Ueber die Festigkeitseigenschaften gestoerter bindiger Boeden*, Copenhagen, 1937, 159 pp.
181. ———, *Subsurface Exploration and Sampling of Soils*, report on the joint research project of the ASCE; the Engineering Foundation; Harvard University; and the U.S. Waterways Experiment Station, Engineering Foundation, New York, 1949, 521 pp.
182. IMMERMAN, HARRY T., Steel Shell Piles for Unusual Foundation, *ENR*, June 3, 1943.
183. INSTITUTION OF STRUCTURAL ENGINEERS, *Specifications for Concrete Pile Driving*, London, 1936.
184. ITERSON, F. K. TH. VAN, Earth Pressure in Mining, *2d. Int. Conf. S.M. & F.E.*, Vol. III, pp. 314–316, 1948.
185. JAKOBSON, B., The Design of Embankments on Soft Clays, *Geotechnique*, London, Vol. I, No. 2, pp. 80–90, 1948.
186. JAKY, J., The Coefficient of Earth Pressure at Rest, *Journal of the Society of Hungarian Architects and Engineers*, Budapest, 1944, pp. 355–358.
187. ———, Pressure in Silos, *2d. Int. Conf. S.M. & F.E.*, Vol. I, pp. 103–107, 1948.
188. JAMIESON, J. A., Grain Pressures in Deep Bins, *Engineering News*, New York, 1904, pp. 236–243.
189. JENKINS, D. S., D. J. BELCHER, L. E. GREGG, and K. B. WOODS, The Origin, Distribution and Airphoto Identification of United States Soils, *CAA Tech. Dev. Report* 52, 1946.
190. JENKINS, HERBERT T., *Soil Mechanics Laboratory Manual*, Comstock Publishing Company, Inc., Ithaca, 1947, 107 pp.

190*a*. Jennings, J. E., Foundations for Buildings in the Orange Free State Goldfields, *Journal, South African Institution of Engineers*, Pretoria, November, 1950; March, 1951.

191. Jenny, Hans, *Factors of Soil Formation*, McGraw-Hill, 1941, 281 pp.

192. Jens, Stifel W., Drainage of Airport Surfaces—Some Basic Considerations, *Trans. ASCE*, 1948, pp. 785–837.

193. Joffe, J. S., *Pedology*, Rutgers University Press, 1936.

194. Johnson, J. W. and C. Martin Riedel, Water Stopped in Alpha Slope by Chemical Sand Solidification, *Coal Age*, New York, July, 1949.

195. Jurgenson, Leo, The Application of Theories of Elasticity and Plasticity to Foundation Problems, *Contrib. S.M., Boston Soc. Civil Engrs.*, 1940, pp. 148–183. Also *J. Boston Soc. Civil Engrs.*, July, 1934.

196. Kimball, William P., Soil Mechanics in Foundation Engineering, *Journal of the Engineering Institute of Canada*, March, 1939.

197. Kimble, Edwin L., A Method of Effecting SR-4 Strain Gage Operation under Water, *Proc. Soc. Exptl. Stress Analysis*, Cambridge, Mass., Vol. III, No. 2, 1946.

198. King, Howard L., Subaqueous Tunnel Construction, *Civil Eng.*, March, 1939. pp. 153–156.

199. Kneas, Frank N., Bearing Value of Soils, *J. of the Franklin Inst.*, Vol. 223, No. 4, April, 1937.

200. Koegler, F. and A. Scheidig, Druckverteilung im Baugrunde, *Bautechnik*, Berlin, 1927–29.

201. ———, and A. Scheidig, *Baugrund und Bauwerk*, Ernst, W. und Sohn, Berlin, 1st ed., 1938, 5th ed., 1948, 288 pp.

202. Koppejan, A. W., B. M. Van Wamelen, and L. J. H. Weinberg, Coastal Flow Slides in the Dutch Province of Zeeland, *2d Int. Conf. S.M. & F.E.*, Vol. V, pp. 89–96, 1948.

203. Krey, H., *Erddruck, Erdwiderstand*, Berlin, 5th ed., 1936, 340 pp.

204. Krynine, D. P., Discussion of Ref. 364, *Trans. ASCE*, 1945, pp. 1175–1178.

205. ———, *Soil Mechanics*, McGraw-Hill, 2d ed., 1947, 511 pp.

206. Labor Department of the State of New York, *Industrial Code Bulletin* 22, 1938.

207. Lee, George Hamor, *An Introduction to Experimental Stress Analysis*, Wiley, 1950.

208. Lee, Charles H., Sealing the Lagoon Lining at Treasure Island with Salt, *Trans. ASCE*, 1941, pp. 577–607.

209. Lee, Donovan H. *Sheet Piling, Cofferdams and Caissons*, Concrete Publ., Ltd., London, 1945, 191 pp.

210. Legget, R. F., *Geology and Engineering*, McGraw-Hill, 1939.

211. Le Gorgeu, M. V., La reconstruction du quai d'accostage des Ferry-boats au port de Dunkerque, *Haventechnick*, Antwerp, 1949.

212. Leimdorfer, Paul, Some Views on the Selection of Steel Sheet Piling, *Proc. XVIIth Int. Navigation Congress*, Lisbon, 1949.

213. Levinton, Zusse, Elastic Foundations Analyzed by the Method of Redund nt Reactions, *Trans. ASCE*, 1949, pp. 40–78.

214. Lobeck, A. K., *Geomorphology*, McGraw-Hill, 1939, 731 pp.

215. Loos, Wilhelm, Comparative Studies of the Effectiveness of Different Methods for Compacting Cohesionless Soils, *1st Int. Conf. S.M. & F.E.*, Vol. III, pp. 174–179, 1936.

216. ———, *Praktische Anwendung der Baugrunduntersuchungen*, Berlin, 1937, 204 pp.
217. LORENZ, H., New Results of Dynamic Investigations of Foundation Soils (in German), *Zeitschrift des Vereins deutscher Ingenieure*, Mar. 24, 1934.
218. LUGEON, MAURICE, *Barrages et géologie*, F. Rouge & Cie., Lausanne, 1933, 138 pp.
219. LYMAN, A. K. B., Compaction of Cohesionless Foundation Soils by Explosives, *Trans. ASCE*, 1942, pp. 1330–1342.
220. MCLEOD, NORMAN W., Airport Runway Evaluation in Canada, *HRB Research Report* 4*B*., October, 1947 (plus 1948 supplement).
221. MACKIN, J. HOOVER, A Geologic Interpretation of the Failure of the Cedar Reservoir, Washington, *Univ. Wash. Eng. Expt. Sta.* Ser. Bull. 107, March, 1941.
222. MASTERS, FRANK M., Timber Friction Pile Foundations, *Trans. ASCE*, 1943, pp. 115–173.
223. MAUTNER, K. W., Structures in Areas Subjected to Mining Subsidence, *Struc. Engr.*, January, 1948, pp. 35–69.
224. MAYER, ARMAND, Washboard Waves on Desert Roads, *Proc. HRB*, 1947, pp. 472–479.
225. MEEM, J. C., The Bracing of Trenches and Tunnels, *Trans. ASCE*, 1908, pp. 1–100.
226. MEYERHOF, G. G., The Settlement Analysis of Building Frames, *Struc. Engr.*, September, 1947.
227. ———, An Investigation of the Bearing Capacity of Shallow Footings on Dry Sand, 2*d. Int. Conf. S.M. & F.E.*, Vol. I. pp. 237–243, 1948.
228. MICHIGAN STATE HIGHWAY DEPARTMENT, *Field Manual of Soil Engineering*, February, 1946.
229. MIDDLEBROOKS, T. A., Fort Peck Slide, *Trans. ASCE*, 1942, pp. 723–764.
230. ———, and WILLIAM H. JERVIS, Relief Wells for Dams and Levees, *Trans. ASCE*, 1947, pp. 1321–1402.
231. Mills, W. H. JR., Suggested Method for Mechanical Analysis of Soil by Elutriation (see Ref. 10).
232. MOHR, H. A., Exploration of Soil Conditions and Sampling Operations, *Harvard University Graduate School of Engineering Pub.*, S.M. Series 21, November, 1943.
233. MOLITOR, DAVID A., Wave-pressures on Sea Walls and Breakwaters, *Trans. ASCE*, 1935, pp. 984–1017.
234. MÖLLER, M., *Grundriss des Wasserbaus*, Leipzig, Vol. I, 1906.
235. MOORE, NORMAN R., The Sardis Dam and Reservoir, *Civil Eng.*, June, 1939.
236. MOORE, RAYMOND C., *Historical Geology*, McGraw-Hill, 1933, 673 pp.
237. MORETRENCH CORPORATION, *Working in the Dry*, New York.
238. MORETTO, ORESTE, Effect of Natural Hardening on the Unconfined Compression Strength of Remolded Clays, 2d *Int. Conf. S.M. & F.E.*, Vol. I, pp. 137–144, 1948.
239. MORSE, FREDERICK T., *Power Plant Engineering and Design*, Van Nostrand, 2d ed., 1942.
240. MOULTON, H. G., Earth and Rock Pressures, *Trans. Am. Inst. Mining Met. Engrs.*, 1920, pp. 327–369.
241. MUELLER-BRESLAU, *Erddruck auf Stuetzmauern*, Kroener, 1906.
242. MULLER, SIEMON W., *Permafrost and Related Engineering Problems*, Edwards Bros., Inc., Ann Arbor, Michigan, 1947, 230 pp.

243. Muhs, H., Erddruckmessungen an einer 24 m. hohen starren Wand, *Bauplanung und Bautechnik*, Berlin, Vol. I, No. 1, pp. 11–16, July, 1947.

244. Nadai, A., *Theory of Flow and Fracture of Solids*, McGraw-Hill, 1950 (revision of *Plasticity*, McGraw-Hill, 1938).

245. *National Bureau of Standards Report BM* 578, Structural, Heat Transfer, and Water Permeability Properties of Five Earth-wall Constructions, Washington, 1941.

246. Newcomb, Wallace K., *Principles of Foundation Design for Engines and Compressors, Trans. ASME*, April, 1951, pp. 307–318.

247. New Jersey Turnpike Authority, (1) *Standard Specifications.* (2) *Contract Documents for Sections* 6 *&* 7, *Contract No.* 2, December, 1949.

248. Newmark, Nathan M., Influence Charts for the Computation of Stresses in Elastic Foundations, *Univ. Illinois Eng. Expt. Sta. Bull. Ser.* 338, 1942.

249. Nicolet, Justin, and V. E. Gunlock, Construction of Chicago's First Subway—Structural Design and Construction of Tubes and Stations, *J. Western Soc. Engrs.*, Vol. 49, No. 2, pp. 111–131, June, 1944.

250. Nixon, I. K., Correspondence on $\phi = 0$ Analysis, *Geotechnique*, London, Vol. I, Nos. 3 and 4, pp. 208 and 272–276, 1949.

251. Obruchev, V. A., *The Formation of Loess* (in Russian), Tomsk, 1911.

252. Ohde, J., Zur Theorie des Erddruckes unter besonderer Beruecksichtigung der Erddruckverteilung, *Bautechnik*, Berlin, No. 10/11, 13, 19, 25, 37, 42, 53/54, 1938.

253. Okey, Charles W., The Subsidence of Muck and Peat Soils in Southern Louisiana and Florida, *Trans. ASCE*, 1918, pp. 396–432.

254. Osterberg, J. O., A Survey of the Frost Heaving Problem, *Civil Eng.*, 1940, pp. 100–102.

255. Pacific Island Engineers, *Report on Quaywall Tests*, Jan. 20, 1949.

256. Palmer, L. A., Discussion of Ref. 378, *Proc. HBR*, 1944.

257. ———, Experiences with Soil Types in Naval Construction, *Proc. ASCE*, January, 1948, pp. 72–83. Also *Trans. ASCE*, 1949, pp. 478–490.

258. ———, and James B. Thompson, The Earth Pressure and Deflection along the Embedded Lengths of Piles Subjected to Lateral Thrust, *2d. Int. Conf. S.M. & F.E.*, Vol. V, pp. 156–161, 1948.

259. Peck, Ralph B., The Measurement of Earth Pressures on the Chicago Subway, *ASTM Bull.*, August, 1941, p. 25.

260. ———, Earth Pressure Measurements in Open Cuts, Chicago (Ill.) Subway, *Trans. ASCE*, 1943, pp. 1008–1036.

261. ———, and O. K. Peck, Experience with Flexible Culverts through Railway Embankments, *2d Int. Conf. S.M. & F.E.*, Vol. II, pp. 95–99, 1948.

262. ———, and Sidney Berman, Measurements of Pressures against a Deep Shaft in Plastic Clay, *2d Int. Conf. S.M. & F.E.*, Vol. III, pp. 300–301, 1948.

263. ———, Letter to G. P. Tschebotarioff, May 28, 1949.

264. Peckworth, H. F., Field Control of Compacted Earth Fill, *Civil Eng.*, April, 1939, pp. 221–223.

264*a*. ———, *Concrete Pipe Handbook*, American Concrete Pipe Assoc., Chicago, 1951.

265. Petterson, K. E., Kajraseti Goteborg des 5[te] Mars 1916, *Tekniske Tidskrift*, Vol. 46, p. 289, July 29, 1916.

266. Pickett, Gerald, and G. K. Ray, Influence Charts for Concrete Pavements, *Proc. ASCE*, Vol. 76, Separate No. 12, April, 1950.

267. Pimm, Gower B. R., Recent Developments in Deep Ground Testing, *Struc. Engr.*, July, 1938, pp. 210–221.

268. ———, The Limitations of Soil Mechanics as Applied to Foundations, *Struc. Engr.*, 1948, pp. 589–604. With discussion in Vol. 27, pp. 147–164 and 238–242, 1949.

269. POLIVKA, MILOS, Running Sand Chemically Solidified, *Western Construction News*, San Francisco, July 15, 1949.

270. PORTER, O. J., Studies of Fill Construction over Mud Flats, Including a Description of Experimental Construction Using Vertical Sand Drains to Hasten Stabilization, 1*st Int. Conf. S.M. & F.E.*, Vol. I, pp. 229–234, 1936.

271. ———, Development of the Original Method for Highway Design, *Trans. ASCE*, 1950, pp. 461–468. (Paper of CBR symposium Ref. 337.)

272. PORTLAND CEMENT ASSOCIATION, *Concrete Piles*, Chicago, 80 pp.

273. ———, *Soil Cement Roads Construction Handbook*, Chicago.

274. PRANDTL, L., Eindringungsfestigkeit und Festigkeit von Schneiden, *Zeitschrift fuer angewandte Mathematik und Mechanik*, Vol. 1, No. 1, pp. 15–20, 1921.

275. PREBUS, A. F., The Electron Microscope, *Colloid Chem.*, Vol. V, 1944.

276. PRENTIS, EDMUND ASTLEY and LAZARUS WHITE, *Underpinning*, Columbia University Press, 2d ed., 1950.

277. PROCTOR, CARLTON S., The Foundations of the San Francisco–Oakland Bay Bridge, 1*st. Int. Conf. S.M. & F.E.*, Vol. III, pp. 183–193, 1936.

278. ———, Bridge Foundations, *Publications of the International Association for Bridge and Structural Engineering*, Zurich, Vol. V, pp. 261–273, 1938.

279. ———, Cap Grouting to Stabilize Foundation on Cavernous Limestone, 2*d Int. Conf. S.M. & F.E.*, Vol. IV, pp. 302–308, 1948.

280. PROCTOR, R. R., Design and Construction of Rolled Earth Dams, *ENR*, Aug. 31; Sept. 7, 21, and 28; 1933; pp. 245–248, 286–289, 348–351, and 372–376.

281. ———, The Relationship between the Foot Pounds per Cubic Foot of Compactive Effort Expended in the Laboratory Compaction of Soils and the Required Compactive Efforts to Secure Similar Results with Sheepsfoot Rollers, 2*d Int. Conf. S.M. & F.E.*, Vol. V, pp. 231–234, 1948.

282. PROCTOR, R. V., and THOMAS WHITE, *Rock Tunneling with Steel Supports*, Commercial Shearing & Stamping Co., Youngstown, Ohio, 1946. Contains five chapters by Karl Terzaghi on "Rock Defects and Loads on Tunnel Supports."

283. RANKINE, W. J. M., On the Stability of Loose Earth, *Trans. Royal Soc. London*, Vol. 147, 1857.

284. RELTON, F. E., Corrugations on Roads, *Roads & Road Construction*, London, Oct. 1, 1938.

285. RENDULIC, L., Ein Beitrag zur Bestimmung der Gleitsicherheit, *Bauingenieur*, Berlin, 1935, No. 19/20.

286. ———, Relation between Void Ratio and Effective Principal Stresses for a Remoulded Silty Clay, 1*st Int. Conf. S.M. & F.E.*, Vol. III, pp. 48–53, 1936.

287. RÉSAL, JEAN, *La poussée des terres*, Paris, 1910.

288. REUSS, *Memoirs of the Imperial Russian Naturalist Society*, Moscow, Vol. 2, pp. 327–337, 1808.

289. RICHART, F. E., A. BRANDTZAEG, and R. L. BROWN, A Study of the Failure of Concrete under Combined Compressive Stresses, *Univ. Illinois Eng. Expt. Sta. Bull. Ser.* 185, 1928.

290. RIMSTAD, I. A., *Zur Bemessung des doppelten Spundbauwerkes*, Copenhagen, 1940, 117 pp.

291. ROBERTS, P. W., and F. A. F. COOKE, Arctic Tower Foundations Frozen into Permafrost, *ENR*, February, 1950.

292. Rodio, M. G., Les Affaissements de la gare transatlantique du Havre, *Bulletin No. 3 du centre d'études et de recherches géotechniques*, Paris, 1935, 55 pp.
293. Rutledge, Philip C., Recent Developments in Soil Testing Apparatus, *Contrib. S.M., Boston Soc. Civil Engrs.*, 1940, pp. 227–257. Also *J. Boston Soc. Civil Engrs.*, October, 1935.
294. ———, Description and Identification of Soil Types, *Proc. Purdue Conf. S.M.*, 1940, pp. 124–129.
295. ———, Theories of Failure of Materials Applied to the Shearing Resistance of Soils, *Proc. Purdue Conf. S.M.*, 1940, pp. 191–204.
296. ———, *Soil Mechanics Fact Finding Survey Progress Report*, review of the cooperative triaxial research program of the War Department, Corps of Engineers, covering the period February, 1940, to May, 1944, *U.S. Waterways Expt. Sta.*, April, 1947, pp. 1–182.
297. Rybakoff, V. I., *Foundation Settlements of Structures* (in Russian), Moscow, 1937, 349 pp.
298. Sampson, E. Jr., *Stabilization of Granular Materials with Controlled Precipitation of Groundwater Type Solutions*, master's thesis, Princeton University, 1950.
299. Samsioe, A. F., Report on the Investigation of the Compressibility of the Ground of the Hydro-electric Power Plant Svir 3, 1*st Int. Conf. S.M. & F.E.*, Vol. I, pp. 41–47, 1936.
300. Sandick, Van, R. A., Nog eens de Campanile di S. Marco te Venetie, *De Ingenieur*, The Hague, 1902.
301. ———, Campanile di San Marco, *De Ingenieur*, The Hague, 1904, p. 183.
302. Scheidig, Alfred, *Der Löss* (in German), 233 pp. Dresden, 1934.
303. ———, Das Bauwerk, *Baugrund und Bauwerk*, Berlin, 1937, Nos. 5, 6, 8.
304. Schmidt, E., *Theoretische und experimentelle Untersuchungen ueber Entstehung und Daempfung von Fundamentschwingungen*, dissertation, Munich, 1921.
305. Schoklitsch, A., *Hydraulic Structures* (translated from German), Am. Soc. Mech. Engrs., Vol. I, 1937, 488 pp.
306. Schuchert, C., and C. O. Dunbar, *Outlines of Historical Geology*, Wiley, 1937, 241 pp.
306*a*. Schultze, Edgar, and Heinz Muhs, *Bodenuntersuchungen fuer Ingenieurbauten*, Springer, Berlin, 1950.
306*b*. Schuyler, James Ross, *Comparison of the Extent of Disturbance Produced by Driving Piles into Plastic Clay to the Disturbance Caused by an Unbalanced Excavation*, master's thesis, Princeton University, January, 1948.
306*c*. ———, Discussion of Ref. 98, *Trans. ASCE*, 1950, pp. 309–312.
307. Seiffert, Rudolf, Untersuchungsmethoden um festzustellen ob sich ein gegebenes Baumaterial fur den Bau eines Erddammes eignet, 1-*er Congrès des Grands Barrages*, Question 2*a*, Rapport 17, Stockholm, 1933.
308. Shepard, E. Raymond, Subsurface Explorations by Geophysical Methods, *ASTM, Proc.*, Vol. 49, pp. 993–1015, 1949.
309. Skempton, A. W., Discussion of Paper on Tunnel Linings, *J. Inst. Civil Engrs.*, Vol. 20, p. 53, March, 1943.
310 ———, Earth Pressure and the Stability of Slopes, *The Principles and Applications of Soil Mechanics*, Inst. Civil Engrs., 1946, pp. 31–61.
311. ———, The Rate of Softening in Stiff Fissured Clays, with Special Reference to London Clay, 2*d Int. Conf. S.M. & F.E.*, Vol. II, pp. 50–53, 1948.
312. ———, Vane Tests in the Alluvial Plane of the River Forth near Grangemouth, *Geotechnique* London, Vol. I, No. 2, pp. 111–124, 1948.

313. Simonds, A. W., and Fred U. Lippold, Treatment of Foundations for Large Dams by Grouting Methods, *Proc. ASCE*, Vol. 76, Separate No. 3, February, 1950.
314. Singer, Max, *Der Baugrund*, Springer, W. 1932, 393 pp.
315. Singstad, Ole, The Queens Midtown Tunnel, *Trans. ASCE*, 1944, pp. 679–762.
316. Smith, William H., Introduction to Symposium on Lateral Earth Pressures on Flexible Retaining Walls, *Proc. ASCE*, January, 1948, pp. 4–9. Also *Trans. ASCE*, 1949, pp. 410–415.
317. Southworth, John S., The Geological Aspects of the Matilja Dam Controversy, *The Mines Magazine*, September, 1949.
318. Spangler, M. G., Horizontal Pressures on Retaining Walls Due to Concentrated Surface Loads, *Iowa State Coll. Agr. Mech. Arts Eng. Expt. Sta. Bull.* 140, 1938.
319. ———, Lateral Pressures on Retaining Walls Caused by Superimposed Loads, *Proc. HRB*, Vol. 18, part II, pp. 57–65, 1938.
320. ———, Underground Conduits—an Appraisal of Modern Research, *Trans. ASCE*, 1948, pp. 316–374.
321. Spencer, Charles B., Drilled in Caissons with Heavy H-cores Carry 16-story Navy Warehouse, *ENR*, Sept. 25, 1941.
322. ———, Steel Braces Hold High Clay Bank in Albany, *ENR*, Mar. 2, 1950.
323. Spilker, A., Mitteilung ueber die Messung der Kraefte in einer Baugrubenaussteifung, *Bautechnik*, Berlin, 1937, No. 1, p. 16.
324. Sprague & Henwood, Inc., Sampling and Sampling Devices and Equipment, *Bulletin* 75*A*, Scranton, Pennsylvania.
325. Squires, L., and W. Squires, *Transactions of the American Institute of Chemical Engineers*, 1937.
326. Steuermann, M., Waermegaenge der Kuehlhausgruendungen, *Bautechnik*, Berlin, Aug. 28, 1936, pp. 547–548.
327. Stewart, Ralph W., Safe Foundation Depths for Bridges to Protect from Scour, *Civil Eng.*, June, 1939.
328. Stokes, Wm. Lee, Glossary of Selected Geologic Terms, *U.S. Geol. Survey Bull.*, (in preparation).
329. Stross, W., Wiederherstellung der Mohamed Aly Moschee in Kairo, *Beton und Eisen*, Berlin, Nov. 20, 1936, pp. 365–374.
330. Stroyer, J. R., Earth Pressure on Flexible Walls, *J. Inst. Civil Engrs.*, 1935–36, pp. 94–139.
331. ———, *Concrete Structures in Marine Work*, Knapp, Drewett & Sons, Ltd., London, 1937, 216 pp.
332. Sullivan, J. D., Physico-chemical Control of Properties of Clays, *Trans. Electrochem. Soc.*, 1939.
333. *Bodenmechanik und neuzeitlicher Strassenbau*, symposium by 24 authors, Volk und Reich Verlag, Berlin, 1936, 108 pp.
334. Foundation Experiences, Tennessee Valley Authority, symposium, *Trans. ASCE*, 1941, pp. 687–848.
335. Unusual Cut-off Problems—Dams of the Tennessee Valley Authority, symposium, *Trans. ASCE*, 1945, pp. 947–1018.
336. Load Tests of Bearing Capacity of Soils, symposium, *ASTM Special Tech. Pub.* 79, 1947.
337. Development of CBR Flexible Pavement Design Methods for Airfields, symposium, *Trans. ASCE*, 1950, pp. 453–590.
338. Symposium of several papers on soil classification, *Proc. ASTM*, 1950.

339. TAMMAN, G., *The States of Aggregation* (English translation), Van Nostrand, 1925.
340. TAN, EK KHOO, Stability of Soil Slopes, *Trans. ASCE*, 1948, pp. 139–180.
341. TAYLOR, DONALD W., Stability Analysis of a Foundation Failure, *Proc. HRB*, 1938, Part II, pp. 93–97.
342. ———, Stability of Earth Slopes, *Contrib. S.M.*, Boston Soc., Civil Engrs., 1940, pp. 337–386. Also *J. Boston Soc. Civil Engrs.*, July, 1937.
343. ———, *Fundamentals of Soil Mechanics*, Wiley, 1948, 700 pp.
344. TCHEKOTILLO, A., Solving the Problem of "Nalyeds" in Permafrost Regions, *ENR*, Nov. 28, 1946.
345. TERZAGHI, KARL, Die Erddruckerscheinungen in oertlich beanspruchten Schuettungen und die Entstehung von Tragkoerpern, *Oesterreichische Wochenschrift fuer oeffentlichen Baudienst*, Vienna, 1919, pp. 194–199, 206–210, 218–223.
346. ———, Old Earth Pressure Theories, *ENR*, Sept. 20, 1920, 632 pp.
347. ———, Die Berechnung der Durchlaessigkeitsziffer des Tones aus dem Verlauf der hydrodynamischen Spannungserscheinungen, *Sitzungsberichte der Akademie der Wissenschaften Abt.* II*a*, Vienna, Vol. 132, 1923.
348. ———, Principles of Soil Mechanics, *ENR*, Dec. 17, 1925, 798 pp.
349. ———, *Erdbaumechanik*, Leipzig, 1925, 397 pp.
350. ———, Principles of Final Soil Classification, *Public Roads*, Washington, 1927, pp. 41–53.
351. ———, The Science of Foundations—its Present and Future, *Trans. ASCE*, 1929.
352. ———, Record Earth Pressure Testing Machine, *ENR*, 1932.
353. ———, Large Retaining Wall Tests, *ENR*, 1934, pp. 136, 259, 316, 403, 503.
354. ———, A Fundamental Fallacy in Earth Pressure Computations, *Contrib. S.M., Boston Soc. Civil Engrs.*, 1940, pp. 277–294. Also *J. Boston Soc. Civil Engrs.*, April, 1936.
355. ———, Stability of Slopes of Natural Clay, 1*st Int. Conf. S.M. & F.E.*, Vol. I, pp. 161–165, 1936.
356. ———, Distribution of the Lateral Pressure of Sand on the Timbering of Cuts, 1*st Int. Conf. S.M. & F.E.*, Vol. I, pp. 211–215, 1936.
357. ———, Settlement of Structures in Europe and Methods of Observation, *Trans. ASCE*, 1938, pp. 1432–1502.
358. ———, Anchored Bulkheads, *Proc. Purdue Conf. S.M.*, 1940.
359. ———, Undisturbed Clay Samples and Undisturbed Clays, *J. Boston Soc. Civil Engrs.*, July, 1941.
360. ———, General Wedge Theory of Earth Pressure, *Trans. ASCE*, 1941, pp. 68–97.
361. ———, Liner-plate Tunnels on the Chicago (Ill.) Subway, *Trans. ASCE*, 1943, pp. 970–1008 and 1090–1097.
362. ———, *Theoretical Soil Mechanics*, Wiley, 1943, 510 pp.
363. ———, Ends and Means in Soil Mechanics, *Journal of the Engineering Institute of Canada*, December, 1944.
364. ———, Stability and Stiffness of Cellular Cofferdams—with Discussions, *Trans. ASCE*, 1945, pp. 1083–1202.
365. ———, and RALPH B. PECK, *Soil Mechanics in Engineering Practice*, Wiley, 1948, 566 pp.
366. THORNLEY, J. H., New Pile Code Sets Load Test Criteria, *ENR*, May 26, 1949.
367. TIMOSHENKO, S., *Theory of Elasticity*, McGraw-Hill, 1934, 416 pp.

368. TOLMAN, CYRUS F., *Ground Water*, McGraw-Hill, 1937, 593 pp.
369. TSCHEBOTARIOFF, GREGORY P., Comparison between Consolidation, Elastic and Other Soil Properties Established from Laboratory Tests and from Observations of Structures in Egypt, *1st. Int. Conf. S.M. & F.E.*, Vol. I, pp. 33–36, 1936.
370. ———, Relation between Observed Inequalities of Settlement of Buildings in Egypt and Theoretical Stress Distribution, Based on Boussinesq Formulas, *1st. Int. Conf. S.M. & F.E.*, Vol. I, pp. 57–61, 1936.
371. ———, Discussion of Reference 357, *Trans. ASCE*, 1938, pp. 1484–1487.
372. ———, Settlement Studies of Structures, *Civil Eng.*, November, 1938, pp. 751–753.
373. ———, Factors Affecting the Accuracy of Settlement Rate Forecasts, *Proc. HRB*, 1938, pp. 120–128.
374. ———, Some Practical Aspects of Soil Shear Testing, *Proc. ASTM*, 1939, pp. 1023–1027.
375. ———, *A Soil and Foundation Study in the United States*, report, Robert Stewart Brooks Fellowship, Princeton University, (unpublished), 1939.
376. ———, Undergraduate Instruction in Soil Mechanics as Part of a Course on Foundations, *Proc. Purdue Conf. S.M.*, 1940, pp. 48–53.
377. ———, Settlement Studies of Structures in Egypt, *Trans. ASCE*, 1940, pp. 919–972.
378. ———, Effect of Vibrations on the Bearing Properties of Soils, *Proc. HRB*, 1944, pp. 405–425.
379. ———, Use of Electric Resistivity Strain Gages over Long Periods of Time, *Proc. Soc. Exptl. Stress Analysis*, Cambridge, Massachusetts, Vol. III, No. 2, pp. 47–52, 1946.
380. ———, *Soil Conditions at the . . . Site*, report to Spencer, White and Prentis, Inc. (unpublished), Aug. 22, 1946.
381. ———, and GEORGE W. MCALPIN, Vibratory and Slow Repetitional Loading of Soils, *Proc. HRB*, 1946, pp. 551–562.
382. ———, and GEORGE W. MCALPIN, The Effect of Vibratory and Slow Repetitional Forces on the Bearing Properties of Soils, *CAA Tech. Dev., Report* 57, October, 1947, 70 pp.
383. ———, and HANS P. WINTERKORN, Testing of Submerged Bitumen-Sand Mixtures by Slow Repetitional Loading, *Proc. HRB*, 1947, pp. 467–471.
384. ———, Large Scale Model Earth Pressure Tests on Flexible Bulkheads, *Proc. ASCE*, January, 1948, pp. 9–48. Also *Trans. ASCE*, 1949, pp. 415–455 and 524–539.
385. ———, and JOHN R. BAYLISS, The Determination of the Shearing Strength of Varved Clays and of Their Sensitivity to Remolding, *2d. Int. Conf. S.M. & F.E.*, Vol. I, pp. 203–207, 1948.
386. ———, and EDWARD R. WARD, The Resonance of Machine Foundations and the Soil Coefficients Which Affect It, *2d. Int. Conf. S.M. & F.E.*, Vol. I, pp. 309–313, 1948.
387. ———, and PHILIP P. BROWN, Lateral Earth Pressure as a Problem of Deformation or of Rupture, *2d Int. Conf. S.M. & F.E.*, Vol. II, pp. 81–86, 1948.
388. ———, and L. A. PALMER, Some Experiences with Tests on Model Piles, *2d. Int. Conf. S.M. & F.E.*, Vol. II, pp. 195–199, 1948.
389. ———, and JAMES R. SCHUYLER, Comparison of the Extent of Disturbance Produced by Driving Piles into Plastic Clay to the Disturbance Caused by an Unbalanced Excavation, *2d Int. Conf. S.M. & F.E.*, Vol. II, pp. 199–205, 1948.

390. ———, and John D. Welch, Effect of Boundary Conditions on Lateral Earth Pressures, *2d Int. Conf. S.M. & F.E.*, Vol. III, pp. 308–313, 1948.
391. ———, Discussion of general report on Section V (Ref. 40), *2d Int. Conf. S.M. & F.E.*, Vol. VI, pp. 103–105, 1948.
392. ———, Discussion of paper Vc3 (Ref. 13), *2d Int. Conf. S.M. & F.E.*, Vol. VI, pp. 108–111, 1948.
393. ———, and John D. Welch, Lateral Earth Pressures and Friction between Soil Minerals, *2d Int. Conf. S.M. & F.E.*, Vol. VII, pp. 135–138, 1948.
394. ———, and Hans F. Winterkorn, Soil Engineering at Princeton University, *2d Int. Conf. S.M. & F.E.*, Vol. VI, pp. 230–233, 1948.
395. ———, *Report to the Bethlehem Steel Co.* (unpublished), Sparrows Point, Nov. 15, 1948.
396. ———, Determination from Bending Strain Measurements of the Distribution of Lateral Earth Pressures against Model Flexible Bulkheads, *Geotechnique*, London, Vol. I, No. 2, pp. 98–111, 1948.
397. ———, *Large Scale Earth Pressure Tests with Model Flexible Bulkheads*, final report to the Bureau of Yards and Docks, U.S. Navy, Princeton University, January, 1949, 272 pp.
398. ———, Discussion of Ref. 98, *Proc. ASCE*, May, 1949.
399. ———, Discussion of Ref. 110, presented at ASCE meeting, Los Angeles, April, 1950.
400. ———, Discussion of Ref. 246, *Trans. ASME*, April, 1951, pp. 315–317.
401. Turnbull, W. J., and H. N. Fisk, Relation of Soil Mechanics and Geology in Foundation Exploration, Lower Mississippi Valley, *2d Int. Conf. S.M. & F.E.*, Vol. III, pp. 3–5, 1948.
402. ———, Utility of Loess as a Construction Material, *2d Int. Conf. S.M. & F.E.*, Vol. V, pp. 97–103, 1948.
403. ———, and John L. McRae, Soil Test Results Shown Graphically, *ENR*, May 25, 1950, pp. 38–39.
404. Twenhofel, W. H., *Principles of Sedimentation*, McGraw-Hill, 1939, 610 pp.
405. Tyrrell, F. C., and L. A. Palmer, Discussion of Ref. 337, *Proc. ASCE*, May, 1949.
406. Urquhart, L. C., and C. E. O'Rourke, *Design of Concrete Structures*, McGraw-Hill, 1940.
407. U.S. Bureau of Reclamation, Drawings No. 40-D-4554 and 40-D-4834, showing typical layout and valve and gage assembly of piezometer terminal well for pore pressure. Drawing No. 285-D-253, Boysen Dam embankment piezometer installation.
408. U.S. Coast and Geodetic Survey, Earthquake Investigations in California 1934/35, *Special Pub.* 201.
409. U.S. Waterways Experimental Station, Conference on Control of Underseepage, Apr. 1, 1945.
410. ———, The California Bearing Ratio Test as Applied to the Design of Flexible Pavements for Airports, *Tech. Mem.* 213-1, 1945.
411. Vassilieff, B. D., *Osnovanya i Fundamenti* (in Russian), Moscow, 1937, 582 pp.
412. Valle-Rodas, Raoul, Capillarity in Sands, *Proc. HRB*, 1944, pp. 389–396.
413. ———, A New Method for the Mechanical Analysis of Soils, *ASTM Bull.*, August, 1945, Vol. 135.
414. Vermeiden, J., Improved Sounding Apparatus, as Developed in Holland since 1936, *2d Int. Conf. S.M. & F.E.*, Vol. I, pp. 281–287, 1948.
415. Vetter, P. C., Design of Pile Foundations, *Trans. ASCE*, 1939, pp. 758–811.

416. WAHLSTROM, ERNEST E., Application of Geology to Tunneling Problems, *Trans. ASCE*, 1948, pp. 1310–1349.
417. WALKER, F. C., and W. W. DAEHN, Ten Years of Pore Pressure Measurements, *2d. Int. Conf. S.M. & F.E.*, Vol. III, pp. 245–250, 1948.
418. ———, and WILLIAM E. COLLINS, Earth Dam Design and Construction Practices of the Bureau of Reclamation, *2d Int. Conf. S.M. & F.E.*, Vol. III, pp. 250–253, 1948.
419. ———, and W. G. HOLTZ, *Comparison between Laboratory Test Results and Behaviour of Completed Embankments and Foundations*, paper presented at ASCE meeting, Los Angeles, May, 1950.
420. WARD, EDWARD R., JOHN R. BAYLISS, and PHILIP P. BROWN, Special Features on Large-scale Earth Pressure Tests, *Proc. ASCE*, January, 1948, pp. 49–57. Also *Trans. ASCE*, 1949, pp. 455–464.
421. WARD, WILLIAM H., The Effect of Vegetation on the Settlement of Structures, Excerpt from the *Proceedings of the Conference on Biology and Civil Engineering*, Institution of Civil Engineers, London, 1948.
422. ———, and E. C. SEWELL, Protection of the Ground from Thermal Effects of Industrial Plant, *Geotechnique*, Vol. II, No. 1, pp. 64–81, June, 1950.
423. WATER RESOURCES COMMITTEE, *Low Dams*, Superintendent of Documents, Washington, D.C., 1938, 431 pp.
424. WEISKOPF, WALTER H., Stresses in Soils under a Foundation, *J. Franklin Inst.*, Vol. 239, No. 6, pp. 446–465, June, 1945.
425. WELCH, JOHN D., *The Results of Tests in the Lateral Earth Pressure Meter, with a Discussion of Comparable Cell Test Data*, master's thesis, Princeton University, January, 1949.
426. WESTERGAARD, H. M., Plastic State of Stress around a Deep Well, *Contrib. S.M., Boston Soc. Civil Engrs.*, 1940, pp. 387–392.
427. ———, New Formulas for Stresses in Concrete Pavements of Airfields, *Trans. ASCE*, 1948, pp. 425–445.
428. WHITE, LAZARUS, *Report to . . . on the Collapse of the . . . Silos* (unpublished), 1940.
429. ———, and EDMUND ASTLEY PRENTIS, *Cofferdams*, Columbia University Press, 2d ed., 1950.
430. WHITE, ROBERT E., Heavy Foundations Drilled into Rock, *Civil Eng.*, January, 1943.
431. WILSON, GUTHLAC, The Calculation of the Bearing Capacity of Footings on Clay, *J. Inst. Civil Engrs.*, Vol. 17, pp. 87–96, 1941.
432. ———, and G. M. J. WILLIAMS, Pavement Bearing Capacity Computed by Theory of Layered Systems, *Proc. ASCE*, Vol. 76, Separate No. 16, May, 1950.
433. WINTERKORN, H. F., and L. D. BAVER, Sorption of Liquids by Soil Colloids, *Soil Science*, Vol. 38, 1934, pp. 291–298; Vol. 40, 1935, pp. 403–419.
434. ———, Surface-chemical Factors Influencing the Engineering Properties of Soils, *Proc. HRB*, 1936.
435. ———, Affinity of Hydrophilic Aggregate for Asphaltic Bitumen, *Industrial and Engineering Chemistry*, Vol. 30, pp. 1362–1368, 1938.
436. ———, and B. B. MOORMAN, A Study of Changes in Physical Properties of Putnam Soil Induced by Ionic Substitution, *Proc. HRB*, Vol. 21, pp. 415–434, 1941.
437. ———, The Condition of Water in Porous Systems, *Soil Science*, August, 1943, pp. 109–115.

438. ———, Principles and Practice of Soil Stabilization, *Colloid Chem.*, Vol. VI, pp. 459–492, 1946.
439. ———, A Laboratory Study of the Soil Stabilizing Effectiveness of Artificial Resins with Special Emphasis on the Aniline-furfural Resin, *CAA Tech. Des. Note* 43, 1947.
440. ———, and GREGORY P. TSCHEBOTARIOFF, Sensitivity of Clay to Remolding and Its Possible Causes, *Proc. HRB*, 1947, pp. 435–442.
441. ———, Fundamental Similarities between Electro-osmotic and Thermo-osmotic Phenomena, *Proc. HRB*, 1947, pp. 443–455.
442. ———, Engineering Uses and Limitations of Pedology for Regional Exploration of Soils, *2d. Int. Conf. S.M. & F.E.*, Vol. I, pp. 8–12, 1948.
443. ———, Soil Stabilization, *2d Int. Conf. S.M. & F.E.*, Vol. V, pp. 209–215, 1948.
444. ———, *Final Report on Beach Stabilization*, submitted to the Bureau of Yards and Docks, Department of the Navy, Nov. 15, 1949.
445. WOODS, K. B., and T. E. SHELBURNE, Pumping of Rigid Pavements in Indiana, *Proc. HRB*, 1943, pp. 301–316.
446. ———, F. H. GREEN, and H. S. SWEET, Pavement Pumping Correlated with Traffic Loads, *Proc. HRB*, 1947, pp. 209–231.
447. WOOLTORTON, D., A Preliminary Investigation into the Subject of Foundations in the "Black Cotton" and "Kyatti" Soils of the Mandalay District, Burma, *1st. Int. Conf. S.M. & F.E.*, Vol. III, pp. 242–256, 1936.
448. WRIGHT, ROY E., Chemical Stabilization of Sand Speeds Driving of 10-ft. Tunnel, *ENR*, Aug. 4, 1949.

NAME INDEX

J

K

L

M

N

O

P

U

V

W

SUBJECT INDEX

D

E

F

G

H

I

O

P

Q

R

S